



**POLITECNICO  
DI TORINO**

DEPARTMENT OF  
MECHANICAL AND  
AEROSPACE ENGINEERING  
(DIMEAS)

**MASTER OF SCIENCE IN AUTOMOTIVE ENGINEERING**

MASTER THESIS

**COMPARISON AND VALIDATION OF SIMULATION  
SOFTWARE FOR SHEET METAL FORMING OF  
AUTOMOTIVE SIDE INTRUSION BEAMS**

Supervisor

Prof. Paolo Minetola

Candidate

Vignesh Tamilarasu

Turin, Italy

July 2018

## **Abstract**

### **Title: Comparison and Validation of Simulation Software for Sheet Metal Forming of Automotive Side Intrusion Beams**

During a forming process, the elasto-plastic stress gradients across the surface build up and result in accumulation of residual stresses. The residual stresses cause the material to bounce back after forming. The resulting deviations from the profile often require manual adjustment before the component is considered acceptable for assembly. Components that do not fit in the final assembly usually need additional manual operations and assembly time. This increases the labour cost and also the overall cost and reduces the effectiveness of the process. The change in the cross section of the component also reduces the efficiency of the component. For example, in case of door reinforcement beam, the change in the cross section of the component, can change the way it absorbs energy in case of a crash leading to possible failures.

Anti intrusion beams are very important elements in the doors of the vehicle. They improve the strength of the door. Also it is a very important structure during the side crash. It absorbs the kinetic energy in case of an impact, thereby protecting the passenger in the vehicle. Here we consider the anti intrusion beam. We consider two components namely, PM13 and MA03. These components are manufactured using the crashform process. During the manufacturing process, the components undergo springback condition. So we simulate the springback with the help of software packages and evaluate the springback compensation. By Reverse Engineering, we scan the component and the dies. The scanned component has some missing or irregular surfaces due to the 3D scanning. So we reconstruct it to improve the geometry of the scanned component.

Simulations are performed in different software packages and the scanned component is compared with CAD model of the component. Numerous simulations with different parameters are considered. Comparisons are made between scanned actual component and simulation parameters, CAD component and simulation parameters, CAD and actual scanned component. These comparisons are made in software packages like Abaqus, Stampack, Autoform, Hyperform. The simulation results from these software packages are compared using the GOM inspect software to know the maximum and minimum distances, mean distance, standard deviation, pointwise evaluation. Also the software provides with the springback during the manufacturing process. It has the capability to evaluate the spring forward. Based on this results, the mould is redesigned. One or more copies of reference component would be produced with each of the different moulds. Now, 3D scanning of the actual geometry of different moulded parts is performed. They are evaluated for the one which is more geometrically similar to the nominal component. This increases the accuracy of the manufactured component. These are simulated in software rather than doing it in real time. It reduces man power, reduces the operational time and also the cost.

This method can be used for best accuracy and prediction capability to help engineers in designing the process more correctly.

## **Declaration**

It is hereby declared that the contents of this thesis are being submitted as a partial fulfillment for the Master of Science Degree in Automotive Engineering by **Vignesh Tamilarasu**, Student ID s218076, at Politecnico di Torino.

---

**PROF. PAOLO MINETOLA**  
*Academic Tutor*

---

**VIGNESH TAMILARASU**  
*Candidate*

**Place:** Torino, Italy

**Date:**

## **Acknowledgement**

I would like to express my gratitude and thank wholeheartedly, my Academic Advisor Prof. Paolo Minetola for being a great support right from providing me the opportunity to do my thesis at Department of Management and Production Engineering (DIGEP). His expertise in the field of Automotive Engineering and in specific to the Computer Aided Manufacturing technology (CAM) is the primary driving force for the successful completion of this thesis. I will never forget the efforts by my Prof. Paolo Minetola and I am fortunate enough to be guided also by his valuable suggestions during the course of this thesis and consequently through the series of presentations.

# Table of Contents

<b>Abstract.....</b>	<b>1</b>
<b>Declaration.....</b>	<b>1</b>
<b>Acknowledgement.....</b>	<b>1</b>
<b>List of Figures.....</b>	<b>1</b>
<b>List of Tables.....</b>	<b>1</b>

## **Chapter One**

<b>1.0 Introduction – Sheet Forming Process.....</b>	<b>1</b>
<b>1.1 The Deep Drawing Process.....</b>	<b>1</b>
<b>1.2 Parameters for Characterization of Metals in Forming Process.....</b>	<b>2</b>
1.2.1 Yield Strength.....	2
1.2.2 Elongation.....	3
1.2.3 Anisotropy.....	4
1.2.4 The Springback.....	4
1.2.5 Formability Curve.....	5
<b>1.3 Process Variables of the Drawing Process.....</b>	<b>6</b>
<b>1.4 Lubricants for the Process.....</b>	<b>6</b>
<b>2.0 Anti intrusion Beam or Side Impact Bar.....</b>	<b>7</b>
<b>2.1 Performance and Materials.....</b>	<b>7</b>
<b>2.2 EURO NCAP Side Impact Test.....</b>	<b>8</b>
<b>3.0 Sheet Metal Forming Simulation.....</b>	<b>9</b>
<b>3.1 Parameters in the Simulation Software Packages.....</b>	<b>9</b>
<b>3.2 Analysis and Comparison of FEA Software used by Polito.....</b>	<b>10</b>
3.2.1 Stampack.....	10
3.2.2 Abaqus.....	11
3.2.3 Comparison of Software.....	12
<b>3.3 Requirements for a Proper Comparison between the Scanning Data and Simulation Results.....</b>	<b>14</b>
<b>4.0 Reverse Engineering.....</b>	<b>15</b>
<b>4.1 Process Procedure for Mathematisation of the Mould Starting from the Scan Data.....</b>	<b>16</b>
4.1.1 Scanning of the Die and Punch.....	18
4.1.2 Definition of Curves Characteristics of the Mould.....	18
4.1.3 Generation of NURBS Surfaces on the Curve Network.....	18
4.1.4 Reconstruction of the Mould CAD Model.....	21

## **Chapter Two**

<b>5.0 Definition of Case Studies.....</b>	<b>23</b>
<b>5.1 Identification of the Input Data Required for Definition of Simulation Models.....</b>	<b>24</b>

<b>6.0</b>	<b>Research, Analysis and Selection of Software.....</b>	<b>24</b>
<b>6.1</b>	<b>Defining the Preliminary Model of Simulation Stampack.....</b>	<b>25</b>
<b>6.2</b>	<b>Characteristics of the Sheet Material.....</b>	<b>26</b>
<b>6.3</b>	<b>Case 1-3D Simulation Shell (CAD Dies, Wire Development Mathematized)..</b>	<b>29</b>
6.3.1	Thickness of Sheet at the End of Forming and Percentage Thinnings.....	30
6.3.2	Formability Analysis.....	31
6.3.3	Performance of the Moulding Force.....	32
6.3.4	Calculation of Elastic Return.....	33
6.3.5	Compensation of the Elastic Return.....	35
<b>6.4</b>	<b>Case 2-Solid 3D Simulation (By Scanning Moulds, Sheet Metal Thickness)..</b>	<b>40</b>
6.4.1	Thickness of the Sheet at the End of Forming.....	41
6.4.2	Formability Analysis.....	42
6.4.3	Contact Pressure.....	43
6.4.4	Performance of the Moulding Force.....	43
6.4.5	Calculation of Elastic Return.....	44
<b>7.0</b>	<b>Scanning of the Actual Geometry of Moulds and Components.....</b>	<b>46</b>
<b>7.1</b>	<b>PM13 Mould 3D Scanning.....</b>	<b>46</b>
7.1.1	Comparison of the Actual Geometry of the Mould with the CAD Model.....	47
<b>7.2</b>	<b>PM13 Component 3D Scanning.....</b>	<b>50</b>
7.2.1	Comparison of the Actual Geometry of the Component with the CAD Model.....	50
<b>7.3</b>	<b>MA03 Mould 3D Scanning.....</b>	<b>51</b>
<b>7.4</b>	<b>MA03 Component 3D Scanning.....</b>	<b>53</b>
7.4.1	Comparison of Actual Geometry of Component with the Scanning of the Surface of the Caliber.....	53
7.4.2	Comparison of the Actual Geometry of the Left Component with the CAD Model.....	54
<b>Chapter Three</b>		
<b>8.0</b>	<b>Refinement of the 3D Simulation Model Shell (PM13).....</b>	<b>56</b>
<b>8.1</b>	<b>Results.....</b>	<b>58</b>
8.1.1	Thickness of the Sheet at the End of Forming and Percentages Thinning.....	58
8.1.2	Formability Analysis.....	59
8.1.3	Performance of the Moulding Force.....	59
8.1.4	Calculation of Elastic Return.....	60
<b>9.0</b>	<b>Evaluation Model on the Second Case Study (MA03).....</b>	<b>62</b>
<b>9.1</b>	<b>Features of the Sheet Material (DP1000).....</b>	<b>63</b>
<b>9.2</b>	<b>Implementation of Gravity in the Model.....</b>	<b>65</b>
<b>9.3</b>	<b>Results.....</b>	<b>67</b>

9.3.1	Thickness of the Sheet at the End of Forming and Percentages Thinning.....	67
9.3.2	Formability Analysis.....	67
9.3.3	Performance of the Moulding Force.....	68
9.3.4	Calculation of Elastic Return.....	68
<b>10.0</b>	<b>Compariosn between BETA and Final Stampack 7.1.....</b>	<b>70</b>
<b>10.1</b>	<b>Comparison of the Results between Two Release for the Case of PM13 Study</b>	
10.1.1	Calculation of Free Elastic Return.....	73
10.1.2	Case Study of PM13.....	74
<b>10.2</b>	<b>Case Study of MA03.....</b>	<b>75</b>

#### Chapter Four

<b>11.0</b>	<b>Introduction to the Comparison of the Simulation Results.....</b>	<b>77</b>
<b>12.0</b>	<b>Simulations of PM13 Component.....</b>	<b>79</b>
<b>12.1</b>	<b>Comparison between Nominal Geometry (CAD) and Real Geometry Resulting from Scanning.....</b>	<b>80</b>
<b>12.2</b>	<b>Comparison between Nominal Geometry (CAD) and Simulation Results....</b>	<b>80</b>
12.2.1	Analysis of 3D Simulations Shell (CAD Dies, Wire Development Mathematized).....	80
12.2.2	Analysis of 3D Simulations Shell (By Scanning Dies, Wire Development Mathematized).....	82
12.2.3	Analysis of 3D Simulations Solid (By Scanning Moulds, Sheet Development with Thickness).....	83
<b>12.3</b>	<b>Comparison between Scanned Actual Geometry and Simulation Result.....</b>	<b>83</b>
12.3.1	Analysis of 3D Simulations Shell (CAD Dies, Wire Development Mathematized).....	83
12.3.2	Analysis of 3D Simulations Shell (By Scanning Dies, Wire Development Mathematized) – Release Final.....	84
12.3.3	Analysis of 3D Simulations Solid (By Scanning Moulds, Development Sheet with a Thickness).....	85
<b>13.0</b>	<b>Simulations of MA03 Component.....</b>	<b>85</b>
<b>13.1</b>	<b>Comparison between Nominal Geometry (CAD) and Real Geometry (Scan Data).....</b>	<b>86</b>
<b>13.2</b>	<b>Comparison between Nominal Geometry (CAD) and Simulation Results....</b>	<b>87</b>
13.2.1	Analysis of 3D Simulations Shell (By Scanning Dies, Wire Development Mathematized).....	87
13.2.2	Analysis of 3D Simulations Shell (CAD Dies, Wire Development Mathematized).....	88
13.2.3	Analysis of 3D Simulations Shell (Moulds from Scanning, Mathermatized Thread Development) – Final Release.....	89
13.2.4	Simulation Autoform (CAD Dies, Wire Development Mathematized).....	90
<b>13.3</b>	<b>Comparison between Scanned Actual Geometry and Simulation Results....</b>	<b>91</b>
13.3.1	Analysis of 3D Simulation Shell (By Scanning Dies, Wire Development Mathematized).....	91

13.3.2	Analysis of 3D Simulations Shell (CAD Dies, Wire Development Mathematized).....	92
13.3.3	Analysis of 3D Simulations Shell (Moulds from Scanning, Mathematized Thread Development) – Final Release.....	92
13.3.4	Simulation Autoform (CAD Dies, Wire Development Mathematized).....	93
<b>14.0</b>	<b>Reconstruction of the Actual Geometry of the Moulds.....</b>	<b>93</b>

**Chapter Five**

<b>15.0</b>	<b>Altair Hyperworks.....</b>	<b>96</b>
<b>15.1</b>	<b>Hyperform.....</b>	<b>96</b>
15.1.1	Capabilities of Hyperform Incremental.....	97
<b>16.0</b>	<b>Hyperform Simulation.....</b>	<b>98</b>
<b>16.1</b>	<b>Case 1 – PM13 Component Simulation.....</b>	<b>100</b>
16.1.1	Geometry Input.....	100
16.1.2	Percentage Thinnings.....	100
16.1.3	Plastic Strain.....	101
16.1.4	Formability Analysis.....	101
16.1.5	Comparison between the CAD and the hyperform simulation.....	102
16.1.6	Comparison between scanned geometry and hyperform simulation.....	103
16.1.7	Comparison Between Nominal Geometry and Simulation Results...	104
16.1.8	Comparison Between Actual Scanned 3D Geometry and Simulation Results.....	104
<b>16.2</b>	<b>Comparison between Hyperform Simulation and Stampack Simulation.....</b>	<b>105</b>
<b>17.0</b>	<b>Conclusion and Next Steps.....</b>	<b>106</b>

**Annex 12.1**

**Annex 12.2**

**Annex 12.3**

**Annex 13.1**

**Annex 13.2**

**Annex 13.3**

**Annex 16.1.7**

**Annex 16.1.8**

**Annex 16.2**

## List of Figures

Fig 1	Deep drawing process steps	2
Fig 2	Deep drawing process parameters	2
Fig 3	Higher yield, lower, middle	3
Fig 4	Specific extensions on stress strain curve	3
Fig 5	Sample specimen obtained from the plate and relative deformation directions	4
Fig 6	Springback	4
Fig 7	Forming limit diagram and formability curve	5
Fig 8	Side impact bar	7
Fig 9	EURO NCAP Side impact test	8
Fig 10	Shaping process analyzed with stampack	11
Fig 11	Capabilities of abaqus	12
Fig 12	Sample abaqus GUI	13
Fir 13	Sample stampack GUI	14
Fig 14	Reverse engineering process	15
Fig 15	Procedure for the scanning of the mould halves	17
Fig 16	Curve characteristics of the mould network	18
Fig 17	Procedure for creation of the network of curves and generation of NURBS Surfaces	19
Fig 18	Reconstructed surface portions of the mould from the curve network	20
Fig 19	Map of deviations of surfaces rebuilt with respect to scan data	20
Fig 20	Procedure for the reconstruction of the 3D CAD model	21
Fig 21	Union of blocks created from NURBS surfaces reconstructed	22
Fig 22	Reconstruction of the complete CAD model of the mould	22
Fig 23	Completion of the CAD model with holes or aesthetic changes	22
Fig 24	Anti-intrusion cross beam (PM13)	23
Fig 25	Anti-intrusion crossbeam (MA03)	23
Fig 26	Definition of the characteristics of the sheet material, 3D shell	26
Fig 27	Definition of characteristics of sheet material, elastic behaviour	27
Fig 28	Definition of characteristics of sheet material, plastic behaviour	27
Fig 29	Definition of characteristics of sheet material, anisotropy	28
Fig 30	Definition of characteristics of sheet material, forming limit curve	28
Fig 31	Definition of characteristics of sheet material, triaxiality failure diagram	29
Fig 32	Geometry input	30
Fig 33	Thickness of the sheet at the end of forming	30
Fig 34	Percentage of thinning	31
Fig 35	Formability FLD – risk of fracture	31
Fig 36	Forming of the results – formation of wrinkles	32
Fig 37	Force on the punch/die during the process	32
Fig 38	Return bound elastic (fast springback)	33
Fig 39	Extent of elastic return-quantitative evaluation (constrained elastic return)	34
Fig 40	Punctual deviations between component calculated with elastic return and bound nominal die side CAD geometry	34

Fig 41	Punctual deviations between component calculated with elastic return constrained and real geometry scanned	35
Fig 42	Software setup screen	36
Fig 43	Geometry obtained by the algorithm springforward	36
Fig 44	Geometry input	37
Fig 45	Return bound elastic (fast springback)	37
Fig 46	Extent of the elastic return quantitative evaluation (constrained elastic return)	38
Fig 47	Punctual deviations between calculated component with mould obtained from springforward with outside shape and nominal CAD geometry die side	38
Fig 48	Punctual deviations between calculated component with mould obtained from springforward with outside shape and real geometry scanned	39
Fig 49	Simulation with and without parting	39
Fig 50	Punctual deviations between calculated component with mould obtained from springforward without outside shape and nominal CAD geometry	40
Fig 51	Punctual deviations between calculated component with mould obtained from springforward without outside shape and real geometry scanned	40
Fig 52	The mould geometry	41
Fig 53	Thickness of the sheet at the end of forming	41
Fig 54	Compare 3D shell vs 3D solid thickness of sheet at the end of forming	42
Fig 55	Formability TFD	42
Fig 56	Contact pressure	43
Fig 57	Force on the punch/die during the process	43
Fig 58	Return bound elastic (fast springback)	44
Fig 59	Extent of the elastic return quantitative evaluation (constrained elastic return)	44
Fig 60	Punctual deviations between nominal CAD model of component and result of simulation with 3D geometry of the real mould	45
Fig 61	Punctual deviations between actual geometry of component and result of simulation with 3D geometry of the real mould	45
Fig 62	Scanner structured light ATOS core 300	46
Fig 63	Scanning of the die (OP40) of PM13 component mould	47
Fig 64	Die OP40-alignment for comparing scan data and CAD model	47
Fig 65	Map of deviations between CAD model and scan data for OP40 die	48
Fig 66	Cricca on the die (OP40) of PM13 left component	48
Fig 67	Punctual deviations between CAD model and scan data for OP40 die	49
Fig 68	Punctual deviations between CAD model and scan data for OP40 punch	49
Fig 69	Deviation on side walls and in section between CAD model and scan data for punch OP40	50
Fig 70	Pointwise deviations between scanned data and CAD model for PM13 cross	51
Fig 71	Deviations at an altitude of section Y=240 mm	51
Fig 72	Scanning of the die (OP20) of the MA03 component mould	52
Fig 73	Scanning of the MA03 component reported on the test gauge	52
Fig 74	Comparison of 3D scan data with respect to points detected on one surface of first component MA03 positioned on the test gauge	53
Fig 75	Punctual deviations of 3D scan data with respect to points detected on one surface of first component MA03 positioned on test gauge	53

Fig 76	Comparison of 3D scan data with respect to points detected on one surface of second component MA03 positioned on the test gauge	54
Fig 77	Punctual deviations of 3D scan data with respect to points detected on one surface of second component MA03 positioned on test gauge	54
Fig 78	Best fit alignment views between scan data of left MA03 and nominal CAD	55
Fig 79	Pointwise deviations between actual geometry of left bar and CAD model	55
Fig 80	Geometry input	56
Fig 81	Condition of contact and friction coefficients	57
Fig 82	Cross section of mould at end of moulding:3D model shell base(left) and 3D model shell top/bottom(right)	57
Fig 83	Sheet thickness at end of forming-3D shell base(top) and 3D model shell top/bottom(bottom)	58
Fig 84	Percentage of thinning-3D shell base(top) and 3D model shell top/bottom(bottom)	59
Fig 85	Formability FLD-3D shell base(top) and 3D model shell top/bottom(bottom)	59
Fig 86	Formation of wrinkles-3D shell base(top) and 3D model shell top/bottom(bottom)	59
Fig 87	Force on punch/die during the process-3D shell base(black curve) and 3D model shell top/bottom(red curve)	60
Fig 88	Position of constraint points (isostatic configuration)	60
Fig 89	Comparison between deformed shape by CAD moulds with isostatic constraint compared to average plane of CAD component PM13	61
Fig 90	Comparison between deformed shape from real moulds with isostatic constraint compared to average plane of CAD component PM13	61
Fig 91	Geometry input-model of moulds,steering column,plate development	62
Fig 92	Condition of contact and friction coefficients	62
Fig 93	Summary of characteristics of sheet material	63
Fig 94	Characteristics of sheet material, density and elastic behaviour	63
Fig 95	Characteristics of sheet material, plastic behavior	64
Fig 96	Characteristics of sheet material, anisotropy	64
Fig 97	Characteristics of sheet material, forming limit curve	65
Fig 98	Cross section of mould showing positioning of development of sheet metal prior to application of gravity(left) and at end of step of applying gravity(right)	65
Fig 99	Placement of development of first application of gravity sheet(top) and at end of phase of application of gravity(bottom)	66
Fig 100	Screenshot of software for implementation of severity in model	66
Fig 101	Thickness of sheet at the end of forming	67
Fig 102	Percentages thinning	67
Fig 103	Formability FLD	68
Fig 104	Forming of the results	68
Fig 105	Force on the punch/die during process	68
Fig 106	Position of constraint points (very static configuration)	68
Fig 107	Comparison between deformed shape from real moulds with constraint hyperstatic compared to average plane of CAD component MA03	69
Fig 108	Pointwise deviations between actual geometry of left bar MA03 and CAD	70

Fig 109	Plate thickness at end of forming results obtained stampack 7.1 final release(top) and beta(bottom)	71
Fig 110	Thinning percent results obtained stampack 7.1 final release(top) and beta(bottom)	71
Fig 111	Formability FLD result obtained stampack 7.1 final release(top) and beta(bottom)	71
Fig 112	Formability FLD result obtained stampack 7.1 final release(top) and beta(bottom)	72
Fig 113	Performance of forming results obtained stampack 7.1 final release(top) and beta(bottom)	72
Fig 114	Force on the punch/die during the process	72
Fig 115	Comparison between deformed shape from real moulds obtained with final release of software compared to average plane of CAD component PM13	73
Fig 116	Screen for setting springback	74
Fig 117	Comparison between deformed shape free from real moulds with elastic return compared to average plane of CAD component PM13	75
Fig 118	Comparison between deformed shape free from real moulds with elastic return compared to average plane of CAD component MA03	76
Fig 119	Comparisons with nominal geometry (CAD) as a reference	78
Fig 120	Comparisons with real geometry (scan data) as a reference	78
Fig 121	MA03 component scan reported on test gauge	90
Fig 122	Network of curves generated for reconstruction of mathematical model of lower mould component of PM13	94
Fig 123	Surfaces rebuilt for reconstruction of mathematical model lower mould of PM13	94
Fig 124	Surfaces rebuilt for reconstruction of mathematical model of upper mould of PM13	95
Fig 125	Surfaces rebuilt for reconstruction of mathematical model of upper mouldMA03	95
Fig 126	Surfaces rebuilt for reconstruction of mathematical model of upper mouldMA03	95
Fig 127	Hyperform interface	97
Fig 128	Hyperworks user profiles	98
Fig 129	Incremental radios – autoprocess	99
Fig 130	Hyperview interface	99
Fig 131	Geometry input	100
Fig 132	Percentage of thinning	100
Fig 133	Plastic strain	101
Fig 134	Formability FLD	101
Fig 135	Forming of the results	101
Fig 136	Surface comparison between hyperform simulation and CAD bottom	102
Fig 137	Surface comparison between hyperform simulation and CAD average	102
Fig 138	Surface comparison between hyperform simulation and CAD top	103
Fig 139	Surface comparison between hyperform simulation and scanned bottom	103
Fig 140	Surface comparison between hyperform simulation and scanned top	104
Fig 141	Surface comparison between stampack simulation and hyperform simulation	105
Fig 142	Experimental procedure to compensate deviations of manufactured component compared to the nominal geometry	107

## List of Tables

Table 1	Comparison between reality and simulation in terms of parameters considered	9
Table 2	Commercial software for the simulation of sheet metal forming process	10
Table 3	Comparison between Abaqus and Stampack	12
Table 4	Calculation time for each simulation stage (PM13)	58
Table 5	Calculation time for each simulation stage (MA03)	67
Table 6	Statistical parameters of distribution of variances obtained with two versions of software	73
Table 7	Calculation time for each simulation stage (PM13)	74
Table 8	Calculation time for each simulation stage (MA03)	75
Table 9	Matrix of possible comparisons on basis of available component models	77
Table 10	Comparison results between the actual surfaces of component and nominal CAD surfaces	80
Table 11	Comparison results between the actual 3D geometry of component and 3D CAD geometry	80
Table 12	Comparison results between the simulation and deformed shape by upper nominal surface	81
Table 13	Comparison results between the simulation and deformed shape by lower nominal surface	81
Table 14	Comparison results between the simulation and deformed shape by average nominal surface	81
Table 15	Comparison results between the simulation and deformed shape by upper nominal surface	82
Table 16	Comparison results between the simulation and deformed shape by lower nominal surface	82
Table 17	Comparison results between the simulation and deformed shape by average nominal surface	82
Table 18	Comparison results between the deformed shape 3D simulation and 3D CAD geometry	83
Table 19	Comparison results between the deformed shape 3D simulation and upper surface of actual 3D scanned geometry	83
Table 20	Comparison results between the deformed shape 3D simulation and lower surface of actual 3D scanned geometry	83
Table 21	Comparison results between the deformed shape 3D simulation and upper surface of actual 3D scanned geometry	84
Table 22	Comparison results between the deformed shape 3D simulation and lower surface of actual 3D scanned geometry	84
Table 23	Comparison results between the deformed shape 3D simulation and actual scanned 3D geometry	85
Table 24	Comparison results between actual surfaces of the component and nominal CAD surfaces	86

Table 25	Comparison results between the simulation and deformed shape by the upper nominal surface	87
Table 26	Comparison results between the simulation and deformed shape by the lower nominal surface	87
Table 27	Comparison results between the simulation and deformed shape by the average nominal surface	87
Table 28	Comparison results between the simulation and deformed shape by the upper nominal surface	88
Table 29	Comparison results between the simulation and deformed shape by the lower nominal surface	88
Table 30	Comparison results between the simulation and deformed shape by the average nominal surface	88
Table 31	Comparison results between the simulation and deformed shape by the upper nominal surface	89
Table 32	Comparison results between the simulation and deformed shape by the lower nominal surface	89
Table 33	Comparison results between the simulation and deformed shape by the average nominal surface	89
Table 34	Comparison results between deformed shape Autoform simulation and nominal CAD surfaces	90
Table 35	Comparison results between deformed shape 3D simulation and the upper surface of actual 3D scanned geometry	91
Table 36	Comparison results between deformed shape 3D simulation and the lower surface of actual 3D scanned geometry	91
Table 37	Comparison results between deformed shape shape 3D simulation and the upper surface of actual 3D scanned geometry	92
Table 38	Comparison results between deformed shape shape 3D simulation and the lower surface of actual 3D scanned geometry	92
Table 39	Comparison results between deformed shape 3D simulation and from the upper surface of actual 3D scanned geometry	92
Table 40	Comparison results between deformed shape 3D simulation and from the lower surface of actual 3D scanned geometry	92
Table 41	Comparison results between deformed shape by simulation Autoform and real surfaces from scan data	93
Table 42	Comparison results between CAD surfaces and hyperform simulation	104
Table 43	Comparison results between actual scanned 3D geometry and hyperform simulation	104
Table 44	Comparison results between stampack simulation and hyperform simulation	105

# Chapter One

## 1 Sheet Forming Process

The term "forming" is a series of mechanical operations to obtain a shaped object, starting from a sheet of metal laminate (Blank), by subjecting the laminate to plastic deformation. Typically the process is divided into three categories:

(i) Shearing                      (ii) Folding and Bending                      (iii) Drawing

Generally the first two operations are performed in the cold, while drawing can operate at cold or hot depending on which degree of viability is greater. Since it is not always possible to reach the final geometry with one of the three techniques, to obtain a finished piece of stamped sheet metal we do one or more of the three operations.

The ordered series of operations designed to transform flat sheet into an object is influenced by:

- Shape of the object to obtain: Simpler the geometry and less deep is the cavity, the shorter will be the sequence of operations to accomplish.
- Size of the object: For thicker metal sheets, especially of hard steel or other deformable materials require a little hot working.
- Characteristics of the material: A very plastic material is adapted to be subjected to a very deep drawing without risk of breakage, while a less plastic material does not allow.

### 1.1 The Deep Drawing Process

Deep drawing is a manufacturing process that is used extensively in the forming of sheet metal into cup or box like structures. Automobile parts such as panels and gas tanks, are among a few of the items. It is performed with a punch and die. The punch is the desired shape of the base of the part, once drawn. The die cavity matches the punch and is a little wider to allow for its passage, as well as clearance. The sheet metal work piece called a blank is placed over the die opening. The punch travels towards the blank. After contacting the work, the punch forces the sheet metal into the die cavity, forming its shape. Theoretically the simple processing of drawing should not alter the initial thickness of the sheet, which should therefore remain equal to that of the initial raw sheet. In reality, thickness of the laminate is also changed heavily.

Material must withstand enormous transformations to maintain continuity of the structure during progressive hardening. Corner radius for deep drawing manufacturing should be sufficient to allow for smooth metal flow. For too small radius, the blank can tear as the material is traveling over the corners. Corner radius optimization should be achieved, because too large radius causes wrinkling.

## DEEP DRAWING OF SHEET METAL

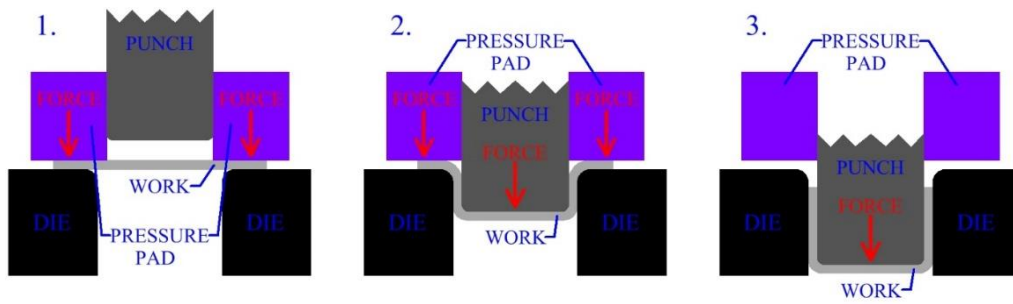


Figure 1 - Deep drawing process steps

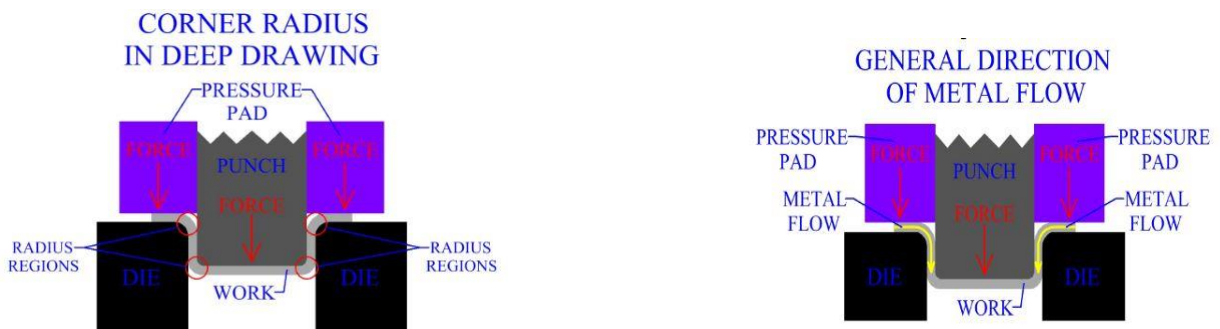


Figure 2 - Deep drawing process parameters

The blank holder must exert maximum pressure allowed by the strength of the material limits. In practice, greater resistance to breakage of the material is in relationship with the cross-section of the same.

## 1.2 Parameters for the Characterization of the Metals in Forming Process

### 1.2.1 Yield Strength

The yield stress is the limit in the  $\sigma$ - $\epsilon$  diagram at which the deformation starts to increase very quickly without an equivalent increase in stress. It thus characterizes the passage of material from the elastic to plastic state, in which the permanent deformations are recorded. A limit of moderate yield facilitates the drawing operation, since it takes before the field of plastic deformation, thus allowing the plasticization of the material.

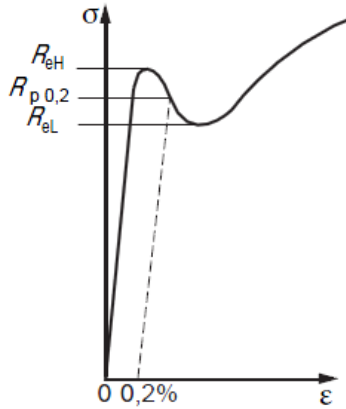


Figure 3 - Higher yield, lower, middle

## 1.2.2 Elongation

This measurement is used to quantify the ductility of material, the ability to absorb inelastic deformations without breaking. At the same strength and hardness, the more ductile materials are best suited to absorb overloads and to be cold-worked by plastic deformation.

To express the deformability of the material, it depends on number of factors such as:

- Intrinsic properties: Chemical composition, Crystalline grain size, Treatment undergone.
- Specimen dimensions: For the same section, the short tubes lengthen more than long ones.
- Breaking position: If the break is not central, the elongation percentage decreases.

It is positive to have a material with high elongation value to respond in an appropriate manner during stretching in moulding.

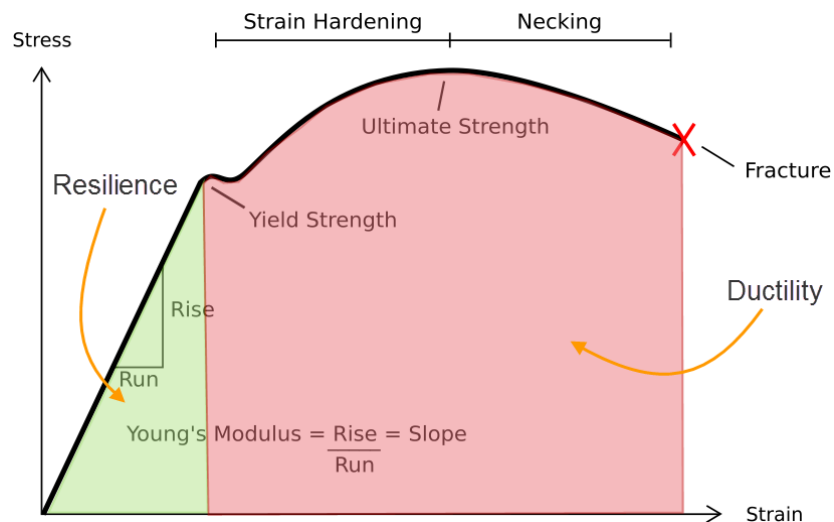


Figure 4 - Explanation specific extensions on the  $\sigma$ - $\epsilon$  diagram

### 1.2.3 Anisotropy

The anisotropy is present not only on the plane of the sheet (planar anisotropy), but also in the direction of its thickness (anisotropy normal or plastic). In reference to the tensile test, evaluating the coefficient of plastic anisotropy, defined according to the formula.

$$R = \frac{\epsilon_W}{\epsilon_T} \quad (2.3)$$

- $\epsilon_W$  is the actual deformation in the width direction of the tube.
- $\epsilon_T$  is the actual deformation in the direction of thickness of the tube.

More the value of R, higher the anisotropy of material. In moulding, the normal plastic anisotropy coefficient R must be very high ( $> 2$ ) for an adequate response of the material during moulding and to avoid the phenomenon of "necking" (thinning in the most deformation points).

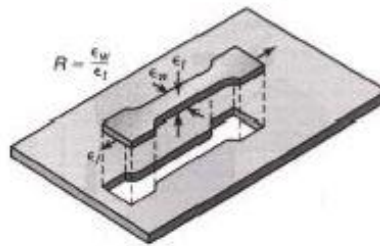


Figure 5 - Sample specimen obtained from the plate and relative deformation directions

### 1.2.4 The Spring back

It is a characteristic of the material especially in the bending process. The mould bend angles must provide for an increase with respect to the workpiece bending angles, in such a way as to compensate for the effects of elastic return and restrict them within certain tolerance range. The simulation tools are used, both for the prediction of the conventional cases of breakage, wrinkles, thinning, and to simulate the secondary operations including the elastic return.

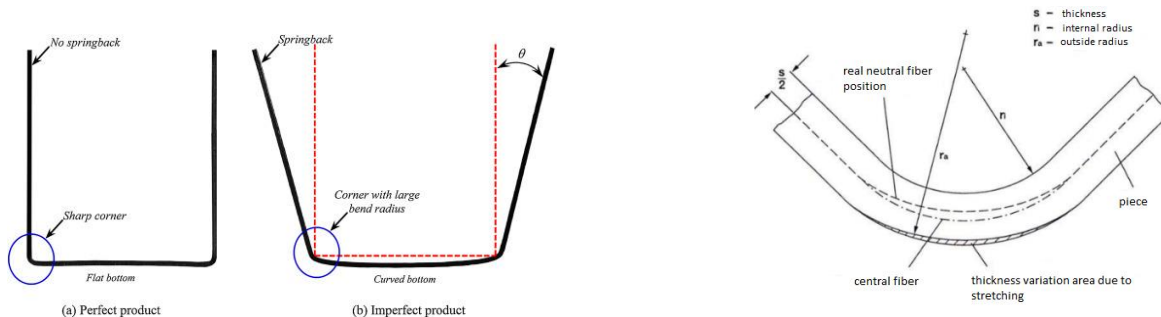


Figure 6 - Springback

In the outer fibers it has stretching which causes a reduction in thickness. In the inner fibers instead, a compression occurs. The compression and stretching actions that occur in the bending

zone must be compensated by an average of "movements" of material. This phenomenon is not uniform and constant. The extent of springback depends strongly in the ratio between the bending radius and the sheet thickness to be bent.

The compensation of surfaces of the mould is implemented in the opposite direction to the elastic return with the same value, by means of an effective algorithm. A successful compensation is strongly linked to a stable moulding process, since the springback is highly influenced by the variations of the process parameters and material.

### 1.2.5 Formability Curve

It indicates the ability of a sheet to be deformed from its initial shape to defined final form. In a generic forming process, there is stretching of the material situations, both at the general level and in localized areas, which in extreme case results in the rupture. Analyzing the total phenomenon, one can identify the key elements in three factors as:

- (i) The material;
- (ii) The process;
- (iii) The shape to be obtained

These curves were recognized as boundaries between combinations of deformations that produced instability and fractures and those which were permitted in forming operations. The formability curve for a particular material is a graphical representation that illustrates the main deformation limit that it could suffer without leading to breakage or to the formation of wrinkles on the workpiece. A schematic FLD, with various linear deformation, fracture limits and states of deformation that produce wrinkling is shown.

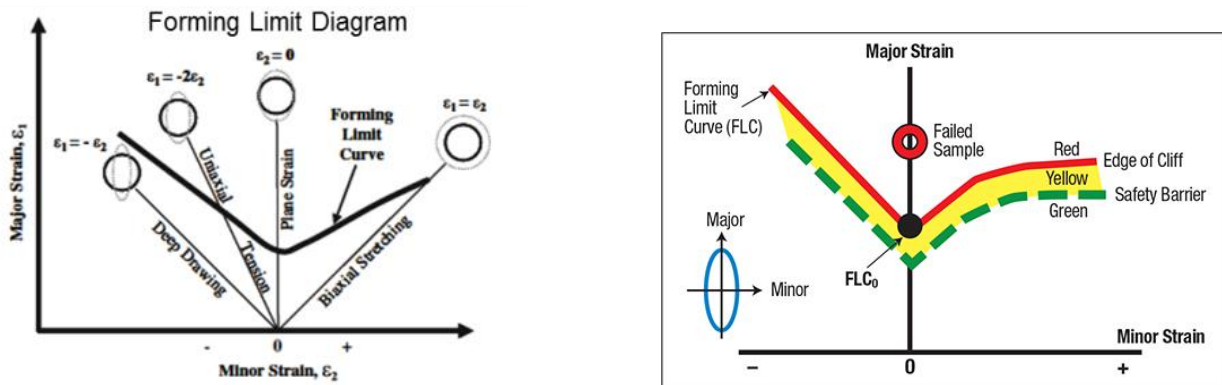


Figure 7 - Forming Limit Diagram and formability curve

Therefore, the type and quality of the chosen material greatly affect the machining process. It is therefore essential to carry out a series of tests on the material itself before it can determine whether it is the most suitable to be formed.

### 1.3 Process Variables of the Drawing Process

- **Spinning speed:** It is variable during the stroke of the punch, reaching maximum impact with the sheet and a null value to the closing of the mould.
- **Reduction ratio:** It is measured using the same variables as drawing ratio. Reduction can be calculated by  $r = (D_b - D_p)/(D_b)$ , where  $D_b$  and  $D_p$  being blank and punch diameters respectively. Often expressed in percentage, the reduction should be 50% or under.
- **Drawing ratio:** Higher the drawing ratio, more extreme the amount of deep drawing. Due to the geometry, forces, metal flow and material properties of the work, there is a limit to the amount of deep drawing that can be performed on a sheet metal blank in a single operation. The drawing ratio is roughly calculated as

$$DR = D_b/D_p$$

where  $D_b$  and  $D_p$  being blank and punch diameters respectively.

The limit to the drawing ratio for an operation is usually 2 or under. Actual limits also depends on the depth of drawing, punch radius, die radius, anisotropy of the sheet and the blank material.

- **Limit value of the spinning ratio:** It indicates the ratio beyond which inevitable fracture of the deep-drawn piece takes place since the required load exceeds the material capacity. Generally, steels by deep drawing admit LDR values between 1.8 and 2.0.

### 1.4 Lubricants for the Process

As described above, in order to transform a laminated sheet into a deep-drawn object, it is necessary to apply an axial force within the forming limits of the material. To prevent breakages on the material and to make the whole process easier, it is necessary that all the surfaces in contact are sufficiently lubricated, in such a way that also prolongs the life of the mould itself.

To deal with such high values of force, the choice of lubricant is very important for successful operations. Under such pressure, the drawing lubricant should:

1. Prevent metal-to-metal adhesion or welding.
2. Cushion the die during the drawing operation.
3. Provide boundary lubrication between the die and workpiece.
4. Cool the die and workpiece.

## 2 Anti Intrusion Beam or Side Impact Bar

An anti-intrusion bar is a passive safety device installed in cars and other ground vehicles, which must protect passengers from side impacts which are particularly dangerous for two reasons:

- a) The location of impact is very close to the passenger, that can be immediately reached by the impacting vehicle.
- b) In many side-impact accidents, the impacting vehicle may be larger, taller, heavier or structurally stiffer than the struck vehicle. The role of an anti-intrusion bar is to absorb the kinetic energy of the colliding vehicle that is partially converted into internal work of the members involved in the crash.

### 2.1 Performance and Materials:

The performance of a side beam is measured by several indicators. The most important are:

- The maximum depth or diameter of the bar must be reasonably small, as the vehicle door does not generally allow much space.
- The Specific Energy Absorption
- The energy efficiency  $\eta$ , which is the ratio between the mean load and the peak load transmitted to vehicle during the impact
- The anti-intrusion bars are generally made of high strength steels. However, some studies indicate that stainless steel 304 might be a better choice, because of its larger plastic field and a larger amount of potentially absorbed energy before fracture
- The cost of the member must be possibly small.



Figure 8 - Side impact bar

## 2.2 EURO NCAP Side Impact Test

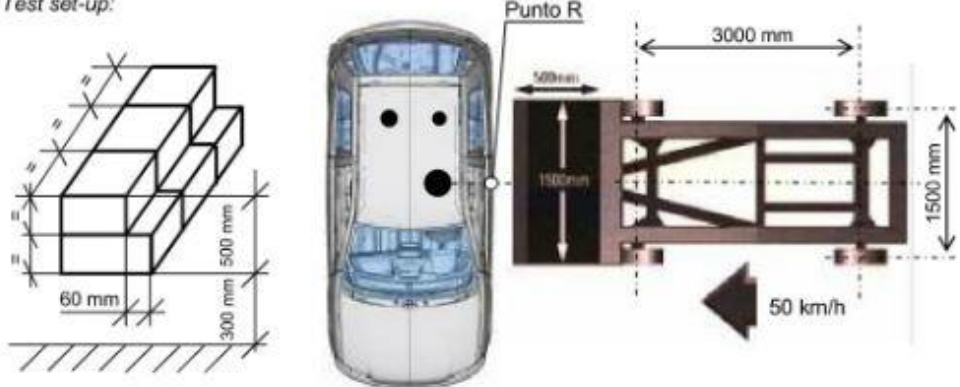
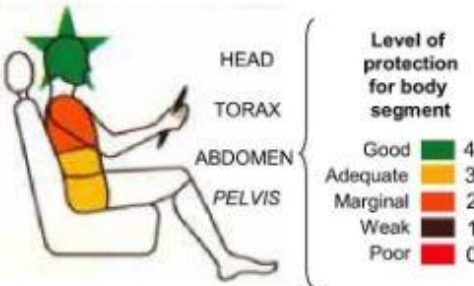
Impact configuration: <b>SIDE</b>	Test name: <b>EURO NCAP</b>	Test type: <b>RATING</b>
<p><i>Test set-up:</i></p> 		
<p><i>Impact speed:</i> <b>50 km/h</b></p>	<p><i>Requirements:</i></p>	
<p><i>Obstacle description:</i></p> <p><b>Mobile Deformable Barrier (MDB)</b>  <b>Mass 950 kg</b>  <b>Perpendicular impact on driver side (trolley x axis centred on R point)</b></p>	<p><u>Biomechanics</u></p>  <p><b>Level of protection for body segment</b></p> <ul style="list-style-type: none"> <li>Good 4</li> <li>Adequate 3</li> <li>Marginal 2</li> <li>Weak 1</li> <li>Poor 0</li> </ul>	
<p><i>Payload typology:</i></p> <p>One EUROSID-2 dummy ( 80 kg )            One P 1 1/2 dummy with CRS (rear left : 11+3 kg)            One P 3 dummy with CRS (rear right: 15+3 kg)            Fuel tank 90% filled (with coloured H<sub>2</sub>O )</p>		
<p><i>Purpose of the test:</i></p> <p>Occupant biomechanical responses            C.R.S behaviour            No doors opening during the impact            Fuel system integrity            Post-crash rescue possibilities</p>		

Figure 9 - EURO NCAP side impact test

### 3. Sheet Metal Forming Simulation

This is a technology to calculate the process of sheet metal stamping, predicting common defects such as splits, wrinkles, spring back and material thinning. Also known as forming simulation, the technology is a specific application of non-linear finite element analysis. The technology has many benefits in the manufacturing industry, especially the automotive industry, where lead time to market, cost and lean manufacturing are critical for the success of a company.

#### 3.1 Parameters considered in the Simulation Software Packages

This provides an overview of what happens in reality and what is taken into account in a simulation model. In principle, the approximations of the simulation model are sufficient to provide good results from the moulding point of view.

*Table 1 - Comparison between reality and simulation in terms of the parameters considered*

<b>Factor</b>	<b>Reality</b>	<b>Simulation</b>	<b>Implementation Difficulties In Simulation</b>
Process Speed	Non-constant	Not considered	High. It requires a dynamic model (Consideration of inertia)
Press	Elastic	Not considered	High
Equipment	Elastic	Rigid or not considered	Average. Increases complexity in the modeling and computing time
Friction	Non-constant	Constant	High. Friction is dependent on lubricant quantity, surface quality of elements involved in contact
Temperature	Non-constant	Not considered	Average. Thermomechanical characterization of material is required and considerably increases the calculation time
Surface characteristics of the blank holder	Non-constant	Not considered	High. The considerations exposed to friction
Material	Complex	Simplified models	High
Material Properties	Non-constant	(Not) Constant	Average. It depends on the materials of the software database customization possibilities

## 3.2 Analysis and Comparison of FEA Software used by Polito

Currently, there are several commercial software packages that allow us to simulate the sheet metal forming process. The key features of the software packages are summarized.

Table 2 - Commercial software for the simulation of sheet metal forming process

	Multistage Forming	Formability	Blank	Die	Springback
	Process	Analysis	Design	Design	Analysis
Fastform	✓	✓	✓	✗	✓
Dynaform	✓	✓	✓	✓	✓
ABAQUS	✓	✓	✗	✗	✓
LS-Dyna	✓	✓	✗	✗	✓
Autoform	✓	✓	✓	✓	✓
Pam-Stamp 2G	✓	✓	✓	✓	✓
Qform 3D	✓	✓	✗	✗	✗
Deform	✗	✗	✗	✗	✓
Hyperform	✓	✓	✓	✓	✓
Openform	✓	✓	✓	✗	✓
Stampack	✓	✓	✓	✗	✓

Below are detailed the characteristics of Stampack and Abaqus software, available at the Polytechnic and used during the project. A brief comparison is presented at the end of this discussion in the form of table.

### 3.2.1 Stampack

It is a software dedicated to the simulation of sheet metal forming processes specific for the hydro-forming applications, coining, bending of tubes, deep drawing, forming parts for the automotive and aeronautical sector.

Implementing Stampack in the process of defining the method reduces the need for creation of physical prototypes to validate design assumptions. Less number of mould tests has an extremely positive impact on the overall costs of the process. The evaluation of the final shape of the component takes into account all the variables that intervene in the process such as pressure, time, coating material, lubrication, pressing, etc, in order to anticipate possible problems on the finished workpiece (cracks, creases, spring back, etc). Available a large database of materials with a simplified user interface.

### Areas of application and main users

The main sectors to use the software, as declared by the developer Quantech ATZ are:

- Automotive and Aerospace
- Home Appliances
- Packaging

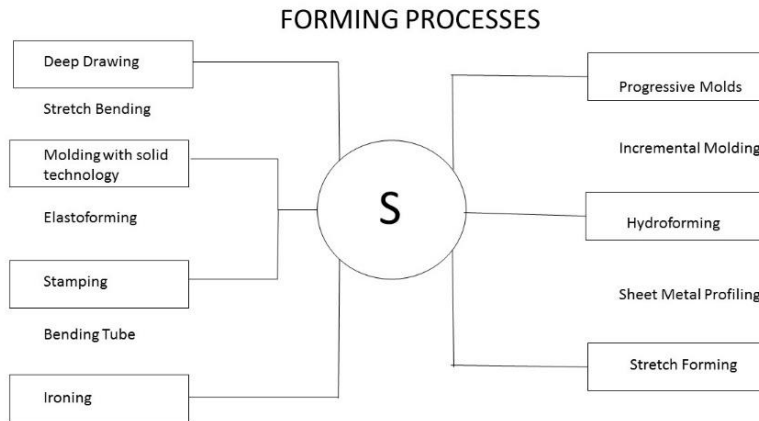


*Figure 10 - Shaping processes analyzed with Stampack*

## Functionality

- Powerful analysis tools of forming process: cracks, surface defects, thickness variation, strains.
- It provides an accurate analysis on the final geometry of the workpiece with the evaluation of the elastic return or with the guidelines on the compensation to be applied to the original geometries. The analysis of the elastic return shows the result of the process speculated moulding and graphically displays the displacement with respect to the theoretical shape caused by springback. It can also have some suggestions to modify the equipment in order to recover the elastic deformation.

### 3.2.2 Abaqus

#### Areas of application and Users

The Abaqus unified FEA product suite offers powerful and complete solutions for complex design problems, covering a broad spectrum of industrial applications. In the automotive industry, for example, the working groups within the design have the ability to consider the full load of the vehicle, dynamic vibration, multibody systems, impact/collision, non-linear static coupling, acoustic/structural coupling via a common model of the data structure and an integrated solver technology.

Below are some examples of use by companies of different sectors:

- Aerospace and Defence
- Consumer goods
- Energy and processes
- Industrial Equipment

## Functionality

- Analysis of the finished and Multiphysics elements: It allows analysis of coupled physical problems (eg. Thermo-mechanical, thermo-electrical, structural-acoustic etc)
- Materials: It can be analyzed by the software using multiple levels of modeling, from purely elastic characterization in complex models up to composites, human tissues.
- Managing assembled: It can define dynamic models multi-component, having the ability to define in detail the contacts between the various bodies - rigid or deformable.
- Fracture: It can be used to evaluate the effect of ballistic impacts and to evaluate the propagation of the fracture in a component during the deformation.



Figure 11 - Capabilities of Abaqus

### 3.2.3 Comparison of Software

The description of the two Stampack and Abaqus software in terms of compliance with the proposed criteria is summarized below.

Table 3 - Comparison between Abaqus and Stampack

Criteria	Abaqus	Stampack
Ability to import mathematized surfaces (CAD 3D file: step, .xt, iges)	Yes	Yes
Ability to import files obtained by scanning surfaces (STL file)	Yes, but simulation in most cases does not come to an end	Yes
Ability to modify the rheological curves directly from SW	Yes, ability to fully define the material (subroutine)	Yes, but only for the models provided within the software

Possibility to simply change the type of calculation to obtain greater or lesser accuracy in the calculation	No	Yes
Simplicity in defining boundary conditions (Drawbead, Control Forces, Coefficient of Friction)	No, there are no tools that simplify their creation	Yes, there are tools that allow you to enter only the characteristic parameters
Possibility / Ease of exporting data to other SW into readable formats	Yes, the most common fromats are available. You can export all of the output data to the exclusion of the relative values of the state variables (Internal software parameters)	Yes, all output data is available in ASCII format. The importability in another environment depends on the third software
Ease of introduction and modification of forms to improve virtual level	No, the changes have to be made on an external CAD software. However, you can upgrade in semi-automatic mode, the Abaqus model	No, the changes have to be made on an external CAD software
Mesh Size Definition	Yes, fully manageable (even variable size, type, accuracy)	Yes, fully manageable (even variable size, type, accuracy)
Indication of good meshing of the particular study	Yes	Yes

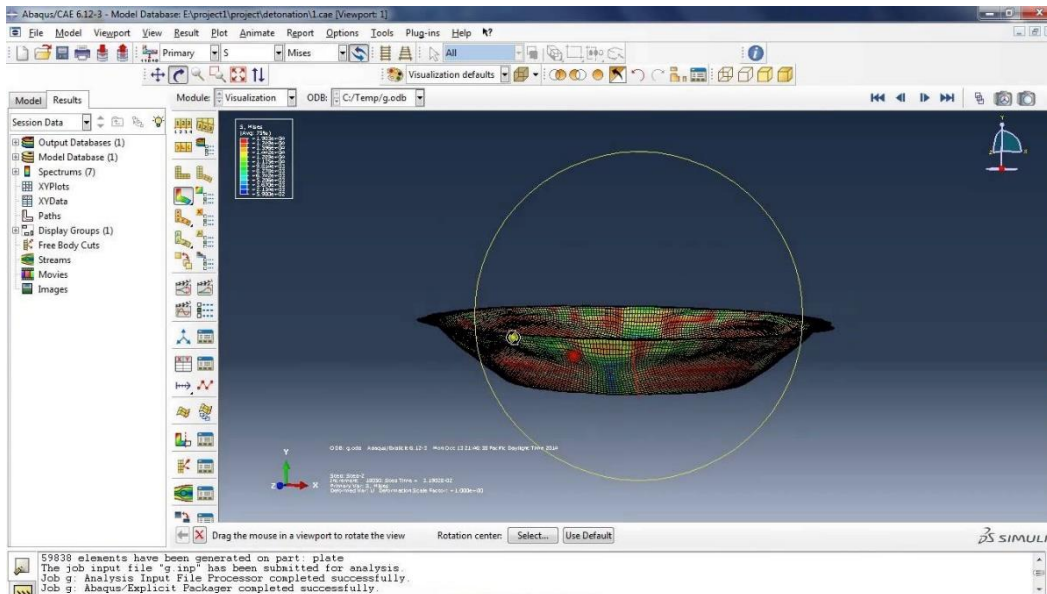


Figure 12 - Sample Abaqus GUI

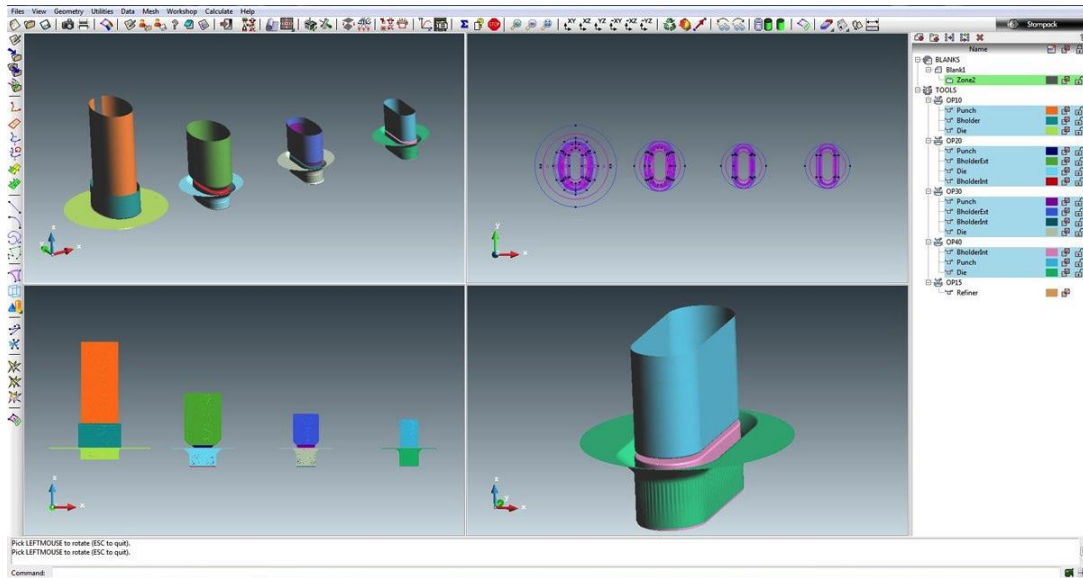


Figure 13 - Sample Stampack GUI

### 3.3 Requirements for a Proper Comparison between the Scanning Data and Simulation Results

The actual geometry of the particular products for PM13 and MA03 components has been acquired by scanning with light in the optical system structured ATOS Core 300.

The scan data in STL format, represent tessellated surfaces by means of the actual 3D geometry or actual components of the products. These surfaces are represented with a triangular mesh that connects the scan points. STL model includes lower surface, upper surface and side surfaces (in the thickness direction). In current versions of the Reverse Engineering software, there is a facility that allows to extract or calculate the average surface starting from triangles of two opposing surfaces. It is advised that the tessellated surfaces do not have a mathematical formulation and surfaces are not ideal because they are the result of the scan of a real object. The calculation for the extraction of the average plane of the STL model is therefore not straightforward.

It has therefore, the following surfaces relative to sheet metal component geometry to be analyzed:

- Nominal geometry of component (CAD): Solid model, middle plane, lower and upper surface
- Scanning of real component (STL model): Solid model, lower surface and upper surface
- Stampack Software: The result of the calculation of the deformed shape as a result of the elastic return is provided on the middle plane
- Autoform Software: The result of the calculation of the deformed shape as a result of the elastic return is provided on the lower or upper surface, depending on how the mould design has taken the reference to the fixed or movable mould for defining the simulation model

- Abaqus Software: The result of the calculation of the deformed shape as a result of the elastic return is provided on the middle plane, on the lower or upper surface, depending on the surface considered in phase of the simulation model definition.

The deformed shape obtained with the Autoform software are not comparable with other, because the data provided by Autoform correspond to a simulation mode which does not correspond to those that can be used within Stampack. The results relate to different levels of the sheet, to the lower surface rather than to the medium or to the top surface plane.

#### 4. Reverse Engineering

As Computer Aided Design (CAD) has become more popular, reverse engineering has become a viable method to create a 3D virtual model of an existing physical part for use in 3D CAD, CAM, CAE or other software packages. It involves measuring an object and then reconstructing it as a 3D model. The physical object can be measured using 3D scanning technologies like CMMs, laser scanners, structured light digitizers or Industrial CT Scanning. The measured data alone, usually represented as a point cloud, lacks topological information and is therefore often processed and modeled into a more usable format such as a triangular-faced mesh, a set of NURBS surfaces or a CAD model. This process needs hardware and software that work together. The hardware is used to measure an object and software reconstructs it as a 3D model.

With the significance of the automotive industry comes the significance of another very important term called Reverse Engineering. It is basically viewed as the process of analyzing a system in various domains in order to make the optimum utilization of the same.

The automotive industry is one of the most significant pillars in the development of a country.

- The automotive industry has a high order of increased need for the re-manufacturing of spares. RE has a feature of enabling discrete geometry that has helped a lot in this field and thereby has gained increasing importance in automotive design.

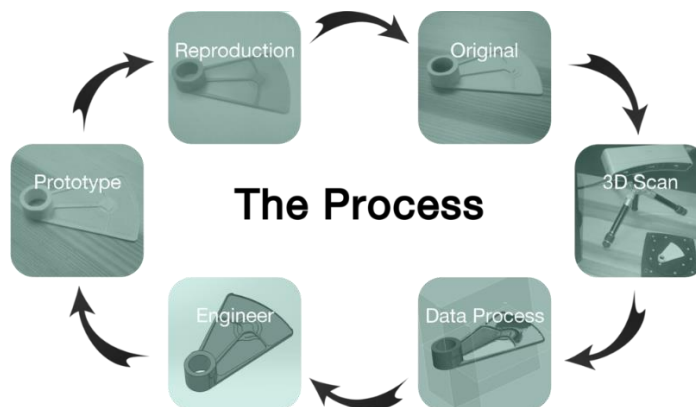


Figure 14 - Reverse Engineering Process

- Reverse Engineering has also helped a lot in applying non-contact and hybrid techniques that is a new technological advancement in the automotive industry. This approach bears an important step by step process involvement as a characterization of geometric forms relating to the automotive manufacturing process.

#### **4.1 Process Procedure for Mathematisation of the Mould starting from the Scan Data**

In general, the design and manufacture of equipment and moulds for the production of components made of metal (eg. Metal stamping) or plastic material (eg. Injection moulding), constitute one of the longer and more expensive phases in the development of a new product. In the modern concurrent engineering approach, the integration of CAD / CAE / CAM technology enables:

- rapid feasibility analysis through the process simulation with CAE tools from 3D CAD model of the component to be printed.
- a simple mould design based on CAD model of the component, also based on the CAE analysis results.
- the definition of the CAM toolpath for milling of the mould surfaces.

To complete the design, use of high material removal rates in roughing and the achievement of optimum dimensional tolerances and low roughness in finishing are sufficient to make the moulds directly usable for the production. Operations in fact, are still needed:

- Polishing (Manual finishing), to eliminate traces of milling operations and ensure the uniformity of surface of the moulds.
- Adjusting, in order to ensure a correct closure (or coupling) of the moulds.
- Compensation for springback, to compensate for deviations between the moulded component and the nominal model encountered during mould tests.

The "real" geometry of the moulds, therefore no longer coincides with the mathematical model of the same. Marginal changes to the moulds which are made directly by the tool maker, are almost never reported on equipment CAD model. Problems may therefore arise when the moulds due to wear or breakage must be replaced, because the lack of alignment between the CAD model of the mould and the physical element involves costs and time losses.

A possible solution to this problem is to use the potential provided by the 3D scanning and reverse engineering techniques to store the actual mathematical model of the moulds through:

- Scan of the die and punch, obtaining in output the relevant point clouds;
- Reconstruction of surfaces from scan data;
- Generation of the 3D model of the moulds;
- The possibility of verifying the particular geometry of the printed starting from CAE analysis carried out considering the real geometry of the equipment.

The CAD model reconstruction procedure of a mould by means of 3D scanning requires carrying out of a series of steps or phases in the following order:

1. Scanning of the active surfaces of the dies (punch and die)
2. Definition of the characteristic curves of the mould
3. Creating surfaces on curved network
4. Generation of the mould CAD model

The indicated stages are sequential, but for the purpose of achievement of a good result, it may be necessary to return to a previous stage to change what has already been partially done and then continue with the procedure for greater success. Generally, three different types of software are:

1. Application software for managing the 3D scanner and export scan data (Phase 1)
2. Reverse Engineering application for generation of curves and surfaces from scan data (Phases 2 and 3)
3. CAD application to create the 3D model of the mould (phase 4)

The Reverse Engineering software allow it to generate the surfaces is the three-dimensional solid model. It advisable to use their own CAD software for the last phase, in order to verify the compatibility between the surfaces or the model generated with the Reverse Engineering software and the CAD application.

In the following is a brief description of the four stages of reconstruction process with a flowchart that describes more in detail the procedure for each of them.

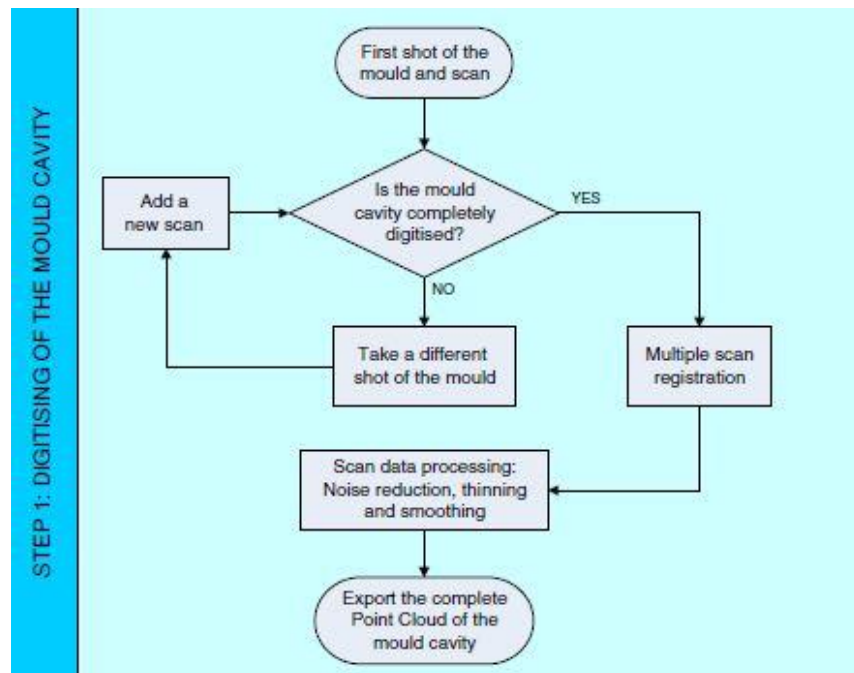


Figure 15 - Procedure for the scanning of the mould halves

### 4.1.1 Scanning of the Die and Punch

In a mould, the most important area is obviously the surfaces that contribute actively to the definition of the particular geometry of the printed. In the operation of the virtual model reconstruction of a mould makes sense, then go to digitize the only relevant part of the figure and those of adjustments can be recovered from the original file or easily redesigned in CAD environment (Figure 15).

### 4.1.2 Definition of Curves Characteristics of the Mould

For the reconstruction of surfaces of the mould from the cloud of points resulting from the 3D scanning equipment, the approach is defined as "curve network based surface". It generates a network on the surface of curves and implements a series of characteristic curves such as the lines of symmetry, style or sharp edges. The definition of such curves (Figure 16) requires the intervention of the operator because the software applications are not able to trace them in an automatic way, starting from the cloud points with satisfactory results.

The operator generates the curves by means of parallel sections to the coordinate axes or through interpolation of the cloud points of the scan data and the end result is much better.

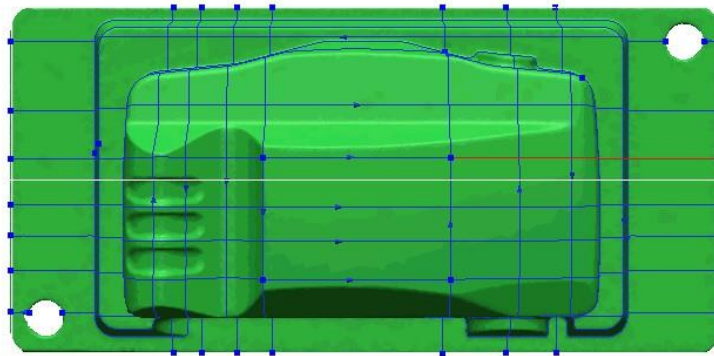


Figure 16 - Curves characteristics of the mould Network

### 4.1.3 Generation of NURBS Surfaces on the Curve Network

The intersection between the curves of the network generates various closed regions (referred to as patches). It should be ensured that the patches, which are generated by the intersection between the curves, do not have large variations of curvature near the edges. If the regions are bounded by four curves, parametric NURBS surfaces are generated without limitations (Figure 17).

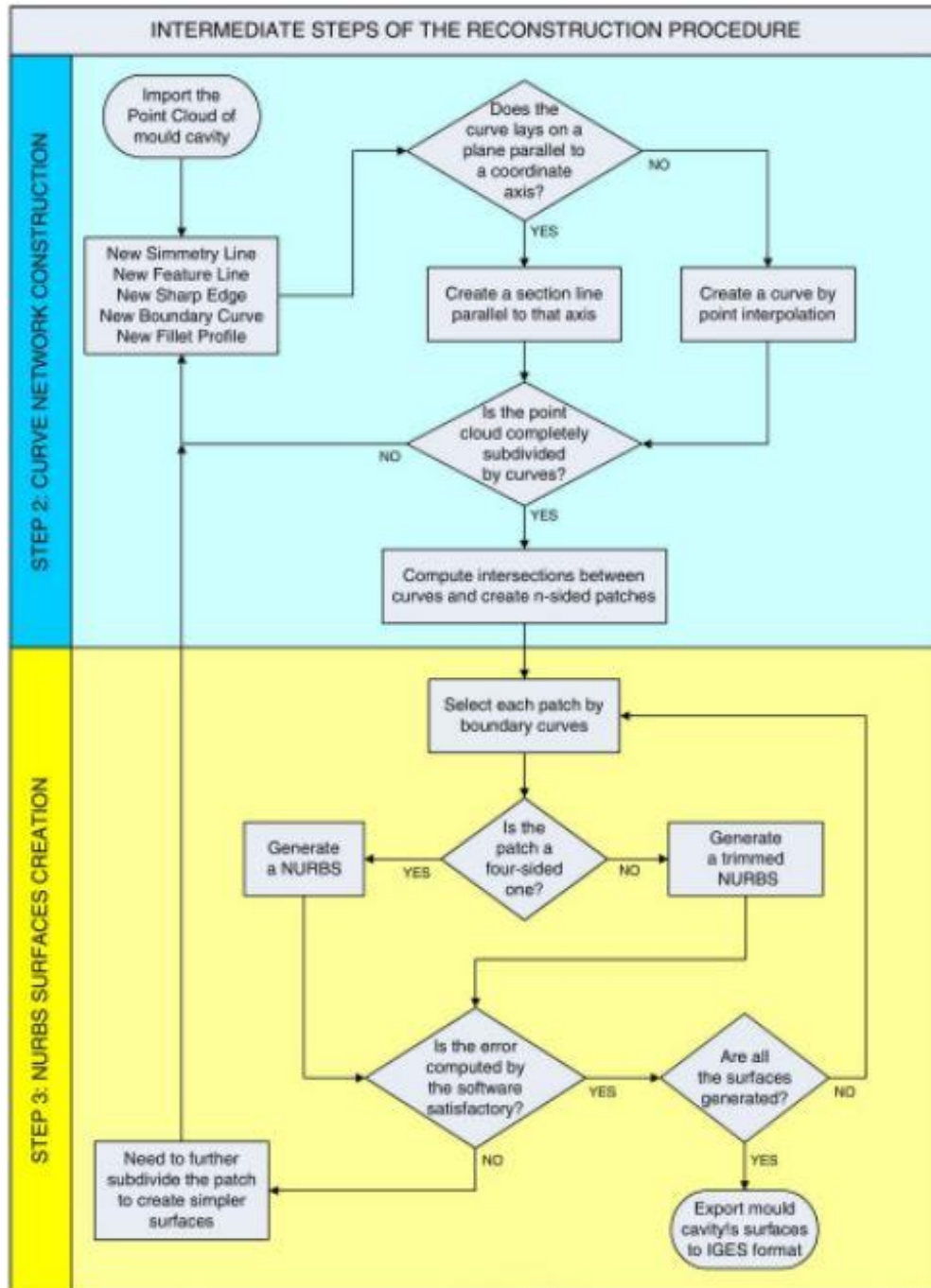


Figure 17 - Procedure for the creation of the network of curves and the generation of NURBS surfaces

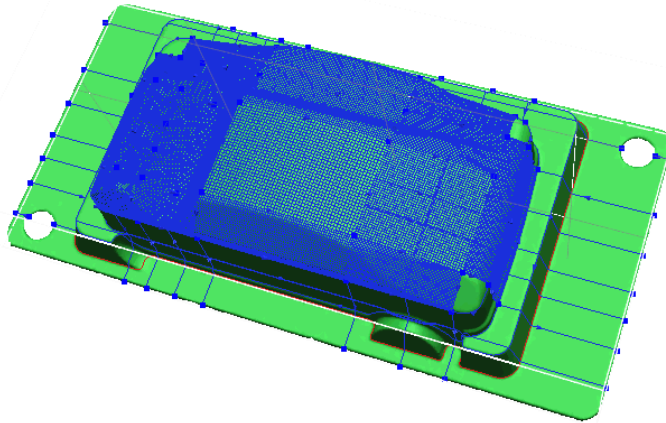


Figure 18 - Reconstructed surface portions of the mould from the curve network

If the number of curves is different, then the software generates a larger surface and then the delimiting of the edge curves (trimmed NURBS) takes place. To be sure that the generated surfaces are continuous and tangent with each other, it is necessary to bind the points on the edge curves.

This constraint limits the degrees of freedom of the algorithm of the surfaces generation. The constraints placed on the sides of the patch, do not allow to go to perfectly adapt the surface to the scan data in the presence of large variations in geometry close to the bound edges. The position of the section curves or style must be in a rational manner defined by the operator trying to coincide, as far as possible, with the edges of the geometry (Figure 16 is Figure 18). For each region starting from the curves on the edge, the surface reconstruction is carried out by Reverse Engineering software on internal points by means of differential calculus algorithms which are able to guarantee continuity and tangency between adjacent surfaces.

At the end of the generation phase of the individual surfaces, it is possible to verify the deviations with respect to the scan data. Normally the deviations are of the order of a few hundredths of a millimeter. If the deviations are excessive, it is necessary to further subdivide the surface into smaller portions and repeat the generation procedure. The overall map of deviations (Figure 19) shows that the deviations are more concentrated in correspondence of the edge surfaces of the individual curves, on which had been set the constraints for the continuity and tangency between neighbouring surfaces.

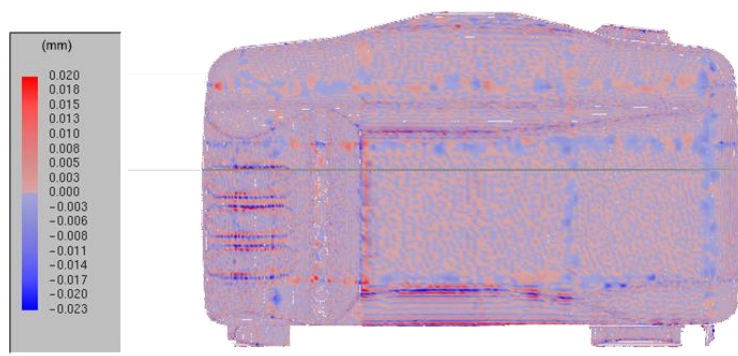


Figure 19 - Map of the deviations of surfaces rebuilt with respect to scan data

#### 4.1.4 Reconstruction of the Mould Cad Model

In reconstructing the CAD model is good to bear in mind that there may be a series of geometric tolerances (symmetry, concentricity, parallelism, squareness, etc.) that constitute essential information for the production of workpiece and for its proper assembly and operation. The NURBS surfaces created with the processing software of point clouds are then exported in IGES format and imported into three-dimensional CAD modeler. The simplest methodology to which you can think of to generate the solid mould starting from the surfaces is to join the surfaces between them and close the model with a lower floor. Since the initial data for the CAD model generation are coming from scans, the edge of the lateral surfaces reconstructed is not perfectly planar. The difference between the Z coordinates of its points varies within a certain range. This variation in addition to the complexity of the surfaces, does not allow the CAD program to unite all the side surfaces with the bottom closure plan.

There is another method for the generation of 3D solid mould. This method is quite simple in conceptual terms and provides positive results, but has the disadvantage of being rather labourious. The strategy is to generate a solid block for each NURBS surface and then insert to build a model for the union of all the blocks that make up the active surface of the mould (Figure 20).

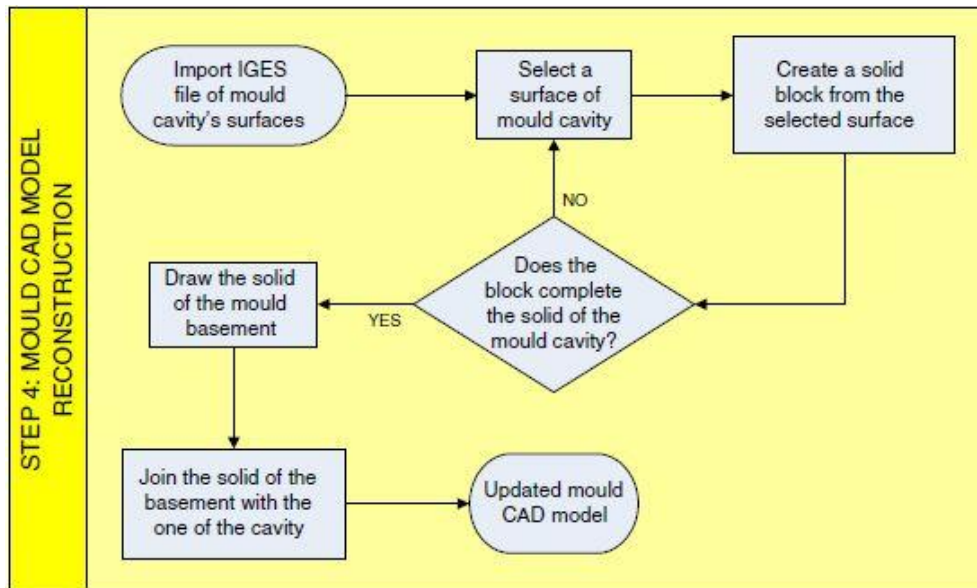


Figure 20 - Procedure for the reconstruction of the 3D CAD model

Each surface is first copied and moved along the direction of moulding. Subsequently, solid block is closed by creating ruled surfaces between the corresponding boundary curves of original surface and the copy. The 3D solid model of the mould is finally generated by combining all the blocks together (Figure 21).



Figure 21 - Union of the blocks created from the NURBS surfaces reconstructed

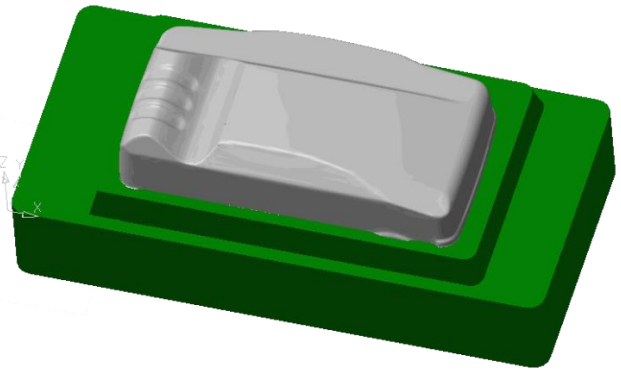


Figure 22- Reconstruction of the complete CAD model of the mould

The mould base is designed using CAD software with the outside surfaces of the figure or closing of the generated mould surfaces as nominal (ideal). The complete 3D CAD model is finally obtained by combining together the solid block of the cavity and that of the base (Figure 22).

Once you obtained the solid mould, it is possible to complete its CAD model with functional geometries (eg: Holes) or subsequent modifications, even possibly to update it as a result of cosmetic changes relating to the particular product (Figure 23).

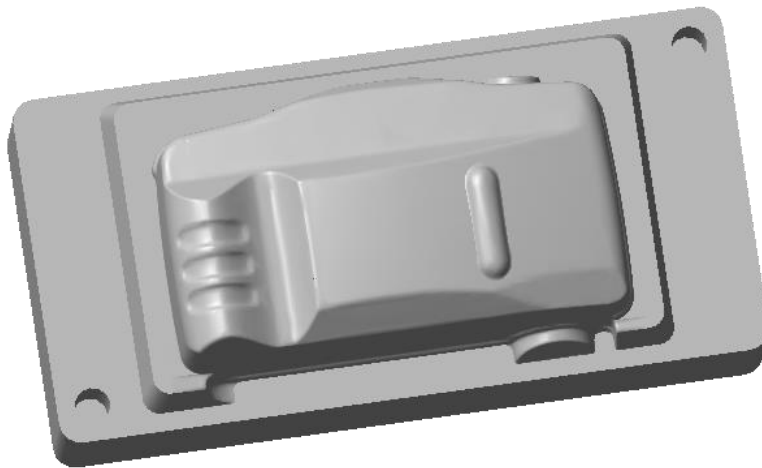


Figure 23 - Completion of the CAD model with holes or aesthetic changes on the product

## Chapter Two

### 5 Definition of case studies

In the first phase of the project it was preceded in accordance with the Company identification of two reference geometries of different level of complexity, chosen as case studies.

The first selected geometry is an anti-intrusion beam (Identified by code PM13). Its geometry is illustrated in Figure 24. This component will be used for the development of the simulation models and for the comparative analysis of the results of different software applications.

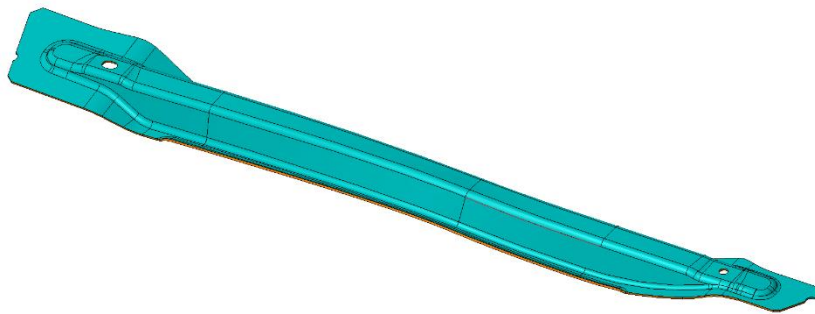


Figure 24 - Anti-intrusion Crossbeam (PM13), DP1200 material, thickness 1.7 mm, size  $800 \times 90 \times 40 \text{ mm}^3$

The second component shown below is also an anti-intrusion beam (Identified by code MA03) but its geometry is more complex and its size is larger than the PM13. This allow us to evaluate the effectiveness of the numerical simulation and the simulation methodology developed with the first geometry.

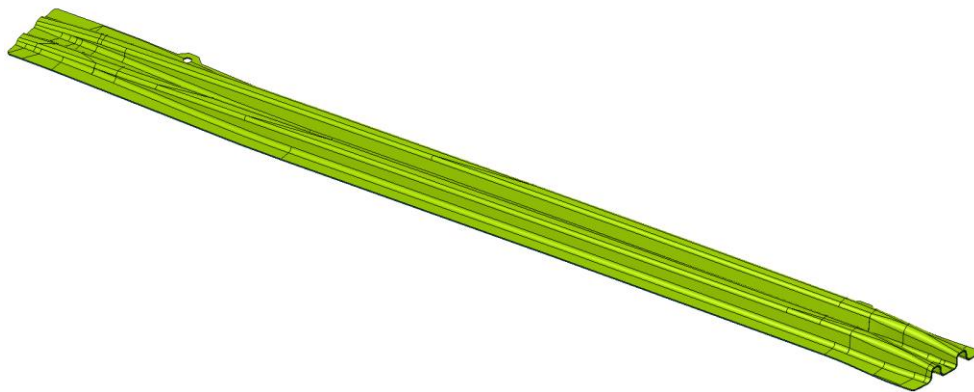


Figure 25 - Anti-intrusion Crossbeam (MA03), DP1000 material, thickness 1.5 mm, size  $1300 \times 125 \times 38 \text{ mm}^3$

## 5.1 Identification of the Input Data Required for the Definition of Simulation Models

It concerns the geometry of the components and / or the mould, the characteristics of the material and the process conditions.

### 1. Geometries of the Component

- 3D CAD model of the component

If available

- 3D CAD model of the mould
- Surfaces in STL format of the die, punch and any complementary elements of mould

### 2. Material Properties

- Sheet thickness [mm]
- Young's modulus [GPa]
- Yield strength [MPa]
- Uniform percentage elongation [%]
- Ultimate Tensile Strength [MPa]
- Density [kg / m<sup>3</sup>]
- Poisson's ratio [-]
- Coefficients of the law of Hollomon
- Resistance factor, K [MPa]
- Work hardening coefficient, n [-]
- Normal anisotropy (directions 0 °, 45 ° and 90 °)

If available

- Experimental results of the tensile test
- Forming limit diagram (FLD) for 3D analysis Shell
- Triaxiality failure diagram (TFD) in the case of 3D analysis Solid

### 3. Process conditions

- Orientation of the veneer (crude) with respect to the direction of rolling

If available

- Velocity profile during the closing of the mould
- Coefficient of friction between die and sheet
- Punch stroke

## 6 Research, Analysis and Selection of Software

In the market there are multiple software solutions for the cold forming simulation of sheet metal - Autoform, ESI PamStamp, ETA Dynaform, FTI FastForm, Altair hyperform, Stampack.

Stampack (<http://stampack.com/>) is a software dedicated to the simulation of specific sheet metal forming processes for molding applications, deep drawing, hydro-forming, coining, bending of tubes directed to components for the automotive and aeronautical industries. Its environment is geared to the convenience and does not require a specific expertise in finite element analysis (FEA). The setting of the process simulation follows a logical sequence that allows users to concentrate on solutions of the problems rather than insertion of parameters for the numerical analysis. The calculation of final shape of the component takes into account the variables involved in the process (pressure, time, coating material and lubrication conditions).

Through integration with VISI environment, modeling tools are available to define the pre- and post-process. Moreover, this interface has been developed specifically for the reduction of the simulation preparation times so as to pass quickly from CAD to the CAE.

The product Abaqus provides powerful and comprehensive solutions for complex design problems and routine, covering a broad spectrum of industrial applications including the molding of sheets (<http://www.3ds.com/products-services/simulia/products/abaqus/>).

Rapidform XOR allows users to go from 3D scan data to fully parametric CAD model. We can process raw 3D scan data into high quality meshes and NURBS surface models in just few minutes. Once the scan data is optimized, you can export high quality meshes. Built for accuracy and speed, it offers real time scan to CAD and scan to scan comparison and industry proven geometric dimension and tolerance. It is the only point cloud software with 100 % repeatable inspection processing in the world.

The GOM Inspect 3D software contains standard alignment functions like RPS alignment, hierarchical alignment based on geometric elements, alignment in a local coordinate system, as well as various best-fit methods such as global best-fit and local best-fit.

The computed polygon meshes describe free-form surfaces and primitives. It can be verified by comparing surfaces with a technical drawing or directly with a CAD data set. A 3D analysis of surfaces as well as a 2D analysis of sections or points can be implemented in the software. I-Inspect suggests suitable measurement principles and inspection criteria to suit the selected element. With I-Inspect, even complex inspection tasks can be implemented quickly and easily.

## 6.1 Defining the Preliminary Model of Simulation Stampack

Following the selection of Stampack as dedicated software for the simulation of the sheet metal stamping and anti-intrusion bar process (**PM13**) as the first case study, it proceeded with the implementation of the numerical simulation model within the environment.

The Stampack software allows you to define the model in two different ways:

- 3D Shell, the sheet is represented by a wireframe blank and the thickness is a property that is assigned to it during the definition of the inputs;
- 3D Solid, the sheet is represented by a solid 3D CAD with volume.

Simulations performed using both approaches are described below. The numerical results with particular attention to the calculation of elastic return of sheet will be presented and analyzed. Final

geometry of the component obtained numerically will be compared with its nominal value and the actual CAD geometry obtained by means of 3D scanning of production component.

- 3D CAD model of active surface of die, for 3D simulation Shell (Case 1)
- STL files of the punch and the die obtained by three-dimensional scanning of the mould used in production, for the type of 3D simulation Solid (Case 2)
- 2D CAD profile sheet metal development provided in .dwg format
- In the mold table mass
- Characteristics of the sheet material
- Process parameters (mold / development friction equal to 0.15)

## 6.2 Characteristics of the Sheet Material

The material used for the simulation is DP1180 and its characteristic parameters were obtained from the files provided by the company (dp1180 susta.mat bars), exported from AutoForm Version 4.6 simulation. In Figure 30, the limit curve of formability (FLC) used as a criterion of breakage in the case of analysis in Shell 3D mode is illustrated. In the case of analysis in Solid 3D mode, it will be used as a criterion for breaking the TFD diagram (Diagram Triaxiality Failure) reported in Figure 31.

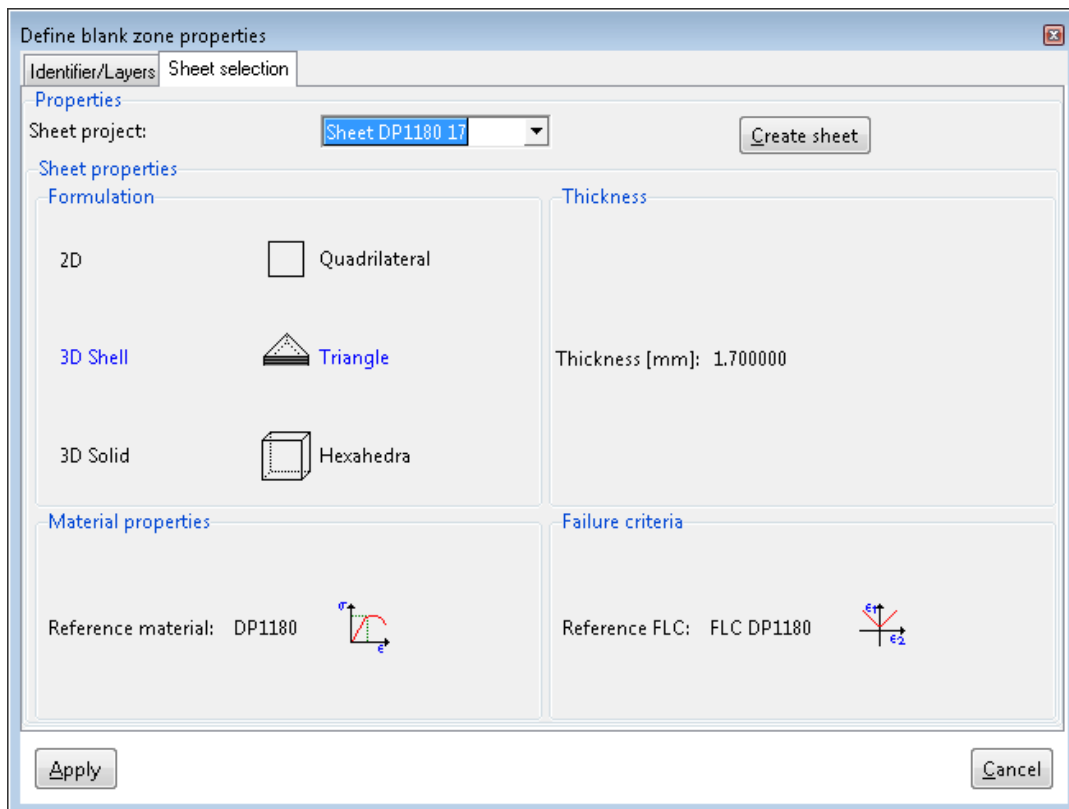


Figure 26 - Definition of the characteristics of the sheet material, 3D Shell

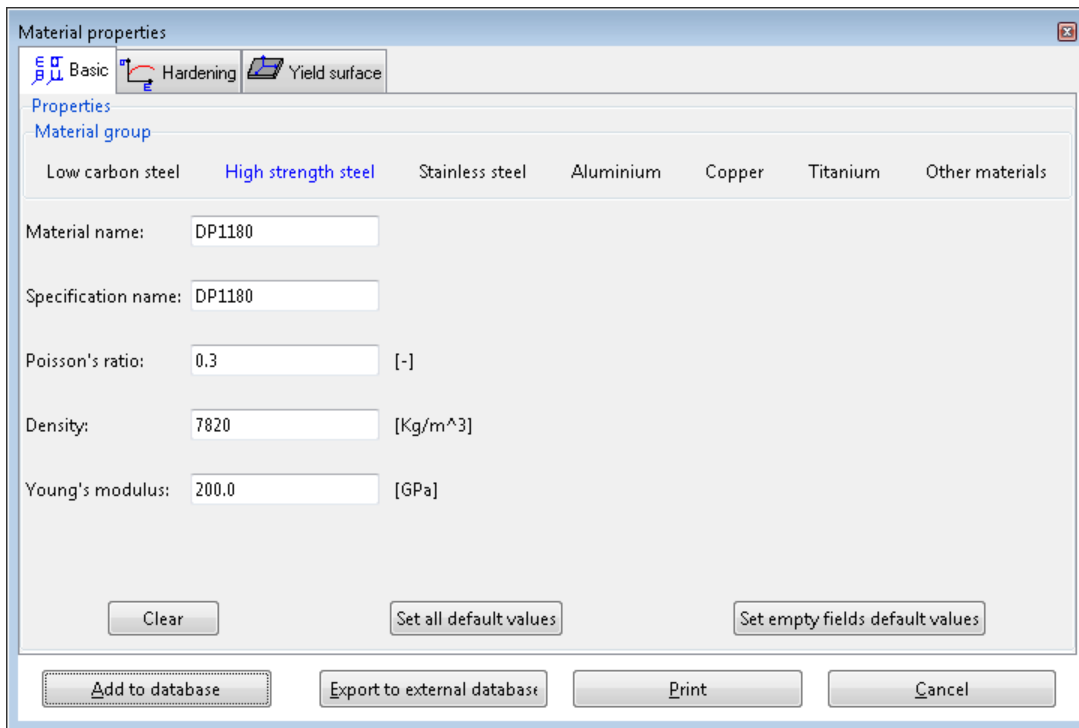


Figure 27 - Definition of the characteristics of the sheet material, elastic behaviour

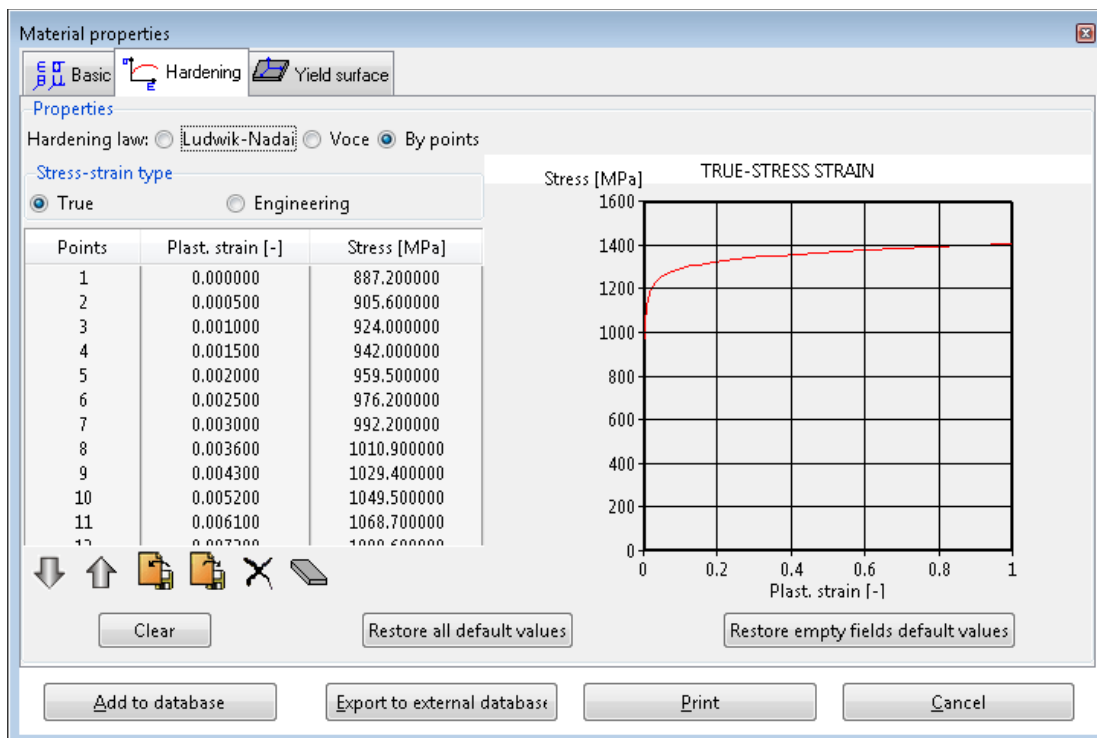


Figure 28 - Definition of the characteristics of the sheet material, plastic behaviour

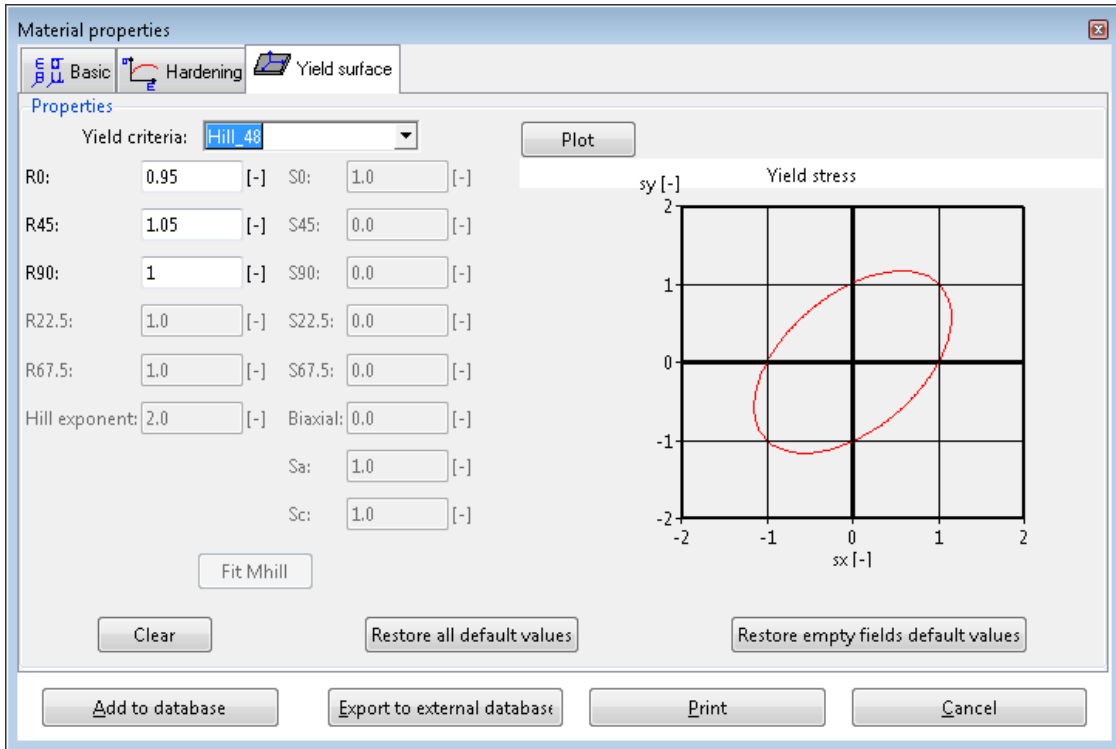


Figure 29 - Definition of the characteristics of the sheet material, anisotropy

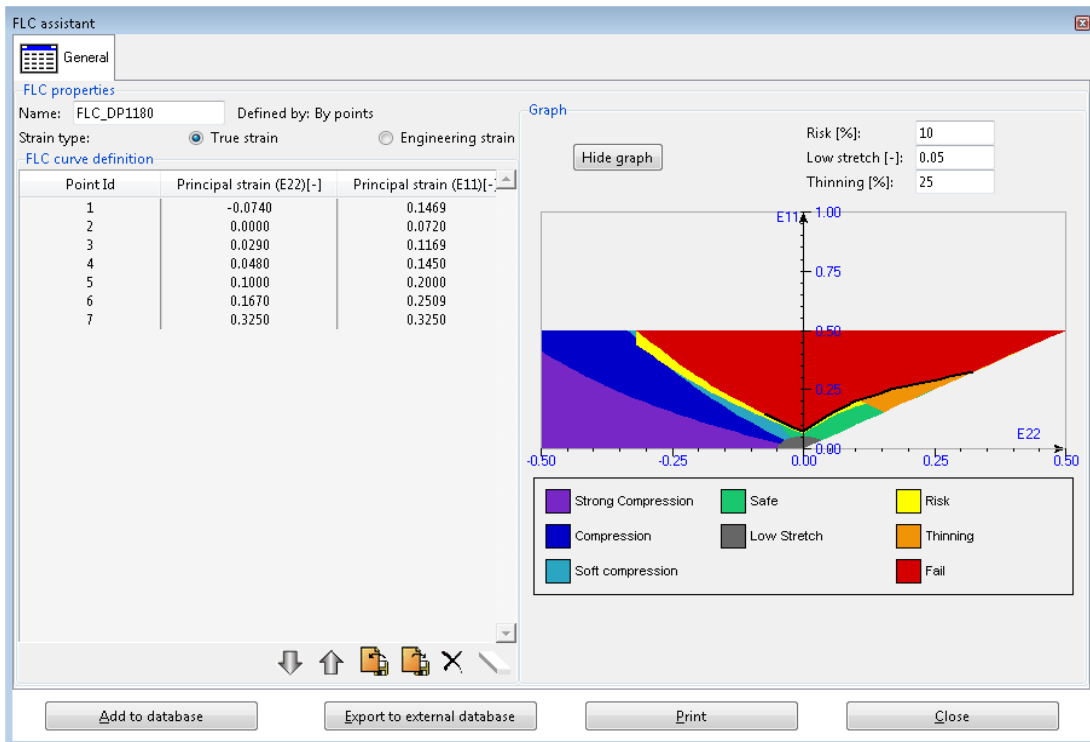


Figure 30 - Definition of the characteristics of the sheet material, forming limit curve

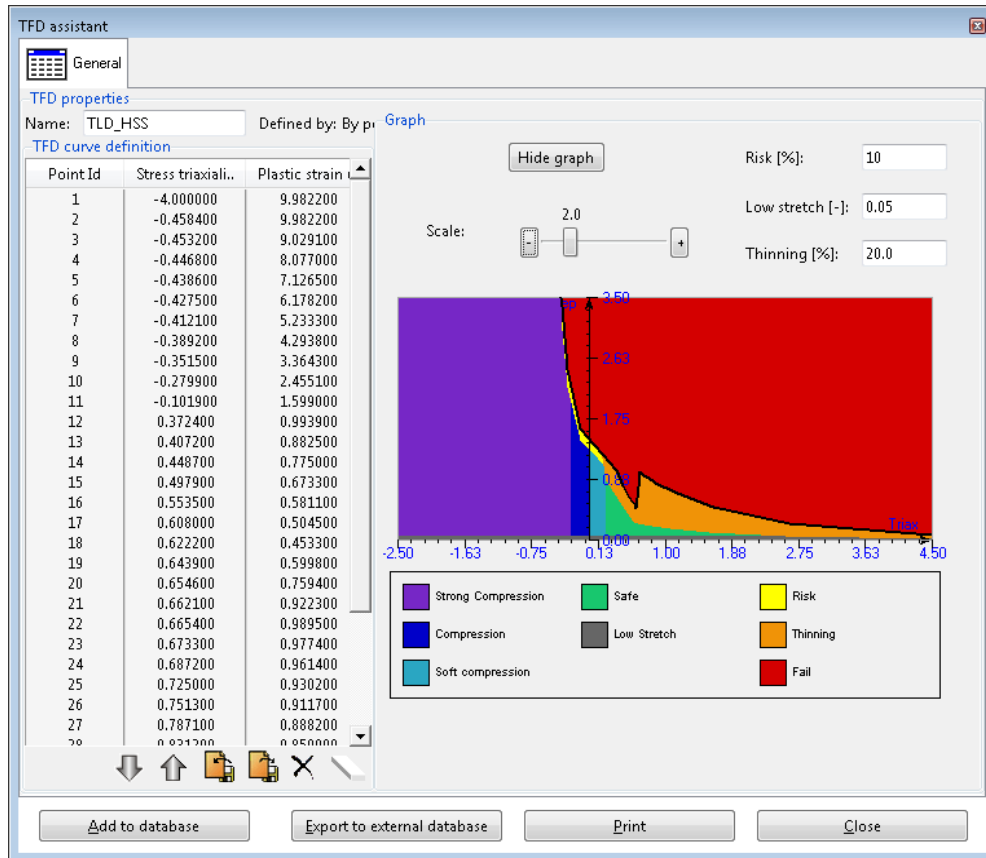


Figure 31 - Definition of the characteristics of the sheet material, triaxiality failure diagram

### 6.3 Case 1 – 3D Simulation Shell (CAD Dies, Wireframe Blank)

In this first case, model is 3D type Shell. The flat surface of the development is obtained from 2D CAD profile. The guides have been created within the CAD environment such as cylinders oriented in the direction of closing of the mold. The number, positions and sizes have been obtained from the mass in the mould table. The input geometries are depicted in Figure 32.

The die, punch and guides were considered as rigid bodies. The sheet is the only deformable body and it is assigned the DP1180 material as features provided. Inside the Stampack software by definition, the die and guide columns are fixed. At the punch it is assigned the motion of displacement until it stops. The software has an explicit solver type in order to avoid inertial effects, the default values of velocity and acceleration are maintained. In this first phase we neglect the effects of gravity.

It assigns a triangular mesh by setting a value of 2 mm on the sheet and leaving the default value for the rigid elements.

The simulation consists of two separate calculations (stage) and consecutive to the step of forming and that of elastic return. The calculation took about 13 minutes for each stage using a workstation with an Intel® Core™ i5-4440 processor @ 3:10 GHz and 8 GB of RAM.

Below are some significant numerical results obtained from the simulation.

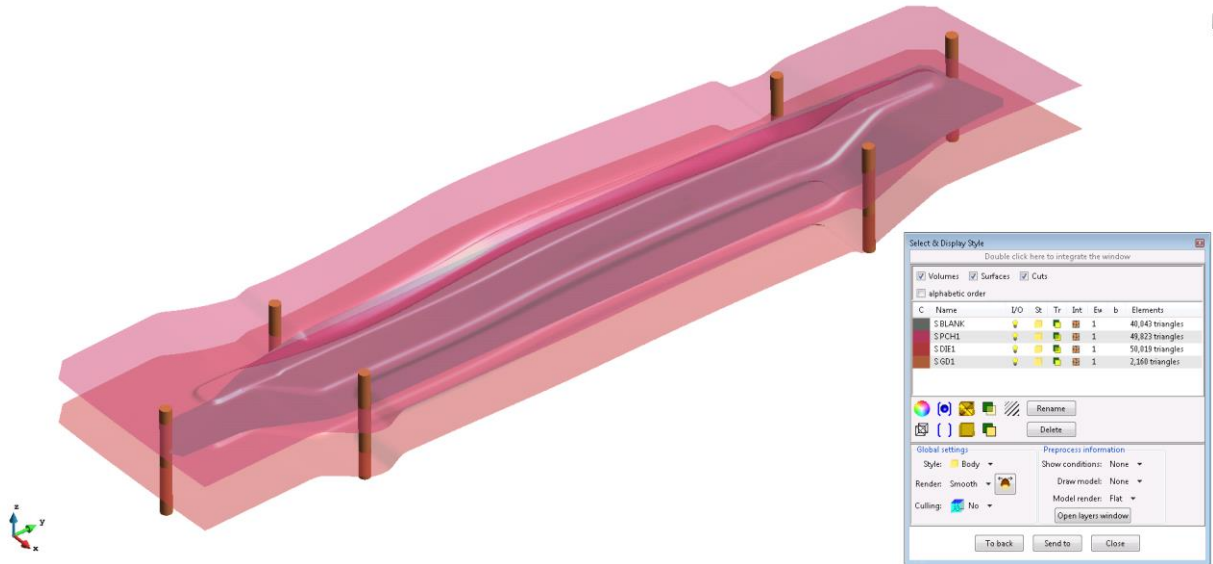


Figure 32 - Geometry input

### 6.3.1 Thickness of Sheet at the End of Forming and Percentage Thinnings

The images represents the result of forming prior to the calculation of the elastic return in terms of the sheet thickness and percentage of thinning. The analysis shows that there are some areas in which it has a thickness variation of more than +/- 5%. This phenomenon is localized at the component wings. These results are comparable with those obtained using AutoForm.

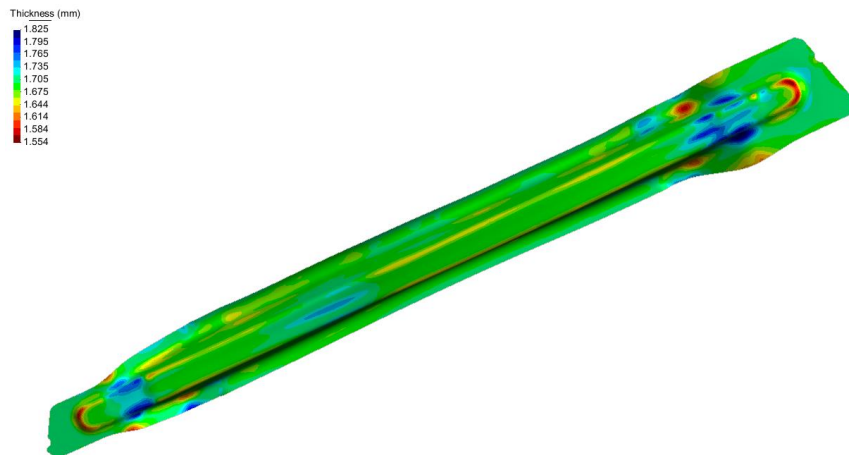


Figure 33 - Thickness of the sheet at the end of forming

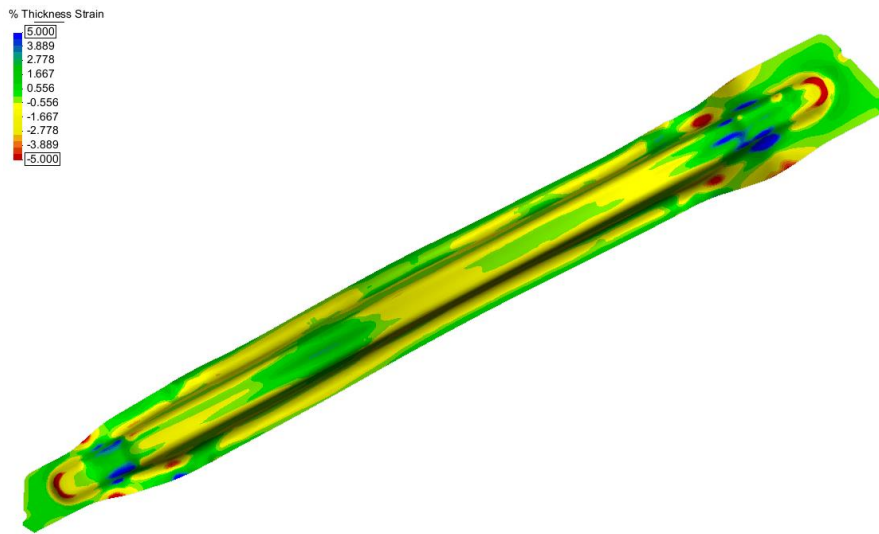


Figure 34 – Percentage of thinning

### 6.3.2 Formability Analysis

The analysis of formability based on FLD curve confirms that the previously highlighted areas from the analysis of thickness are critical. You can identify two areas at risk of fracture in warm colors in Figure 35. Similarly in Figure 36, represents areas where there is a high probability of formation of wrinkles. These trends are comparable with those obtained using AutoForm.

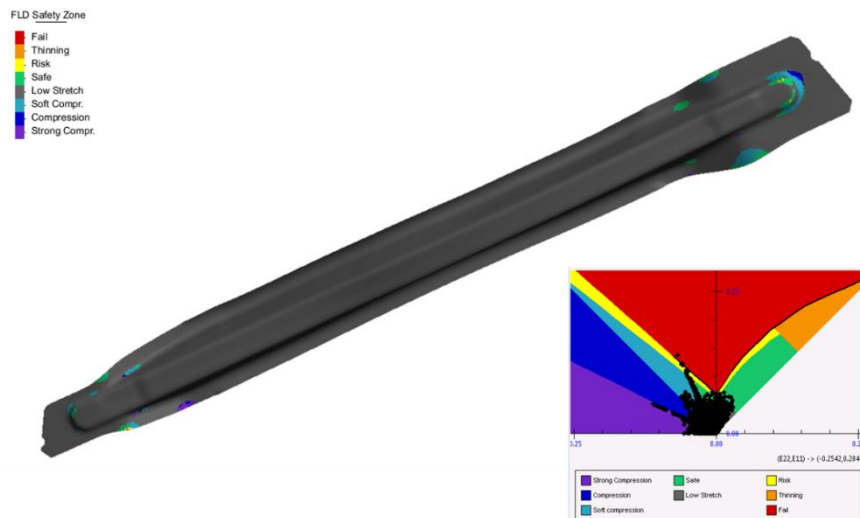


Figure 35 - Formability FLD – risk of fracture

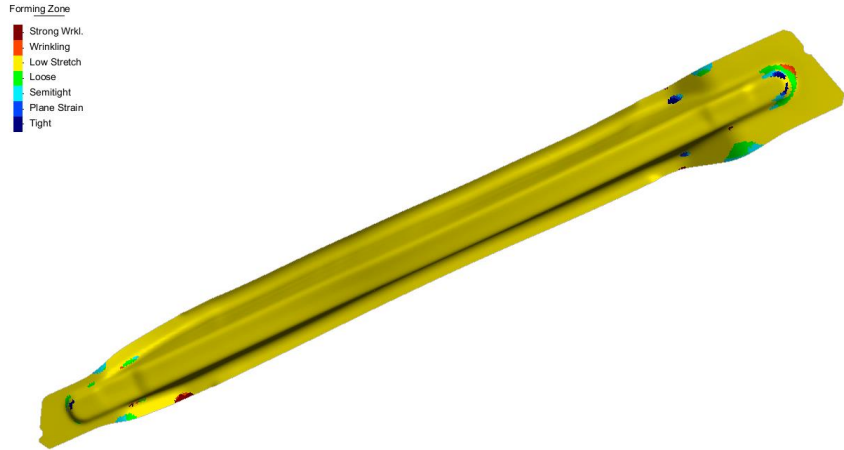


Figure 36 - Forming of the results – formation of wrinkles

### 6.3.3 Performance of the Moulding Force

It derives the slope of the force on the punch / die during the forming process as a function of simulated time in the form of graph. It is necessary to derive the force as a function of the displacement if it does not match the real time in simulation. For this purpose, it considers a linear relationship between the displacement of the punch and simulation time. The maximum value of force is equal to about 280 Ton, next to the same value obtained by AutoForm.

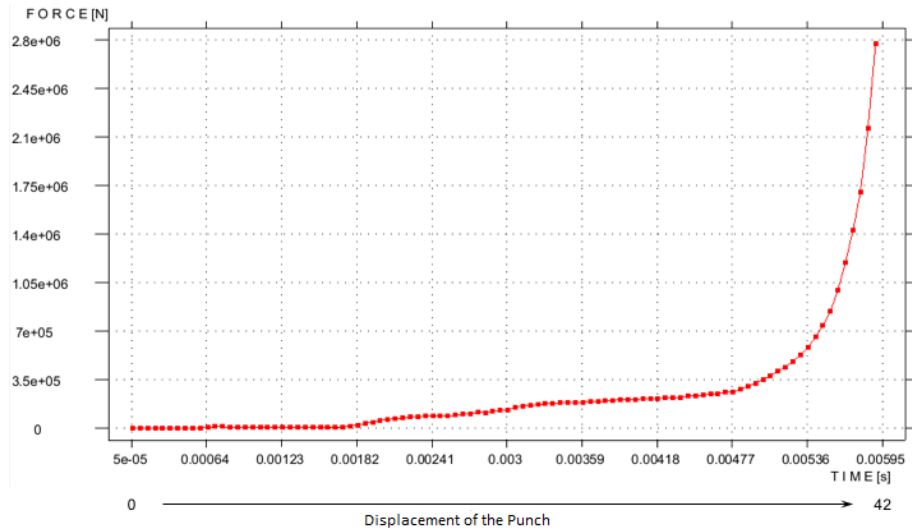


Figure 37 - Force on the punch / die during the process

### 6.3.4 Calculation of Elastic Return

We proceed with the calculation of the elastic return. Two different computational approaches can be used with Stampack.

- **Fast springback** : In this approach, the software does not take into consideration the contact between mold and molded part. The mold is virtually eliminated and the system calculates the elastic return of the sheet taking account of the constrained points. For this purpose it is necessary to define an adequate number of points bound as if the object is placed instantly on a measuring gauge.
- **Explicit springback** (or free springback) : In this approach, the software takes into account the contact between mold and molded part in the process which is the only constraint. The computation time is very high (in the order of a few hours).

In this first phase we followed the first approach and we bound 4 points positioned in the central zone of development. It will be evaluated under the influence of number and position of constraint points.

Springback results are represented in Figure 38 and Figure 39. Figure 38 illustrates geometry of the component as a result of elastic recoil (grey area), while the red line identifies component profile at the end of molding operation alone. Figure 39 allows to quantify the displacement suffered by the different areas of the component as a result of the calculation of elastic return in the form of coloured map. The global maximum displacement of nodes as a result of elastic return are equal to about 6 mm and localized on the wings. It detects a discrepancy in terms of performance and value compared to the simulation performed with AutoForm.



Figure 38 - Return bound elastic (fast springback)



Figure 39 - The extent of elastic return - Quantitative evaluation (constrained elastic return)

A further validation is accomplished by comparing the results obtained from the software with the nominal and real geometry of the metal component. Having assumed as a reference surface for the Shell 3D simulation that of the die, the results of the comparison will be limited to compare the geometry of the component from the side of the die neglecting the thickness effect.

In Figure 40, you can see that the calculated deviations from the CAD model are contained and exceed the millimeter only in certain localized areas.

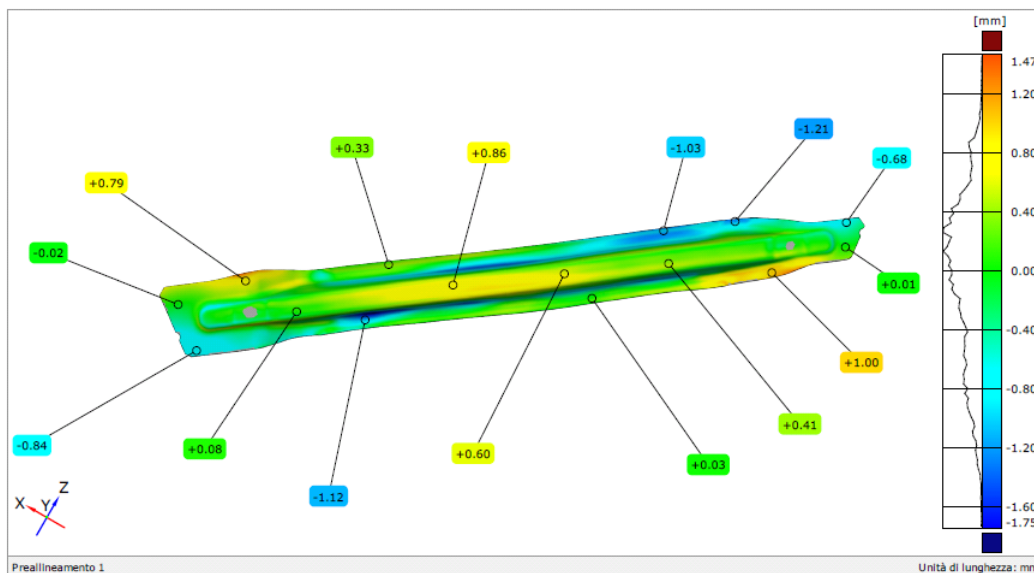


Figure 40 - Pointwise deviations between component calculated with elastic return and bound nominal die side CAD geometry

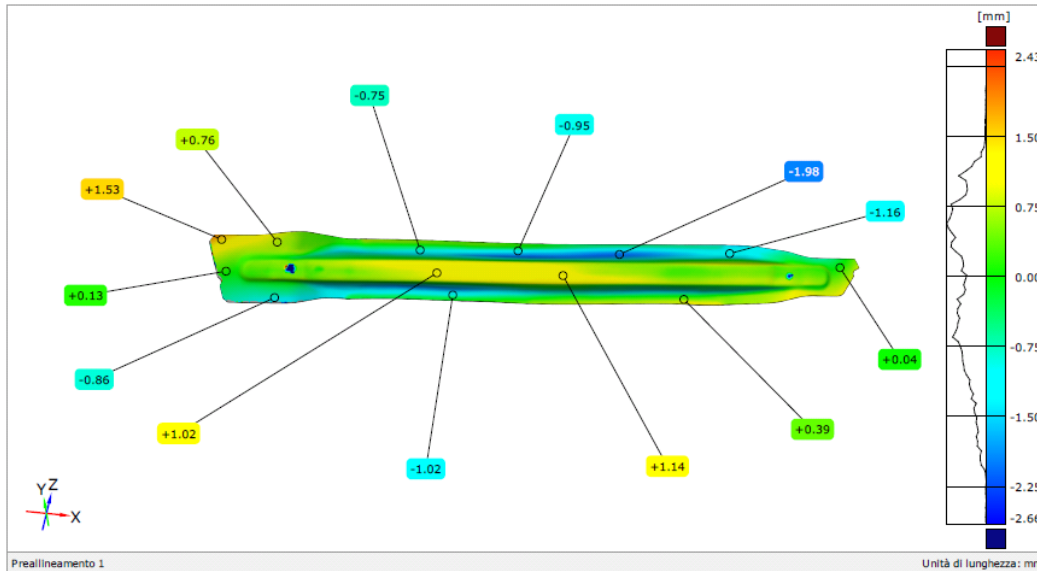


Figure 41 - Pointwise deviations between component calculated with elastic return constrained and real geometry scanned

The differences with respect to the geometry of the real component, which is considered as a die side surface are higher (Figure 41). This difference is not surprising, if one takes into account the fact that the simulation has been carried out starting from the CAD model of the mould, which does not coincide with that of the real mold.

### 6.3.5 Compensation of the Elastic Return

To evaluate the ability of springback compensation of geometric mould taking into account the springback effects, a Shell 3D simulation which has been activated during the calculation of the elastic return of the springforward algorithm is carried out (Figure 42). It should be noted that this algorithm can be activated only in the case of constrained elastic recovery (springback fast).

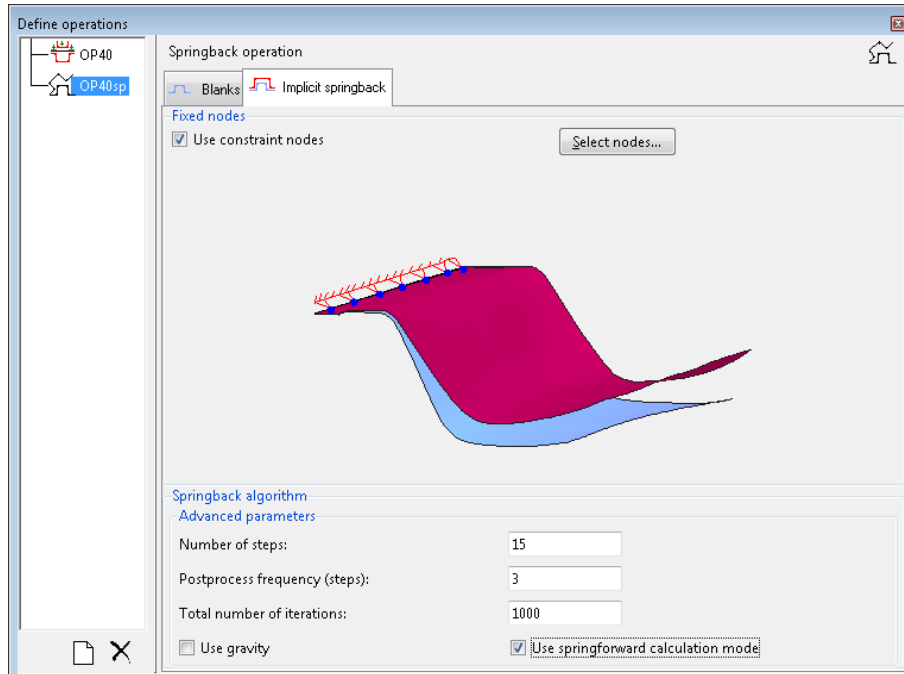


Figure 42 - Software setup screen

In Figure 43, one can observe the calculated geometry. Examining the position of the red line, which identifies the profile of the component at the end of molding operation only with respect to the gray surface, you can clearly observe the result induced by the application of the algorithm of springforward. In fact their mutual position is opposite to that which would result from the calculation of the elastic return (Figure 38).

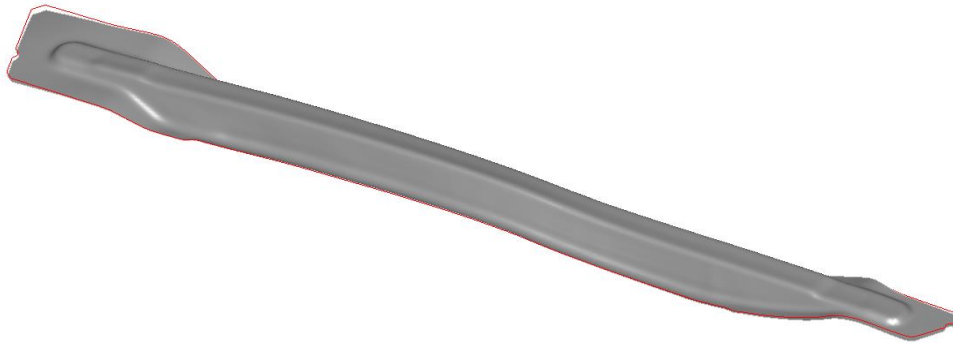
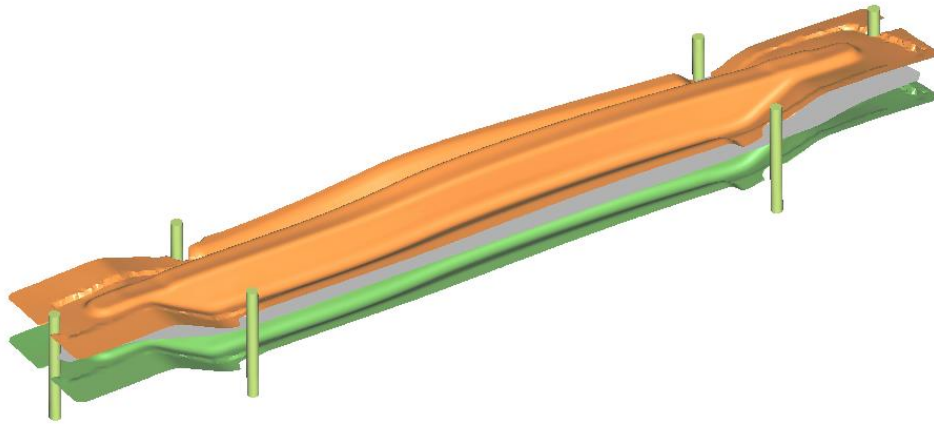


Figure 43 - Geometry obtained by the algorithm springforward

In order to perform the simulation it is necessary to start from the geometry of Figure 43 and shaping the outside figure. The die was obtained by filling the active surface of springforward calculated using the algorithm with the outside surfaces of the figure. The processing was performed using STL files. The surface of the punch was obtained simply by copying the die, since the software works whereas the wireframe blank, without modeling the thickness. The flat surface of the development is obtained from 2D CAD profile. The guides have been created within the CAD environment such as cylinders oriented in the direction of closing of the mould. The number,

positions and sizes have been obtained from the mass in the mold table. The input geometries are depicted in Figure 44.



*Figure 44 - Geometry Input*

The simulation was conducted using the same material and the same process conditions described in the preceding paragraphs. The springback results are represented in Figure 45 in the form of component geometry and in Figure 46 it represents the global displacement of the nodes that occurs during springback. The global maximum displacements of the nodes as a result of the elastic return are located on the wings and their trends partly it differs with that shown in Figure 39 that makes the non flawed mould.

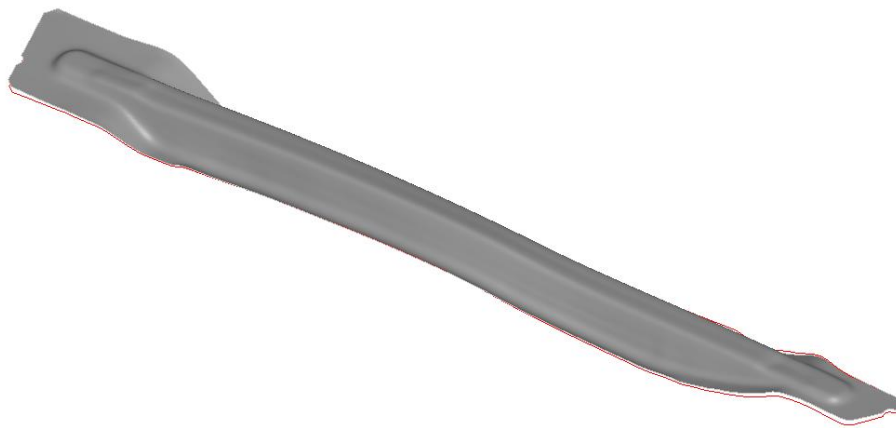


*Figure 45 - Return bound elastic (fast springback)*



Figure 46 - The extent of the elastic return Quantitative evaluation (constrained elastic return)

The colored maps that represent the deviations between the geometry obtained by the simulation and the nominal CAD model (Figure 47) and the real object (Figure 48). They reveal that following a first loop springback compensation there is a reduction of deviations in some areas of the workpiece and an increase in others.

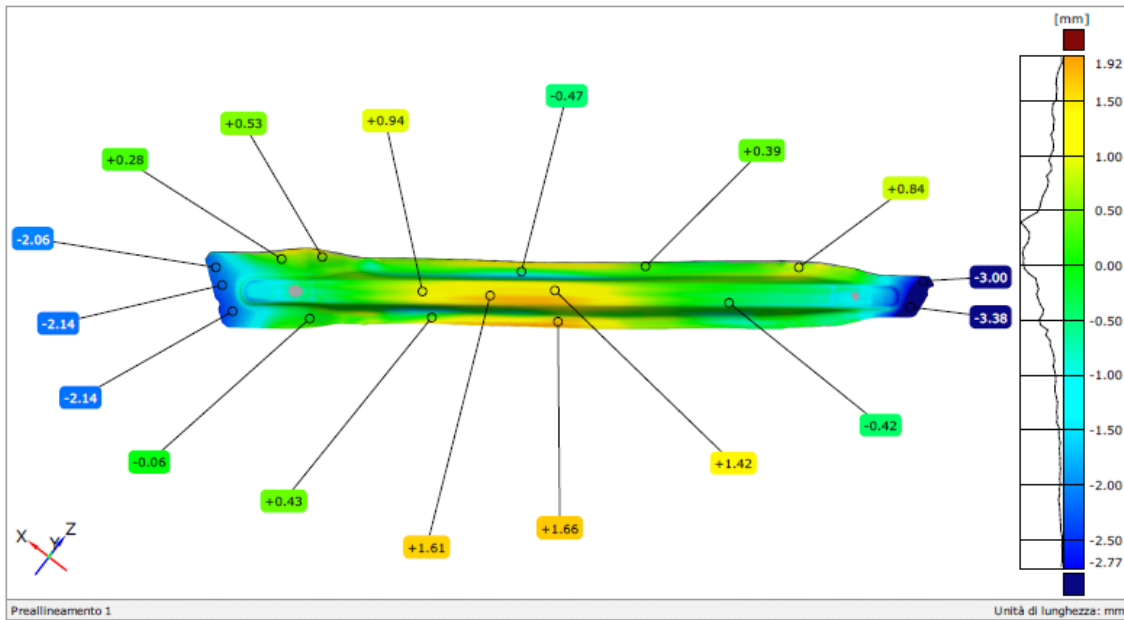


Figure 47 - Pointwise deviations between calculated component with mould obtained from springforward with outside shape and nominal CAD geometry die side

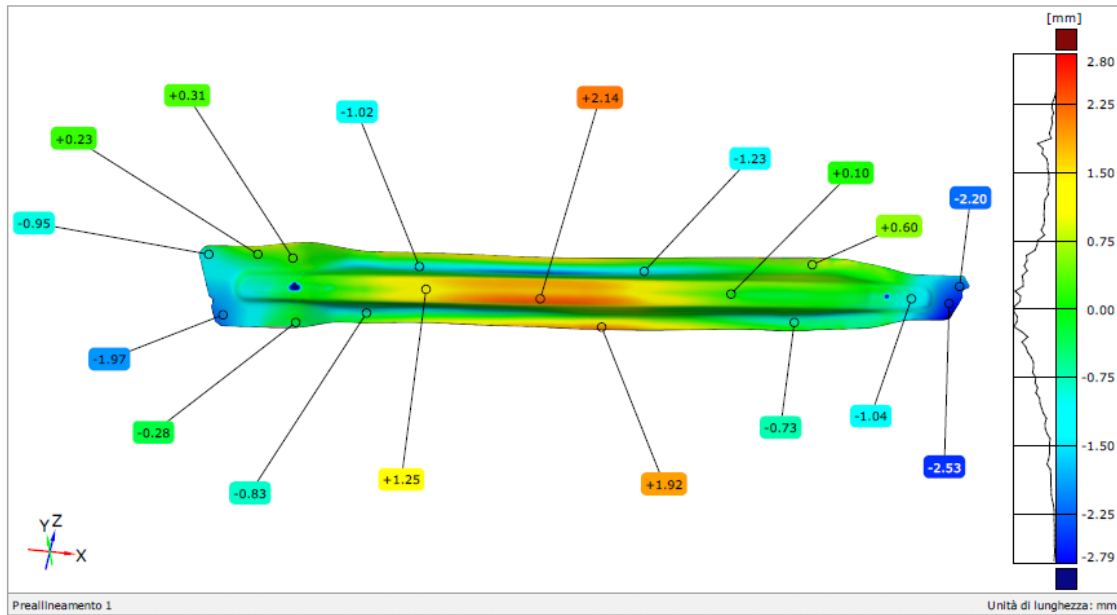


Figure 48 - Pointwise deviations between calculated component with mould obtained from springforward with outside shape and real geometry scanned

Beyond the quantitative values obtained from this single iteration of virtual springback compensation of the mould, the results go in the direction to change the geometry of the mould in order to obtain a component that is more similar to the real one and less to the nominal CAD model. Compared to previous results Figure 40 and Figure 41, Deviations from the CAD model (Figure 47) are higher and those with respect to the lower scan data (Figure 48).

From the two images below, it is clear the role of "guide" played by the outside shape during the moulding step.

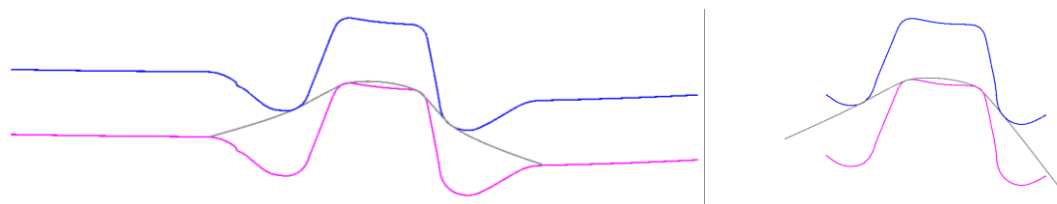


Figure 49 - Simulation with and without parting

In fact solving the simulation (for example forming and calculation of the springback) without considering the presence of an outside figure - the geometry obtained from the calculation of springforward is used as die and punch - are obtained deviations from nominal CAD (Figure 50) and the actual geometry (Figure 51) greater to those obtained from the simulations performed with the mould without parting plane (Figure 47 and Figure 48).

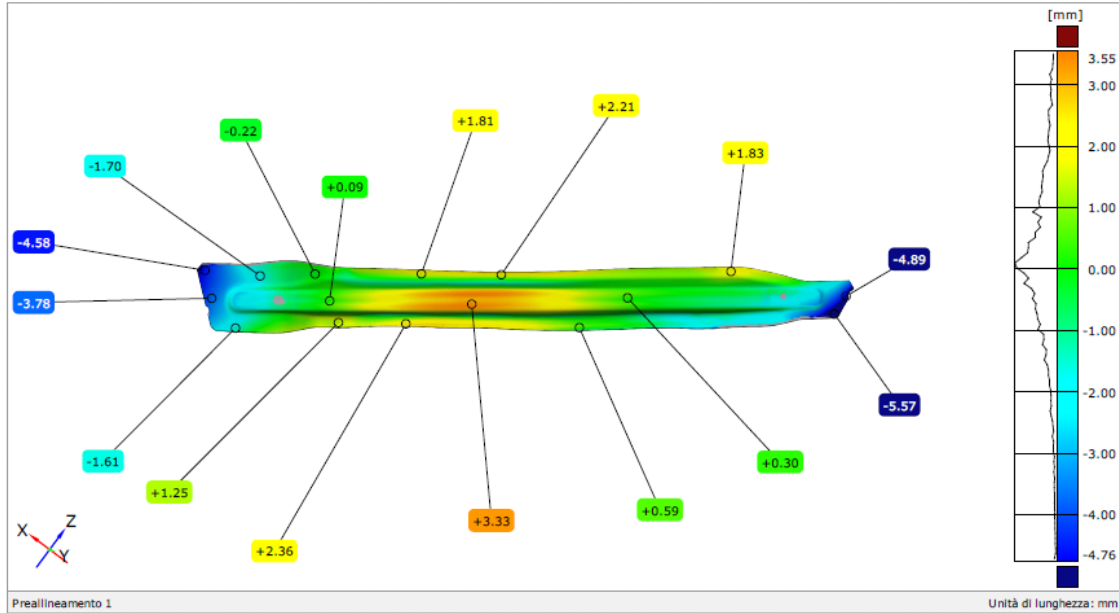


Figure 50- Pointwise deviations between calculated component with mould obtained from springforward without outside shape and nominal CAD geometry

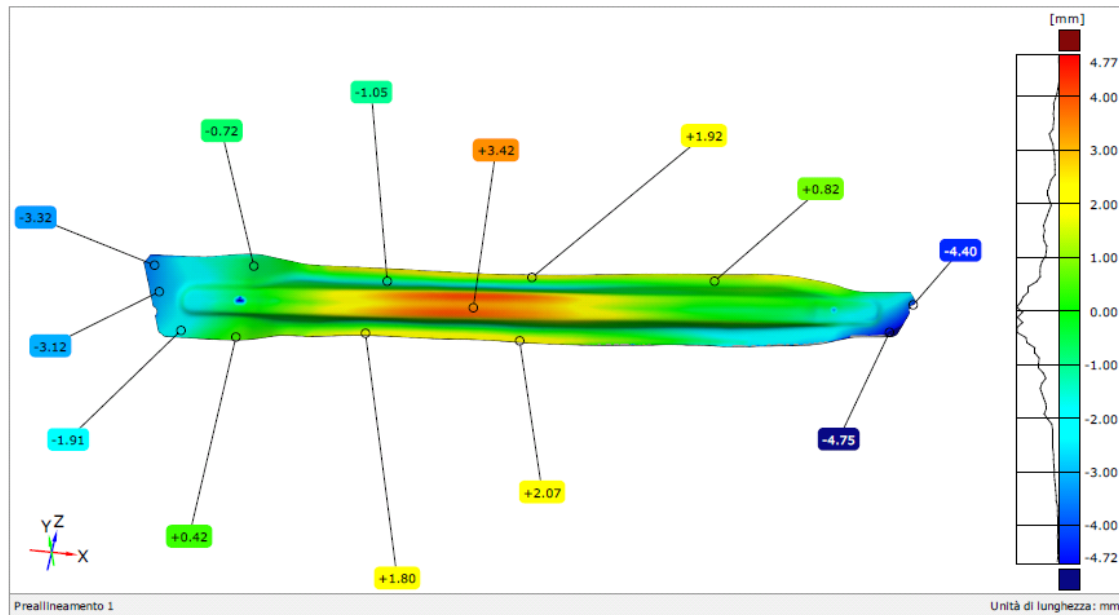


Figure 51 - Pointwise deviations between calculated component with mould obtained from springforward without outside shape and real geometry scanned

## 6.4 Case 2 – Solid 3D Simulation (By Scanning Moulds, Sheet Metal Thickness)

The model is 3D type Solid. The active surfaces of the die and the punch were obtained by three-dimensional scanning. The sheet was obtained from 2D CAD profile using extrusion operation. The guides have been created within the CAD environment such as cylinders oriented in the

direction of closing of the mould. The number, positions and sizes have been obtained from the mass in the mold table. The input geometries are depicted in Figure 52.

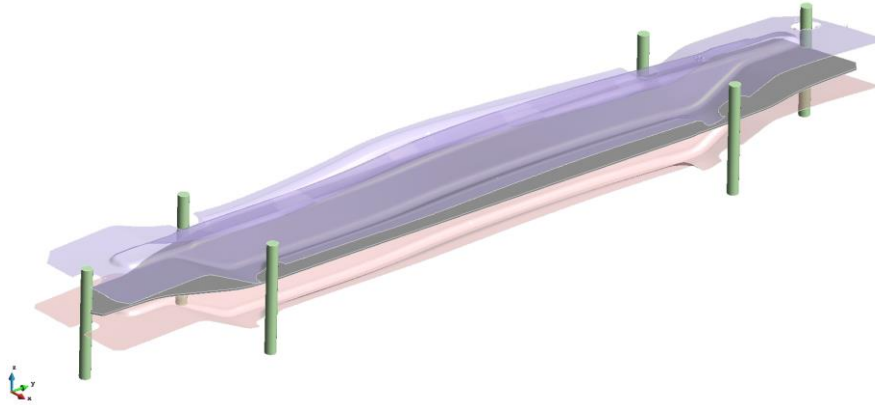


Figure 52 - The mould geometry

The modeling is analogous to the previous case, with the following differences:

- in the characterization of the material it uses TFD curve as a criterion of rupture
- the sheet metal is a semistructured hexahedral type

The simulation consists of two separate calculations (stage) and consecutive to the step of forming and that of elastic return. The calculation took approximately 90 minutes for the stage of forming and 30 minutes for the stage of springback calculation.

Below are some significant numerical results obtained from the simulation

### 6.4.1 Thickness of the Sheet at the End of Forming

Figure 53 shows the result of forming prior to the calculation of the elastic return in terms of the sheet thickness. The trends are comparable with those of Shell 3D simulation.

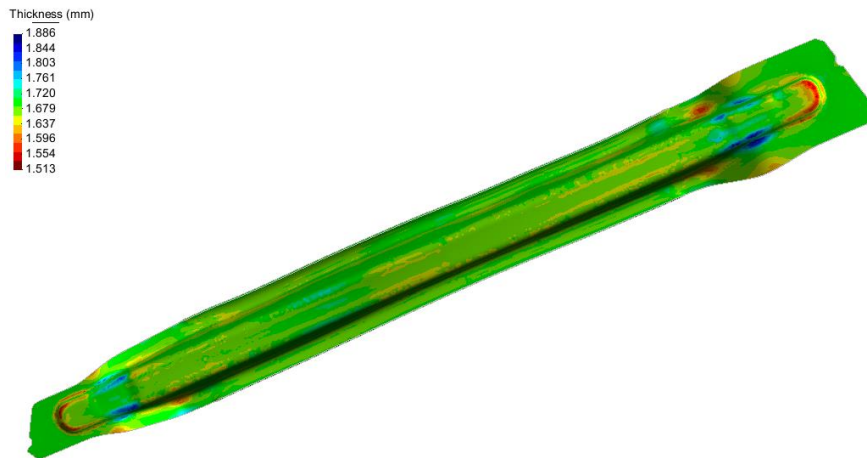


Figure 53 - Thickness of the sheet at the end of forming

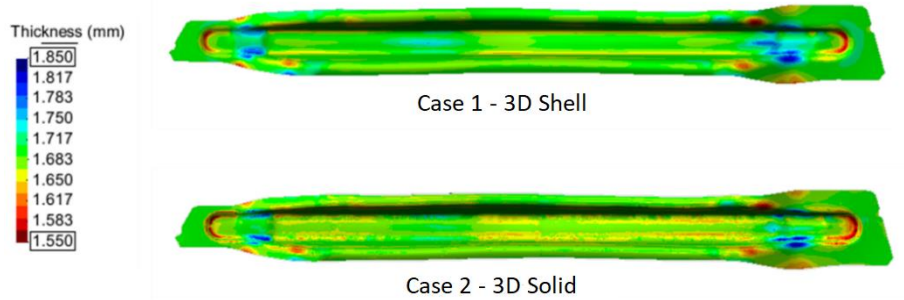


Figure 54- Compare 3D Shell vs 3D Solid thickness of the sheet at the end of forming

## 6.4.2 Formability Analysis

The analysis of formability based on TFD curve does not identify any risk of rupture area. Unlike Shell 3D simulation, it will show large areas of compression at the spokes.

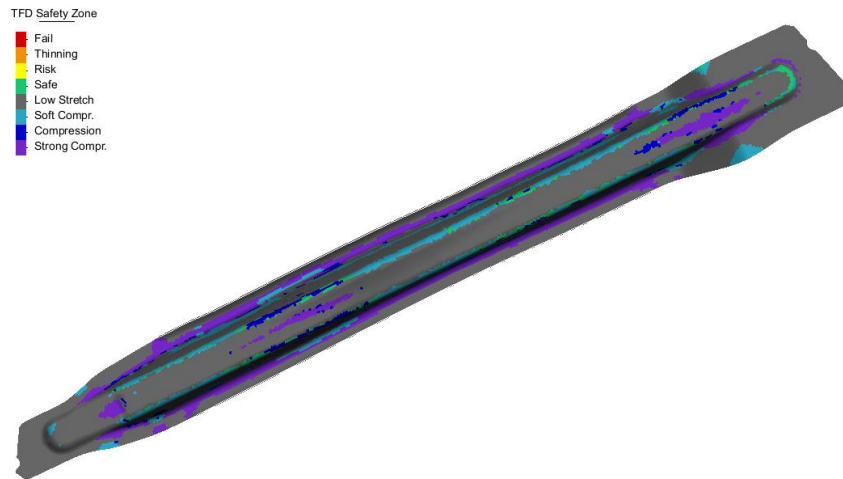


Figure 55 - formability TFD

### 6.4.3 Contact Pressure

Different mould inserts are not perfectly aligned, this causes non-uniform distribution of contact pressure. There was a zone of non-continuity corresponding to center of the component.

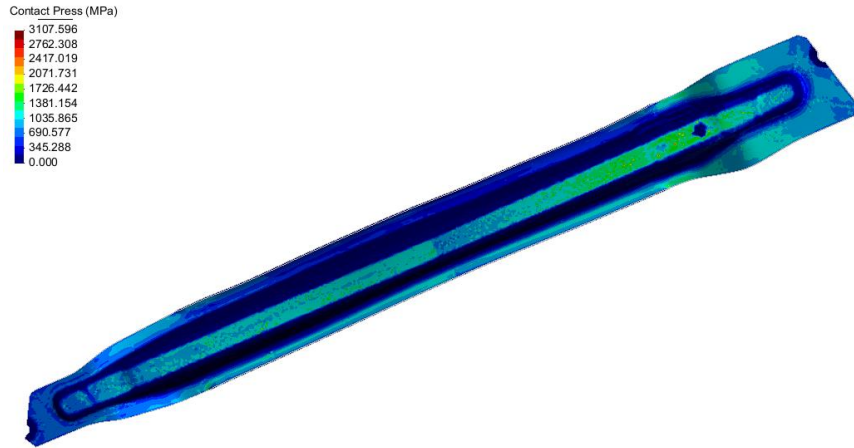


Figure 56 - Contact pressure

### 6.4.4 Performance of the Moulding Force

The trend is quite comparable with that obtained by the 3D simulation Shell.

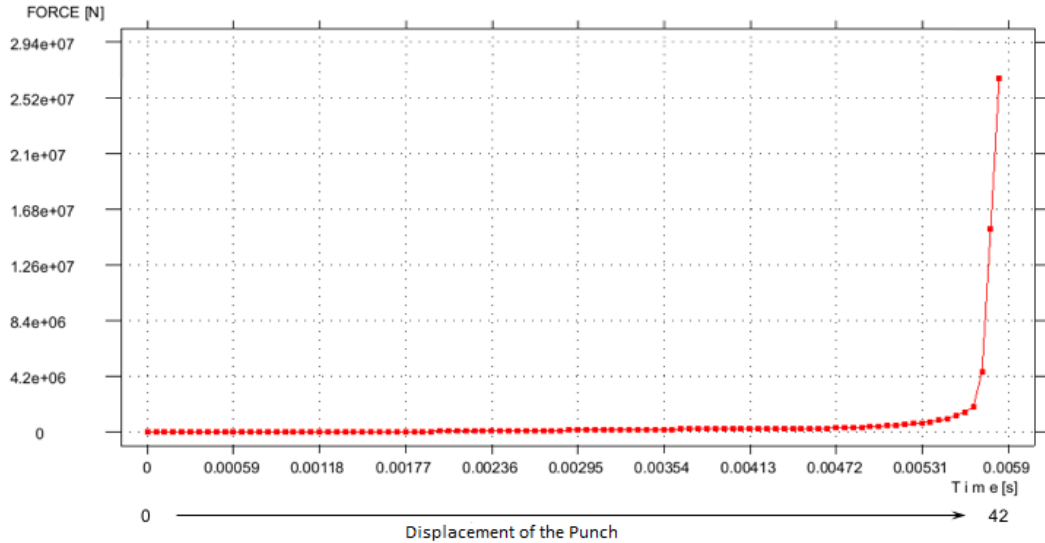


Figure 57 - Force on the punch / die during the process

## 6.4.5 Calculation of Elastic Return

Similar to the case 3D Shell, after simulating moulding of the component, we proceed with the calculation of the elastic return. We operate in fast springback (constrained elastic return) mode or explicit mode springback (free elastic return). In this first phase considering first approach, we bound 4 points positioned in the central zone of development. The result of the calculation of elastic return will depend on the number and position of the constraint points.



Figure 58 - Return bound elastic (fast springback)

The springback results are represented in Figure 58 and Figure 59. The red lines identify the edges of the component at the end of molding operation alone. The global maximum displacement of the nodes as a result of the elastic return are equal to about 2.5 mm and localized on the wings. It detects a discrepancy in terms of performance and value compared to the Shell 3D simulations performed with Stampack and AutoForm.

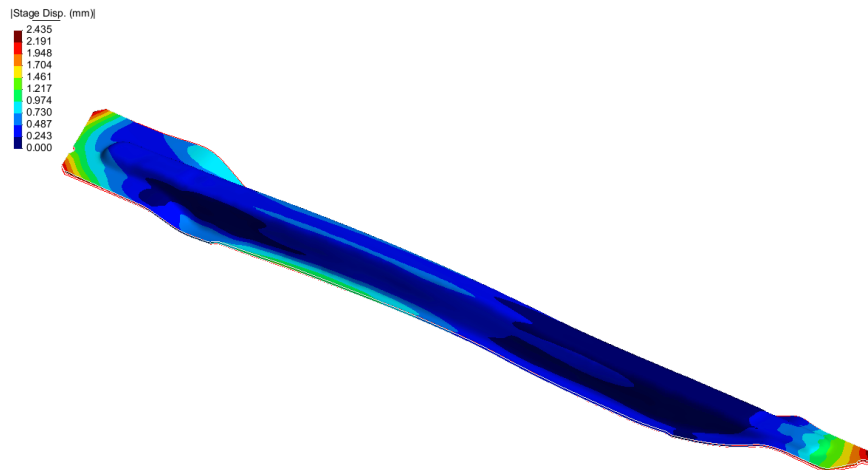


Figure 59 - the extent of the elastic return Quantitative evaluation (constrained elastic return)

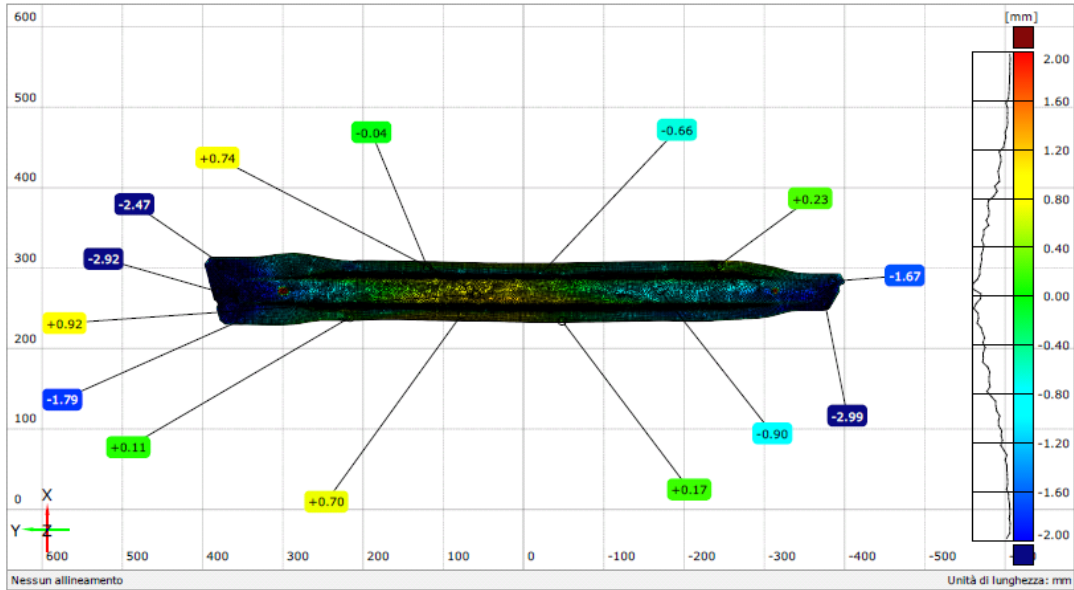


Figure 60- Pointwise Deviations between nominal CAD model of the component and the result of simulation with 3D geometry of the real mold

Comparison of the results of Solid 3D simulation with the 3D CAD model of the component (Figure 60) and with the actual geometry of the component (Figure 61), leading to considerations analogous to those already described above for the first loop with springforward algorithm (Figure 47 and Figure 48). The deviations from the CAD model are higher than those evaluated with respect to the actual geometry of the component, consistent with the fact that we have used the real geometry of the die and punch for 3D simulation Solid.

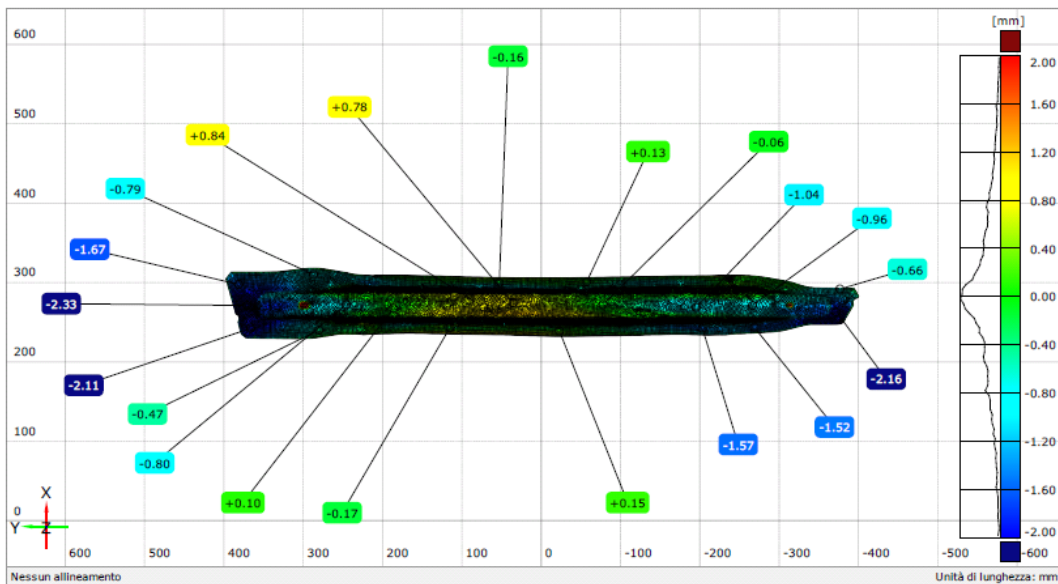


Figure 61 - Pointwise Deviations between actual geometry of the component and the result of simulation with 3D geometry of the real mould

## 7 3D Scanning of the Actual Geometry of Moulds and Components

The finishing operations cause a mismatch between the physical mould and its mathematical model. A possible solution to this problem is to employ the potential provided by the Reverse Engineering and from the non-contact scan to acquire the real geometry of the mould and the molded component. The scanning equipment repeated at an interval of time can be used to monitor the wear of the moulds and the possible impact that it may have on the geometry of the component. For the activity, the scanner Atos Core 300 has been used.



Figure 62 - Scanner structured light ATOS Core 300

The preliminary operations to the scanning phase are opacification of surfaces and to detect the arrangement of markers. The use of a spray powder of the type of those used for the detection of cracks with penetrating liquids, it is necessary on metal surfaces in order to reduce the reflection of the surface and improve the contrast for the acquisition in gray tones carried out by cameras of the 3D optical scanner. The application of the markers, consisting of adhesive stamps representing a white circle of 1.5 mm diameter on a black field, serves to create a network of fixed reference points on the object scanned, so the image management software is able to report and to align automatically the views of different areas that are acquired in succession from different angles.

### 7.1 PM13 Mold 3D Scanning

The mold of PM13 is scanned at the establishment of PMC Automotive Bruino. On this occasion, we have detected and acquired the following geometries:

- Upper surface development of left and right components shown on die operation OP30
- Geometry of the punch operation OP40 crash-forming
- Geometry of the die operation OP40 crash-forming
- Upper surface of moulded components right and left positioned on the operation OP50 vacuum references

- As seen from Figure 63, in fact, due to the protruding position of extractors, it was not possible to report on the operation OP40 mold.

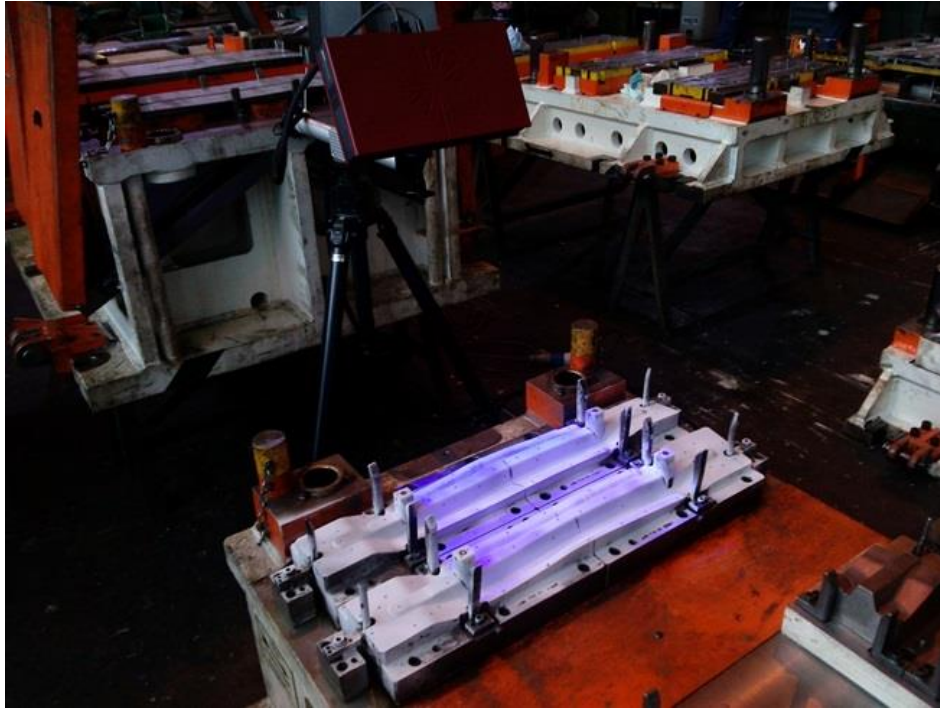


Figure 63 - Scanning of the die (OP40) of the PM13 component mould

### 7.1.1 Comparison of the Actual Geometry of the Mould with the Cad Model

The CAD geometry of die should correspond to that used for the milling of the die, while the CAD geometry of the punch coincides with that of the die, as the existing offset between the punch and die is assigned directly in the definition phase of the milling tool path.

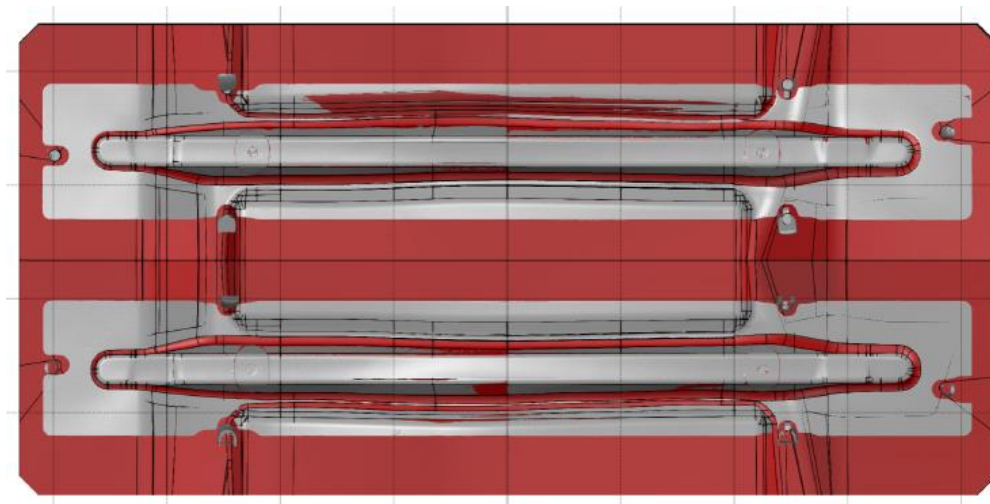


Figure 64 - Die OP40 - Alignment for comparing the scan data and CAD model

After alignment of Best Fit models, the comparison of actual geometry of the die with the CAD model of the same shows the greatest differences are localized at junctions on the bottom that follow the profile of the bar. The majority of surfaces deviates from the CAD model in a range of  $\pm 0.20\text{mm}$  interval. The blue colour line more pronounced that we see at the top of Figure 65. It corresponds to a crack present on the left of the component die. The presence of this crack had already been identified by the naked eye during a first investigation carried out at the plant in Bruino (Figure 66).

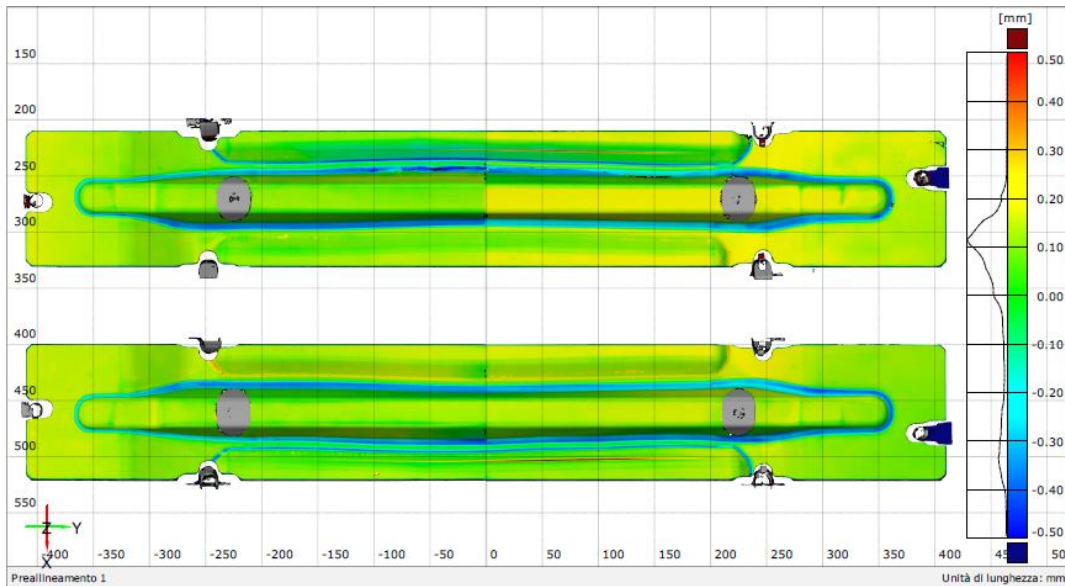


Figure 65 - Map of deviations between the CAD model and the scan data for the OP40 die



Figure 66 - Cricca on the die (OP40) of the PM13 left component

In Figure 67 are reported, for completeness, some values of pointwise deviations for the die.

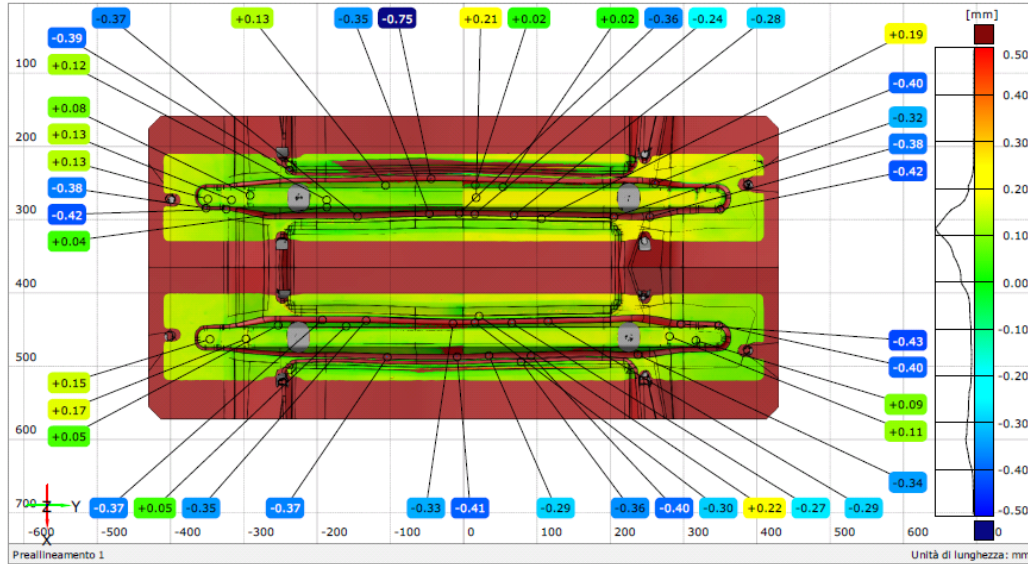


Figure 67 – Pointwise deviations between CAD model and scan data for the OP40 die

It is reported, the comparison between actual geometry of the punch with the sole reference CAD model identical to that of the die. Such a comparison, allows to highlight the offsets that have been defined between the die and punch to take account of the thickness of the component.

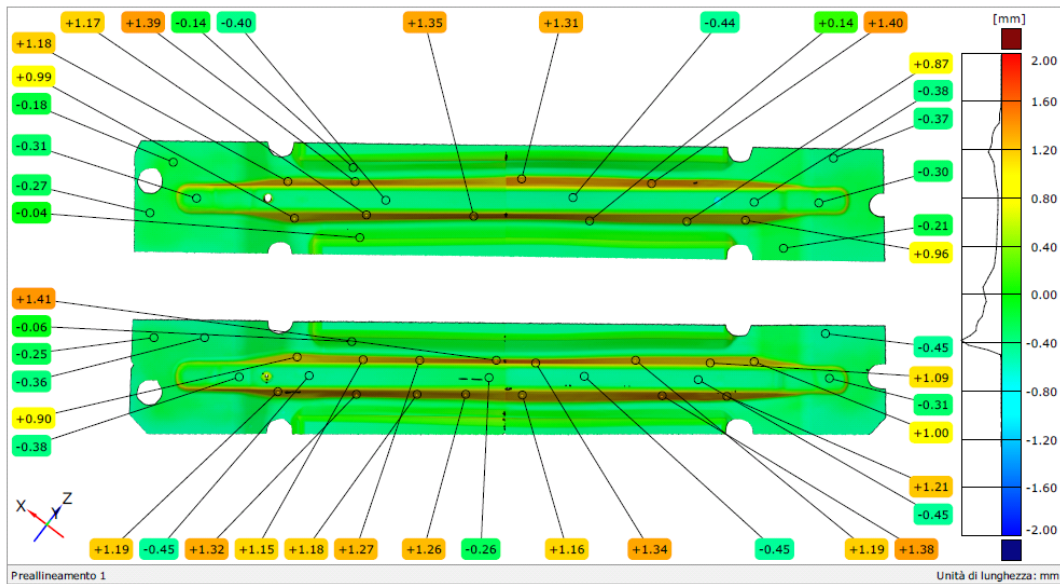


Figure 68 - Pointwise deviations between CAD model and scan data for the OP40 punch

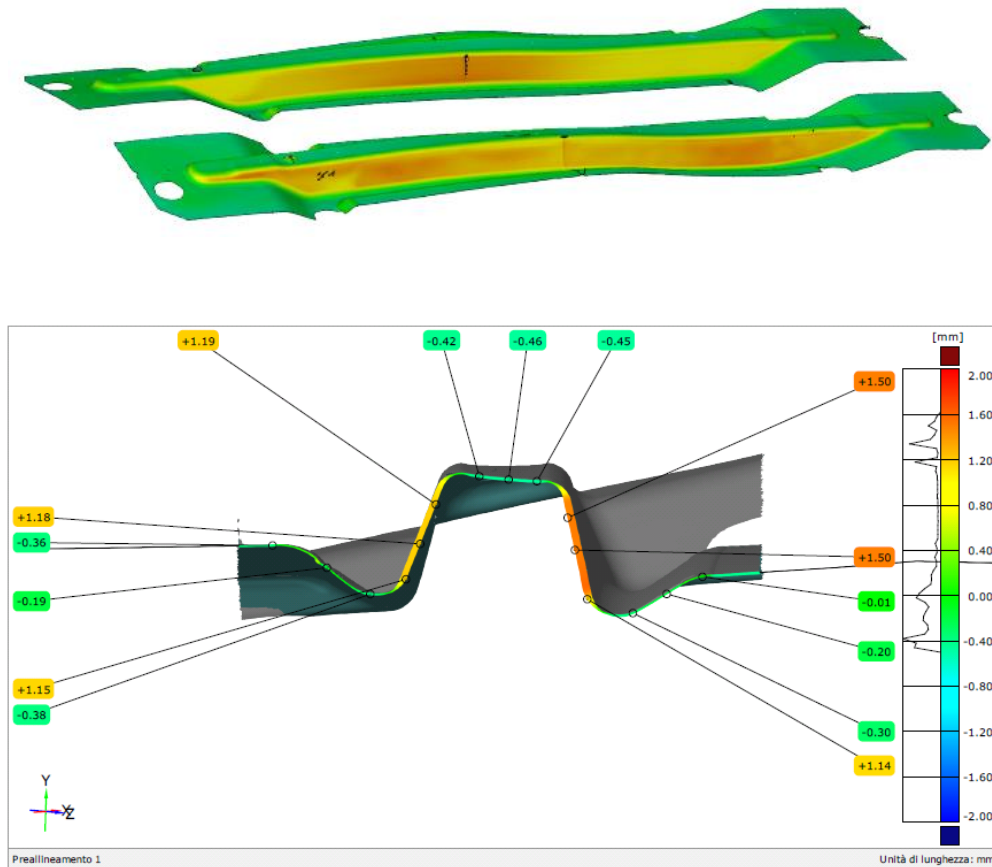


Figure 69- Deviation on side walls and in a section between CAD model and scan data for punch OP40

## 7.2 PM13 Component 3D Scanning

### 7.2.1 Comparison of the Actual Geometry of the Component with the CAD Model

The comparison between the actual geometry of the component acquired by the scanner ATOS Core and 3D CAD model shows a good dimensional quality of PM13 crosspiece (Figure 70).

The component variances with sign amounted on average around 0.10 mm. The largest deviations are recorded in correspondence with the head and tail fins, where the real surface is more bent (lower because the deviations are negative) than that of the CAD model. Another area in which the deviations are marked is that of the junction that runs along the entire contour of the workpiece.

Analyzing the cross section in correspondence with the plane  $Y = 240$  mm, it can occur as the effect of variation of fitting on the mould, causing a geometric variation localized on the component (Figure 71).

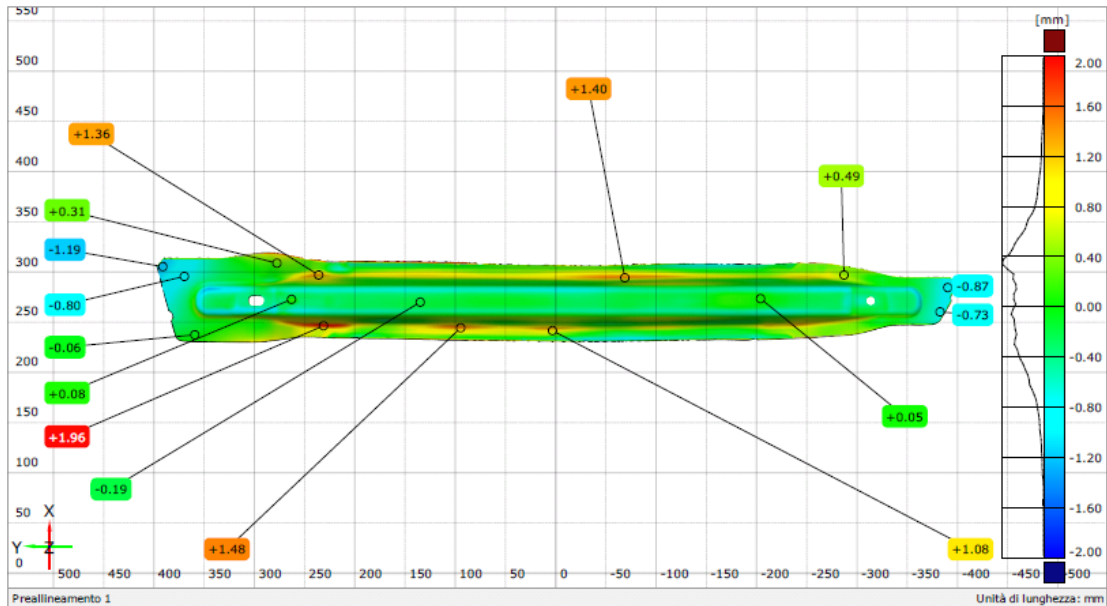


Figure 70 – Pointwise deviations between the scanned data and CAD model for PM13 cross

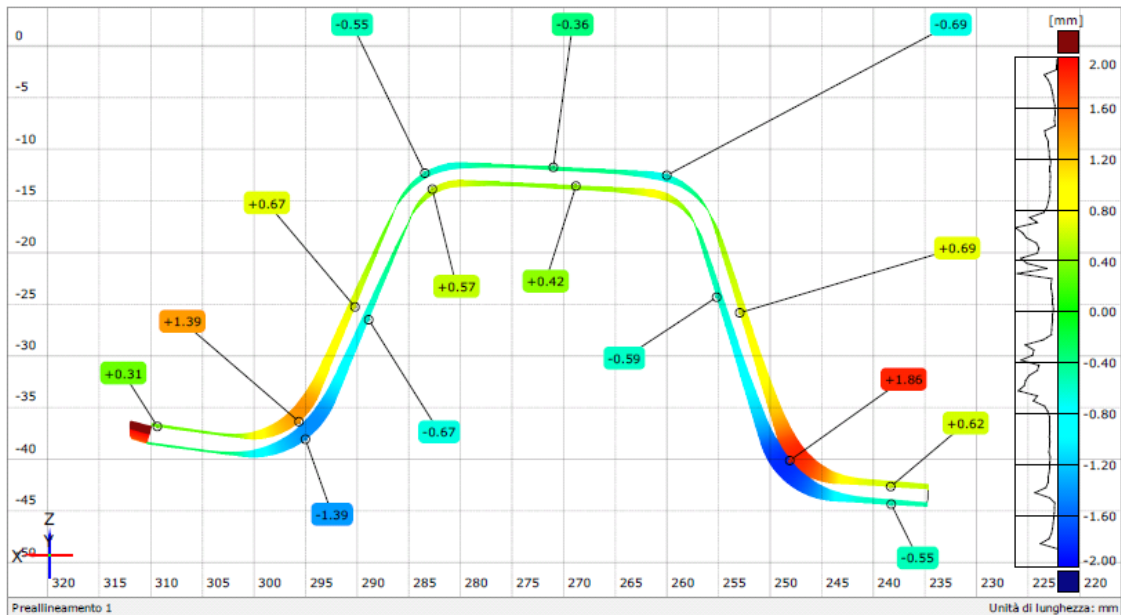


Figure 71 - Deviations at an altitude of section Y = 240 mm

### 7.3 MA03 Mould 3D Scanning

The mould of the MA03 is scanned at the plant Sall New Chivasso. On this occasion, we have detected and acquired the following geometries:

- Upper surface development of left and right components shown on die operation OP20
- Geometry of the punch operation OP20 crash-forming

- Geometry of the die operation OP20 crash-forming
- Upper surface of moulded components right and left positioned on die operation OP20
- Upper surface of molded components right and left positioned on test gauges (Figure 72).



*Figure 72 - Scanning of the die (OP20) of the MA03 component mould*

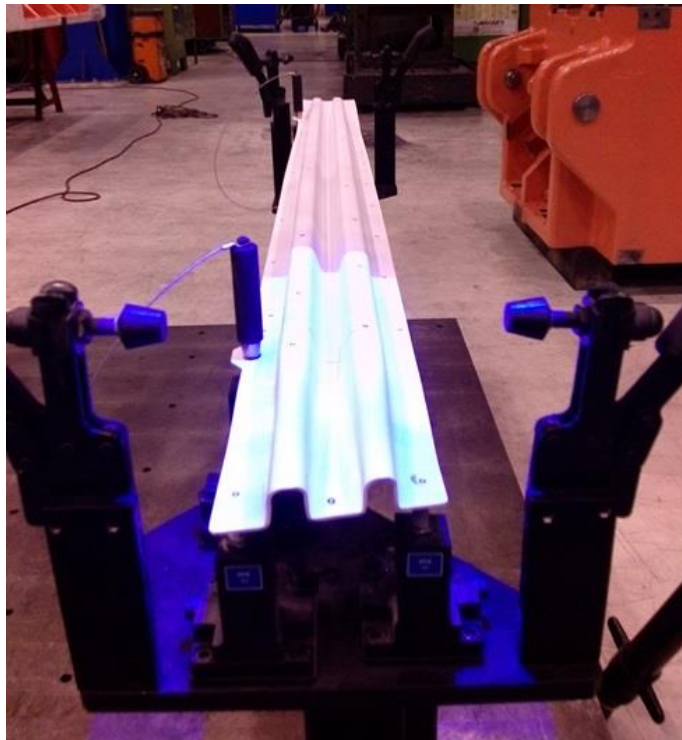


*Figure 73 - Scanning the MA03 component reported on the test gauge*

## 7.4 MA03 Component 3D Scanning

### 7.4.1 Comparison of Actual Geometry of Component with the Scanning of the Surface of the Caliber

In a preliminary phase, the 3D geometry of the individual bars as detected at the Polytechnic, was compared with the scan performed on the control caliber at New Sall.

By superimposing the scanned data of the first sheet with the surface detected in New Sall, the component appears rotated along the diagonal which joins the edge at the bottom left with the one in the upper right (Figure 74).

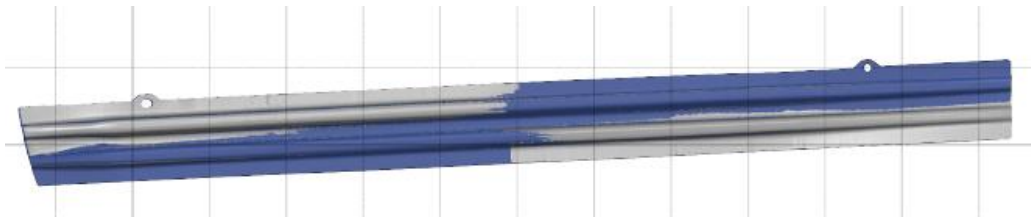


Figure 74 - Comparison of 3D scan data with respect to the points detected on one surface of the first component MA03 positioned on the test gauge

The effect is also confirmed by the analysis of variances that are positive on one side of the diagonal and negative on the other (Figure 75).

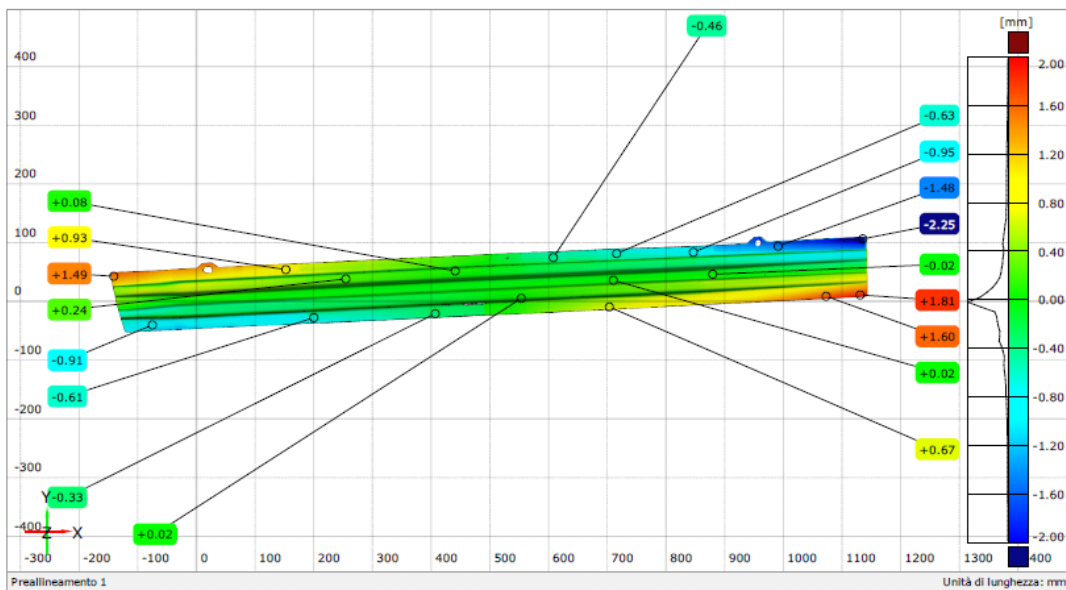


Figure 75 - Pointwise deviations of 3D scan data with respect to the points detected on one surface of the first component MA03 positioned on the test gauge

The same effect of deformation along the diagonal as a result of the support used to lock the sheet metal during the scan appears evident also for the second component (Figure 76).

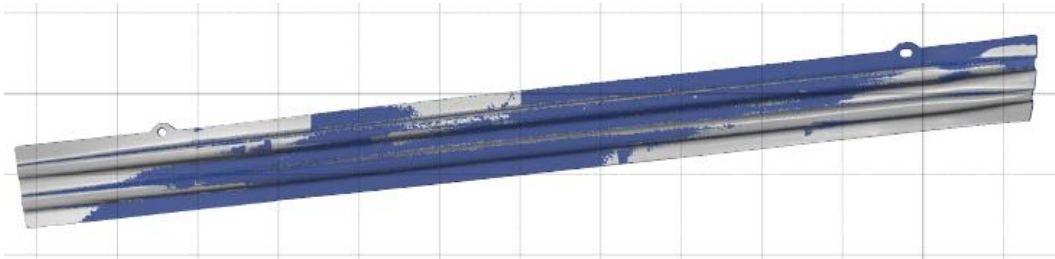


Figure 76 - Comparison of 3D scan data with respect to the points detected on one surface of the second component MA03 positioned on the test gauge

In the second case the deviations are of a lower magnitude (Figure 77).

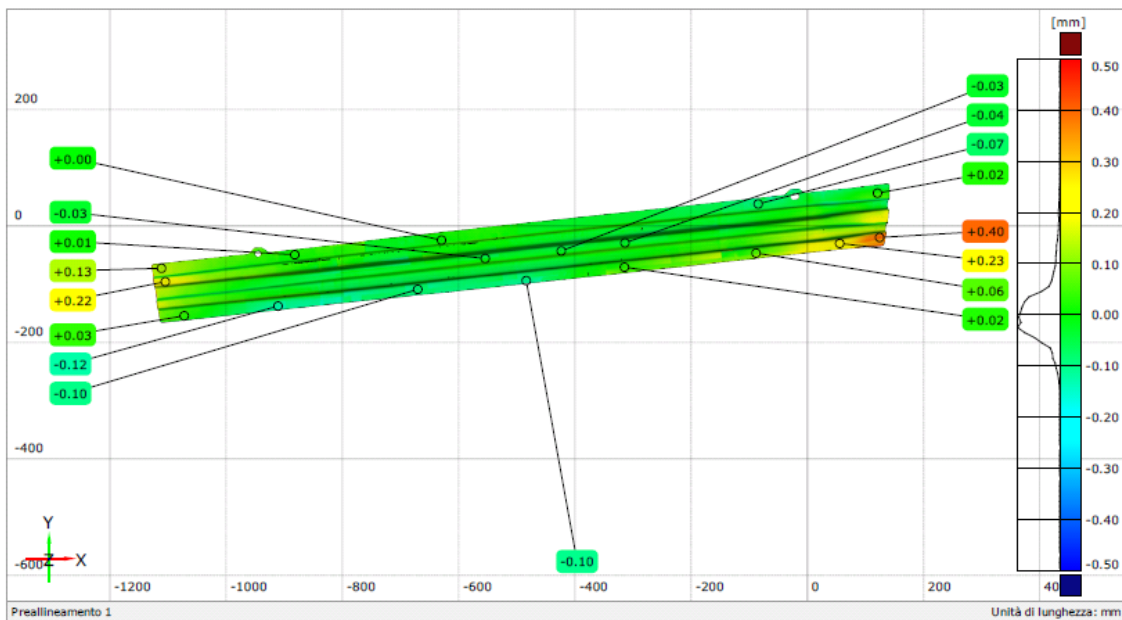


Figure 77 - Pointwise deviations of 3D scan data with respect to the points detected on one surface of the second component MA03 positioned on the test gauge

Among the detected differences between the scans of the two MA03 crossbars, it will be considered only the best case, namely that of the second component, the left.

## 7.4.2 Comparison of the Actual Geometry of the Left Component with the Cad Model

The views in Figure 78 reports the result of best fit alignment between the actual geometry of the anti-intrusion bar MA03 left and the corresponding nominal CAD model.

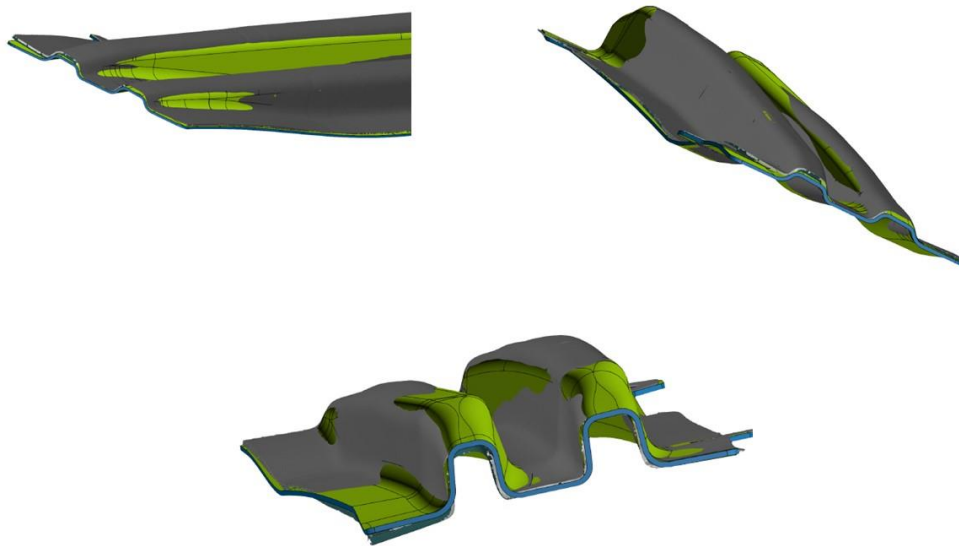


Figure 78 - Best Fit alignment views between scan data of the left MA03 bar and nominal CAD model

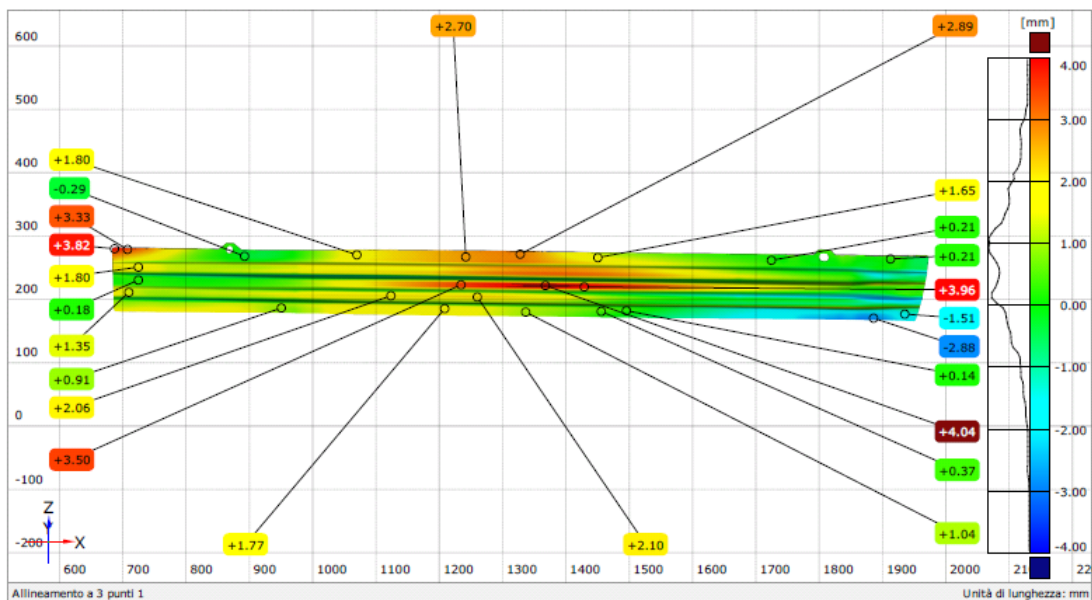


Figure 79 - Pointwise deviations between the actual geometry of the left bar and the CAD model

The differences are evident and are in the color map Figure 79. We note again a tendency to twist along the diagonal, because the top left deviations are positive and negative in the lower right. There is deviations of a few millimeters even in the central area of the bar. Such deviations are positive and indicates bending of the component, which tends to have a belly or hump in the middle. The same effect has been detected in the establishment of production and assembly of Daimler in Germany and it is due to interference with the other elements of sheet metal of the door group of which the MA03 bar is a part.

## Chapter Three

### 8 Refinement of the 3D Simulation Model Shell (PM13)

At the conclusion of the preliminary definition of simulation models it was found that:

- 3D Shell does not allow the use of actual geometry of mould obtained by scanning.
- 3D Solid used to introduce the actual geometry of the moulds. This leads to a deformed shape less representative of the real object, with an average deviation of +0.12 mm and a standard deviation of 0.89 mm. The timing of implementation and calculation are considerably higher (about 5 times) and the convergence of the model especially during the calculation of the elastic return, is often problematic.

From a comparison with the distributor of Stampack Company, emerged a solution combining the advantages of a 3D Shell model in terms of modeling simplicity and speed of calculation with the possibility of considering the thickness of sheet in contact and the actual geometry of moulds . It defined a new 3D Shell simulation model implementing a new function: the contact condition Top / Bottom. The following changes were introduced:

- introduction of the real geometry of the moulds;
- positioning of the moulds considering an offset equal to the thickness of the sheet in the closed position;
- definition of the contact condition Top / Bottom.

The new 3D model is visible in Shell Figure 80 while Figure 81 shows the window with the contact condition Top / Bottom and coefficients of friction.

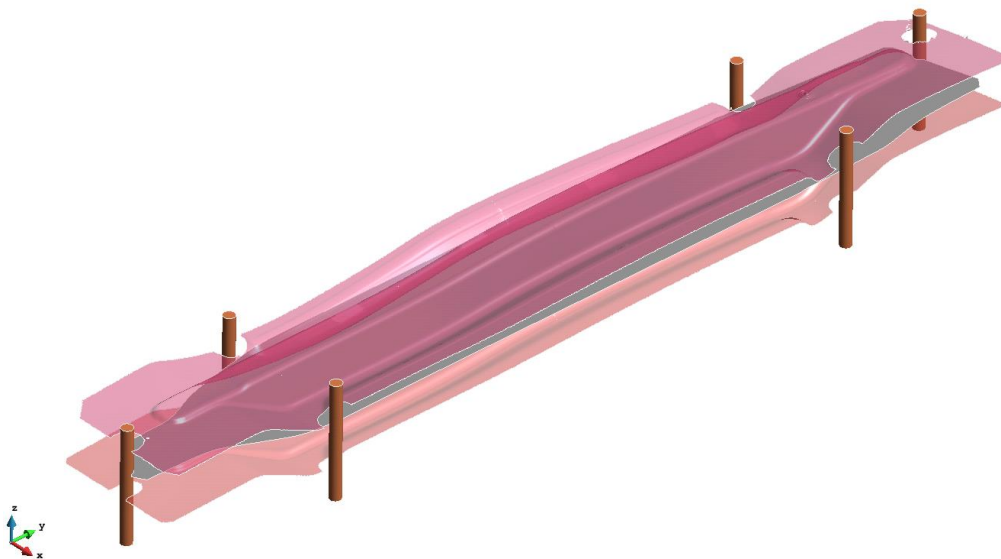


Figure 80 - Geometry Input

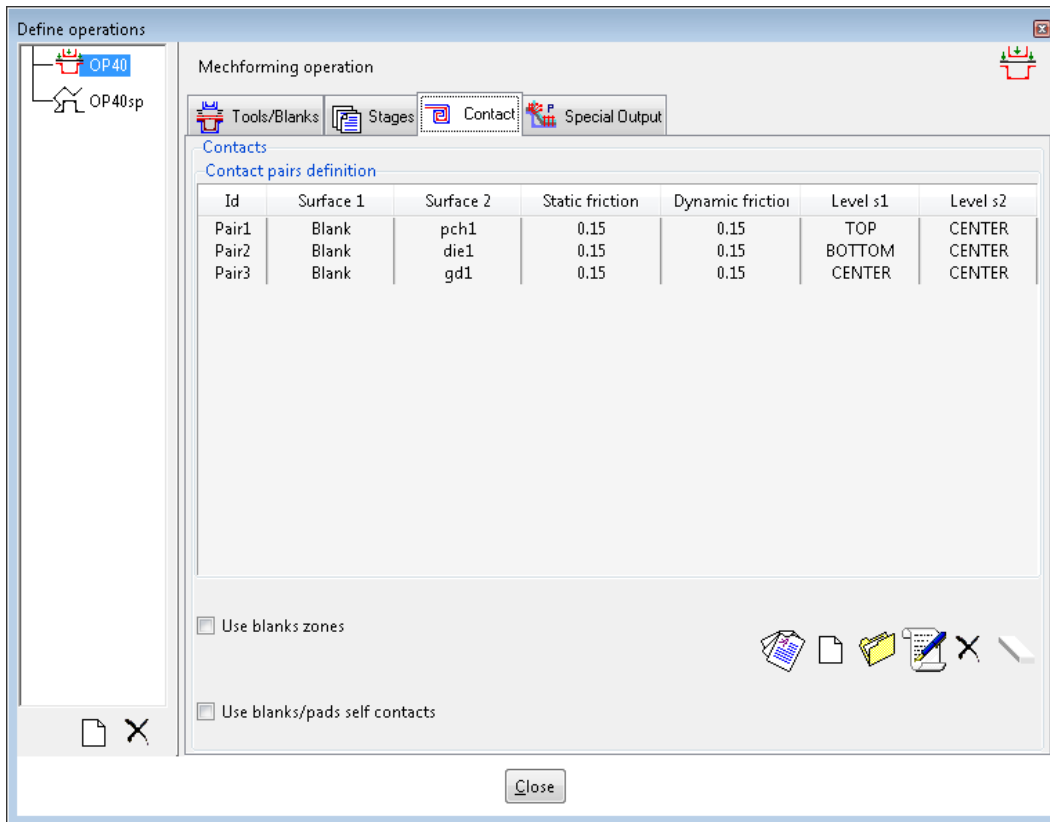


Figure 81 - Condition of contact and friction coefficients

In the following figures, in the first case the sheet thickness is not taken into account during the forming and the moving die half comes running up to the stop on the fixed mould half. In the second case, instead, it takes into account the thickness of the sheet; the irregularities of the real moulds and is clearly visible that the wireframe blank is positioned about halfway offset.

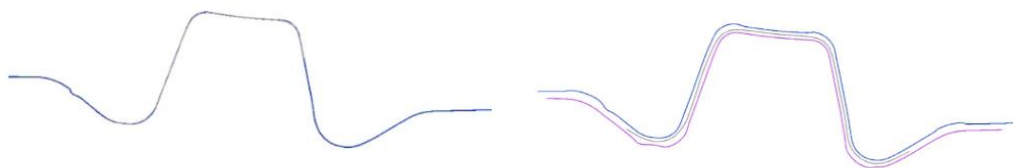


Figure 82 - Cross section of the mould at the end of moulding: 3D model Shell base (left) and the 3D model Shell Top / Bottom (right)

Table 4 shows the computation time for each stage relatively to different simulation models so far analyzed. We can see that from the point of view of time, the 3D model Shell Top / Bottom guarantees the rapidity of calculation of a 3D model Shell base with the possibility of using the actual geometries of the typical mould of a 3D Solid.

Table 4 - Calculation time for each simulation stage (PM13)

Operation simulated	Solver	Processing time
<i>3D Shell base (moulds CAD)</i>		
• Forming	Explicit	15 '40 "
• Back bound elastic	Implicit	15 '29 "
	Total	35 '09 "
<i>3D Solid (real moulds)</i>		
• Forming	Explicit	1h 27 '13 "
• Back bound elastic	Implicit	1h 22 '31 "
	Total	2h 49 '44 "
<i>3D Shell TOP / BOTTOM (real moulds)</i>		
• Forming	Explicit	31 '34 "
• Back bound elastic	Implicit	22 '56 "
	Total	54 '30 "

## 8.1 Results

Below are some significant numerical results obtained from the simulation.

### 8.1.1 Thickness of the Sheet at the End of Forming and Percentages Thinning

Figure 83 represents the result of forming prior to the calculation of the elastic return in terms of the sheet thickness. Figure 84 shows the analogous information in the form of percentages thinning. The results are comparable with those obtained from the 3D model based Shell.

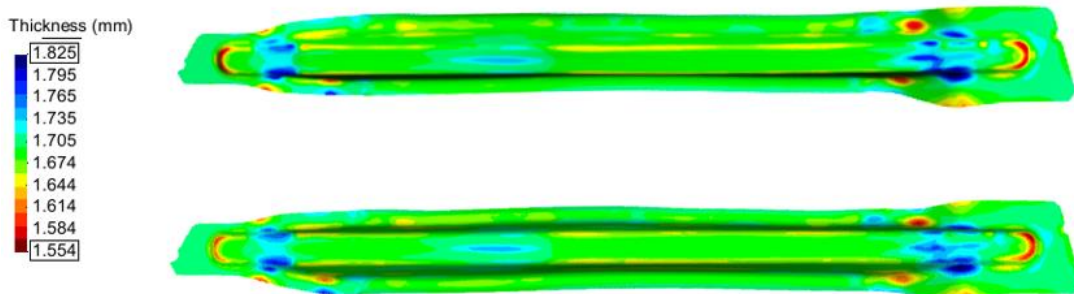


Figure 83 - Sheet thickness at the end of forming - 3D Shell base (top) and the 3D model Shell Top / Bottom (bottom)

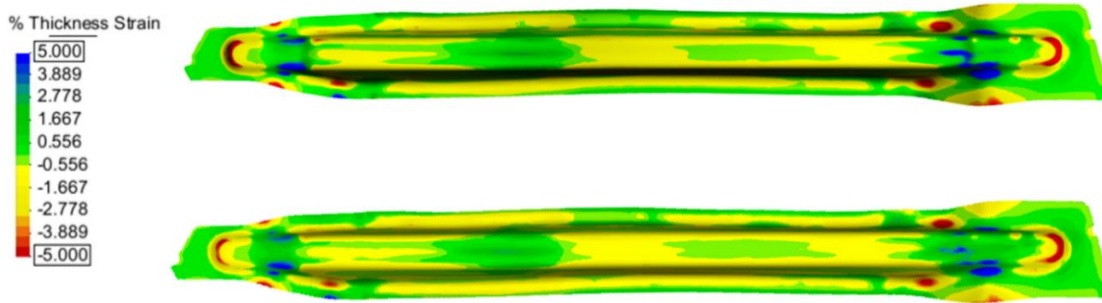


Figure 84 – Percentage of thinning - 3D Shell base (top) and 3D model Shell Top / Bottom (bottom)

## 8.1.2 Formability Analysis



Figure 85 - formability FLD - 3D Shell base (top) and 3D model Shell Top / Bottom (bottom)

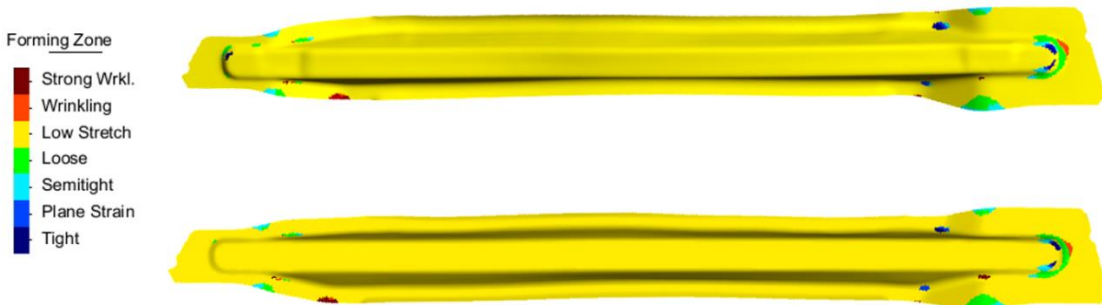


Figure 86 – Formation of wrinkles 3D Shell base (top) and 3D model Shell Top / Bottom (bottom)

## 8.1.3 Performance of the Moulding Force

The maximum force value is approximately 295 tons in the case of real mould, next to the same value obtained from the 3D model based Shell. The trend is entirely comparable (Figure 87).

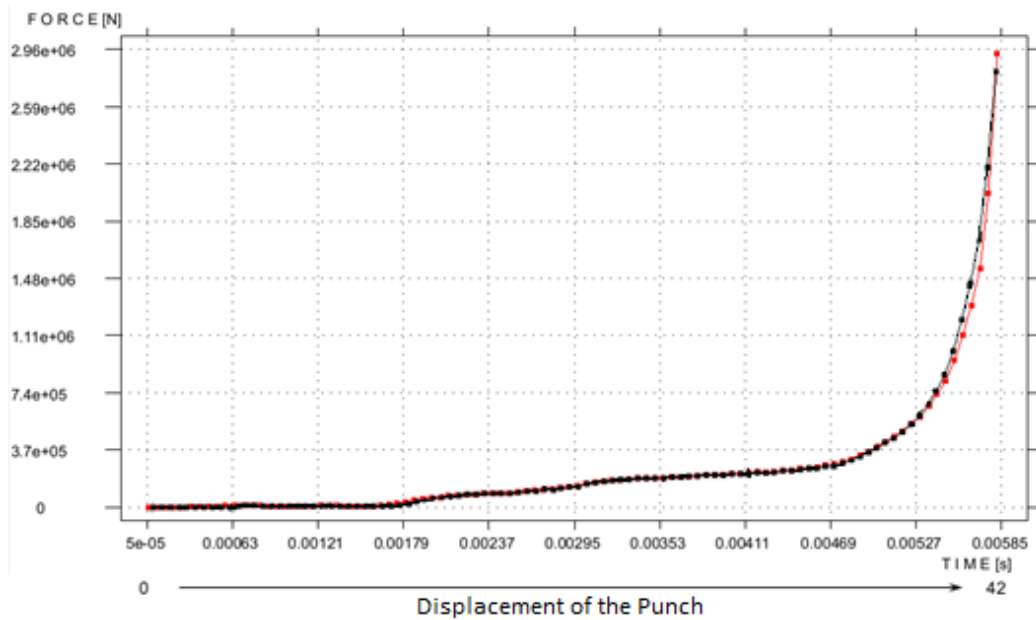


Figure 87 - Force on the punch / die during the process 3D Shell base (black curve) and 3D model Shell Top / Bottom (red curve)

### 8.1.4 Calculation Of Elastic Return

The springback calculation was performed considering an isostatic constraint configuration represented in Figure 88.

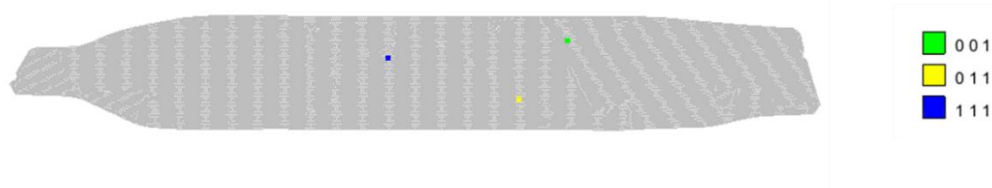


Figure 88 - Position of constraint points (isostatic configuration)

The comparison with the nominal geometry (average floor extracted from the 3D CAD model of the component) highlights the limitations arising from the use of CAD nominal surface of the mould without offset between the punch and die, which also does not take into account the springback. It is noted that for comparison is not possible to use the average plane of the STL model obtained by scanning the real component, as the extraction and the calculation of such a plane is not allowed by the version of the software inspection and testing used.

The Pointwise deviations between the springback deformation with isostatic constraint from CAD moulds and the average CAD plane are reported in Figure 89. The average deviation is of -0.21 mm with a standard deviation of 0.67 mm.

The Pointwise deviations between the springback deformation with isostatic constraint by using the scanning moulds and the average CAD plane are reported in Figure 90. The average deviation is of -0.01 mm with a standard deviation of 0.32 mm.

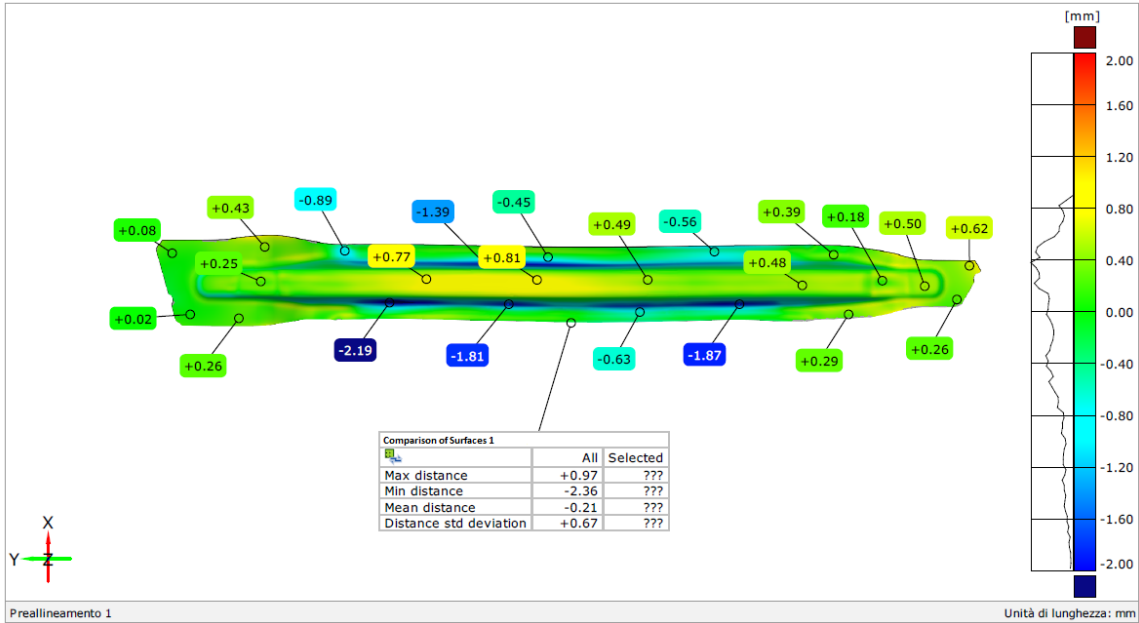


Figure 89 - Comparison between the deformed shape by CAD moulds with isostatic constraint compared to the average plane of the CAD component PM13

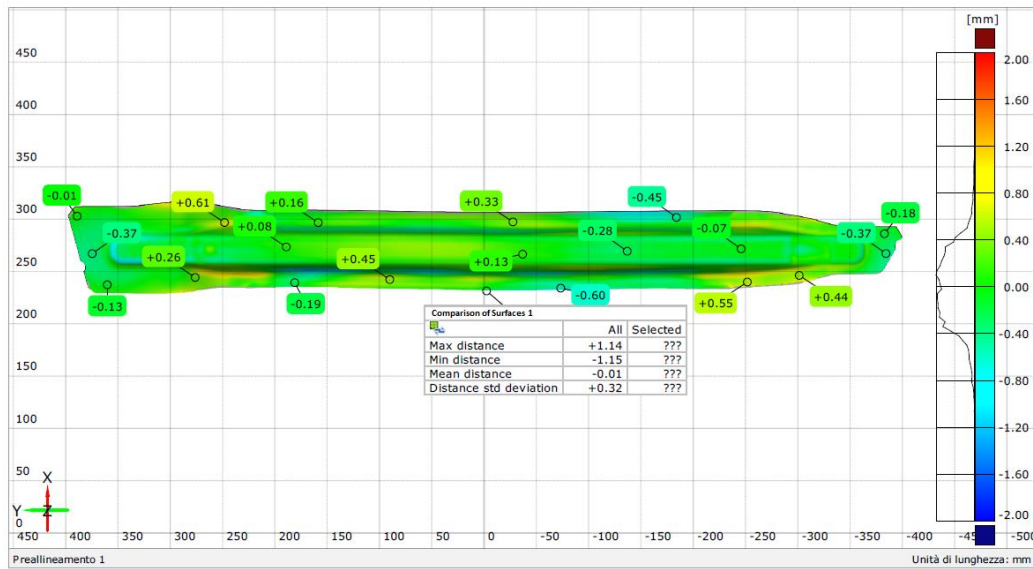


Figure 90 - Comparison between the deformed shape from real moulds with isostatic constraint compared to the average plane of the CAD component PM13

It is therefore evident that the simulation of the component moulding which considers the actual geometry of the moulds process (including offset between the punch and die and springback compensation) provides results consistent with actual process of moulding, although a comparison limit remains the comparison with the plane average CAD and not with the midplane of the real component. We reserve the right to seek a procedure for defining and midplane extraction from the scanned data in STL format. Downstream of such extraction, it will be possible to validate the results of the Figure 89 and Figure 90 also with respect to the actual geometry of the component.

## 9 Evaluation Model on the Second Case Study (MA03)

This case study is an anti-intrusion bar (identified by code MA03) of more complex geometry and larger in size compared to the case PM13. It evaluates robustness of numerical simulation model developed with the first geometry. This presents the 3D model of Shell Top / Bottom. The moulds had already been scanned during the first activities of the project. In the model Stampack the two mould halves and guide columns were important as STL file extracted from appropriate cloud points in the scan after decimation to decrease the number of the mesh nodes.

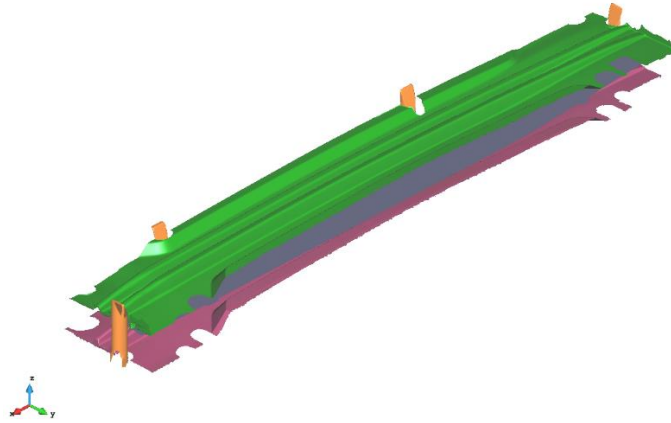


Figure 91- Geometry Input- Complete model of moulds, steering columns and plate development set

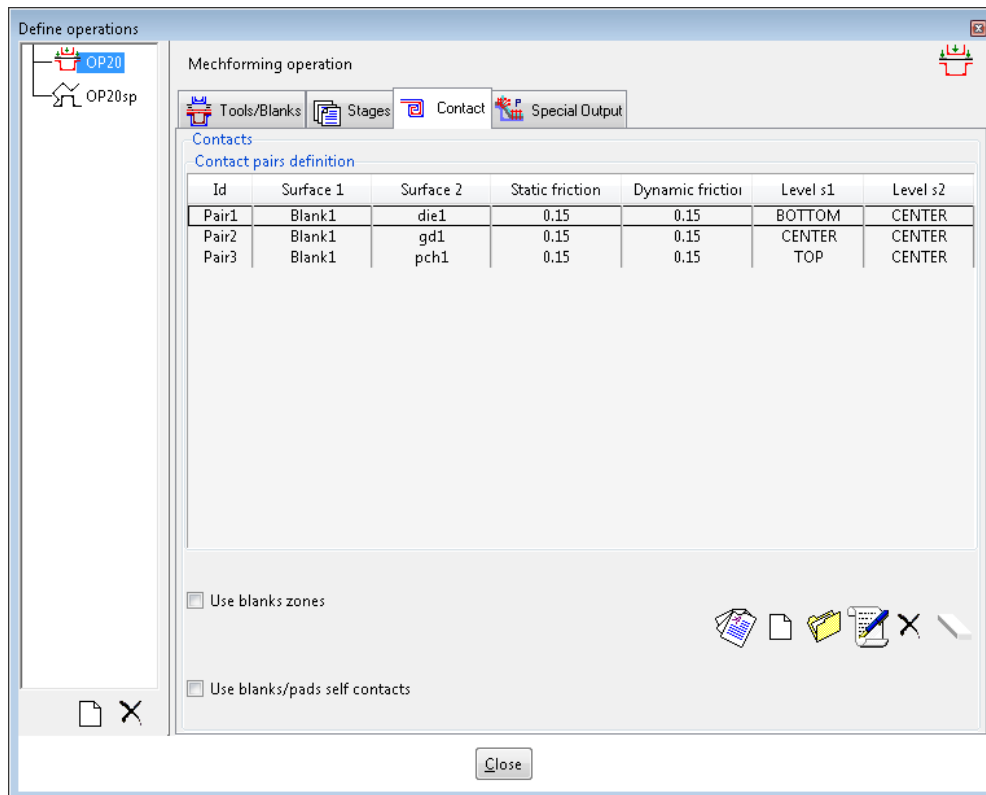


Figure 92 - Condition of contact and friction coefficients

## 9.1 Features of the Sheet Material (DP1000)

The material used for the simulation is a DP1000 and its characteristic parameters were obtained from the Stampack database. The thickness of the sheet metal of 1.5 mm is considered.

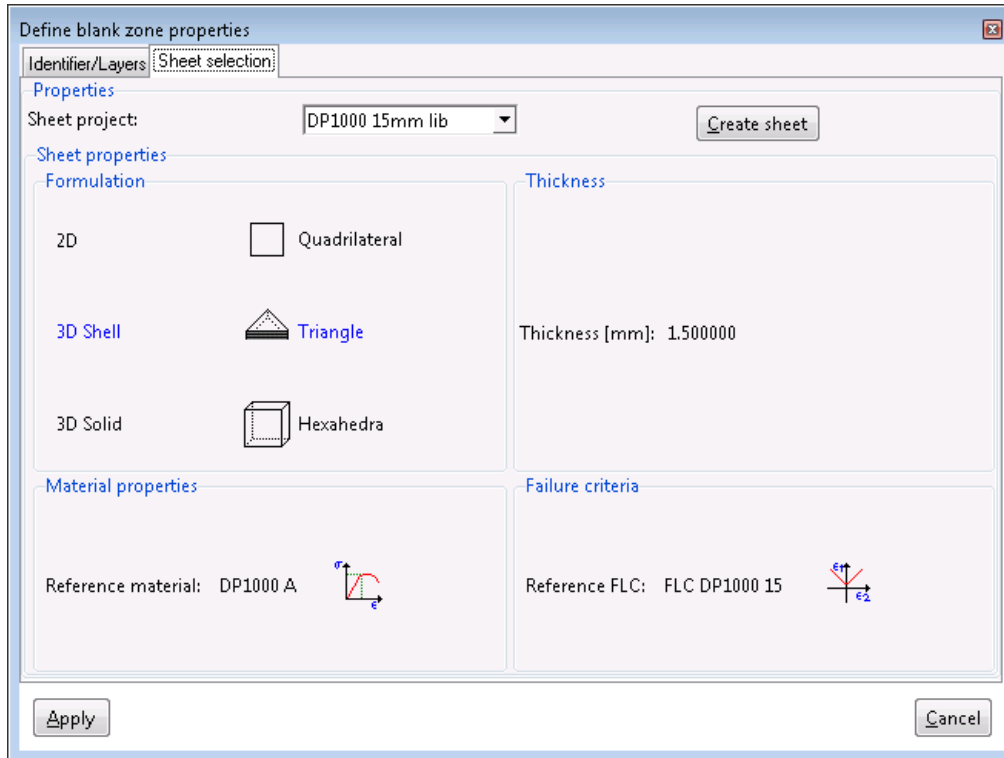


Figure 93 - Summary of characteristics of the sheet material

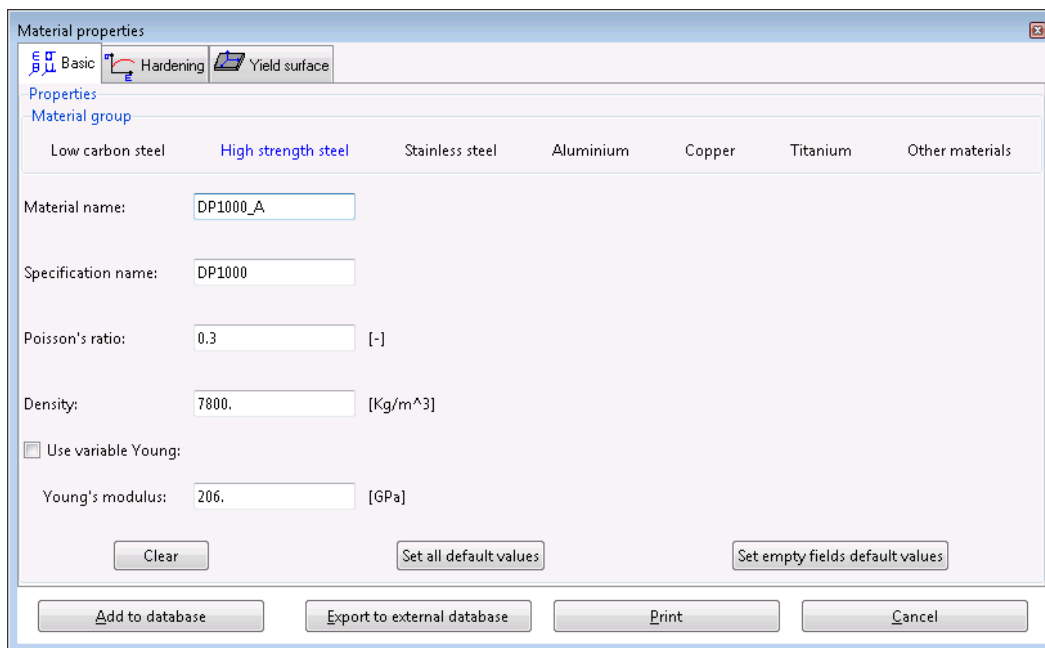


Figure 94 - Characteristics of the sheet material, density and elastic behaviour

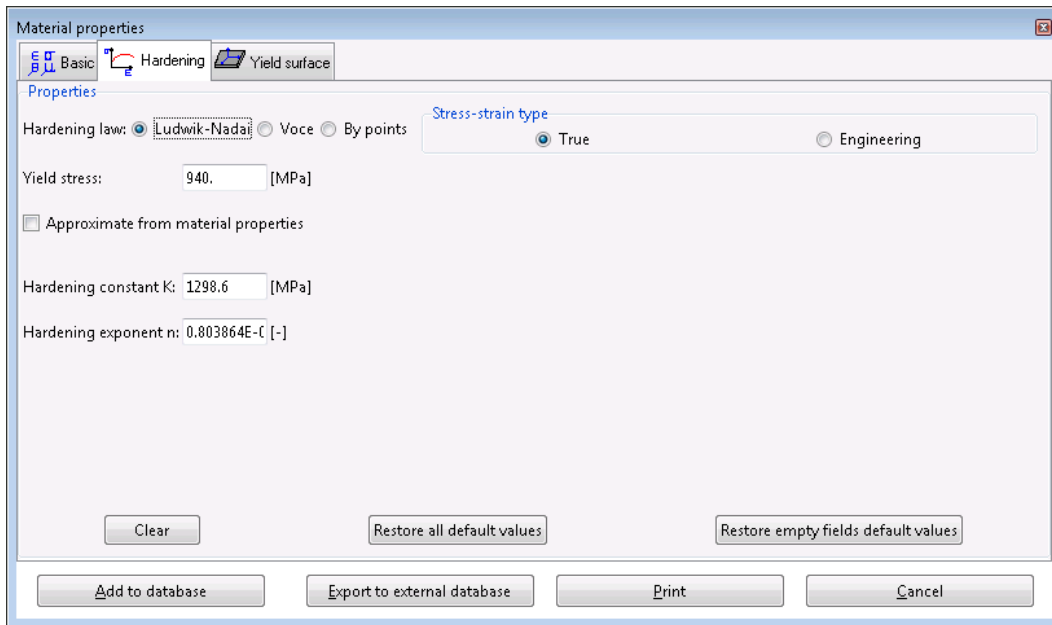


Figure 95 - Characteristics of the sheet material, plastic behaviour

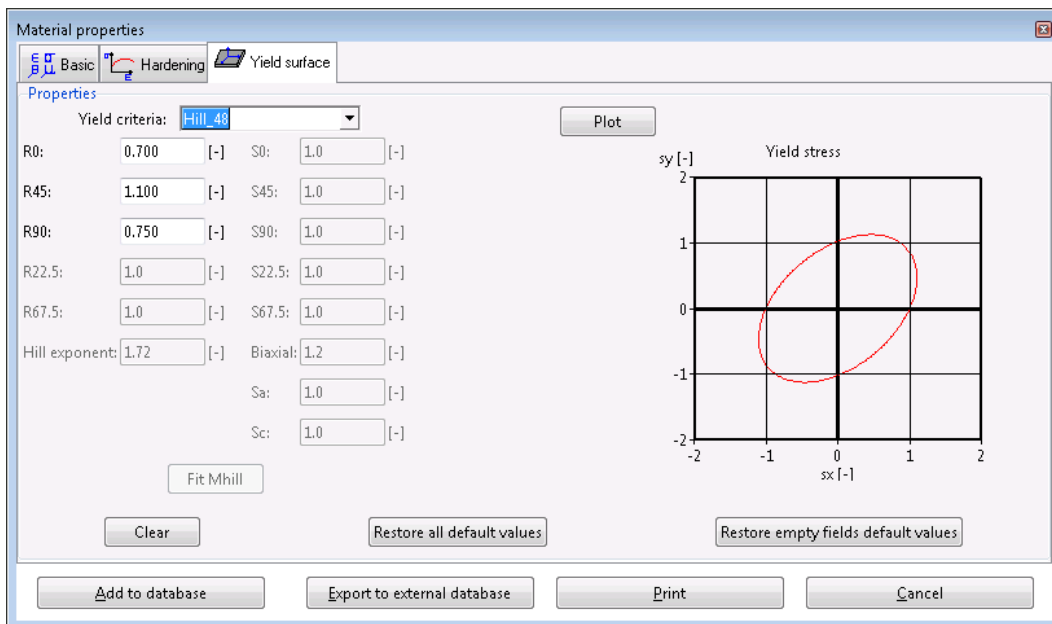


Figure 96 - Characteristics of the sheet material, anisotropy

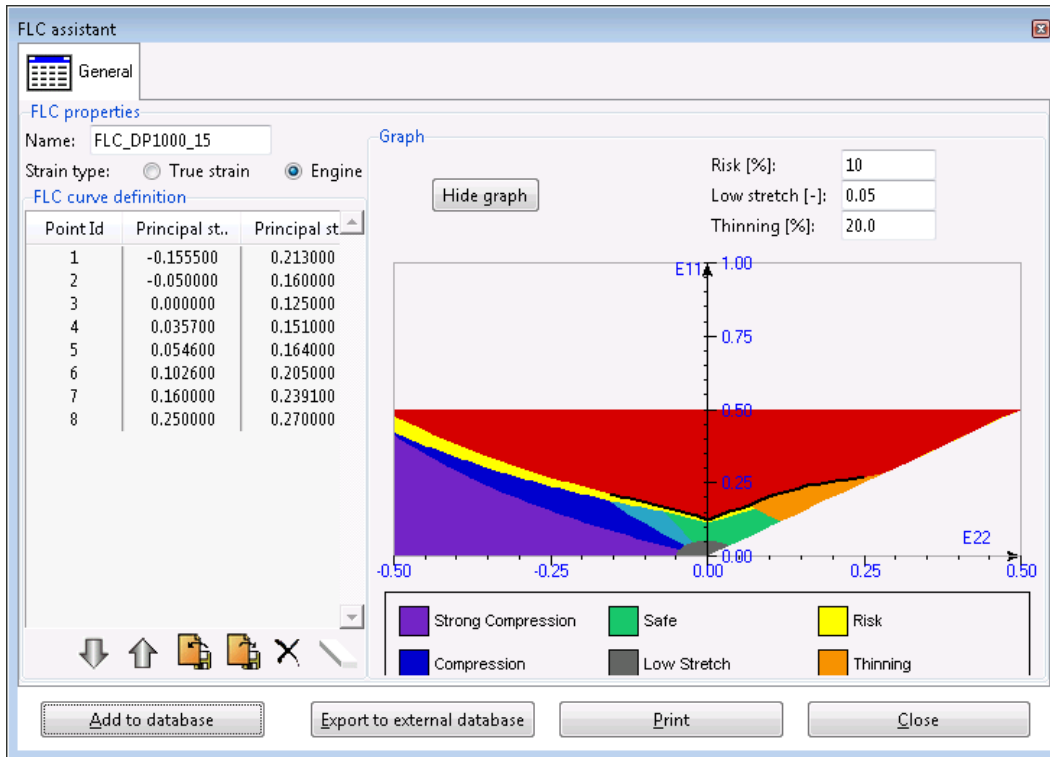


Figure 97 - Characteristics of the sheet material, forming limit curve

## 9.2 Implementation of Gravity in the Model

The geometry of the moulds and size of the component examined make it necessary to introduce in the model simulation of gravity, prior to the forming step. The sheet development is in fact initially oriented in the model perpendicularly to the direction of closure, but in reality the sheet rests on the surface of fixed mould half leaning and curving on the basis of points of support. The sheet displacement under the effect of gravity is constrained by contact with the guide columns, as well as by the geometry of mould. Figure 98 and Figure 99 shows the geometry of the model before and after the application of gravity. The violet line in Figure 99 represents the contour of the sheet at the end of the forming phase.



Figure 98 - Cross section of the mould showing the positioning of the development of sheet metal prior to the application of gravity (left) and at the end of the step of applying the gravity (right)

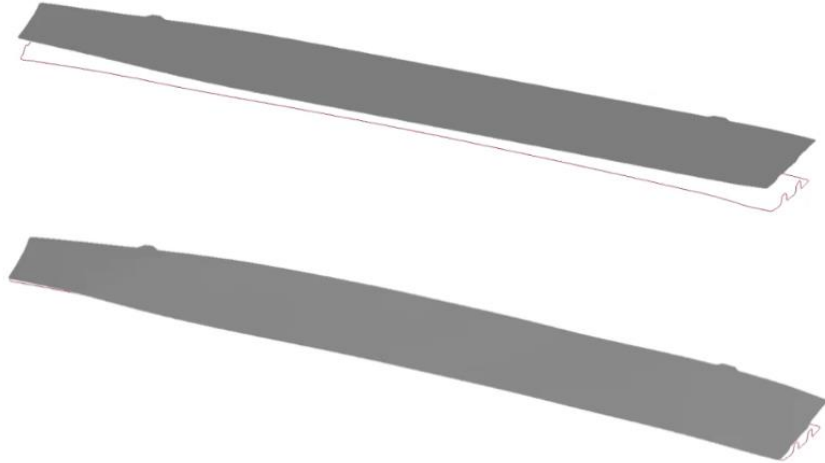


Figure 99 - Placement of the development of the first application of gravity sheet (top) and at the end of the phase of application of gravity (bottom). The contour of the sheet at the end of the forming phase is represented by the violet line

Figure 100 is the screen of the software for implementing the severity in the model with its parameters. In the specific gravity, it is applied for 0.3 seconds, enough time to position the sheet metal development on the fixed mould half and allow stabilization. The simulation is performed with dynamic solver, to take account of inertia and fluctuations. The simulation then continues as described for the case of previous study for the forming step. The contribution of gravity is again taken into account in the calculation of the elastic return.

Table 5 shows the calculation time of the stages of application of gravity, forming and elastic return. It is however to be considered that it is a preliminary calculation to define the initial condition of the sheet. This calculation is performed only once and is not repeated in case you want to evaluate the effect of new moulding parameters.

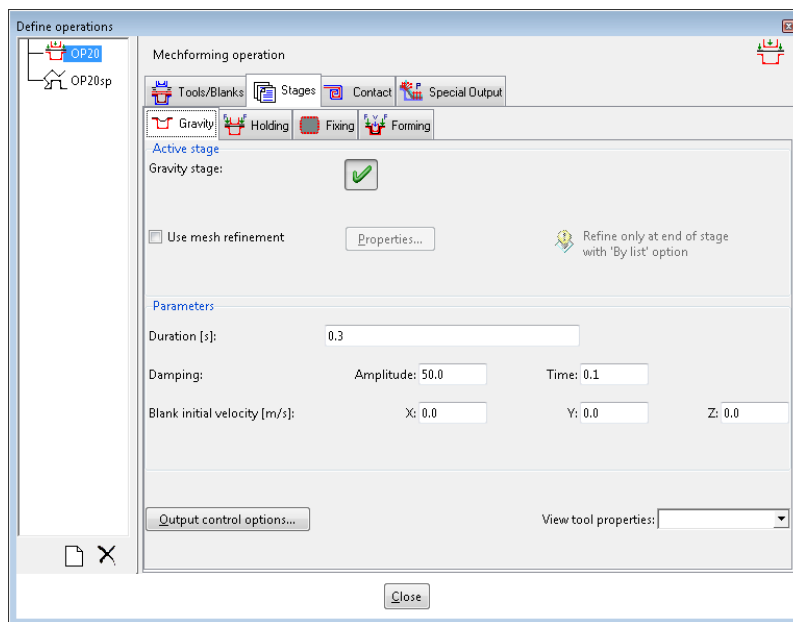


Figure 100 - Screenshot of the software for the implementation of severity in the model

Table 5 - Calculation time for each simulation stage (MA03)

Operation simulated	Solver	Processing time
Severity	Explicit	9h 9 '35 "
Forming	Explicit	34 '25 "
Back bound elastic (hyperstatic)	Implicit	1h 15 '56 "

## 9.3 Results

### 9.3.1 Thickness of the Sheet at the End of Forming and Percentages Thinning

By analyzing, there are large areas in which there is thinning to 5%. This phenomenon is localized in correspondence of projections of the component in an asymmetrical way, focusing in the upper prominence in the view. With reference to Figure 102, are observed some areas (the right end) with more than 4% thickening, index of possible sheet metal wrinkle.

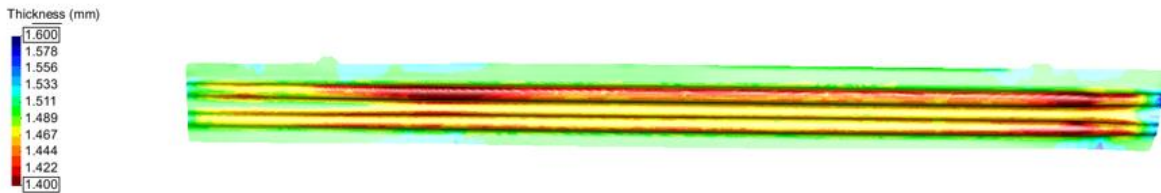


Figure 101 - Thickness of the sheet at the end of forming

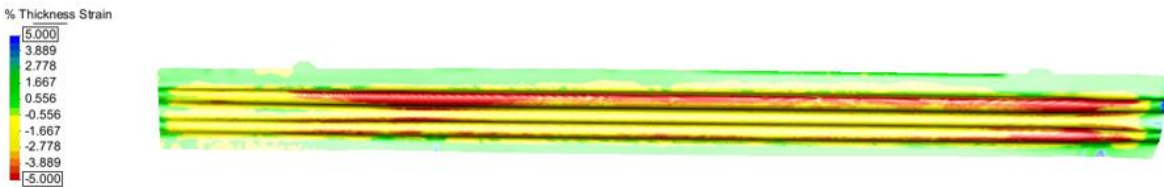


Figure 102 - Percentages thinning

### 9.3.2 Formability Analysis

The analysis of formability based on FLD curve confirms the results highlighted by the analysis of the thicknesses (Figure 103). No evidence of a risk of rupture areas while they detect two areas in which it is highly likely the formation of wrinkles (Figure 104).



Figure 103 - Formability FLD



Figure 104 - Forming of the results

### 9.3.3 Performance of the Moulding Force

It shows the trend of the force on the punch / die during the forming process in the form of graph. The graph is provided as a function of simulated time. The maximum force value is approximately 620 tons. The graph has a first rising section which corresponds to the forming of the central part of the projections in the longitudinal direction, then an almost constant distance (about 200 tons) when it is completed the forming of the side areas, mainly on the left in the view. Finally, the force increases exponentially when it comes to closing.

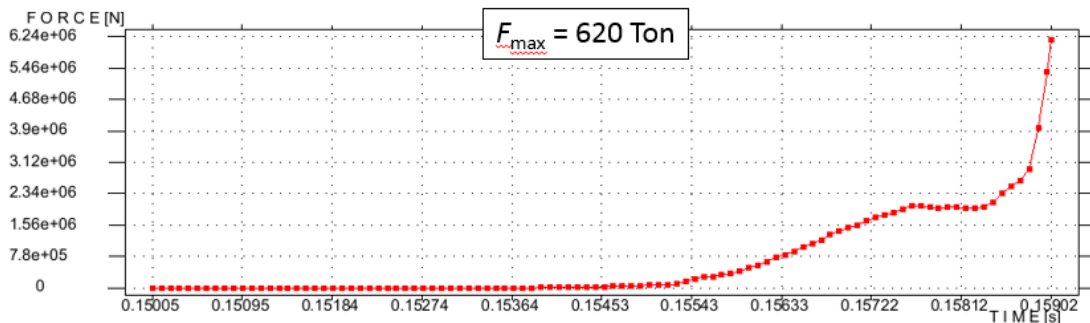


Figure 105 - Force on the punch / die during the process

### 9.3.4 Calculation of Elastic Return

The springback calculation was performed in a hyperstatic constraint configuration, represented in Figure 106. It was not possible to calculate in isostatic mode because of a convergence problem.

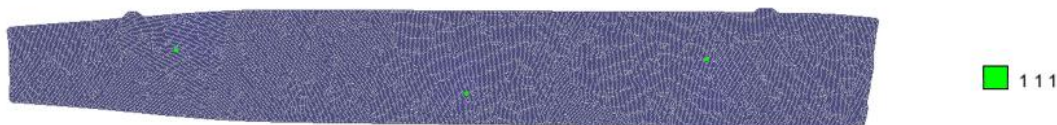


Figure 106 - Position of constraint points (very static configuration)

The comparison with the nominal geometry (average floor extracted from the 3D CAD model of the component) and deformed shape by springback with hyperstatic constraint from real moulds is shown in Figure 107. The Pointwise deviations show a maximum of nearly 24 mm in correspondence of the angle at the bottom on the side where the projections have greater dimension. It is confirmed the effect of warping of the central bar area. In fact, the negative deviations are reduced entities, while the average value of deviations is positive (+7.53 mm, standard deviation of +6.40 mm).

In order to estimate the error of calculation of the downstream of the elastic return, software should compare the deformed shape with the midplane of the real component, not directly available from raw scan data for the problems described above in paragraph 8.1.4. In fact, as already highlighted, the actual geometry of the component presents deviations of a few millimeters with respect to the nominal CAD. For completeness these deviations are replicated in Figure 108. It can be seen how the warping of the workpiece is similar morphologically, but it is difficult to distinguish and quantify the contribution of deviation resulting from the calculation of software other than that due to springback of the moulds.

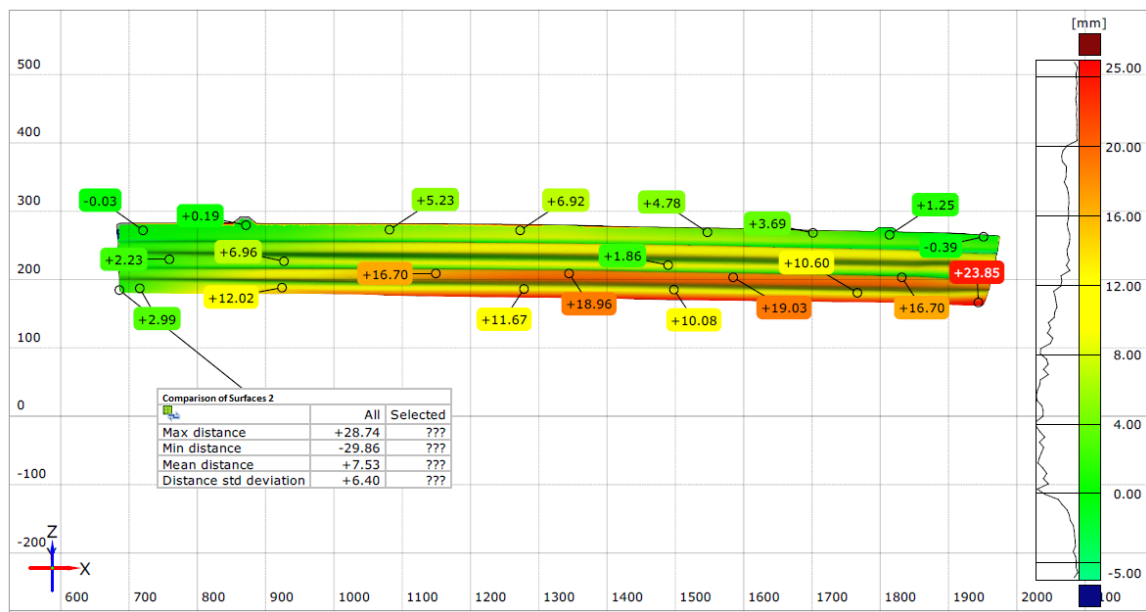


Figure 107 - Comparison between the deformed shape from real moulds with constraint hyperstatic compared to the average plane of the CAD component MA03

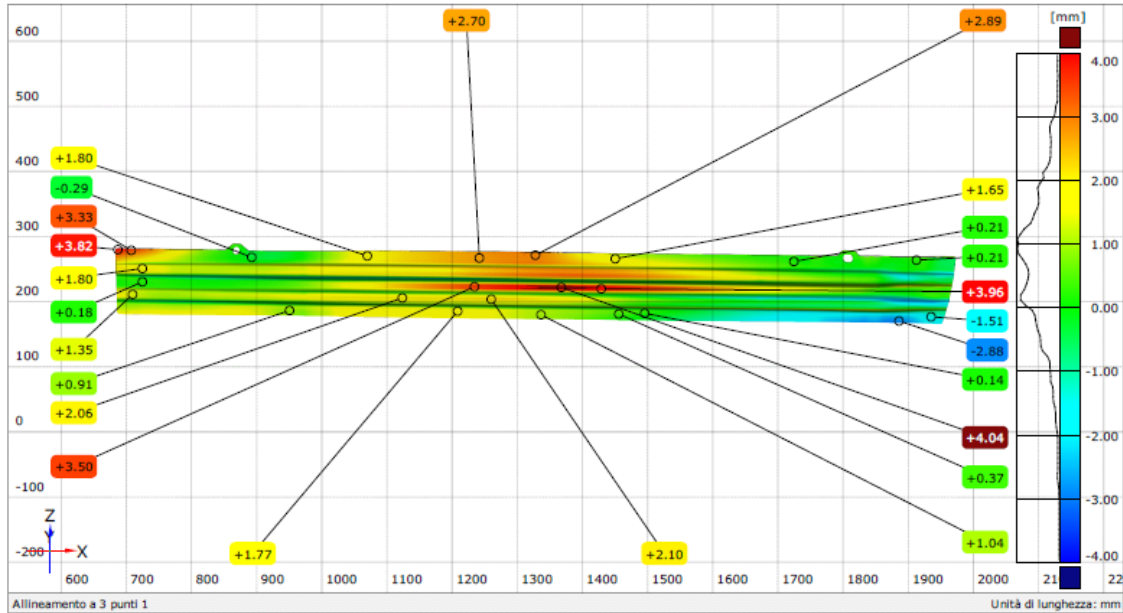


Figure 108 - Pointwise deviations between the actual geometry of the left bar MA03 and the CAD model

## 10 Comparison between BETA and Final Stampack 7.1

In the course of research activity, the final version of Stampack software (release 7.1) got released. The final release, in addition to removing minor bugs, solves the convergence problem that manifested itself in beta release, relating to the calculation of the free spring back.

### 10.1 Comparison of the Results between the Two Releases for the Case of PM13 Study

To verify the correspondence of the results of simulations carried out with beta version, with those obtained using the final version, it is made to re-run the calculation with final version of software for the case of PM13 study, described in paragraph 1 at the beginning of this document.

Below is the comparison of the most significant results in terms of:

- thickness of the sheet at the end of forming (Figure 109)
- thinning rates (Figure 110)
- formability FLD (Figure 111 and Figure 112)
- trend of forming (Figure 113)
- trend of the force as a function of the stroke of the movable half-mould (Figure 114)
- elastic return in isostatic constraint condition (Figure 115)

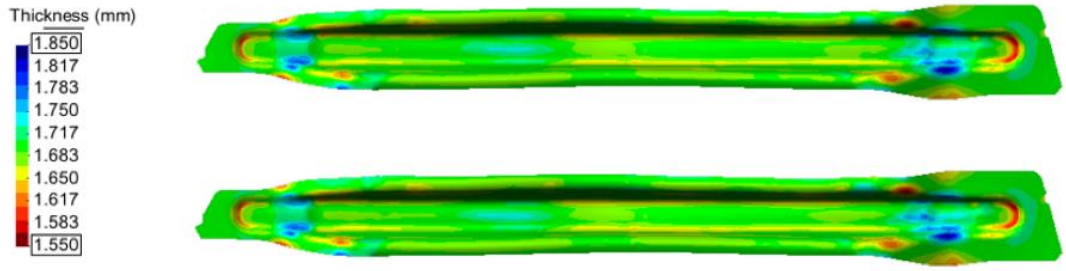


Figure 109 - Plate thickness at the end of forming results obtained Stampack 7.1 final release (top) and beta (bottom)

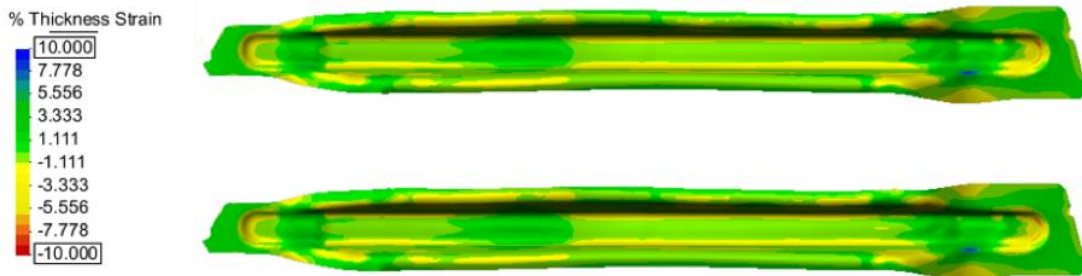


Figure 110 - Thinning percent results obtained Stampack 7.1 final release (top) and beta (bottom)



Figure 111 - Formability FLD result obtained Stampack 7.1 final release (top) and beta (bottom)

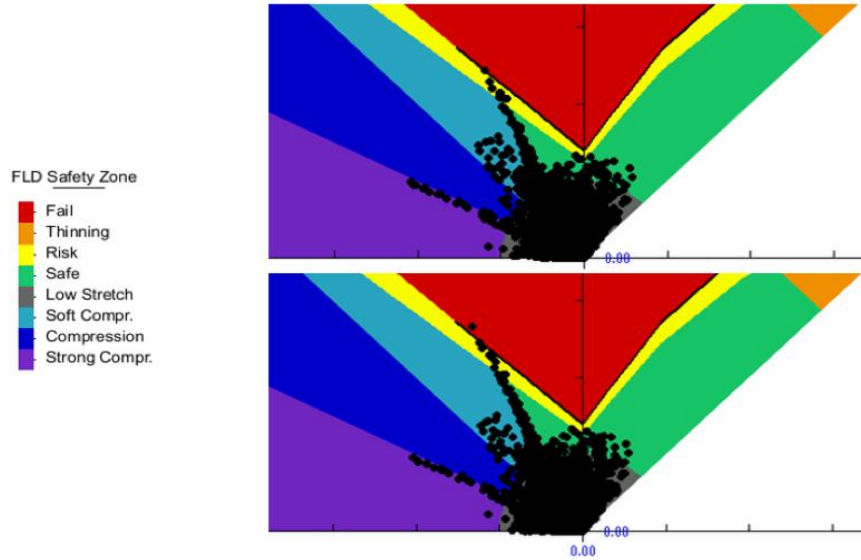


Figure 112 - Formability FLD result obtained Stampack 7.1 final release (top) and beta (bottom)

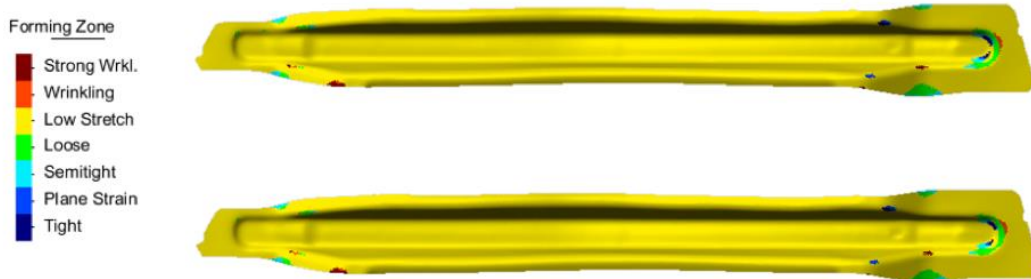


Figure 113 - Performance of forming results obtained Stampack 7.1 final release (top) and beta (bottom)

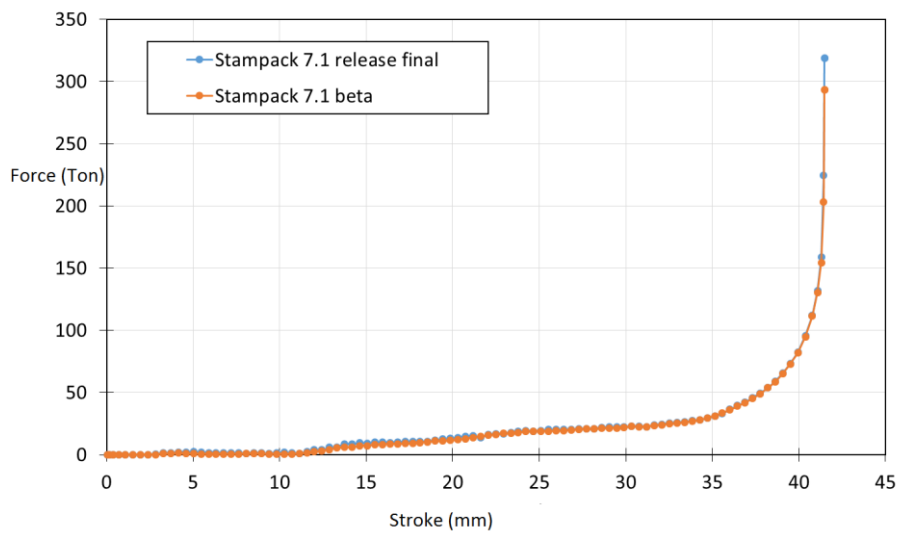


Figure 114 - Force on the punch / die during the process

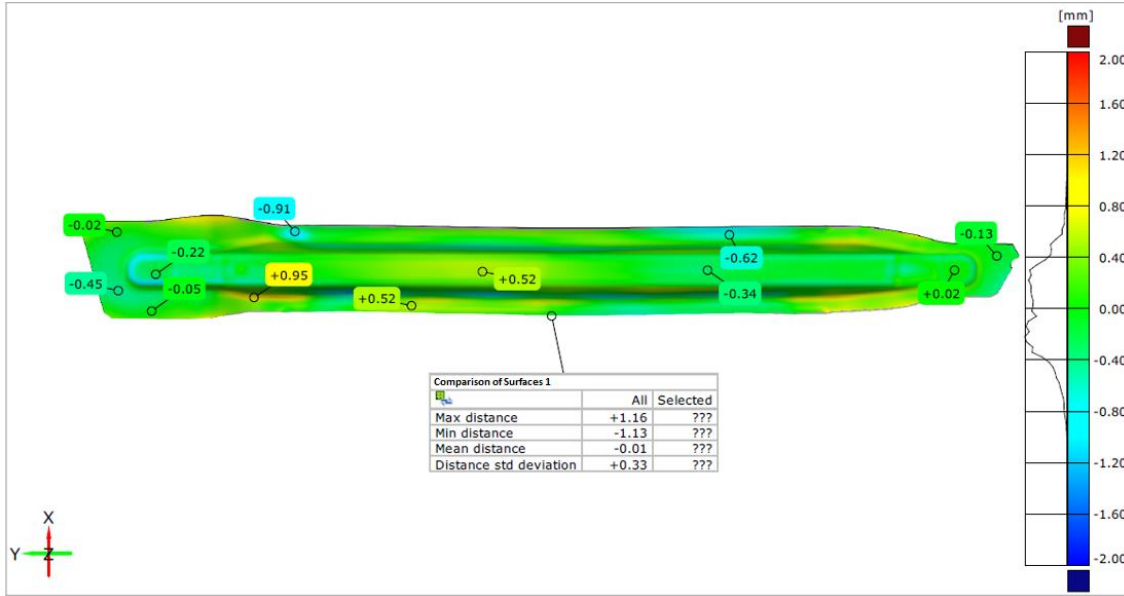


Figure 115 - Comparison between the deformed shape from real moulds obtained with the final release of the software compared to the average plane of the CAD component PM13

The Pointwise deviations in Figure 115 are almost identical to those obtained with beta version of the software and previously reported in Figure 90. Even the statistical distribution of the values of variances are the same for two versions of the software, such as from the Table 6.

Table 6 - Statistical parameters of distribution of variances obtained with the two versions of the software

Parameter	Beta Version	Final Release
Maximum deviation	+1.14 mm	+1.16 mm
Minimum deviation	-1.15 mm	-1.13 mm
Medium deviation	-0.01 mm	-0.01 mm
Standard deviation	+0.32 mm	+0.33 mm

### 10.1.1 Calculation of Free Elastic Return

For calculating the free springback simply disable all constraint points in the previously created template (Figure 116). Then the results of free elastic return calculation, for the two cases of PM13 and MA03 study and the comparison with nominal / actual geometries are presented. For the MA03 case, it considers the effect of gravity even in the calculation of elastic return.

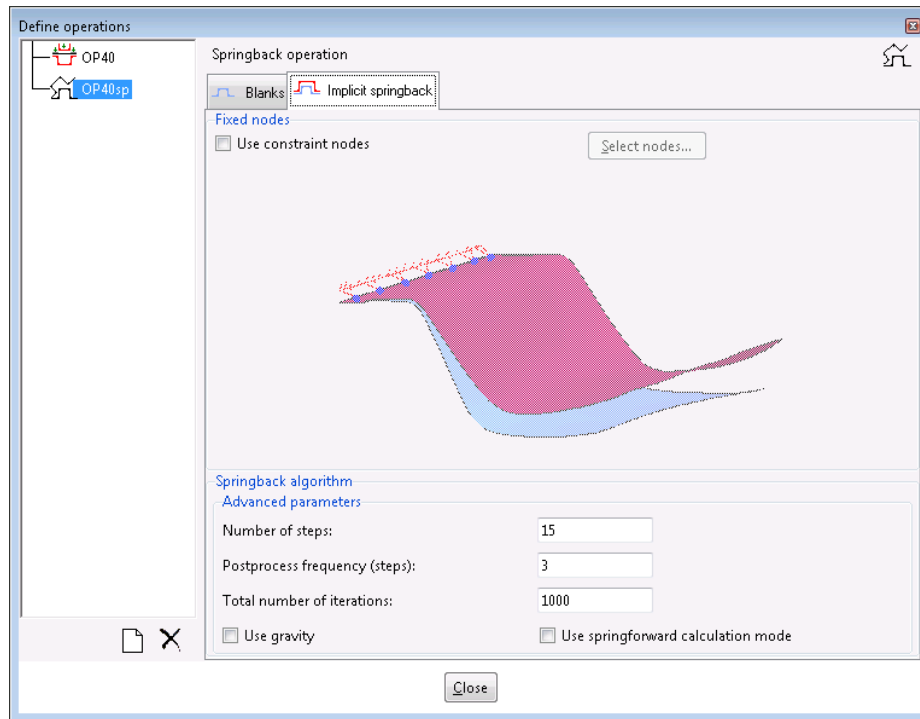


Figure 116 - Screen for setting springback

### 10.1.2 Case Study Of PM13

The calculation time is increased by 50% compared to the same calculation with a constraint condition and is now comparable with the time required for calculation of the forming phase.

Table 7 - Calculation time for each simulation stage (PM13)

Operation simulated	Solver	Processing time
Forming	Explicit	31 '34 "
Back bound elastic (isostatic)	Implicit	22 '56 "
Back Elastic Free	Implicit	33 '26 "

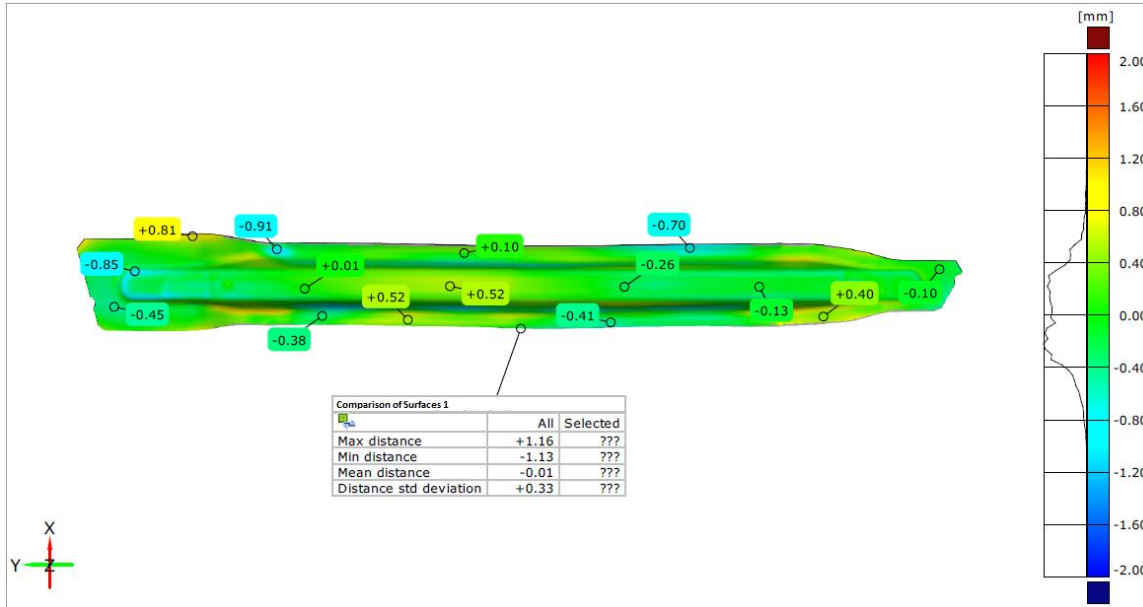


Figure 117 - Comparison between the deformed shape free from real moulds with elastic return compared to the average plane of the CAD component PM13

Figure 117 is in fact identical to those obtained in the case of elastic return bound isostatic (Figure 115). From the point of view of calculation time, it is preferable to operate in constrained mode because it allows a saving of time equal to approximately 30%.

## 10.2 Case Study of MA03

It is noted that the calculation time for the free elastic return is approximately three times longer than the time required in case of constrained elastic return. The timing of the calculation of elastic return bound increases with decreasing the number of constraint points. This increase is an instability in the calculation index, probably related to the geometry of the component itself.

Table 8 - Calculation time for each simulation stage (MA03)

Operation Simulated	Solver	Processing time
Severity	Explicit	9h 9 '35 "
Forming	Explicit	34 '25 "
Back bound elastic (hyperstatic, 6 pts)	Implicit	36 '19 "
Back bound elastic (hyperstatic, 3 pts)	Implicit	1h 15 '56 "
Back Elastic Free	Implicit	3h 8 '22 "

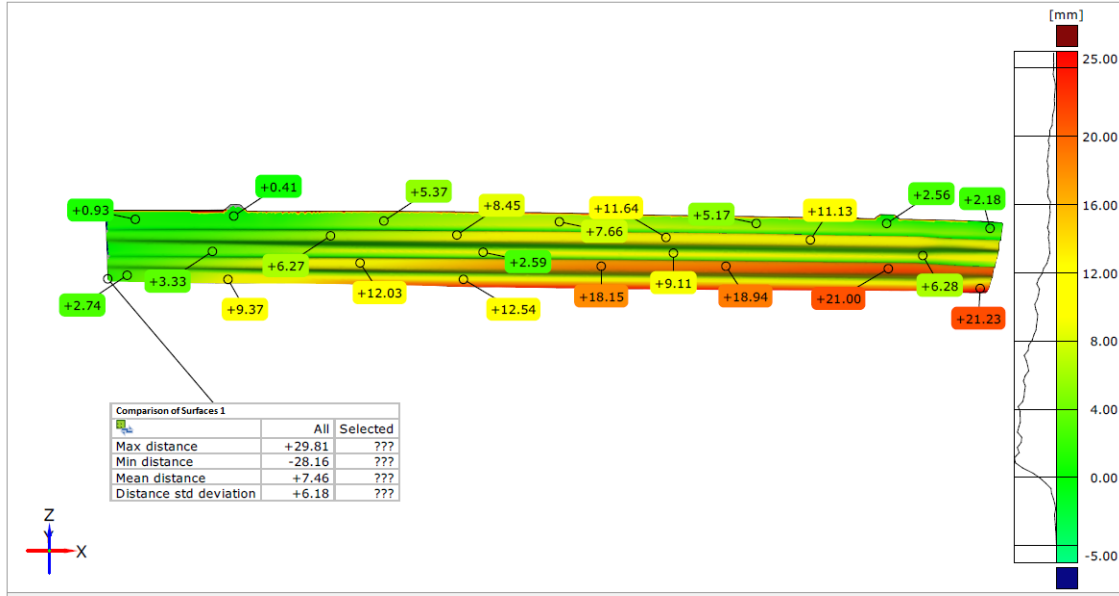


Figure 118 - Comparison between the deformed shape free from real moulds with elastic return compared to the average plane of the CAD component MA03

Figure 118 is similar to those obtained in the case of elastic return bound hyperstatic (Figure 107). From the point of view of calculation time, it is preferable to operate in constrained mode because it allows saving of time without much change in the results.

# Chapter Four

## 11 Introduction to the Comparison of the Simulation Results

The data provided by Autoform correspond to a simulation mode does not correspond to those that can be used within Stampack: the results refer to different levels of the sheet, ie to the lower surface rather than the mid-plane or to the upper surface .

The scan data in STL format, represent tessellated surfaces by means of the actual 3D geometry or actual components of the products. These surfaces are represented with a triangular mesh that connects the scan points and the STL model includes lower surface, upper surface and side surfaces (in the thickness direction). In current versions of the Reverse Engineering software, there is a facility that allows to extract or calculate the average surface starting from triangles of two opposing surfaces. It is advised that the tessellated surfaces do not have a mathematical formulation and surfaces are not ideal because they are the result of the scan of a real object. The calculation for the extraction of the average plane of the STL model is therefore not straightforward as in the CAD model. As regards the possibility to compare the results of forming simulation and calculation of the elastic return by means of different analyzed software, Table 9 shows the comparison matrix

*Table 9 - Matrix of possible comparisons on the basis of the available component models*

Geometry component	CAD Model Nominal Geometry (IGES/STEP files)	3D Scanning Real Geometry (STL file)	Autoform Simulation Elastic return	Stampack Simulation Elastic return
<b>3D Solid</b>	Available	Available	No	Available
<b>Medium Plane</b>	Available	No	No	Available
<b>Top Surface</b>	Available	Available	Available**	No
<b>Lower Surface</b>	Available	Available	Available**	No

**\*\*ORANGE** : It indicates that the availability of the component of the geometry model is subjected to the surface considered in phase of the simulation model definition.

- Stampack Software: The result of the calculation of the deformed shape as a result of the elastic return is provided on the middle plane;
- Autoform Software: The result of the calculation of the deformed shape as a result of the elastic return is provided on the lower or upper surface, depending on the mould design taken as a reference to the fixed or movable mould for defining the simulation model.

For the comparison of the simulation results we proceeded to three types of comparisons, as a function of the geometries available listed above:

- a) Comparison between nominal geometry (CAD) and real geometry resulting from scanning
- b) Comparison between nominal geometry (CAD) and simulation results (Figure 119).

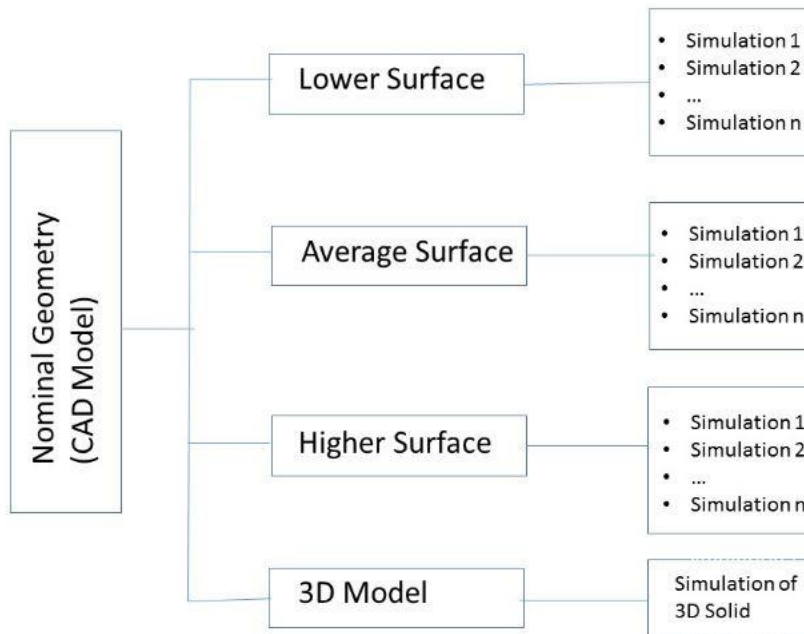


Figure 119 - Comparisons with nominal geometry (CAD) as a reference

- c) Comparison between actual geometry (scanned result) and simulation results (Figure 120).

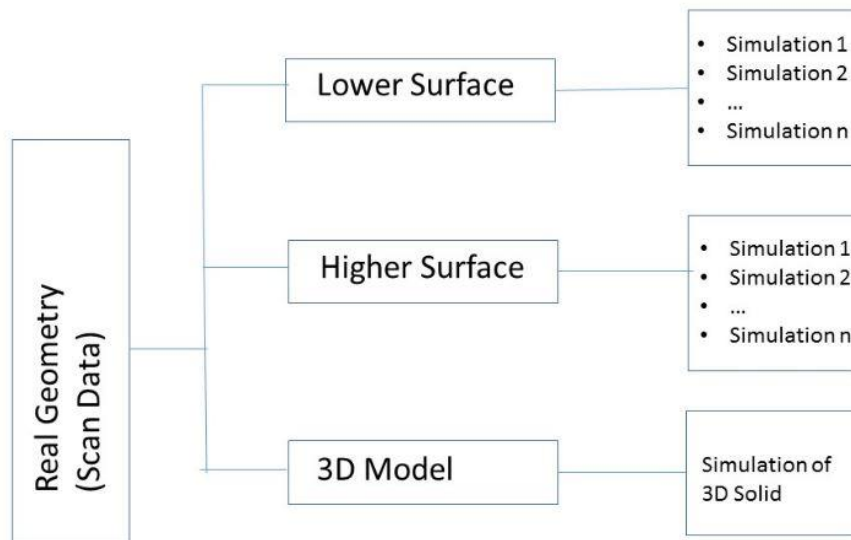


Figure 120 - Comparisons with real geometry (scan data) as a reference

It is important to highlight that, in order to make meaningful comparisons of the results, it is important that the reference is always the same (nominal or actual geometry). The results of the comparisons are summarized in tabular form, in which are shown the following data:

- **Max distance** [mm]: Maximum recorded distance.
- **Min distance** [mm]: Minimum recorded distance.
- **Mean distance** [mm]: Average value of the distance  $\bar{d} = \frac{\sum_{i=1}^n d_i}{n}$ , compared with the number n of points and value of the distance of the i-th point.  $\bar{d} = \frac{\sum_{i=1}^n d_i}{n}$
- **Distance std deviation** [mm]: Value of the standard deviation of distances,  $\sigma_d = \sqrt{\frac{\sum_{i=1}^n (d_i - \bar{d})^2}{n-1}}$
- **Area of valid distance** [mm<sup>2</sup>]: Surface area to consider for the results of comparison in the range of minimum-maximum deviation (typically - / + 5 or 10 or 20 mm).

The chromatic maps related to the data in the tables are attached to the bottom of this report.

## 12 Simulations of PM13 Component

With regard to PM13 anti-intrusion bar, with the version 7.1 beta Stampack software available at Politecnico, forming process was simulated in one step (crash forming) and was calculated the deformation of component as a result of elastic return under the following conditions:

3D Simulation Shell (CAD dies, wireframe blank)

1. Simulation - Configuration isostatic (3 points -321 rule) - PM13\_1b\_sp\_321
2. Simulation - Configuration hyperstatic (3 points -X, Y and Z locked) - PM13\_1b\_sp\_333
3. Simulation - Free configuration - PM13\_1b\_sp\_free.stl
4. Simulation - Configuration with Virtual compensation - PM13\_1b\_sp\_SF.stl

3D Simulation Shell (by scanning dies, wireframe blank)

5. Simulation - Configure hyperstatic - PM13\_2scan\_c\_topbot
6. Simulation – Not locked - PM13\_2scan\_c\_topbot\_f
7. Simulation - Configuration isostatic - PM13\_2scan\_c\_topbot\_i
8. Simulation - Configuration isostatic virtual compensation without parting plane - PM13\_4tools\_da\_sf.stl
9. Simulation – Not locked with virtual compensation with parting plane - PM13\_4tools\_da\_sf\_ff.stl
10. Simulation - Configuration isostatic final release - PM13\_gd\_321\_release.stl

3D Simulation Solid (by scanning Moulds, sheet development with a thickness)

Simulation only - Configuration isostatic - PM13\_3scan\_3D\_sp\_T.stl

The results of the comparisons are summarized in tables and maps of the comparisons are attached to the report respecting the numbering of the section. For example, the maps relating to Section 12.1 of the table data, are provided in Annex 12.1.

## 12.1 Comparison between Nominal Geometry (CAD) and Real Geometry Resulting from Scanning

Table 10 - Comparison results between actual surfaces of the component and nominal CAD surfaces

Reference Nominal CAD Surface	Compared Real Scanned Geometry	Max distance (mm)	Min distance (mm)	Mean fair (mm)	Std deviation (mm)	Area of Valid Distance (mm <sup>2</sup> )
lower	lower	1.90	-1.50	-0.04	0.60	78988
lower	higher	2.67	-2.93	-0.07	0.86	78786
Average	lower	1.75	-1.32	-0.02	0.57	78609
Average	higher	2.21	-2.58	-0.01	0.70	78560
higher	lower	1.70	-1.60	-0.03	0.64	78143
higher	higher	1.96	-2.39	0.06	0.61	78128

Table 11 – Comparison results between actual 3D geometry of the component and 3D CAD geometry

Reference Nominal CAD	Max distance (mm)	Min distance (mm)	Mean distance (mm)	Std deviation (mm)	Area of Valid Distance (mm <sup>2</sup> )
3D Model	2.54	-4.80	0.07	0.62	159210

Comparisons between actual geometry of moulded part and nominal geometry of CAD model confirm that moulding process does not present problems and there is a good correspondence between the two geometries. PM13 component is produced in compliance with specification from tolerances imposed no particular problems or high percentages of non-conforming parts.

The average error on the full 3D model and compared to the individual surfaces is a few hundredths of a millimeter and even the spread of data is reduced and limited to about six tenths of a millimeter. Higher standard deviations are recorded in comparisons between opposing surfaces or mismatched, the type lower than average or higher than upper surface.

## 12.2 Comparison between Nominal Geometry (CAD) and Simulation Results

### 12.2.1 Analysis of 3D Simulations Shell (CAD Dies, Wireframe blank)

In this set of comparisons, the simulations were carried out considering the nominal CAD geometry of the moulds.

Table 12 – Comparison results between the simulation and deformed shape by the upper nominal surface

Reference Nominal CAD Surface - Higher	Max distance (mm)	Min distance (mm)	Mean distance (mm)	Std deviation (mm)	Area of Valid Distance (mm <sup>2</sup> )
Simulation 1	1.15	-2.86	-0.03	0.58	77395
Simulation 2	1.90	-3.01	-0.02	0.67	77417
Simulation 3	2.77	-3.75	-0.18	1.15	77560
Simulation 4	4.18	-8.42	-0.35	1.96	77334

Table 13 – Comparison results between the simulation and deformed shape by the lower nominal surface

Reference Nominal CAD Surface - Lower	Max distance (mm)	Min distance (mm)	Mean distance (mm)	Std deviation (mm)	Area of Valid Distance (mm <sup>2</sup> )
Simulation 1	0.82	-1.84	0.03	00.37	77332
Simulation 2	1.58	-1.99	-0.01	00.49	77393
Simulation 3	2.42	-4.19	-0.29	1.16	77493
Simulation 4	3.67	-8.59	-0.60	2.04	77377

Table 14 - Comparison results between the simulation and deformed shape by the average nominal surface

Reference Nominal CAD Surface - Average	Max distance (mm)	Min distance (mm)	Mean distance (mm)	Std deviation (mm)	Area of Valid Distance (mm <sup>2</sup> )
Simulation 1	0.97	-2.36	-0.03	0.45	77549
Simulation 2	1.72	-2.5	-0.02	0.55	77628
Simulation 3	2.57	-3.91	-0.15	1.13	77719
Simulation 4	3.88	-8.54	-0.31	1.96	77543

Comparison between the results of different simulations carried out by the Stampack software and reference surfaces of nominal CAD model of the component show that there is still a good correspondence between the compared geometries. The simulations that provide the best results are the 1 and the 2, ie those performed with the calculation of the elastic return with isostatic constraint and hyperstatic respectively. For these simulations the dispersion of the results is still in line with the values of the comparisons between the actual geometry of the component and the nominal (section 12.1 above). The area in which the distance falls within the minimum-maximum range in Table 14 is slightly greater than that obtained in comparison with the other surfaces (Tables 12 and 13). This result is justified by the fact that the Stampack software provides the calculation result of the deformed shape as a result of elastic return on the average plane.

## 12.2.2 Analysis of 3D Simulations Shell (By Scanning Dies, Wireframe blank)

Table 15 - Comparison results between the simulation and deformed shape by the upper nominal surface

Reference Nominal CAD Surface - Higher	Max distance (mm)	Min distance (mm)	Mean distance (mm)	Std deviation (mm)	Area of Valid Distance (mm <sup>2</sup> )
Simulation 5	1.99	-2.17	0.00	0.55	78029
Simulation 6	2.56	-3.88	-0.18	1.12	77544
Simulation 7	1.17	-1.66	0.00	0.42	78037
Simulation 8	3.88	-5.00	-0.30	1.64	76316
Simulation 9	2.24	-3.26	-0.18	1.06	77771
Simulation 10	1.23	-1.64	-0.02	0.42	78031

Table 16 - Comparison results between the simulation and deformed shape by the lower nominal surface

Reference Nominal CAD Surface - Lower	Max distance (mm)	Min distance (mm)	Mean distance (mm)	Std deviation (mm)	Area of Valid Distance (mm <sup>2</sup> )
Simulation 5	1.78	-1.47	-0.02	0.54	78260
Simulation 6	2.28	-4.27	-0.24	1.20	77538
Simulation 7	1.42	-1.10	-0.01	0.45	78363
Simulation 8	3.54	-6.66	-0.43	1.66	76646
Simulation 9	1.93	-3.87	-0.32	1.05	78057
Simulation 10	1.36	-1.14	-0.02	0.44	78299

Table 17 – Comparison results between the simulation and deformed shape by the average nominal surface

Reference Nominal CAD Surface - Average	Max distance (mm)	Min distance (mm)	Mean distance (mm)	Std deviation (mm)	Area of Valid Distance (mm <sup>2</sup> )
Simulation 5	1.90	-1.67	0.01	0.51	78392
Simulation 6	2.38	-4.07	-0.14	1:14	77718
Simulation 7	1.20	-1.15	0.00	0.38	78430
Simulation 8	3.72	-6.43	-0.25	1.64	76675
Simulation 9	2.12	-3.47	-0.14	1:01	78169
Simulation 10	1.16	-1.13	-0.01	0.39	78397

In this set of comparisons, the simulations were carried out considering the actual geometry of the scan from the moulds.

The simulations that provide the best results are 7 and 10, carried out using isostatic configuration. As already mentioned, the area whose distance falls within the minimum-maximum range in Table 17 is slightly greater than that obtained in comparison with the other surfaces (Tables 15 and 16).

This result is justified by the fact that the Stampack software provides the calculation result of the deformed shape as a result of elastic return on the average plane.

### 12.2.3 Analysis of 3D Simulations Solid (By Scanning Moulds, Sheet Development With Thickness)

Table 18 – Comparison results between the deformed shape 3D simulation and 3D CAD geometry

Reference Nominal CAD	Max distance (mm)	Min distance (mm)	Mean distance (mm)	Std deviation (mm)	Area of Valid Distance (mm <sup>2</sup> )
3D Model	3.80	-3.46	00.03	1.18	157015

The result of the calculation of the deformed shape as a result of the elastic return with a 3D simulation model, provides very similar results to those of Table 11 and referring to the comparison between the actual 3D Geometry of PM13 component and the reference nominal CAD.

The range of variation for the result of the simulation are slightly wider and the area in which the distance falls within the minimum-maximum range is slightly lower. The average deviation is still the order of a few hundredths of a millimeter.

## 12.3 Comparison Between Actual Geometry (Scanned Result) and Simulation Results

This section presents a series of comparisons between simulations and real geometry that may be considered as cross-analysis between those in Section 12.1 (comparing actual geometry and CAD) and in Section 12.2 (Simulations and CAD).

### 12.3.1 Analysis of 3D Simulations Shell (CAD Dies, Wireframe blank)

Table 19 – Comparison results between the deformed shape 3D simulation and upper surface of actual 3D scanned geometry

Reference 3D scanning Surface - Higher	Max distance (mm)	Min distance (mm)	Mean distance (mm)	Std deviation (mm)	Area of Valid Distance (mm <sup>2</sup> )
Simulation 1	2.19	-4.99	-0.45	1.09	75648
Simulation 2	2.58	-5.00	-0.44	1.15	75634
Simulation 3	3.23	-5.00	-0.19	1.26	75672
Simulation 4	4.68	-10.00	-0.04	1.96	75885

Table 20 – Comparison results between the deformed shape 3D simulation and lower surface of actual 3D scanned geometry

Reference 3D scanning Surface - Lower	Max distance (mm)	Min distance (mm)	Mean distance (mm)	Std deviation (mm)	Area of Valid Distance (mm <sup>2</sup> )
Simulation 1	4.93	-3.50	-0.02	0.76	75587
Simulation 2	5.00	-4.33	0.00	0.86	75546
Simulation 3	4.91	-4.99	0.27	1.16	75631

Simulation 4	10.00	-9.03	0.41	1.83	75587
--------------	-------	-------	------	------	-------

In this set of comparisons, simulations were carried out considering the nominal CAD geometry of the moulds. The reference for comparison is the actual geometry of the component obtained from the scan. Therefore, only the upper and lower surfaces are available, but not the middle.

The simulations that provide the best results are 1 and 2, ie those performed with the calculation of the elastic return with isostatic constraint and hyperstatic respectively. For these simulations, the numerical values and dispersion of the results are slightly different depending on whether you take the upper or lower surface as a reference. The dispersion of the results in comparison with the lower reference surface is less than that of the corresponding comparison with the upper surface. However, Stampack software provides the result of the calculation of deformed shape of elastic return on average plane, so none of the previous comparisons would be correct.

### 12.3.2 Analysis of 3D Simulations Shell (By Scanning Dies, Wireframe blank) - Release Final

Table 21 – Comparison results between the deformed shape 3D simulation and upper surface of actual 3D scanned geometry

Reference 3D scanning Surface - Higher	Max distance (mm)	Min distance (mm)	Mean distance (mm)	Std deviation (mm)	Area of Valid Distance (mm2)
Simulation 5	3.08	-5.00	-0.23	0.74	76467
Simulation 6	3.00	-4.98	-0.05	1.09	75719
Simulation 7	1.81	-5.00	-0.21	0.57	76589
Simulation 8	4.37	-4.99	-0.16	1.59	75000
Simulation 9	3.83	-5.00	-0.20	1.10	76361
Simulation 10	2.43	-5.00	-0.22	0.59	76562

Table 22 – Comparison results between the deformed shape 3D simulation and lower surface of actual 3D scanned geometry

Reference 3D scanning Surface - Lower	Max distance (mm)	Min distance (mm)	Mean distance (mm)	Std deviation (mm)	Area of Valid Distance (mm2)
Simulation 5	4.90	-4.68	0.03	0.62	76438
Simulation 6	4.10	-4.99	0.25	1.13	75661
Simulation 7	4.99	-4.93	0.01	0.39	76686
Simulation 8	9.99	-9.91	0.35	1.62	75047
Simulation 9	4.87	-4.90	0.21	0.96	76421
Simulation 10	4.94	-4.99	0.01	0.42	76606

In this set of comparisons, the simulations were carried out considering the actual geometry of the scan from the moulds.

Comparisons between the results of various simulations performed using the Stampack software and reference surfaces of the actual geometry of the component are in line with the results obtained

for comparisons of the previous section 12.2.2. This confirms that the simulations that provide the best results are the 7 and 10.

It is therefore of the same simulation, carried out with same parameters and same constraints. From the corresponding rows of Tables 15, 16 and 17 is then confirmed that the same simulation conditions, the version of the software does not affect the calculation of the deformed shape. As already pointed out above, the dispersion of the results in comparison with the bottom reference surface is reduced compared to that of the corresponding comparison with the upper surface.

### 12.3.3 Analysis of 3D Simulations Solid (3D Scanned moulds, 3D blank with Thickness)

Table 23 – Comparison results between the deformed shape 3D simulation and actual scanned 3D geometry

Reference 3D scanning	Max distance (mm)	Min distance (mm)	Mean distance (mm)	Std deviation (mm)	Area of Valid Distance (mm <sup>2</sup> )
3D Model	18.96	-17.76	-0.05	1.34	151280

The result of the calculation of the deformed shape as a result of the elastic return with a 3D simulation model, provides worse results to those of the preceding Tables 11 and 18.

The range of variation for the result of the simulation, in this case are wider and the area in which the distance falls within the minimum-maximum range is less than the previous. The average deviation is still the order of a few hundredths of a millimeter.

## 13 Simulations of MA03 Component

With regard to the MA03 anti-intrusion bar, the version 7.1 beta Stampack software available at the Politecnico was used to simulate the forming process in a single pass (crash forming) and calculated the deformation of component as a result of elastic return under following conditions:

### 3D Simulation Shell (by scanning dies, wireframe blank)

1. Simulation - Configuration hyperstatic (3 points -bloccati X, Y and Z) with gravity - MA03\_2scan\_svi\_CAD\_bg
2. Simulation - Configuration isostatic (3 points -321 rule) without severity - MA03\_2scan\_svi\_CAD\_bm
3. Simulation - Configuration isostatic (3 points -321 rule) with gravity - MA03\_2scan\_svi\_CAD\_cg
4. Simulation - Configuration hyperstatic (3 -X, Y and Z locked) without gravity - MA03\_2scan\_svi\_CAD\_cm
5. Simulation - Configuration hyperstatic (3 points -bloccati X, Y and Z) without gravity in the calculation of the elastic return - MA03\_2scan\_svi\_CAD\_dg

6. Simulation - Configuration hyperstatic with gravity with guide columns - MA03\_2scan\_svi\_CAD\_gg

7. Simulation - Configuration hyperstatic with gravity without guide columns - MA03\_2scan\_svi\_CAD\_gm

Shell 3D Simulation (CAD dies, wireframe blank)

8. Simulation - hyperstatic configuration without gravity - MA03\_1cad\_svi\_CAD

9. Simulation - hyperstatic configuration with gravity - MA03\_1cad\_svi\_CAD\_g

3D Simulation Shell (Moulds from scanning, mathematized thread development) - Final Release

10. Simulation – hyperstatic configuration of the test gauge gravity final releases - MA03\_gd\_gr\_calibro

11. Simulation - Not locked gravity final release - MA03\_gd\_gr\_free

Simulation Autoform (CAD dies, wireframe blank)

Simulation software carried out by means of Autoform.

The results of the comparisons are summarized in tables and maps of the comparisons are attached to the report respecting the numbering of the section. For example, the maps relating to Section 13.1 of the table data, are provided in Annex 13.1.

### 13.1 Comparison Between Nominal Geometry (CAD) and Real Geometry (Scan Data)

Table 24 – Comparison results between actual surfaces of the component and nominal CAD surfaces

Reference Nominal CAD Surface	Compared 3D scanning surface	Max distance (mm)	Min distance (mm)	Mean distance (mm)	Std deviation (mm)	Area of Valid Distance (mm2)
lower	lower	19.38	-19.88	0.36	1.30	207835
lower	higher	17.53	-19.78	2.02	1.21	207623
Average	lower	18.72	-19.86	-0.33	1.23	208013
Average	higher	19.65	-19.65	1.30	1.17	207879
higher	lower	18.08	-19.82	-1.10	1.24	207782
higher	higher	16.85	-19.88	0.52	1.20	207719

Comparisons between actual geometry of component and nominal geometry of CAD model confirm that moulding process allows to produce the component MA03 with larger deviations than those observed for other component analyzed (PM13). Geometry of MA03 component is more complex and it is known that the tuning process of the moulds was longer and more costly.

The average error is correctly lowest for the comparison between corresponding surfaces: lower / upper and lower / higher. In cross comparisons between the other surfaces, the lower the real

surface is also very similar to the average plane of the 3D CAD model. The dispersion of the results for the various comparisons is approximately constant, or varies in a very narrow range from 1.17 mm to 1.30 mm. In this case the component has a thickness of 1.5 mm and then compared to PM13 component (thickness 1.7 mm), the difference between the nominal geometry of the three upper surfaces and lower average is slightly reduced. In addition, the larger process tolerances, are reflected in a greater dispersion of the deviations between the real component and the nominal CAD geometry.

## 13.2 Comparison Between Nominal Geometry (CAD) and Simulation Results

### 13.2.1 Analysis of 3D Simulations Shell (By Scanning Dies, Wireframe blank)

Table 25 - Comparison results between the simulation and deformed shape by the upper nominal surface

Reference Nominal CAD Surface - Higher	Max distance (mm)	Min distance (mm)	Mean distance (mm)	Std deviation (mm)	Area of Valid Distance (mm <sup>2</sup> )
Simulation 1	14.94	-19.99	0.18	3.93	205047
Simulation 2	19.83	-19.91	-0.89	4.92	201772
Simulation 3	12.70	-19.99	-0.07	4.67	202724
Simulation 4	8.61	-19.97	-0.19	3.09	207543
Simulation 5	11.82	-19.85	-0.04	3.37	207224
Simulation 6	19.73	-20.00	-1.39	5.50	203880
Simulation 7	19.95	-20.00	-0.76	4.51	205442

Table 26 - Comparison results between the simulation and deformed shape by the lower nominal surface

Reference Nominal CAD Surface - Lower	Max distance (mm)	Min distance (mm)	Mean distance (mm)	Std deviation (mm)	Area of Valid Distance (mm <sup>2</sup> )
Simulation 1	15.48	-20.00	0.22	4.03	205990
Simulation 2	17.08	-19.97	-0.76	4.72	202270
Simulation 3	13.02	-20.00	0.46	5.01	204368
Simulation 4	8.38	-19.20	0.19	3.27	207113
Simulation 5	8.97	-19.23	0.40	3.56	207236
Simulation 6	18.98	-20.00	-1.41	4.56	204144
Simulation 7	19.05	-20.00	-1.43	4.08	204060

Table 27 - Comparison results between the simulation and deformed shape by the average nominal surface

Reference Nominal CAD Surface - Average	Max distance (mm)	Min distance (mm)	Mean distance (mm)	Std deviation (mm)	Area of Valid Distance (mm <sup>2</sup> )
Simulation 1	8.57	19.97	0.05	3.64	207232

Simulation 2	19.52	-20.00	-0.86	4.87	202323
Simulation 3	12.88	-20.00	0.18	4.59	203978
Simulation 4	7.82	-19.99	-0.04	3.25	207072
Simulation 5	15.36	-19.92	0.16	3.22	207533
Simulation 6	19.18	-20.00	-1.16	4.74	204647
Simulation 7	19.97	-20.00	-0.84	6.42	202853

In this set of comparisons, the simulations were carried out considering the actual geometry of the scan from the moulds.

The average value of the deviation varies from a few tenths of a millimeter up to one millimeter, while the dispersion of the results is wider than that of PM13 and component ranges in the range between 3 and 6 mm. The best match between the compared geometries, whatever the CAD surface used for comparison, is always obtained by the simulation 4, one performed in hyperstatic configuration neglecting the effect of gravity in the process of forming.

The simulation 5 which neglects the effect of gravity even in the calculation of the elastic return, provides very similar results to the previous ones. It can therefore be concluded that the effect of the gravity added in the calculation of the elastic return of the PM13 component has no influence on the simulation results.

### 13.2.2 Analysis of 3D Simulations Shell (CAD Dies, Wireframe blank)

*Table 28 - Comparison results between the simulation and deformed shape by the upper nominal surface*

Reference Nominal CAD Surface - Higher	Max distance (mm)	Min distance (mm)	Mean distance (mm)	Std deviation (mm)	Area of Valid Distance (mm <sup>2</sup> )
Simulation 8	18.96	-19.39	0.12	2.66	207433
Simulation 9	19.93	-19.72	-0.10	1.65	207281

*Table 29 - Comparison results between the simulation and deformed shape by the lower nominal surface*

Reference Nominal CAD Surface - Lower	Max distance (mm)	Min distance (mm)	Mean distance (mm)	Std deviation (mm)	Area of Valid Distance (mm <sup>2</sup> )
Simulation 8	19.99	-19.86	1.17	3.96	204497
Simulation 9	19.79	-19.84	00.13	1.94	206946

*Table 30 - Comparison results between the simulation and deformed shape by the average nominal surface*

Reference Nominal CAD Surface - Average	Max distance (mm)	Min distance (mm)	Mean distance (mm)	Std deviation (mm)	Area of Valid Distance (mm <sup>2</sup> )
Simulation 8	10.79	-19.28	0.16	2.56	207280
Simulation 9	19.67	-19.91	-0.08	2.21	208411

In this set of comparisons, the simulations were carried out considering the nominal CAD geometry of the moulds.

Comparison between the result of different simulations carried out by Stampack software and the reference surfaces of nominal CAD model of the component show that, compared to the actual geometry of the moulds (section 13.2.1), the deviations have a reduced dispersion. The simulation that provides the closest results to the nominal geometry of the component is simulation 9, regardless of the reference surface considered. This simulation is performed in hyperstatic configuration considering the effect of gravity in the process of forming.

### 13.2.3 Analysis of 3D Simulations Shell (Moulds From Scanning, Mathematized Thread Development) - Final Release

Table 31 - Comparison results between the simulation and deformed shape by the upper nominal surface

Reference Nominal CAD Surface - Higher	Max distance (mm)	Min distance (mm)	Mean distance (mm)	Std deviation (mm)	Area of Valid Distance (mm <sup>2</sup> )
Simulation 10	19.98	-19.98	-1.05	6.22	198089
Simulation 11	9.32	-20.00	-0.41	4.65	205942

Table 32 - Comparison results between the simulation and deformed shape by the lower nominal surface

Reference Nominal CAD Surface - Lower	Max distance (Mm)	Min distance (Mm)	Mean distance (Mm)	Std deviation (Mm)	Area of Valid Distance (Mm <sup>2</sup> )
Simulation 10	20.00	-20.00	-1.32	6.50	197146
Simulation 11	19.19	-19.99	-0.55	5.37	204878

Table 33 - Comparison results between the simulation and deformed shape by the average nominal surface

Reference Nominal CAD Surface - Average	Max distance (mm)	Min distance (mm)	Mean distance (mm)	Std deviation (mm)	Area of Valid Distance (mm <sup>2</sup> )
Simulation 10	20.00	-20.00	-1.19	6.96	194956
Simulation 11	7.79	-19.99	-0.12	4.74	205542

In this set of comparisons, the simulations were carried out considering the actual geometry of the scan from the moulds.

Having previously verified for PM13 component that there were no differences in the calculation results of the two versions Beta Release and Final Release Stampack software, the final release was used to perform two additional simulations. Simulation 10 considers the calculation of the elastic return into free configuration, while simulation 11 considers a hyperstatic configuration with the constraints localized in the same areas in which the real part is bound on the gauge control (Figure 121).

Of the two simulations, the second configuration provides a geometry that is greater correspondence with the nominal CAD geometry of the component.

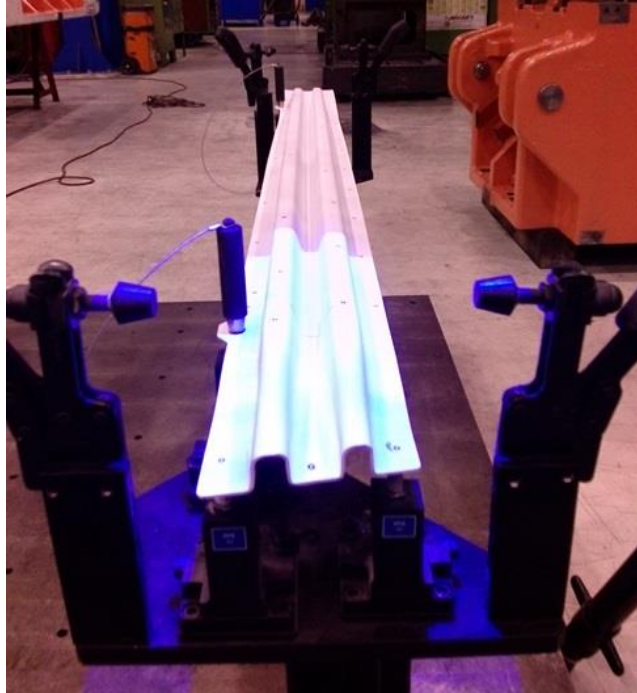


Figure 121 - MA03 component scan reported on the test gauge

### 13.2.4 Simulation Autoform (CAD Dies, Wireframe blank)

Table 34 – Comparison results between deformed shape of Autoform Simulation and nominal CAD surfaces

Reference Nominal CAD Surface	Compared Surface Autoform	Max distance (mm)	Min distance (mm)	Mean distance (mm)	Std deviation (mm)	Area of Valid Distance (mm <sup>2</sup> )
lower	lower	15.66	-15.48	0.94	3.30	205000
Average	lower	13.76	-7.02	0.01	3.06	206681
higher	lower	18.25	-10.41	0.40	4.01	202259

Here, simulations considering the CAD nominal geometry of the moulds and simulations have been carried out using the Autoform software.

The deviations which are obtained from the comparison between the deformed shape of Autoform and surfaces of the nominal CAD model MA03 component are similar to those obtained for the simulations with the Stampack software. In particular, results should be compared with those of the simulations 8 and 9 of section 13.2.2. The statistical values of distribution of deviations are similar for the two software both in terms of average value of dispersion of the results and also with regard to the area in which the distance falls within the minimum-maximum range.

Apparently the calculation of the deformed shape of Autoform, which considers the lower surface of the sheet, provides a geometry that is greater than the nominal CAD correspondence with the

middle plane. The average deviation is only 0.01mm, the standard deviation is lower and the area in which the distance falls within the minimum-maximum range is more extensive with respect to comparisons with the lower or upper surface.

### 13.3 Comparison Between Actual Geometry (Scanned Data) and Simulation Results

This section presents a series of comparisons that may be considered as cross-analysis between those in Section 13.1 and those in Section 13.2, because after comparing actual geometry and CAD (section 13.1) and simulations and CAD (section 13.2), we are comparing simulations and actual geometry.

#### 13.3.1 Analysis of 3D Simulations Shell (By Scanning Dies, Wireframe blank)

Table 35 – Comparison results between deformed shape 3D simulation and the upper surface of actual 3D scanned geometry

Reference 3D scanning Surface - Higher	Max distance (mm)	Min distance (mm)	Mean distance (mm)	Std deviation (mm)	Area of Valid Distance (mm <sup>2</sup> )
Simulation 1	17.54	-20.00	-0.95	4.15	205059
Simulation 2	19.90	-20.00	-1.05	5.29	200812
Simulation 3	18.99	-20.00	-0.46	5.02	202563
Simulation 4	18.88	-20.00	-1.07	4.01	205900
Simulation 5	15.18	-20.00	-0.23	4.45	205040
Simulation 6	19.91	-20.00	-1.45	4.80	203070
Simulation 7	19.92	-20.00	-1.17	4.61	204372

Table 36 – Comparison results between deformed shape 3D simulation and the lower surface of actual 3D scanned geometry

Reference 3D scanning Surface - Lower	Max distance (mm)	Min distance (mm)	Mean distance (mm)	Std deviation (mm)	Area of Valid Distance (mm <sup>2</sup> )
Simulation 1	19.77	-19.99	0.43	3.48	204809
Simulation 2	19.85	-19.86	-0.12	4.63	200983
Simulation 3	19.91	-20.00	00.39	4.23	202937
Simulation 4	19.69	-19.67	-0.06	2.94	205216
Simulation 5	19.70	-19.60	0.35	3.11	204860
Simulation 6	19.96	-20.00	-0.70	4.37	202208
Simulation 7	19.99	-19.99	-0.54	3.58	202820

In this set of comparisons, the simulations were carried out considering the actual geometry of the scan from the moulds. The reference for comparison is the actual geometry of the component obtained from the scan. Therefore, only the upper and lower surfaces are available.

It is confirmed as mentioned in section 13.2.1 that the simulations that provide best results are 4 and 5, namely those performed with the calculation of elastic return in hyperstatic configuration

with and without the effect of gravity. For these simulations, dispersion of results is lower compared to other simulations and is best if we take as reference the lower surface of the component. However, Stampack software provides result of the calculation of deformed elastic return on average plane, so none of the previous comparisons would be correct.

### 13.3.2 Analysis of 3D Simulations Shell (CAD Dies, Wireframe blank)

Table 37 – Comparison results between deformed shape 3D simulation and the upper surface of actual 3D scanned geometry

Reference 3D scanning Surface - Higher	Max distance (mm)	Min distance (mm)	Mean distance (mm)	Std deviation (mm)	Area of Valid Distance (mm <sup>2</sup> )
Simulation 8	20.00	-20.00	-1.00	4.25	202406
Simulation 9	19.99	-20.00	-0.91	4.19	202516

Table 38 - Comparison results between deformed shape 3D simulation and the lower surface of actual 3D scanned geometry

Reference 3D scanning Surface - Lower	Max distance (mm)	Min distance (mm)	Mean distance (mm)	Std deviation (mm)	Area of Valid Distance (mm <sup>2</sup> )
Simulation 8	19.92	-19.89	-0.20	3.21	202233
Simulation 9	19.55	-19.85	-0.11	2.13	203391

In this set of comparisons, simulations were carried out considering the nominal CAD geometry.

Comparisons between results of various simulations performed using Stampack software and reference surfaces of actual geometry of the component does not deviate much from the results of the previous section 13.2.2. Of the two, simulation that provides the best results is the simulation 9, which considers a hyperstatic configuration and effect of gravity in the process of forming.

### 13.3.3 Analysis of 3D Simulations Shell (Moulds From Scanning, Mathematized Thread Development) - Final Release

Table 39-Comparison results between deformed shape 3D simulation and from the upper surface of actual 3D scanned geometry

Reference 3D scanning Surface - Higher	Max distance (mm)	Min distance (mm)	Mean distance (mm)	Std deviation (mm)	Area of Valid Distance (mm <sup>2</sup> )
Simulation 10	19.99	-20.00	-0.71	5.27	200810
Simulation 11	19.85	-20.00	-0.39	4.40	205164

Table 40-Comparison results between deformed shape 3D simulation and from the lower surface of actual 3D scanned geometry

Reference 3D scanning Surface - Lower	Max distance (mm)	Min distance (mm)	Mean distance (mm)	Std deviation (mm)	Area of Valid Distance (mm <sup>2</sup> )
Simulation 10	19.93	-20.00	0.45	5.17	199715
Simulation 11	19.96	-19.96	0.61	3.55	203940

In this set of comparisons, the simulations were carried out considering the actual geometry of the scan from the moulds. The two simulations were performed with the release Final version 7.1 Stampack.

Out of the two, simulation 11 provides the best results which considers hyperstatic configuration with constraints localized in same areas in which the real part is bound on the gauge control (Figure 121). As already pointed out above, the dispersion of the results in comparison with the bottom reference surface is reduced compared to that of the corresponding comparison with the upper surface.

### 13.3.4 Simulation Autoform (CAD Dies, Wireframe blank)

Table 41 - Comparison results between the deformed shape by simulation Autoform and real surfaces from scan data

Reference 3D scanning Surface	Compared Surface Autoform	Max distance (mm)	Min distance (mm)	Mean distance (mm)	Std deviation (mm)	Area of Valid Distance (mm <sup>2</sup> )
lower	lower	19.97	-19.87	0.27	3.66	201238
higher	lower	18.56	-20.00	-0.83	4.65	202640

In this set of comparisons, simulations considering CAD nominal geometry of the moulds and simulations have been carried out using Autoform software.

The deviations which are obtained from the comparison between the deformed shape of Autoform and the actual surfaces of the MA03 component are worse than those obtained with respect to the surfaces of the nominal CAD geometry (section 13.2.4).

Compared to values of Table 34, corresponding comparisons have higher average deviation, a greater dispersion of results and a smaller area in which distance falls within the minimum-maximum range.

As already pointed out for the Stampack software results, also in this case, there is a greater correspondence between the simulation result and geometry of the lower surface of MA03.

## 14 Reconstruction of the Actual Geometry of the Moulds

The actual surfaces of the moulds for PM13 and MA03 components were mathematized starting from the scan data.

For reconstruction of the CAD mould surfaces, "network-based surface curves" or surface based on a network of curves approach was used. It generates a network on the surface of curves and implements on building a series of characteristic curves, for example, the lines of symmetry, those of style or sharp edges (Figure 122).

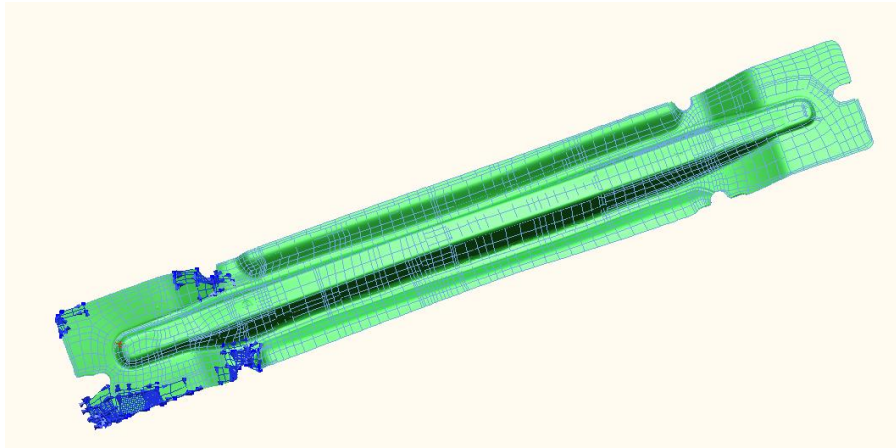


*Figure 122 - Network of curves generated for reconstruction of mathematical model of the lower mould component of PM13*

The intersection between the curves of the network generates various closed regions (referred to as patches). It should be ensured that the patches which are generated by the intersection between the curves, do not have large variations of curvature near the edges. If the regions are bounded by four curves, parametric NURBS surfaces are generated without limitations.

Figures 123 and 124 are the results of reconstruction of surfaces of the moulds for the PM13 component. Figures 125 and 126 are the results of reconstruction of surfaces of the moulds for the MA03 component.

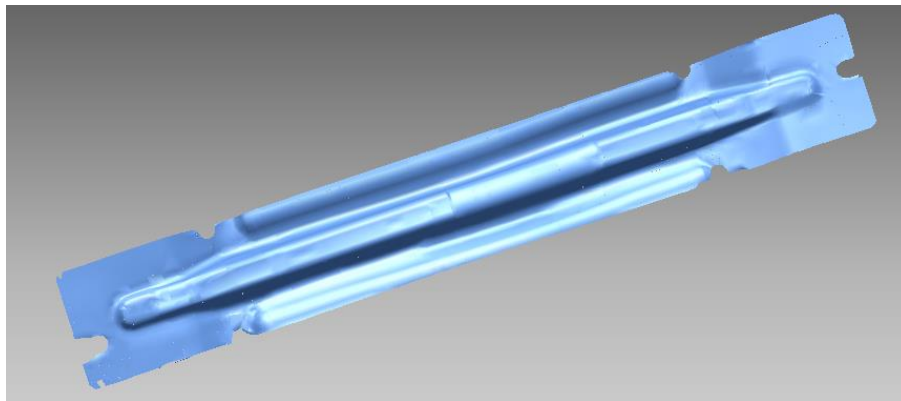


*Figure 123 - Surfaces rebuilt for the reconstruction of mathematical model of the lower mould of PM13*

The surfaces were generated in a manner faithful with respect to scan data and cannot be considered as ideal surfaces free of imperfections. The aim of reconstruction is to be able to use the actual geometry of the moulds in order to verify, by means of simulation, the correspondence between the numerical calculation of deformed shape by elastic return and the actual geometry of the moulded part.

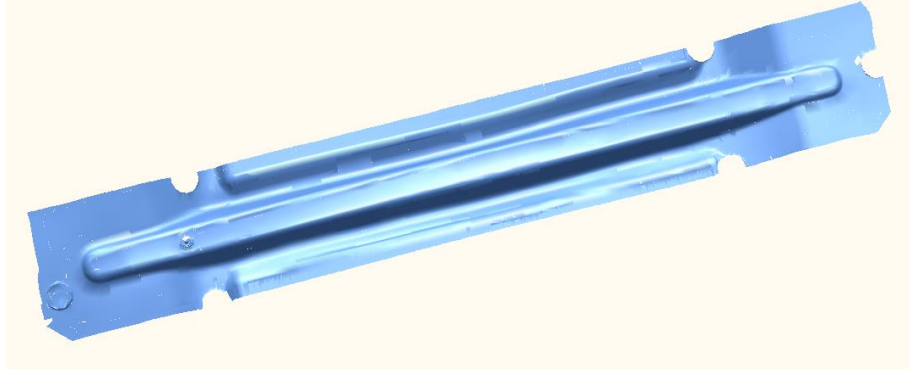


*Figure 124 - Surfaces rebuilt for the reconstruction of mathematical model of the upper mould of PM13*

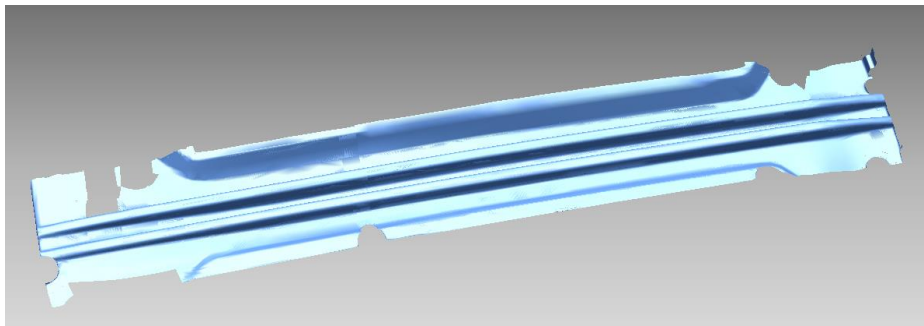


*Figure 125 - Surfaces rebuilt for the reconstruction of mathematical model of the lower mould of MA03*

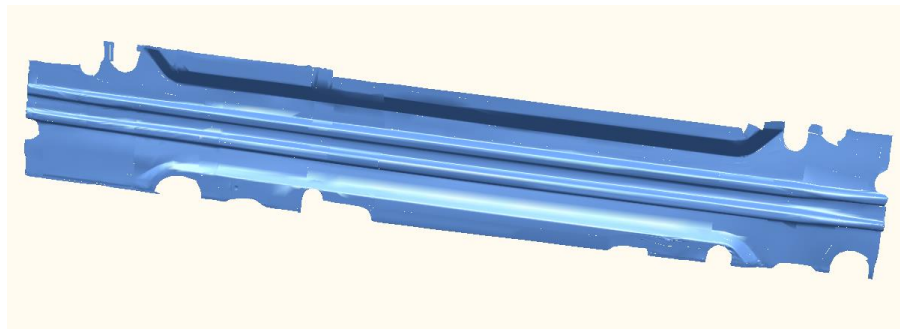


*Figure 126 - Surfaces rebuilt for the reconstruction of mathematical model of the upper mould of MA03*

Moreover, it is not necessary that the surfaces are free of localized defects, because they have aesthetic value or modeling purposes and editing using CAD software. It will however be evaluated later if surface imperfections prevent the proper completion of the CAD model discretization process and creation of the mesh for the moulding simulation.

### **Additional Testing of PM13 Component in Hyperform**

#### **15 Altair Hyperworks**

This is the version of the Altair Hyperworks 2017. Altair is the most comprehensive, open architecture CAE simulation platform in the industry, offering the best technologies to design and optimize high performance, weight efficient and innovative products. Hyperworks includes best in class modelling, linear and non linear analysis, structural and system level optimization, metal forming solver, fluid and multibody dynamics simulation, electromagnetic compatibility, Multiphysics analysis, model based development and data management solutions.

#### **15.1 Hyperform**

Altair Hyperform is an industry proven comprehensive simulation software solution for stamping and tooling industries. It allows to engineer and optimize all aspects of stamped product development cycle from concept design to finished part for metals and composites.

Hyperform is a comprehensive solution with specialized features to analyse and optimize each phase of the product development cycle. Also integrated to reap benefits of simultaneous engineering minimizing total cost.

Hyperform leverages years of Altair's experience in manufacturing simulation, process design and combines several of Altair's state of the art technologies from geometry manipulation to model setup, fast, reliable and scalable finite element solver, optimization technology, powerful post processing in an intuitive and natural workflow familiar to designers and engineers for efficient stamping product and process development.

Hyperform provides best Return of Investment in its class with functionality and affordability to meet demands of customers varying from individual analysts, tool shops to large OEM. It is highly efficient comprehensive platform for the stamping product development cycle.

Customers worldwide have benefitted using Hyperform to

- Improve the product design for easy manufacture at early concept stage.
- Develop reliable and robust tooling that minimize die tryouts and press down time resulting in quality parts conforming requirement.
- Thereby, maximizing efficiency and significantly reducing cost and time for product development.

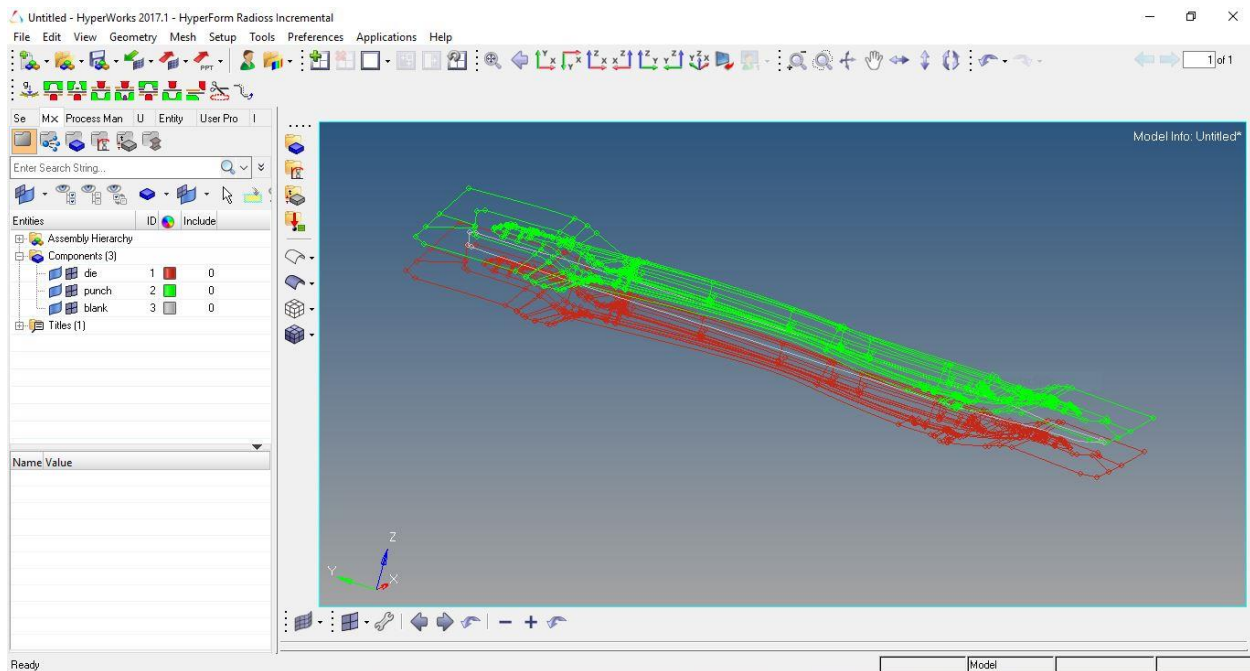


Figure 127 Hyperform interface

### 15.1.1 Capabilities of Hyperform Incremental :

- Automatic tool creations based on process type from die face design.
- User friendly and intuitive interface for designers and engineers to setup models for all sheet forming process types including hot stamping with quenching.
- Single user interface to setup forming process for blanks of different types.
- Users can create their own custom process and store it as templates for quick reuse and share them to establish uniform modelling practices in a team.
- Fast, robust, accurate and scalable incremental solver radios provides quick and best in class forming and springback results.
- Efficient result interpretation in hyperview with special tools for forming relevant post processing like FLD, draw in, springback displacement relevant to fixture points, springback compensation, blank shape prediction.
- Simplified interface to setup optimization of process parameters, blank shape, tooling parameter in stamping process for forming feasibility and springback using Hyperstudy with radioss.
- Trim line and blank shape optimization to support net shape manufacturing.
- Die structure topology optimization using radioss with optistruct for maximum tool life and lightweight.

## Applications

- Aviation
- Automotive
- Smartphone drop test simulation
- Ship building

## 16 Hyperform Simulation

There are so many user profiles within the hyperform. Here we choose, the Application as Manufacturing Solutions. Since we deal with the crashform and simulation of the blank component, we choose the Hyperform - Incremental Radioss.

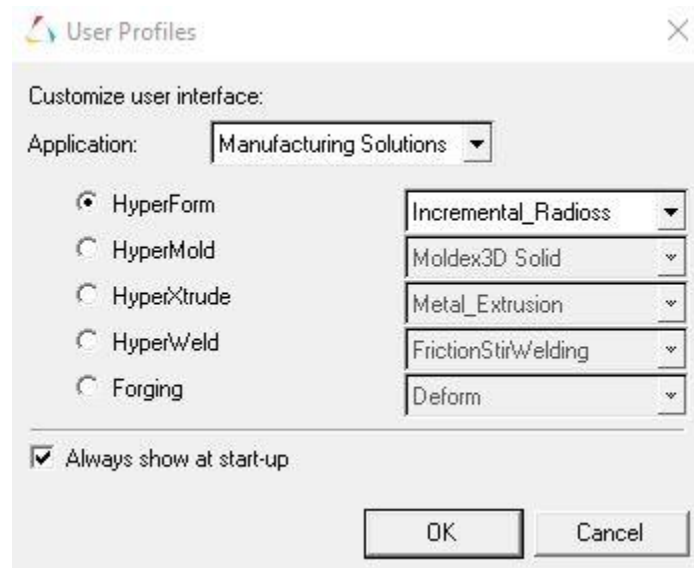


Figure 128 Hyperworks user profiles

Then we should choose the type of mesh needed to get the best results. For the blank simulation, Hyperform experts suggests to use the type B Mesh. Now we choose the type of process in the Autoprocess. We choose the crashform. Then the input paramters – Material and thickness are given. The blank, punch and the die are assigned accordingly. Autoposition calculates the required distance between the punch and die. If there is no penetration interference error, then we confirm it to be the distance and the simulation is run. The mesh size can be smaller to get more accurate results of the process. The drawback of having smaller mesh size is that it takes higher computational time. Also when the mesh size is too small, this version provided with some stability issues while running the simulation.

Once the simulation is done, loading the animation file in Hyperview enables us to view how the blank is getting deformed in real time process. Also the results can be generated by loading any one of the animations files.

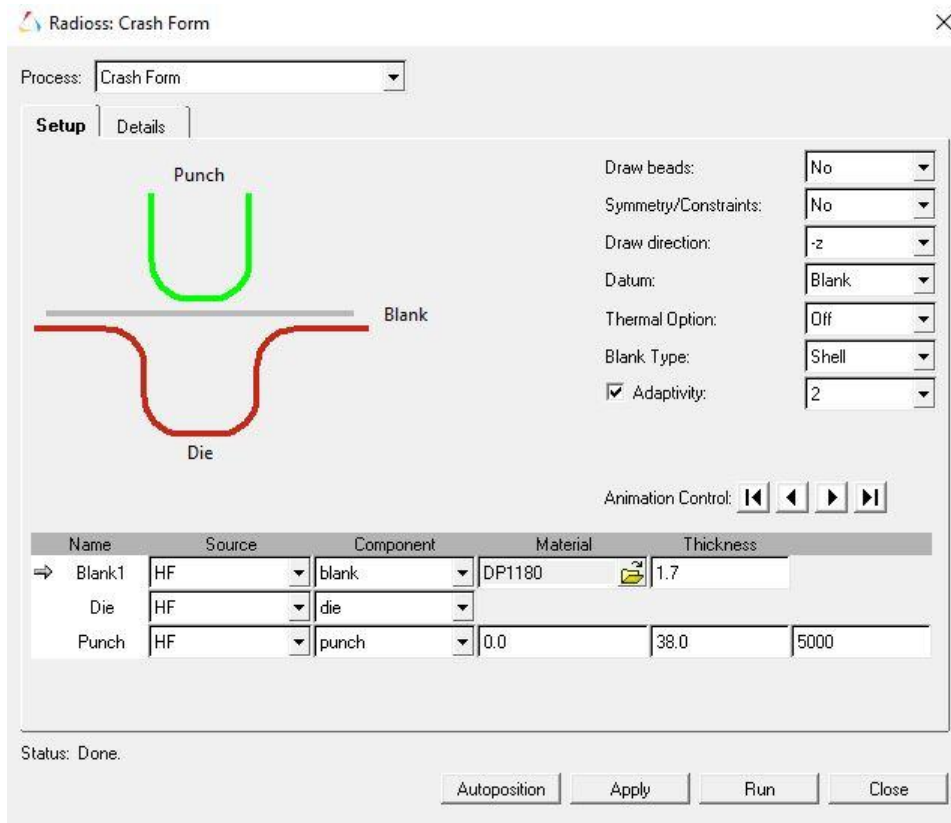


Figure 129 Incremental radioss – Autoprocess

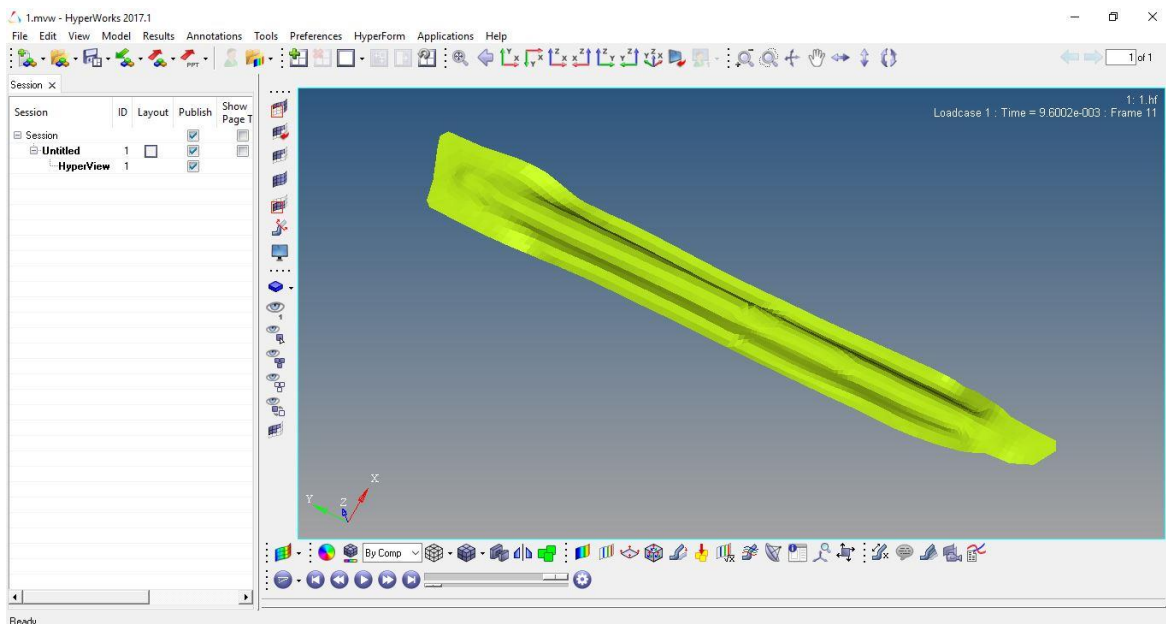


Figure 130 Hyperview interface

## 16.1 Case 1 - PM13 Component Simulation

### 16.1.1 Geometry Input

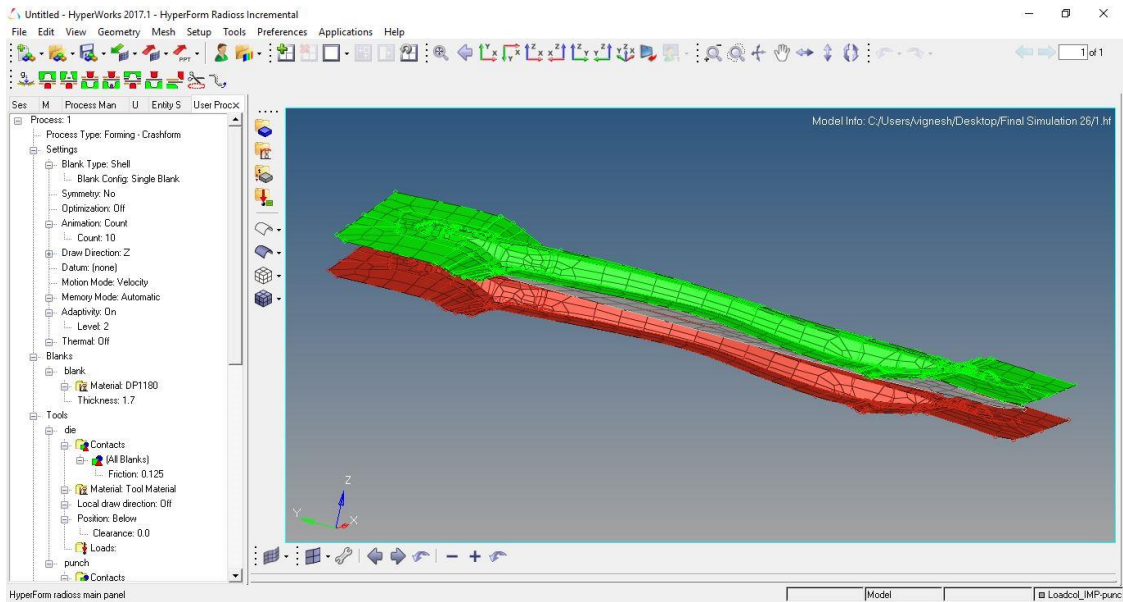


Figure 131 Geometry input

### 16.1.2 Percentage Thinnings

The image represents the result of forming prior to the calculation of the elastic return in terms of the percentage of thinning. The analysis shows that there are some areas in which it has a thickness variation of more than +/- 2.5%.

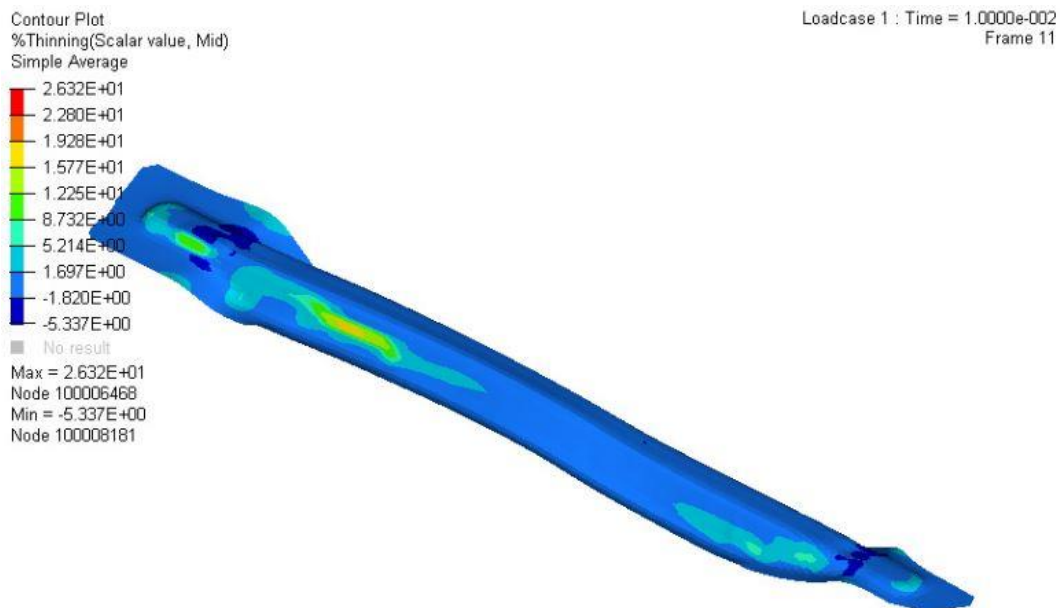


Figure 132 Percentage of thinning

### 16.1.3 Plastic Strain

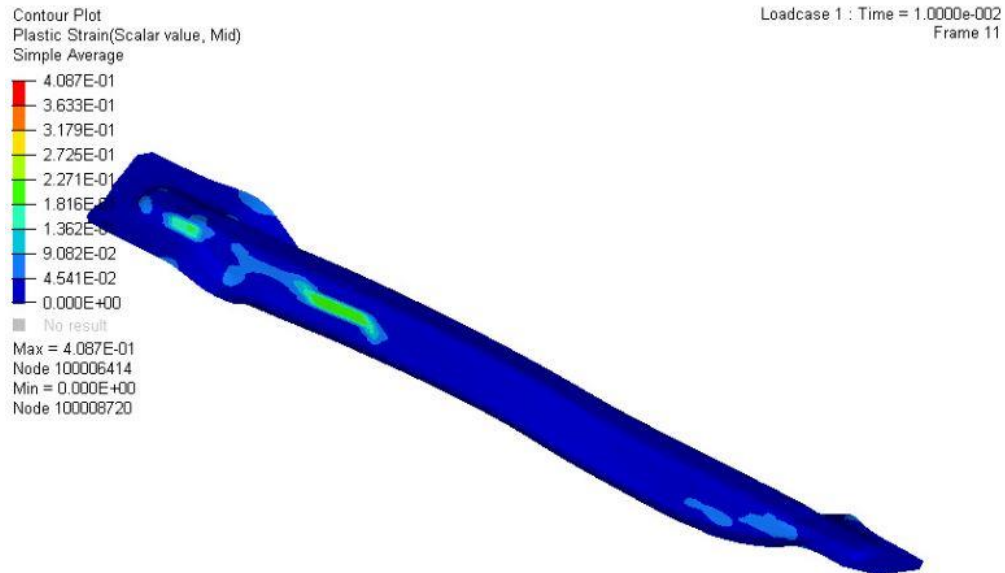


Figure 133 Plastic strain

### 16.1.4 Formability Analysis

The analysis of formability based on FLD curve confirms there is certain areas of failure and certain areas of compression. It is due to the improper clearance between the die and the punch, thereby restricting the material flow during the crashform process.

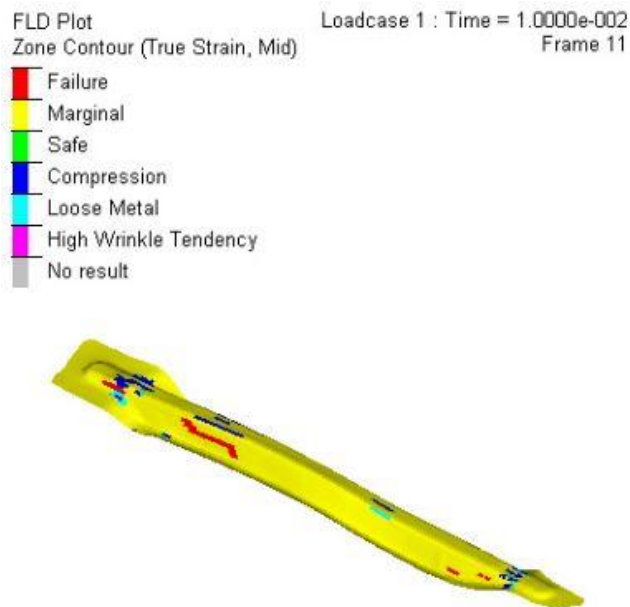


Figure 134 Formability FLD

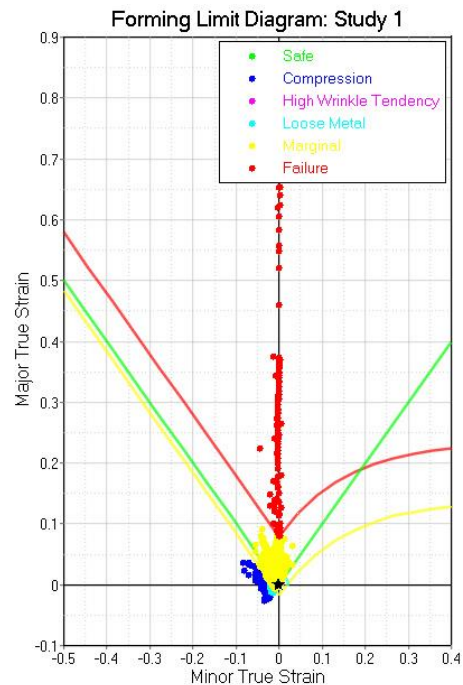


Figure 135 Forming of the results

### 16.1.5 Comparison between the CAD and the Hyperform Simulation

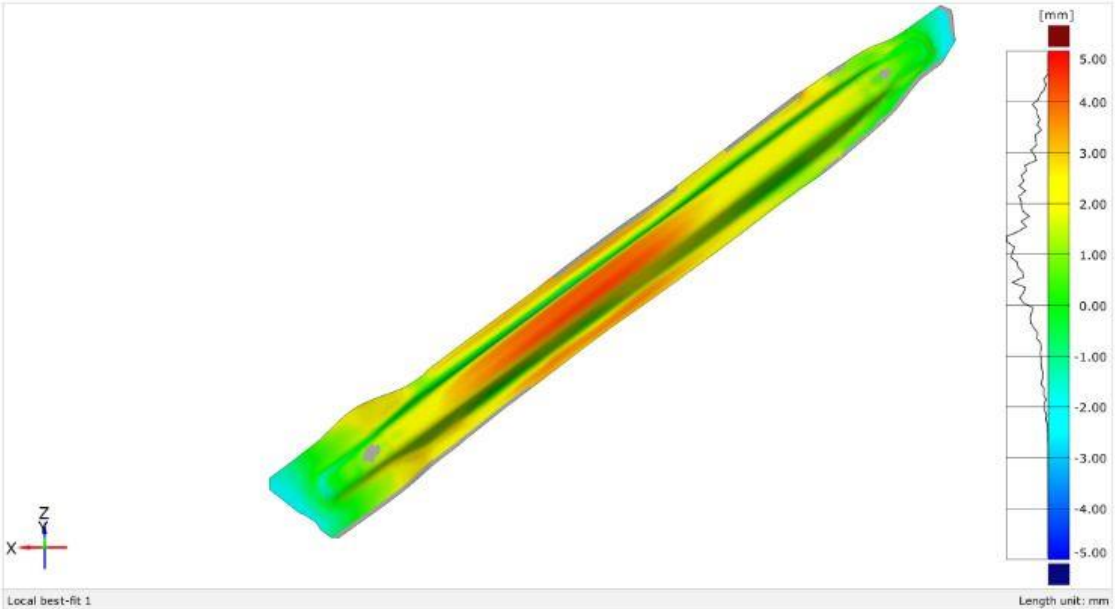


Figure 136 Surface comparison between hyperform simulation and CAD bottom

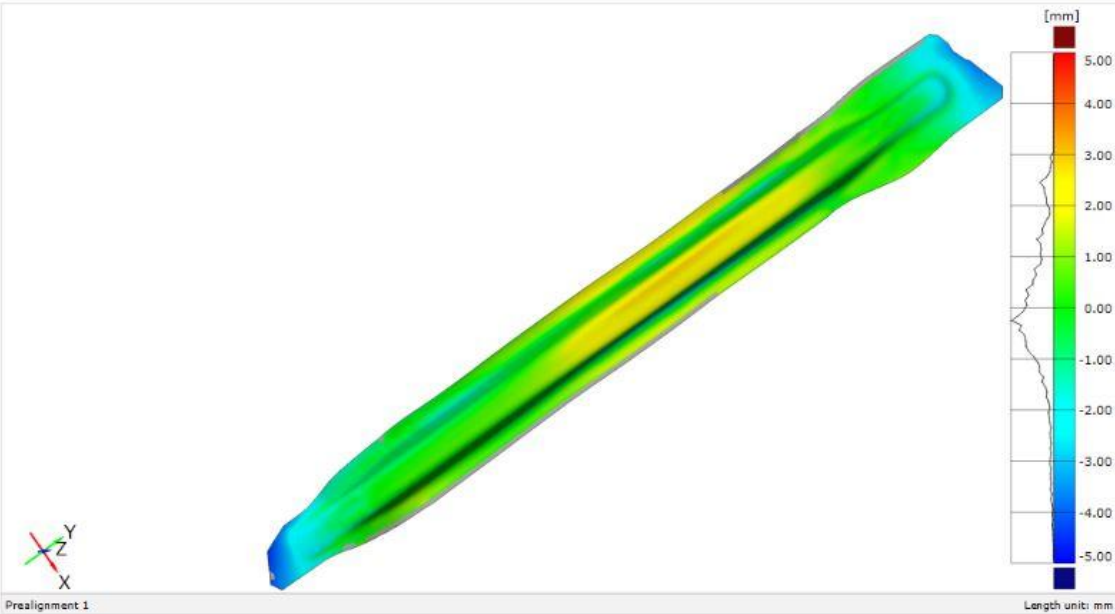


Figure 137 Surface comparison between hyperform simulation and CAD average



Figure 138 Surface comparison between hyperform simulation and CAD top

## 16.1.6 Comparison between the scanned geometry and the Hyperform Simulation

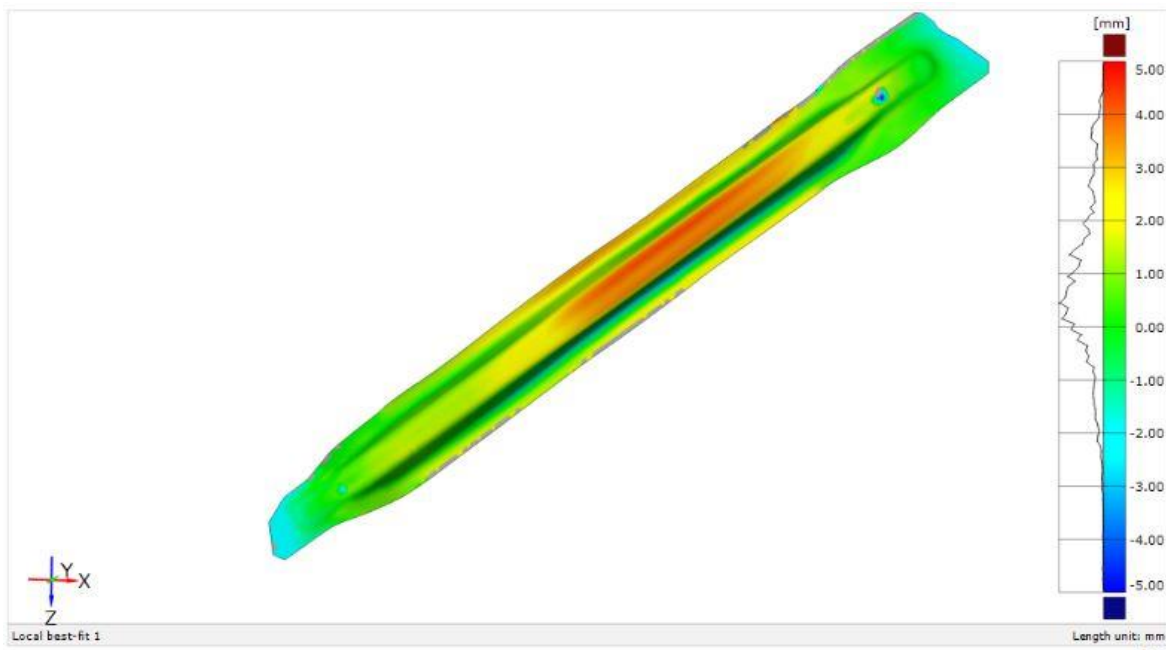


Figure 139 Surface comparison between hyperform simulation and scanned bottom

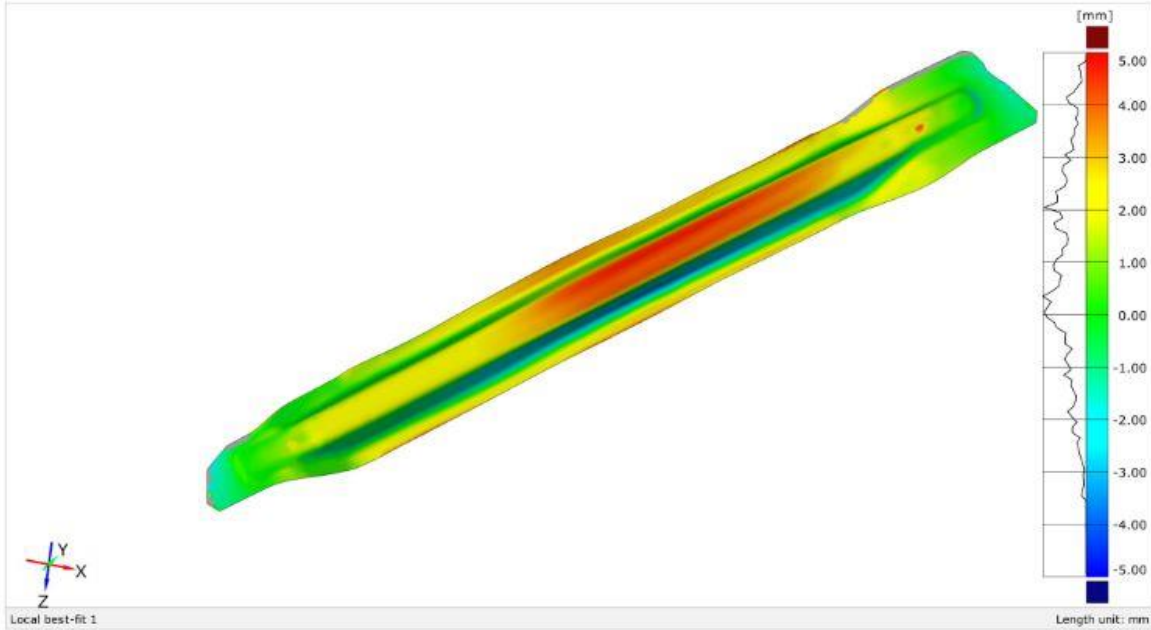


Figure 140 Surface comparison between hyperform simulation and scanned top

### 16.1.7 Comparison Between Nominal Geometry (CAD) and Simulation Results

Table 42 - Comparison results between CAD surfaces and hyperform simulation

Reference Nominal CAD Surface	Max distance (mm)	Min distance (mm)	Mean distance (mm)	Std deviation (mm)	Area of Valid Distance (mm <sup>2</sup> )
Lower	4.47	-2.67	1.15	1.31	78348.63
Average	2.98	-4.57	-0.12	1.26	78110.29
Upper	4.26	-3.28	0.78	1.39	77780.90

### 16.1.8 Comparison Between Actual Scanned 3D Geometry and Simulation Results

Table 43 - Comparison results between actual scanned 3D geometry and hyperform simulation

Reference 3D Scanning Surface	Max distance (mm)	Min distance (mm)	Mean distance (mm)	Std deviation (mm)	Area of Valid Distance (mm <sup>2</sup> )
Lower	5.00	-4.66	1.18	1.38	76718.81
Higher	4.76	-4.60	0.69	1.81	76158.21

## 16.2 Comparison Between Best Results From Hyperform Simulation and Stampack Simulation

We have one simulation in hyperform which is exported in stl format. Out of all the simulations of the PM13 component in stampack software, the simulation 7 is chosen to be the best with minimum mean distance and standard deviation combinations and with higher area of valid distance. So the corresponding simulation file is considered. The two files from the stampack and hyperform are compared in the GOM inspect software. The result is as follows.



Figure 141 Surface comparison between stampack simulation and hyperform simulation

Table 44 - Comparison results between stampack simulation and hyperform simulation

Reference Stampack & Hyperform Simulation	Max distance (mm)	Min distance (mm)	Mean distance (mm)	Std deviation (mm)	Area of Valid Distance (mm <sup>2</sup> )
Lower	2.72	-4.15	-0.02	1.19	78256.29

## 17.0 Conclusion and Next Steps

Different software packages for forming simulation consider different starting surface for the blank (bottom surface, middle surface, upper surface) for calculation of the simulation according to the 3D shell model. Also the deformed shape that they return is referred to the starting surface they consider. Therefore, even if the thickness of the components is reduced, the comparison between the deformed ones is not theoretically correct, at least quantitatively. The comparison could be considered in terms of quality, compared to the variation in shape. However, it must be considered that the alignment influences the results of the comparison. This aspect introduces a further element of variability, that cannot be checked previously and that, together with the different starting surface, it is not able to provide a suitable scientific comparison.

In order to overcome this problem, it would be necessary to develop an experimental activity to compare the real deformations obtained from the simulation carried out with the different software packages even starting from different surfaces. In fact the ultimate aim and utility is that, the tools for the forming simulation should suggest to the industrial user the definition of the geometry of the dies in an appropriate manner to compensate the springback from forming. With the aid of the simulation, the geometry compensated by the dies should provide a final component that, despite the springback, has a geometry corresponding to that required by the drawing. After the calculation of springback deformation (springback simulation), the simulation software has the possibility to calculate (simulation of springforward) the optimal geometry of the dies. This operation is defined as a "virtual compensation", since the springforward calculation should eliminate or at least reduce the experimental setup steps of the dies, during which the toolmaker is forced to spoil the mould to compensate the deviations of the manufactured component when compared to the nominal shape required. The manual operation is based on the experience and know-how of the process and may require different iterations to modify the mould shape with lengthening of the setup and delivery times as well as costs.

The experimental activity to be developed with non-negligible costs is shown in the diagram in Figure 142. Starting from the definition of a benchmarking geometry, a forming simulation should be performed with each of the analyzed software packages (Stampack, Autoform, Hyperform) with its own methods. The simulation of forming would be followed by the calculation of the springback and then virtual compensation of the mould (springforward). In addition to the dies having the nominal geometry of the component, four other moulds should be produced, each having the optimized geometry corresponding to the springforward result. One or more copies of the reference component would be produced with each of the different moulds. Now, 3D scanning of the actual geometry of different moulded parts is performed. Then they are evaluated for the one which is more geometrically similar to the nominal component. The best results are chosen and this activity allows to validate the software which gives the best result to improve the accuracy of estimation and compensation of the elastic return of the crashforming operation.

So, an experimental activity needs to be carried out to correlate numerical results of different software tools to experimental evidence for increasing the reliability of virtual design of forming dies.

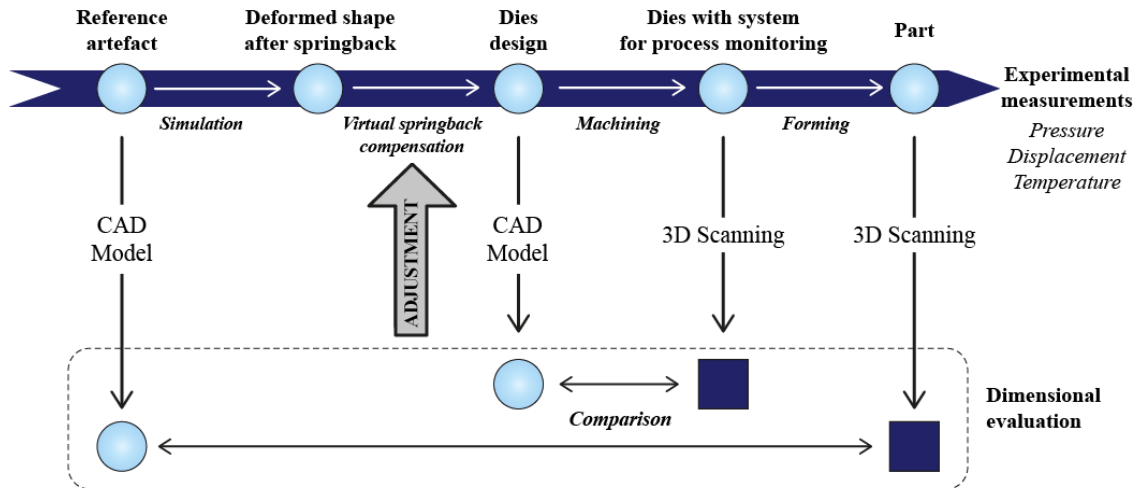


Figure 142 Experimental procedure to compensate deviations of manufactured component compared to the nominal geometry

The results of this thesis can be summarized as in the following,

- Depending on how we constrain the part for springback evaluation in the software packages, we get different results. After the simulation we should compare among the different results by checking the surface and variation on the results.
- We used nominal geometry of the tools but it would be more correct to use the actual geometry that was retrieved by reverse engineering and 3D Scanning. This difference should improve the accuracy of the results. This is one of the next important steps to be developed.
- In this project, by using different software packages for forming simulation, we studied and evaluated the springback in the process and came to a conclusion on the best configuration to be used, based on the evaluated results. Another important future step should be the evaluation of the compensation (spring forward) capability of each software.
- In addition to the previous results, the MA03 component should be simulated using the Hyperform software and the springback and forward prediction capability should be evaluated for that package as well.

## ANNEX 12.1

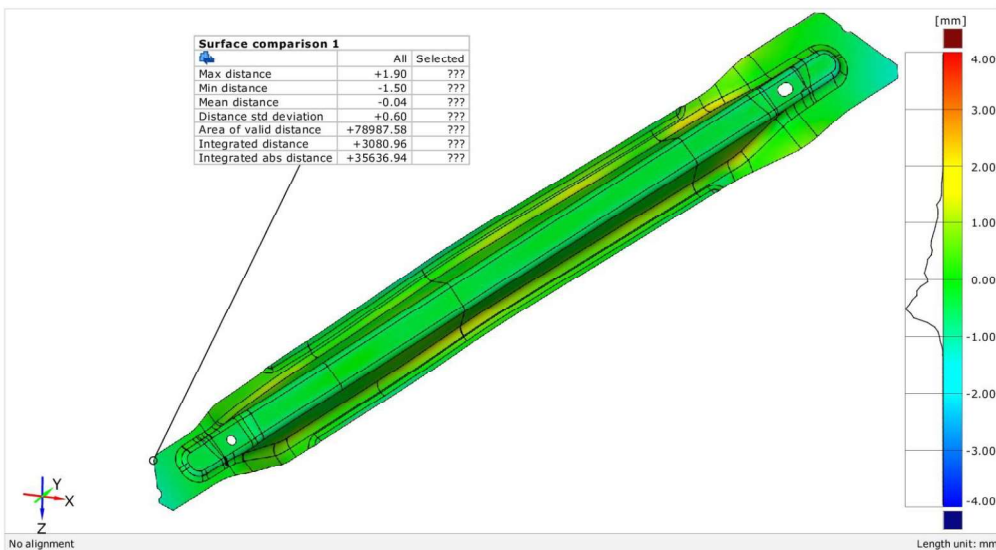
### COMPARISON OF NOMINAL GEOMETRY (CAD) AND REAL GEOMETRY RESULTING FROM SCAN

#### CAD lower\_real lower

Generated with GOM Inspect V8



Surface Comparison on CAD

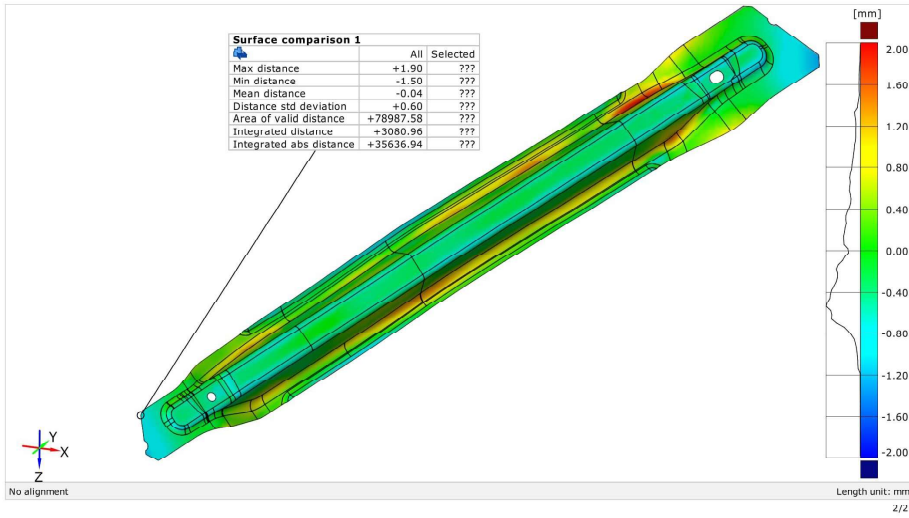


# CAD lower\_real lower

Generated with GOM Inspect V8



## Surface Comparison on CAD

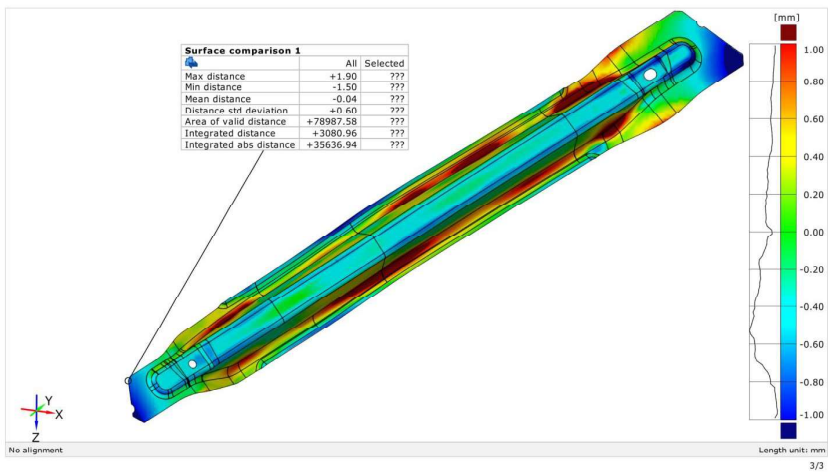


# CAD lower\_real lower

Generated with GOM Inspect V8



## Surface Comparison on CAD

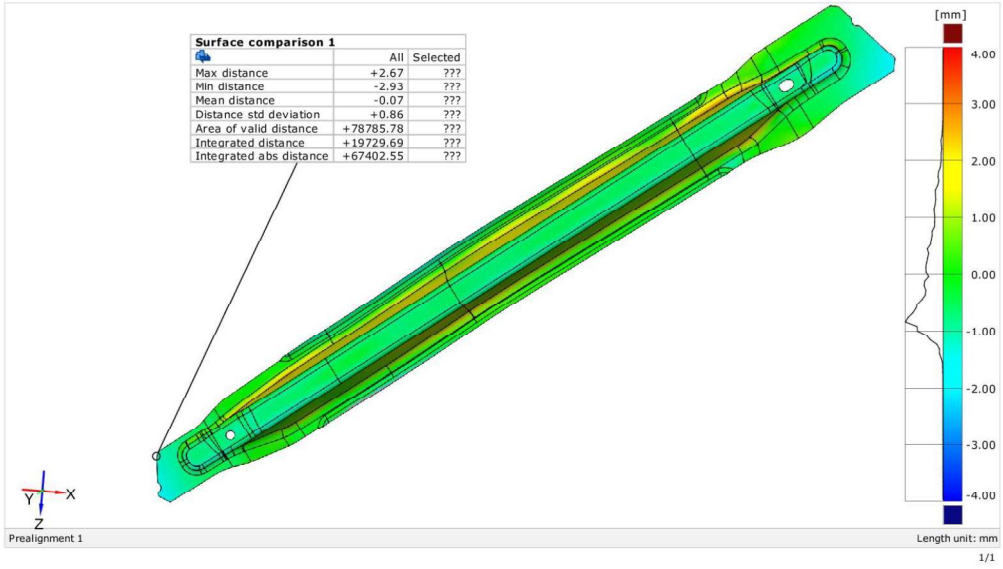


# CAD lower\_real higher

Generated with GOM Inspect V8



Surface Comparison on CAD

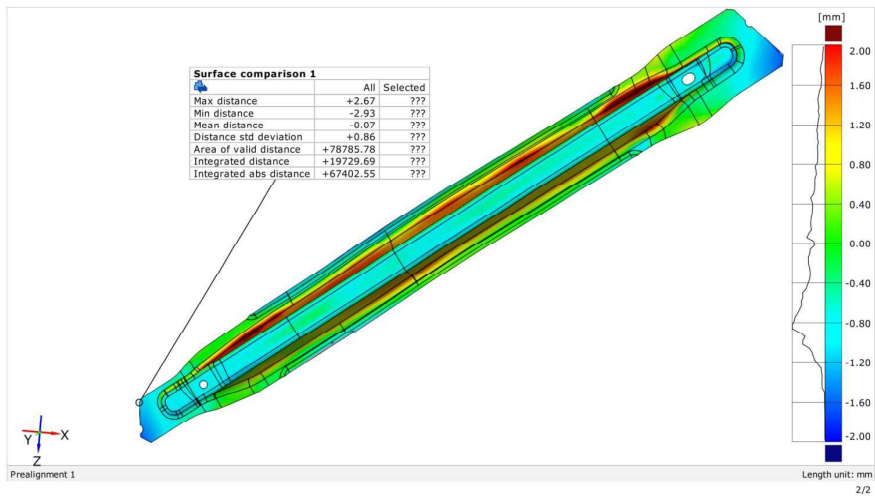


# CAD lower\_real higher

Generated with GOM Inspect V8



Surface Comparison on CAD

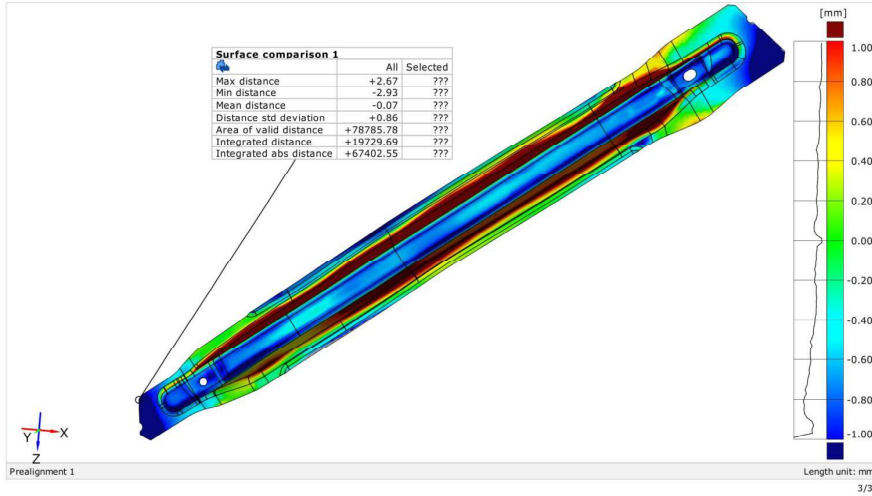


# CAD lower\_real higher

Generated with GOM Inspect V8



Surface Comparison on CAD

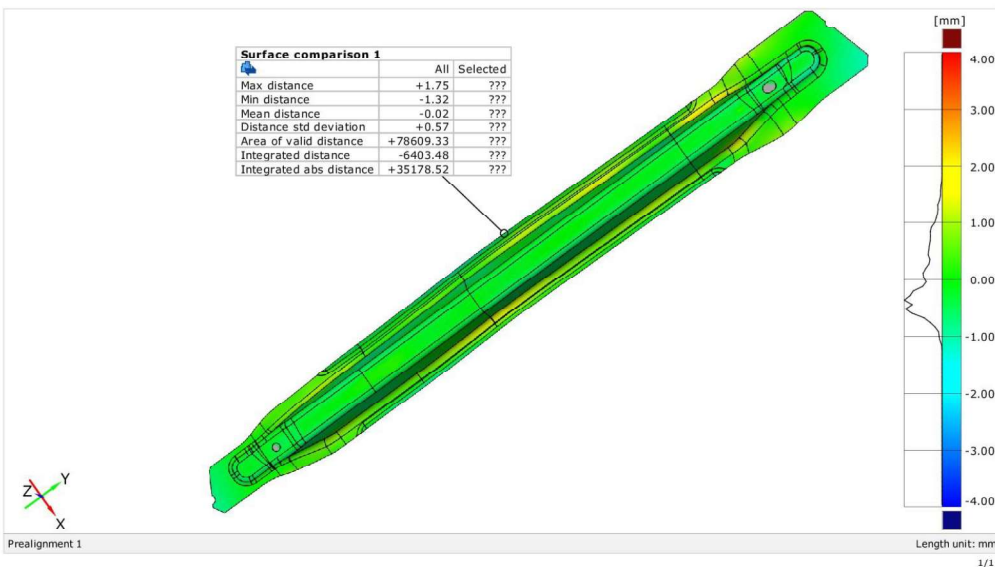


# CAD average\_real lower

Generated with GOM Inspect V8



Surface Comparison on CAD

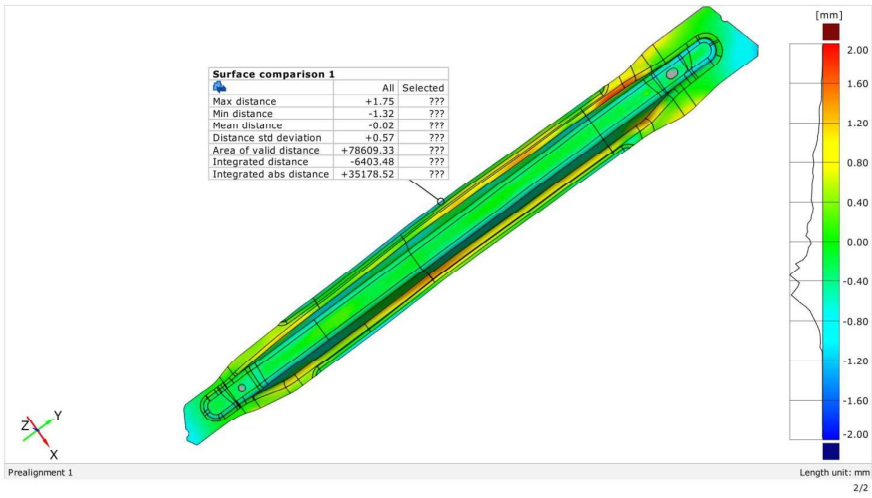


# CAD average\_real lower

Generated with GOM Inspect V8



Surface Comparison on CAD

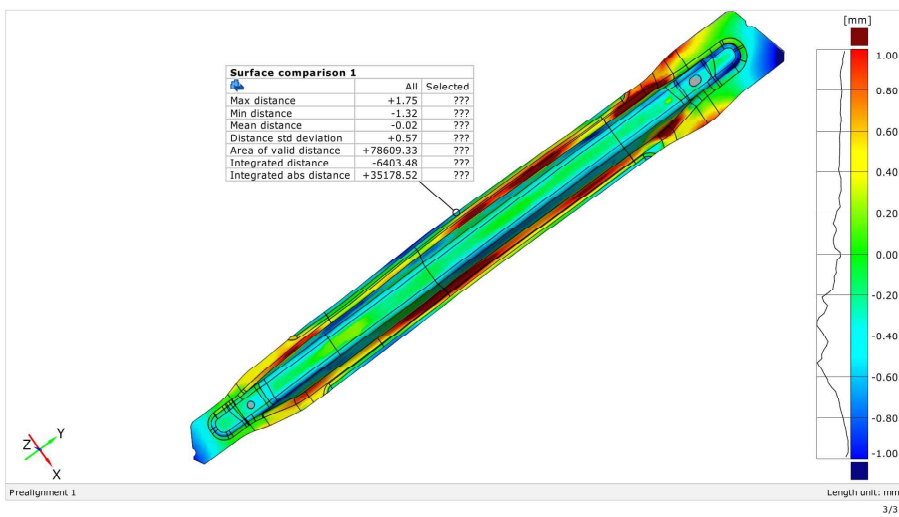


# CAD average\_real lower

Generated with GOM Inspect V8



Surface Comparison on CAD

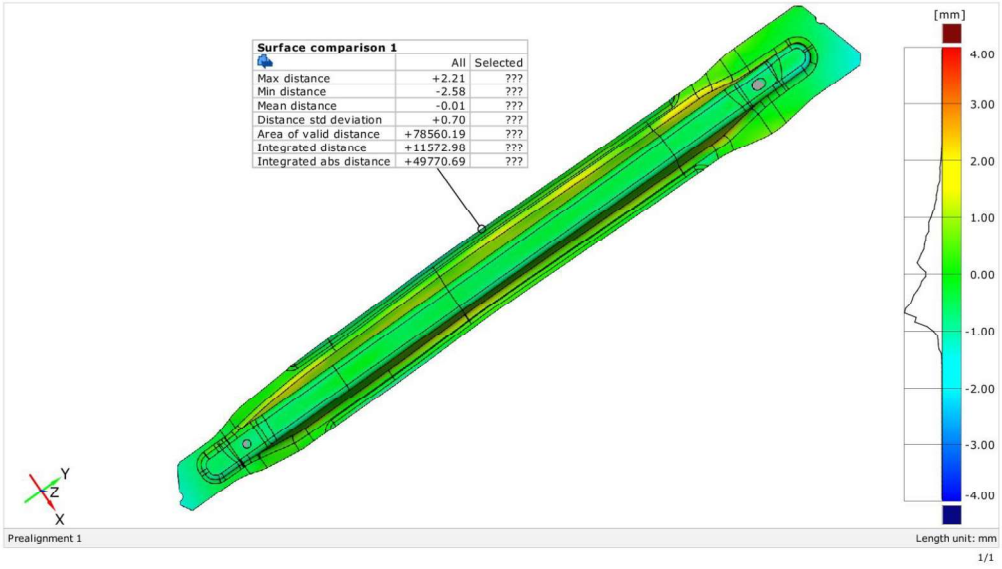


# CAD average\_real higher

Generated with GOM Inspect V8



Surface Comparison on CAD

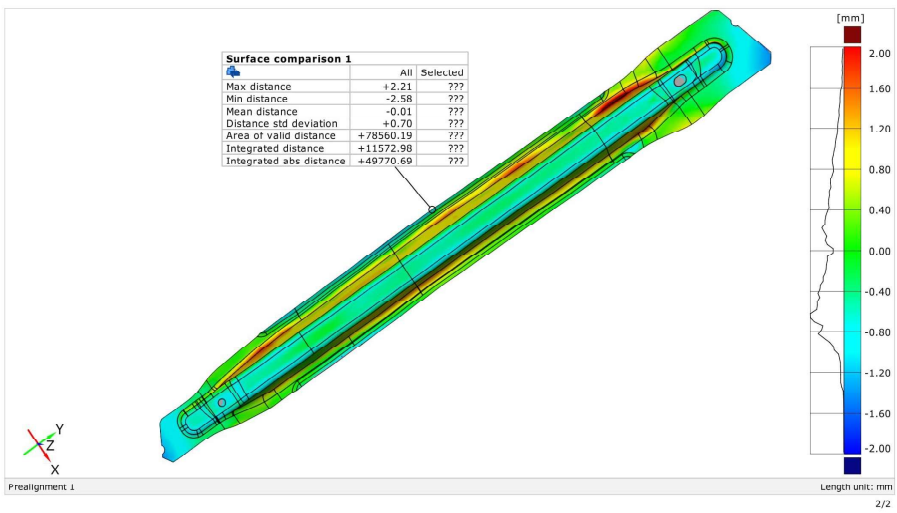


# CAD average\_real higher

Generated with GOM Inspect V8



Surface Comparison on CAD

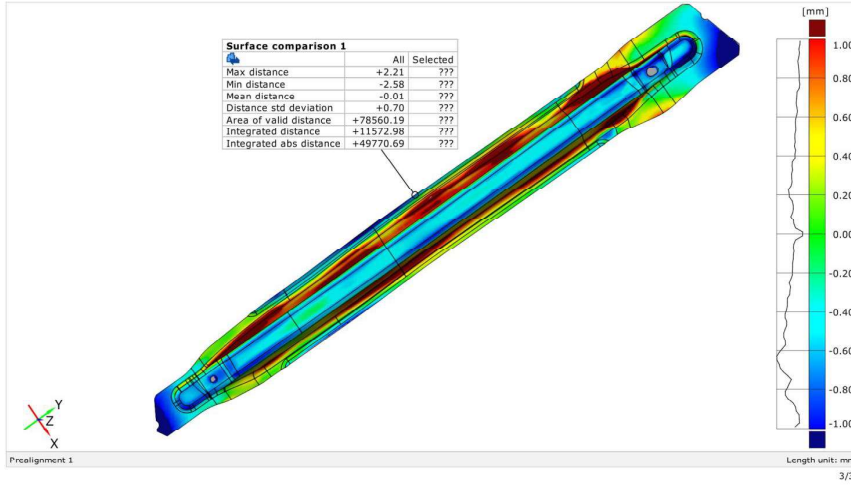


# CAD average\_real higher

Generated with GOM Inspect V8



Surface Comparison on CAD

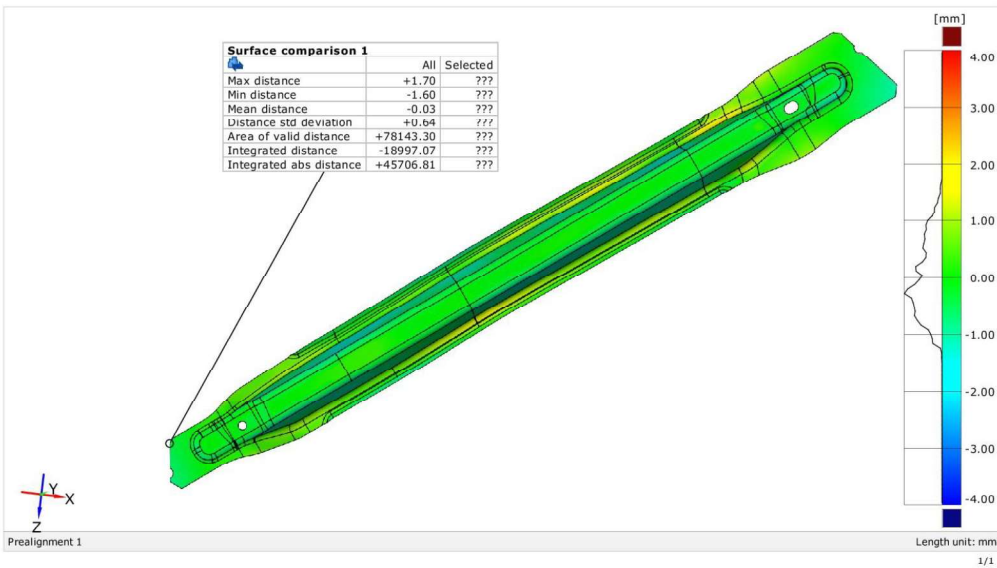


# CAD higher\_real lower

Generated with GOM Inspect V8



Surface Comparison on CAD

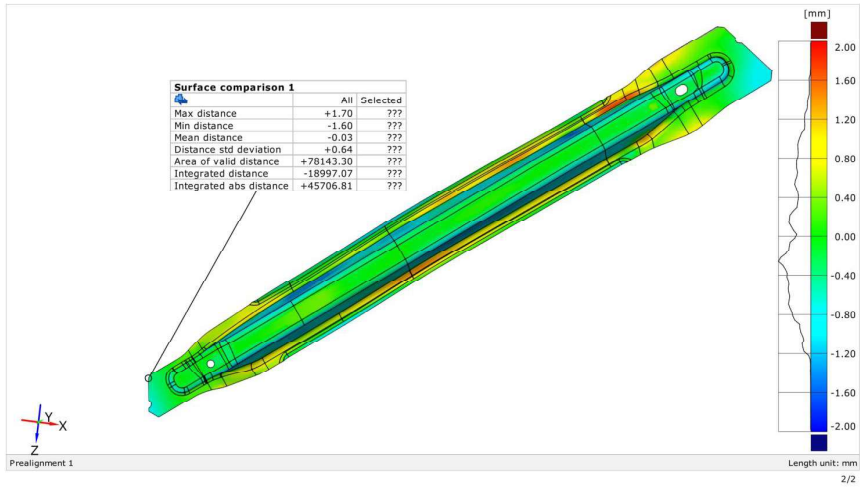


# CAD higher\_real lower

Generated with GOM Inspect V8



## Surface Comparison on CAD

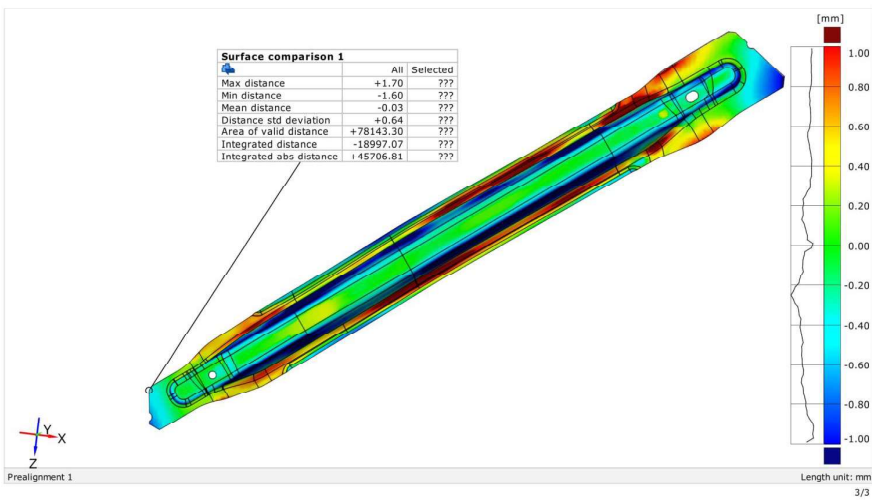


# CAD higher\_real lower

Generated with GOM Inspect V8



## Surface Comparison on CAD

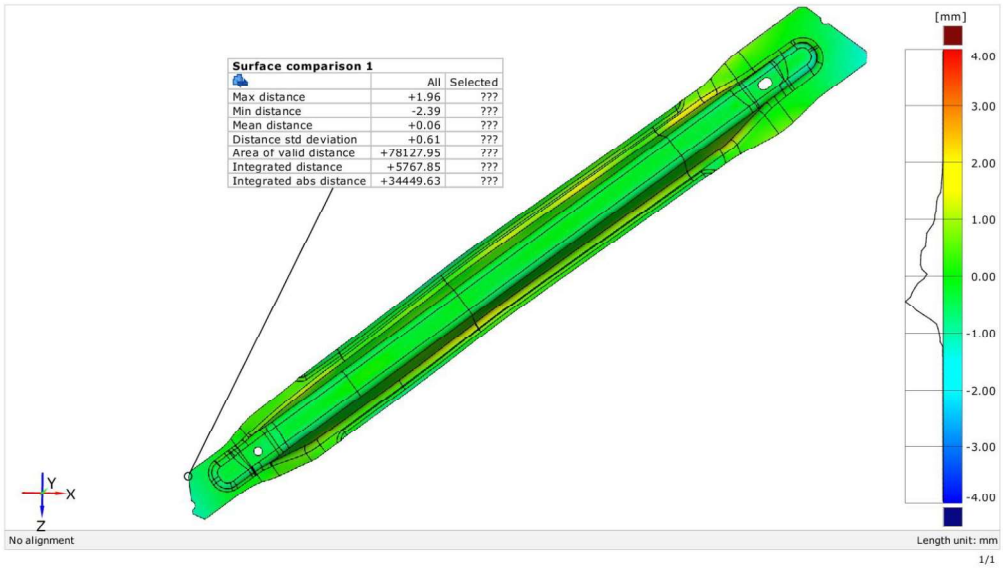


# CAD higher\_real higher

Generated with GOM Inspect V8



Surface Comparison on CAD

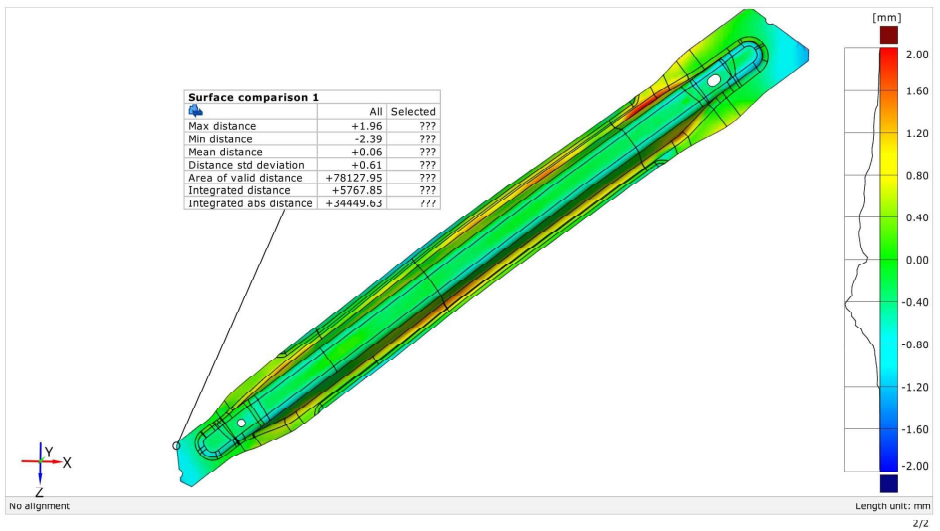


# CAD higher\_real higher

Generated with GOM Inspect V8



Surface Comparison on CAD

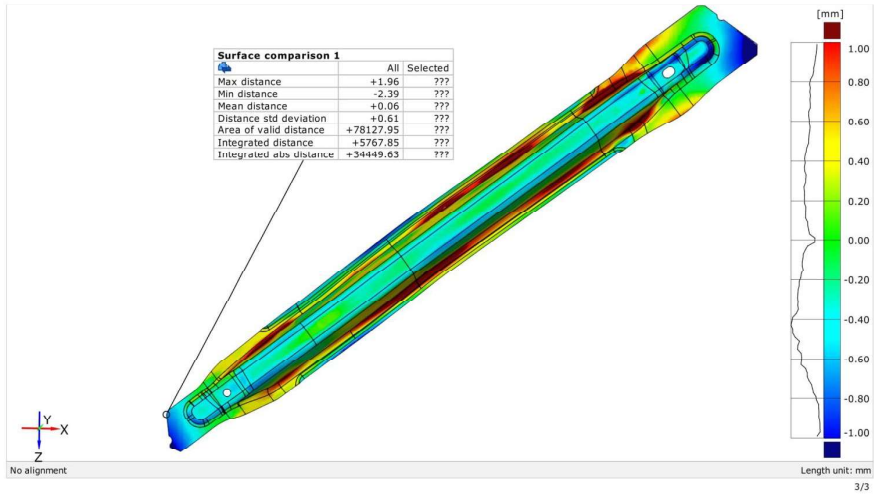


# CAD higher\_real higher

Generated with GOM Inspect V8



## Surface Comparison on CAD

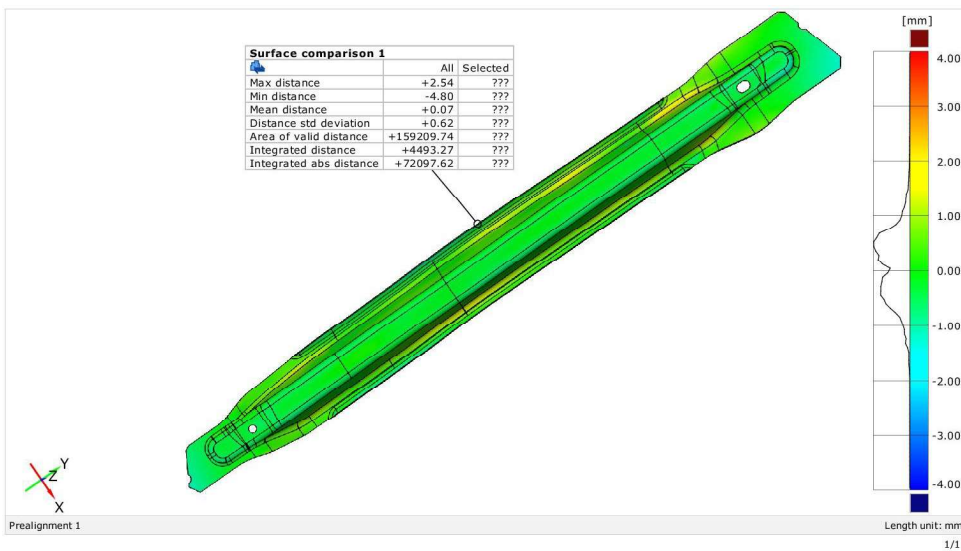


# 3D CAD Part\_real 3D

Generated with GOM Inspect V8



## Surface Comparison on CAD

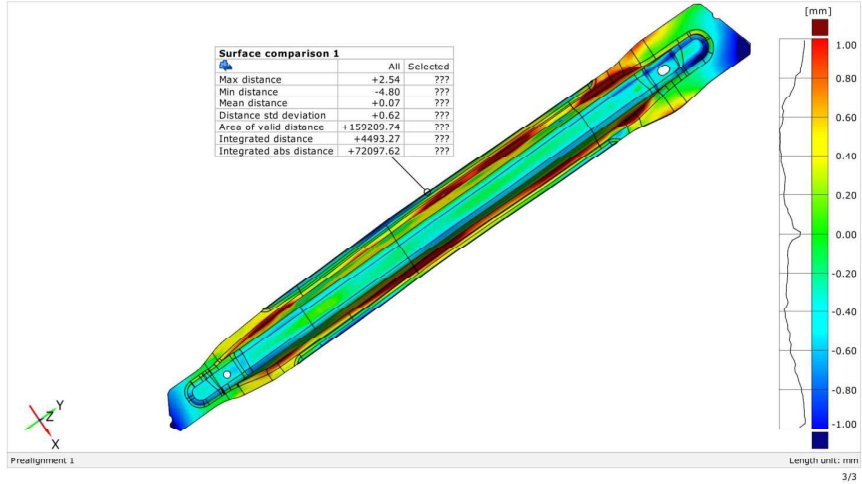


# 3D CAD Part\_real 3D

Generated with GOM Inspect V8



## Surface Comparison on CAD

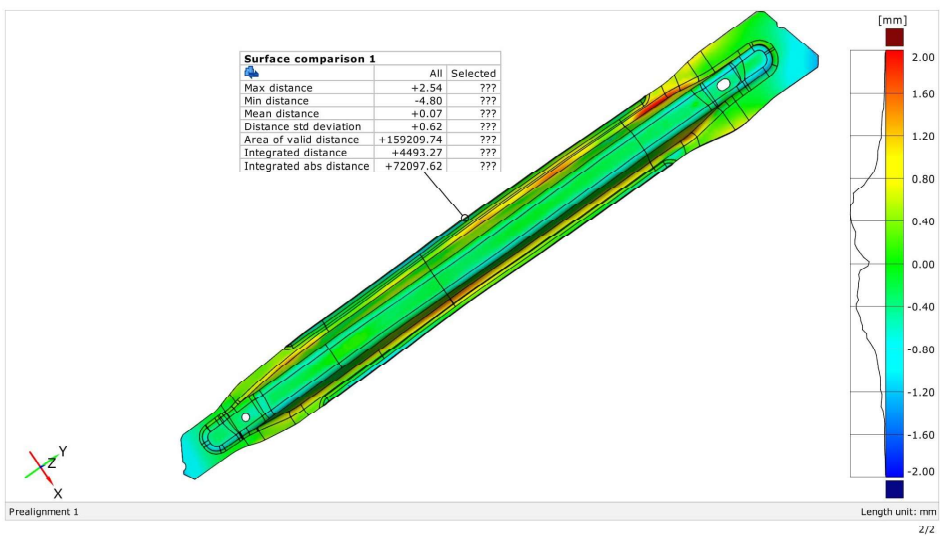


# 3D CAD Part\_real 3D

Generated with GOM Inspect V8



## Surface Comparison on CAD



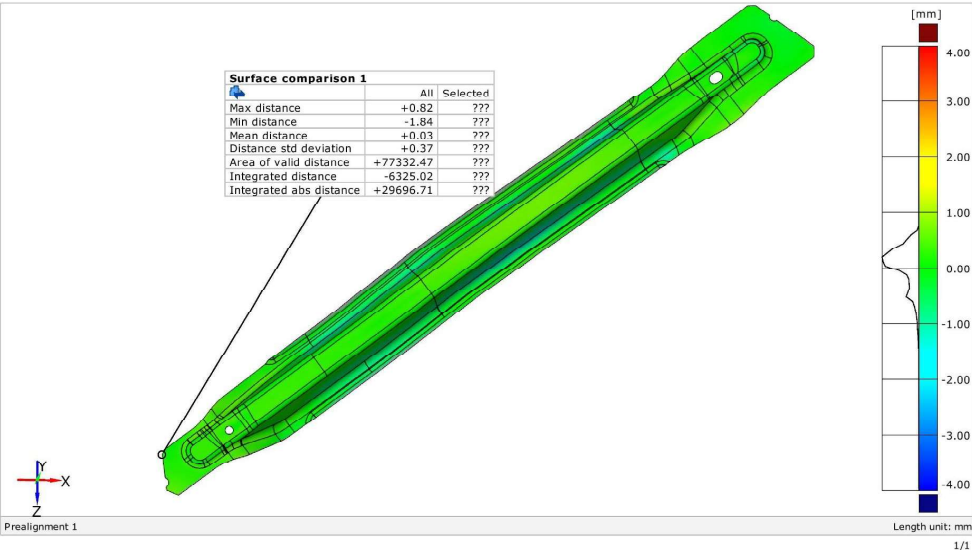
# ANNEX 12.2 COMPARISON OF NOMINAL GEOMETRY (CAD) AND SIMULATION RESULTS

## CAD lower\_simulation 1

Generated with GOM Inspect V8



Surface Comparison on CAD

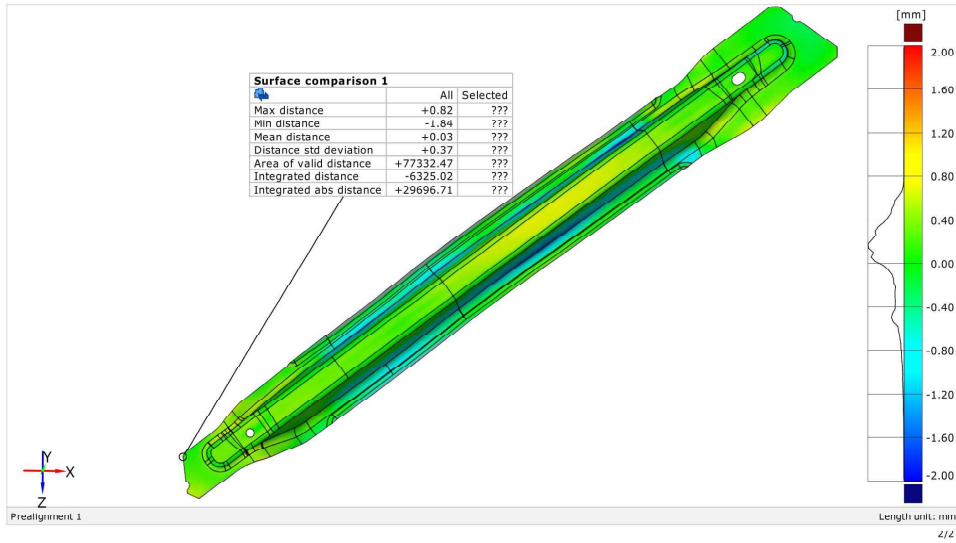


# CAD lower\_simulation 1

Generated with GOM Inspect V8



## Surface Comparison on CAD

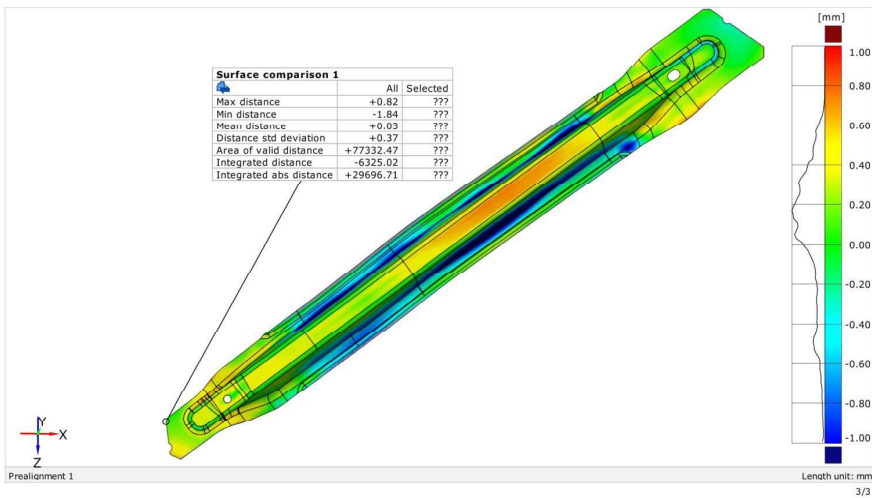


# CAD lower\_simulation 1

Generated with GOM Inspect V8



## Surface Comparison on CAD

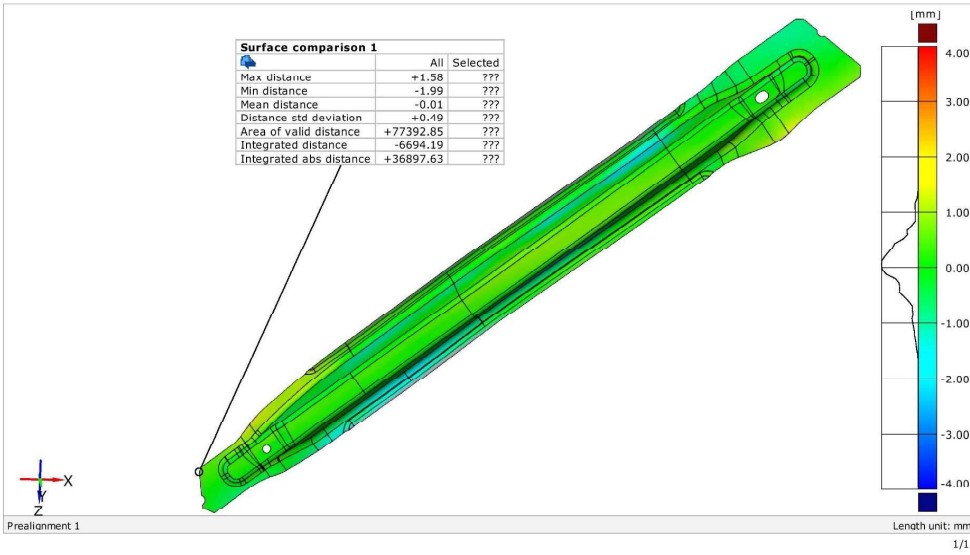


# CAD lower\_simulation 2

Generated with GOM Inspect V8



## Surface Comparison on CAD

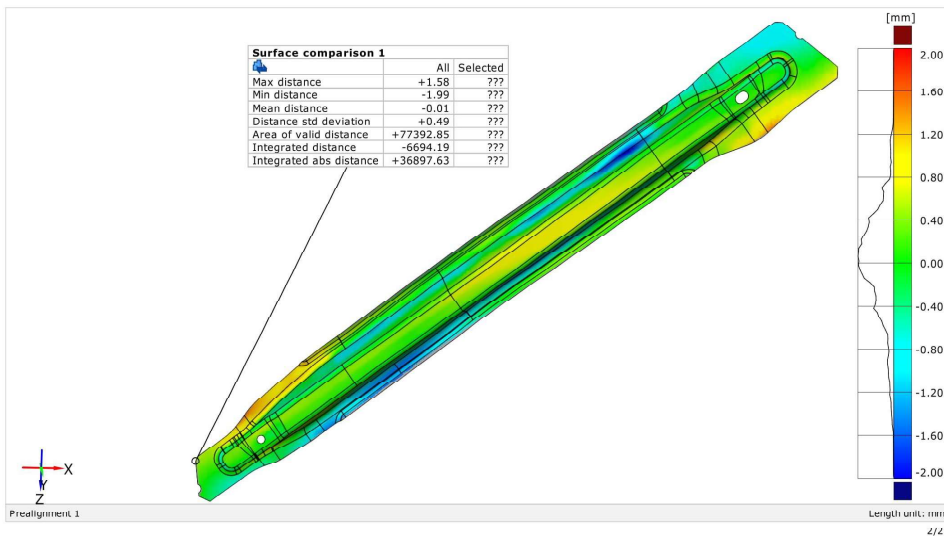


# CAD lower\_simulation 2

Generated with GOM Inspect V8



## Surface Comparison on CAD

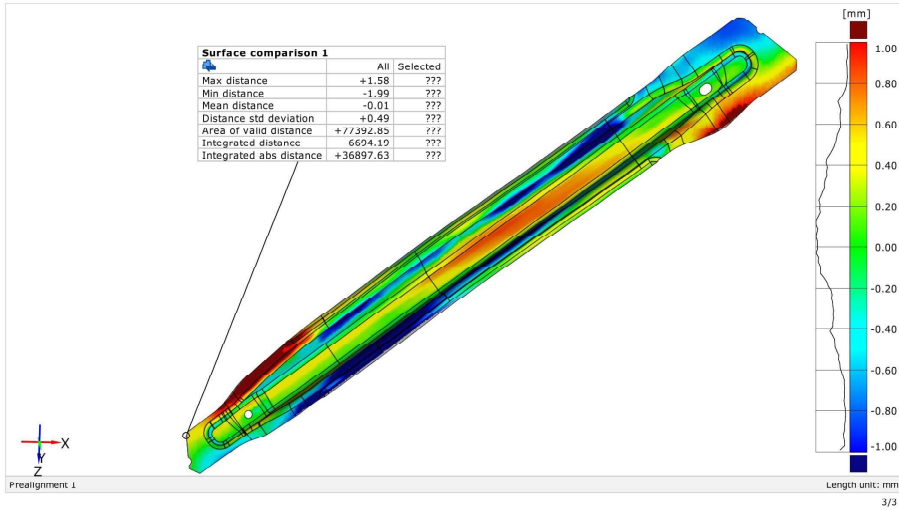


## CAD lower\_simulation 2

Generated with GOM Inspect V8

gom

Surface Comparison on CAD

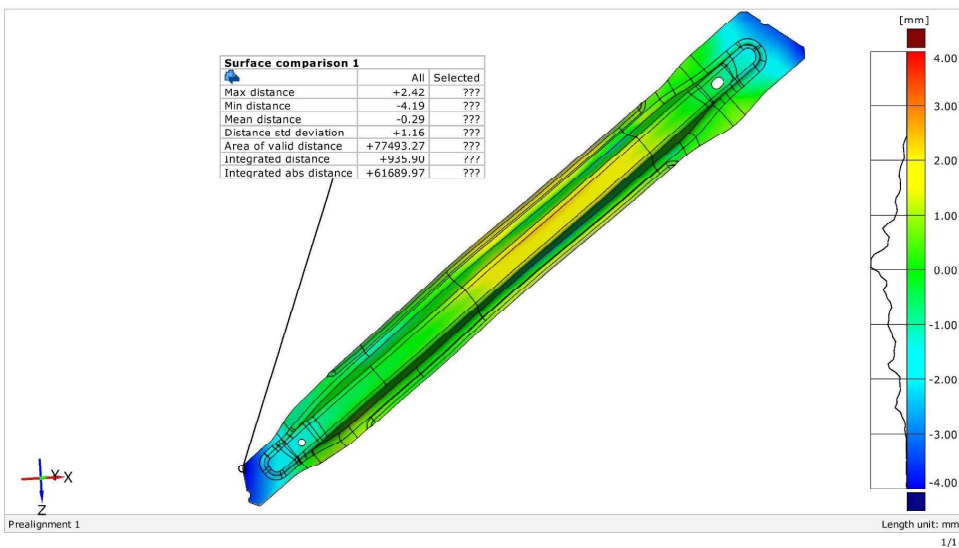


## CAD lower\_simulation 3

Generated with GOM Inspect V8

gom

Surface Comparison on CAD

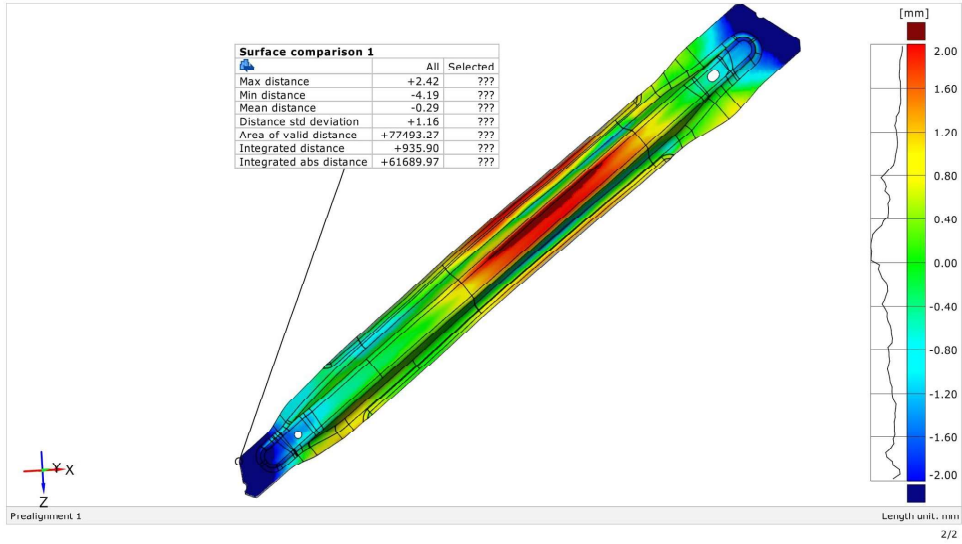


# CAD lower\_simulation 3

Generated with GOM Inspect V8



## Surface Comparison on CAD

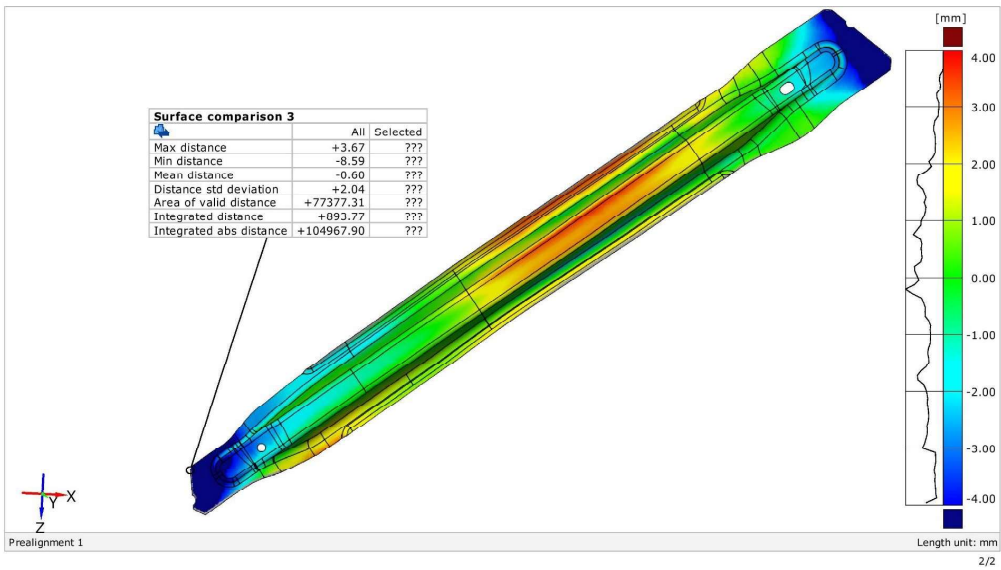


# CAD lower\_simulation 4

Generated with GOM Inspect V8



## Surface Comparison on CAD

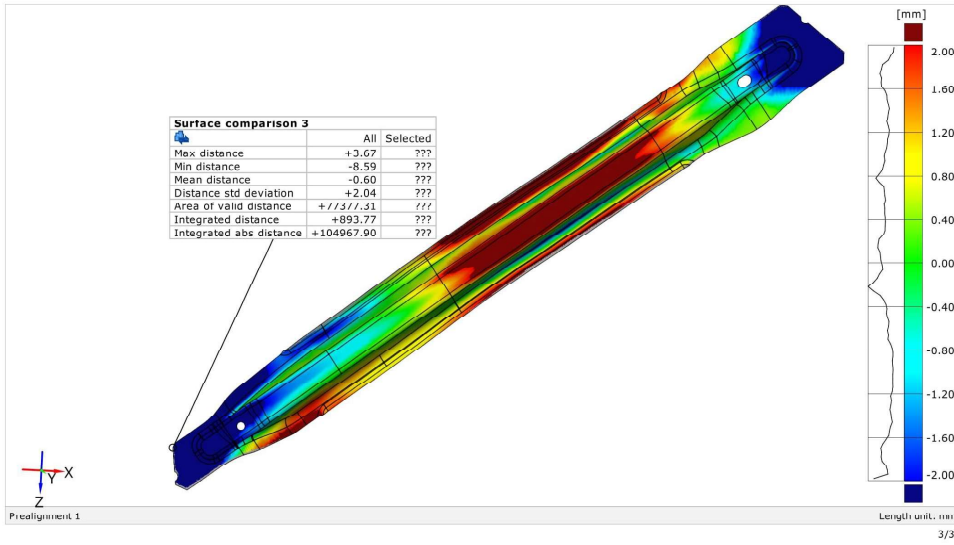


# CAD lower\_simulation 4

Generated with GOM Inspect V8



## Surface Comparison on CAD

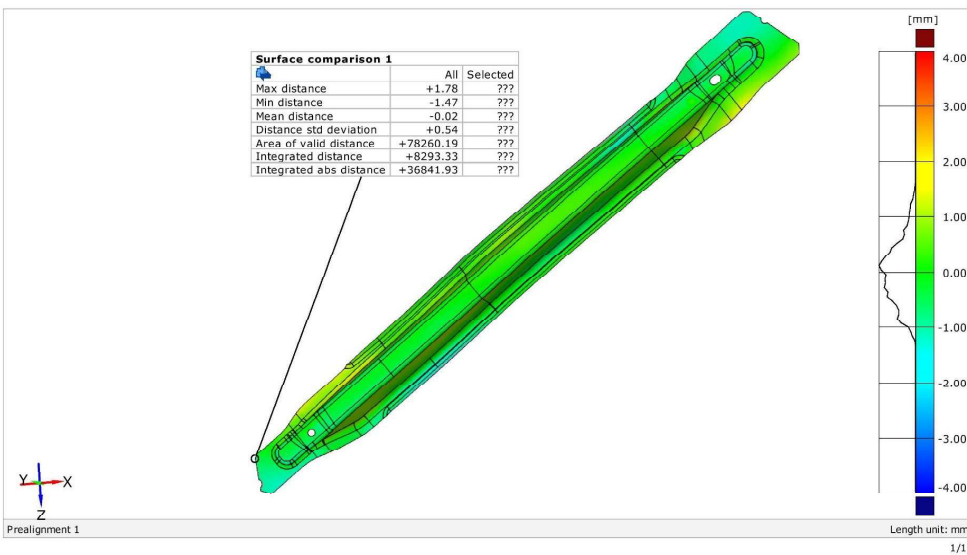


# CAD lower\_simulation 5

Generated with GOM Inspect V8



## Surface Comparison on CAD

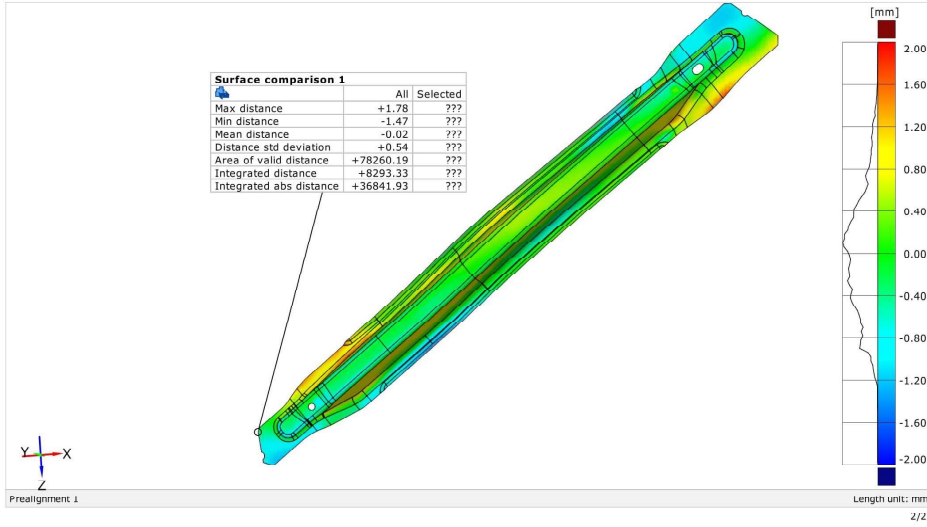


# CAD lower\_simulation 5

Generated with GOM Inspect V8



## Surface Comparison on CAD

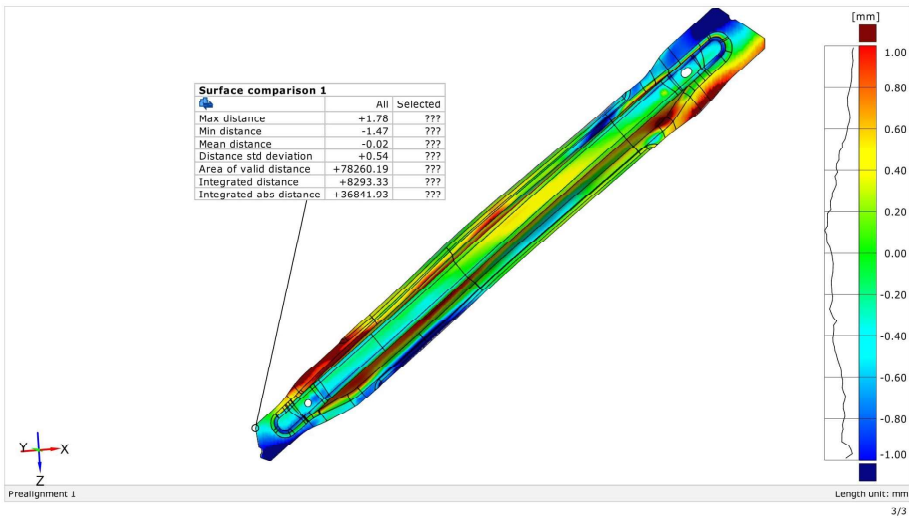


# CAD lower\_simulation 5

Generated with GOM Inspect V8



## Surface Comparison on CAD

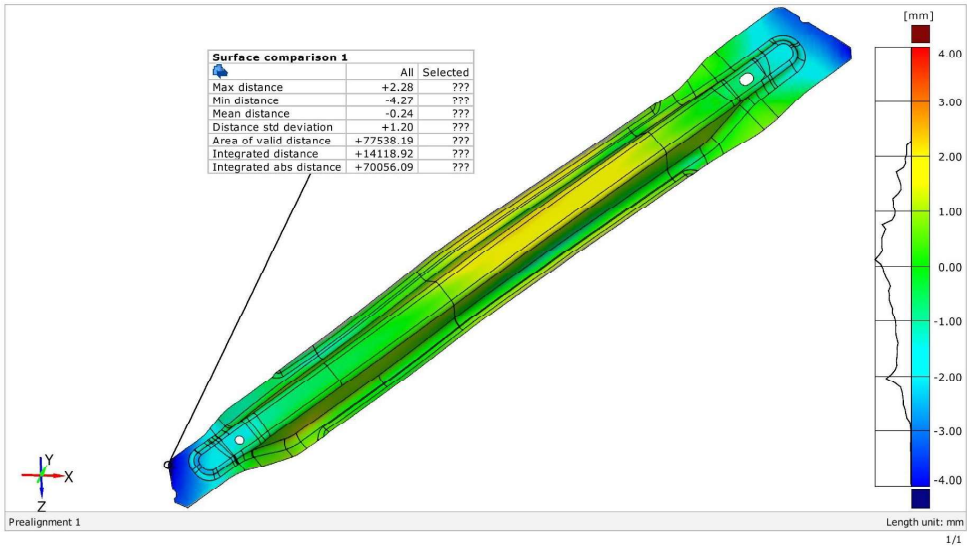


# CAD lower\_simulation 6

Generated with GOM Inspect V8



Surface Comparison on CAD

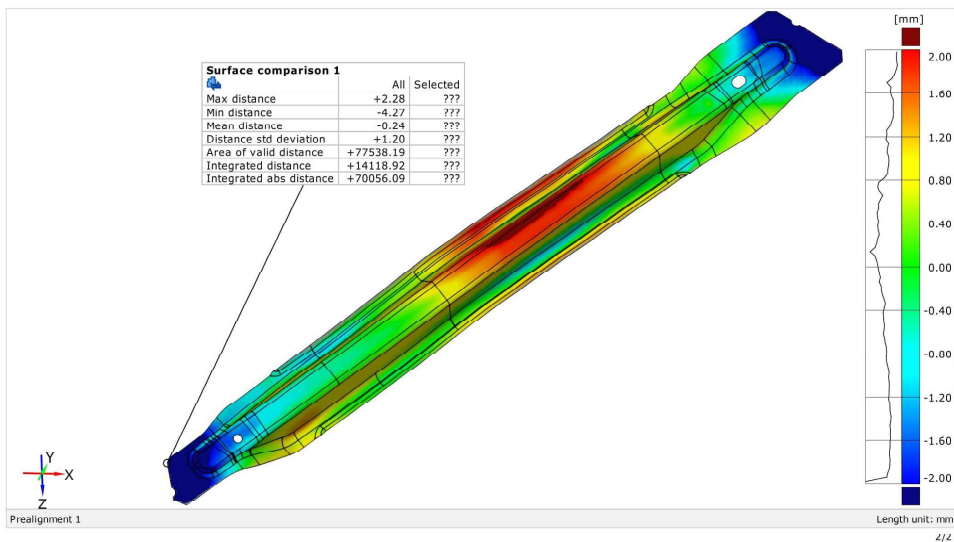


# CAD lower\_simulation 6

Generated with GOM Inspect V8



Surface Comparison on CAD

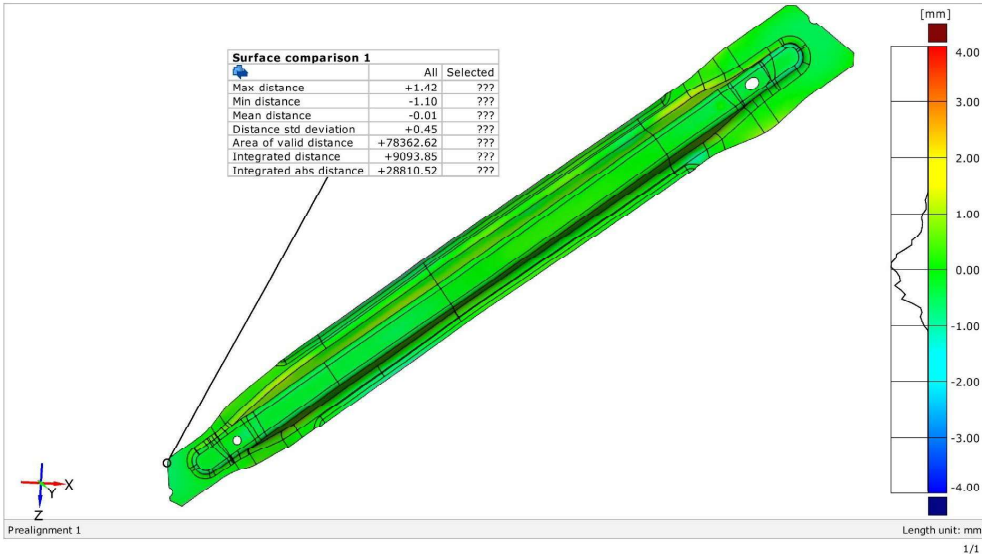


# CAD lower\_simulation 7

Generated with GOM Inspect V8



Surface Comparison on CAD

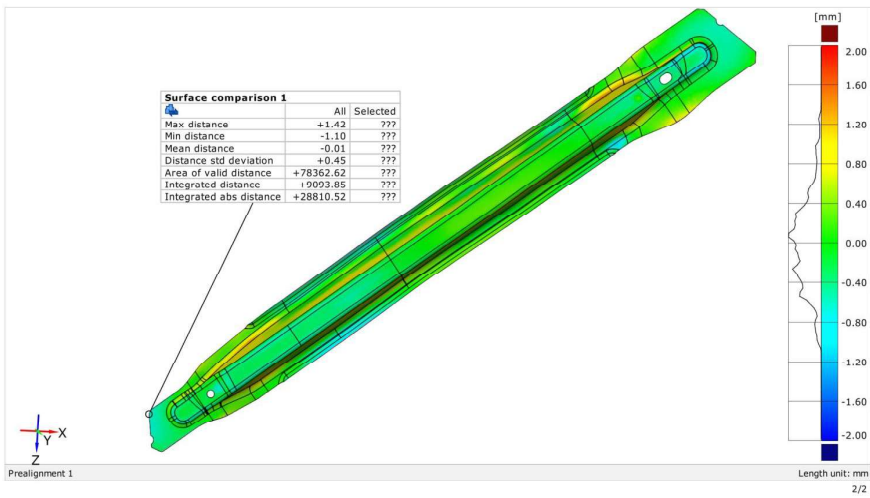


# CAD lower\_simulation 7

Generated with GOM Inspect V8



Surface Comparison on CAD

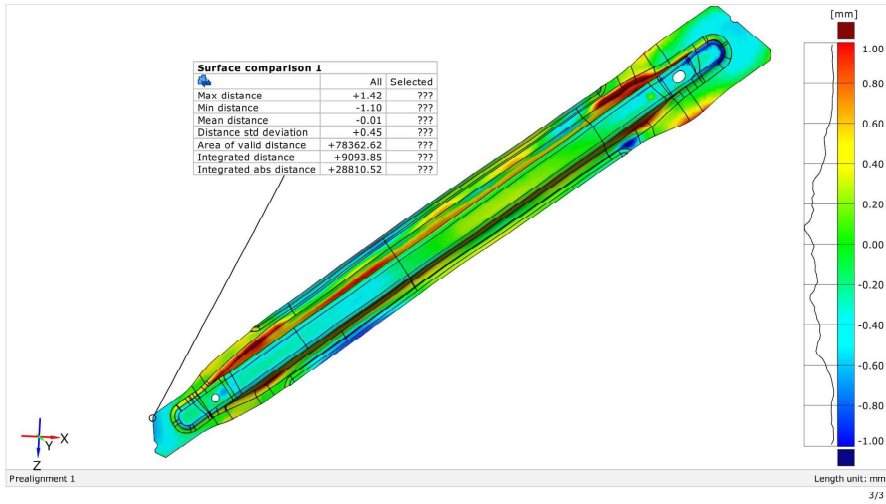


# CAD lower\_simulation 7

Generated with GOM Inspect V8



## Surface Comparison on CAD

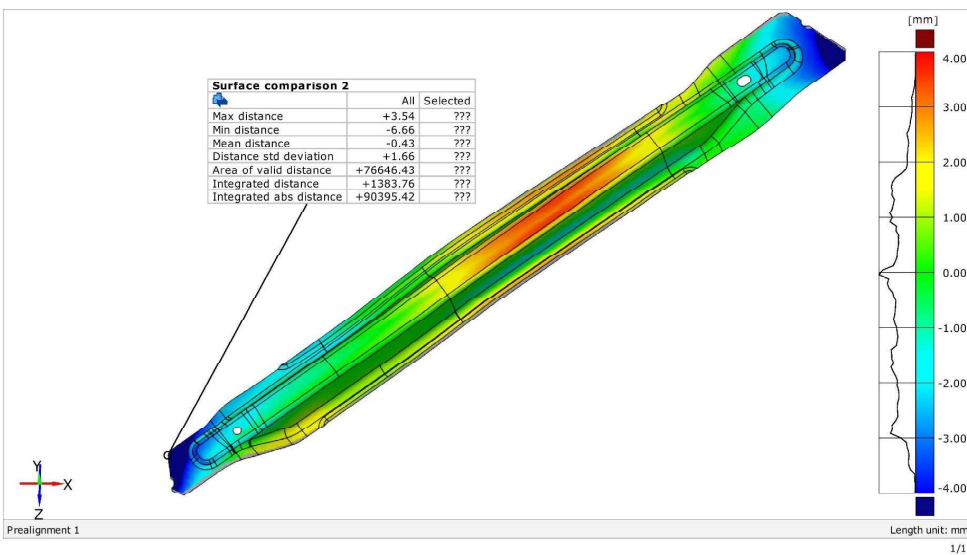


# CAD lower\_simulation 8

Generated with GOM Inspect V8



## Surface Comparison on CAD

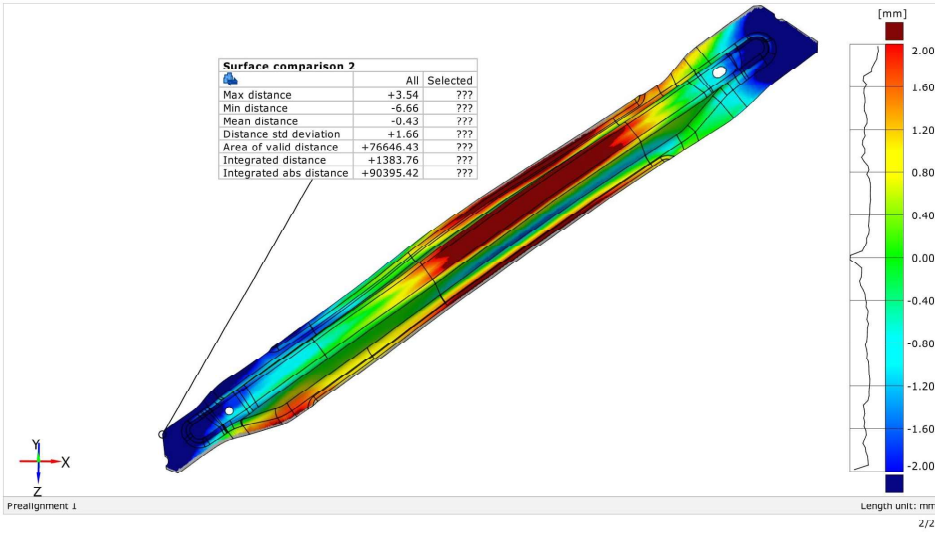


# CAD lower\_simulation 8

Generated with GOM Inspect V8



## Surface Comparison on CAD

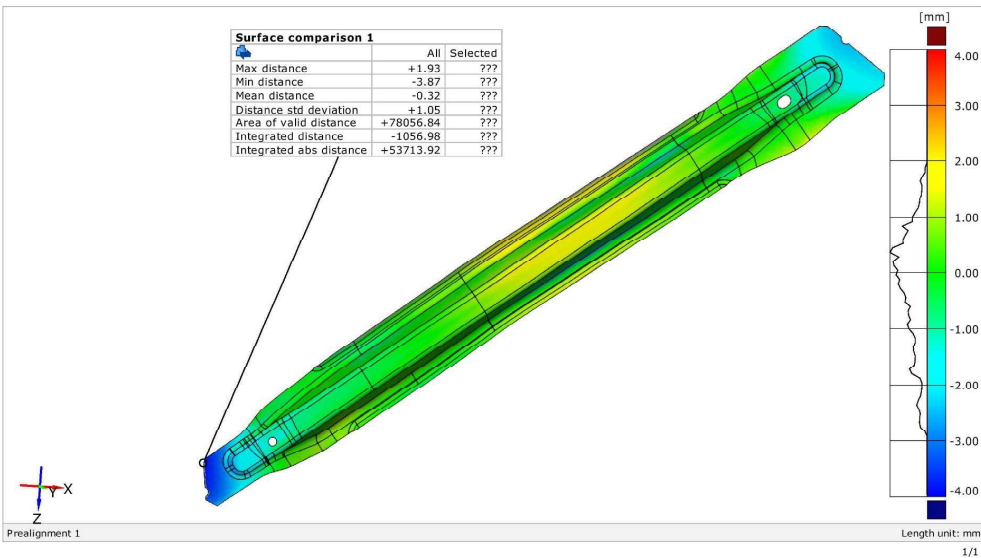


# CAD lower\_simulation 9

Generated with GOM Inspect V8



## Surface Comparison on CAD

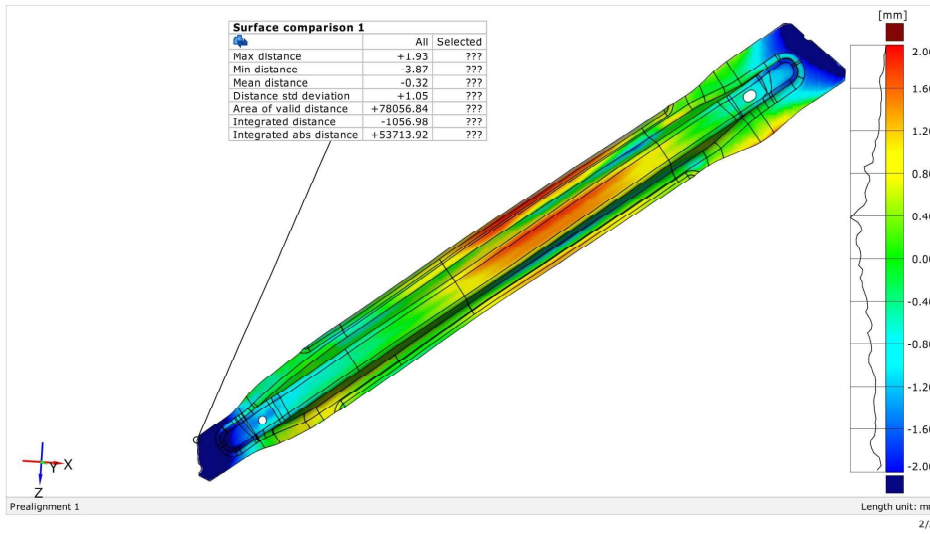


# CAD lower simulation 9

Generated with GOM Inspect V8



## Surface Comparison on CAD

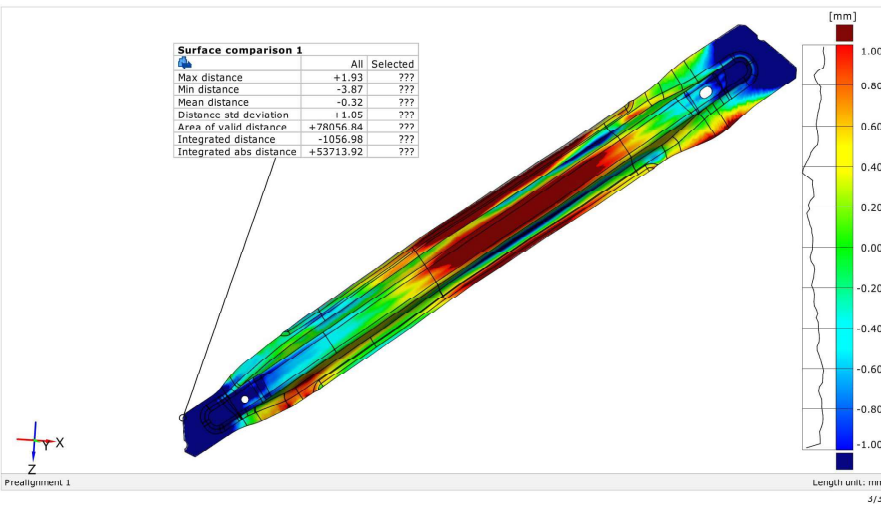


# CAD lower\_simulation 9

Generated with GOM Inspect V8



## Surface Comparison on CAD

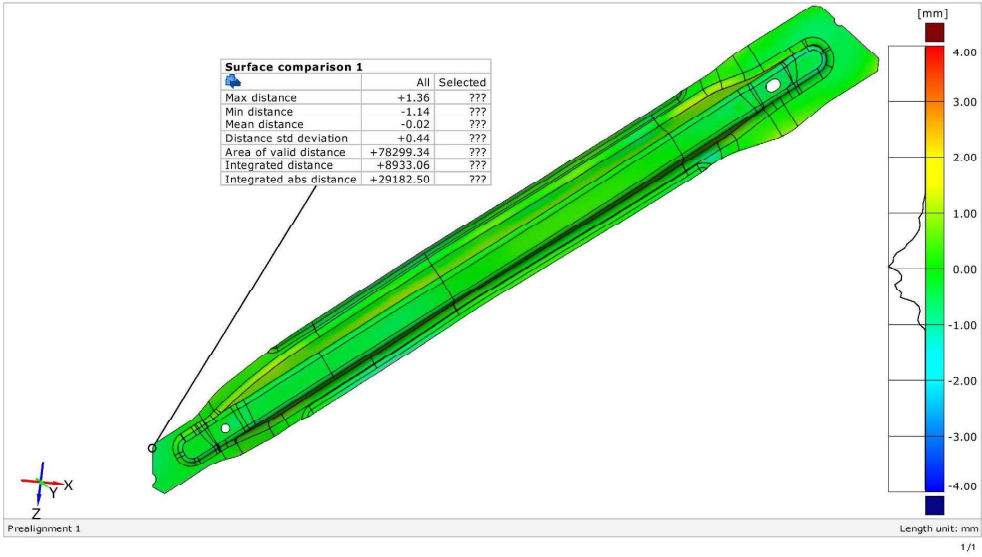


# CAD lower\_simulation 10

Generated with GOM Inspect V8



## Surface Comparison on CAD

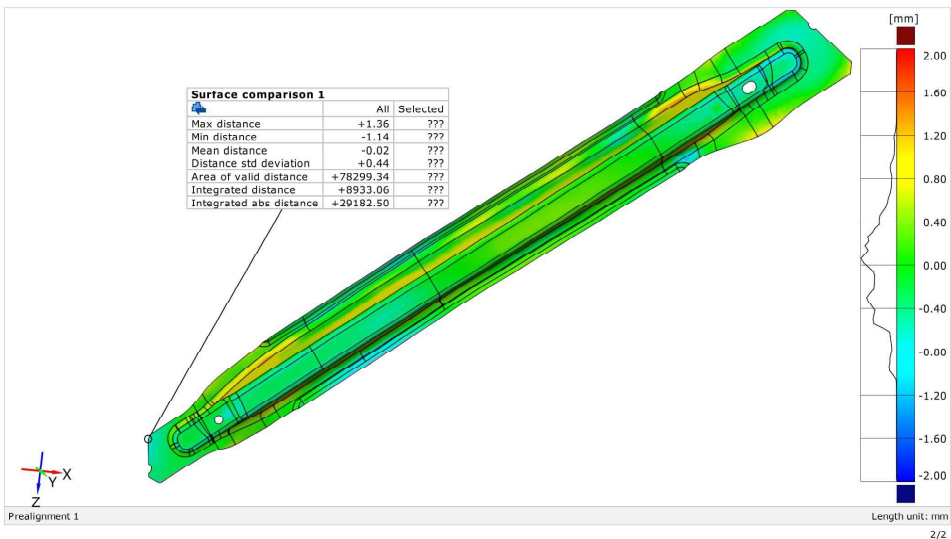


# CAD lower\_simulation 10

Generated with GOM Inspect V8



## Surface Comparison on CAD

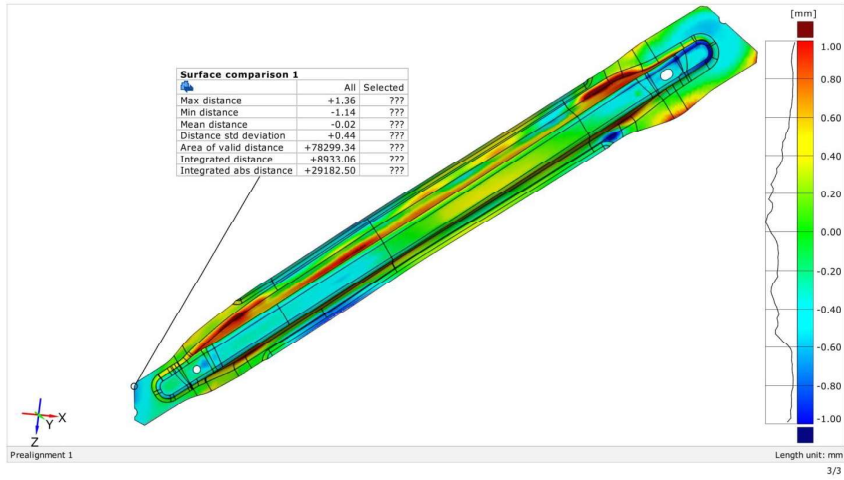


# CAD lower\_simulation 10

Generated with GOM Inspect V8



Surface Comparison on CAD

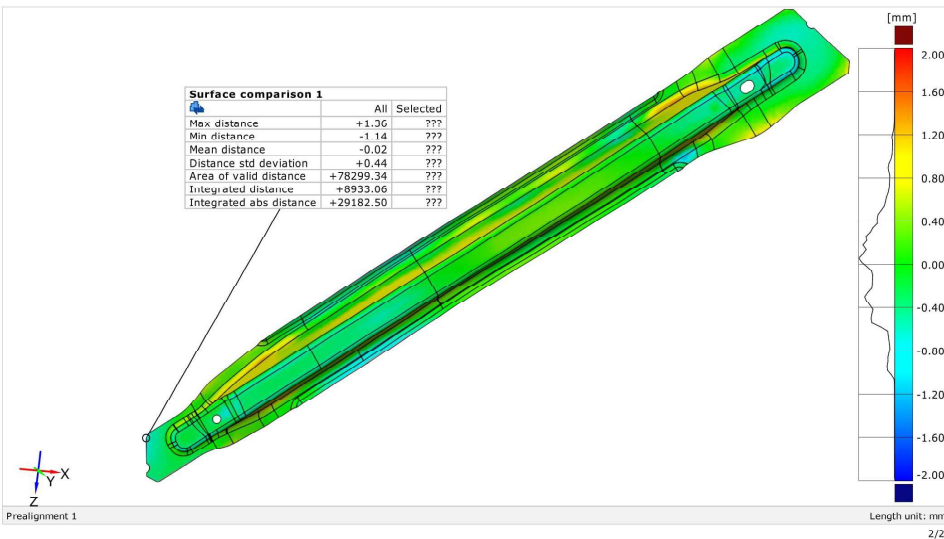


# CAD lower\_simulation 10

Generated with GOM Inspect V8



Surface Comparison on CAD

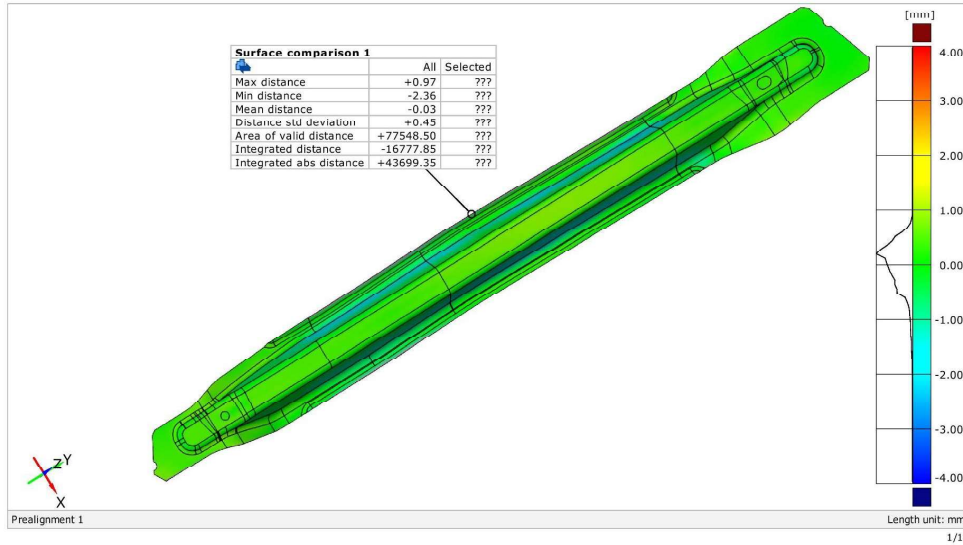


# CAD average\_simulation 1

Generated with GOM Inspect V8



Surface Comparison on CAD

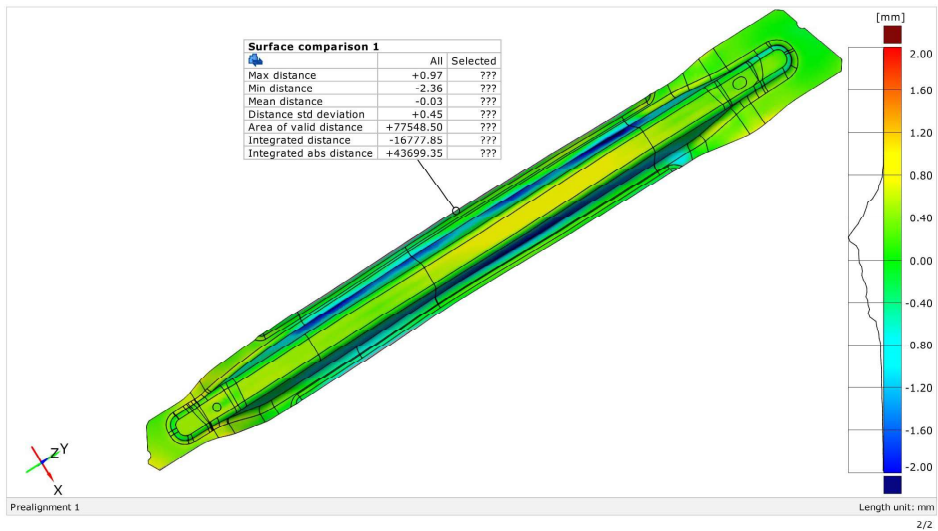


# CAD average\_simulation 1

Generated with GOM Inspect V8



Surface Comparison on CAD

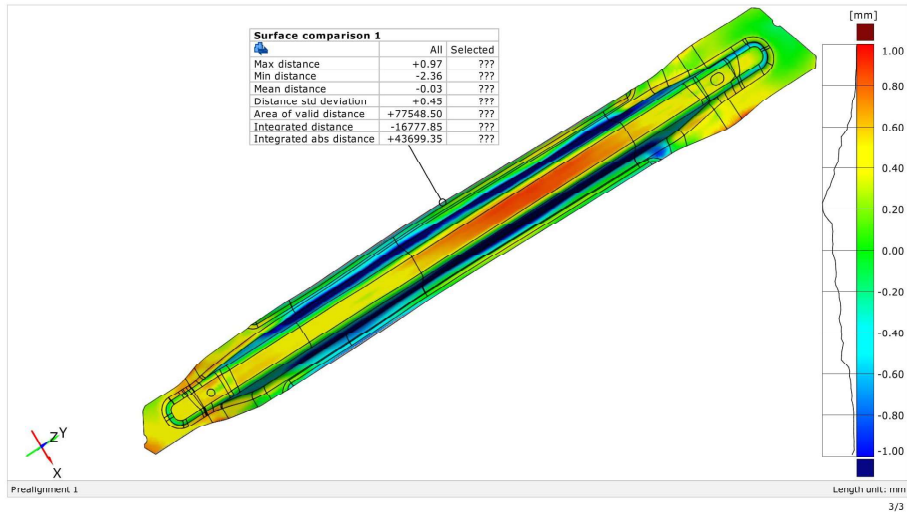


## CAD average\_simulation 1

Generated with GOM Inspect V8

gom

Surface Comparison on CAD

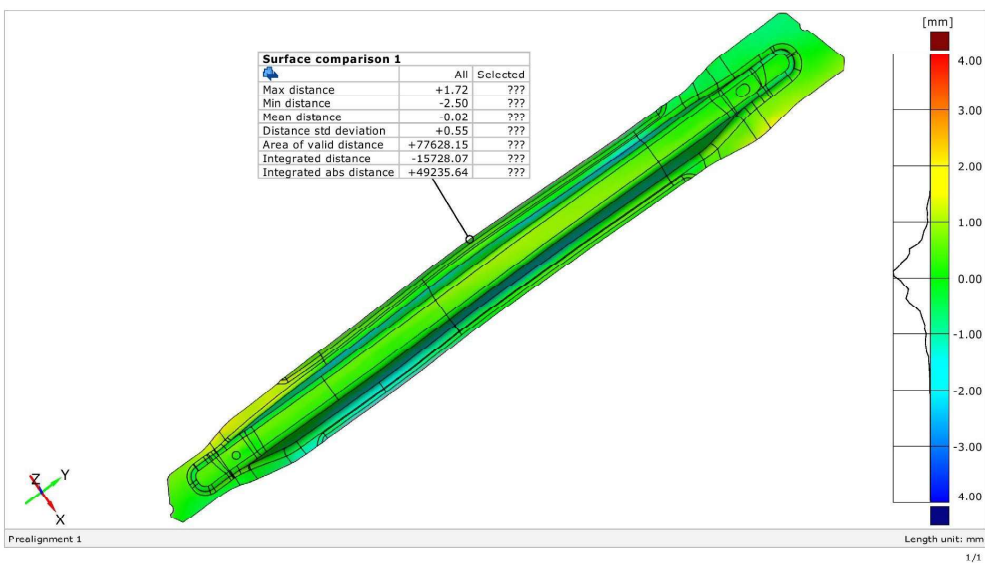


## CAD average\_simulation 2

Generated with GOM Inspect V8

gom

Surface Comparison on CAD

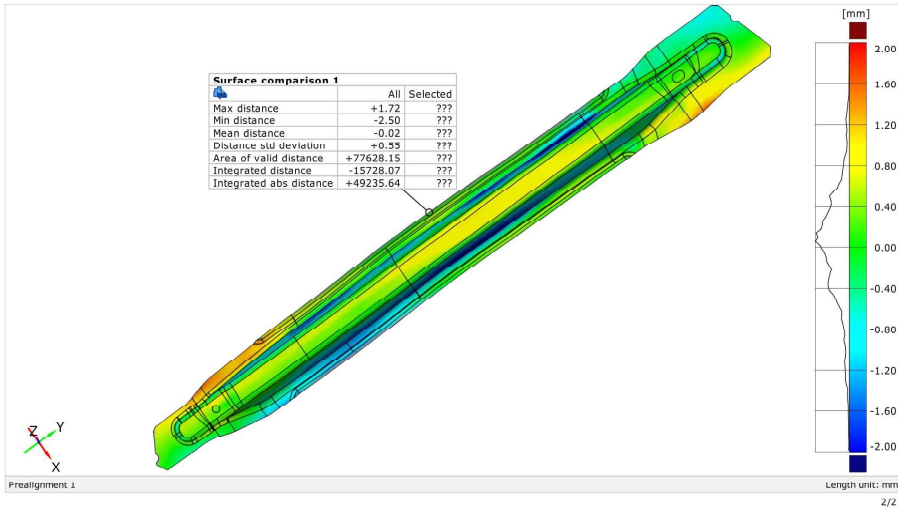


# CAD average\_simulation 2

Generated with GOM Inspect V8



Surface Comparison on CAD

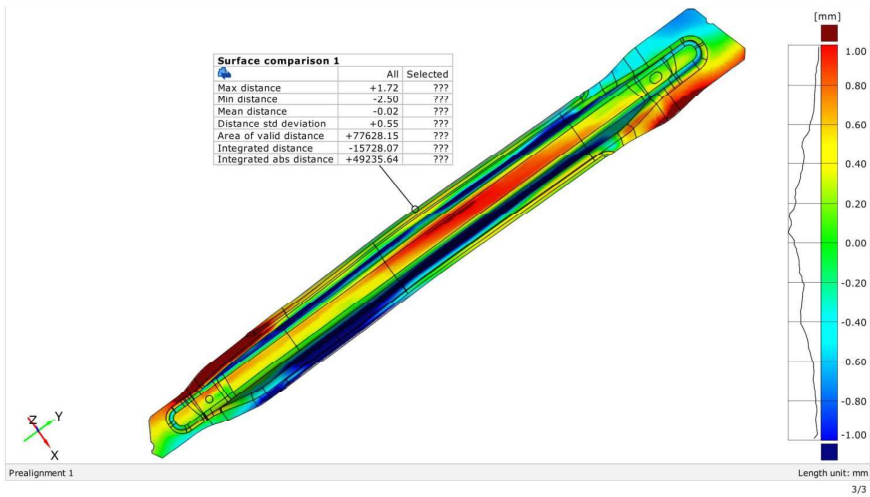


# CAD average\_simulation 2

Generated with GOM Inspect V8



Surface Comparison on CAD

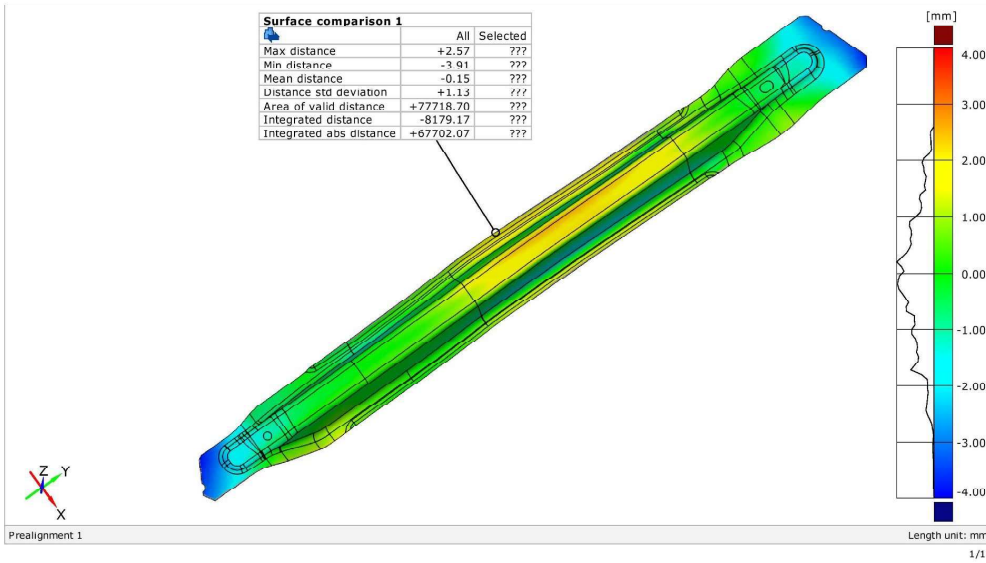


# CAD average\_simulation 3

Generated with GOM Inspect V8



Surface Comparison on CAD

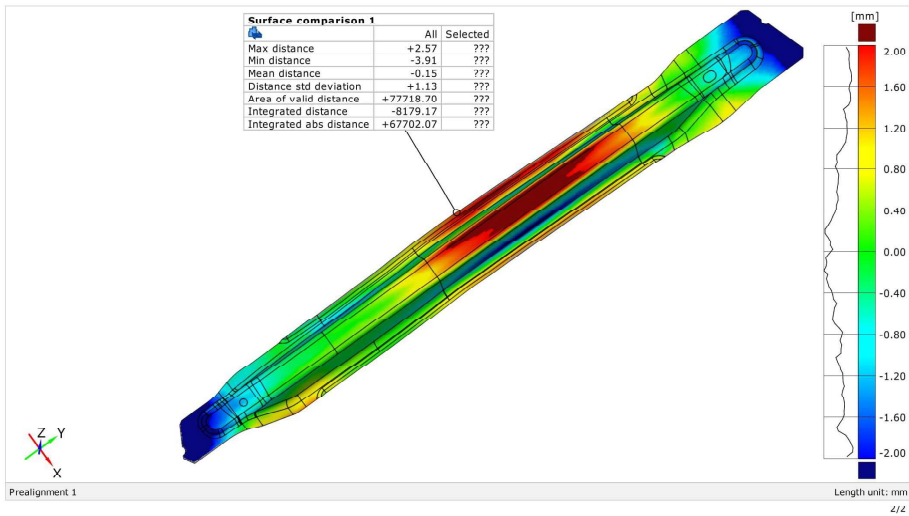


# CAD average\_simulation 3

Generated with GOM Inspect V8



Surface Comparison on CAD

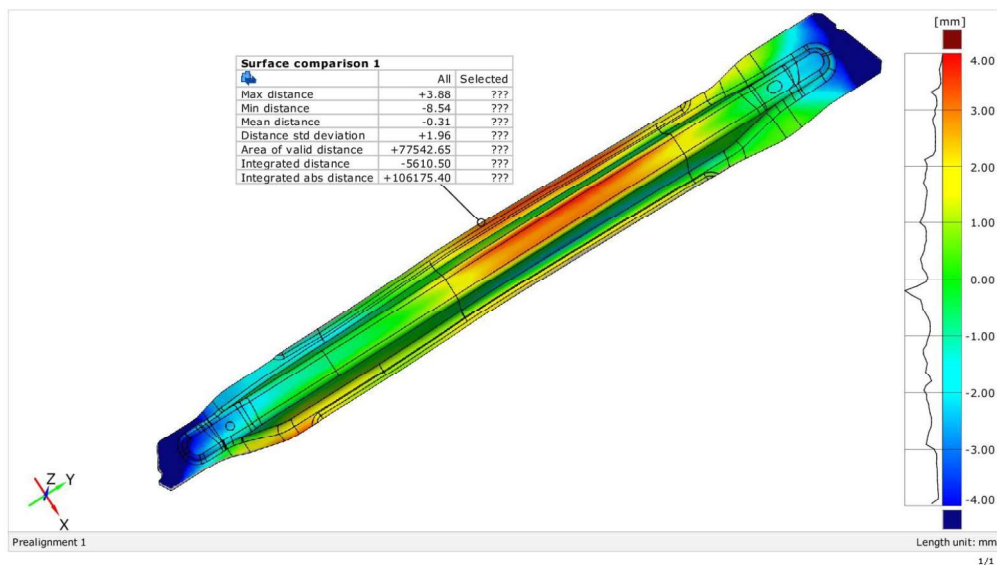


# CAD average\_simulation 4

Generated with GOM Inspect V8



Surface Comparison on CAD

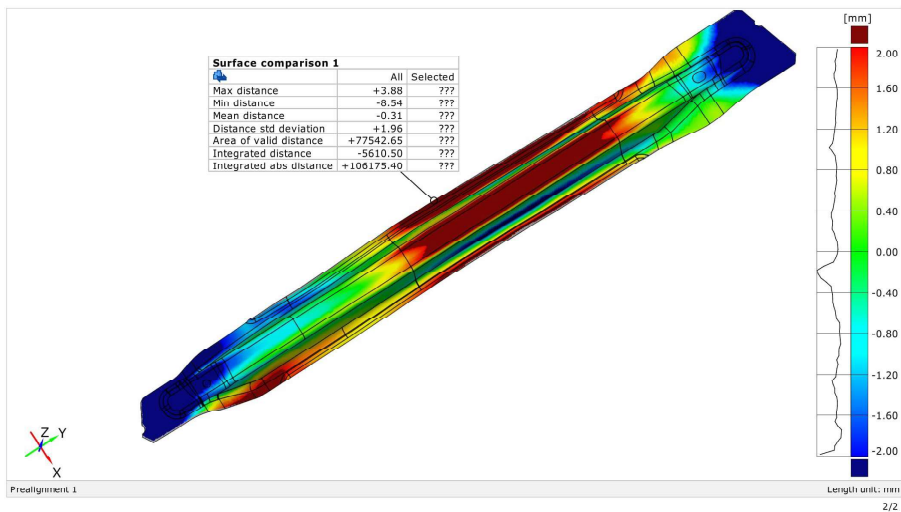


# CAD average\_simulation 4

Generated with GOM Inspect V8



Surface Comparison on CAD

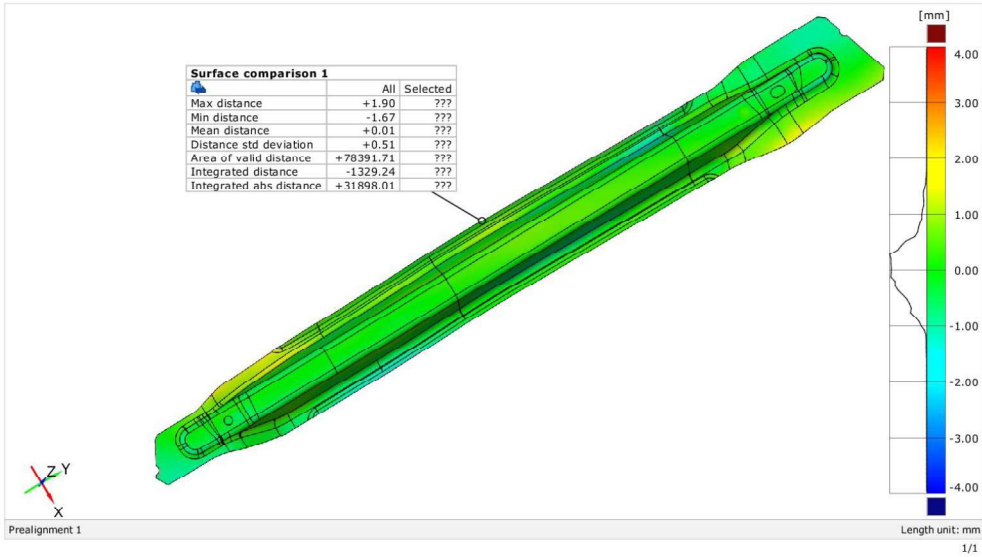


# CAD average\_simulation 5

Generated with GOM Inspect V8

gom

Surface Comparison on CAD

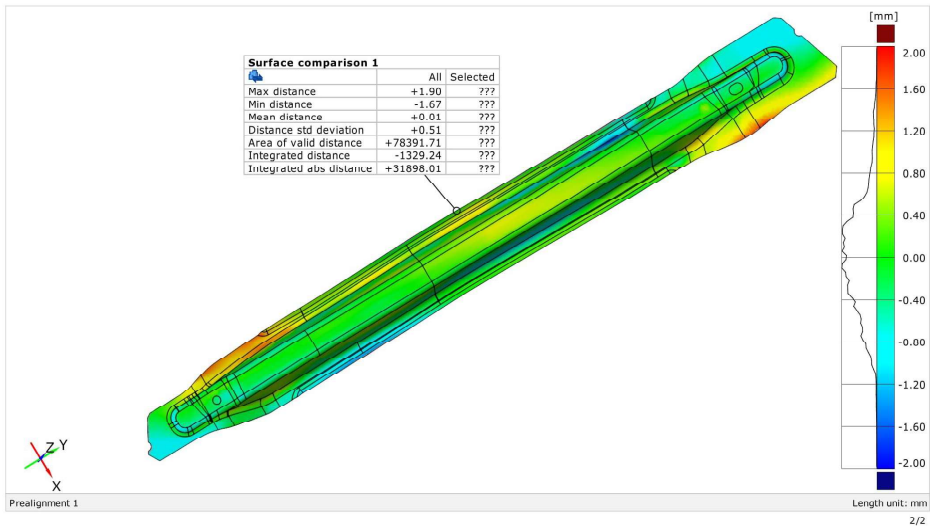


# CAD average\_simulation 5

Generated with GOM Inspect V8

gom

Surface Comparison on CAD

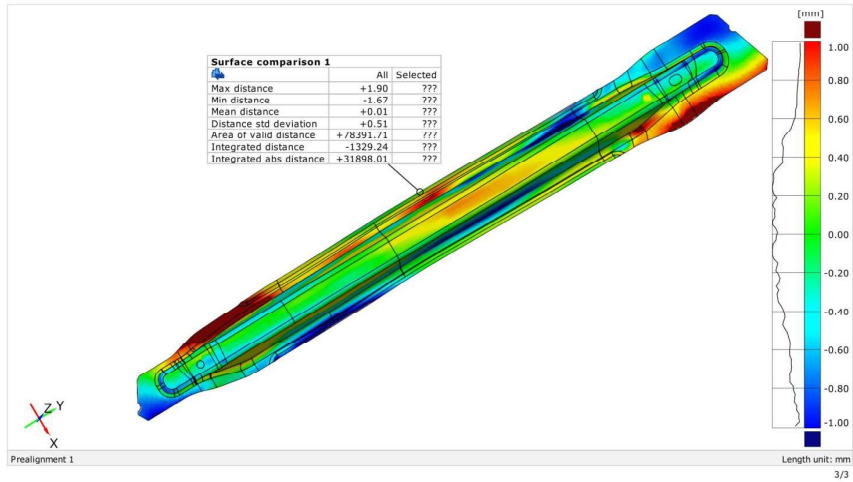


## CAD average\_simulation 5

Generated with GOM Inspect V8

gom

Surface Comparison on CAD

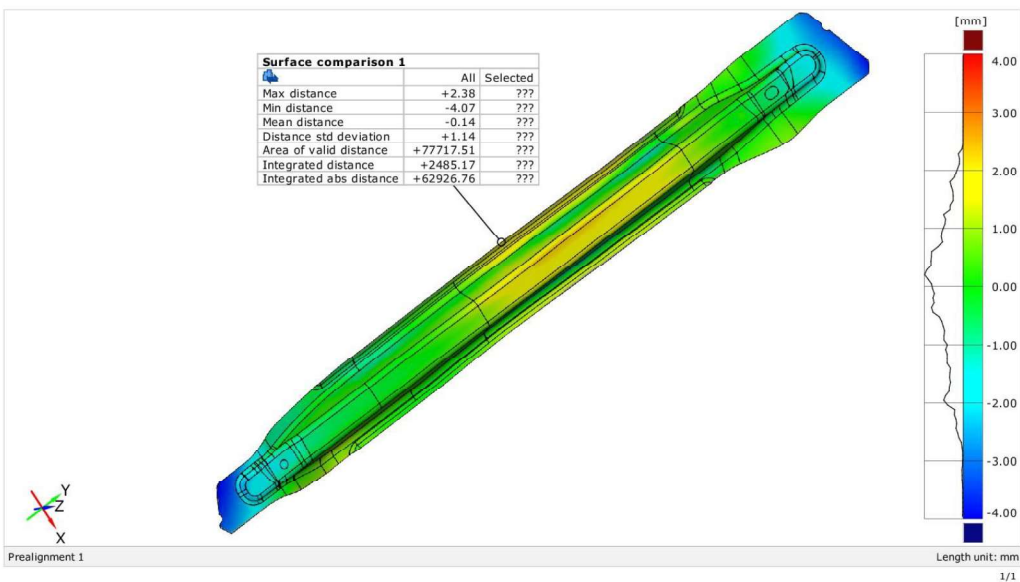


## CAD average\_simulation 6

Generated with GOM Inspect V8

gom

Surface Comparison on CAD

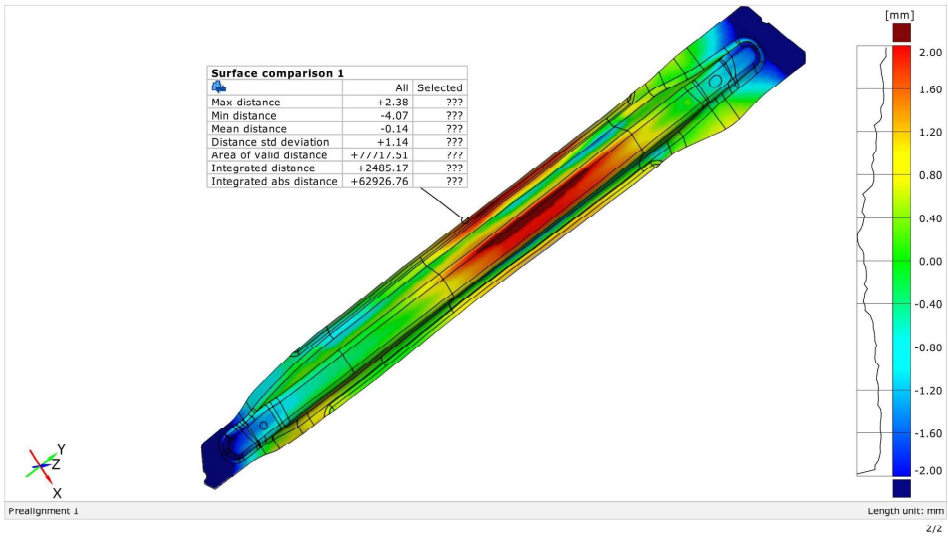


# CAD average\_simulation 6

Generated with GOM Inspect V8



## Surface Comparison on CAD

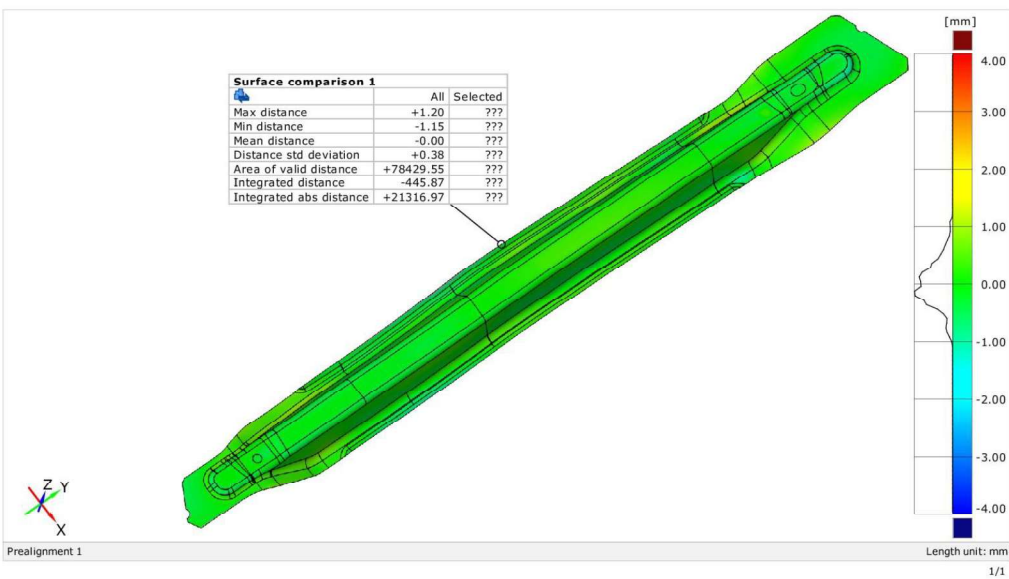


# CAD average\_simulation 7

Generated with GOM Inspect V8



## Surface Comparison on CAD

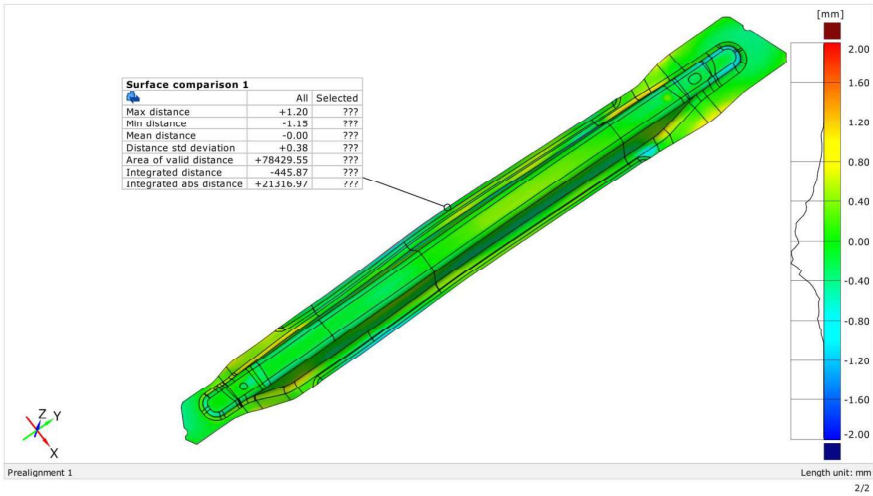


# CAD average\_simulation 7

Generated with GOM Inspect V8



Surface Comparison on CAD

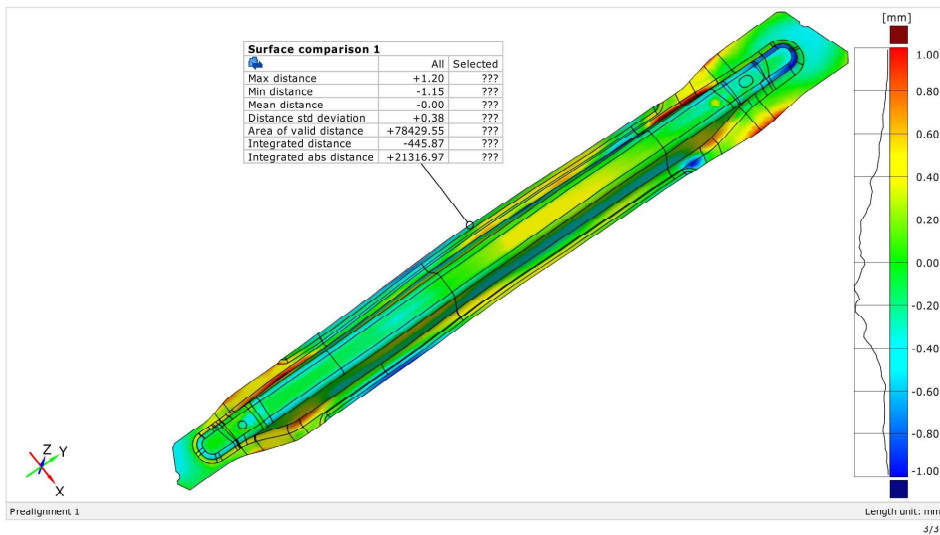


# CAD average\_simulation 7

Generated with GOM Inspect V8



Surface Comparison on CAD

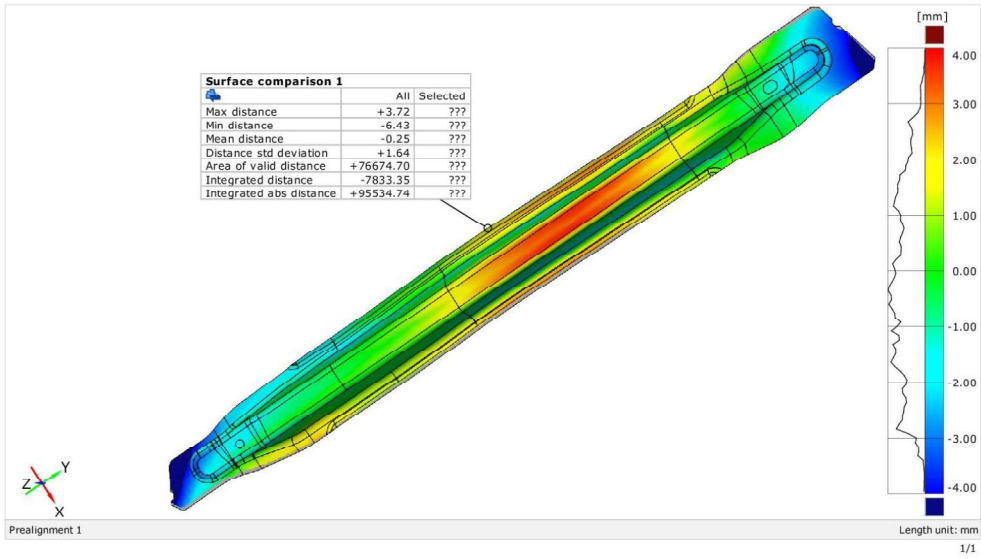


# CAD average\_simulation 8

Generated with GOM Inspect V8



Surface Comparison on CAD

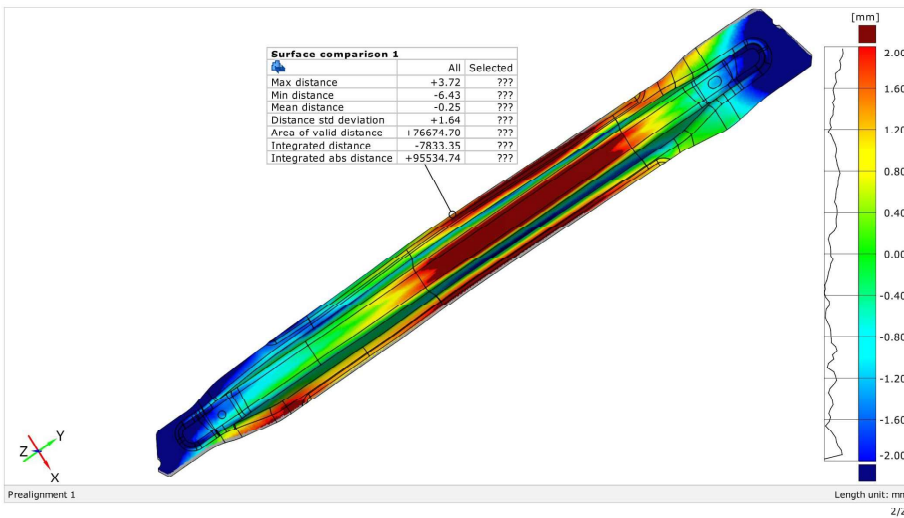


# CAD average\_simulation 8

Generated with GOM Inspect V8



Surface Comparison on CAD

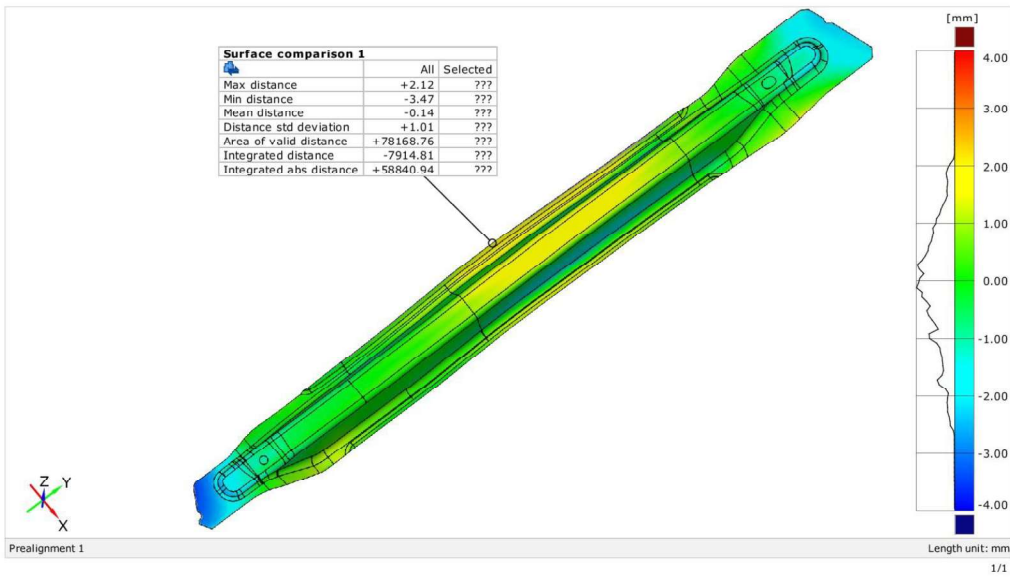


# CAD average\_simulation 9

Generated with GOM Inspect V8



## Surface Comparison on CAD

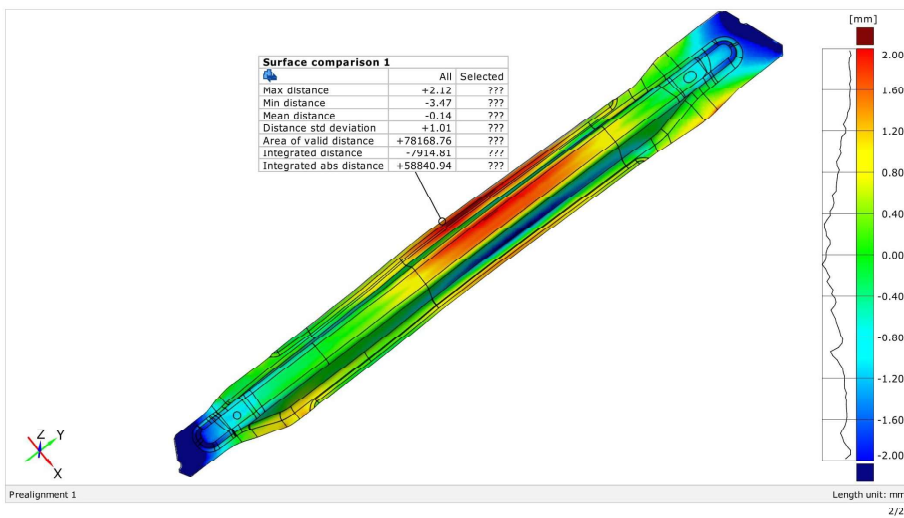


# CAD average\_simulation 9

Generated with GOM Inspect V8



## Surface Comparison on CAD

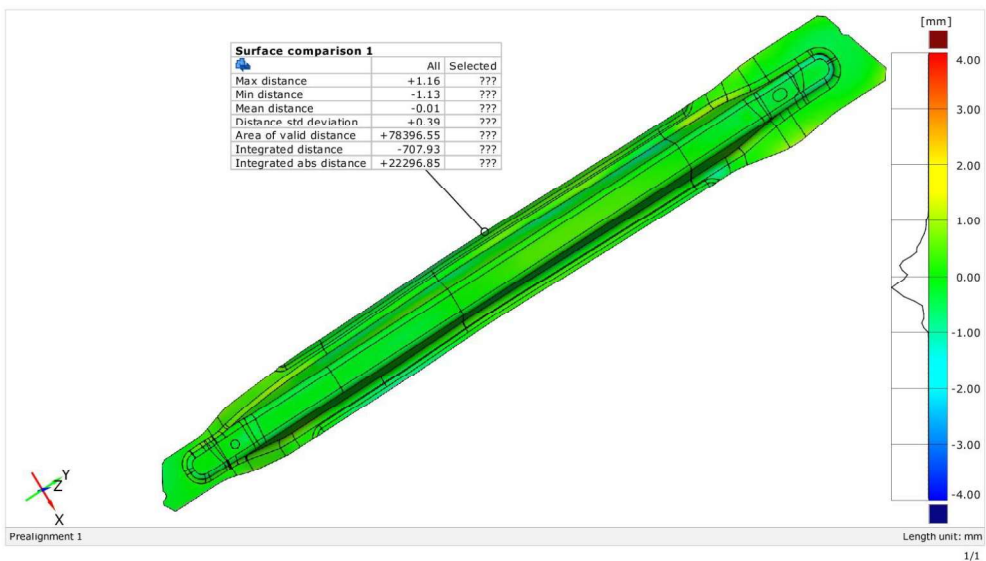


# CAD average\_simulation 10

Generated with GOM Inspect V8



Surface Comparison on CAD

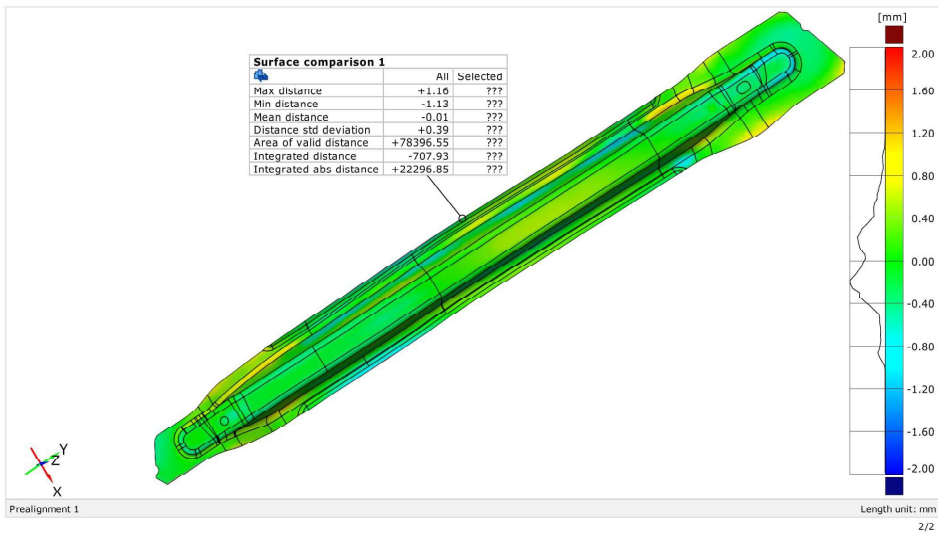


# CAD average\_simulation 10

Generated with GOM Inspect V8



Surface Comparison on CAD

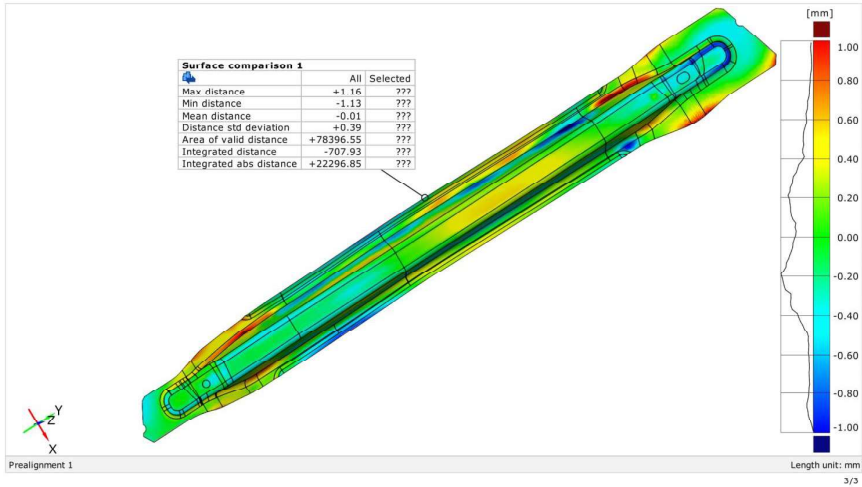


# CAD average\_simulation 10

Generated with GOM Inspect V8



Surface Comparison on CAD

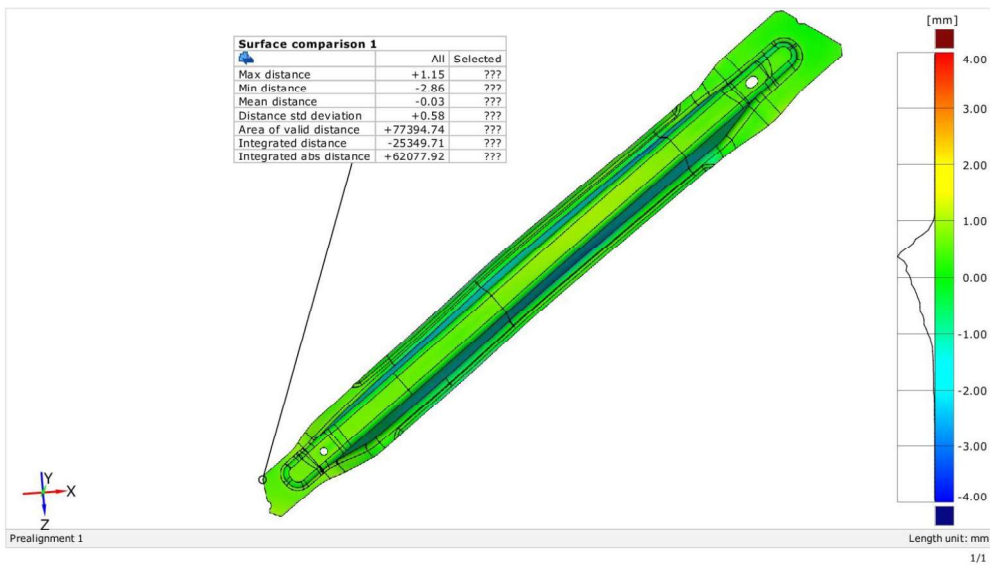


# CAD higher\_simulation 1

Generated with GOM Inspect V8



Surface Comparison on CAD

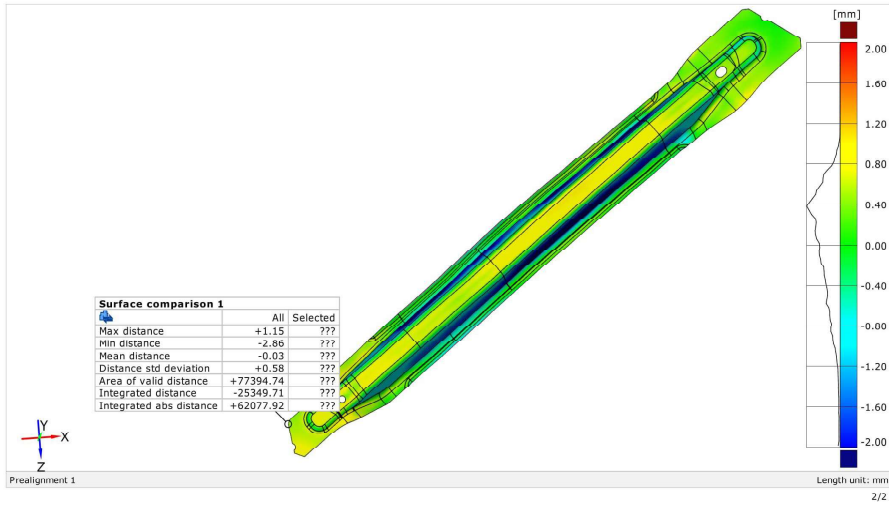


# CAD higher\_simulation 1

Generated with GOM Inspect V8



Surface Comparison on CAD

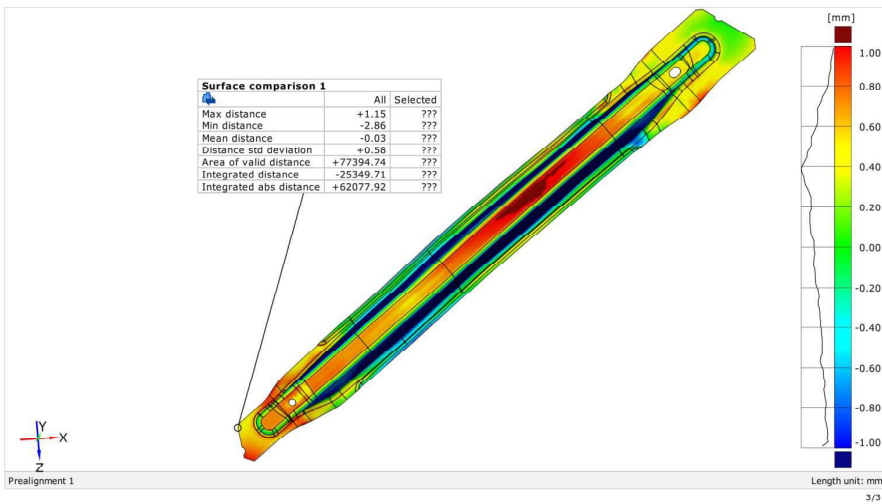


# CAD higher\_simulation 1

Generated with GOM Inspect V8



Surface Comparison on CAD

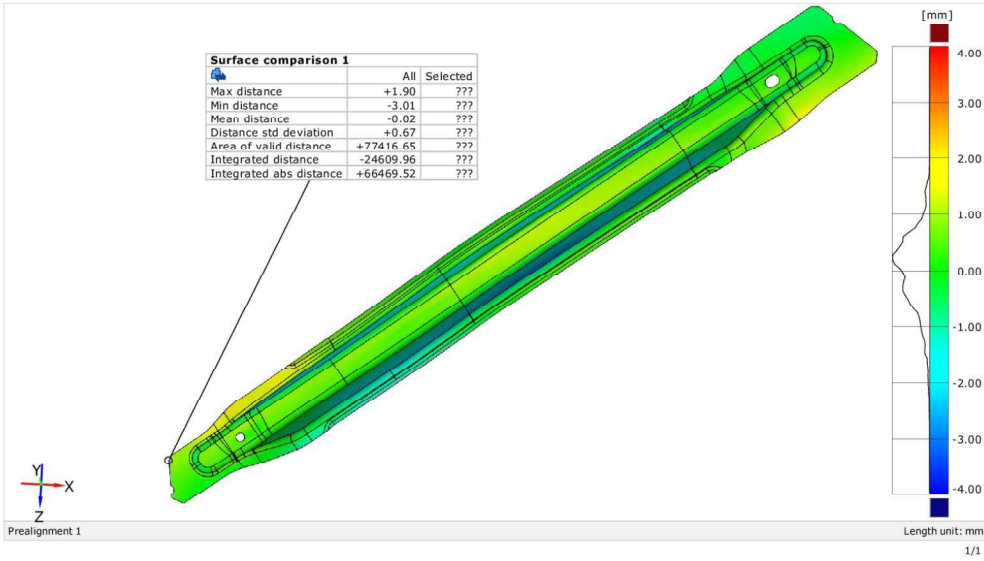


## CAD higher\_simulation 2

Generated with GOM Inspect V8

gom

Surface Comparison on CAD

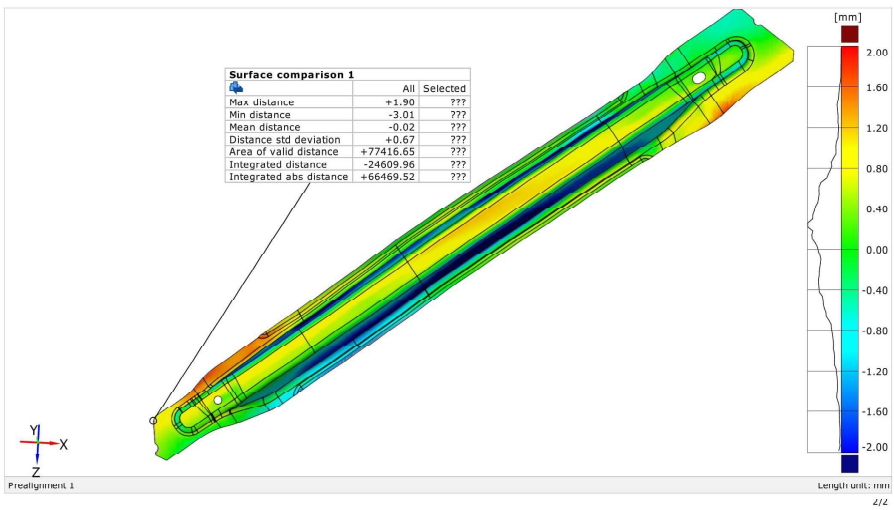


## CAD higher\_simulation 2

Generated with GOM Inspect V8

gom

Surface Comparison on CAD

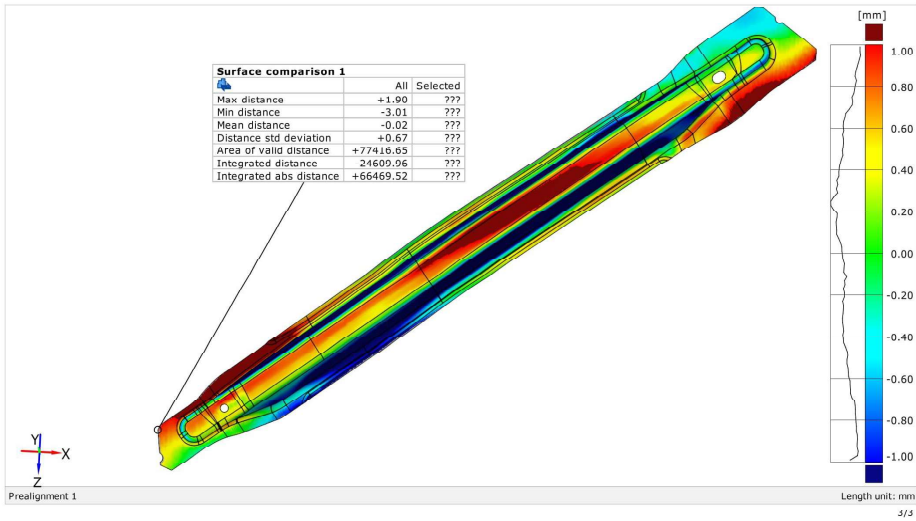


## CAD higher\_simulation 2

Generated with GOM Inspect V8

gom

Surface Comparison on CAD

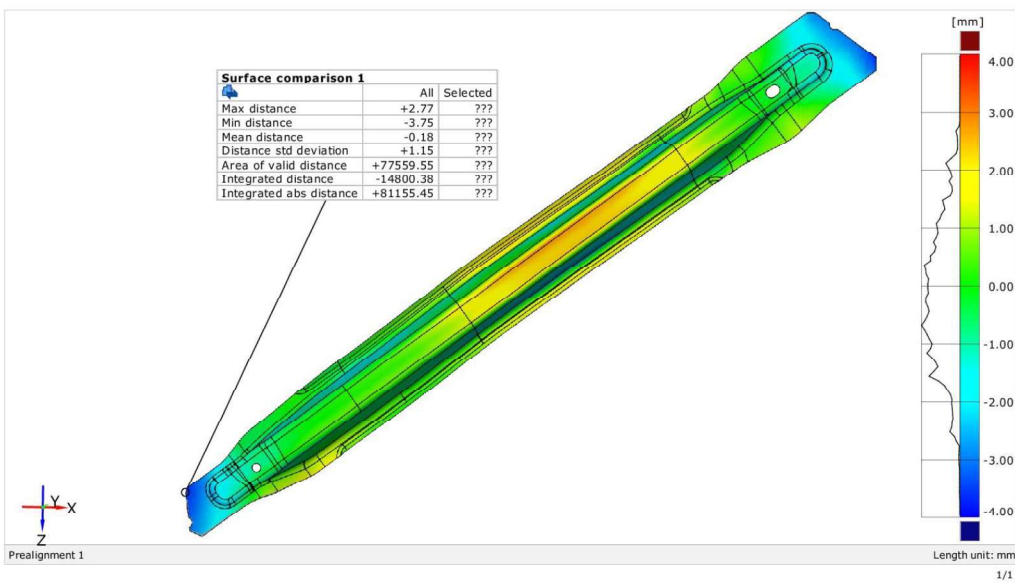


## CAD higher\_simulation 3

Generated with GOM Inspect V8

gom

Surface Comparison on CAD

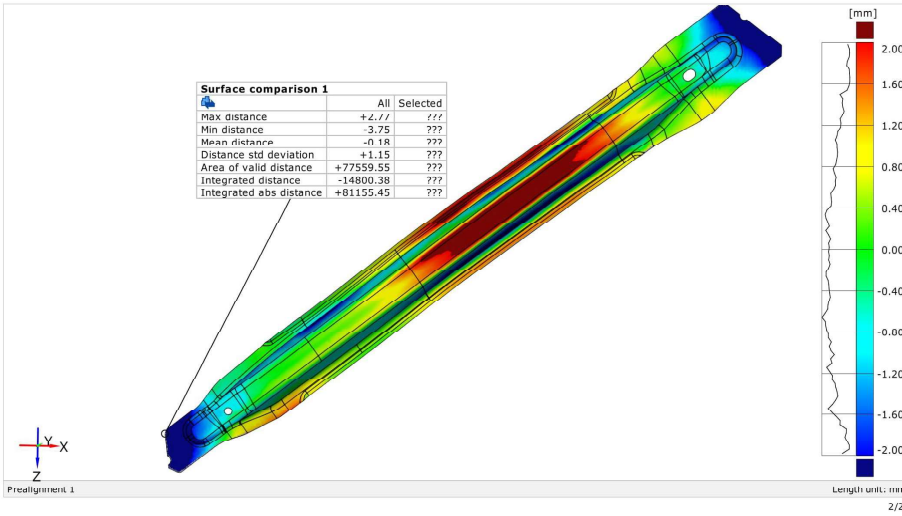


### CAD higher\_simulation 3

Generated with GOM Inspect V8



Surface Comparison on CAD

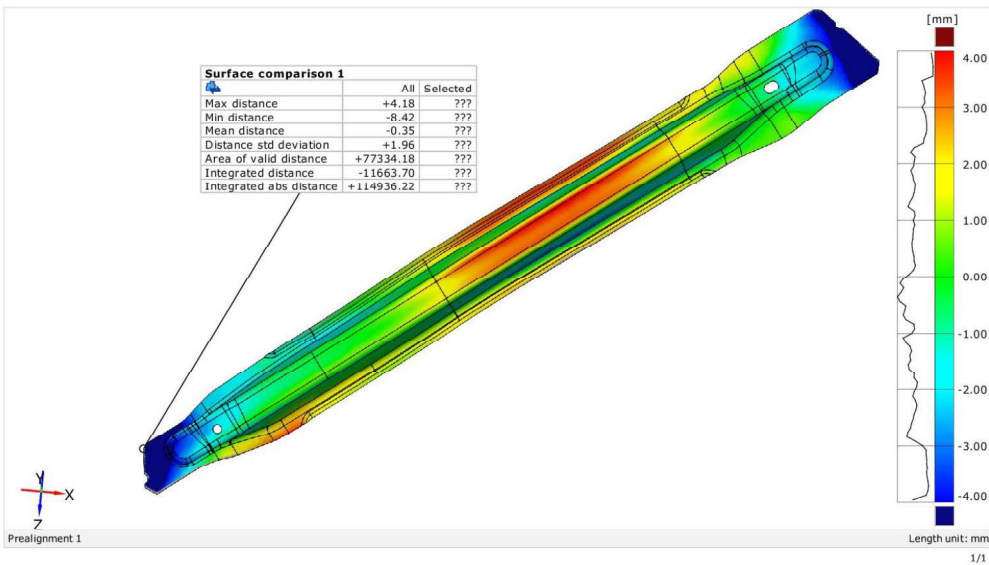


### CAD higher\_simulation 4

Generated with GOM Inspect V8



Surface Comparison on CAD

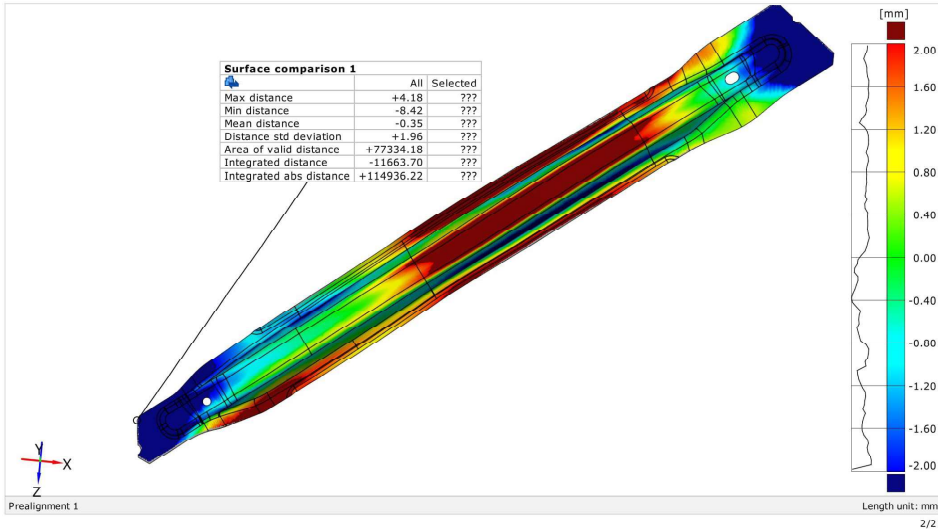


# CAD higher\_simulation 4

Generated with GOM Inspect V8



## Surface Comparison on CAD

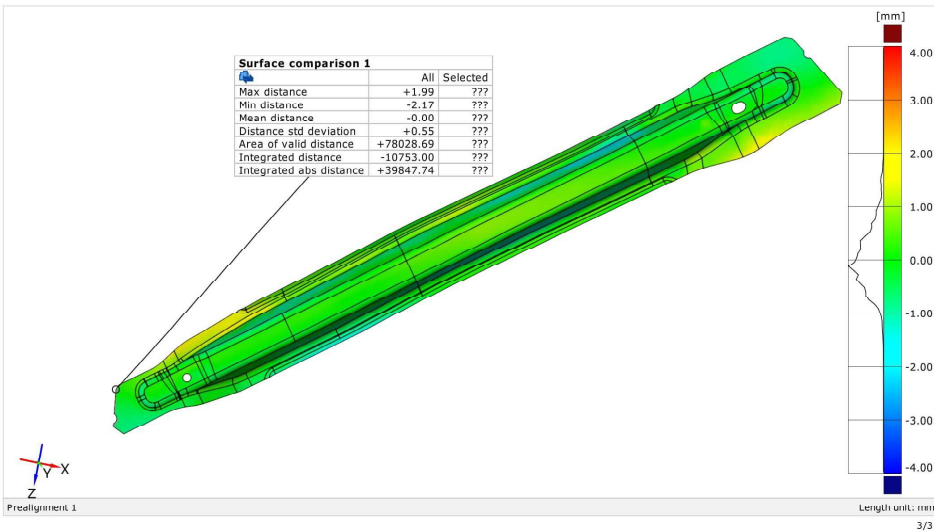


# CAD higher\_simulation 5

Generated with GOM Inspect V8



## Surface Comparison on CAD

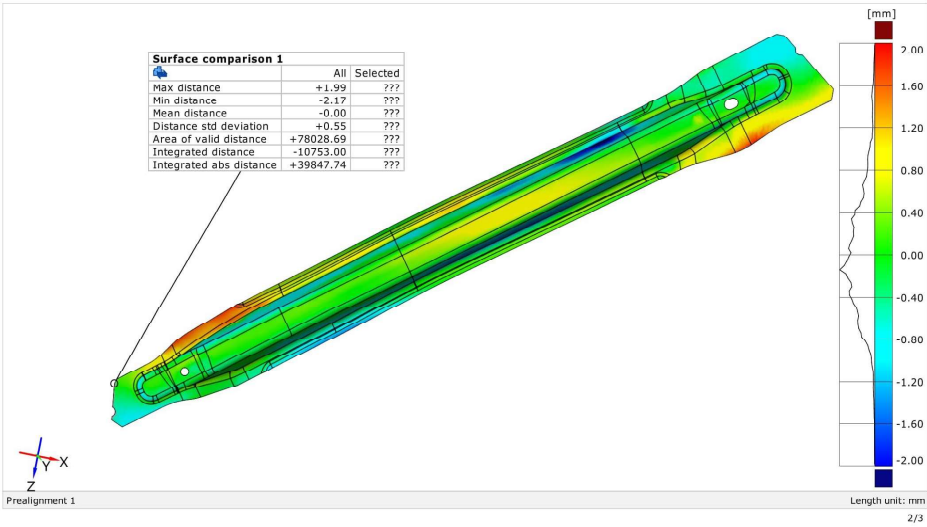


# CAD higher\_simulation 5

Generated with GOM Inspect V8



## Surface Comparison on CAD

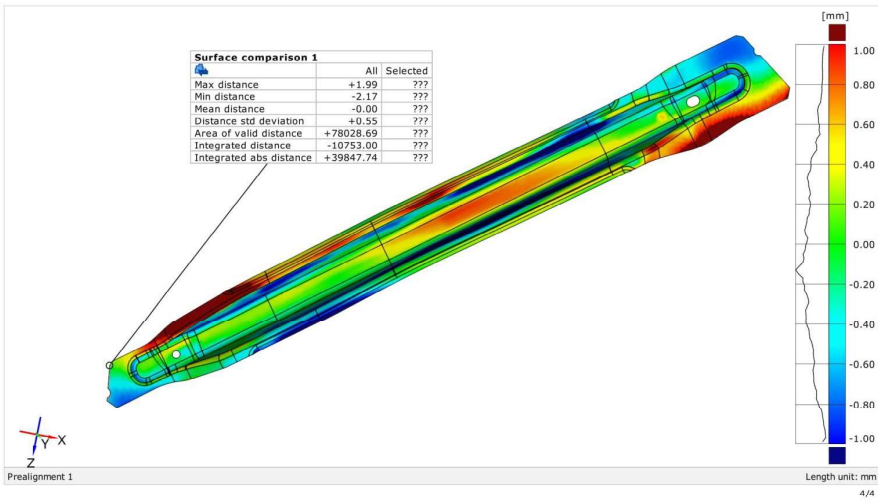


# CAD higher\_simulation 5

Generated with GOM Inspect V8



## Surface Comparison on CAD

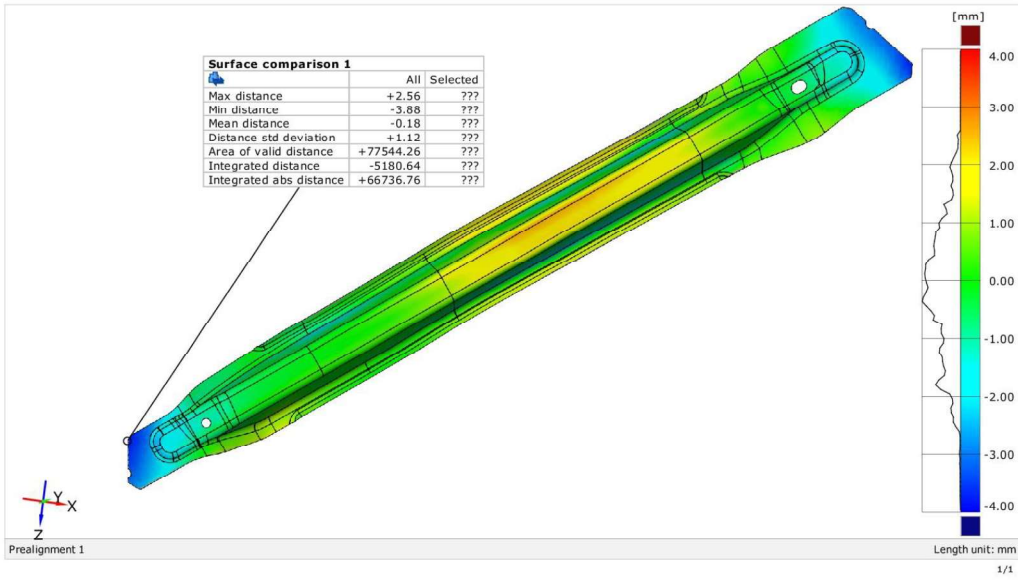


# CAD higher\_simulation 6

Generated with GOM Inspect V8



## Surface Comparison on CAD

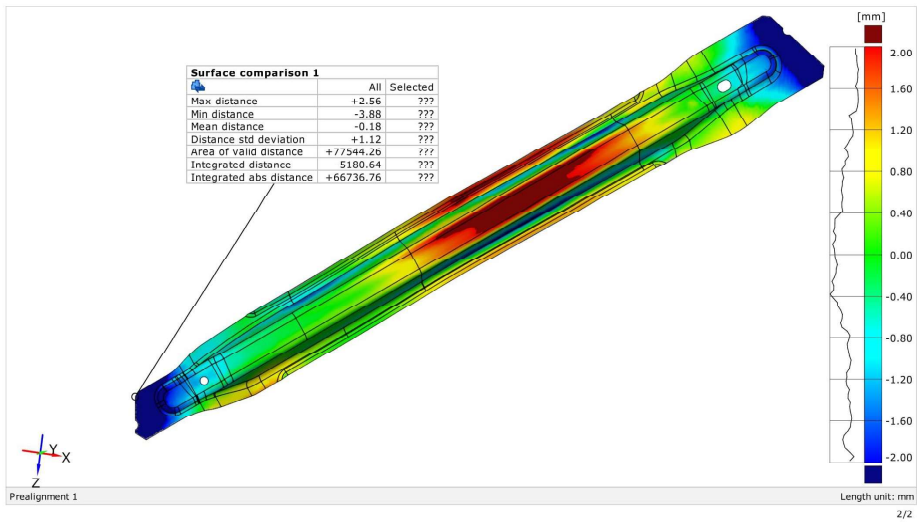


# CAD higher\_simulation 6

Generated with GOM Inspect V8



## Surface Comparison on CAD

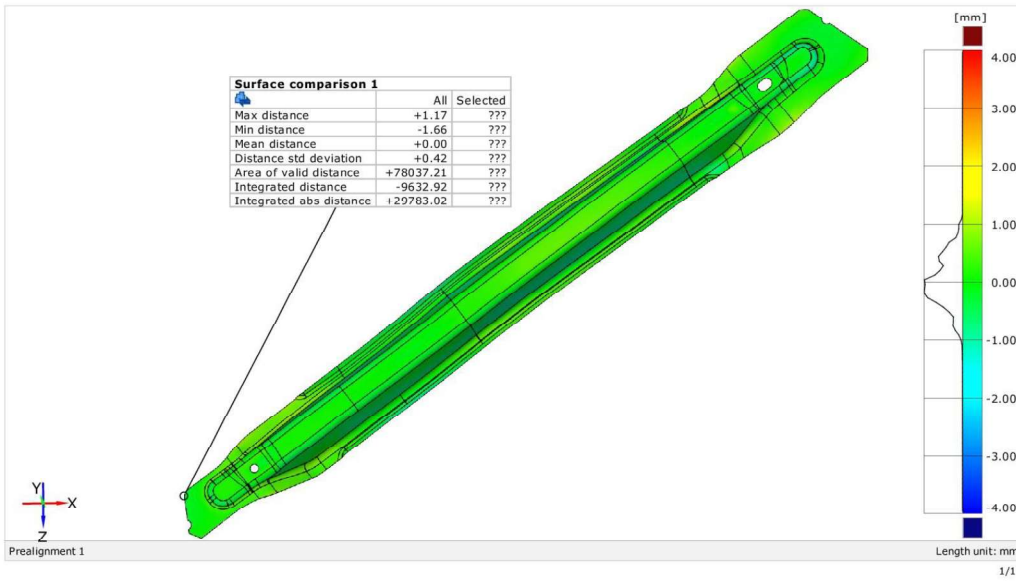


# CAD higher\_simulation 7

Generated with GOM Inspect V8



## Surface Comparison on CAD

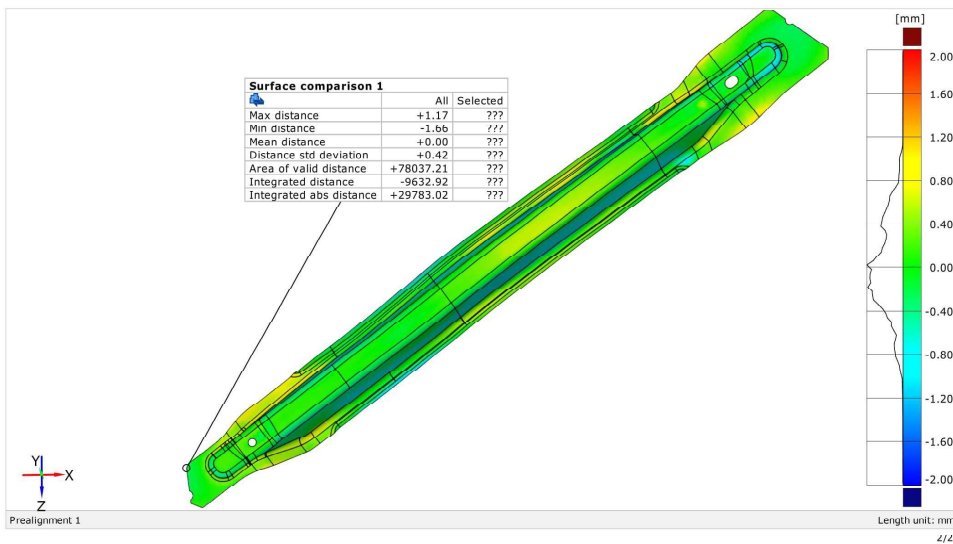


# CAD higher\_simulation 7

Generated with GOM Inspect V8



## Surface Comparison on CAD

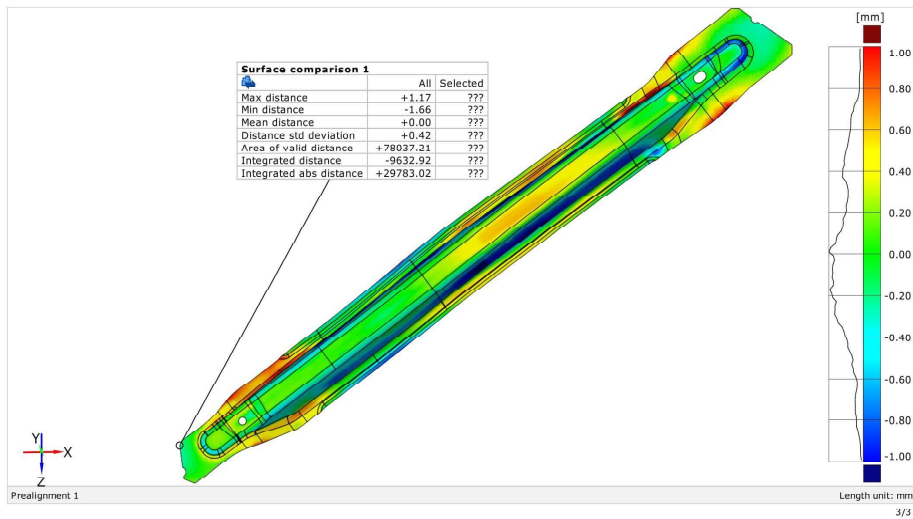


## CAD higher\_simulation 7

Generated with GOM Inspect V8

gom

Surface Comparison on CAD

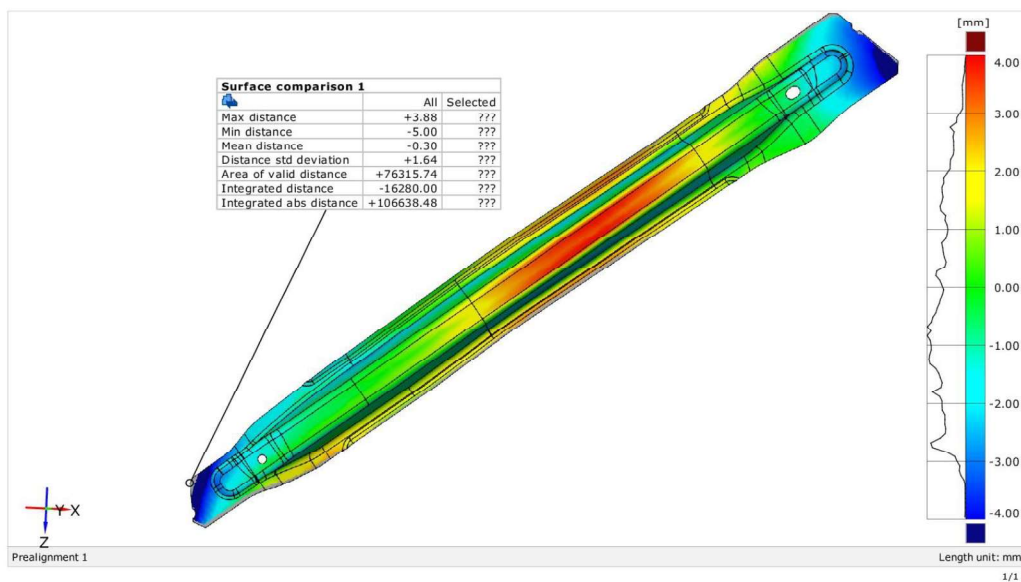


## CAD higher\_simulation 8

Generated with GOM Inspect V8

gom

Surface Comparison on CAD

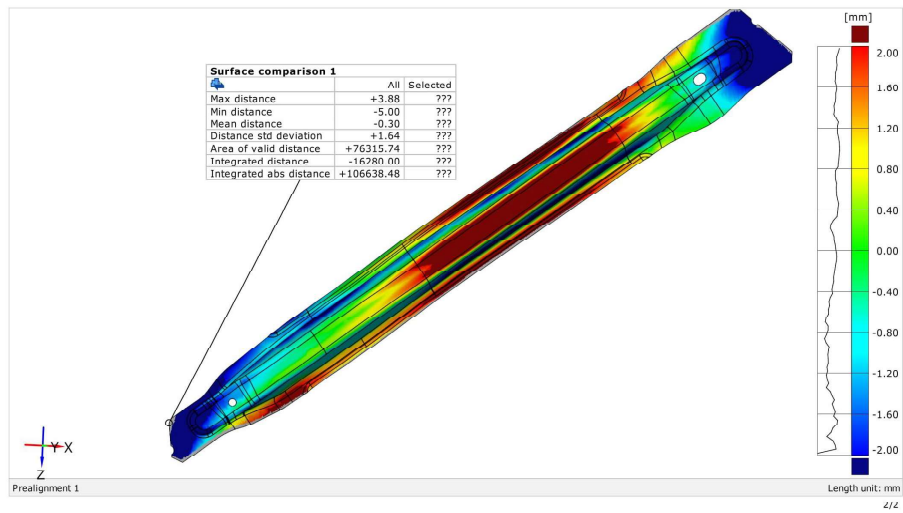


## CAD higher\_simulation 8

Generated with GOM Inspect V8

gom

Surface Comparison on CAD

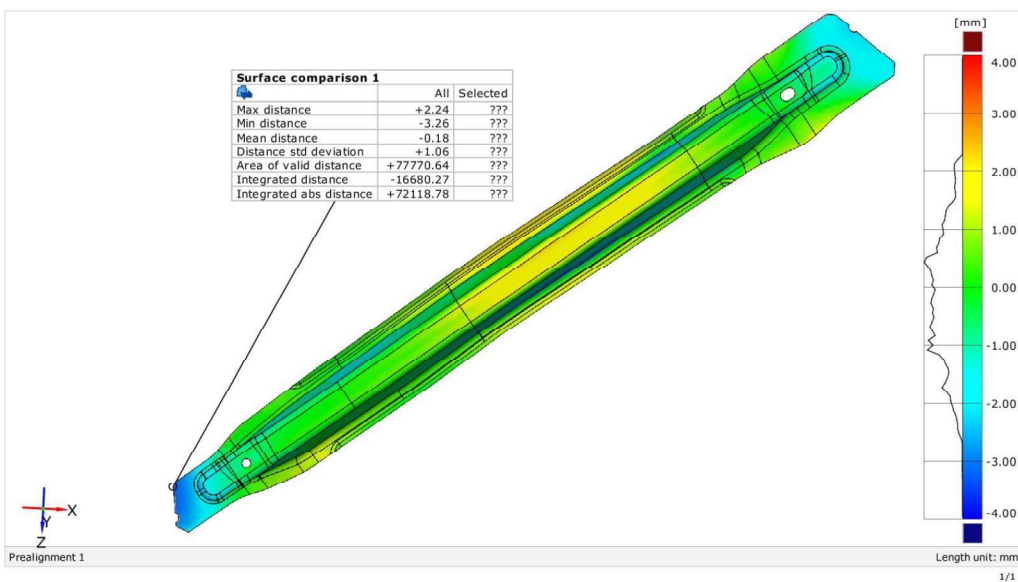


## CAD higher\_simulation 9

Generated with GOM Inspect V8

gom

Surface Comparison on CAD

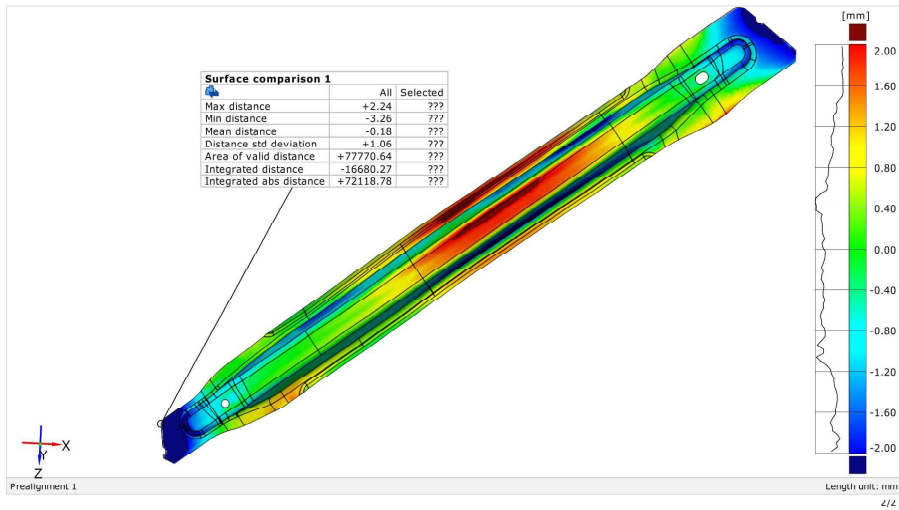


## CAD higher\_simulation 9

Generated with GOM Inspect V8

gom

Surface Comparison on CAD

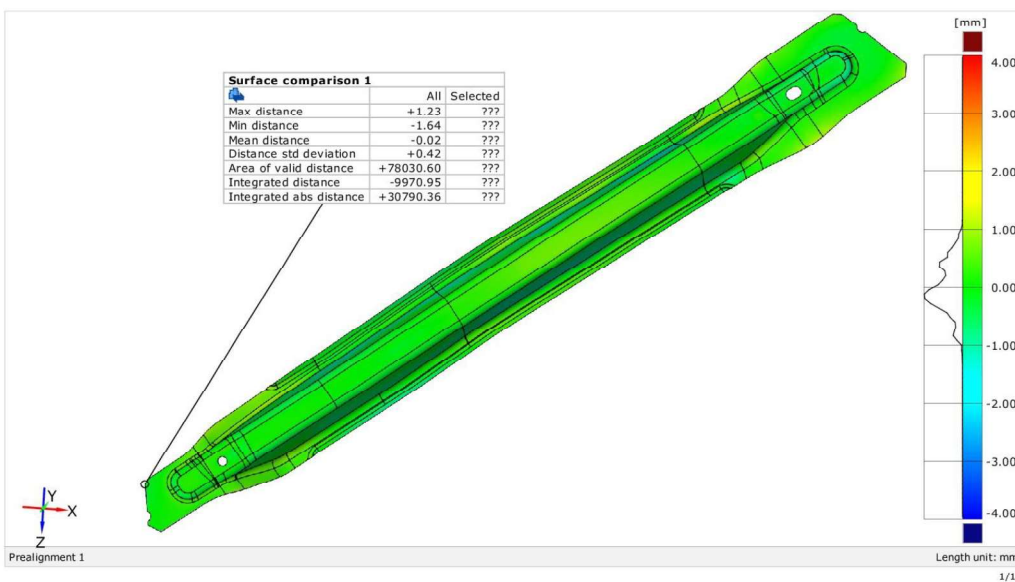


## CAD higher\_simulation 10

Generated with GOM Inspect V8

gom

Surface Comparison on CAD

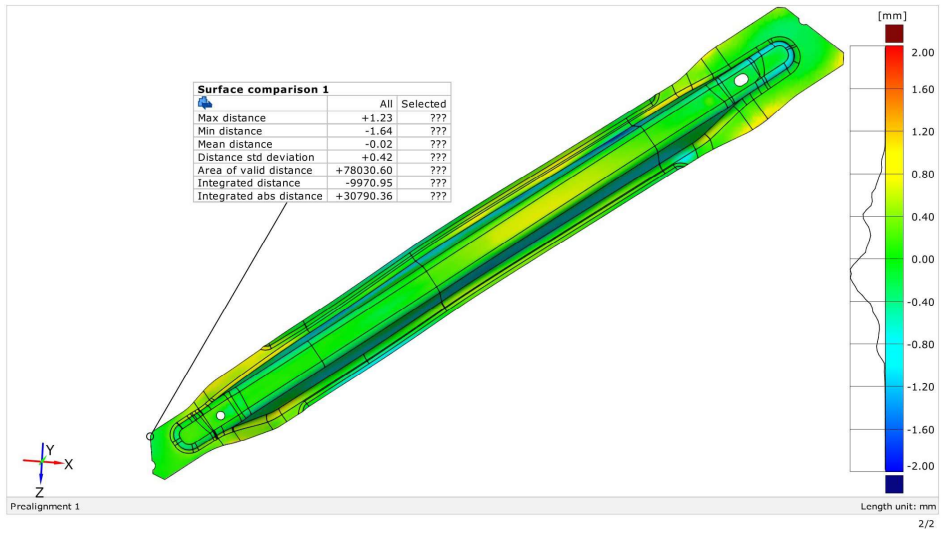


# CAD higher\_simulation 10

Generated with GOM Inspect V8



Surface Comparison on CAD

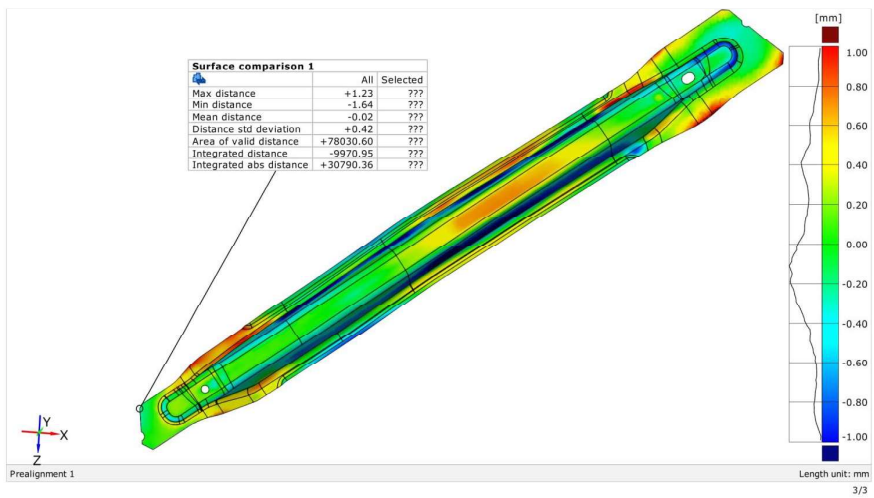


# CAD higher\_simulation 10

Generated with GOM Inspect V8



Surface Comparison on CAD

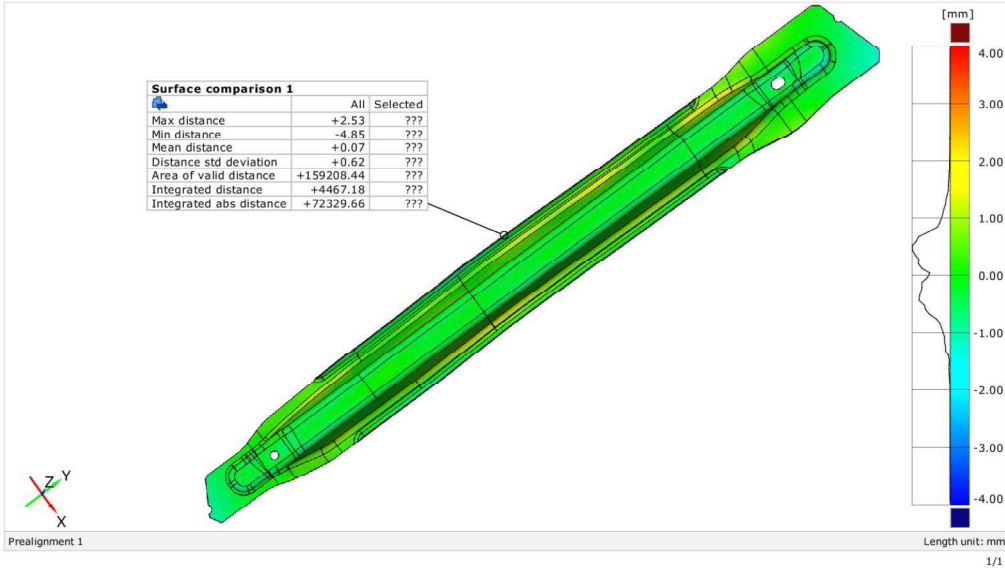


# 3D CAD\_simulation 3D

Generated with GOM Inspect V8



## Surface Comparison on CAD

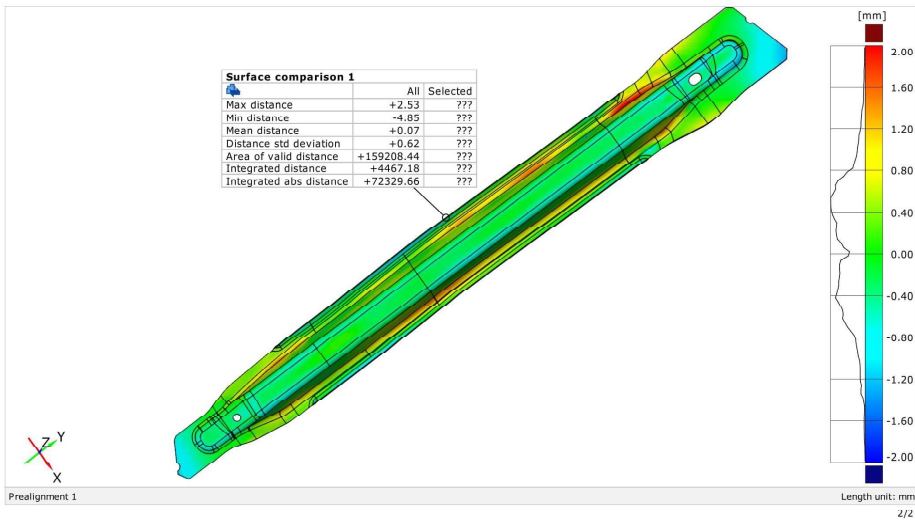


# 3D CAD\_simulation 3D

Generated with GOM Inspect V8



## Surface Comparison on CAD

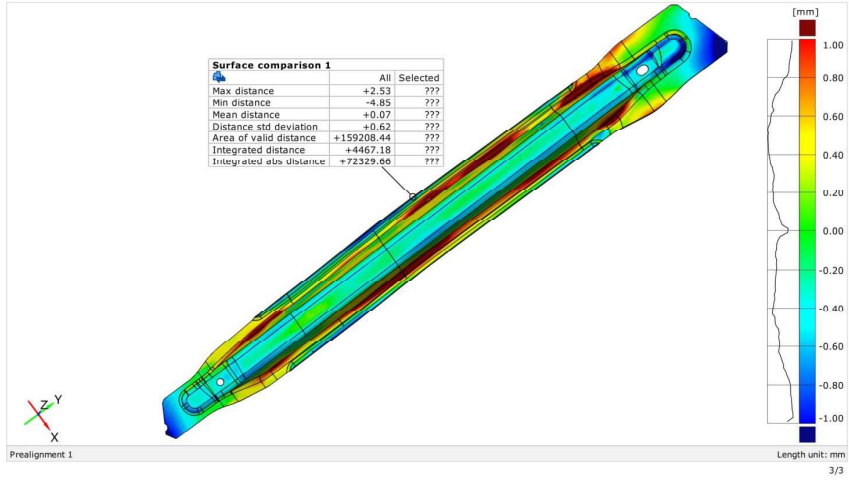


# 3D CAD\_simulation 3D

Generated with GOM Inspect V8



## Surface Comparison on CAD



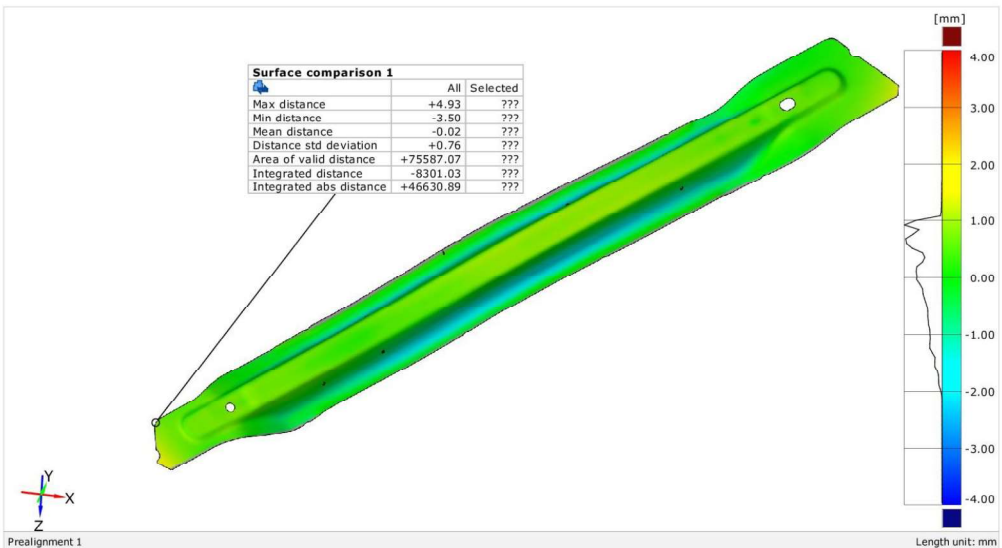
# ANNEX 12.3 COMPARISON OF REAL GEOMETRY RESULTING FROM SCAN AND SIMULATION RESULTS

## 3D real PM13 lower\_simulation 1

Generated with GOM Inspect V8



Surface Comparison on CAD

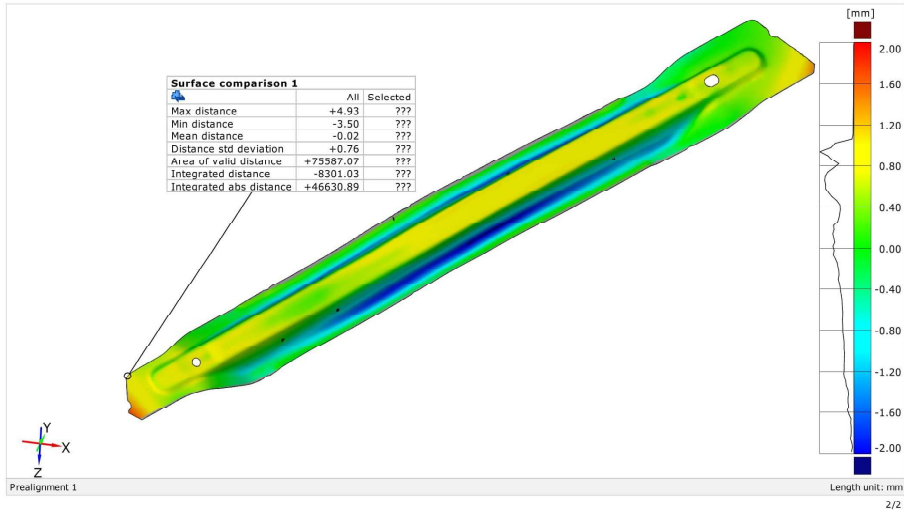


# 3D real PM13 lower\_simulation 1

Generated with GOM Inspect V8



Surface Comparison on CAD

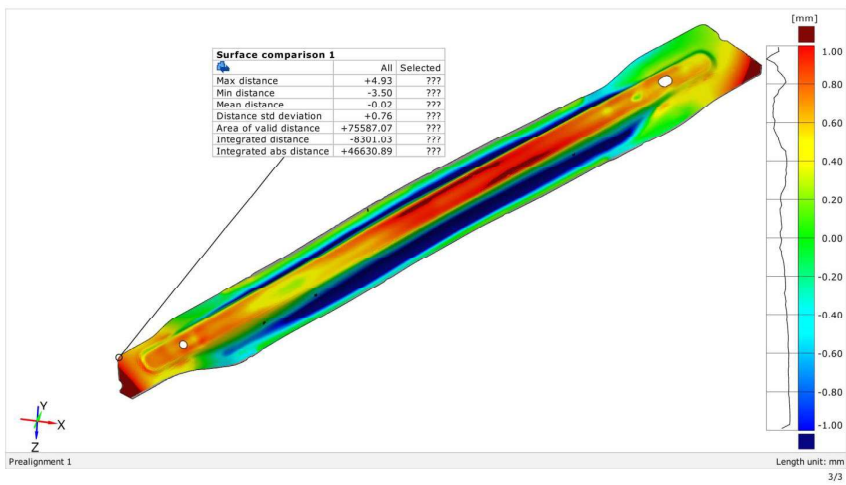


# 3D real PM13 lower\_simulation 1

Generated with GOM Inspect V8



Surface Comparison on CAD

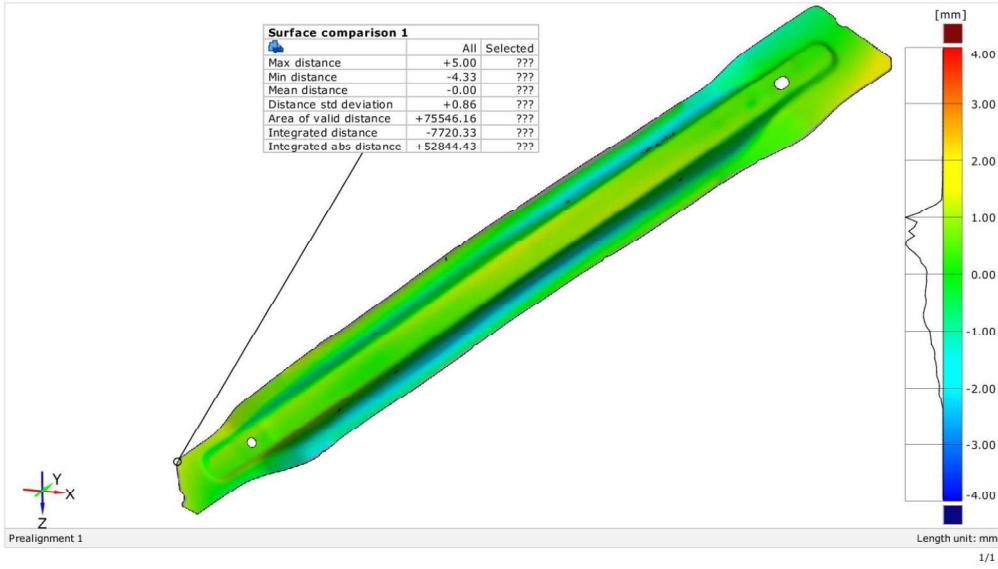


# 3D real PM13 lower\_simulation 2

Generated with GOM Inspect V8



Surface Comparison on CAD

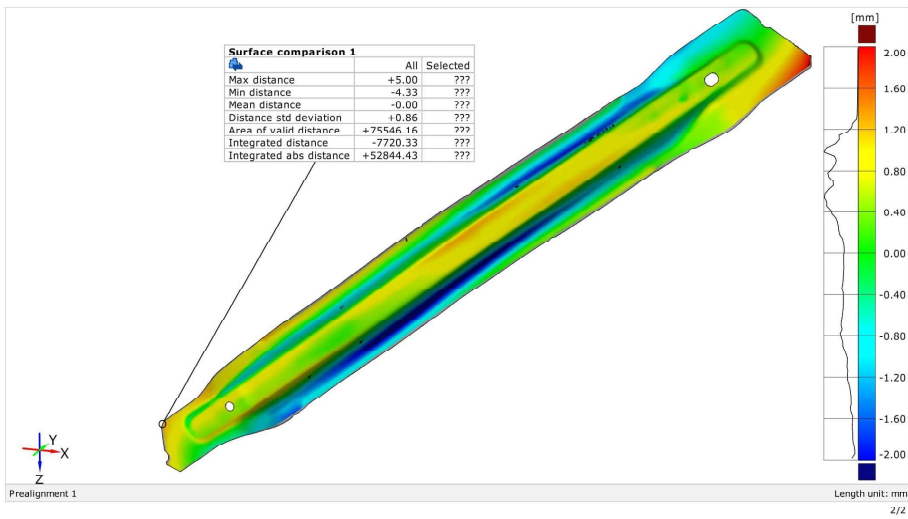


# 3D real PM13 lower\_simulation 2

Generated with GOM Inspect V8



Surface Comparison on CAD

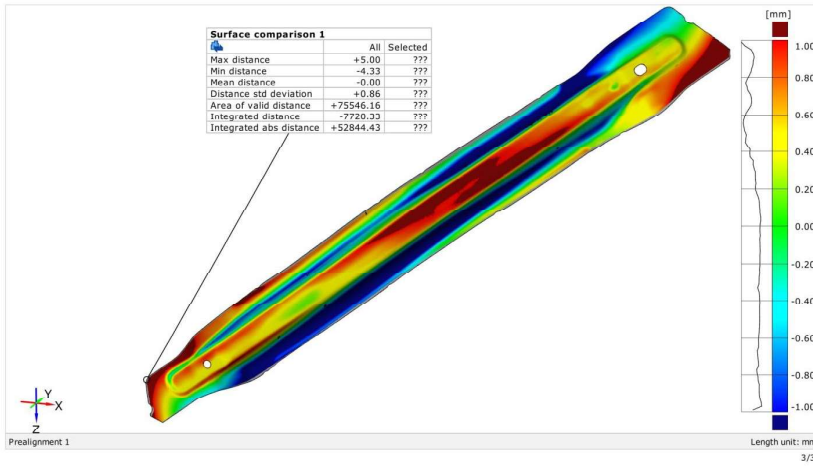


### 3D real PM13 lower\_simulation 2

Generated with GOM Inspect V8



Surface Comparison on CAD

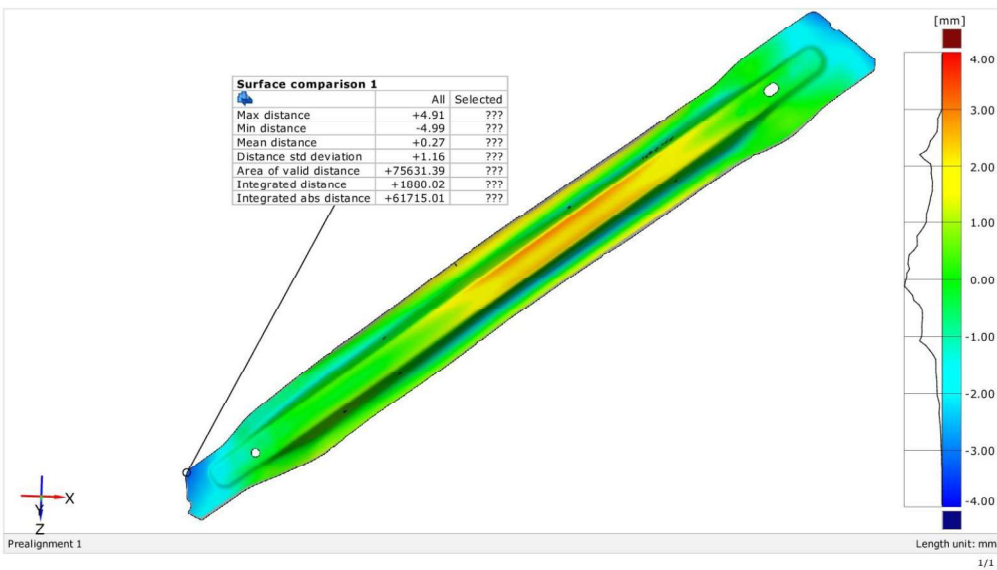


### 3D real PM13 lower\_simulation 3

Generated with GOM Inspect V8



Surface Comparison on CAD

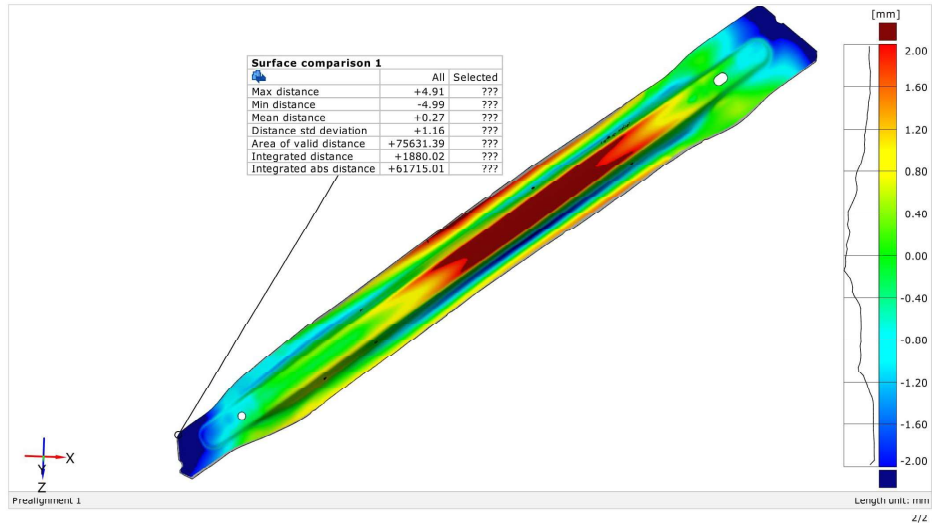


### 3D real PM13 lower\_simulation 3

Generated with GOM Inspect V8



Surface Comparison on CAD

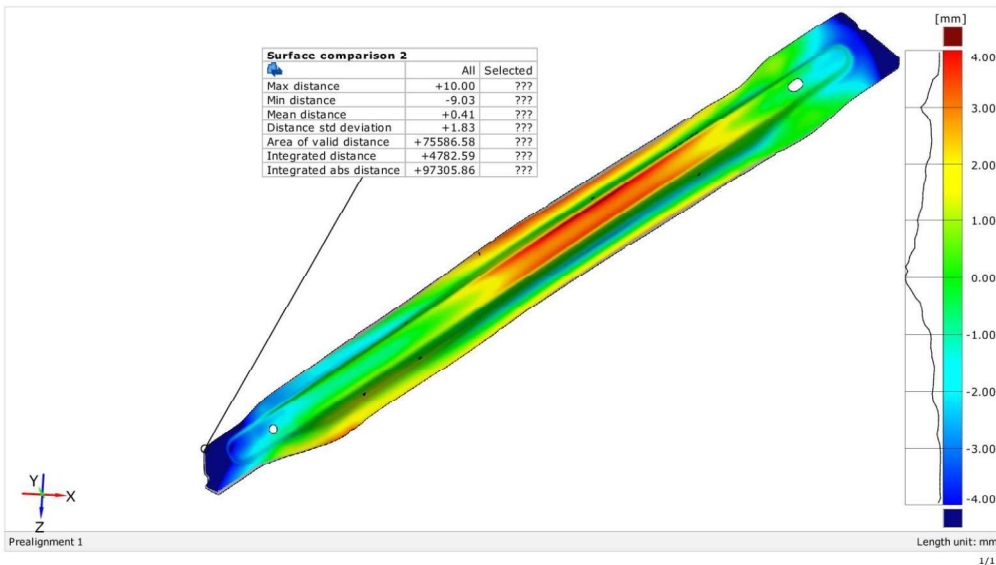


### 3D real PM13 lower\_simulation 4

Generated with GOM Inspect V8



Surface Comparison on CAD

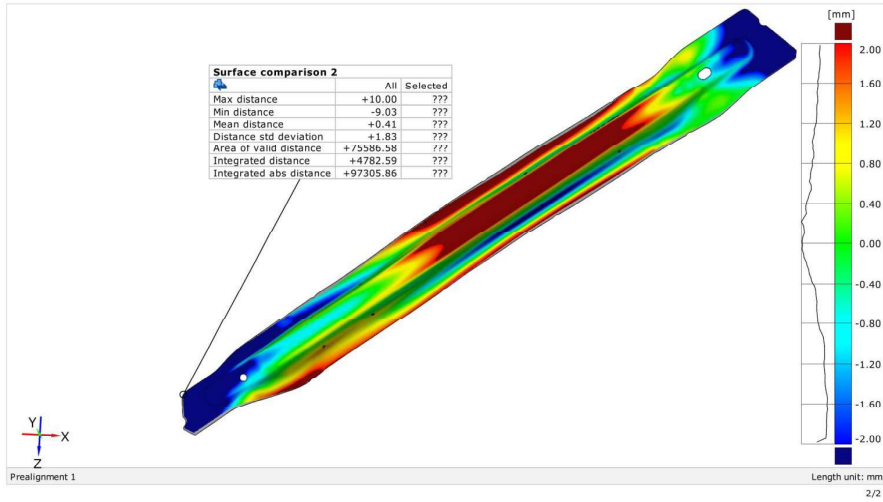


### 3D real PM13 lower\_simulation 4

Generated with GOM Inspect V8



Surface Comparison on CAD

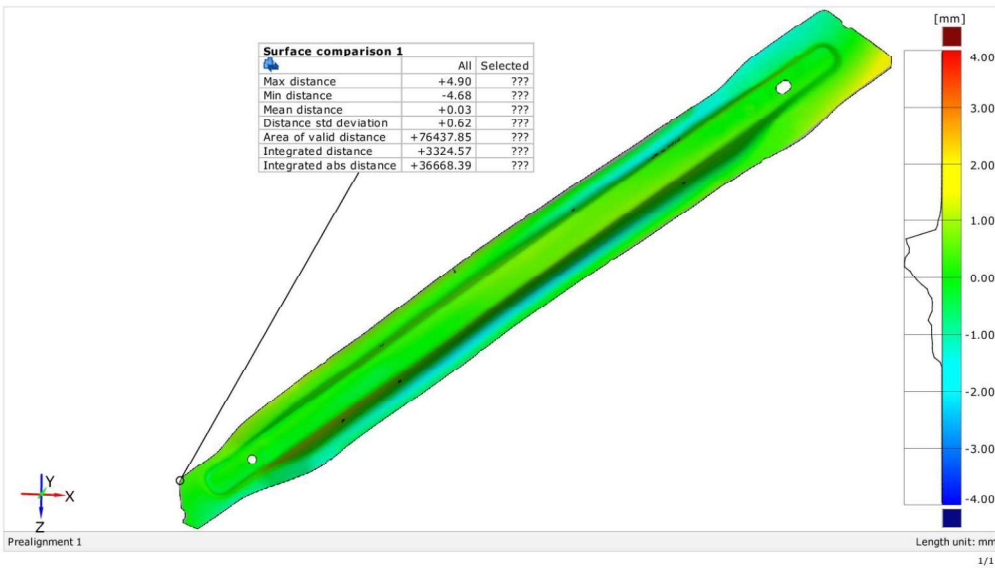


### 3D real PM13 lower\_simulation 5

Generated with GOM Inspect V8



Surface Comparison on CAD

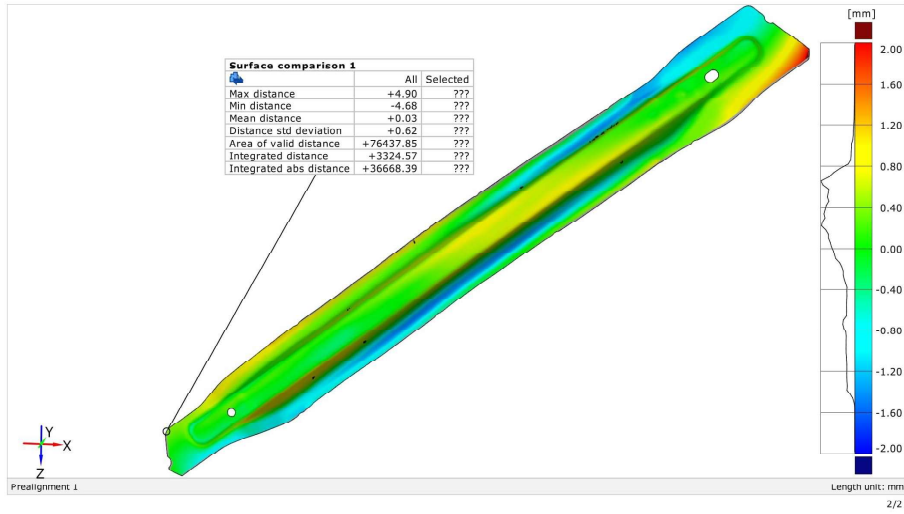


# 3D real PM13 lower\_simulation 5

Generated with GOM Inspect V8



Surface Comparison on CAD

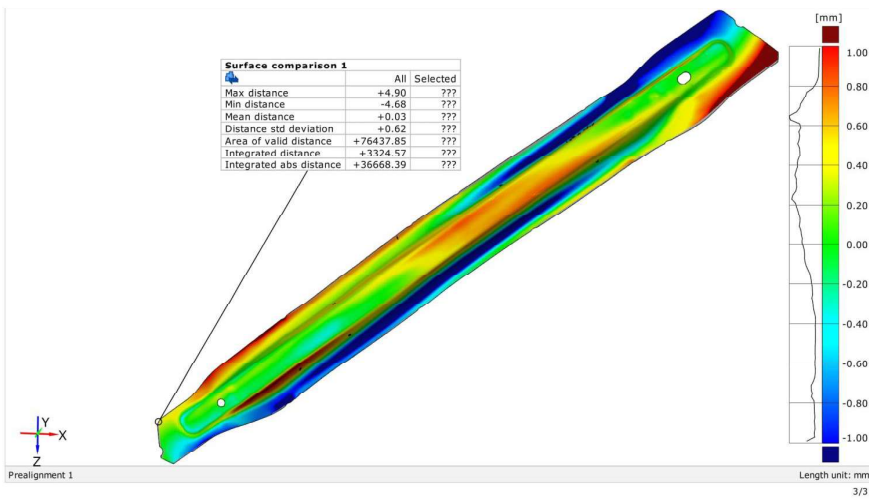


# 3D real PM13 lower\_simulation 5

Generated with GOM Inspect V8



Surface Comparison on CAD

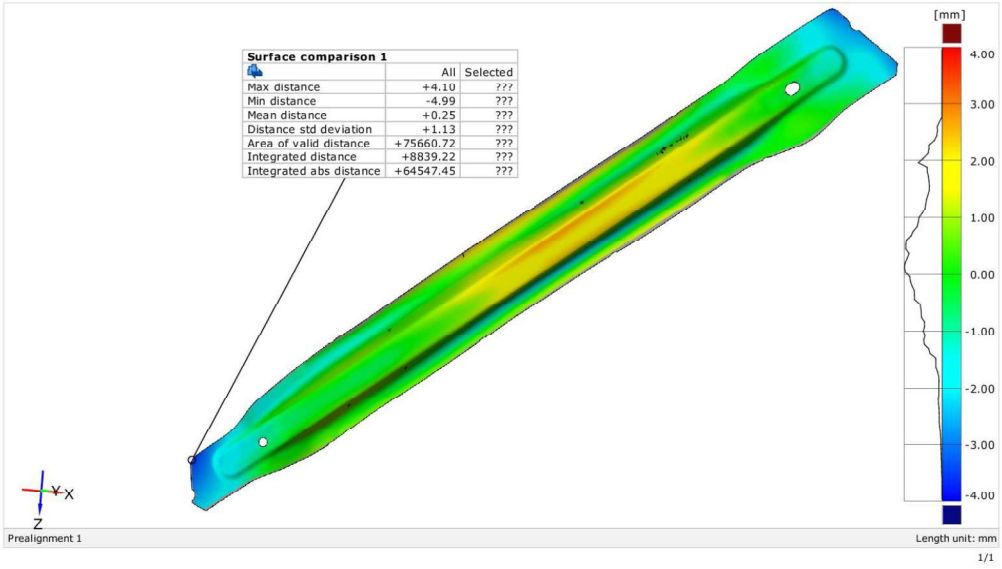


# 3D real PM13 lower\_simulation 6

Generated with GOM Inspect V8



Surface Comparison on CAD

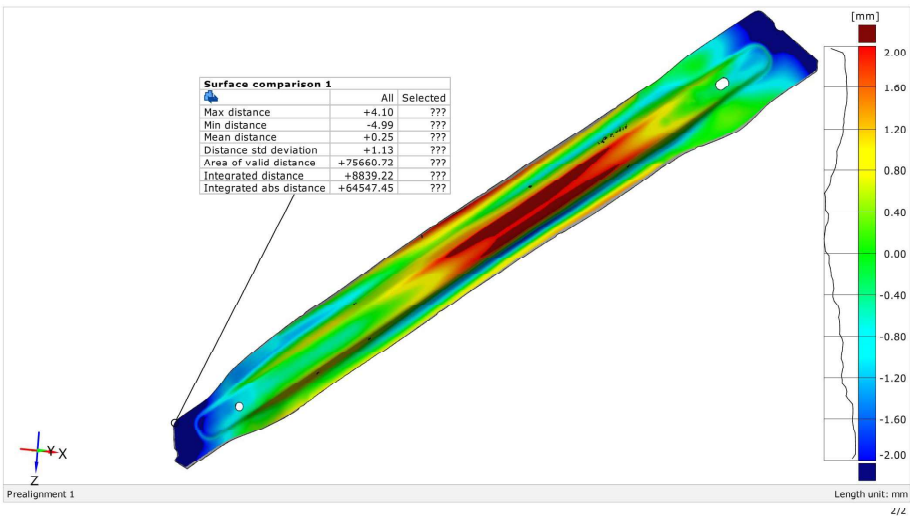


# 3D real PM13 lower\_simulation 6

Generated with GOM Inspect V8



Surface Comparison on CAD

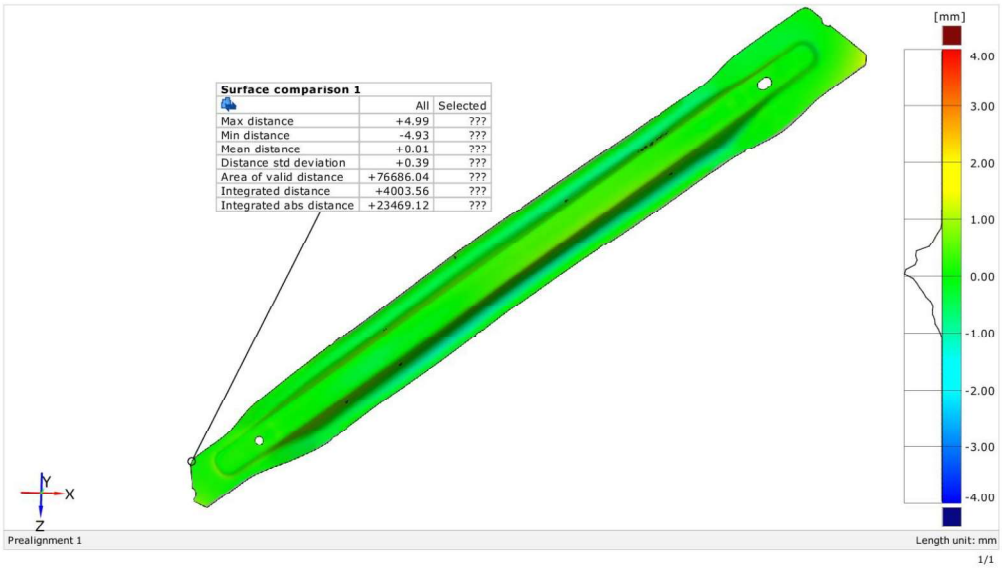


# 3D real PM13 lower\_simulation 7

Generated with GOM Inspect V8



Surface Comparison on CAD

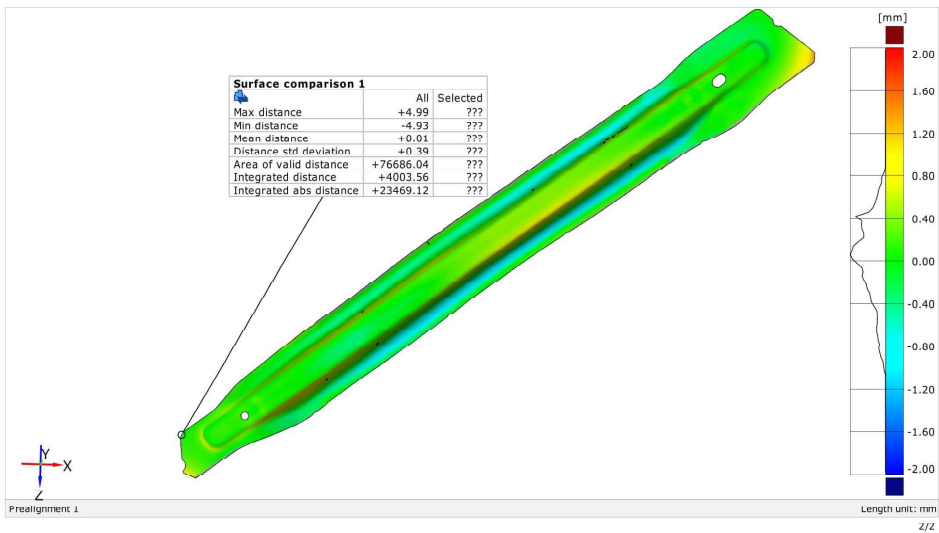


# 3D real PM13 lower\_simulation 7

Generated with GOM Inspect V8



Surface Comparison on CAD

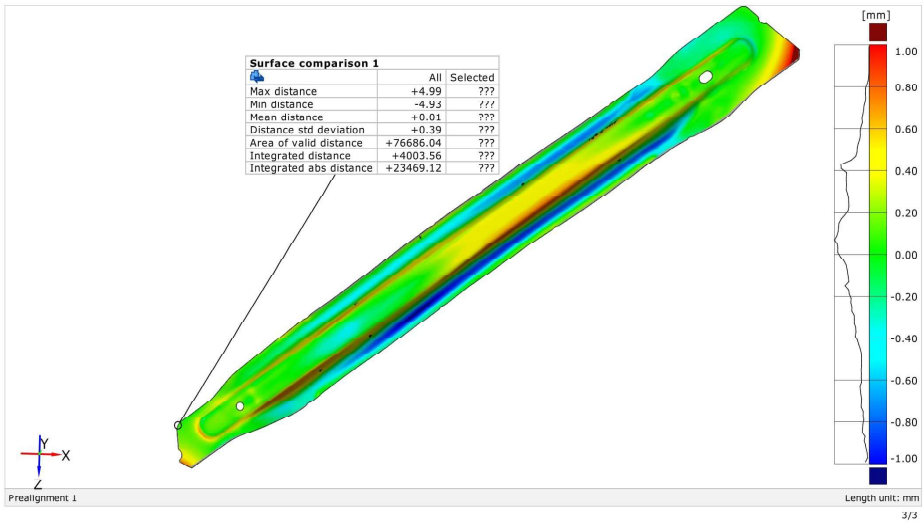


### 3D real PM13 lower\_simulation 8

Generated with GOM Inspect V8



#### Surface Comparison on CAD

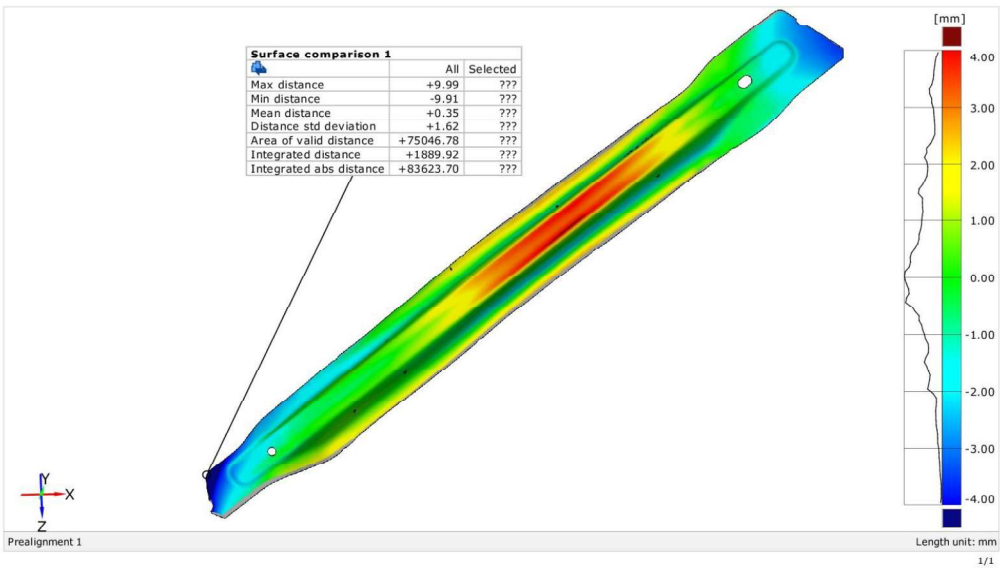


### 3D real PM13 lower\_simulation 8

Generated with GOM Inspect V8



#### Surface Comparison on CAD

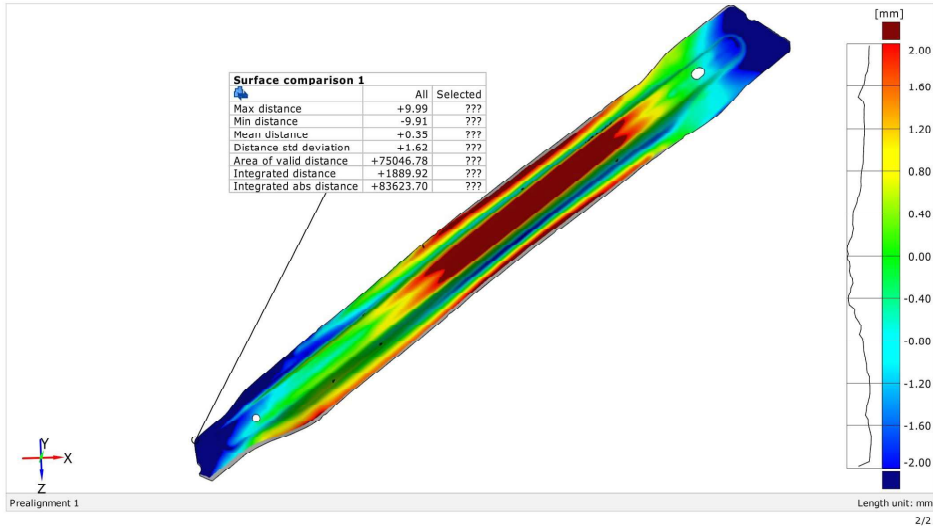


### 3D real PM13 lower\_simulation 8

Generated with GOM Inspect V8



Surface Comparison on CAD

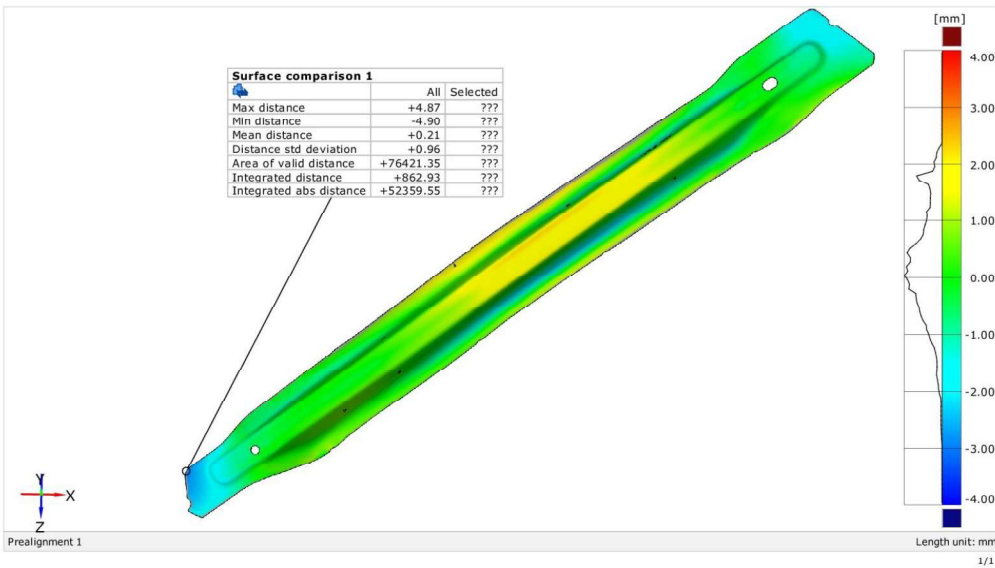


### 3D real PM13 lower\_simulation 9

Generated with GOM Inspect V8



Surface Comparison on CAD

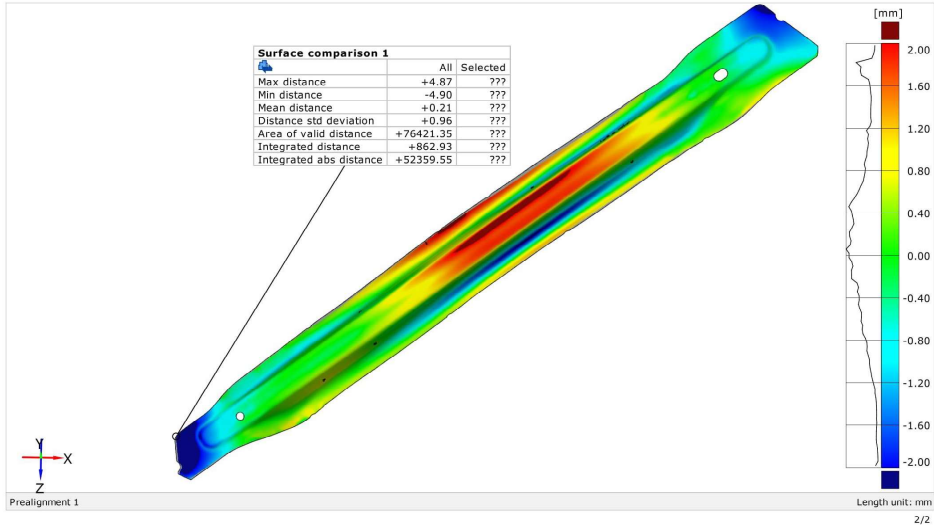


### 3D real PM13 lower\_simulation 9

Generated with GOM Inspect V8



Surface Comparison on CAD

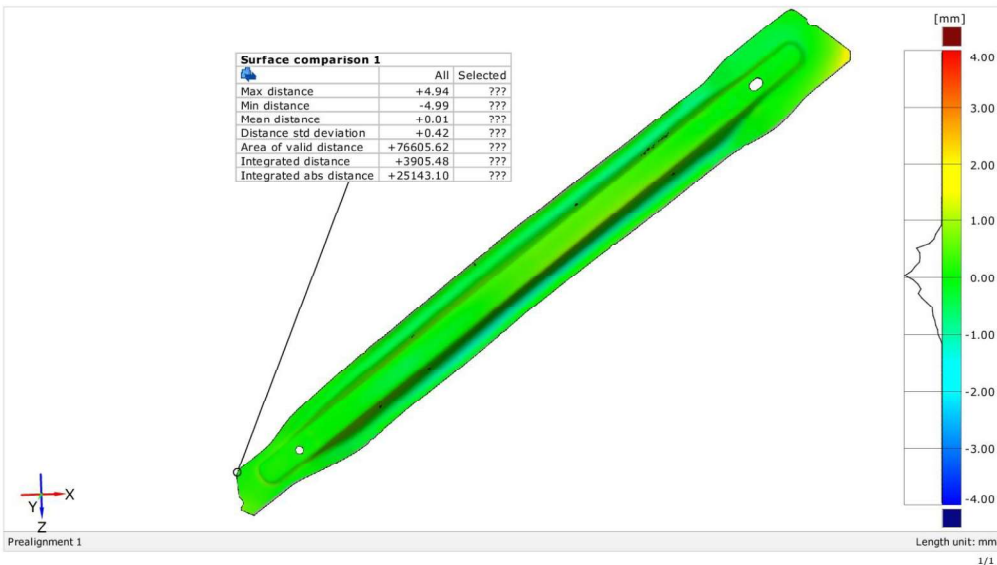


### 3D real PM13 lower\_simulation 10

Generated with GOM Inspect V8



Surface Comparison on CAD

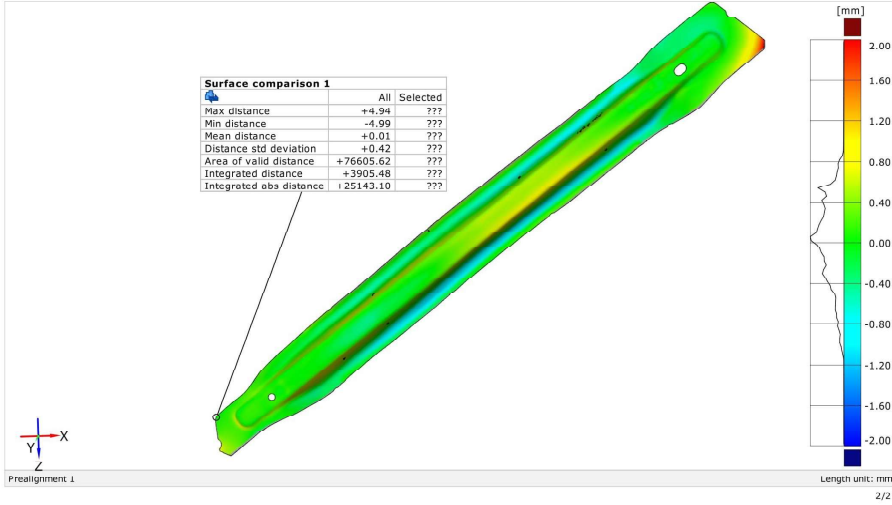


# 3D real PM13 lower\_simulation 10

Generated with GOM Inspect VR



Surface Comparison on CAD

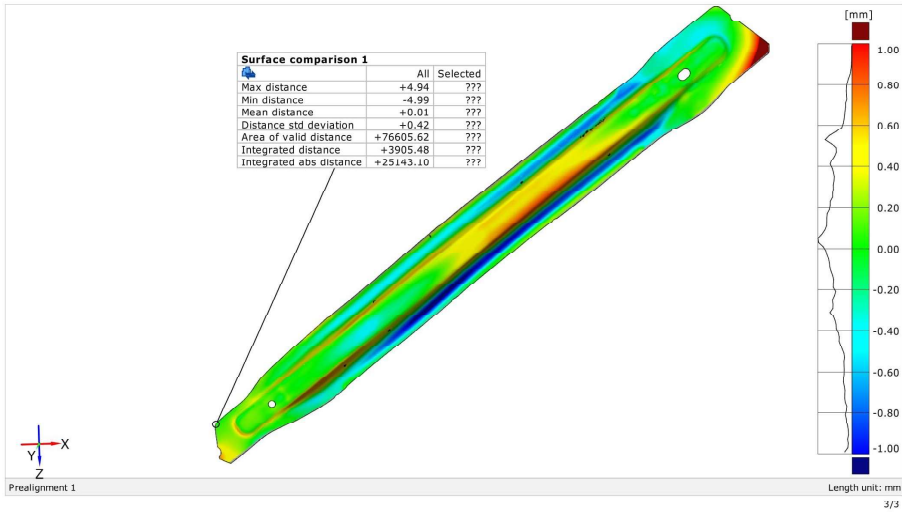


# 3D real PM13 lower\_simulation 10

Generated with GOM Inspect VR



Surface Comparison on CAD

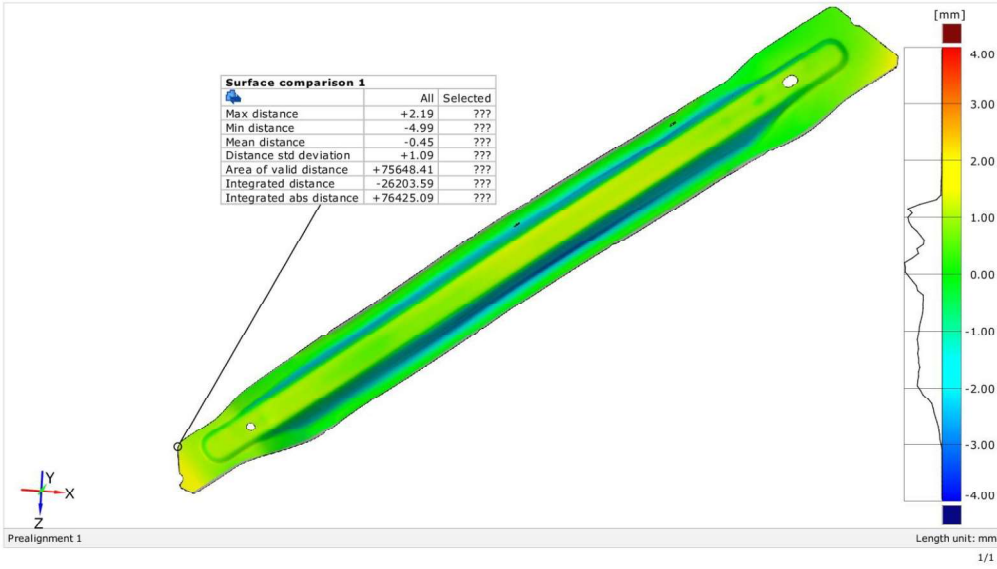


# 3D real PM13 higher\_simulation 1

Generated with GOM Inspect V8



Surface Comparison on CAD

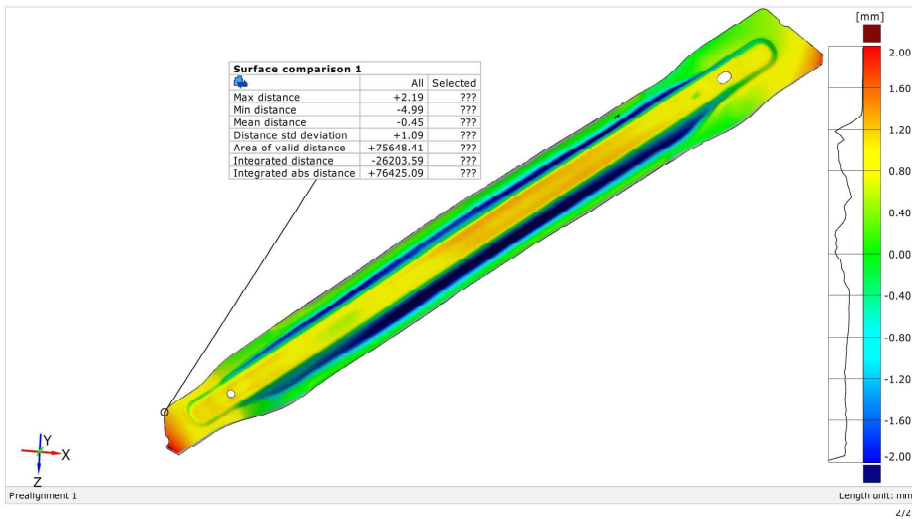


# 3D real PM13 higher\_simulation 1

Generated with GOM Inspect V8



Surface Comparison on CAD

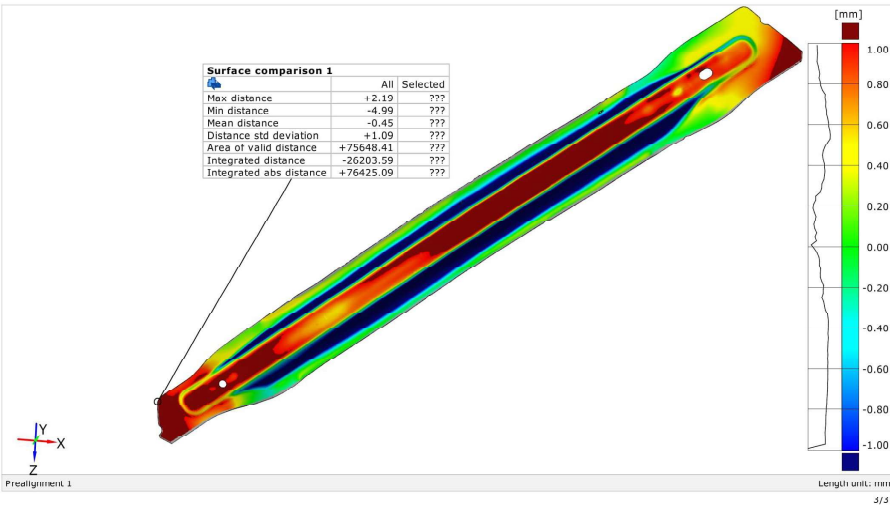


# 3D real PM13 higher\_simulation 1

Generated with GOM Inspect V8



Surface Comparison on CAD

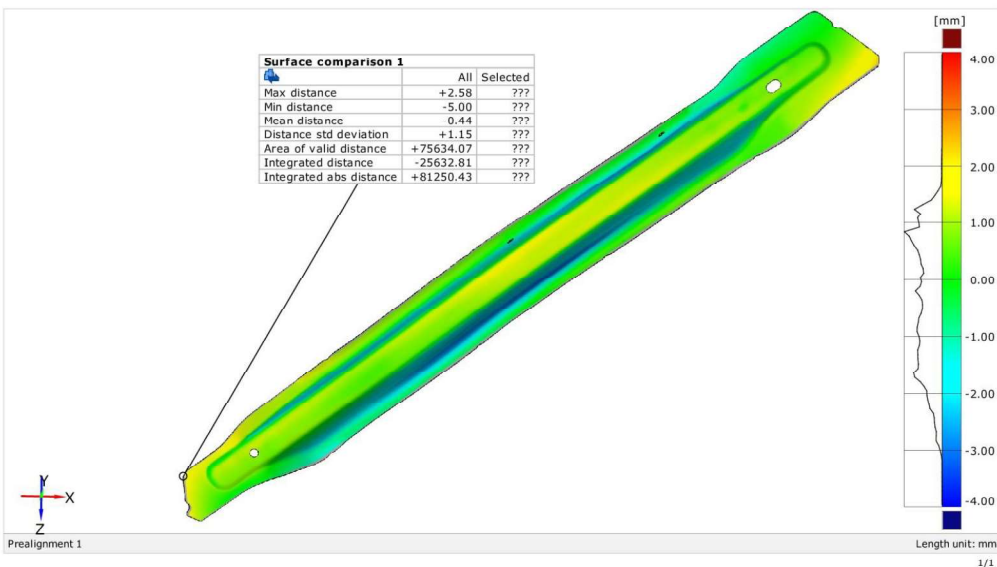


# 3D real PM13 higher\_simulation 2

Generated with GOM Inspect V8



Surface Comparison on CAD

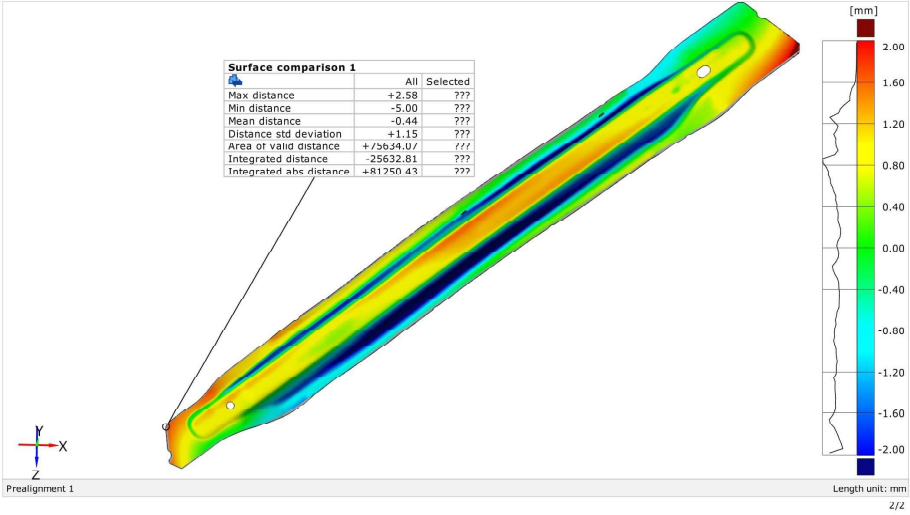


# 3D real PM13 higher\_simulation 2

Generated with GOM Inspect V8



## Surface Comparison on CAD

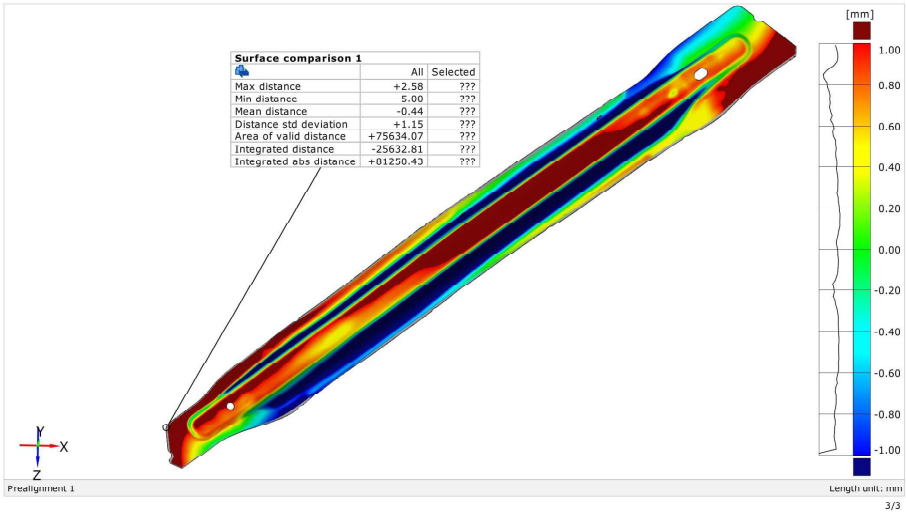


# 3D real PM13 higher\_simulation 2

Generated with GOM Inspect V8



## Surface Comparison on CAD

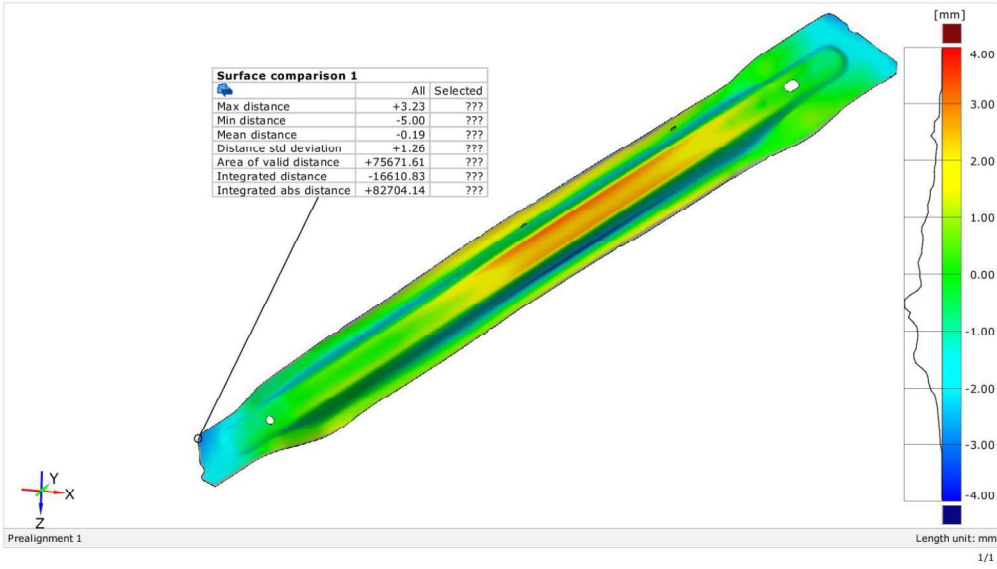


### 3D real PM13 higher\_simulation 3

Generated with GOM Inspect V8



Surface Comparison on CAD

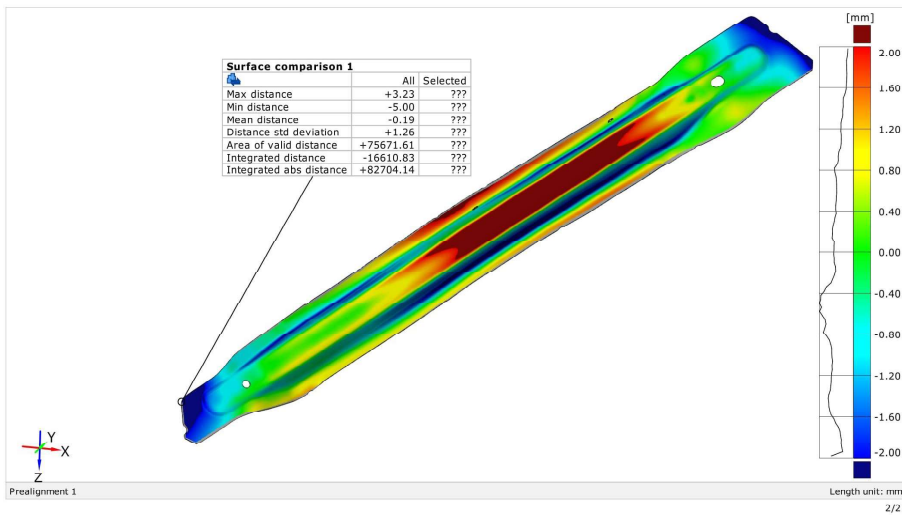


### 3D real PM13 higher\_simulation 3

Generated with GOM Inspect V8



Surface Comparison on CAD

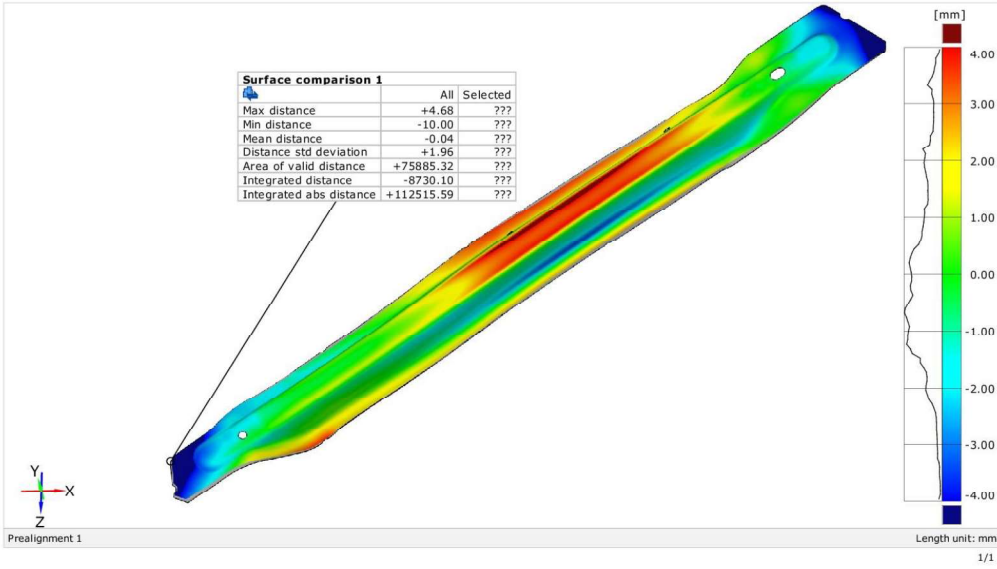


# 3D real PM13 higher\_simulation 4

Generated with GOM Inspect V8



Surface Comparison on CAD

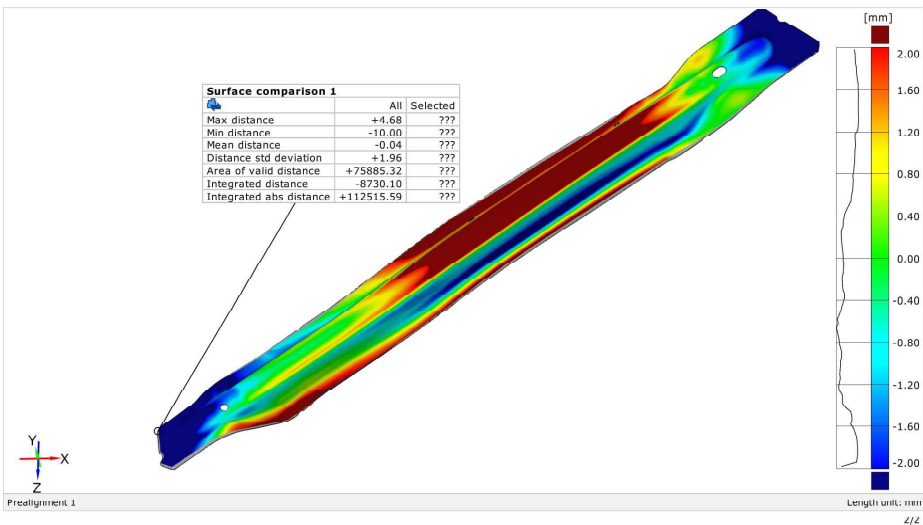


# 3D real PM13 higher\_simulation 4

Generated with GOM Inspect V8



Surface Comparison on CAD

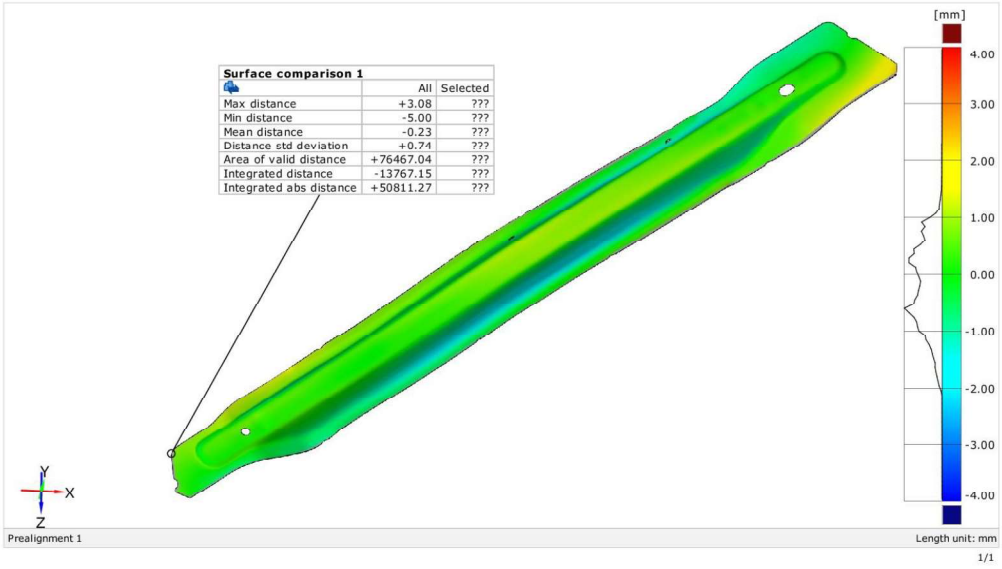


# 3D real PM13 higher\_simulation 5

Generated with GOM Inspect V8



Surface Comparison on CAD

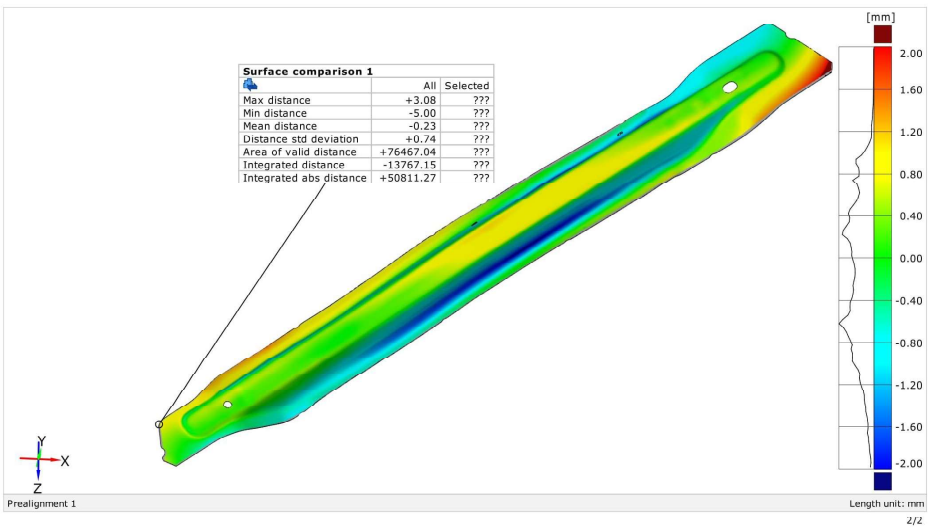


# 3D real PM13 higher\_simulation 5

Generated with GOM Inspect V8



Surface Comparison on CAD

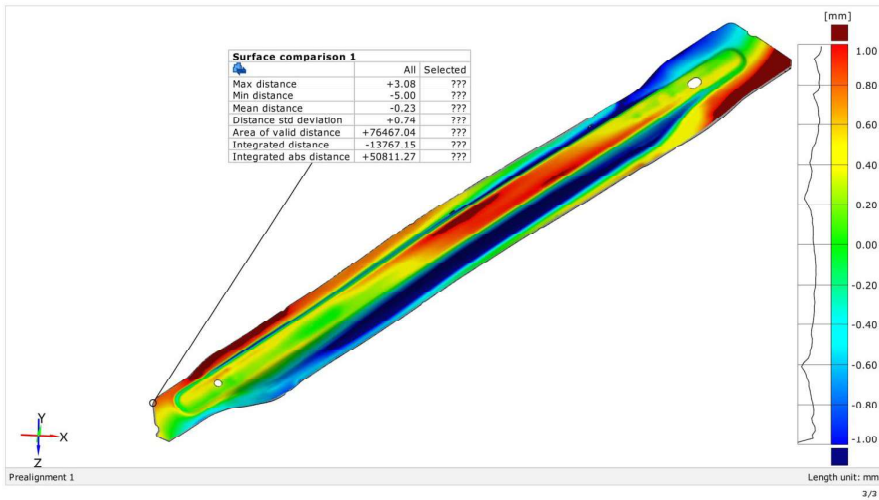


### 3D real PM13 higher\_simulation 5

Generated with GOM Inspect V8



Surface Comparison on CAD

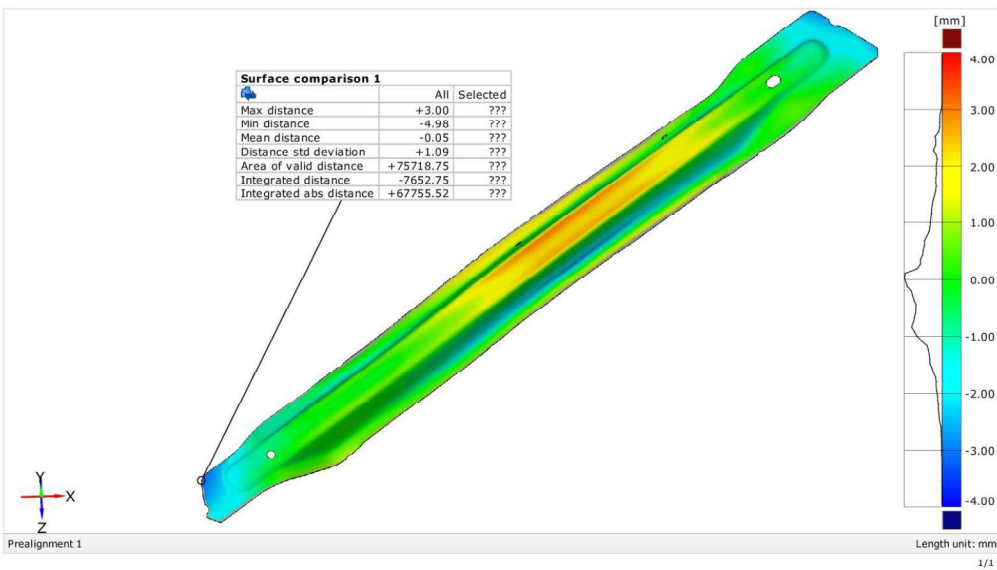


### 3D real PM13 higher\_simulation 6

Generated with GOM Inspect V8



Surface Comparison on CAD

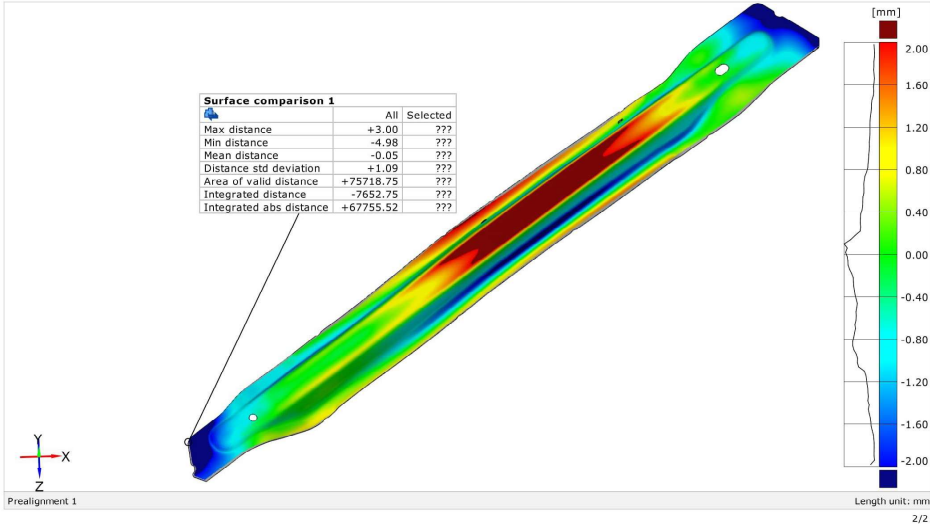


# 3D real PM13 higher\_simulation 6

Generated with GOM Inspect V8



Surface Comparison on CAD

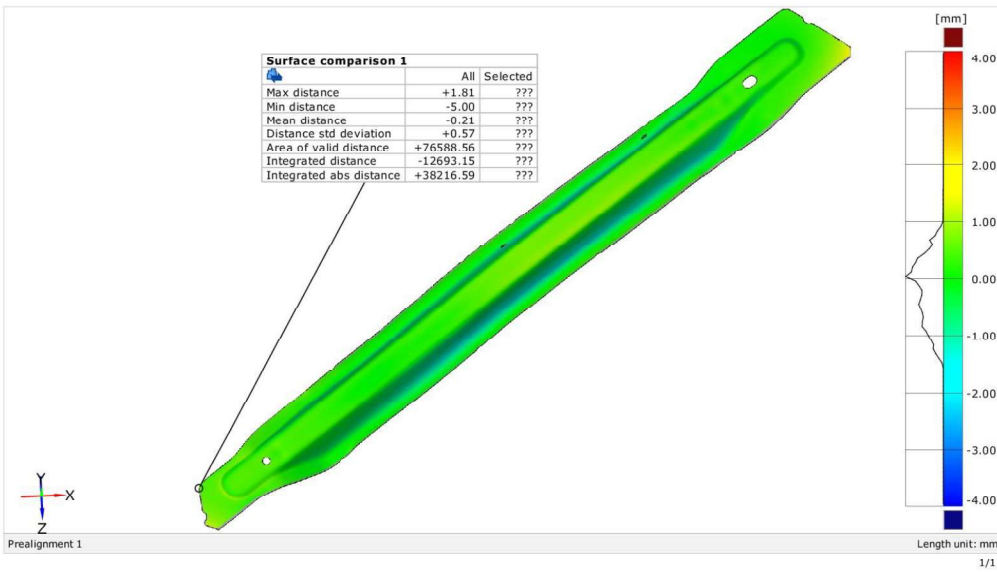


# 3D real PM13 higher\_simulation 7

Generated with GOM Inspect V8



Surface Comparison on CAD

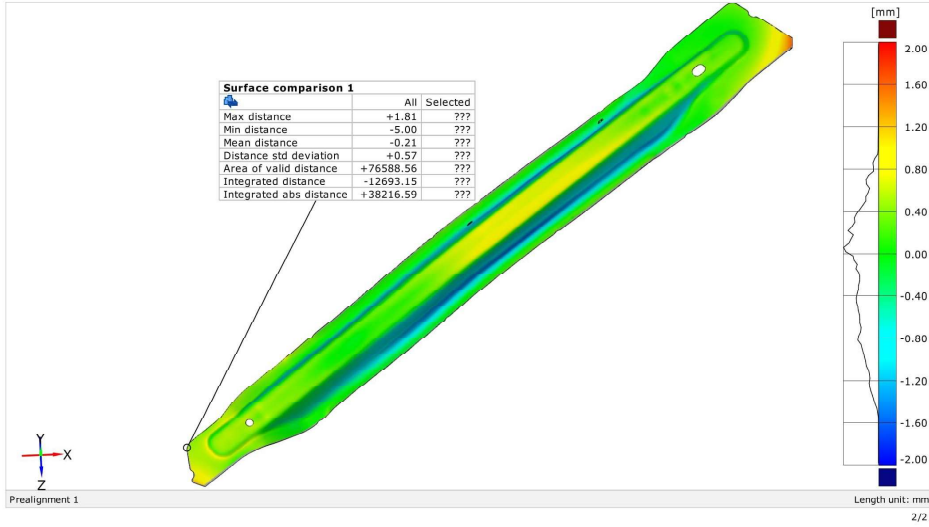


# 3D real PM13 higher\_simulation 7

Generated with GOM Inspect V8



Surface Comparison on CAD

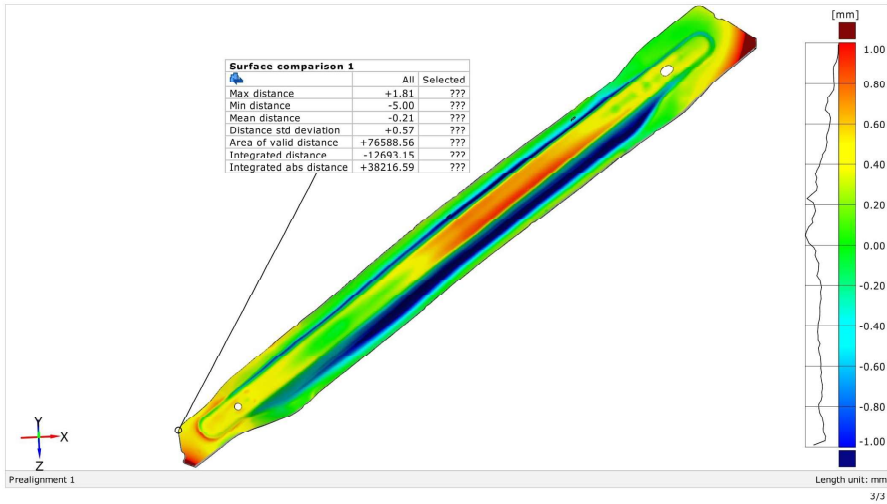


# 3D real PM13 higher\_simulation 7

Generated with GOM Inspect V8



Surface Comparison on CAD

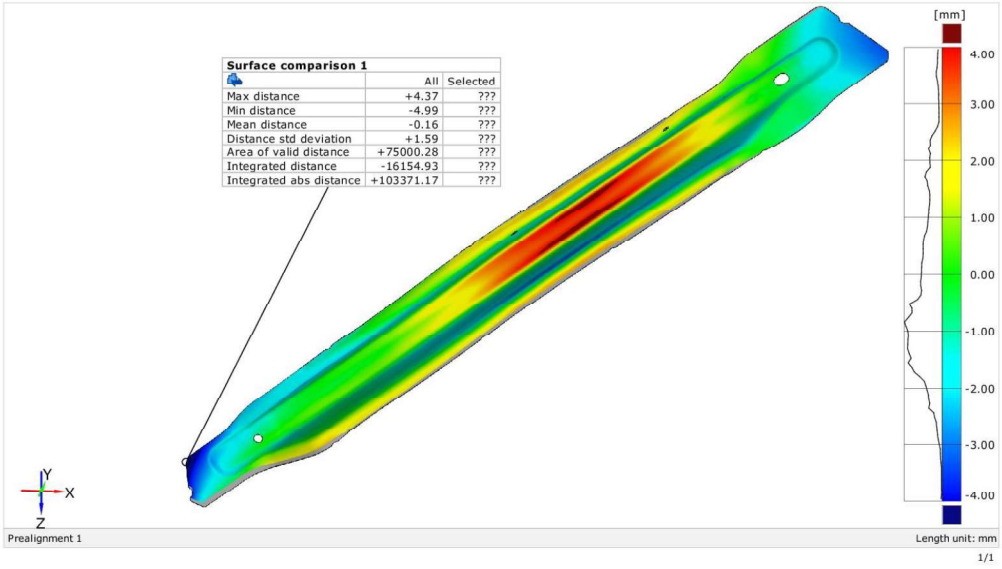


# 3D real PM13 higher\_simulation 8

Generated with GOM Inspect V8



Surface Comparison on CAD

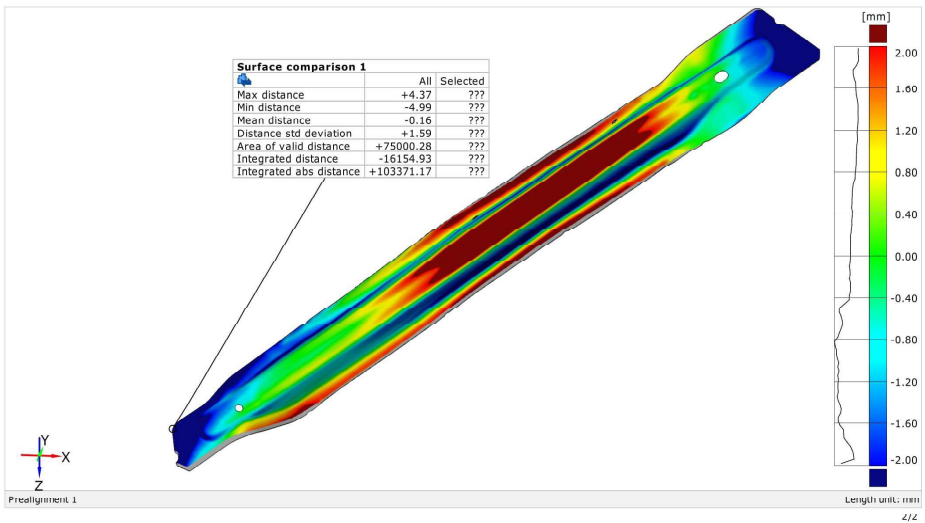


# 3D real PM13 higher\_simulation 8

Generated with GOM Inspect V8



Surface Comparison on CAD

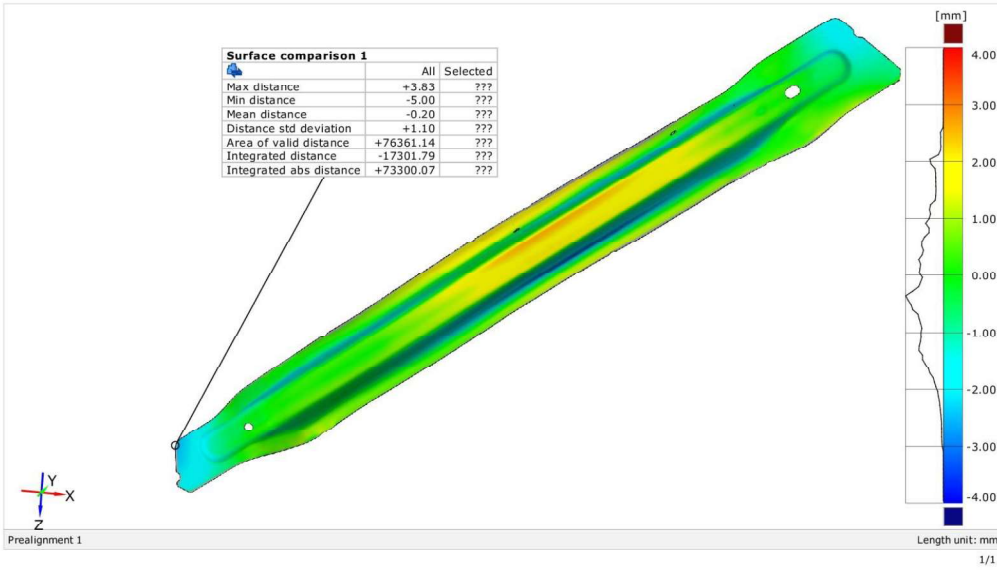


# 3D real PM13 higher\_simulation 9

Generated with GOM Inspect V8



Surface Comparison on CAD

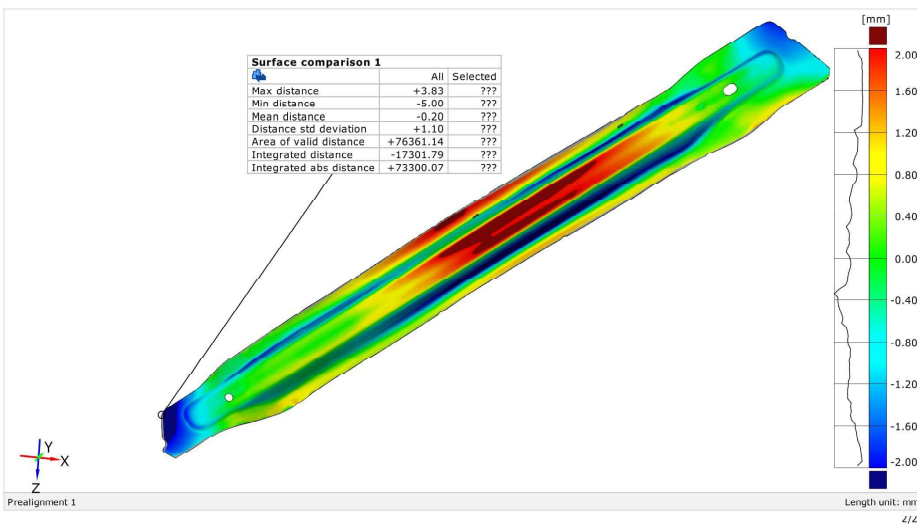


# 3D real PM13 higher\_simulation 9

Generated with GOM Inspect V8



Surface Comparison on CAD

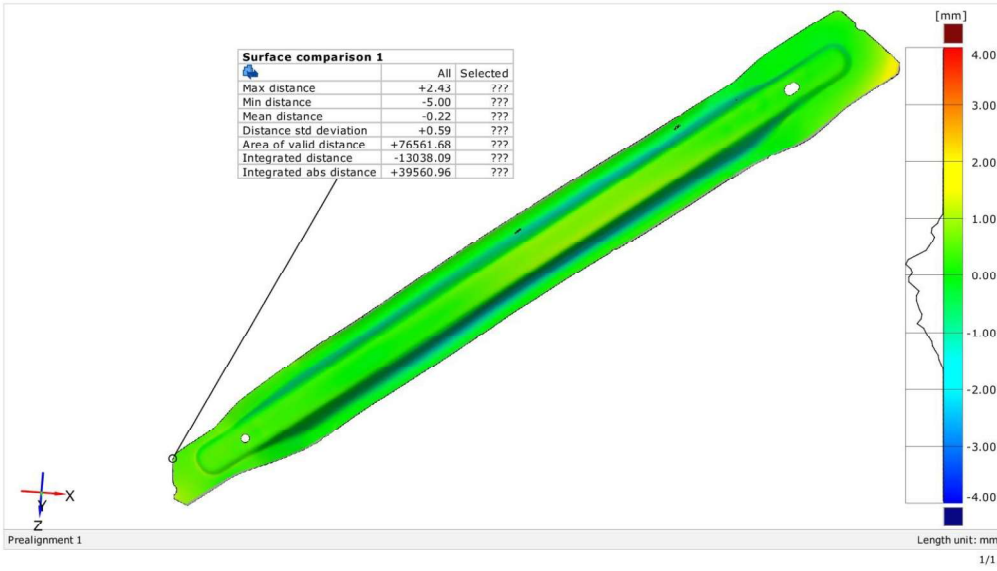


# 3D real PM13 higher\_simulation 10

Generated with GOM Inspect V8



Surface Comparison on CAD

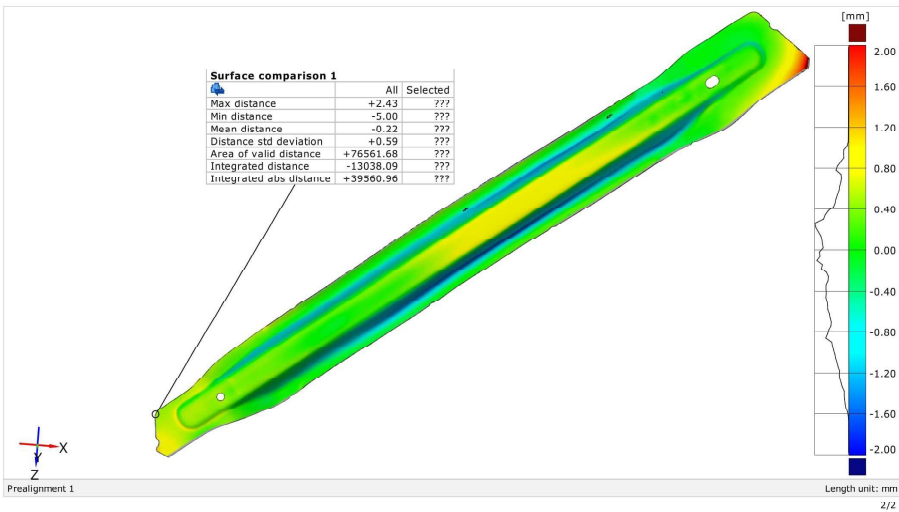


# 3D real PM13 higher\_simulation 10

Generated with GOM Inspect V8



Surface Comparison on CAD

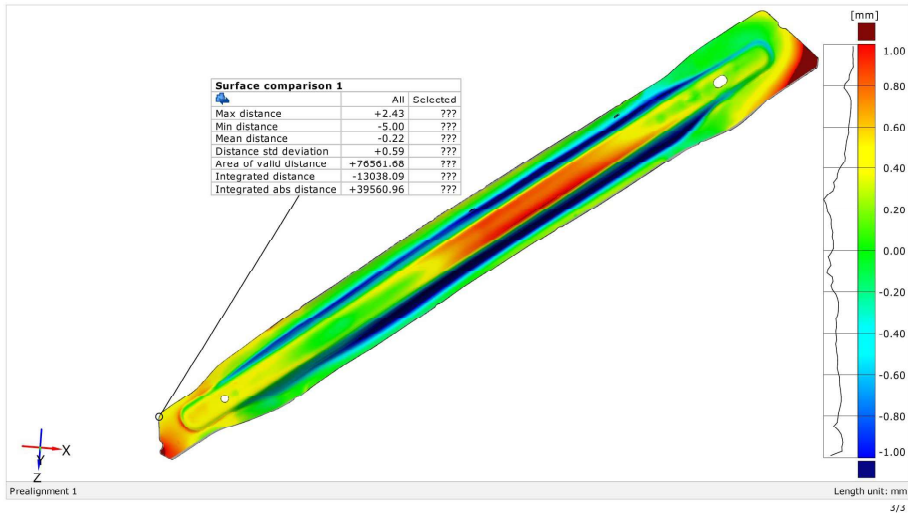


# 3D real PM13 higher\_simulation 10

Generated with GOM Inspect V8



Surface Comparison on CAD

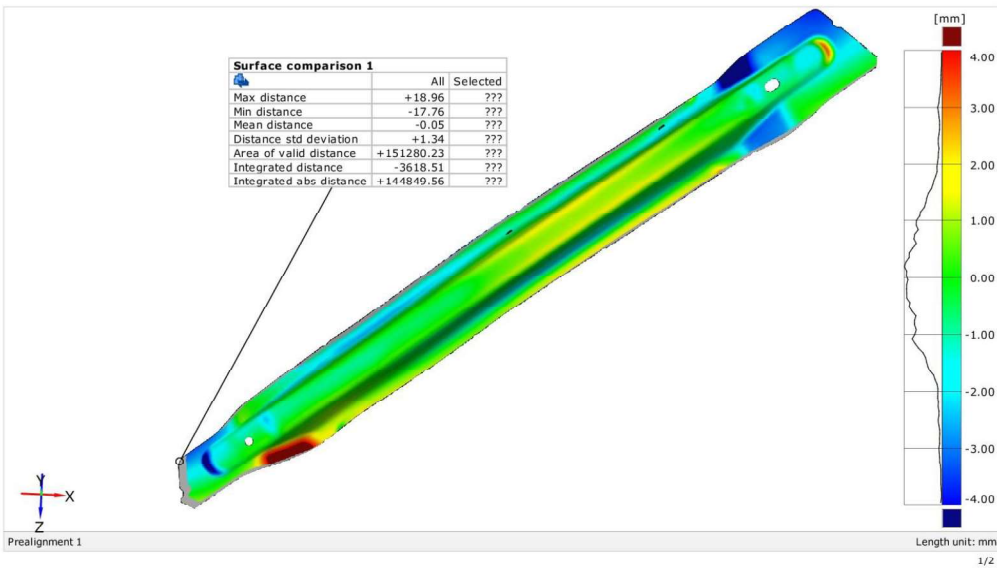


# 3D real\_simulation 3D

Generated with GOM Inspect V8



Surface Comparison on CAD

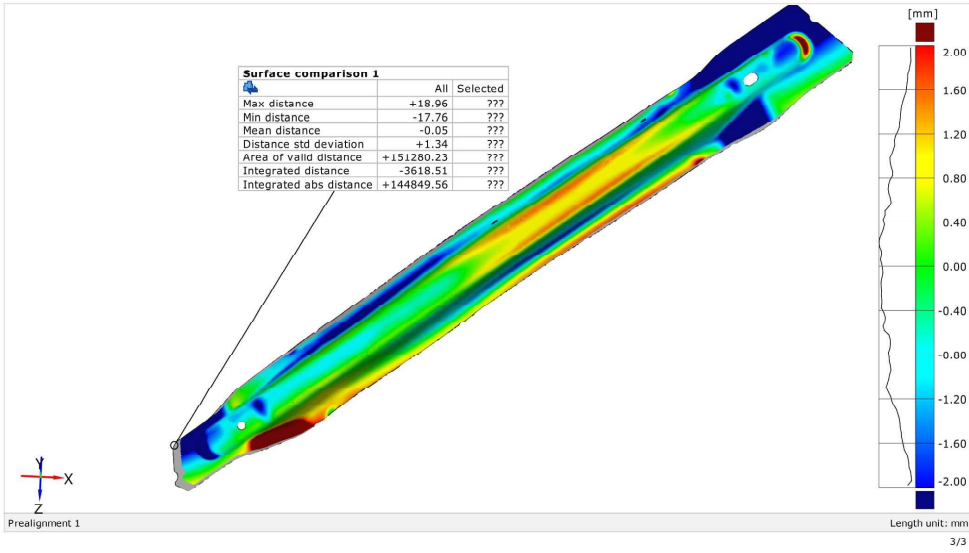


# 3D real\_simulation 3D

Generated with GOM Inspect V8



## Surface Comparison on CAD

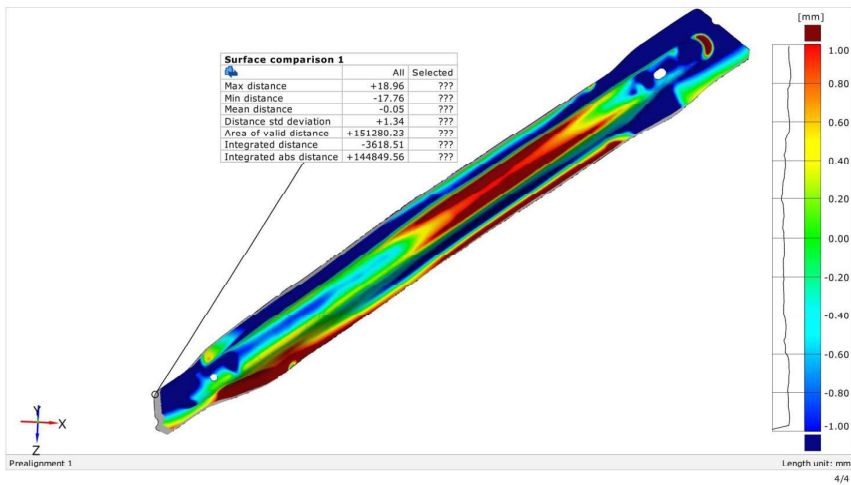


# 3D real\_simulation 3D

Generated with GOM Inspect V8



## Surface Comparison on CAD



# ANNEX 13.1

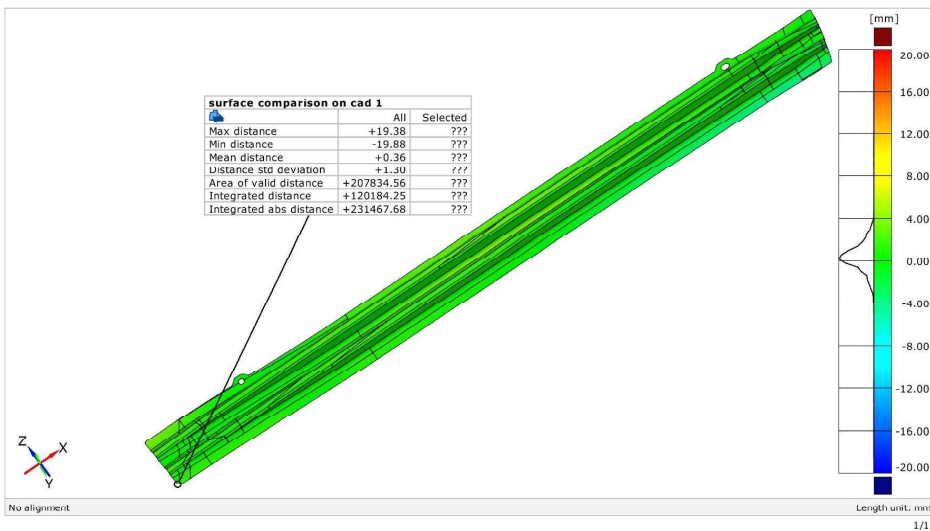
## COMPARISON OF NOMINAL GEOMETRY (CAD) AND REAL GEOMETRY RESULTING FROM SCAN

### CAD lower\_3D real MA03 lower

Generated with GOM Inspect V8



surface comparison on cad

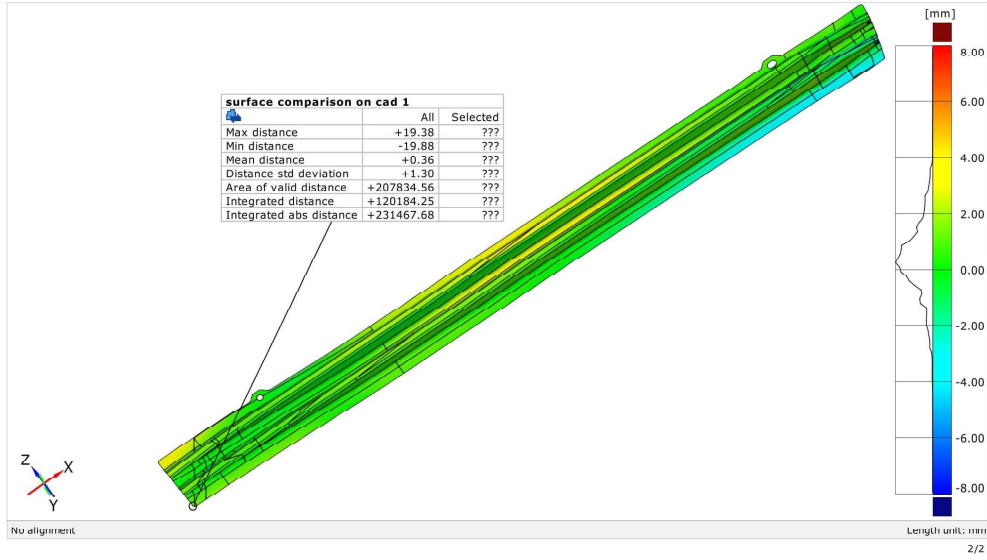


# CAD lower\_3D real MA03 lower

Generated with GOM Inspect V8



## Surface Comparison on CAD

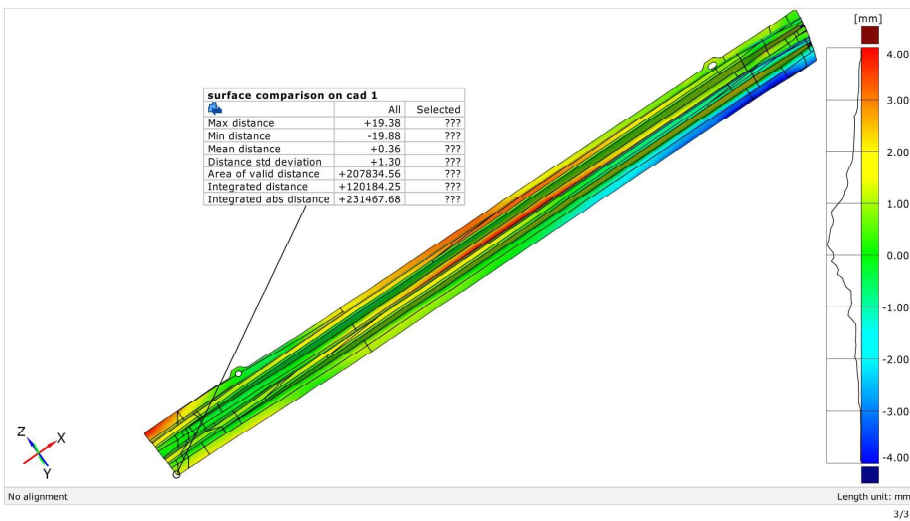


# CAD lower\_3D real MA03 lower

Generated with GOM Inspect V8



## Surface Comparison on CAD

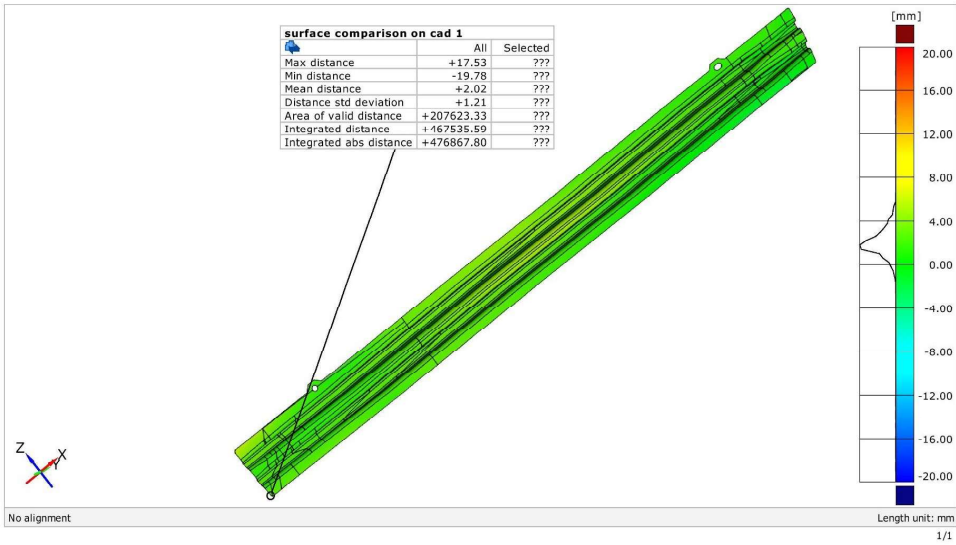


# CAD lower\_3D real MA03 higher

Generated with GOM Inspect V8



surface comparison on cad

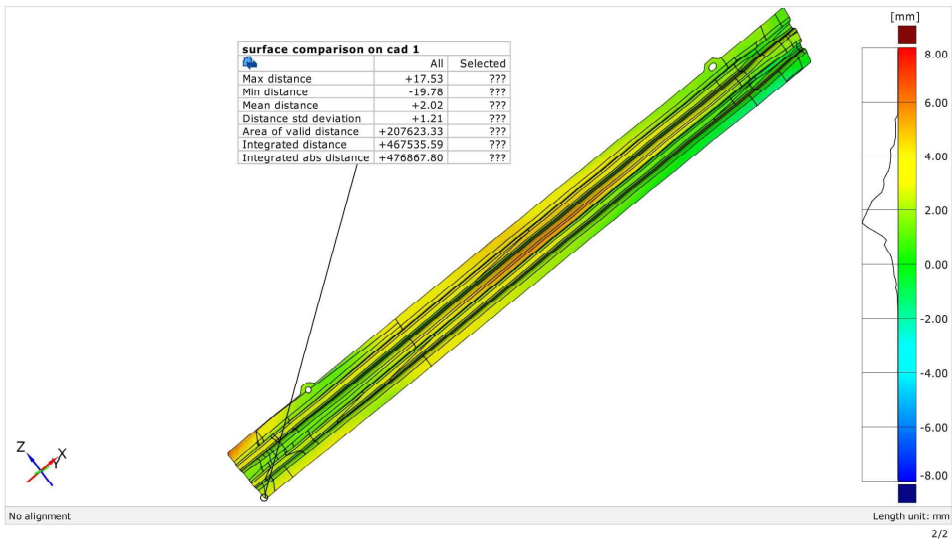


# CAD lower\_3D real MA03 higher

Generated with GOM Inspect V8



Surface Comparison on CAD

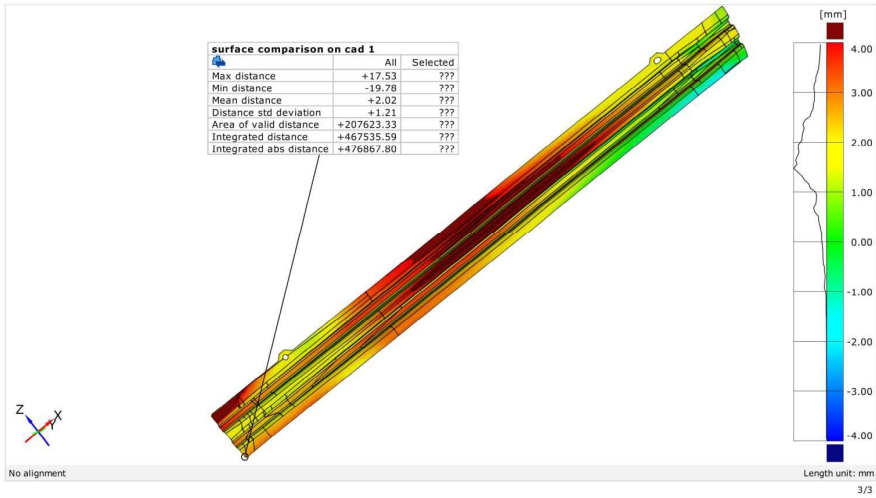


# CAD lower\_3D real MA03 higher

Generated with GOM Inspect V8



Surface Comparison on CAD

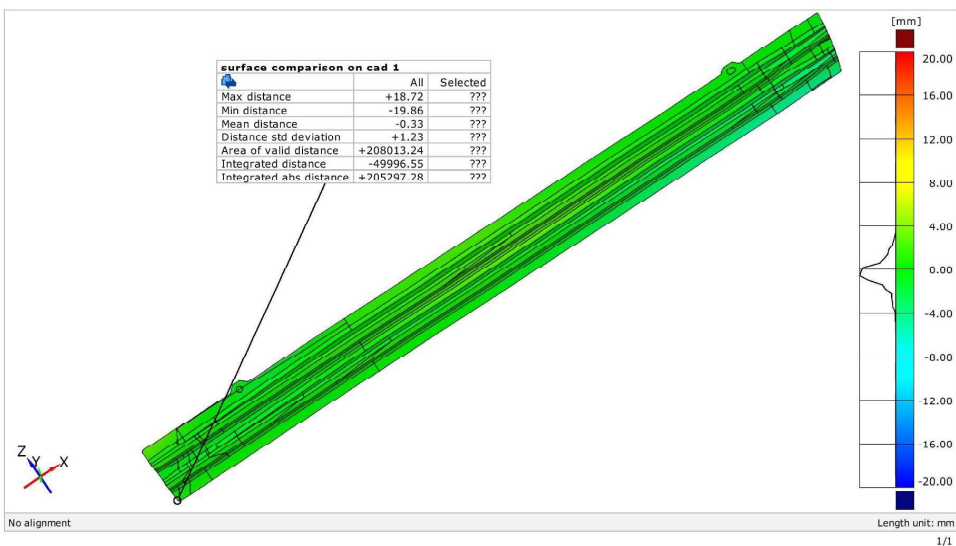


# CAD average\_3D real MA03 lower

Generated with GOM Inspect V8



surface comparison on cad

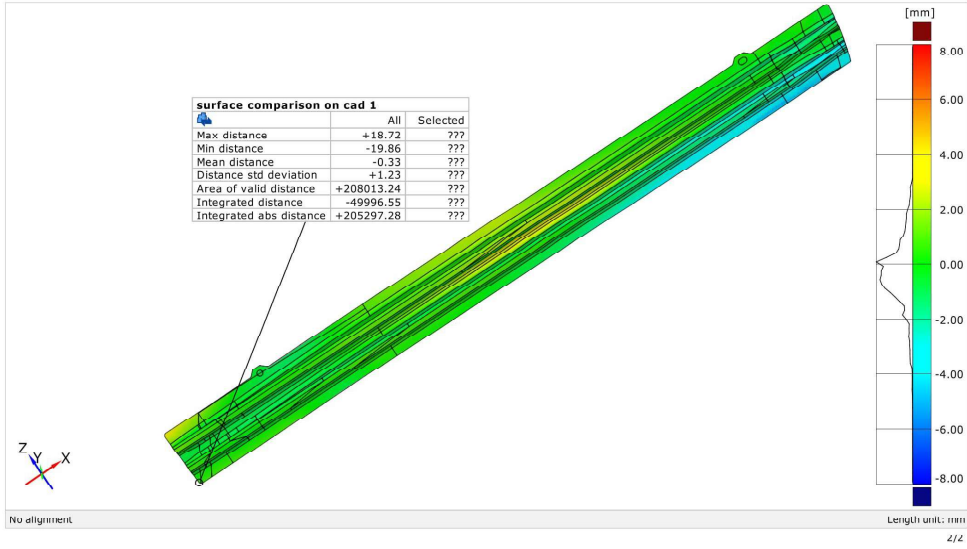


# CAD average\_3D real MA03 lower

Generated with GOM Inspect V8



## Surface Comparison on CAD

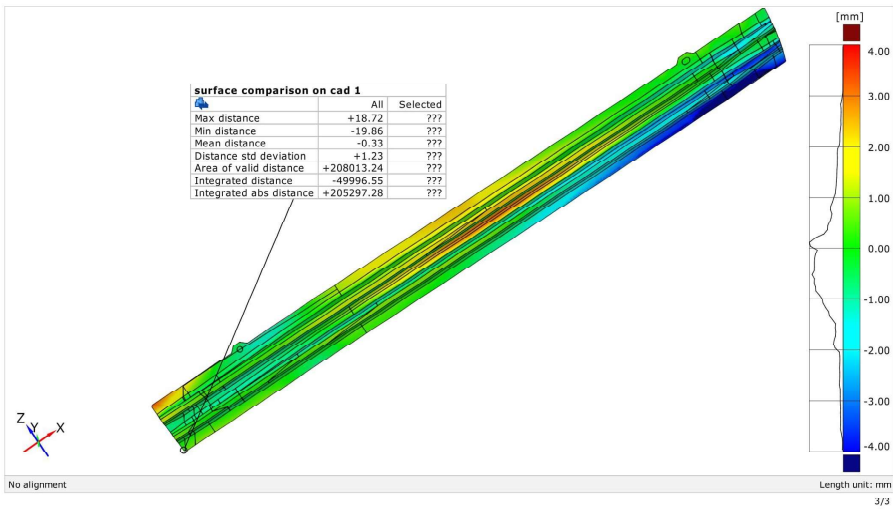


# CAD average\_3D real MA03 lower

Generated with GOM Inspect V8



## Surface Comparison on CAD

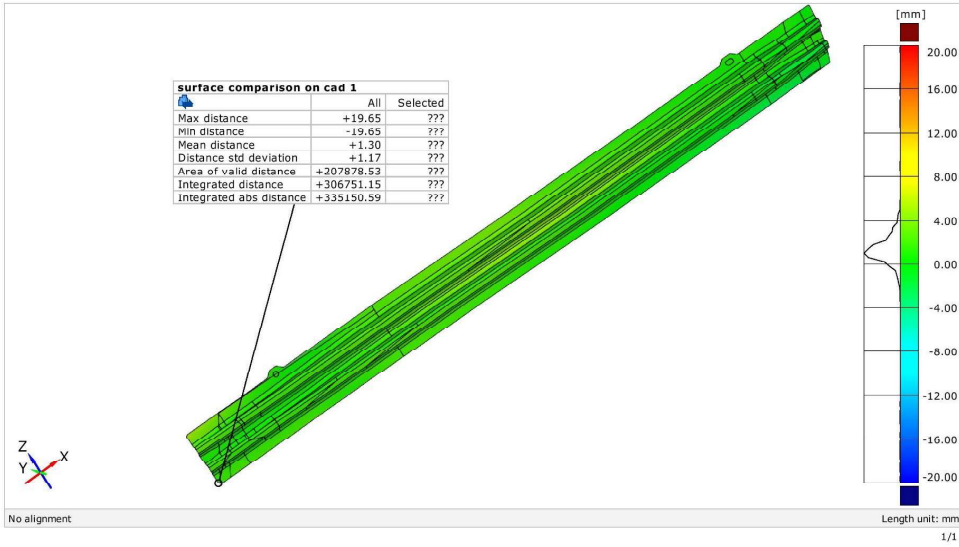


# CAD average\_3D real MA03 higher

Generated with GOM Inspect V8



surface comparison on cad

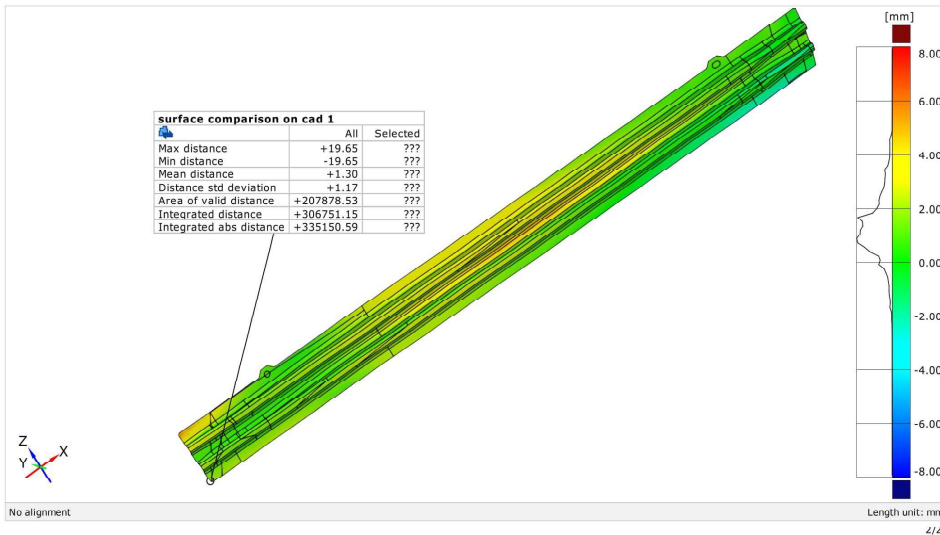


# CAD average\_3D real MA03 higher

Generated with GOM Inspect V8



Surface Comparison on CAD

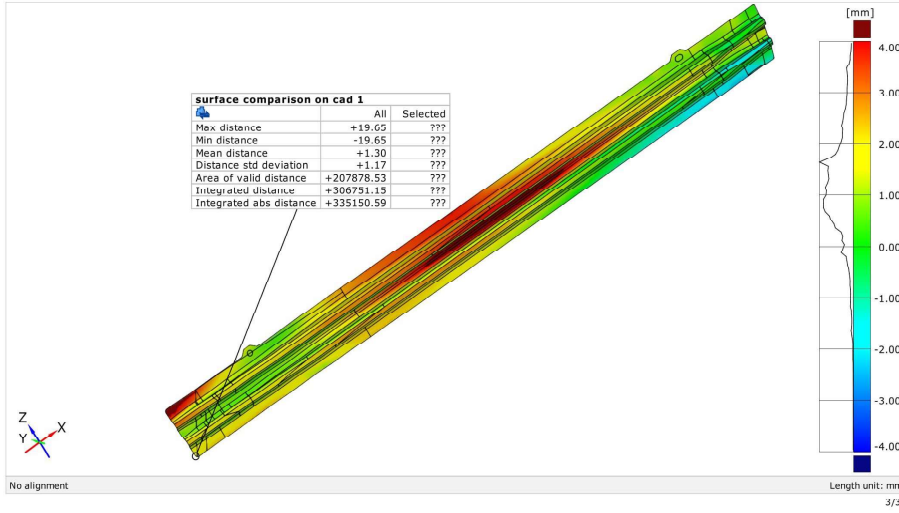


# CAD average\_3D real MA03 higher

Generated with GOM Inspect V8



Surface Comparison on CAD

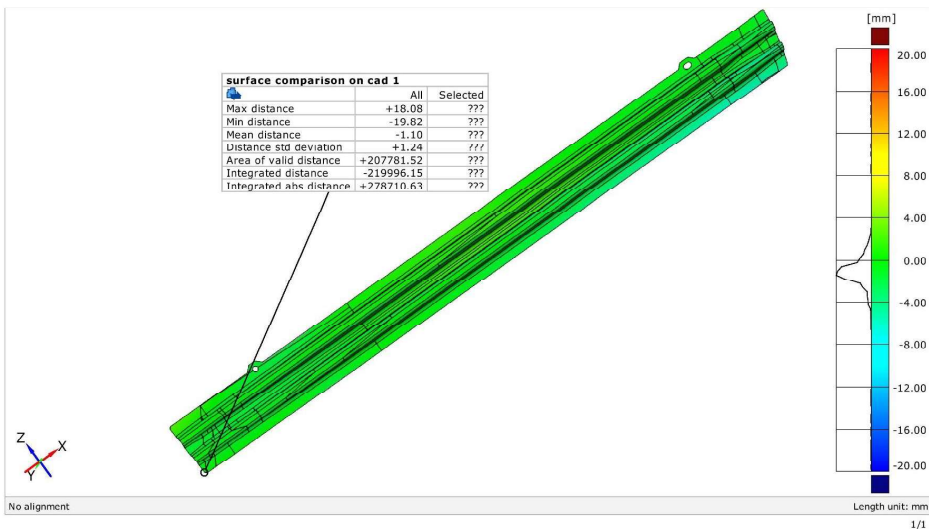


# CAD higher\_3D real MA03 lower

Generated with GOM Inspect V8



surface comparison on cad

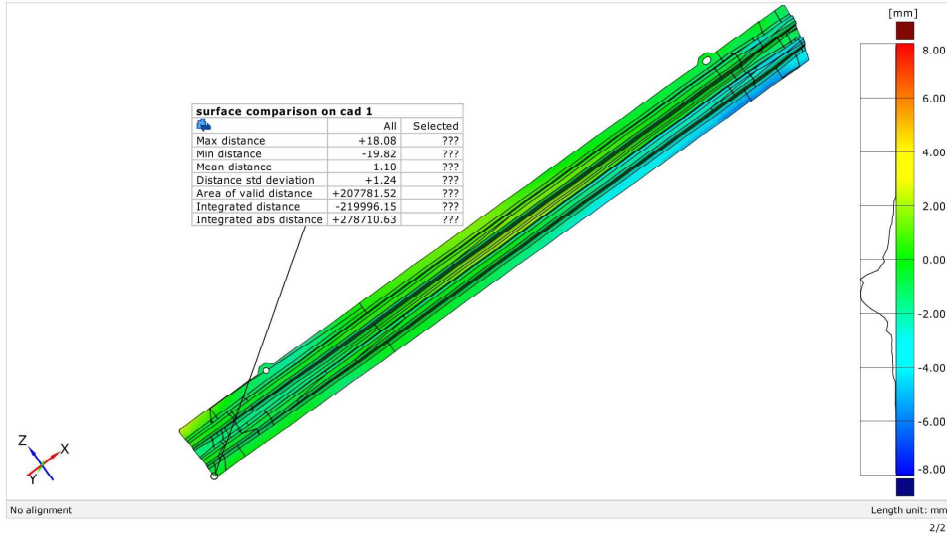


# CAD higher\_3D real MA03 lower

Generated with GOM Inspect V8



## Surface Comparison on CAD

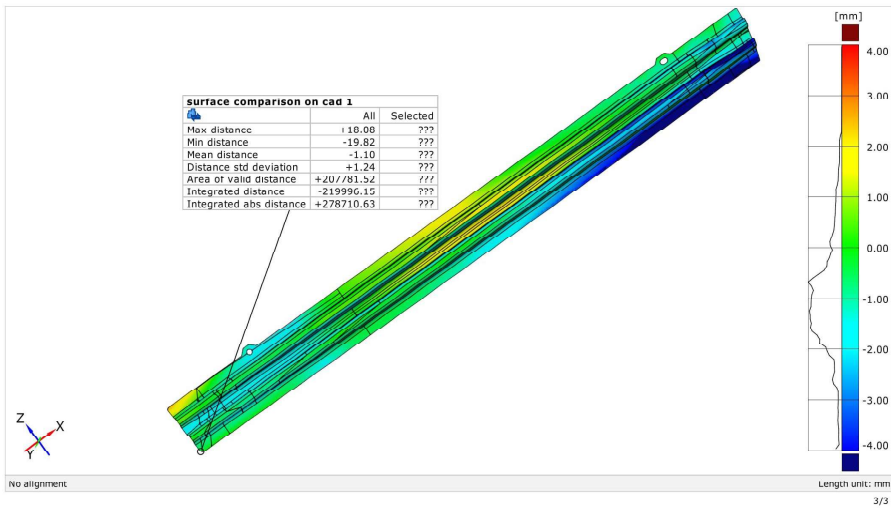


# CAD higher\_3D real MA03 lower

Generated with GOM Inspect V8



## Surface Comparison on CAD

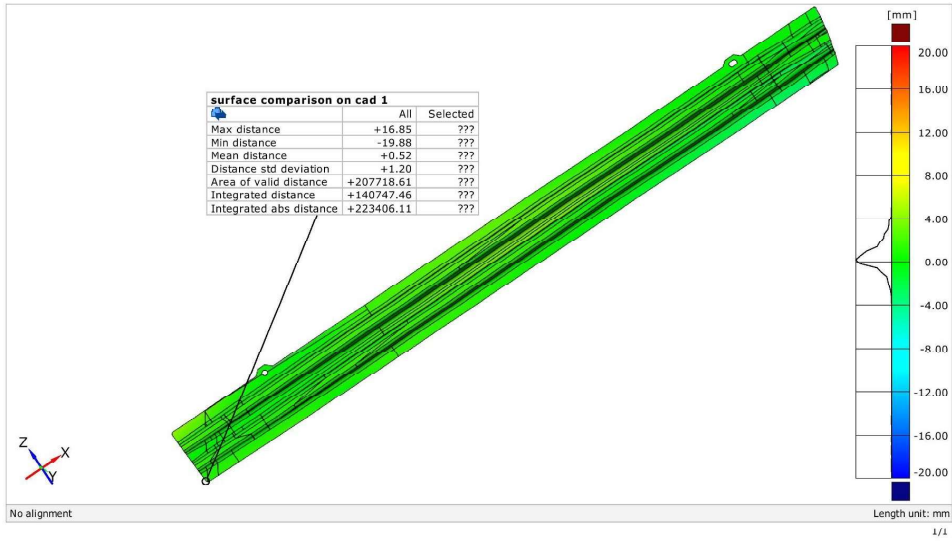


# CAD higher\_3D real MA03 higher

Generated with GOM Inspect V8



surface comparison on cad

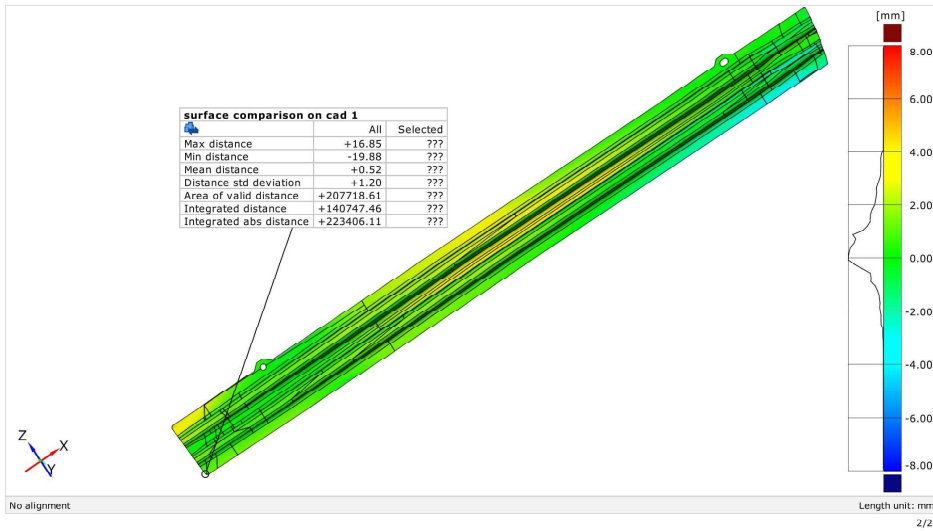


# CAD higher 3D real MA03 higher

Generated with GOM Inspect V8



Surface Comparison on CAD

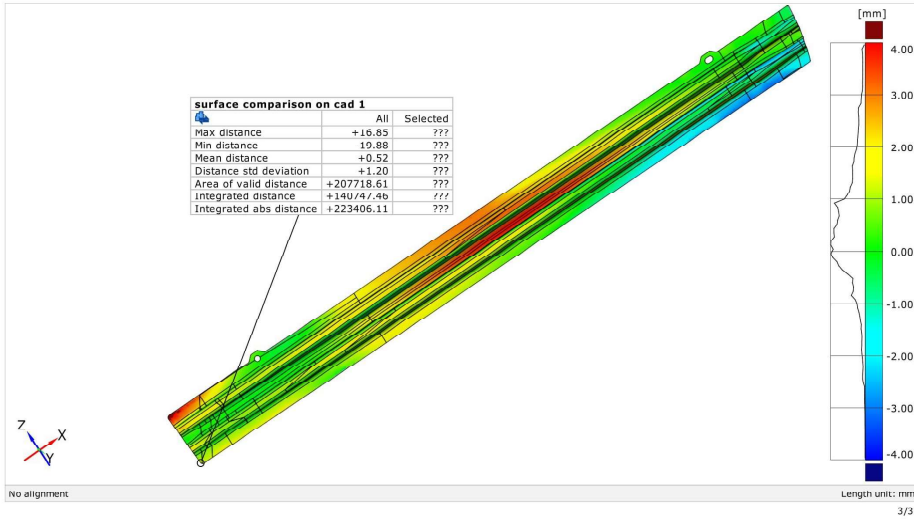


# CAD higher\_3D real MA03 higher

Generated with GOM Inspect V8



## Surface Comparison on CAD



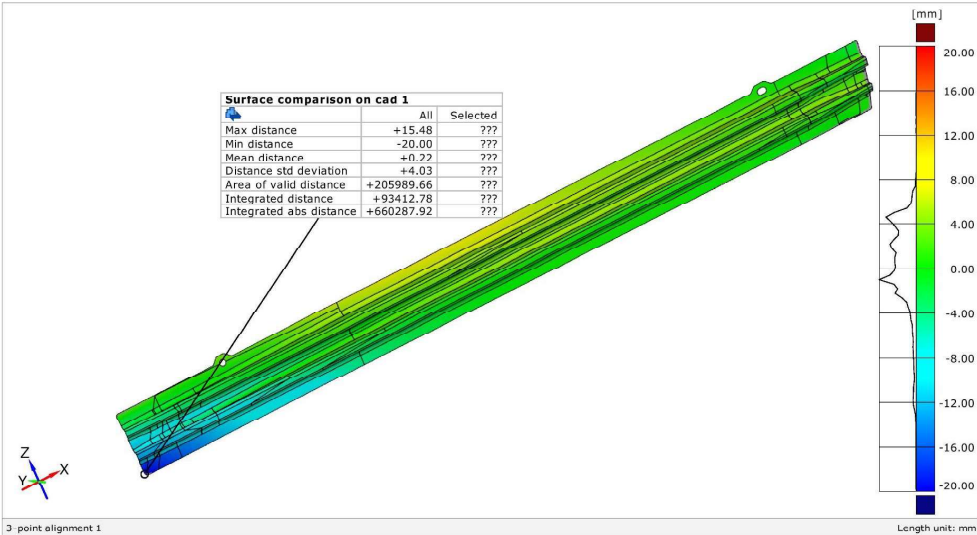
# ANNEX 13.2 COMPARISON BETWEEN CAD (NOMINAL) AND SIMULATION RESULTS

## CAD lower\_simulation 1

Generated with GOM Inspect V8



surface comparison on cad

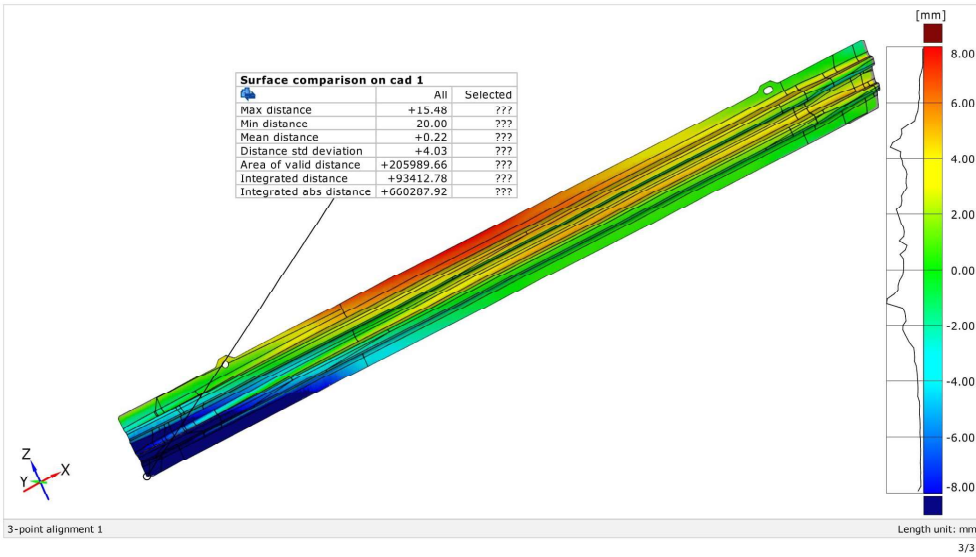


# CAD lower\_simulation 1

Generated with GOM Inspect VR



## Surface Comparison on CAD

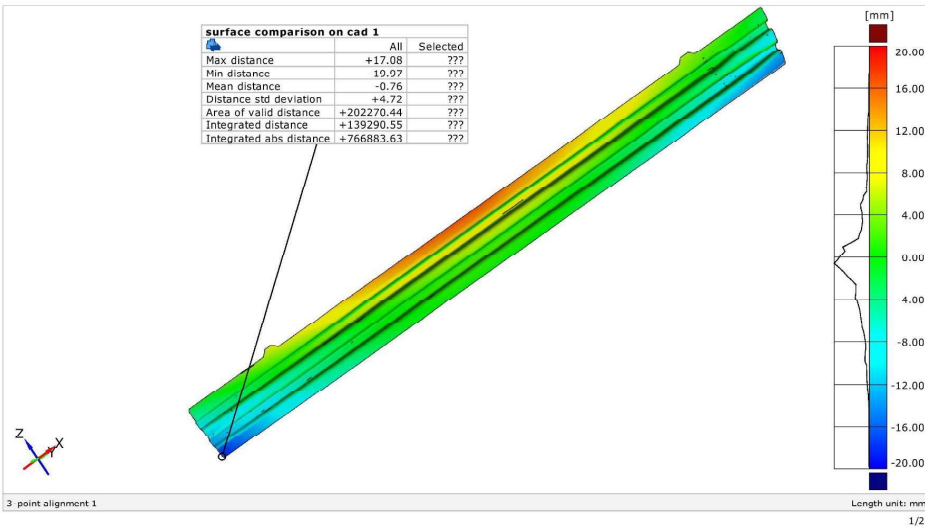


# CAD lower\_simulation 2

Generated with GOM Inspect V8



## surface comparison on cad

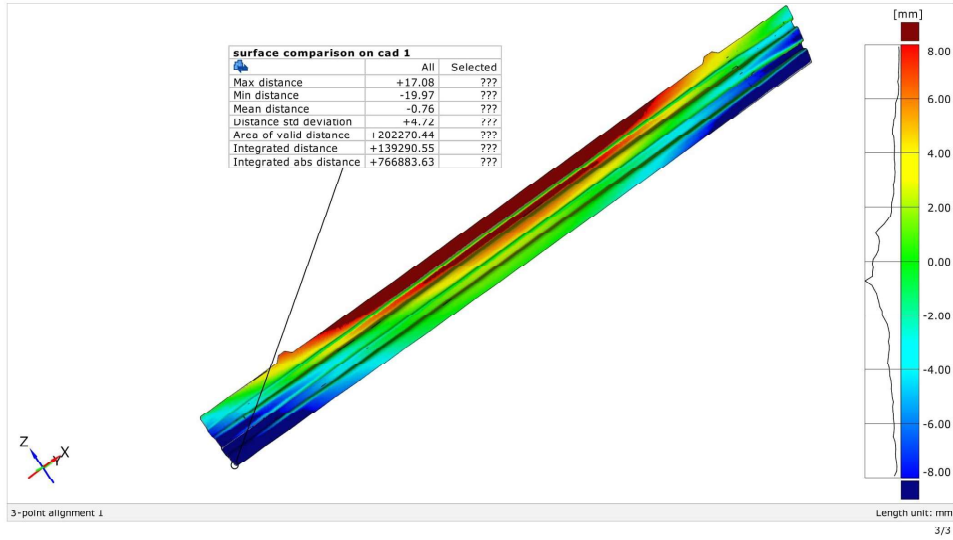


## CAD lower\_simulation 2

Generated with GOM Inspect V8



### Surface Comparison on CAD

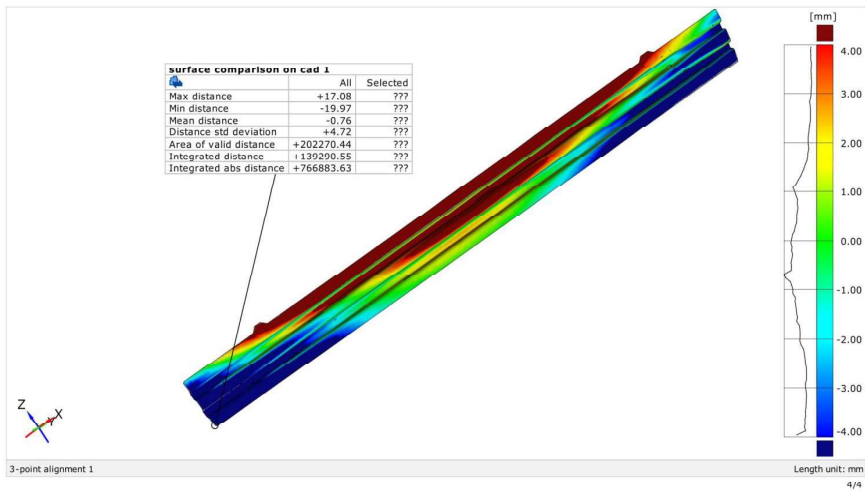


## CAD lower\_simulation 2

Generated with GOM Inspect V8



### Surface Comparison on CAD

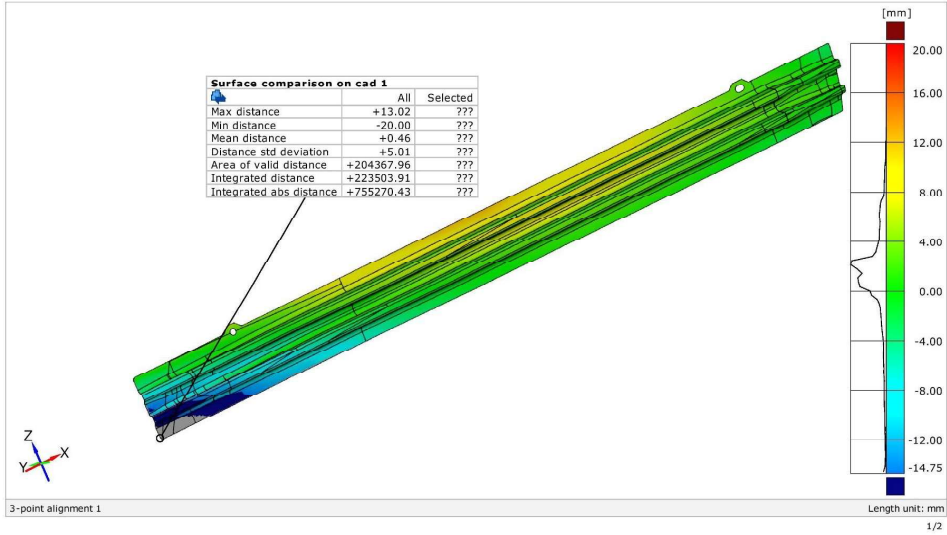


# CAD lower\_simulation 3

Generated with GOM Inspect V8



surface comparison on cad

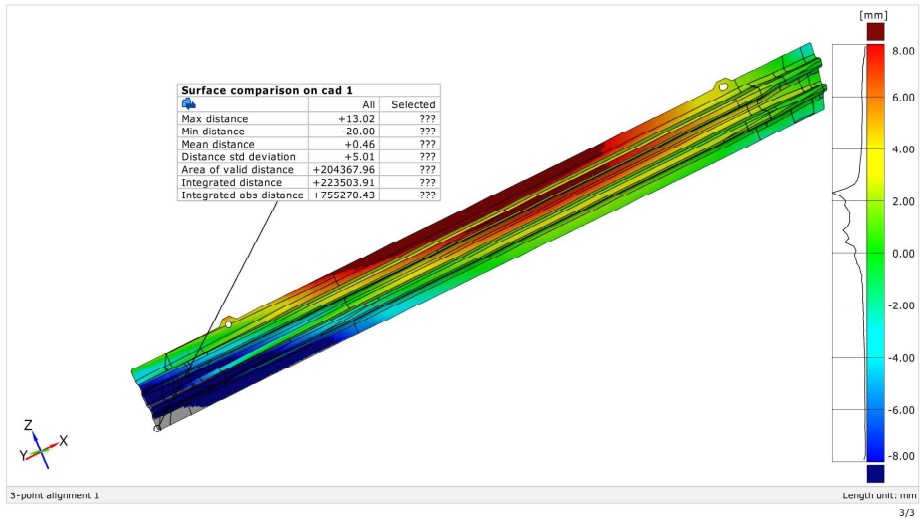


# CAD lower\_simulation 3

Generated with GOM Inspect V8



Surface Comparison on CAD

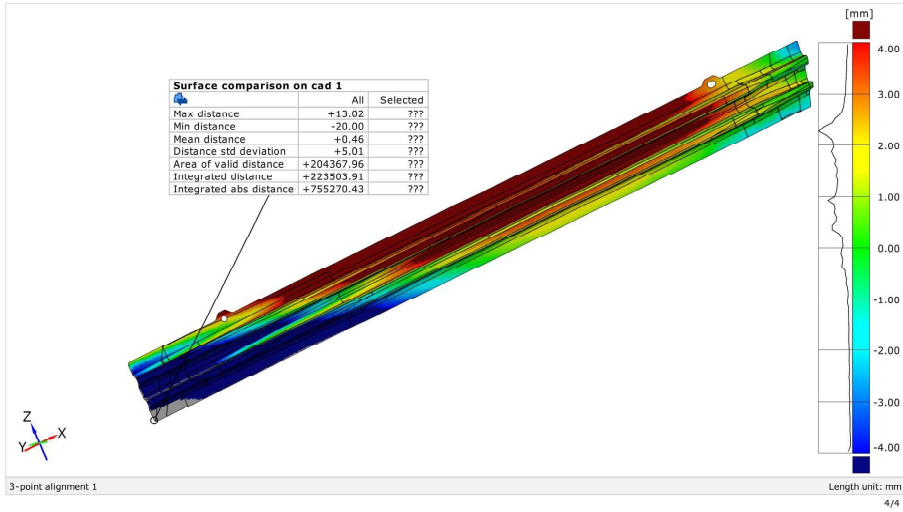


# CAD lower\_simulation 3

Generated with GOM Inspect V8



## Surface Comparison on CAD

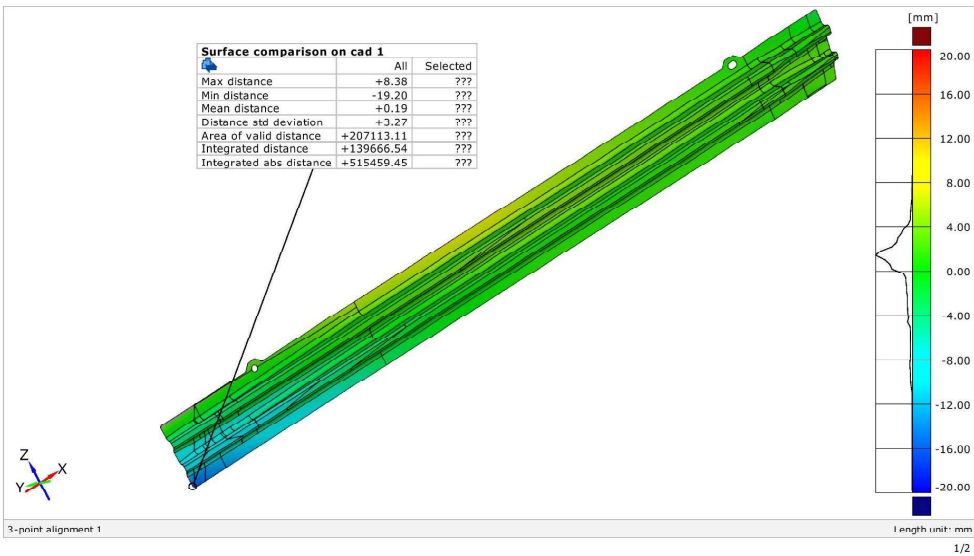


# CAD lower\_simulation 4

Generated with GOM Inspect V8



## surface comparison on cad

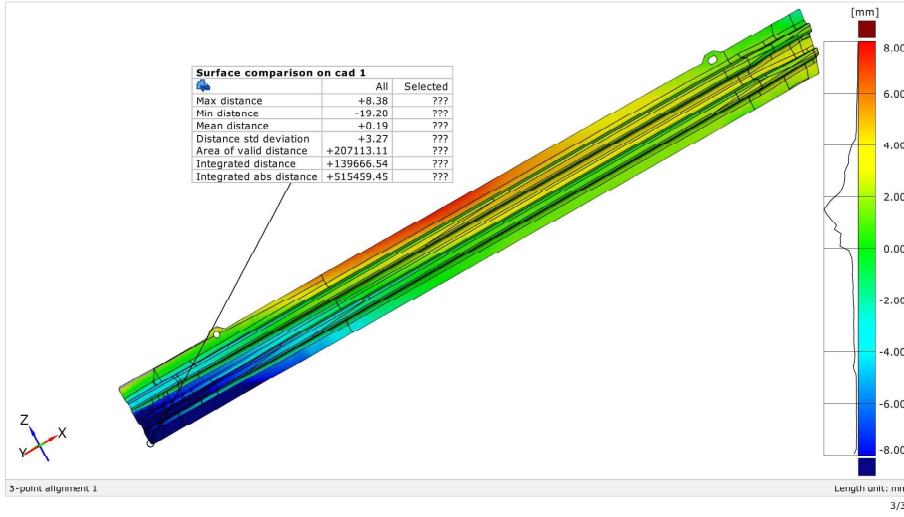


# CAD lower\_simulation 4

Generated with GOM Inspect V8



## Surface Comparison on CAD

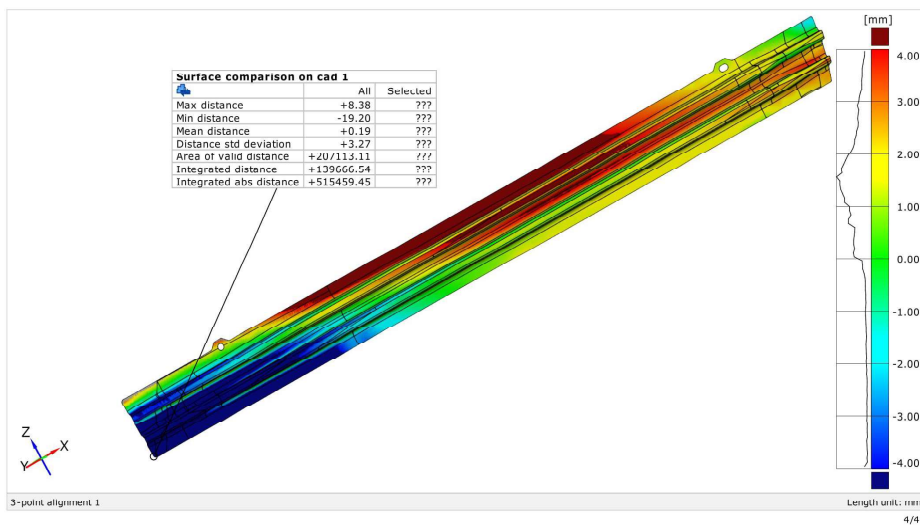


# CAD lower\_simulation 4

Generated with GOM Inspect V8



## Surface Comparison on CAD

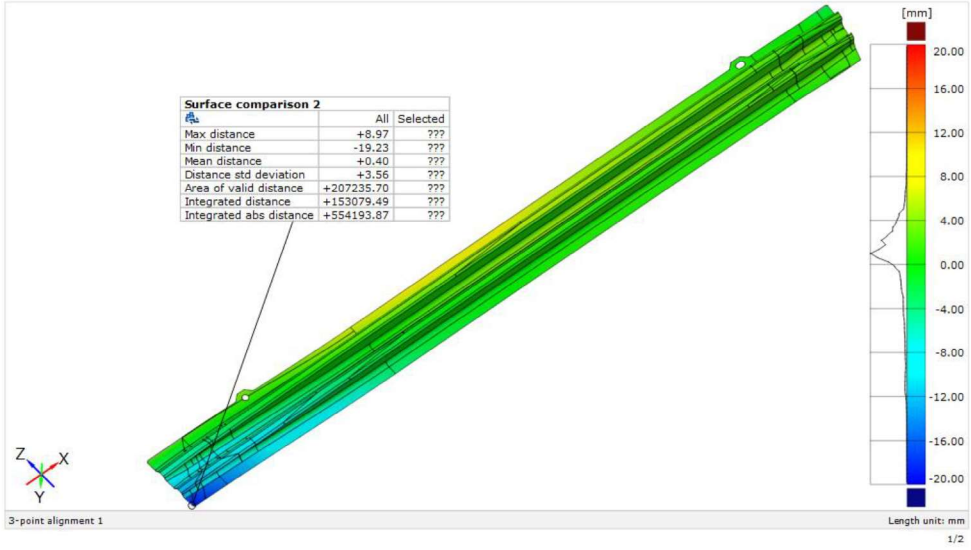


# CAD lower\_simulation 5

Generated with GOM Inspect V8



surface comparison on cad

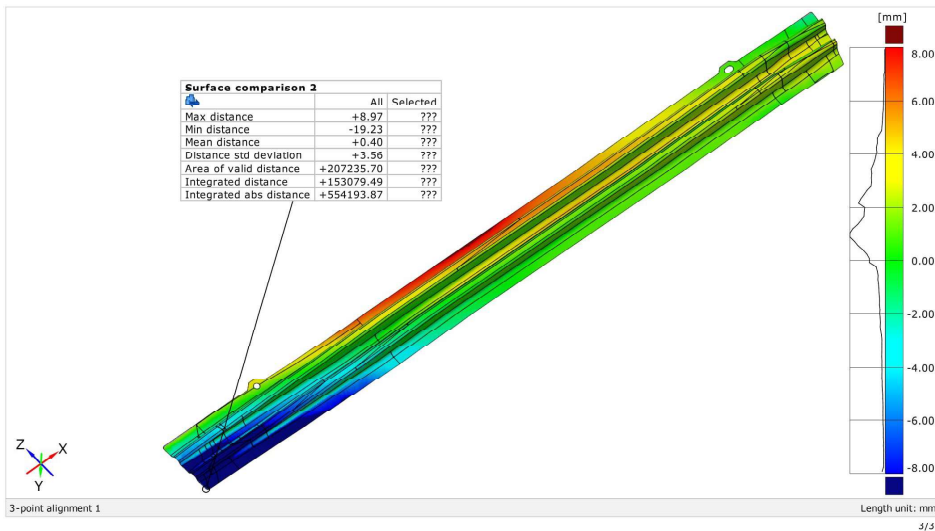


# CAD lower\_simulation 5

Generated with GOM Inspect V8



Surface Comparison on CAD

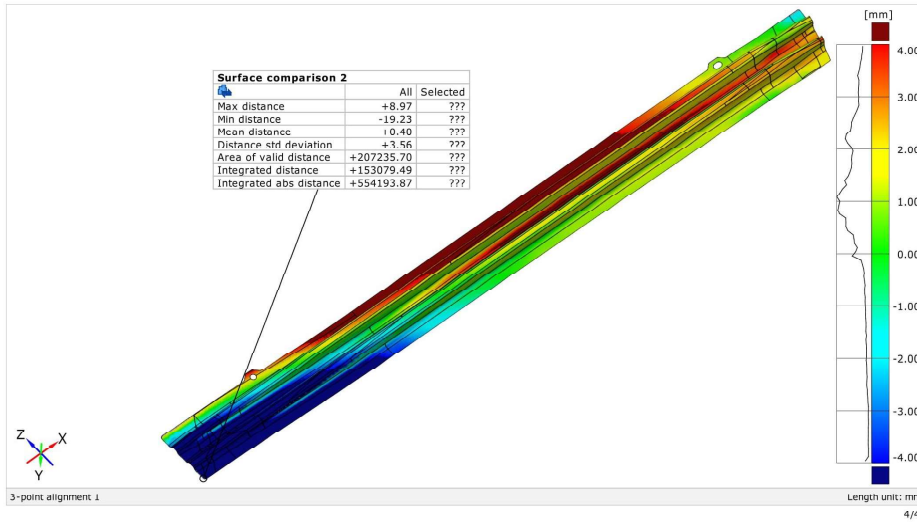


# CAD lower\_simulation 5

Generated with GOM Inspect V8



Surface Comparison on CAD

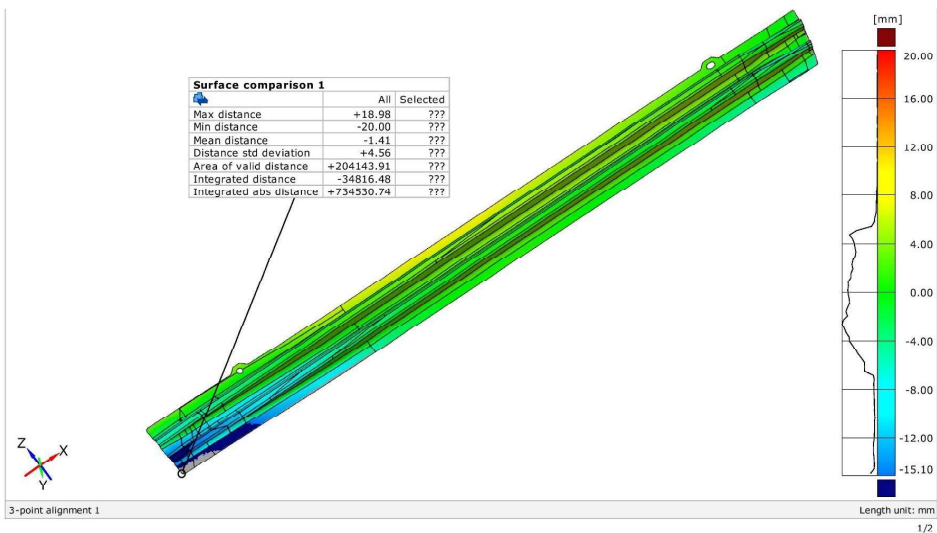


# CAD lower\_simulation 6

Generated with GOM Inspect V8



surface comparison on cad

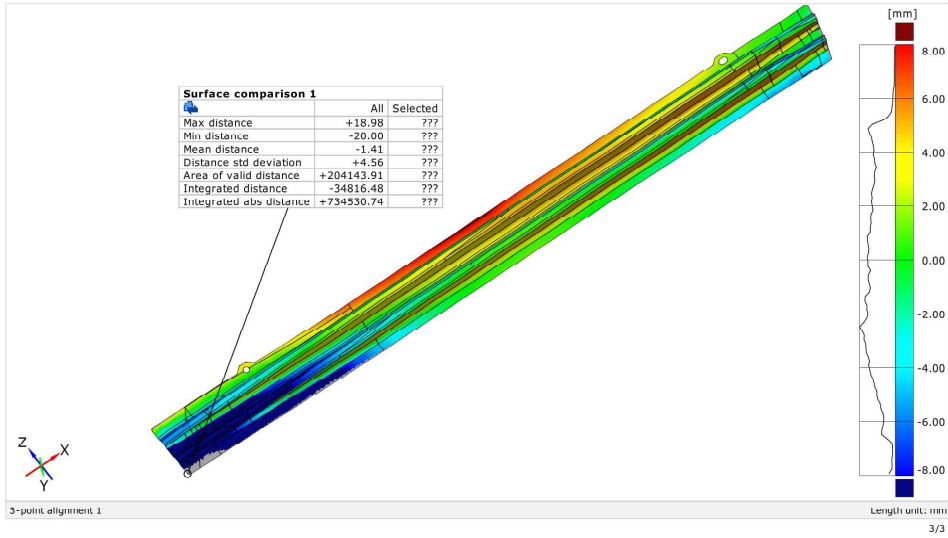


# CAD lower\_simulation 6

Generated with GOM Inspect V8



Surface Comparison on CAD

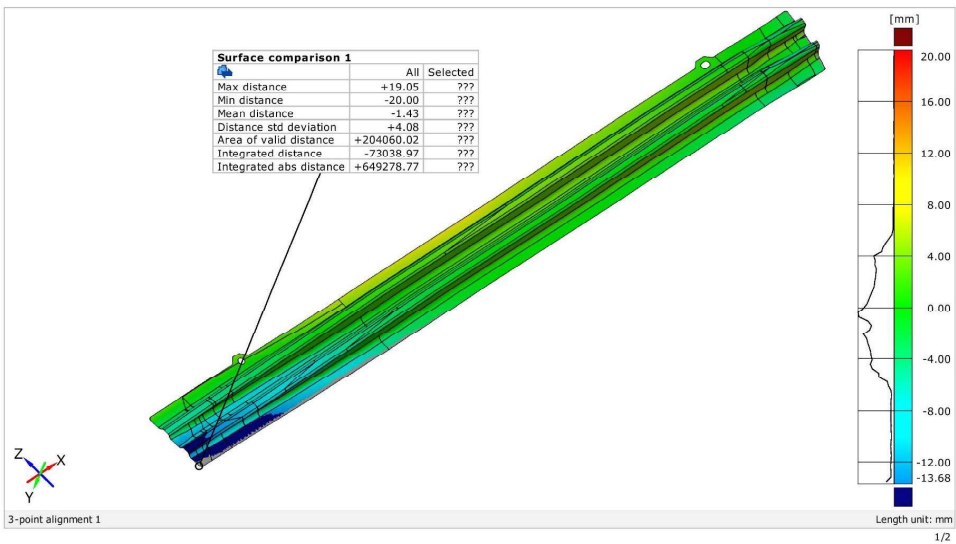


# CAD lower\_simulation 7

Generated with GOM Inspect V8



surface comparison on cad

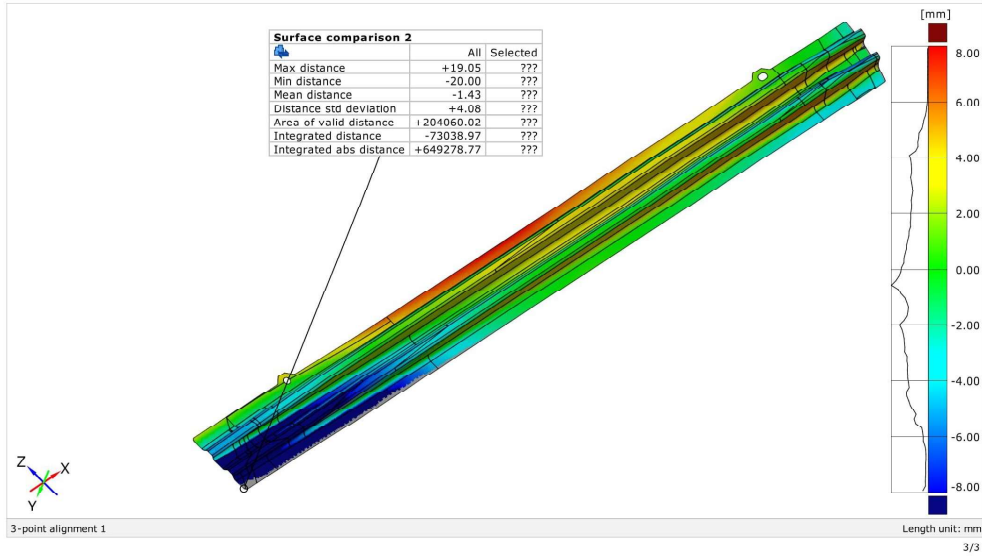


# CAD lower\_simulation 7

Generated with GOM Inspect V8



## Surface Comparison on CAD

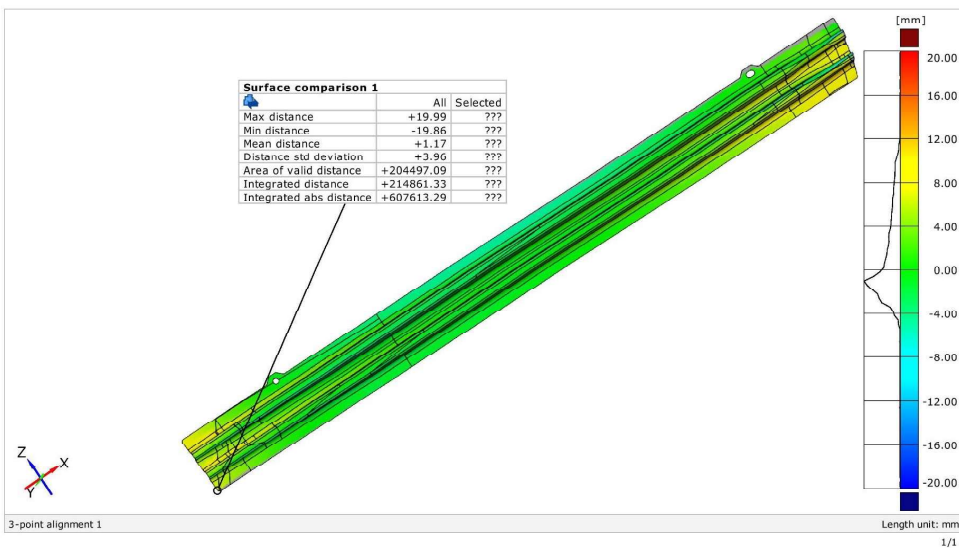


# CAD lower\_simulation 8

Generated with GOM Inspect V8



## Surface Comparison on CAD

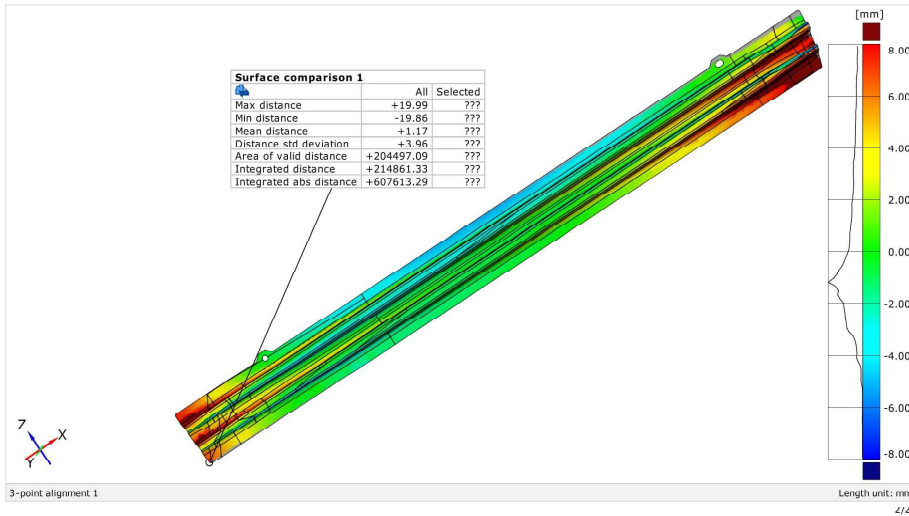


# CAD lower\_simulation 8

Generated with GOM Inspect V8



## Surface Comparison on CAD

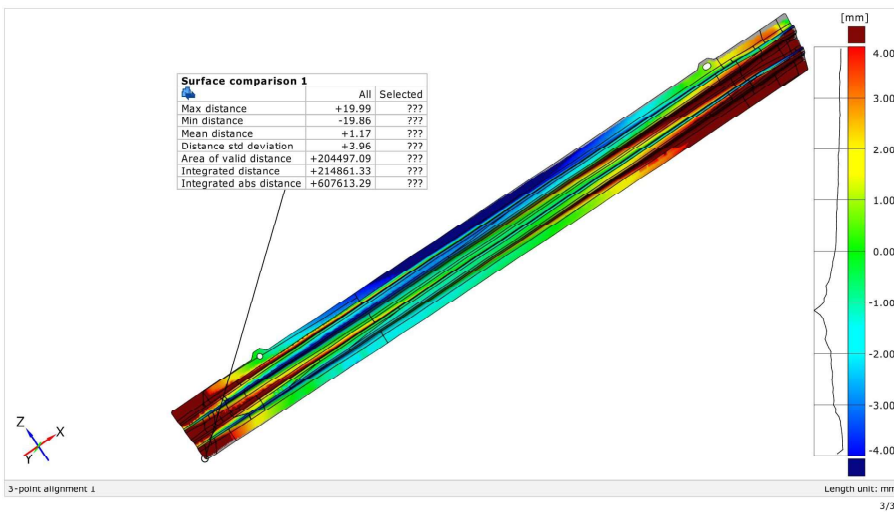


# CAD lower\_simulation 8

Generated with GOM Inspect V8



## Surface Comparison on CAD

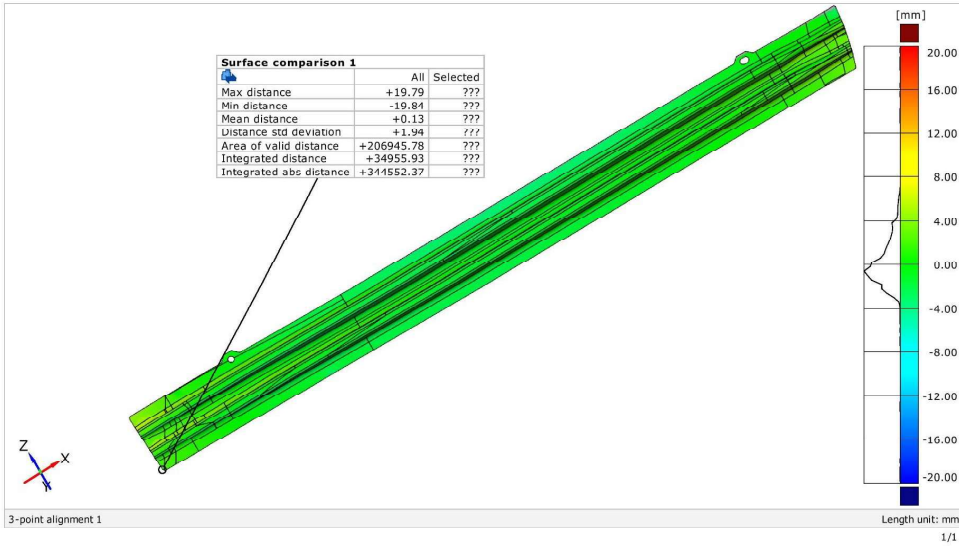


# CAD lower\_simulation 9

Generated with GOM Inspect V8



## Surface Comparison on CAD

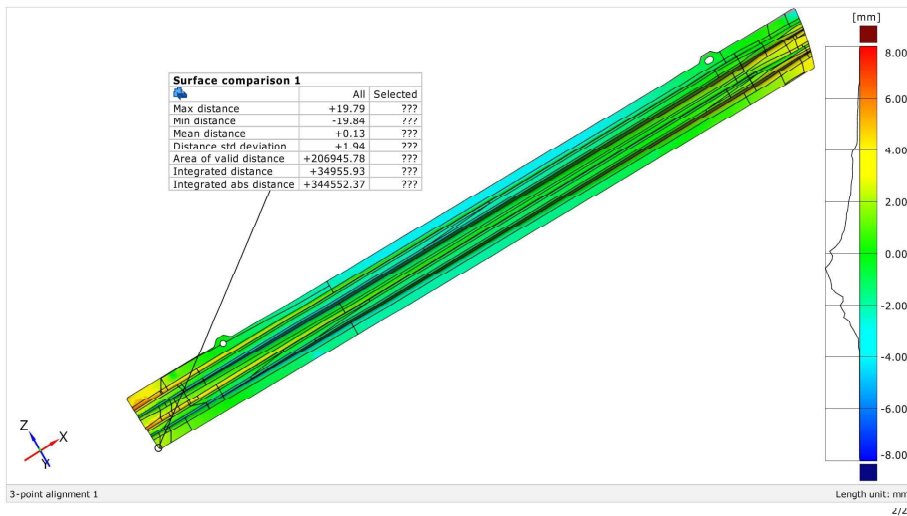


# CAD lower\_simulation 9

Generated with GOM Inspect V8



## Surface Comparison on CAD

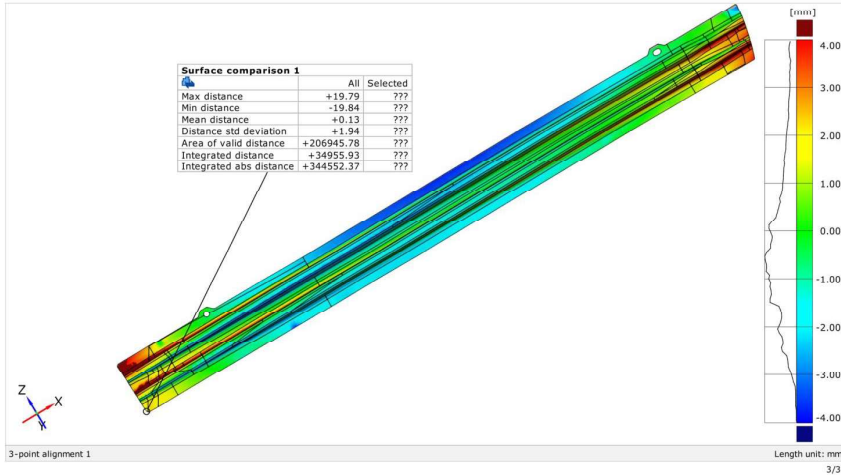


## CAD lower\_simulation 9

Generated with GOM Inspect V8



Surface Comparison on CAD

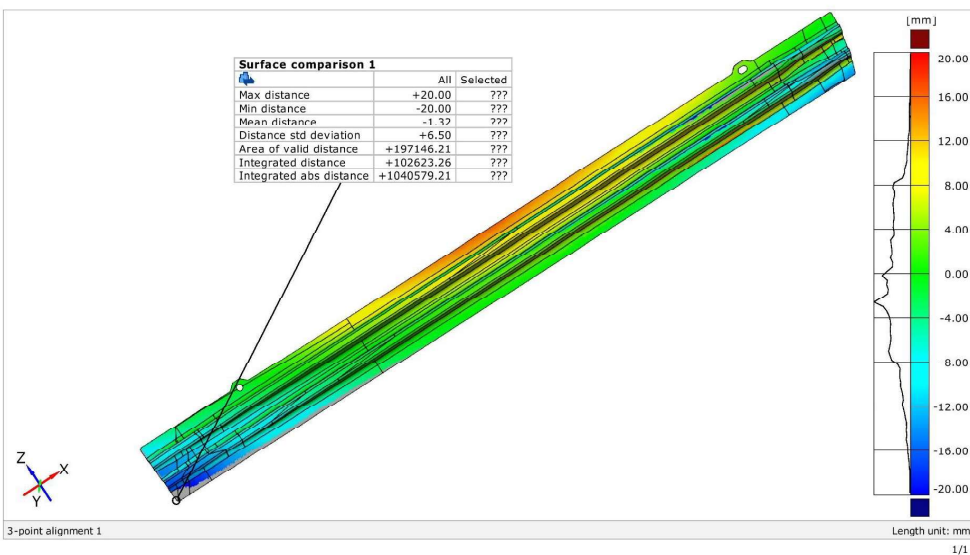


## CAD lower\_simulation 10

Generated with GOM Inspect V8



Surface Comparison on CAD

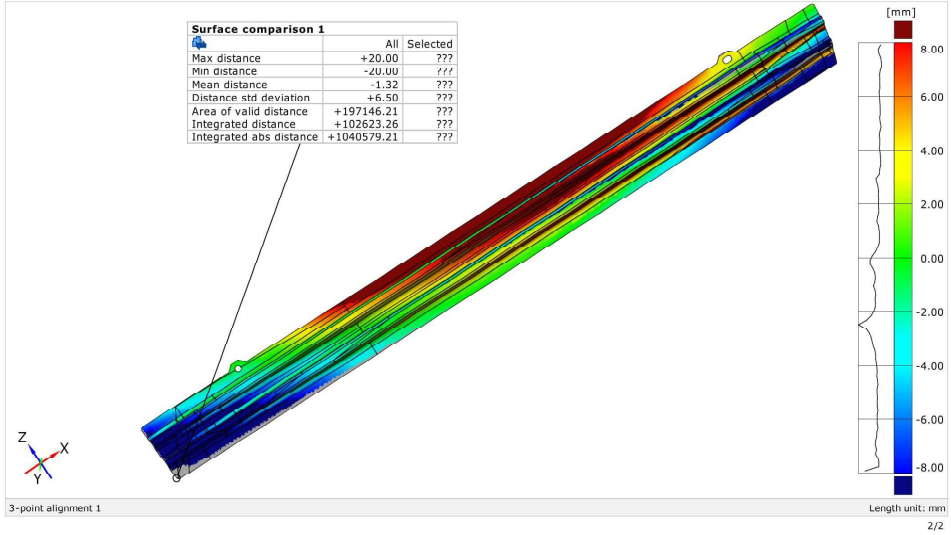


# CAD lower\_simulation 10

Generated with GOM Inspect V8



## Surface Comparison on CAD

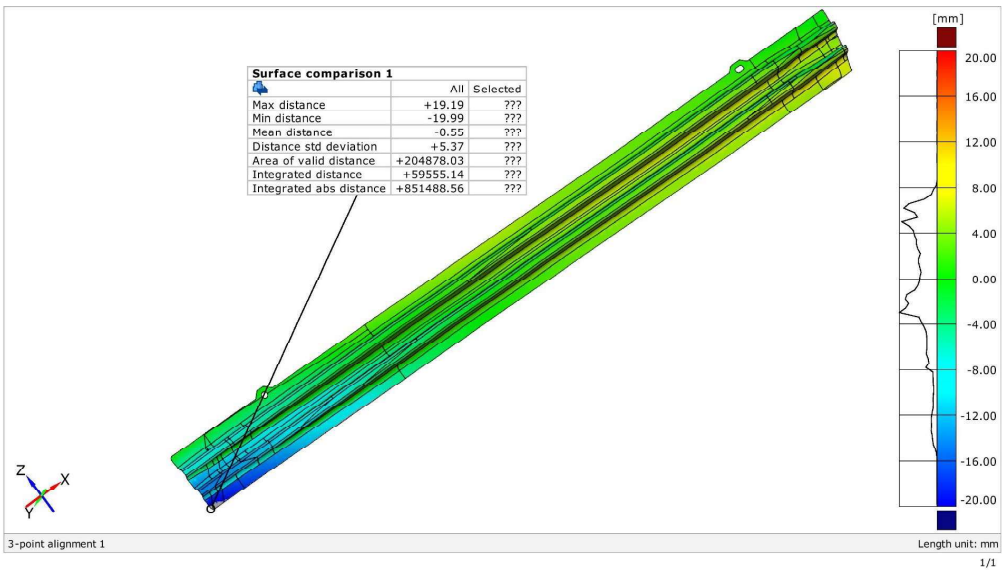


# CAD lower\_simulation 11

Generated with GOM Inspect V8



## Surface Comparison on CAD

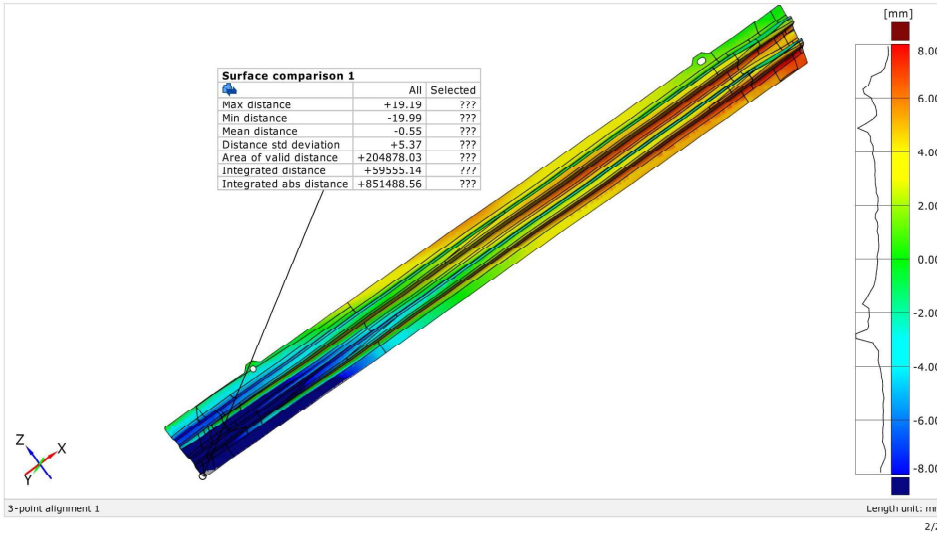


# CAD lower\_simulation 11

Generated with GOM Inspect V8



## Surface Comparison on CAD

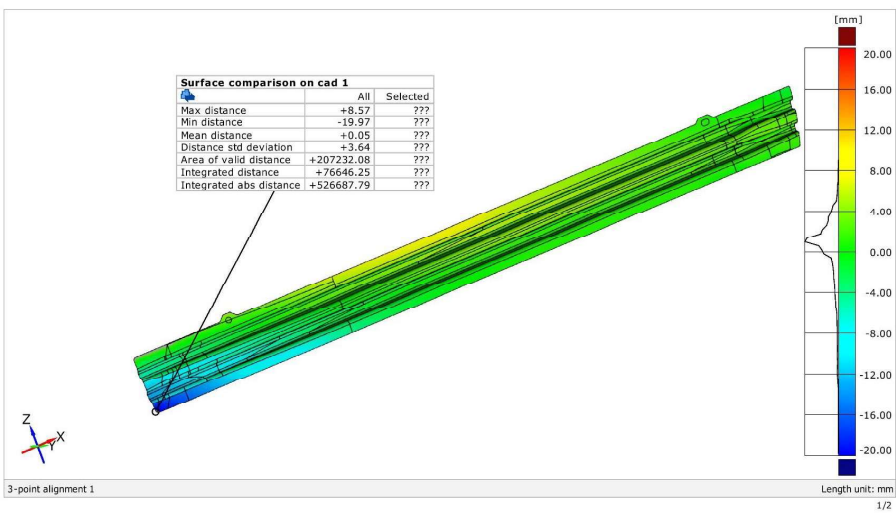


# CAD average\_simulation 1

Generated with GOM Inspect V8



## surface comparison on cad

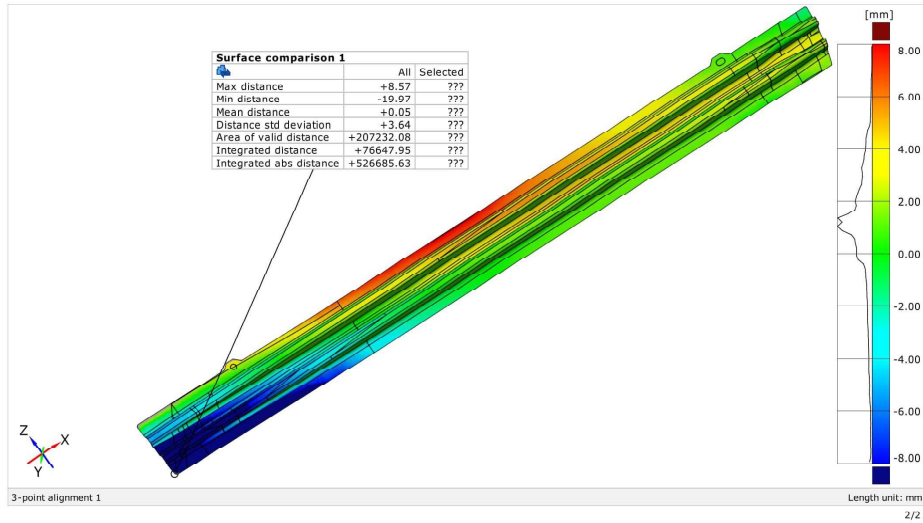


# CAD average\_simulation 1

Generated with GOM Inspect V8



Surface Comparison on CAD

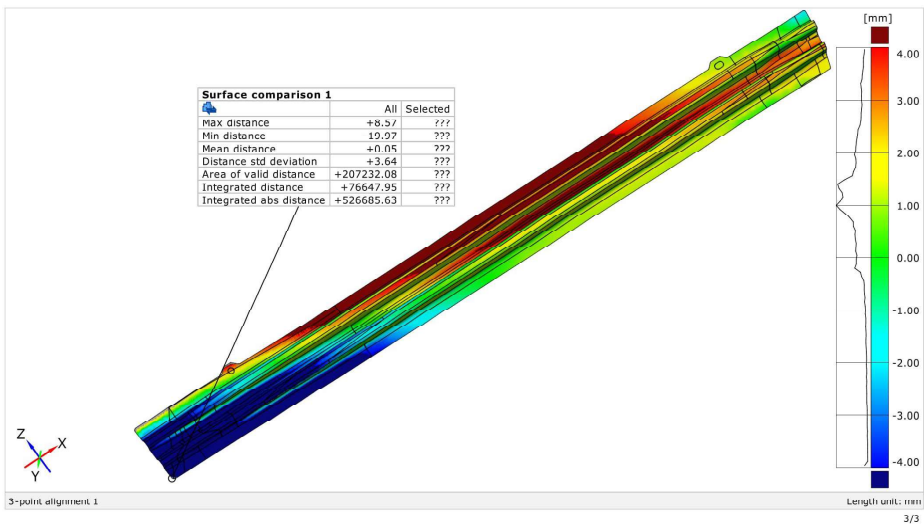


# CAD average\_simulation 1

Generated with GOM Inspect V8



Surface Comparison on CAD

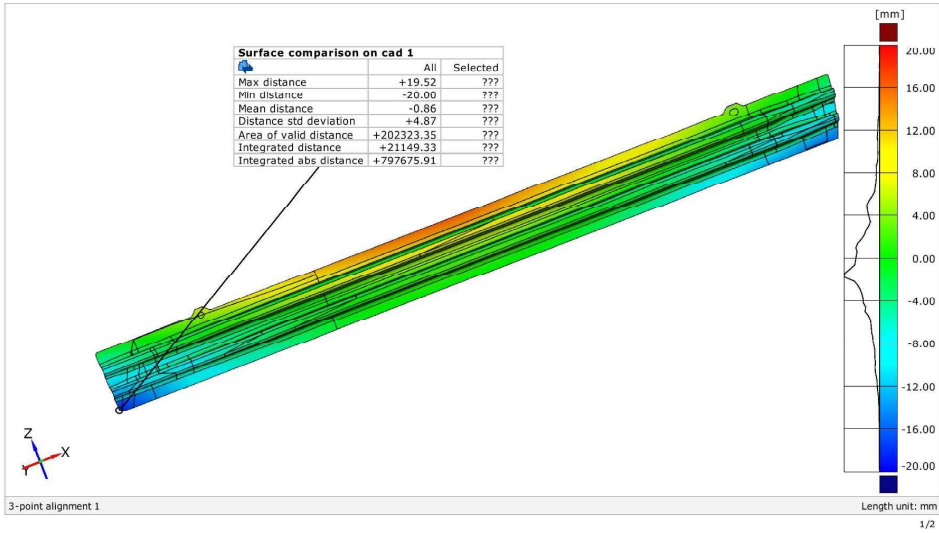


## CAD average\_simulation 2

Generated with GOM Inspect V8

gom

surface comparison on cad

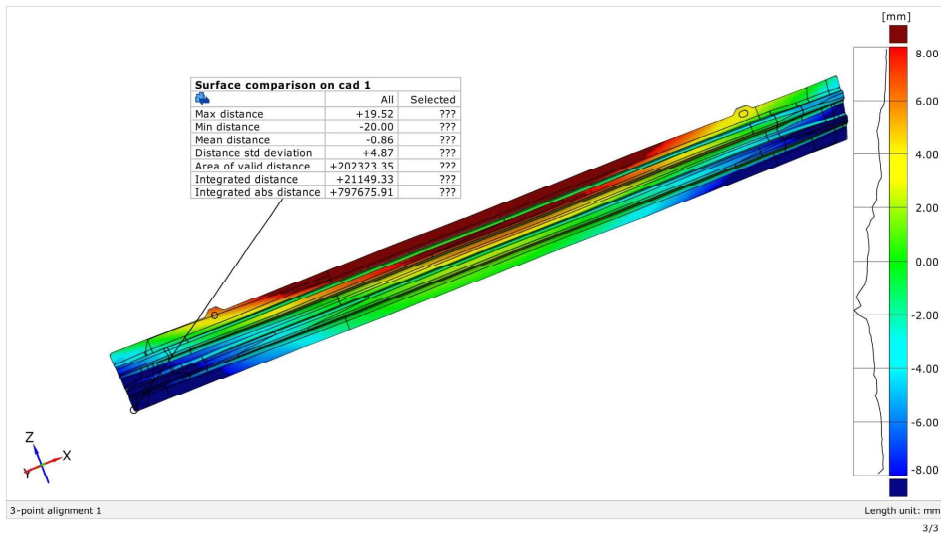


## CAD average\_simulation 2

Generated with GOM Inspect V8

gom

Surface Comparison on CAD

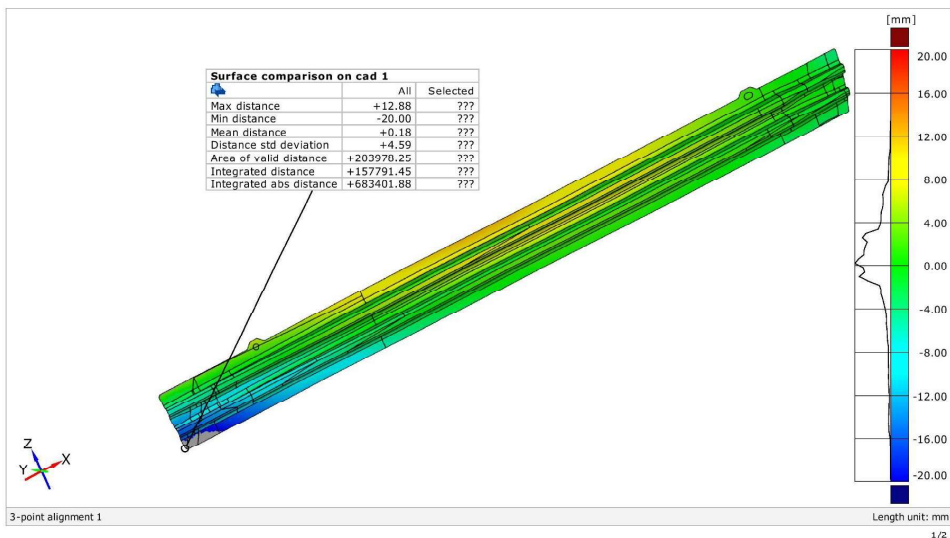


# CAD average\_simulation 3

Generated with GOM Inspect V8



surface comparison on cad

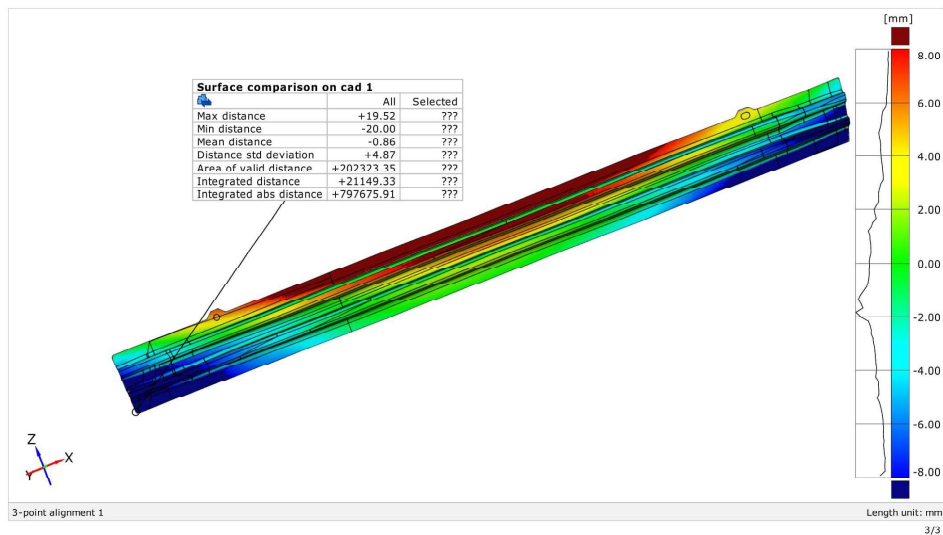


# CAD average\_simulation 3

Generated with GOM Inspect V8



Surface Comparison on CAD

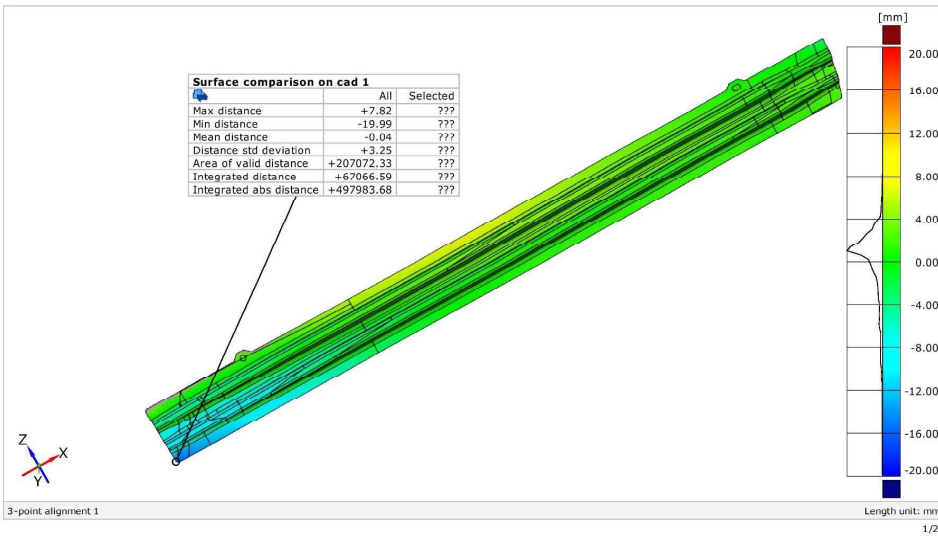


# CAD average\_simulation 4

Generated with GOM Inspect V8



surface comparison on cad

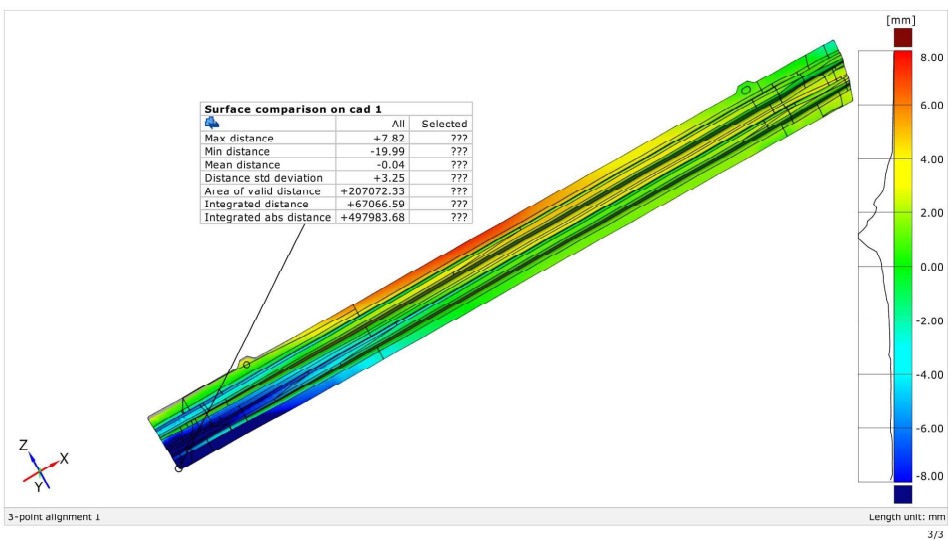


# CAD average\_simulation 4

Generated with GOM Inspect V8



Surface Comparison on CAD

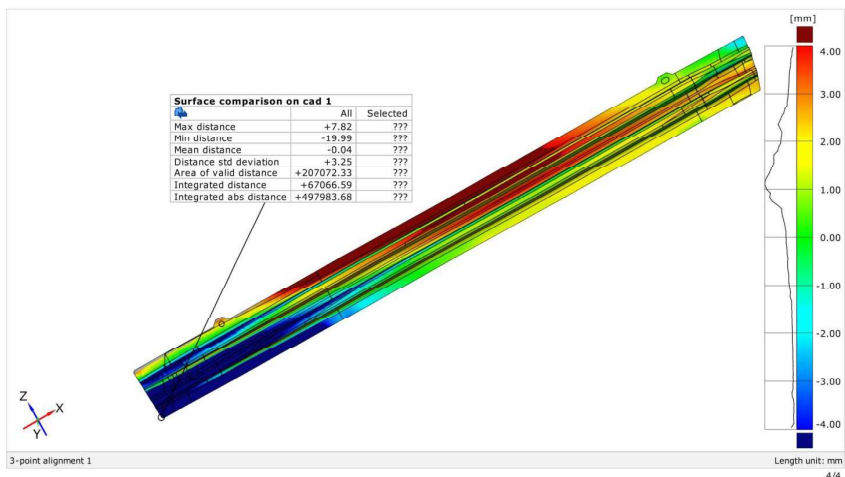


## CAD average\_simulation 4

Generated with GOM Inspect V8



Surface Comparison on CAD

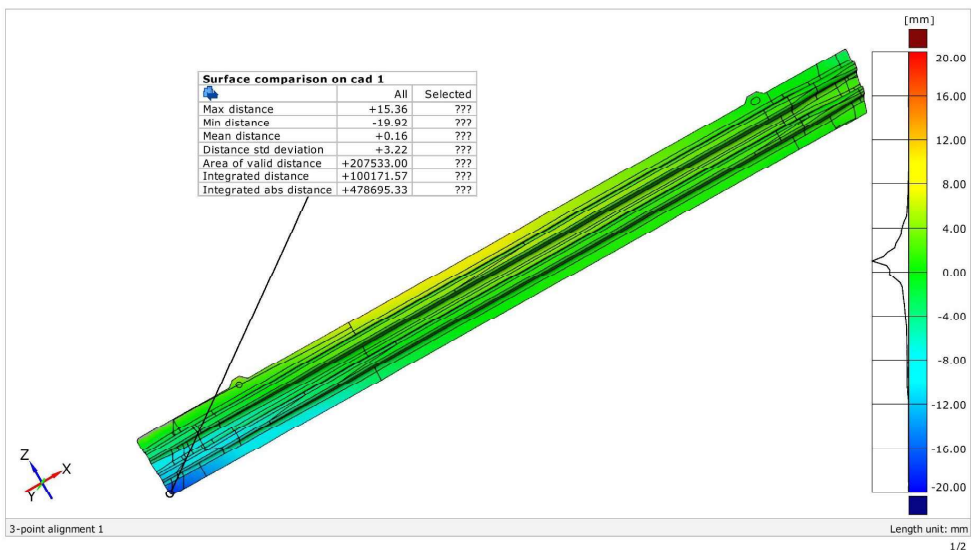


## CAD average\_simulation 5

Generated with GOM Inspect V8



surface comparison on cad

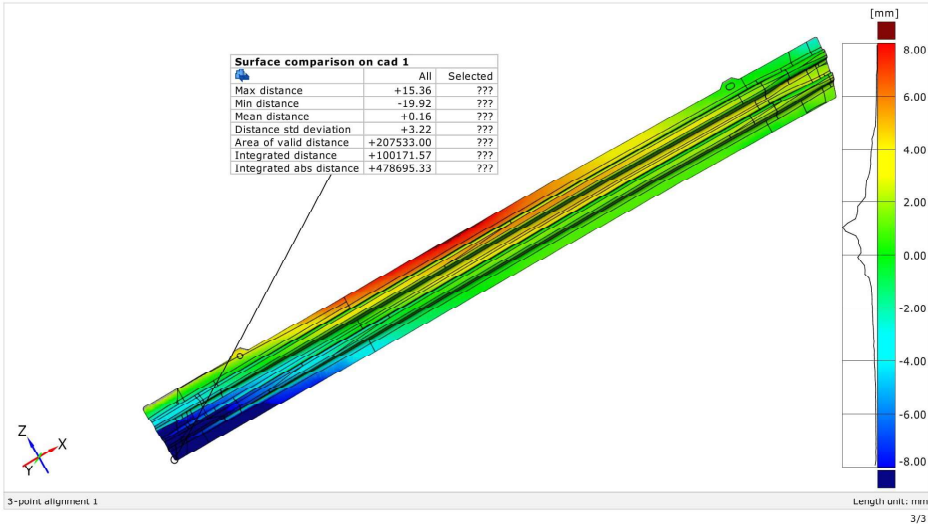


# CAD average\_simulation 5

Generated with GOM Inspect V8



## Surface Comparison on CAD

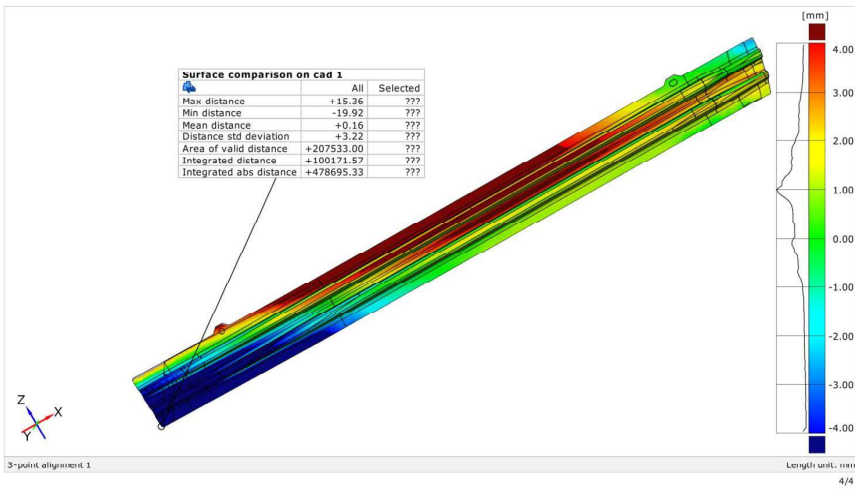


# CAD average\_simulation 5

Generated with GOM Inspect V8



## Surface Comparison on CAD

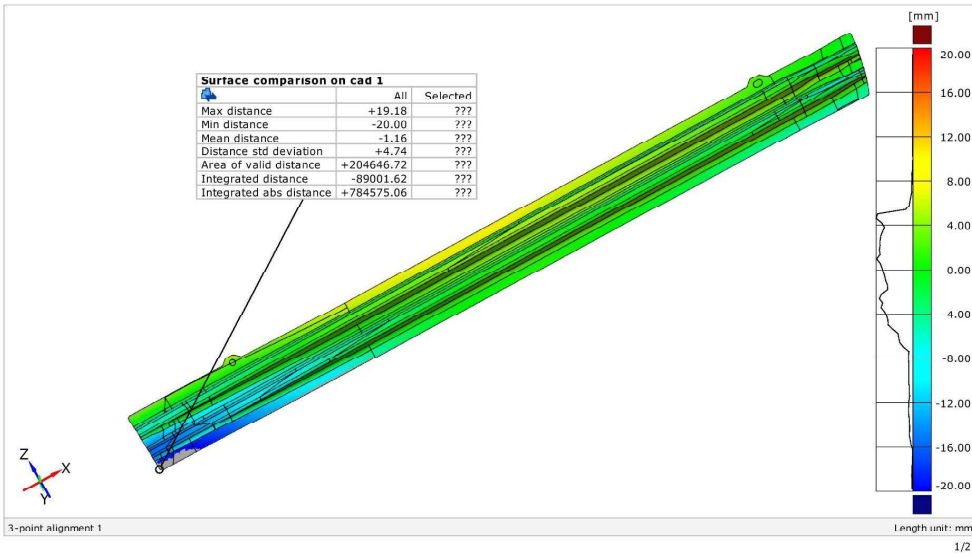


# CAD average\_simulation 6

Generated with GOM Inspect V8



surface comparison on cad

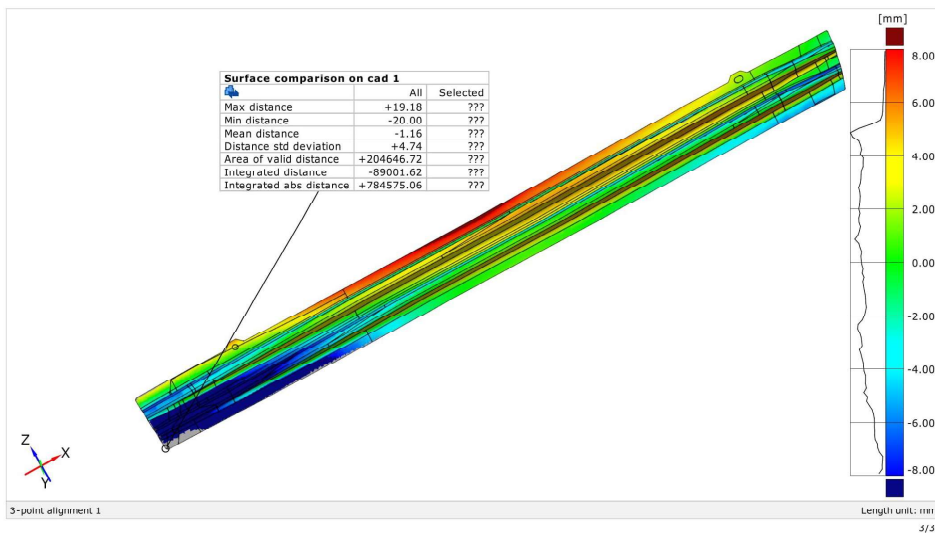


# CAD average\_simulation 6

Generated with GOM Inspect V8



Surface Comparison on CAD

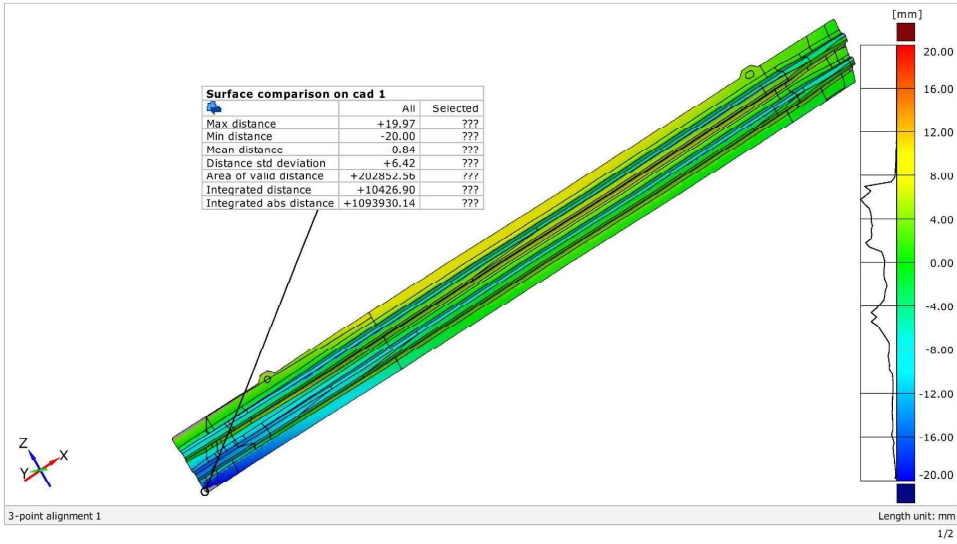


# CAD average\_simulation 7

Generated with GOM Inspect V8



surface comparison on cad

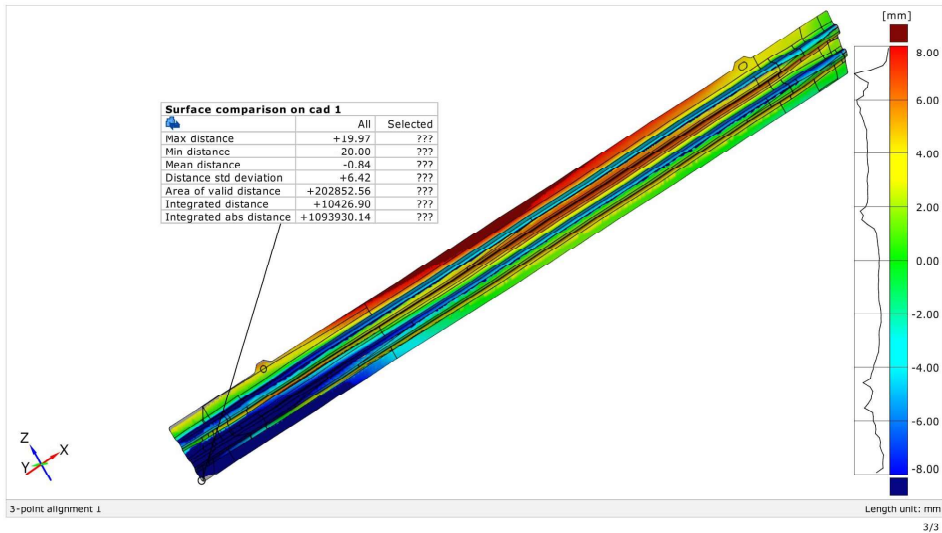


# CAD average\_simulation 7

Generated with GOM Inspect V8



Surface Comparison on CAD

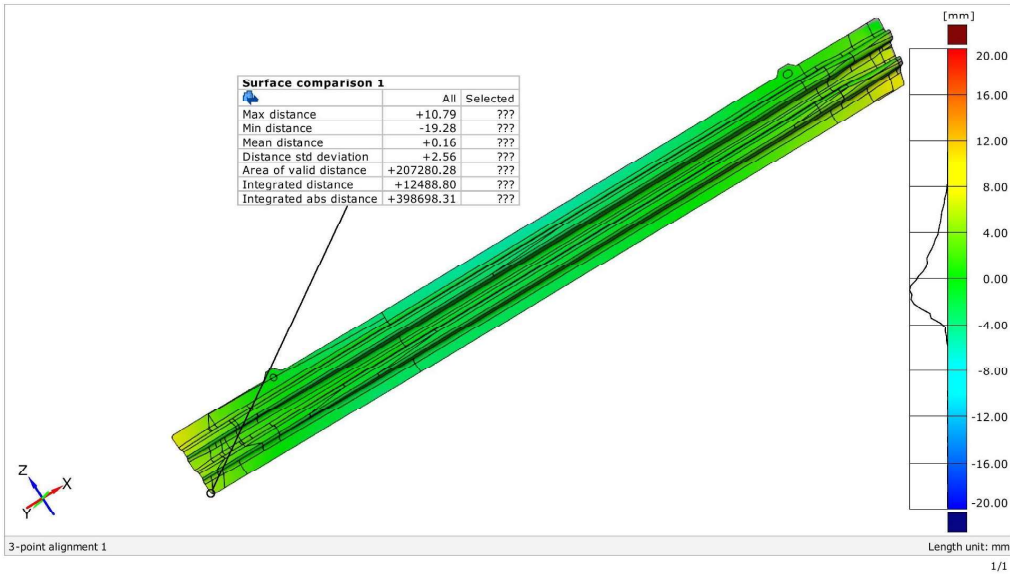


# CAD average\_simulation 8

Generated with GOM Inspect v8



## Surface Comparison on CAD

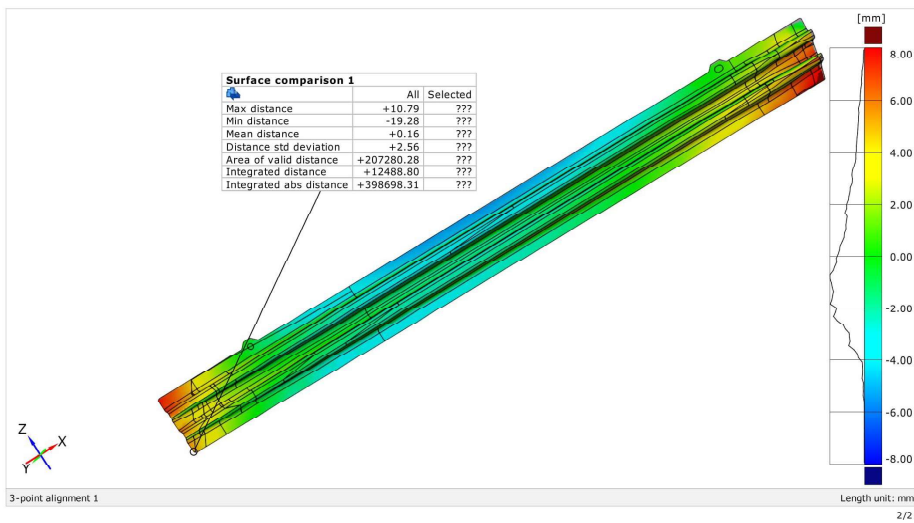


# CAD average\_simulation 8

Generated with GOM Inspect v8



## Surface Comparison on CAD

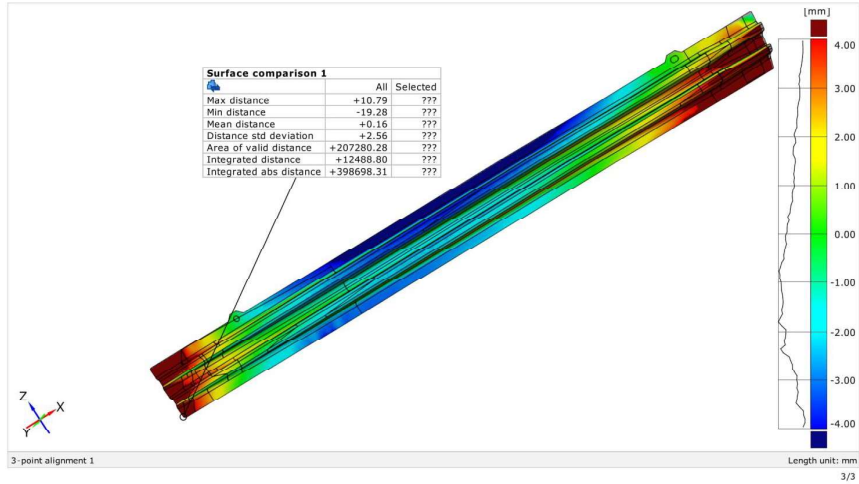


## CAD average\_simulation 8

Generated with GOM Inspect V8

gom

Surface Comparison on CAD

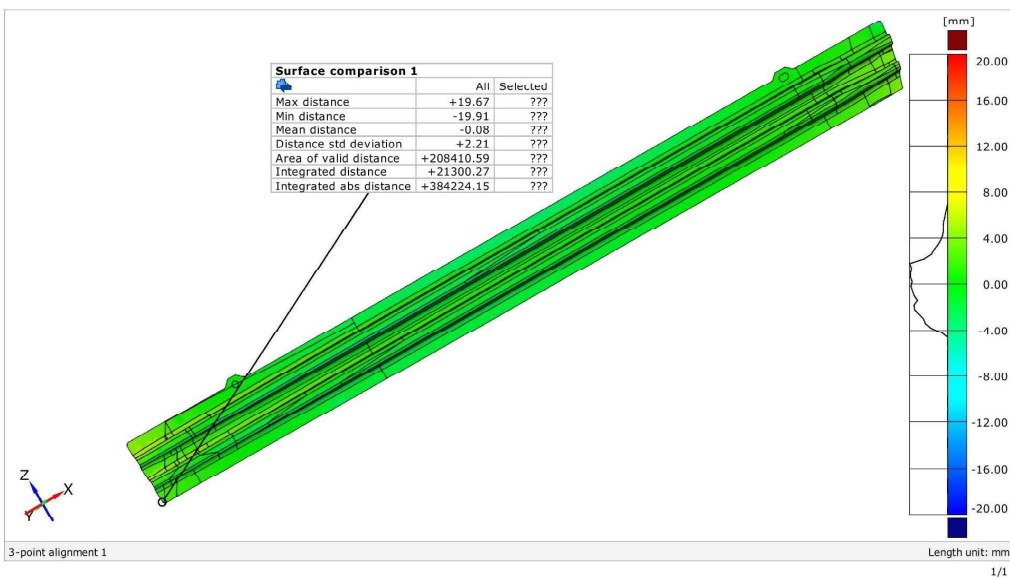


## CAD average\_simulation 9

Generated with GOM Inspect V8

gom

Surface Comparison on CAD

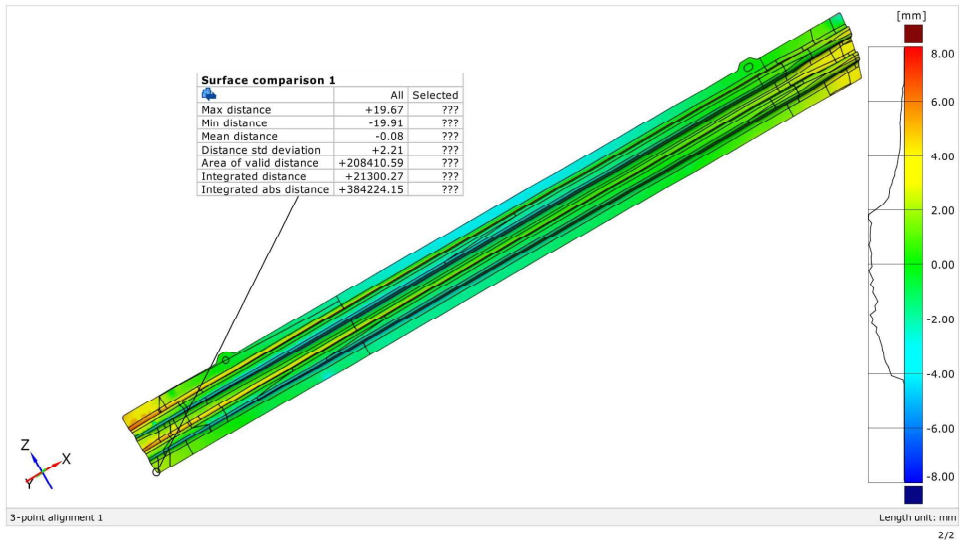


# CAD average\_simulation 9

Generated with GOM Inspect V8



Surface Comparison on CAD

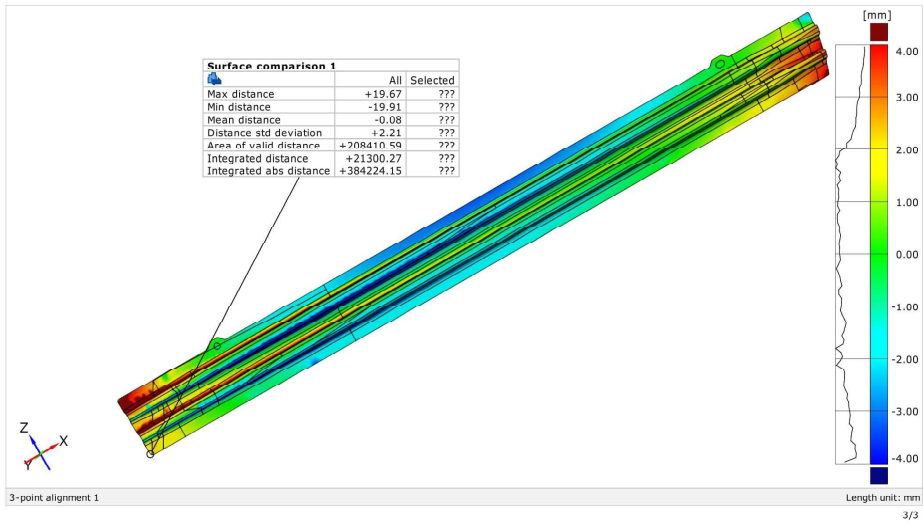


# CAD average\_simulation 9

Generated with GOM Inspect V8



Surface Comparison on CAD

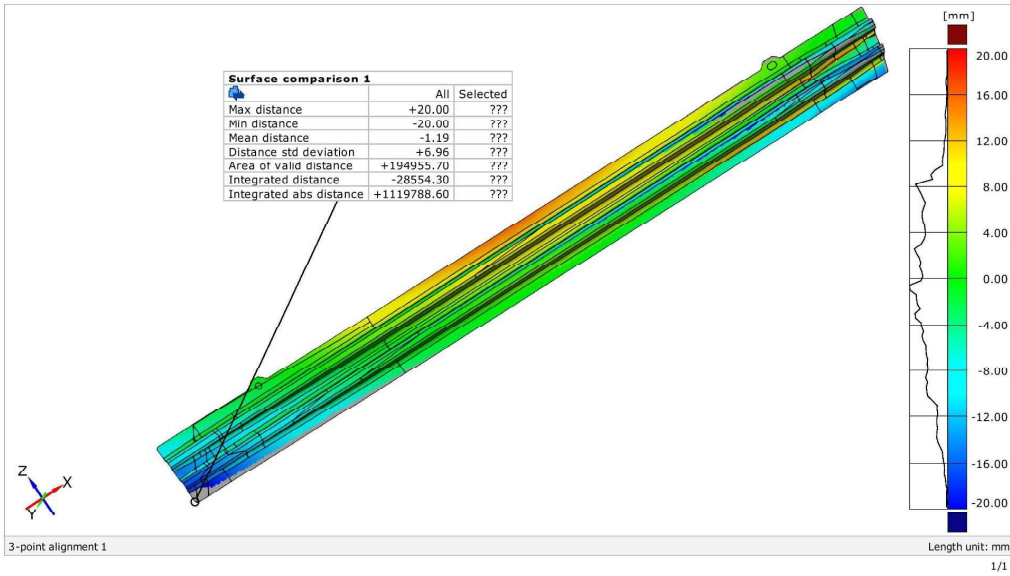


# CAD average\_simulation 10

Generated with GOM Inspect V8



## Surface Comparison on CAD

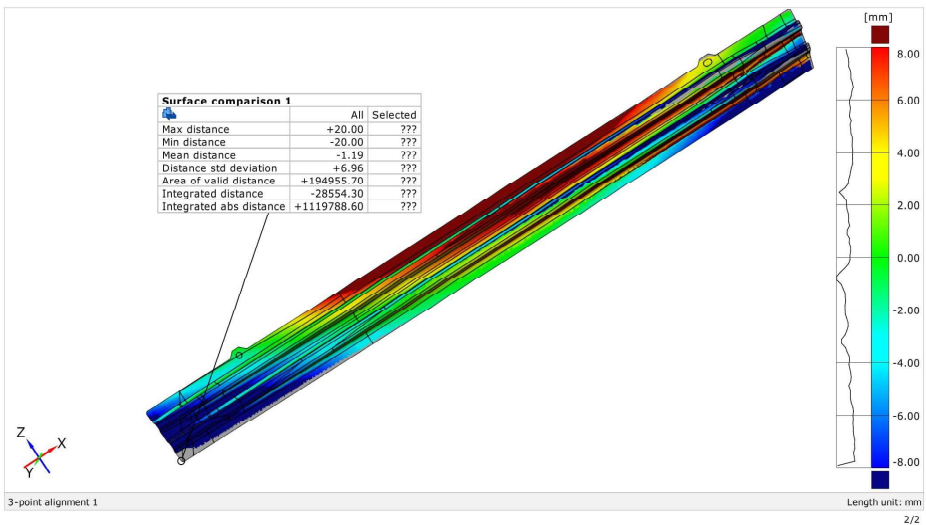


# CAD average\_simulation 10

Generated with GOM Inspect V8



## Surface Comparison on CAD

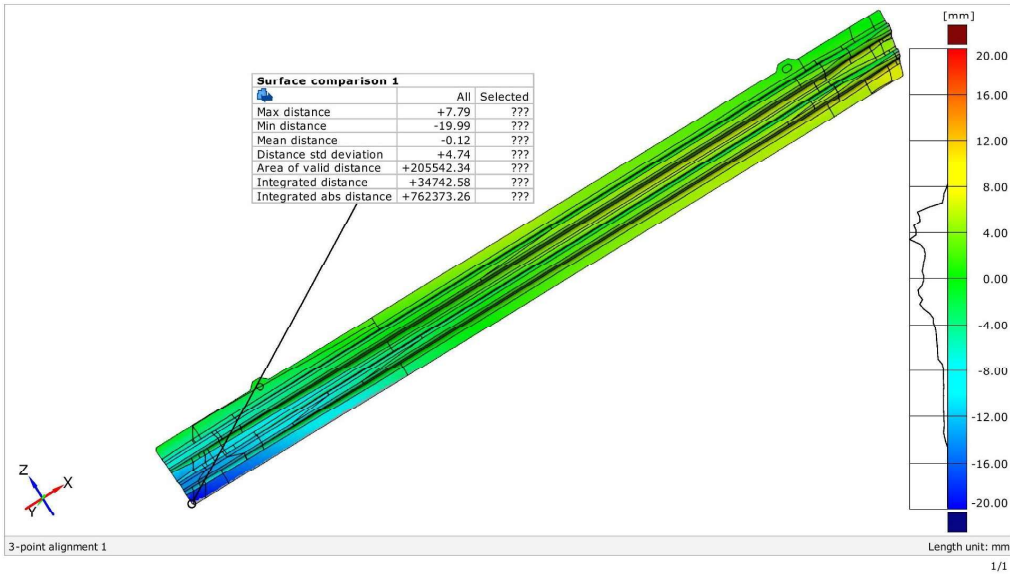


# CAD average\_simulation 11

Generated with GOM Inspect v8



## Surface Comparison on CAD

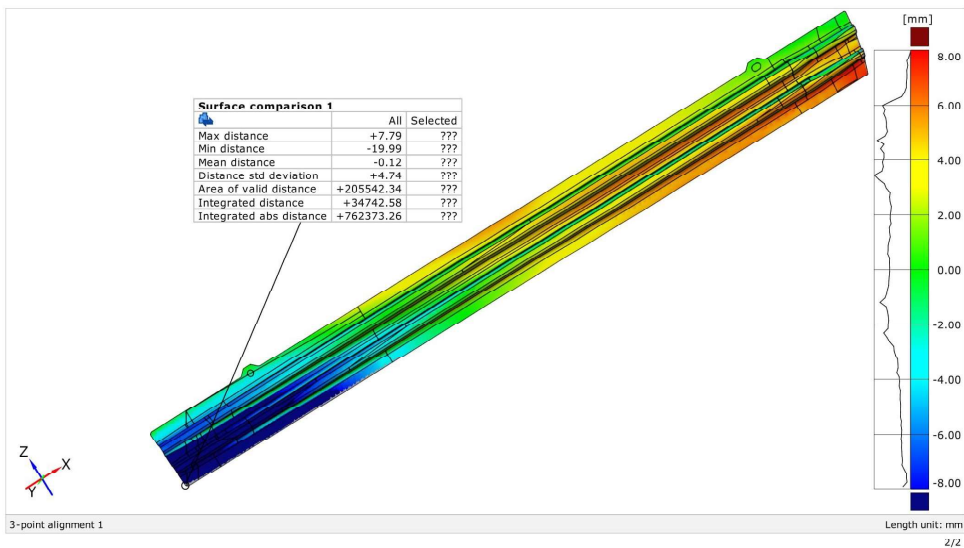


# CAD average\_simulation 11

Generated with GOM Inspect v8



## Surface Comparison on CAD

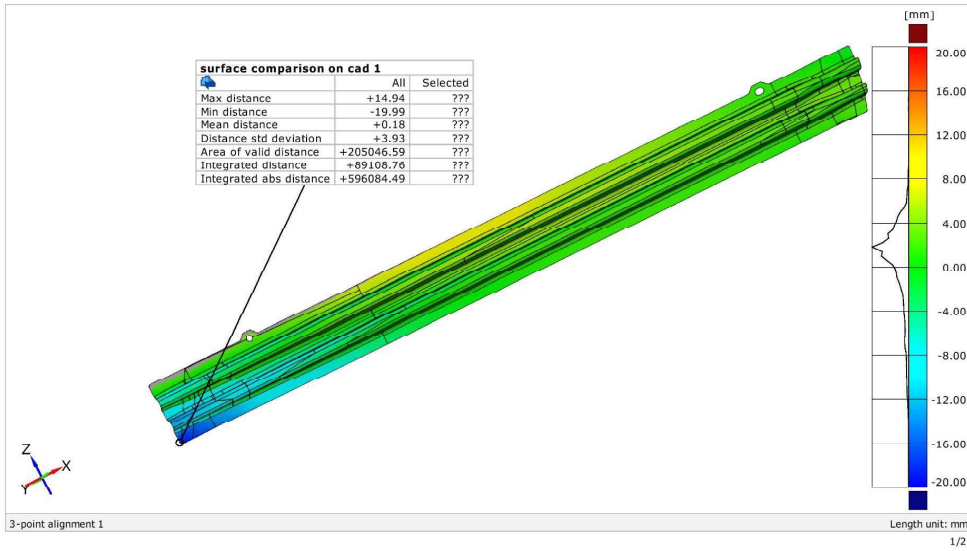


# CAD higher\_simulation 1

Generated with GOM Inspect V8



surface comparison on cad

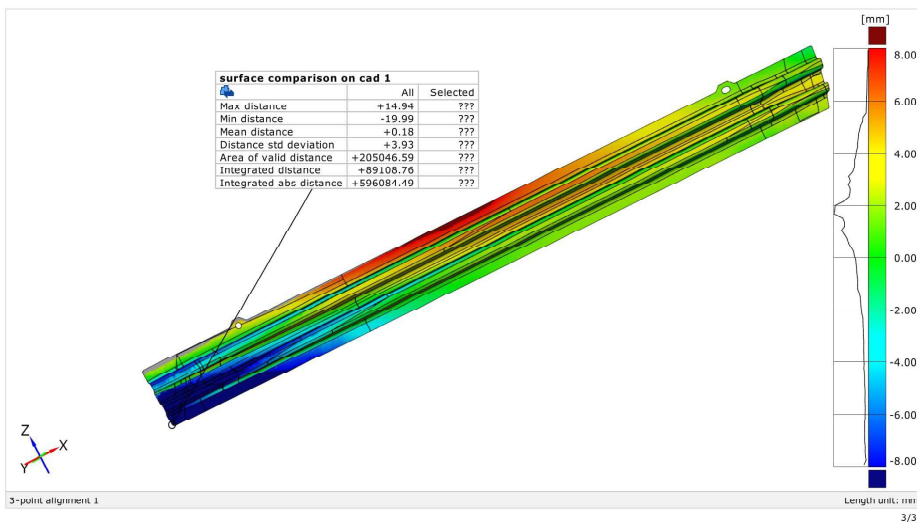


# CAD higher\_simulation 1

Generated with GOM Inspect V8



Surface Comparison on CAD

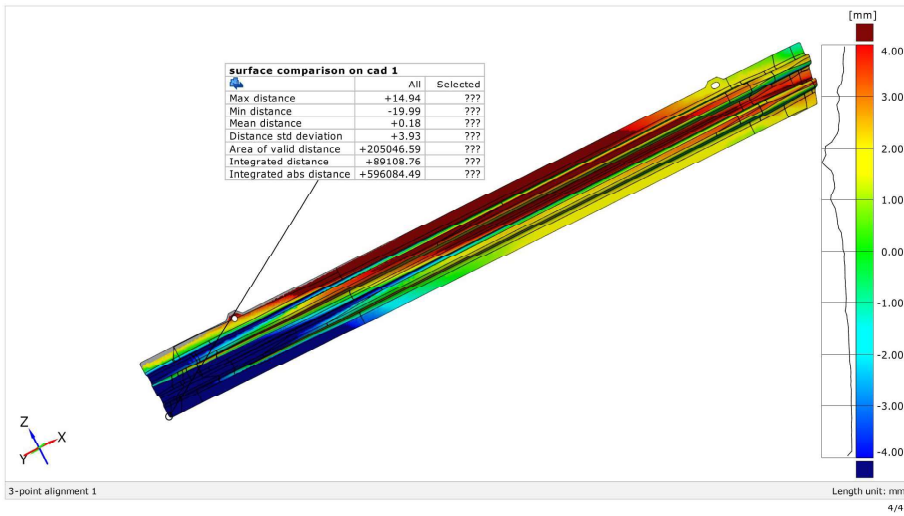


# CAD higher\_simulation 1

Generated with GOM Inspect V8



Surface Comparison on CAD

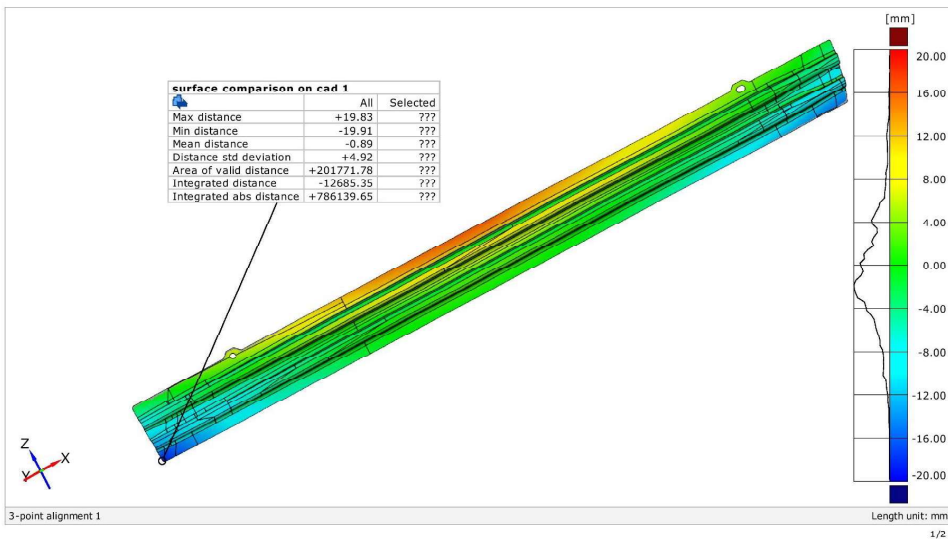


# CAD higher\_simulation 2

Generated with GOM Inspect V8



surface comparison on cad

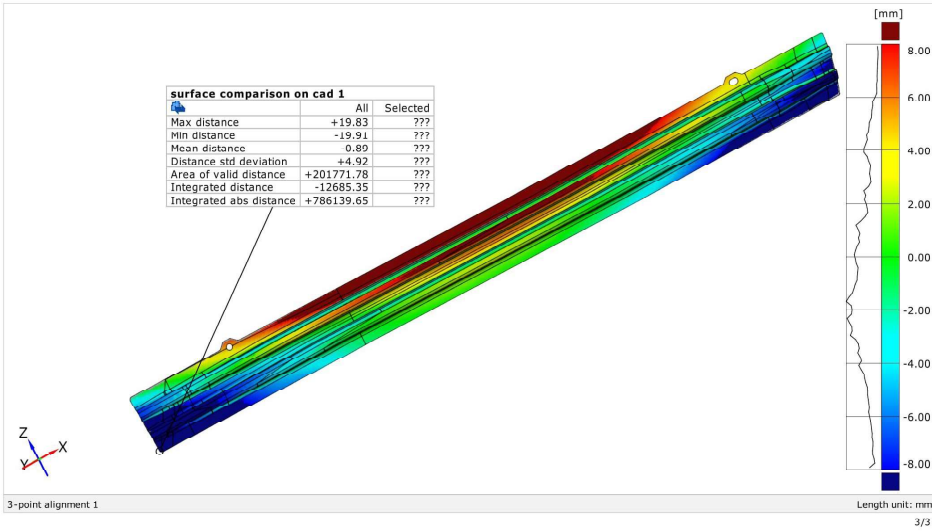


## CAD higher\_simulation 2

Generated with GOM Inspect V8



Surface Comparison on CAD

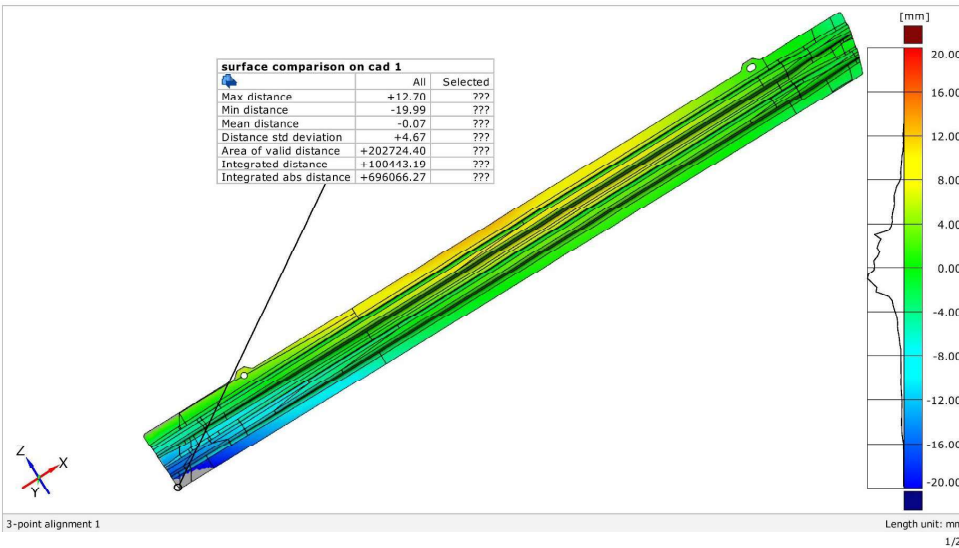


## CAD higher\_simulation 3

Generated with GOM Inspect V8



Surface comparison on CAD

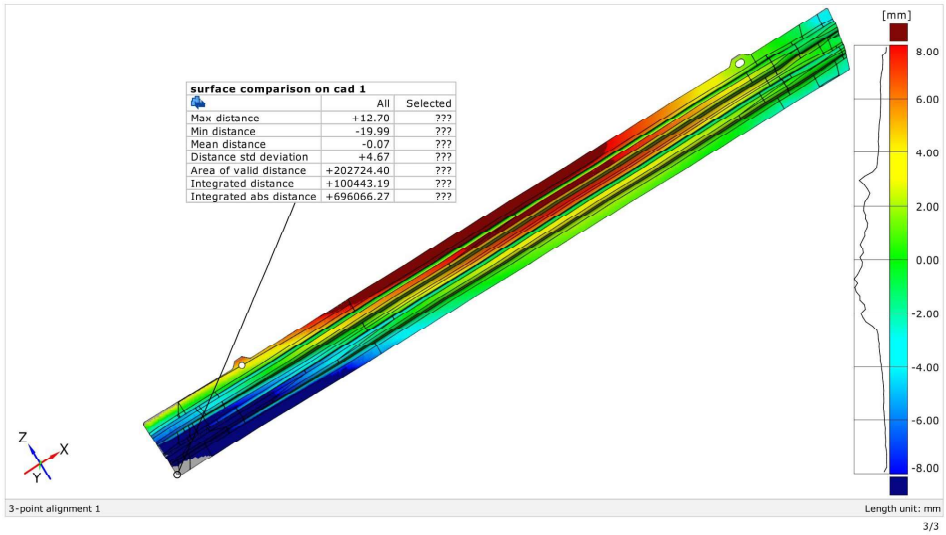


# CAD higher\_simulation 3

Generated with GOM Inspect V8



## Surface Comparison on CAD

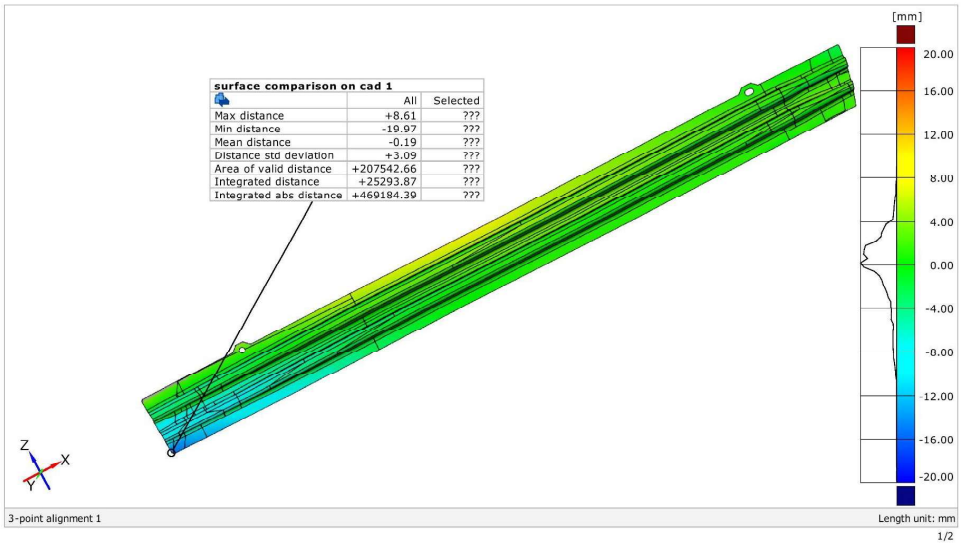


# CAD higher\_simulation 4

Generated with GOM Inspect V8



## surface comparison on cad

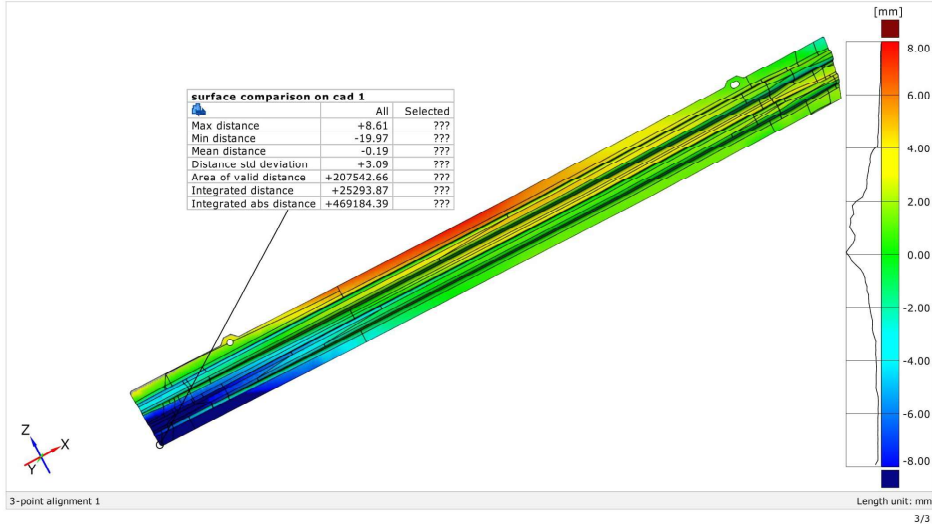


# CAD higher\_simulation 4

Generated with GOM Inspect V8



## Surface Comparison on CAD

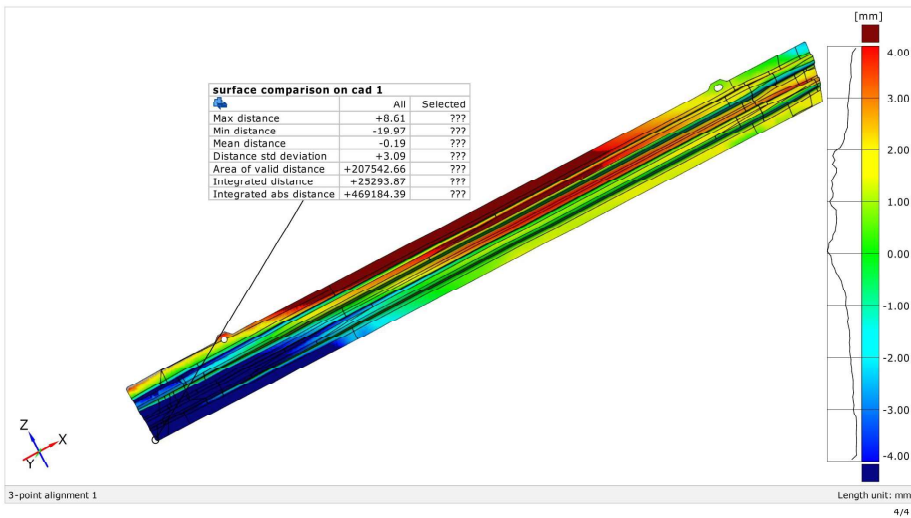


# CAD higher\_simulation 4

Generated with GOM Inspect V8



## Surface Comparison on CAD

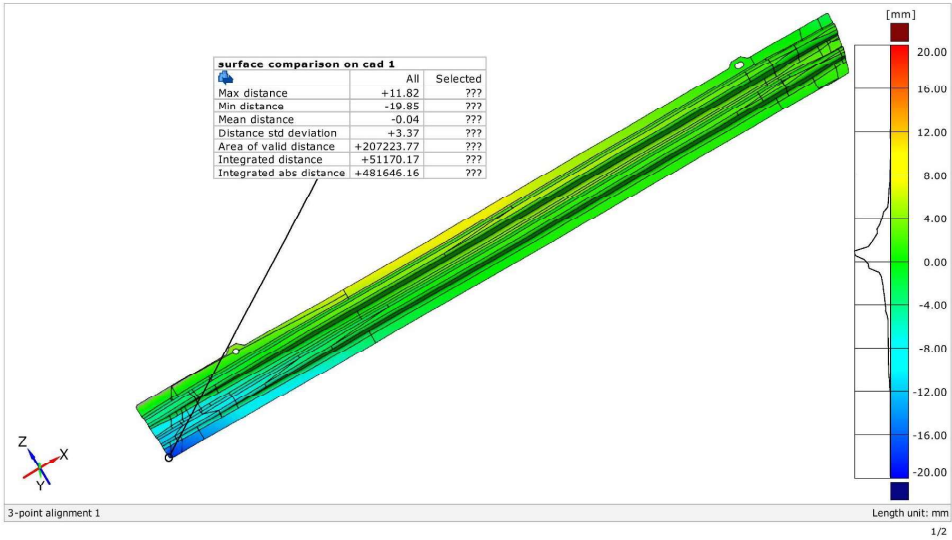


# CAD higher\_simulation 5

Generated with GOM Inspect V8



surface comparison on cad

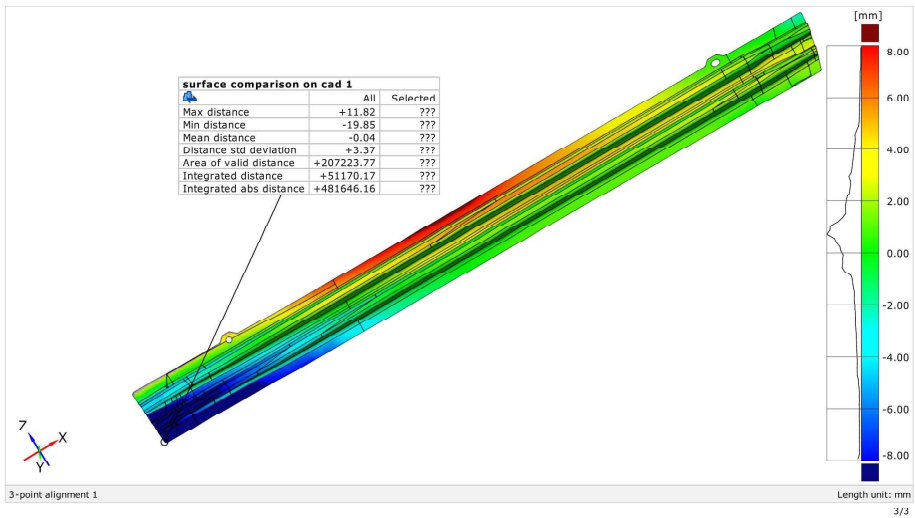


# CAD higher\_simulation 5

Generated with GOM Inspect V8



Surface Comparison on CAD

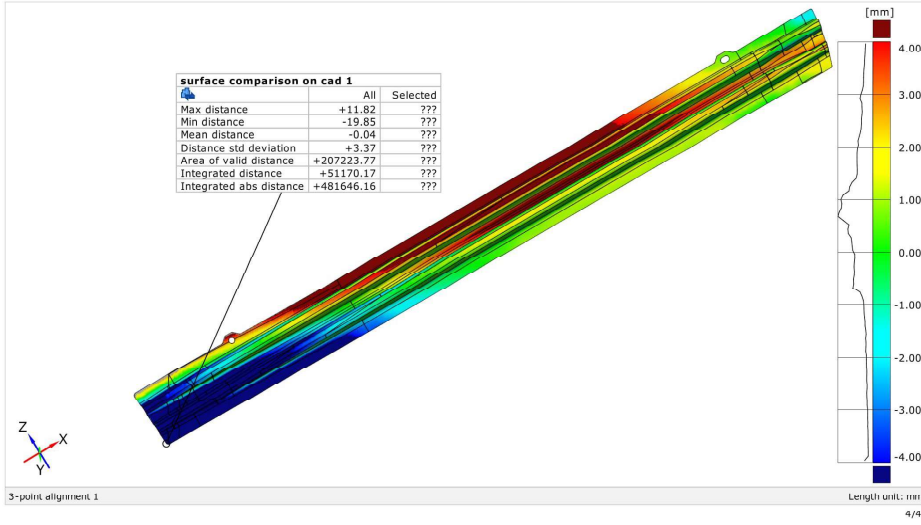


# CAD higher\_simulation 5

Generated with GOM Inspect V8



## Surface Comparison on CAD

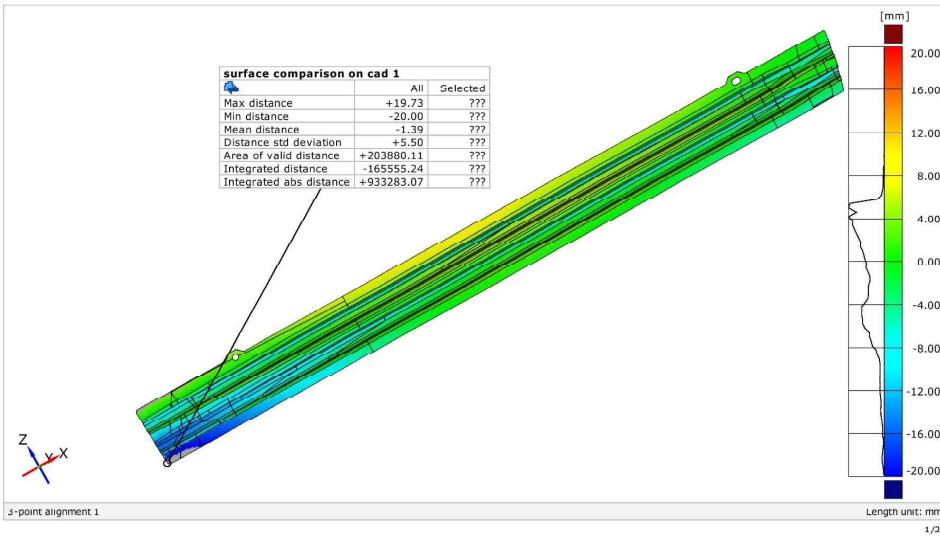


# CAD higher\_simulation 6

Generated with GOM Inspect V8



## surface comparison on cad

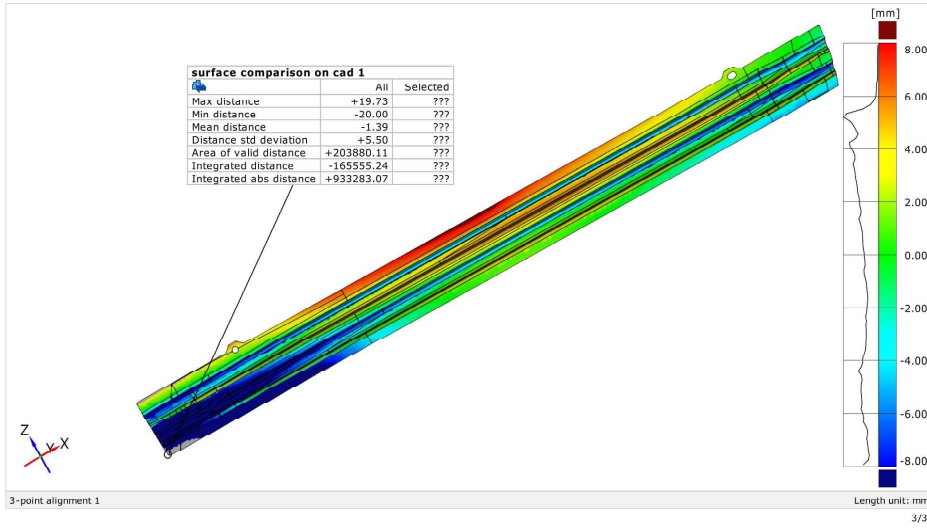


# CAD higher\_simulation 6

Generated with GOM Inspect V8



## Surface Comparison on CAD

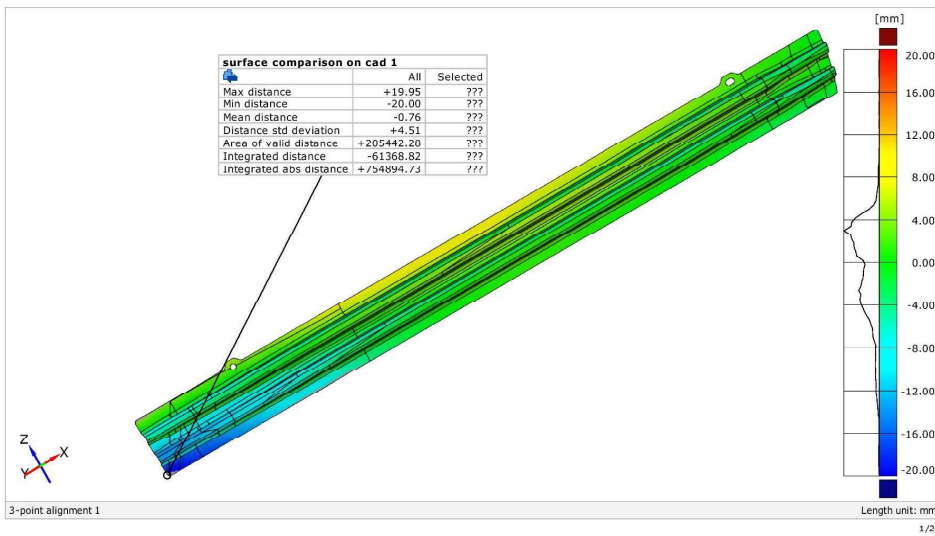


# CAD higher\_simulation 7

Generated with GOM Inspect V8



## surface comparison on cad

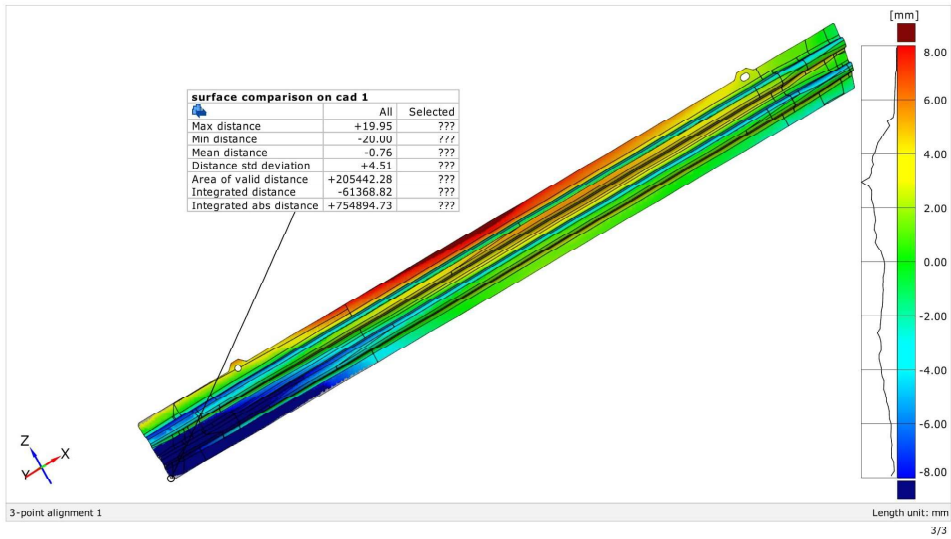


# CAD higher\_simulation 7

Generated with GOM Inspect V8



## Surface Comparison on CAD

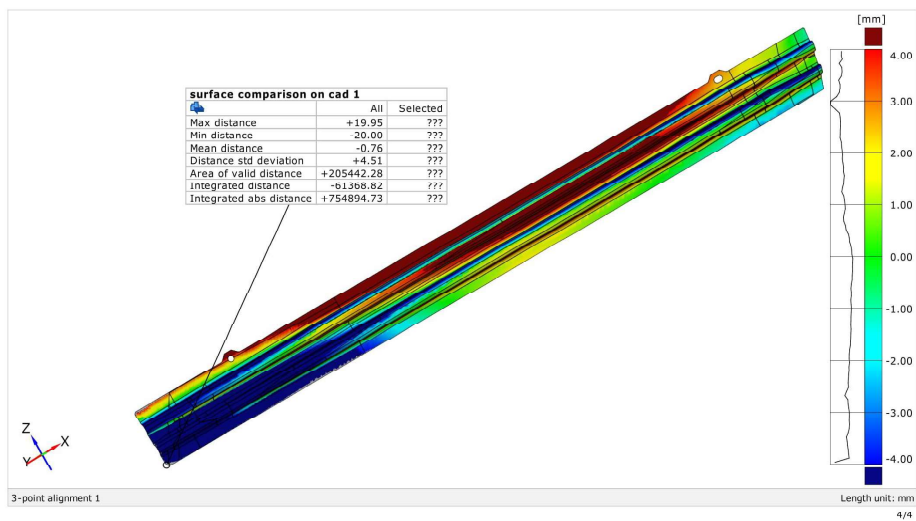


# CAD higher\_simulation 7

Generated with GOM Inspect V8



## Surface Comparison on CAD

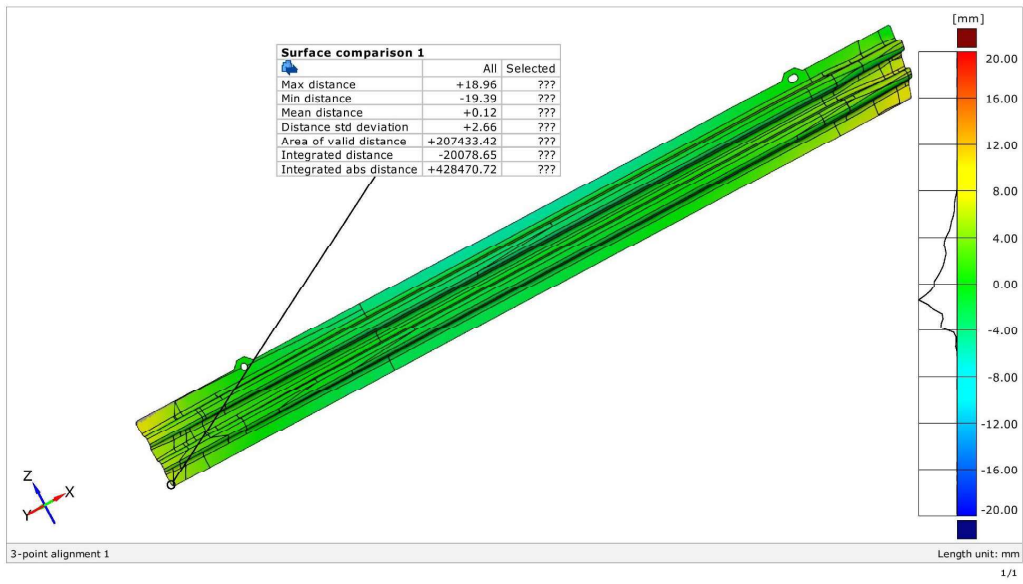


# CAD higher\_simulation 8

Generated with GOM Inspect V8



## Surface Comparison on CAD

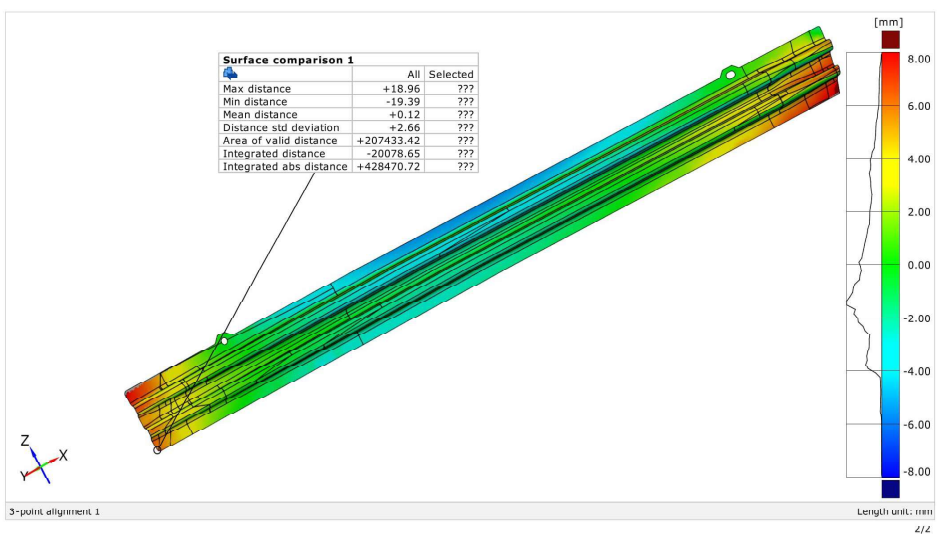


# CAD higher\_simulation 8

Generated with GOM Inspect V8



## Surface Comparison on CAD

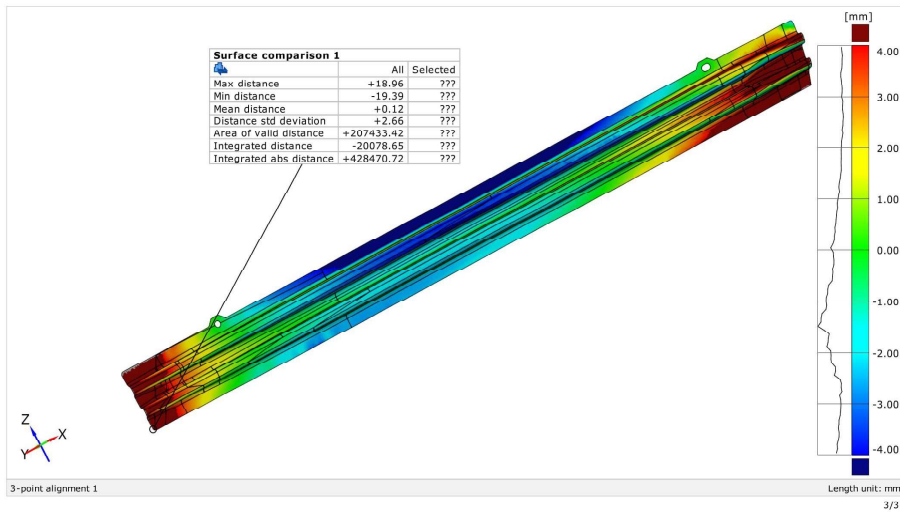


# CAD higher\_simulation 8

Generated with GOM Inspect V8



Surface Comparison on CAD

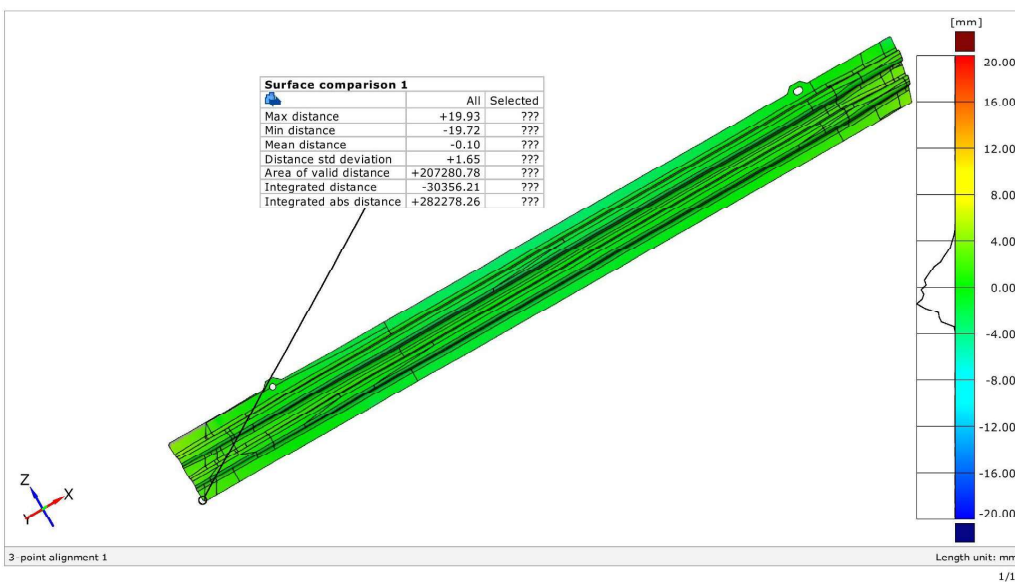


# CAD higher\_simulation 9

Generated with GOM Inspect V8



Surface Comparison on CAD

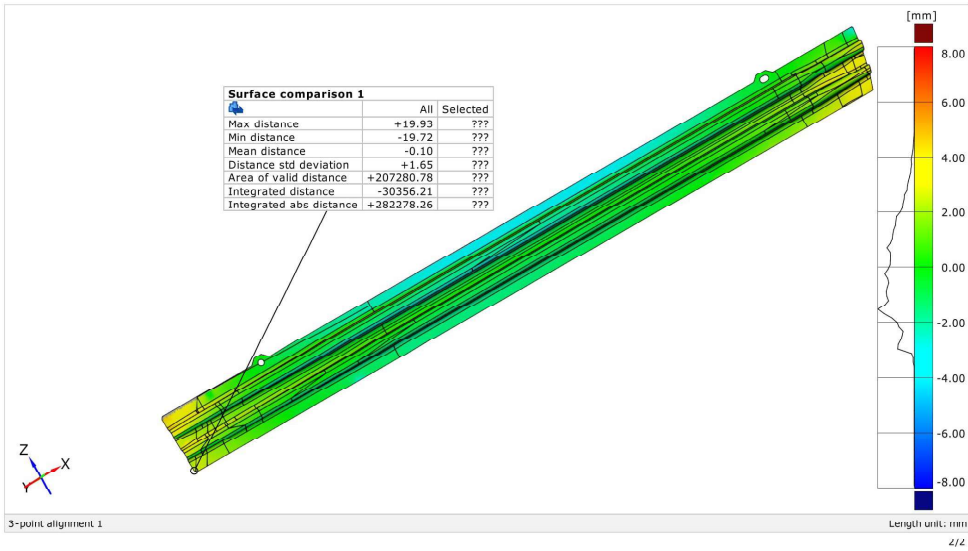


# CAD higher\_simulation 9

Generated with GOM Inspect V8



## Surface Comparison on CAD

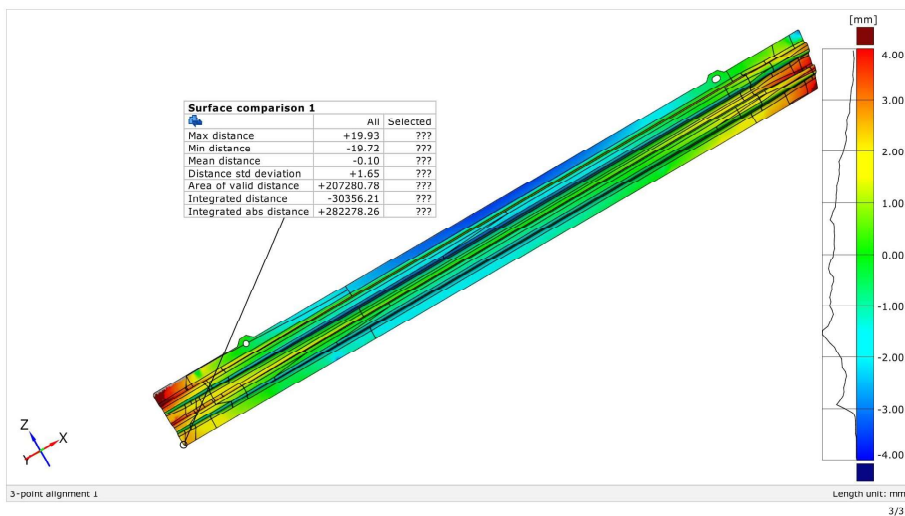


# CAD higher\_simulation 9

Generated with GOM Inspect V8



## Surface Comparison on CAD

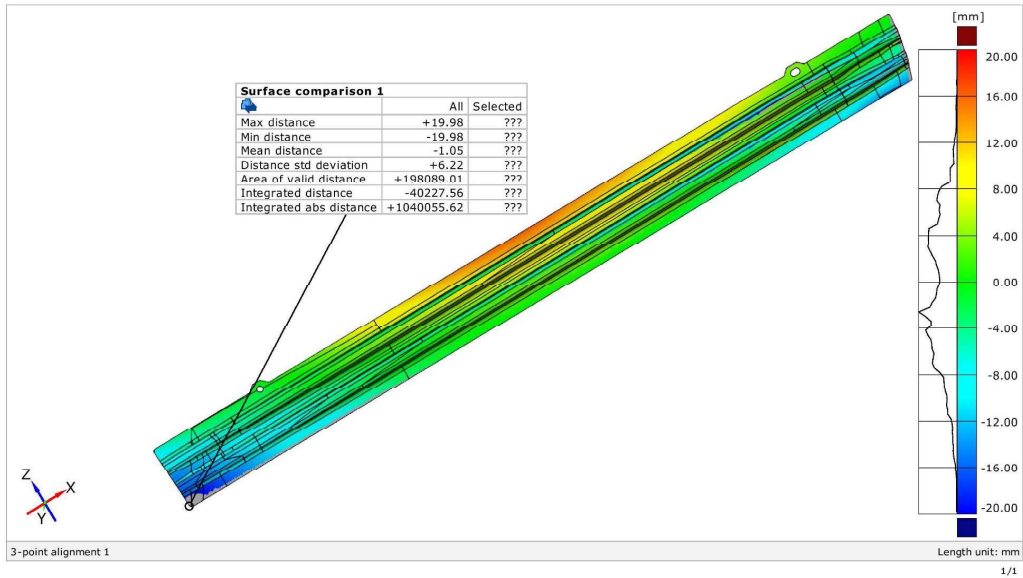


# CAD higher\_simulation 10

Generated with GOM Inspect V8



## Surface Comparison on CAD

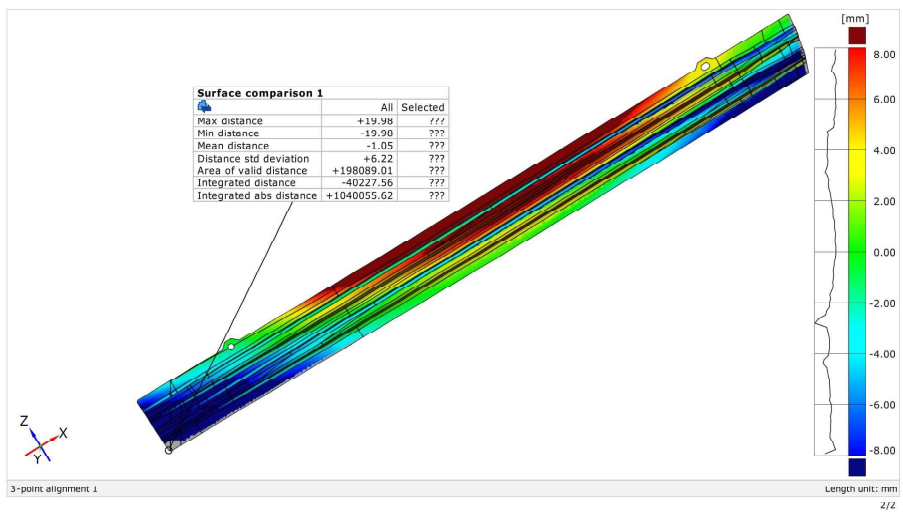


# CAD higher\_simulation 10

Generated with GOM Inspect V8



## Surface Comparison on CAD

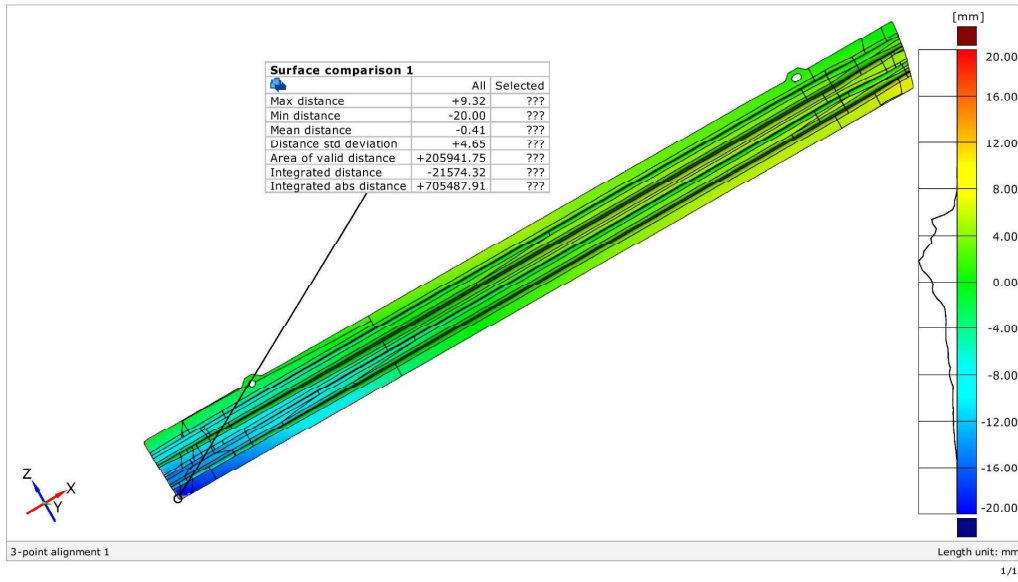


# CAD higher\_simulation 11

Generated with GOM Inspect V8



## Surface Comparison on CAD

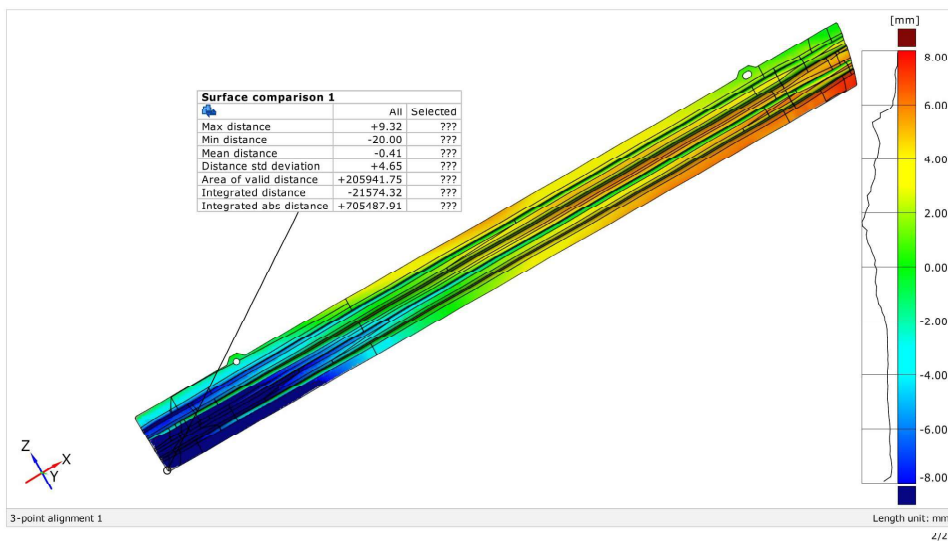


# CAD higher\_simulation 11

Generated with GOM Inspect V8



## Surface Comparison on CAD

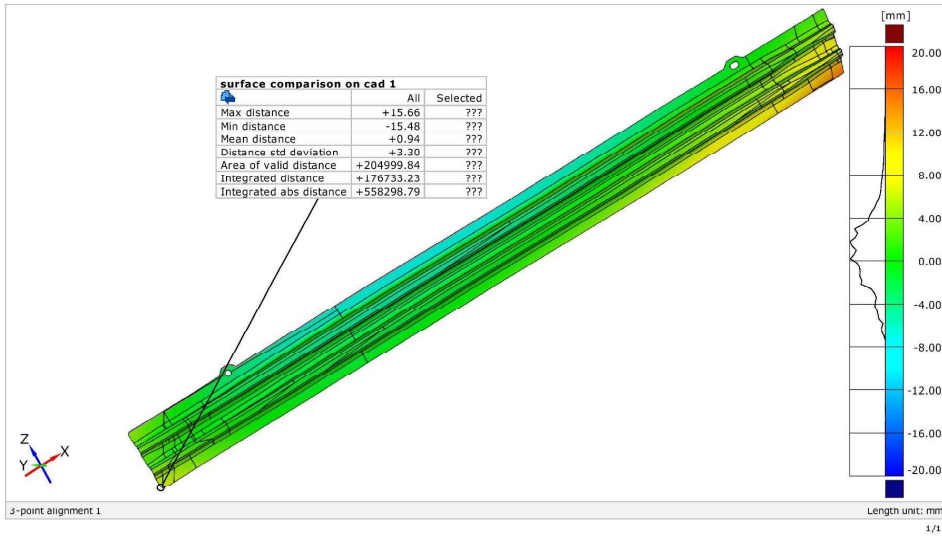


# CAD lower\_simulation Autoform

Generated with GOM Inspect V8



surface comparison on cad

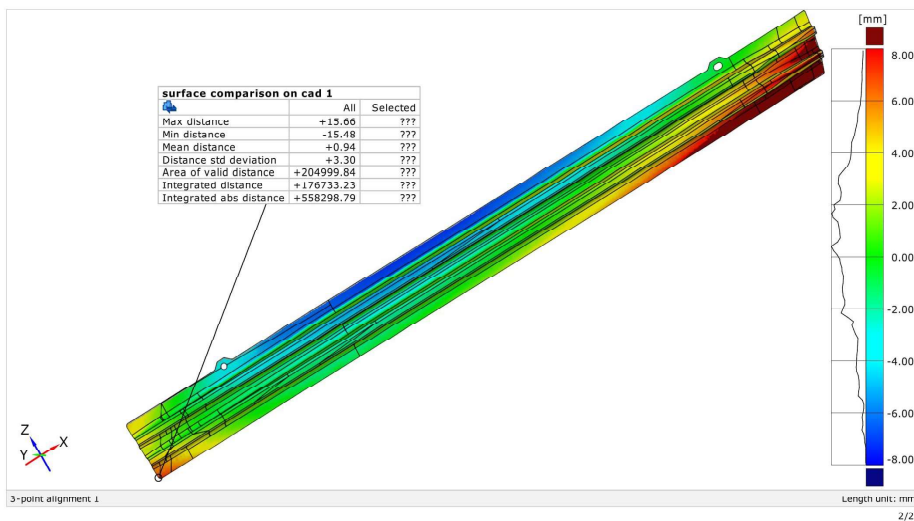


# CAD lower\_simulation Autoform

Generated with GOM Inspect V8



Surface Comparison on CAD

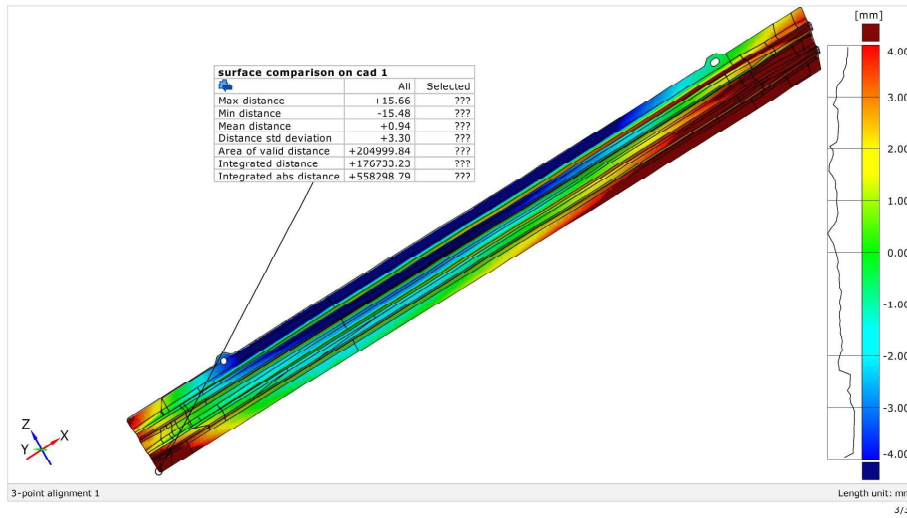


# CAD lower\_simulation Autoform

Generated with GOM Inspect V8



## Surface Comparison on CAD

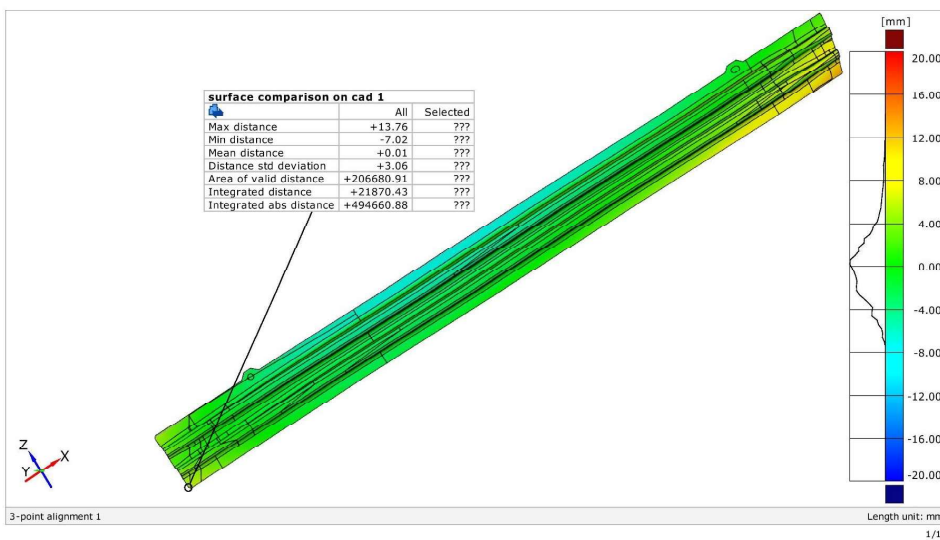


# CAD average\_simulation Autoform

Generated with GOM Inspect V8



## surface comparison on cad

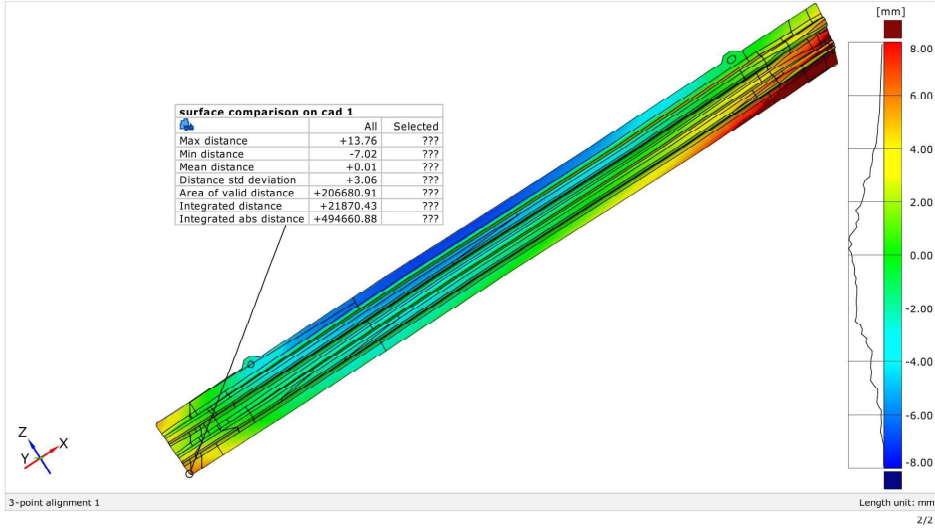


# CAD average\_simulation Autoform

Generated with GOM Inspect V8



## Surface Comparison on CAD

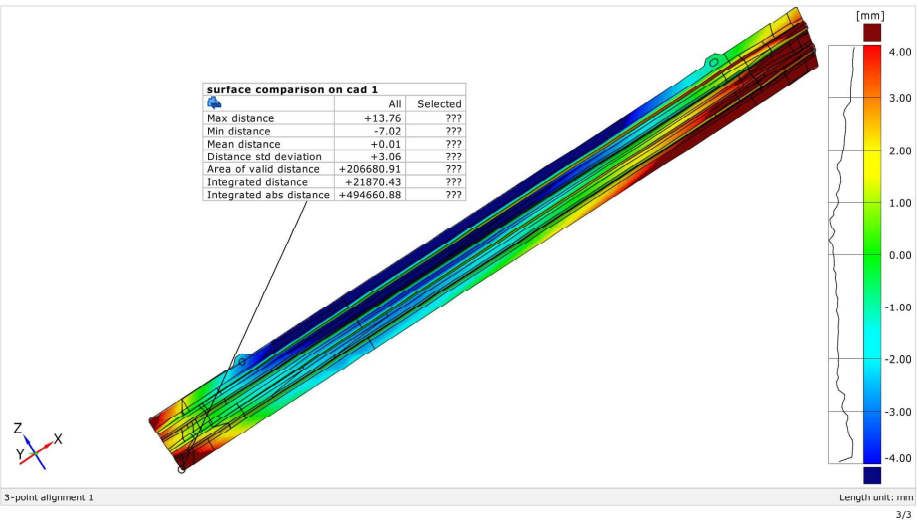


# CAD average\_simulation Autoform

Generated with GOM Inspect V8



## Surface Comparison on CAD

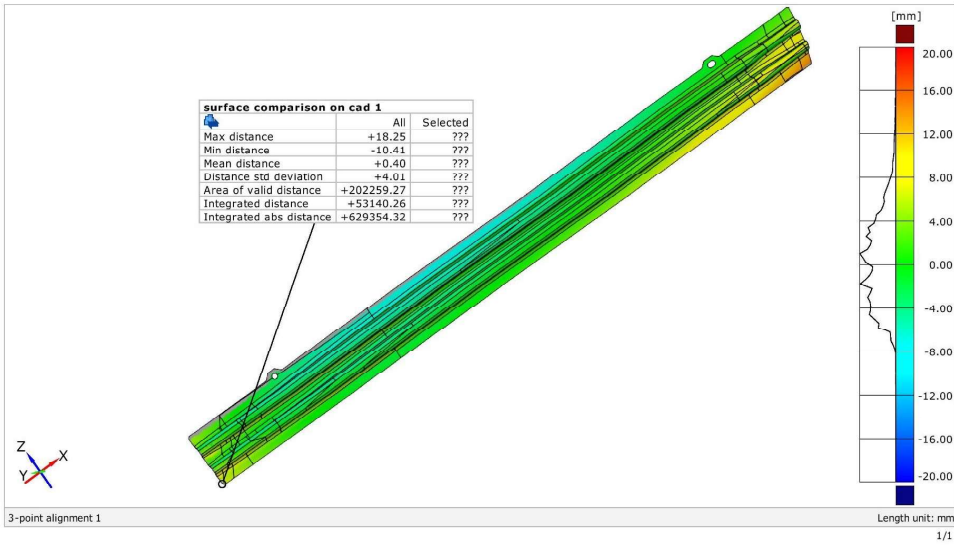


# CAD higher\_simulation Autoform

Generated with GOM Inspect V8



surface comparison on cad

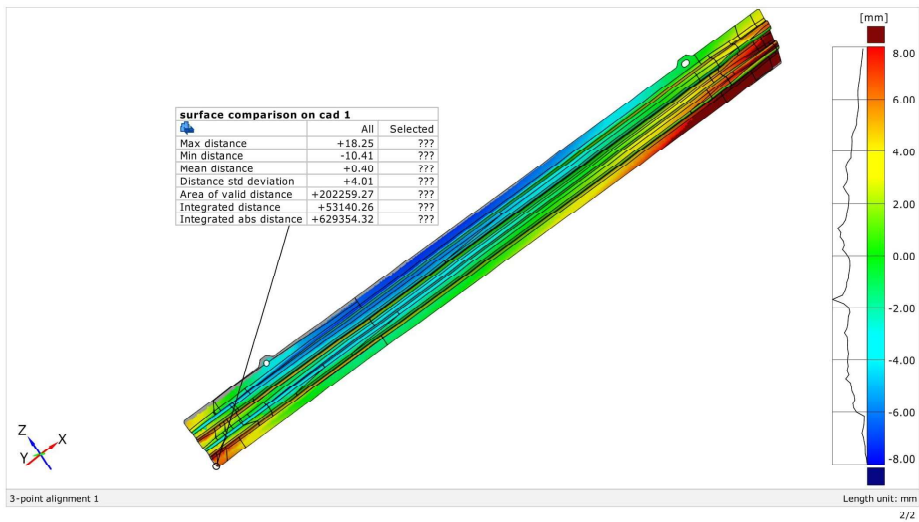


# CAD higher\_simulation Autoform

Generated with GOM Inspect V8



Surface Comparison on CAD

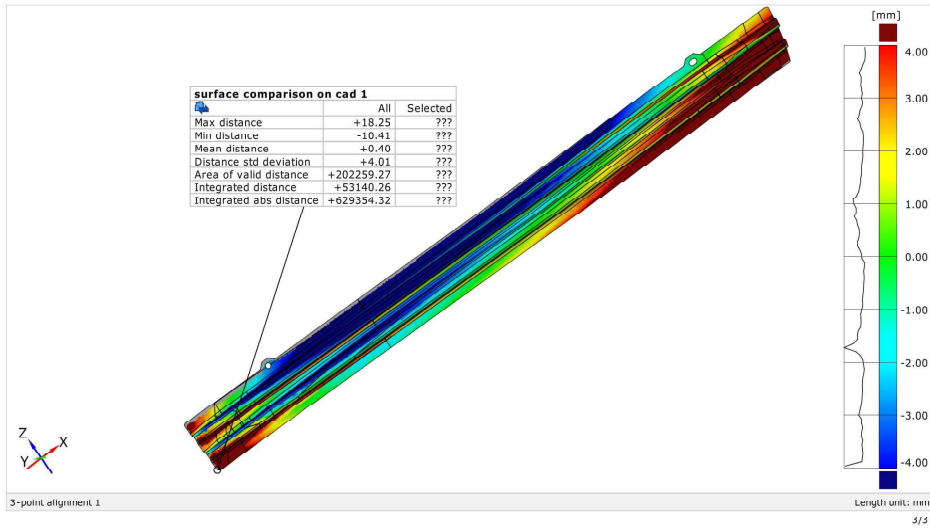


# CAD higher\_simulation Autoform

Generated with GOM Inspect V8



## Surface Comparison on CAD



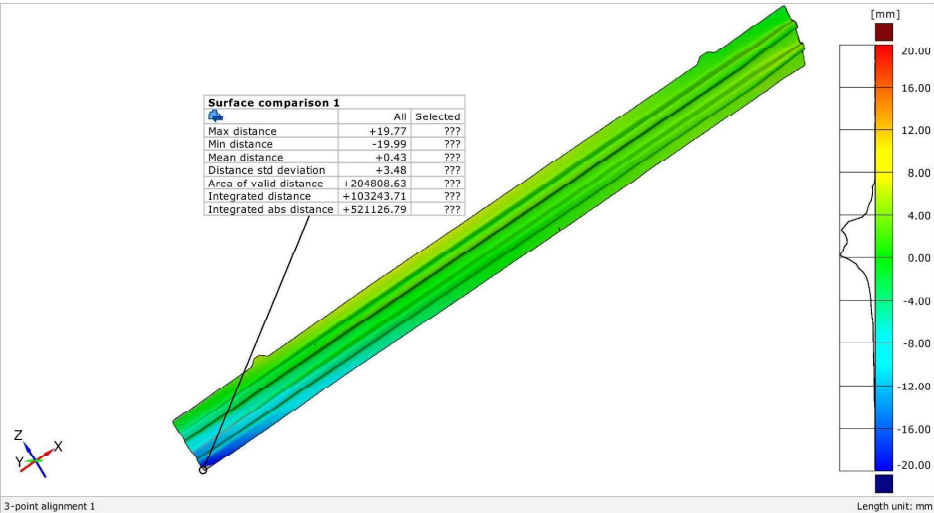
# ANNEX 13.3 COMPARISON OF REAL GEOMETRY RESULTING FROM SCAN AND SIMULATION RESULTS

## 3D real MA03 lower\_simulation 1

Generated with GOM Inspect V8



surface comparison on cad

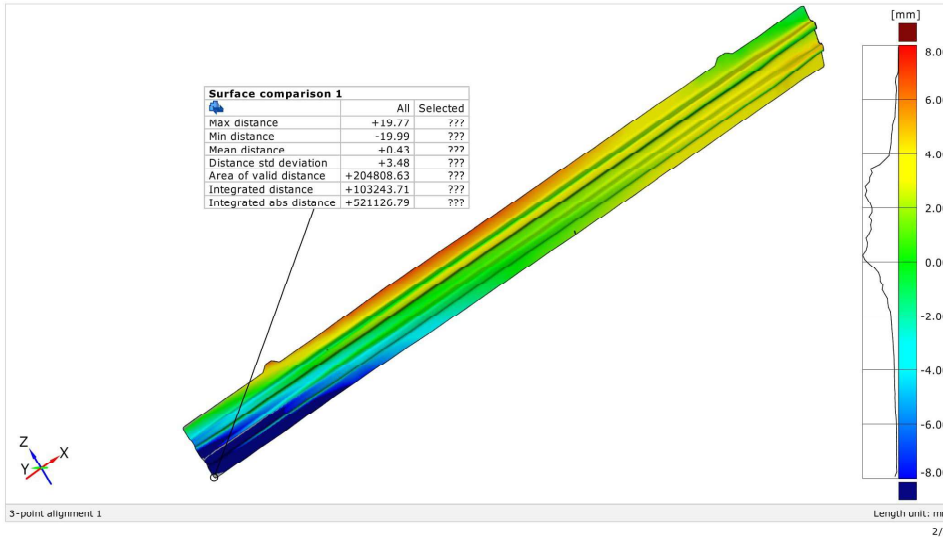


# 3D real MA03 lower\_simulation 1

Generated with GOM Inspect V8



Surface Comparison on CAD

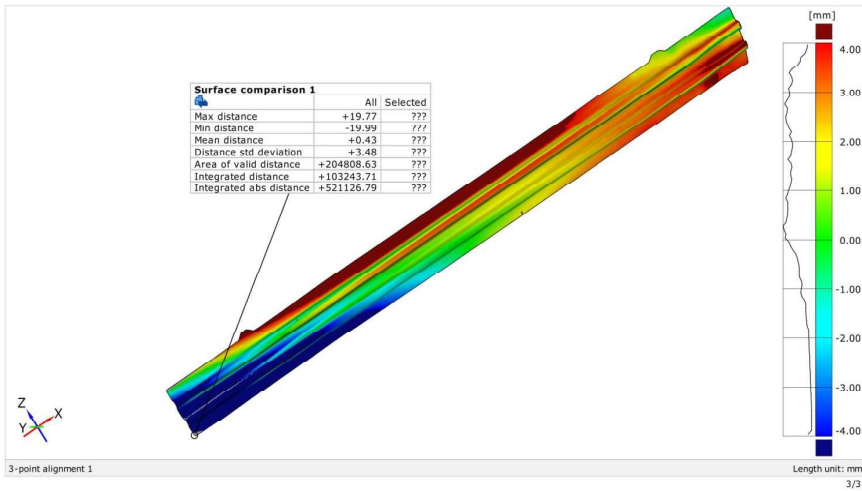


# 3D real MA03 lower\_simulation 1

Generated with GOM Inspect V8



Surface Comparison on CAD

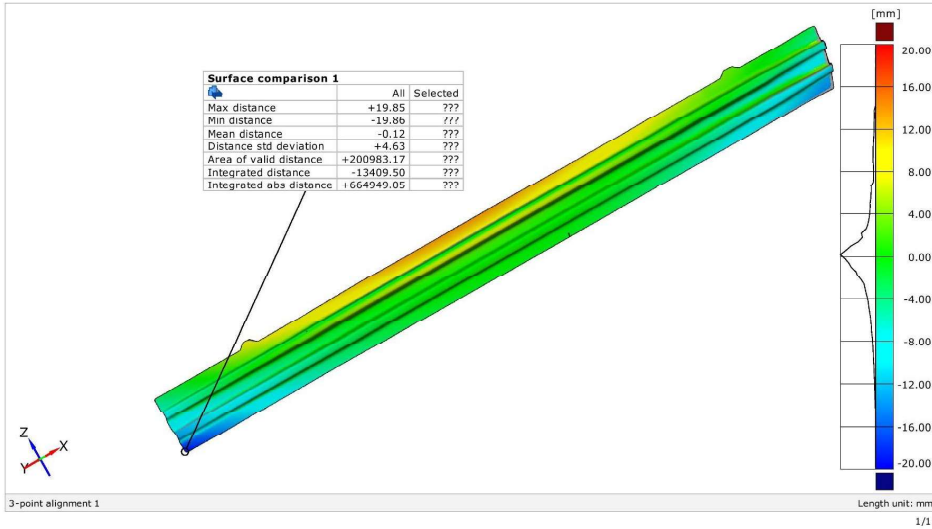


# 3D real MA03 lower\_simulation 2

Generated with GOM Inspect V8



surface comparison on cad

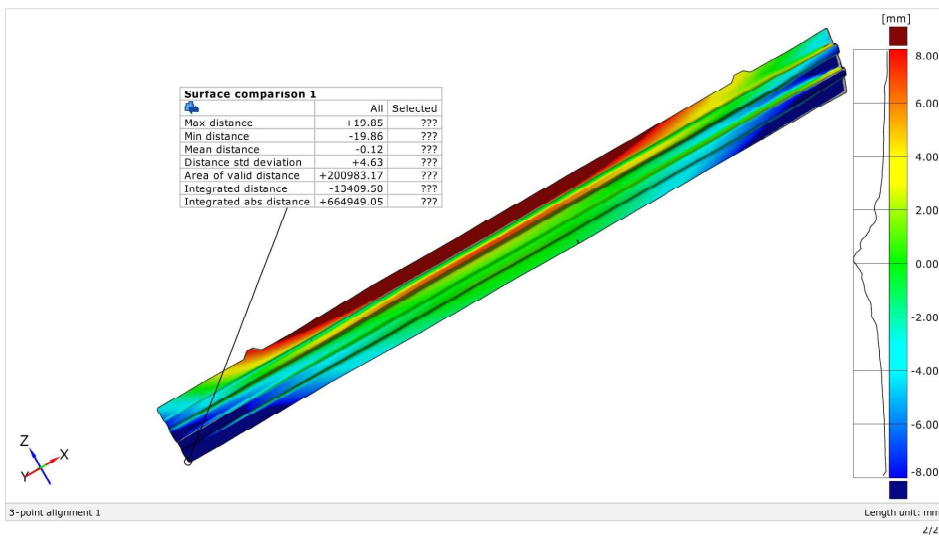


# 3D real MA03 lower\_simulation 2

Generated with GOM Inspect V8



Surface Comparison on CAD

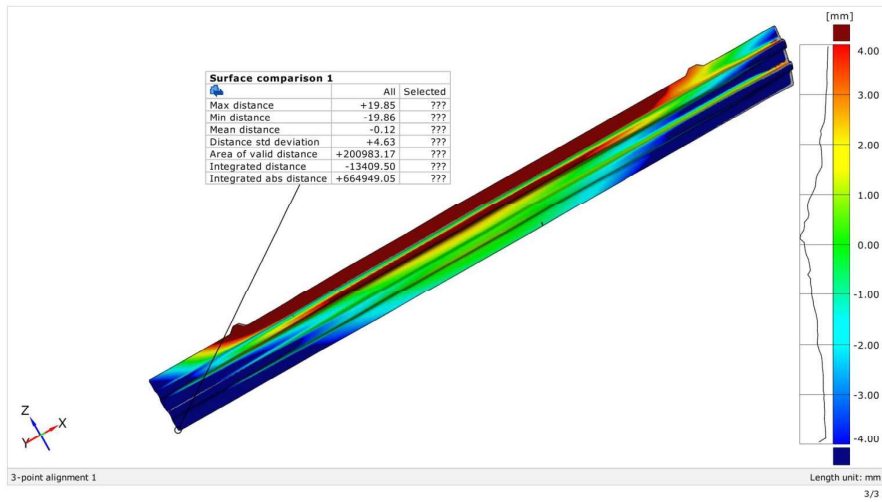


### 3D real MA03 lower\_simulation 2

Generated with GOM Inspect V8



Surface Comparison on CAD

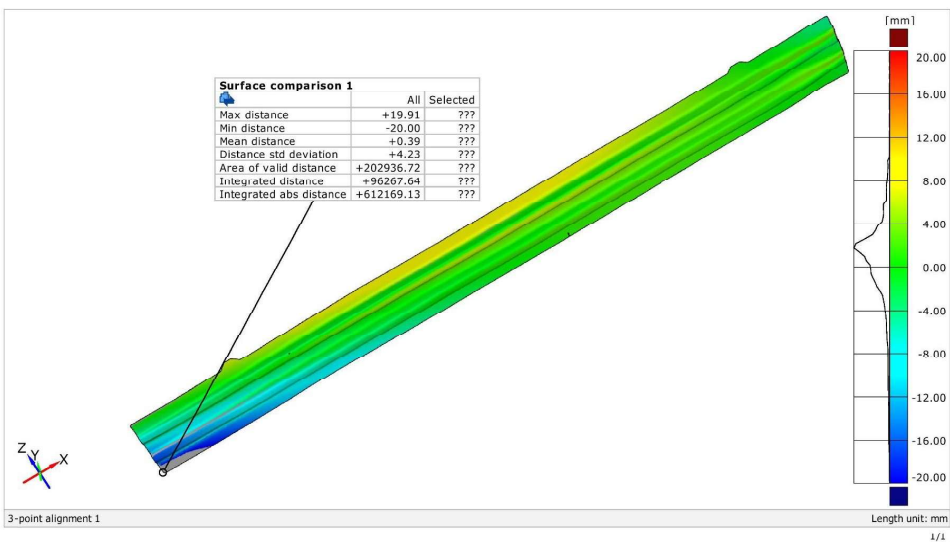


### 3D real MA03 lower\_simulation 3

Generated with GOM Inspect V8



surface comparison on cad

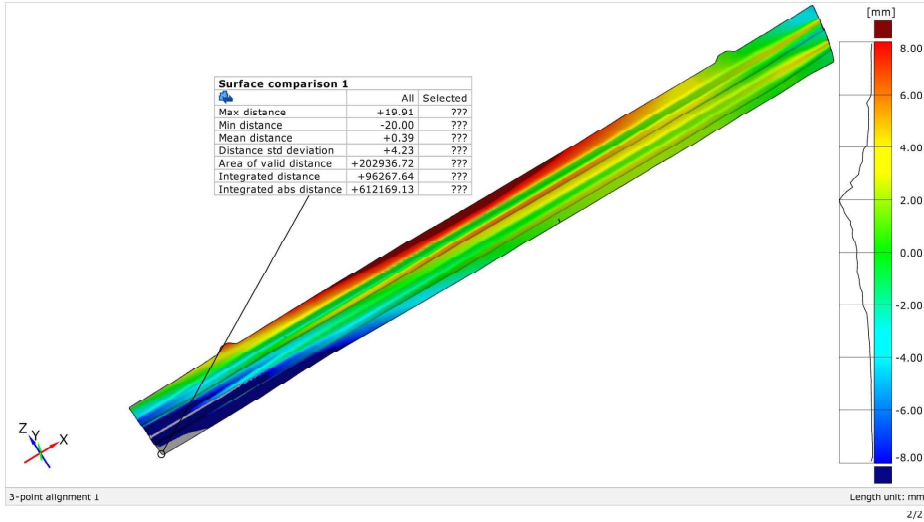


### 3D real MA03 lower\_simulation 3

Generated with GOM Inspect V8



Surface Comparison on CAD

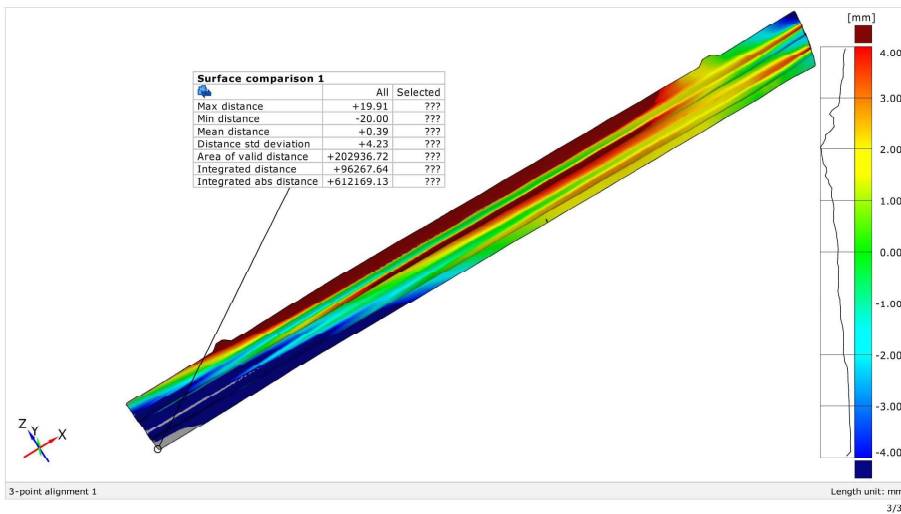


### 3D real MA03 lower\_simulation 3

Generated with GOM Inspect V8



Surface Comparison on CAD

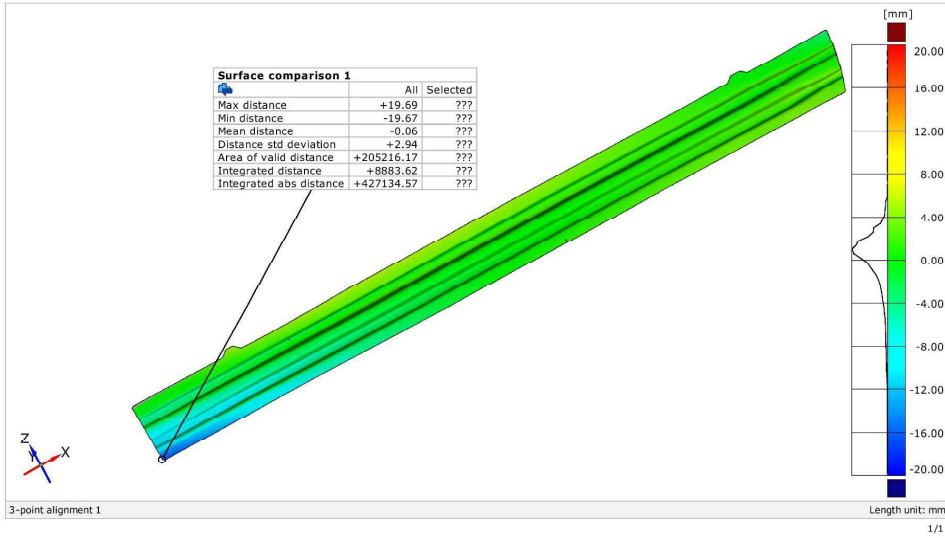


# 3D real MA03 lower\_simulation 4

Generated with GOM Inspect V8



surface comparison on cad

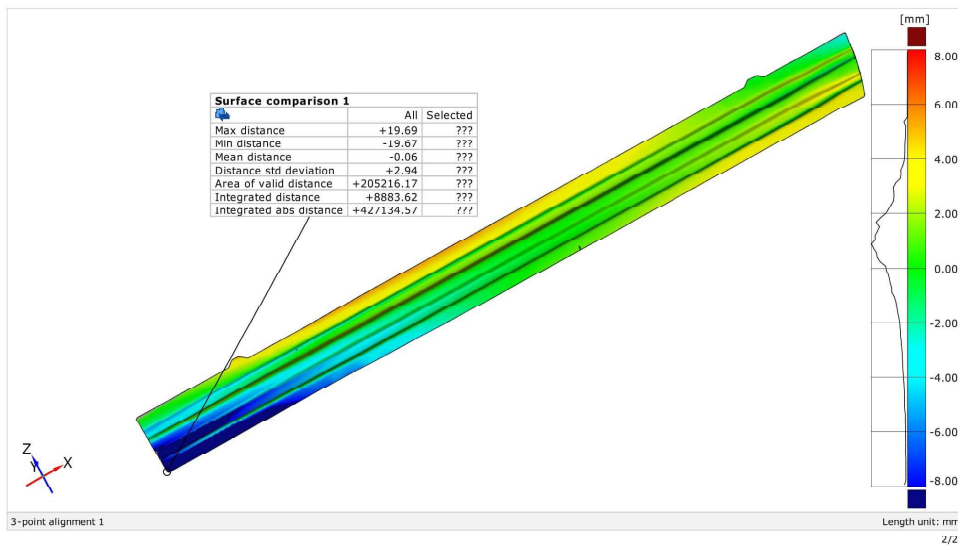


# 3D real MA03 lower\_simulation 4

Generated with GOM Inspect V8



Surface Comparison on CAD

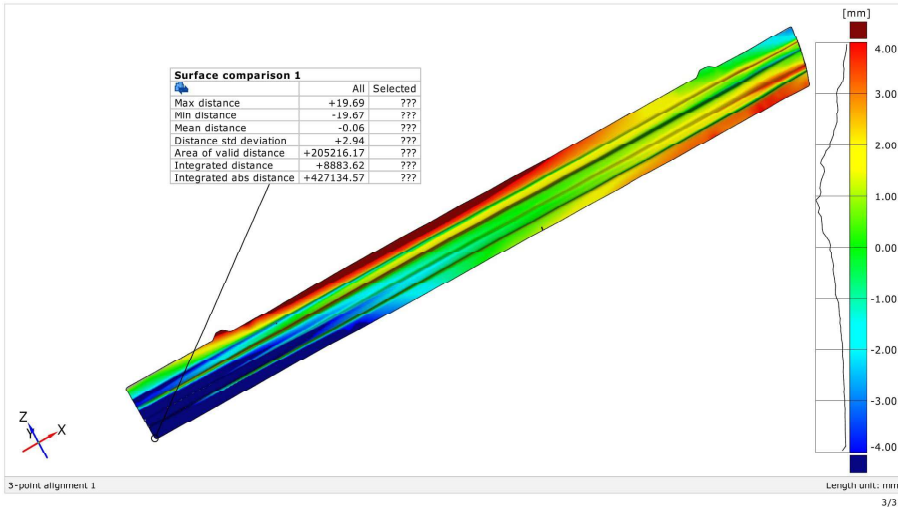


### 3D real MA03 lower\_simulation 4

Generated with GOM Inspect V8



Surface Comparison on CAD

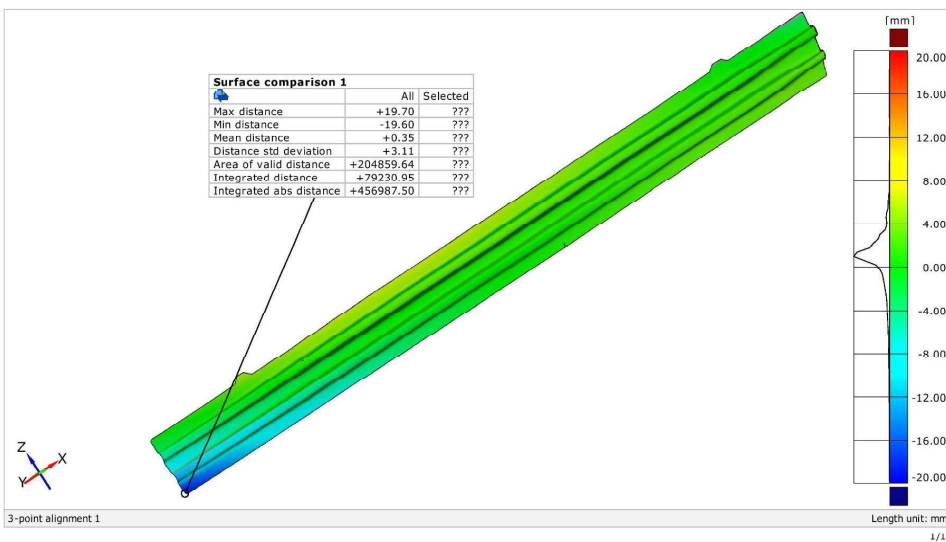


### 3D real MA03 lower\_simulation 5

Generated with GOM Inspect V8



surface comparison on cad

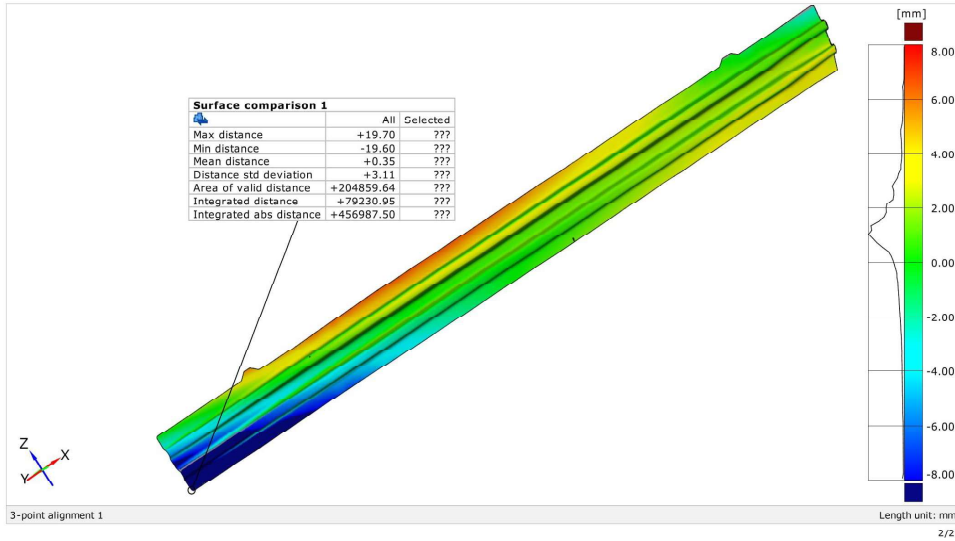


# 3D real MA03 lower\_simulation 5

Generated with GOM Inspect V8



## Surface Comparison on CAD

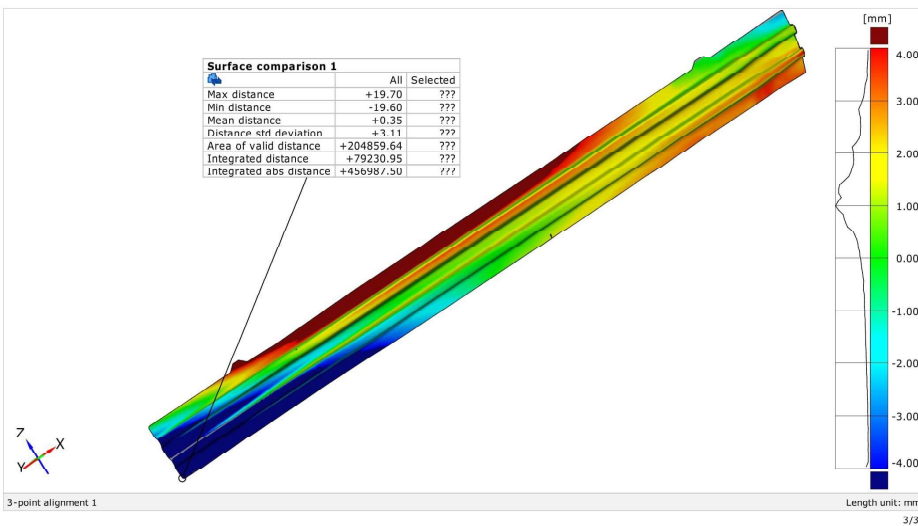


# 3D real MA03 lower\_simulation 5

Generated with GOM Inspect V8



## Surface Comparison on CAD

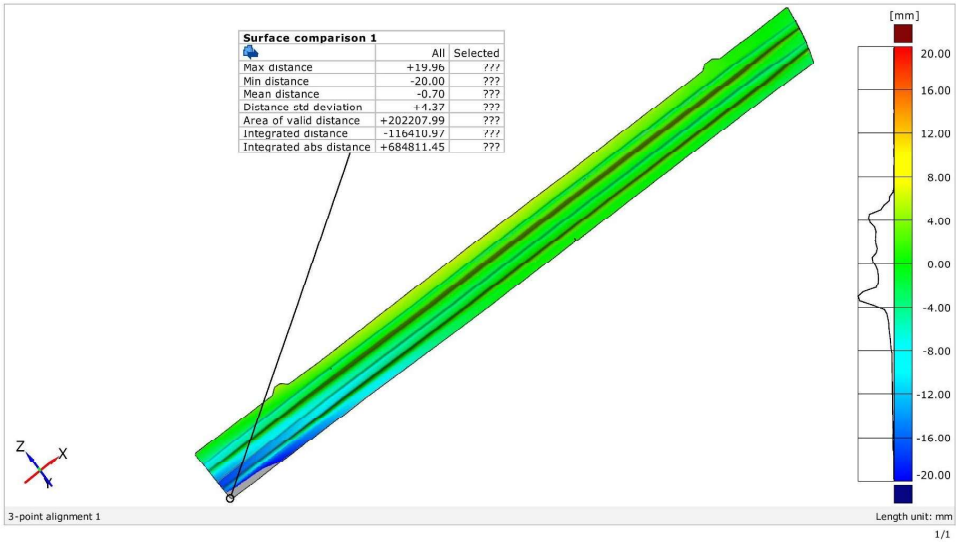


# 3D real MA03 lower\_simulation 6

Generated with GOM Inspect V8



surface comparison on cad

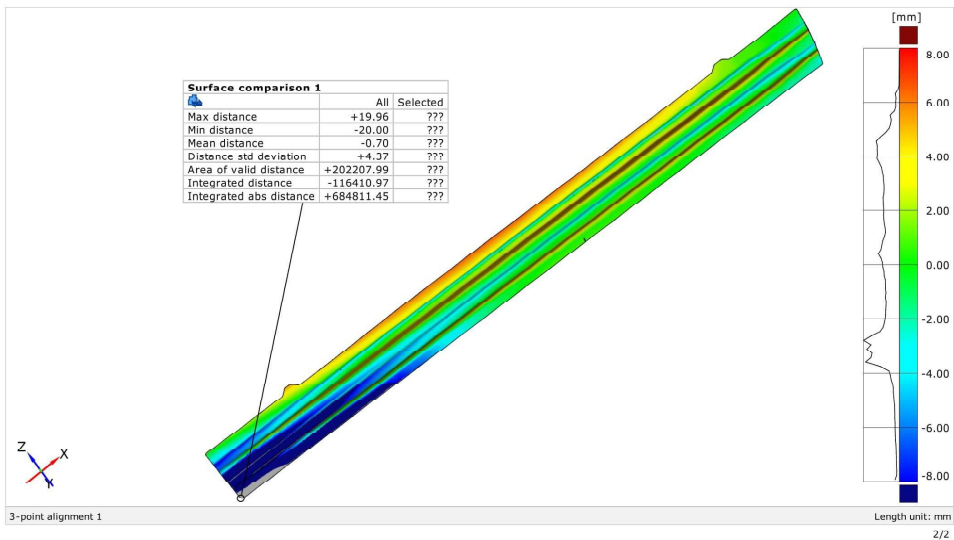


# 3D real MA03 lower\_simulation 6

Generated with GOM Inspect V8



Surface Comparison on CAD

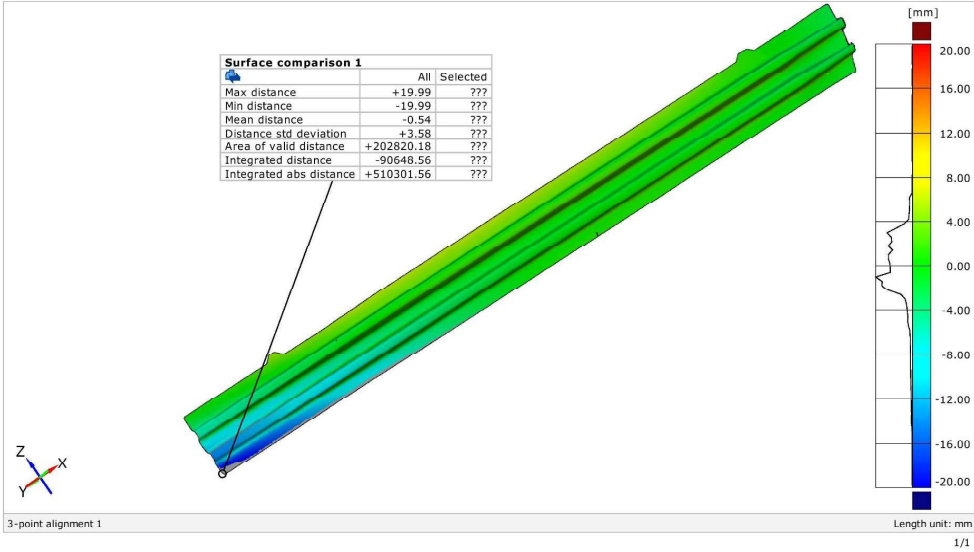


# 3D real MA03 lower\_simulation 7

Generated with GOM Inspect V8



surface comparison on cad

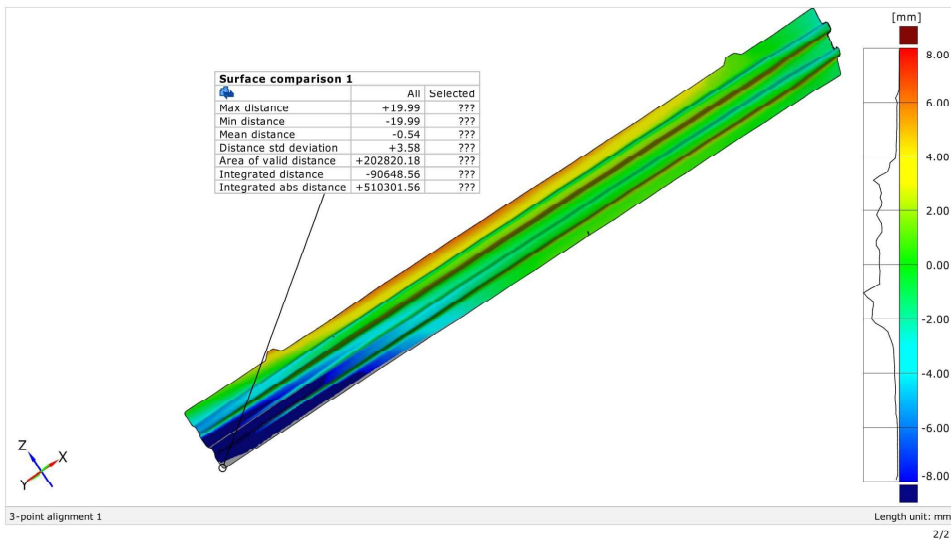


# 3D real MA03 lower\_simulation 7

Generated with GOM Inspect V8



Surface Comparison on CAD

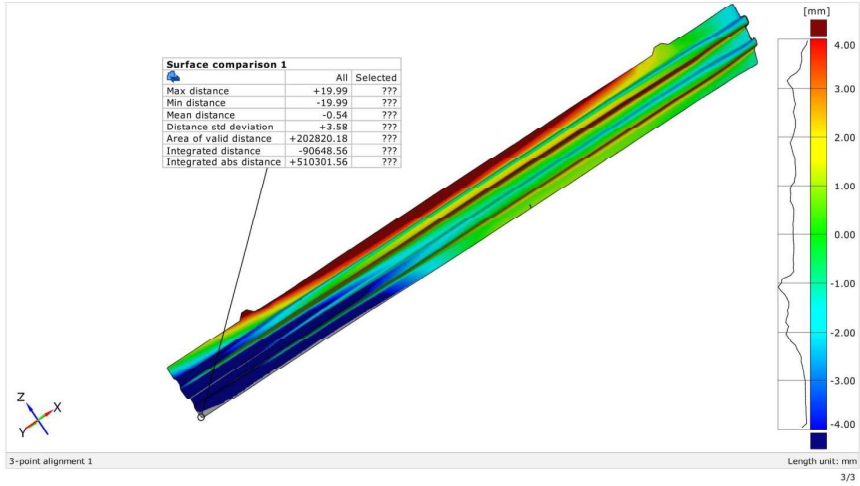


### 3D real MA03 lower\_simulation 7

Generated with GOM Inspect V8



Surface Comparison on CAD

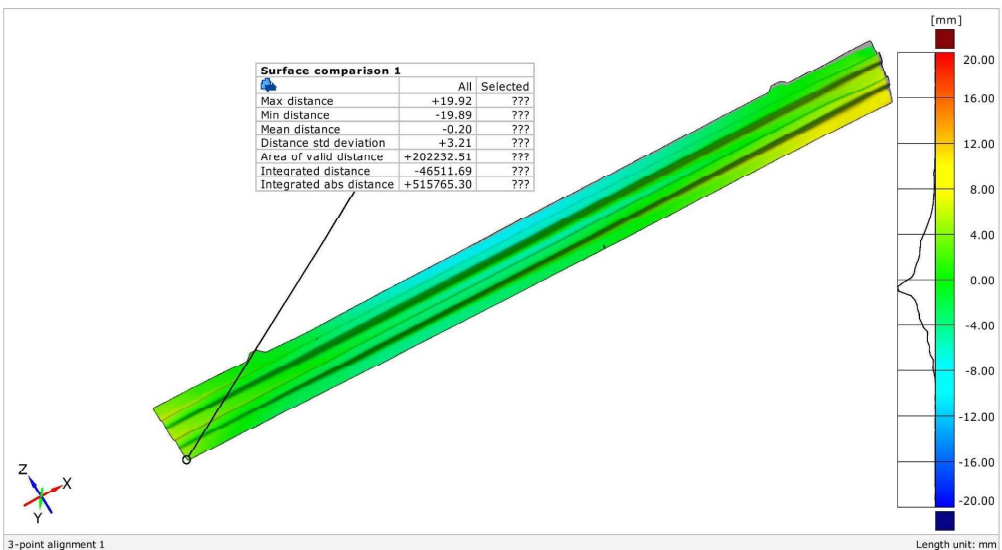


### 3D real MA03 lower\_simulation 8

Generated with GOM Inspect V8



Surface Comparison on CAD

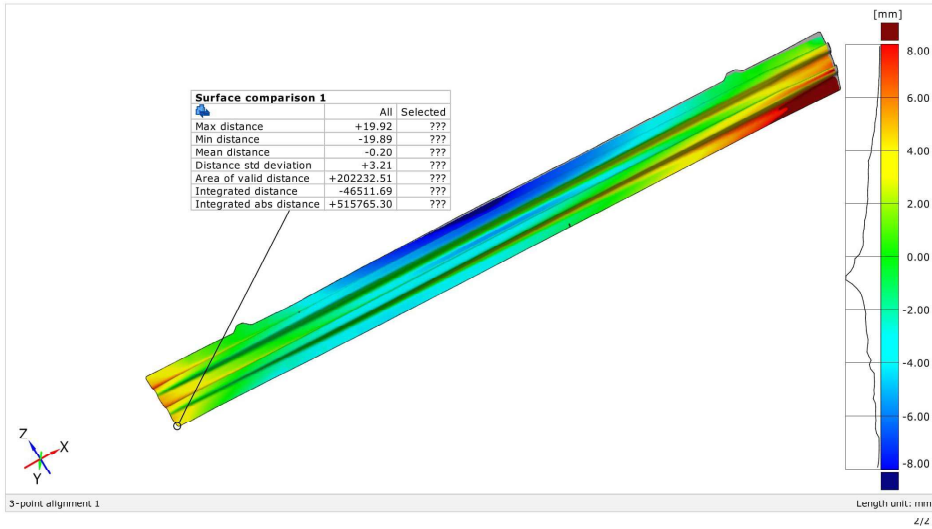


# 3D real MA03 lower\_simulation 8

Generated with GOM Inspect V8



Surface Comparison on CAD

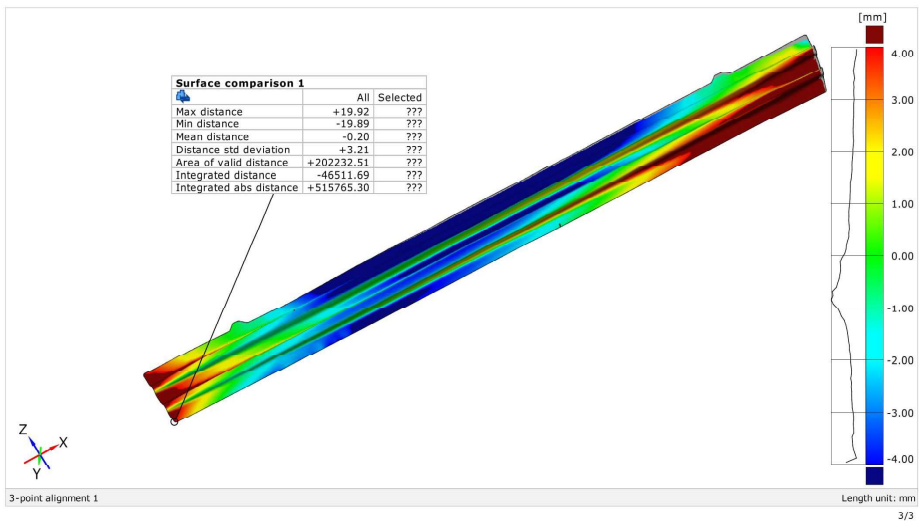


# 3D real MA03 lower\_simulation 8

Generated with GOM Inspect V8



Surface Comparison on CAD

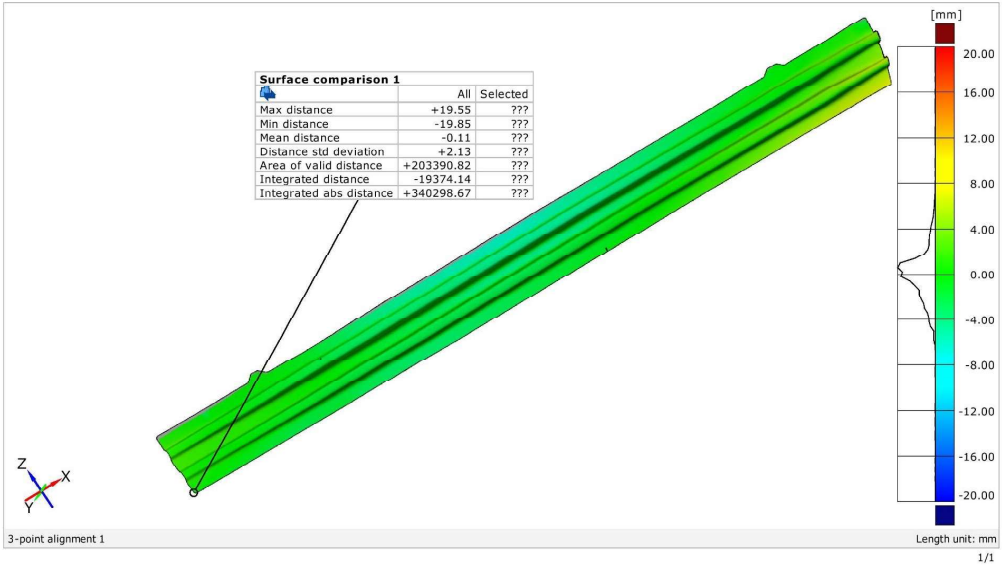


# 3D real MA03 lower\_simulation 9

Generated with GOM Inspect V8



Surface Comparison on CAD

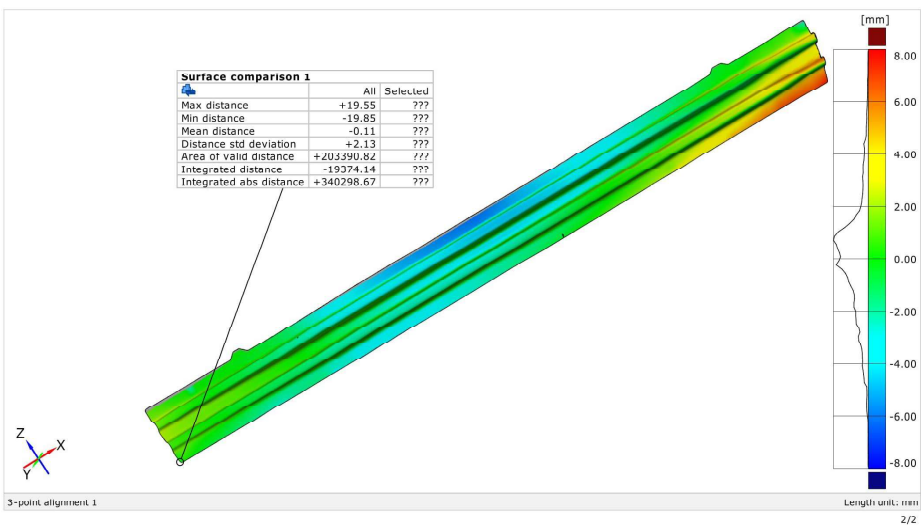


# 3D real MA03 lower\_simulation 9

Generated with GOM Inspect V8



Surface Comparison on CAD

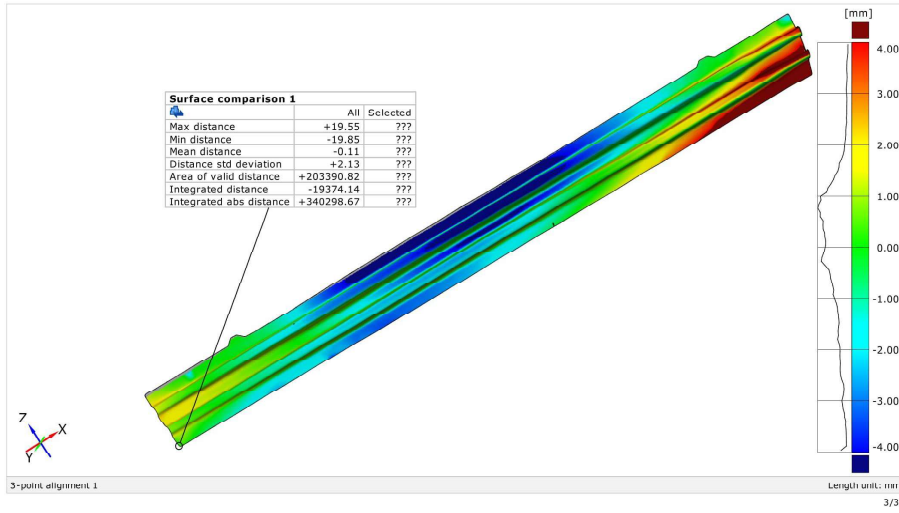


# 3D real MA03 lower\_simulation 9

Generated with GOM Inspect V8



Surface Comparison on CAD

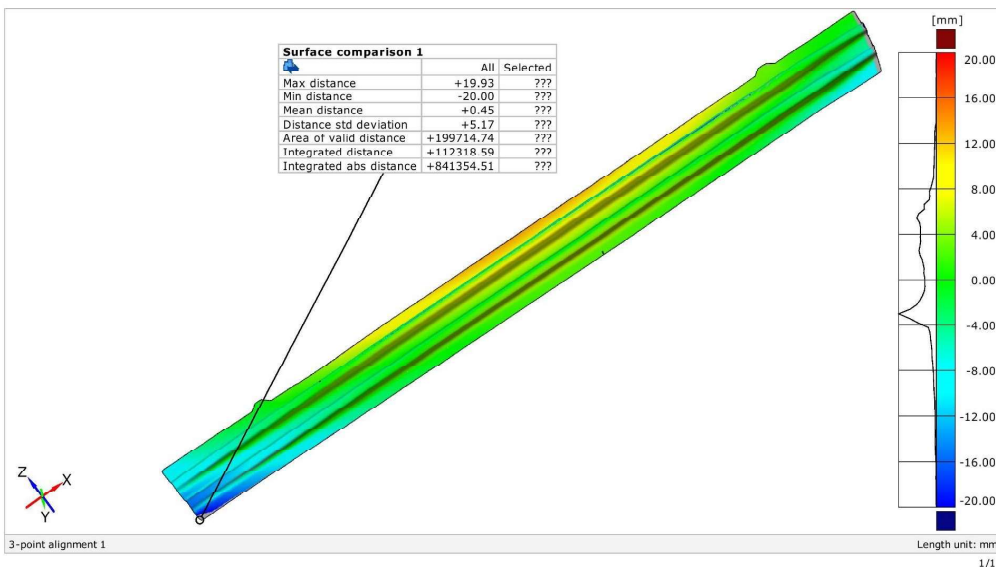


# 3D real MA03 lower\_simulation 10

Generated with GOM Inspect V8



Surface Comparison on CAD

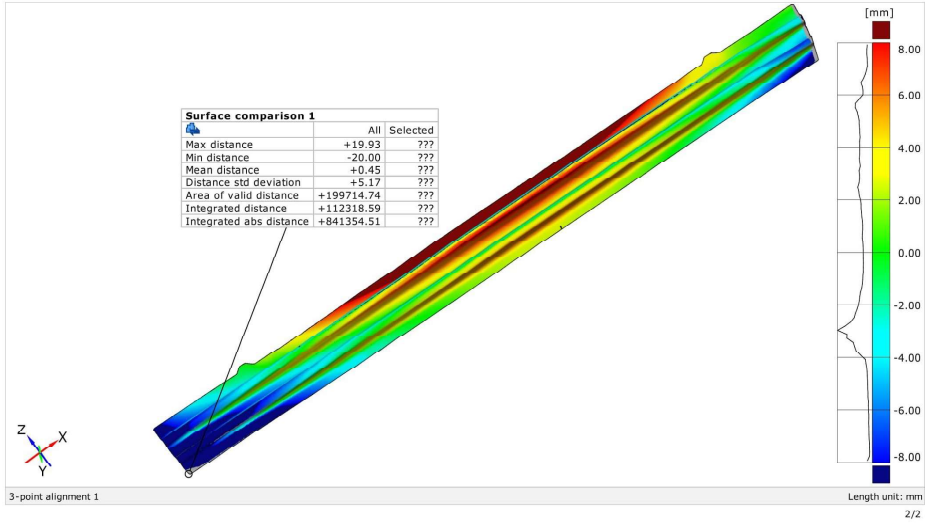


### 3D real MA03 lower\_simulation 10

Generated with GOM Inspect V8



Surface Comparison on CAD

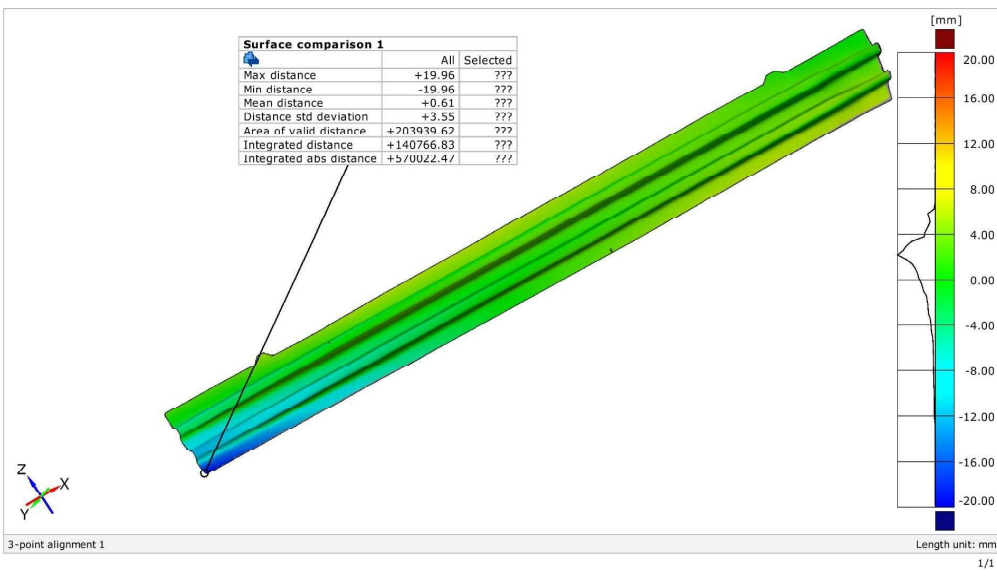


### 3D real MA03 lower\_simulation 11

Generated with GOM Inspect V8



Surface Comparison on CAD

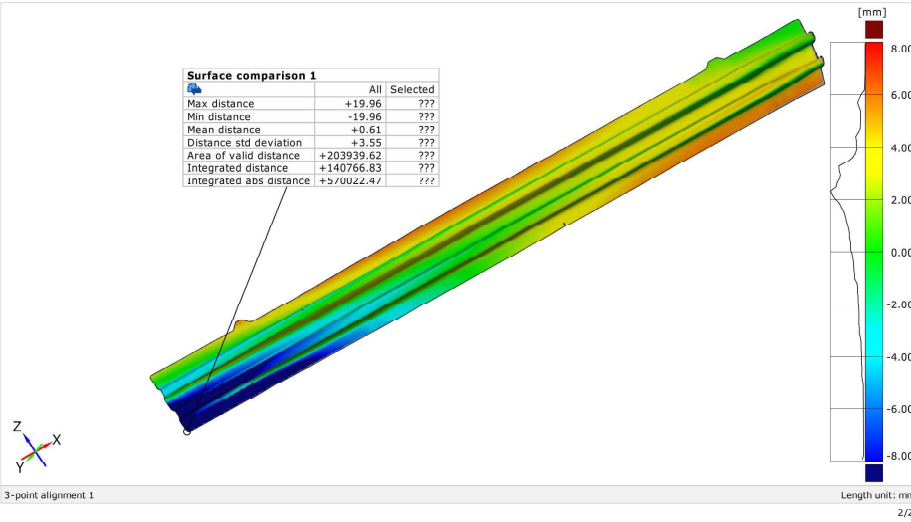


# 3D real MA03 lower\_simulation 11

Generated with GOM Inspect V8



Surface Comparison on CAD

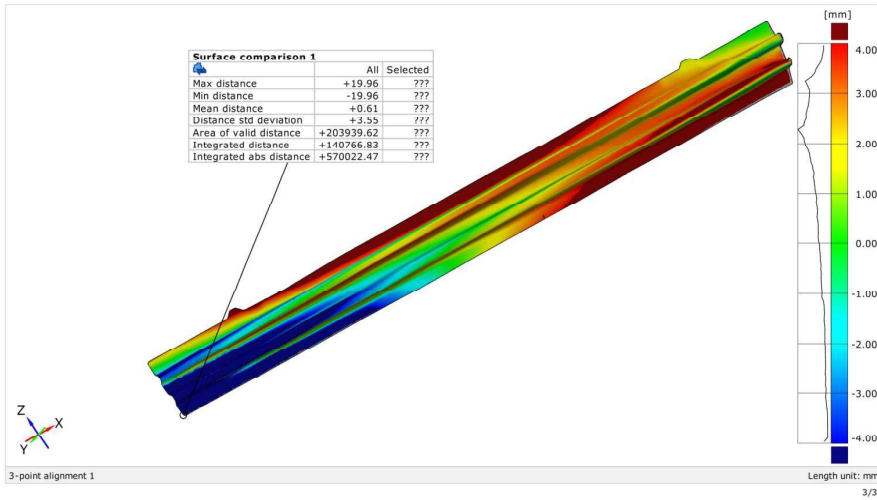


# 3D real MA03 lower\_simulation 11

Generated with GOM Inspect V8



Surface Comparison on CAD

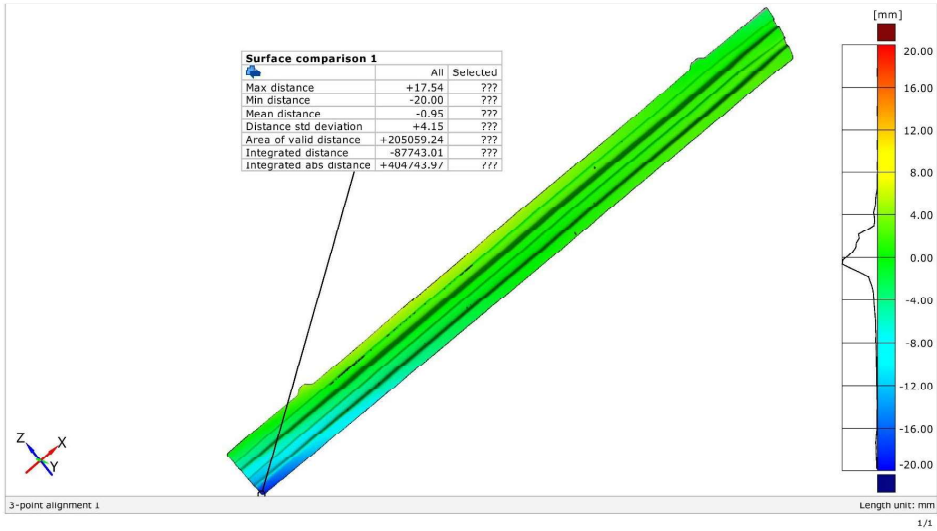


# 3D real MA03 higher\_simulation 1

Generated with GOM Inspect V8



surface comparison on cad

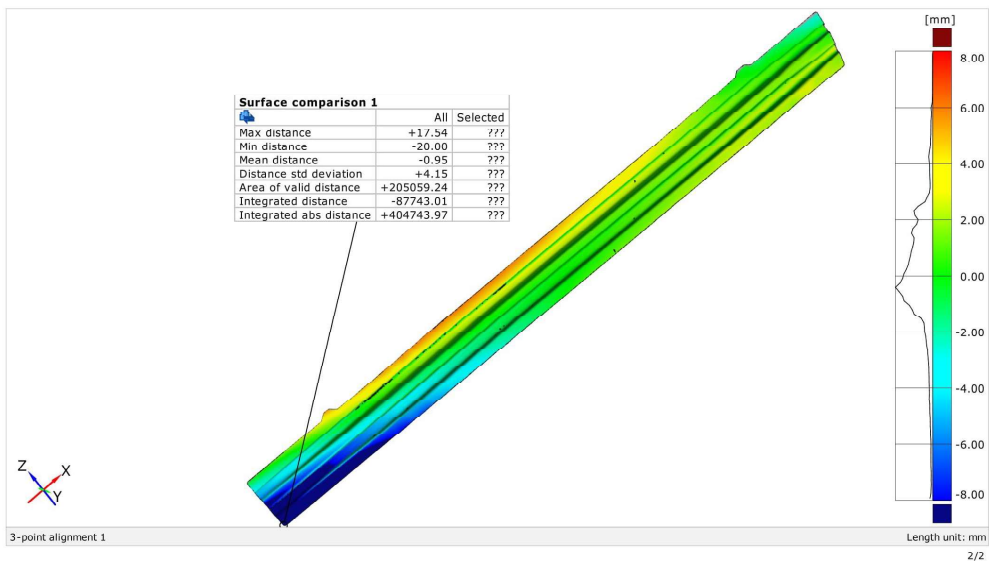


# 3D real MA03 higher\_simulation 1

Generated with GOM Inspect V8



Surface Comparison on CAD

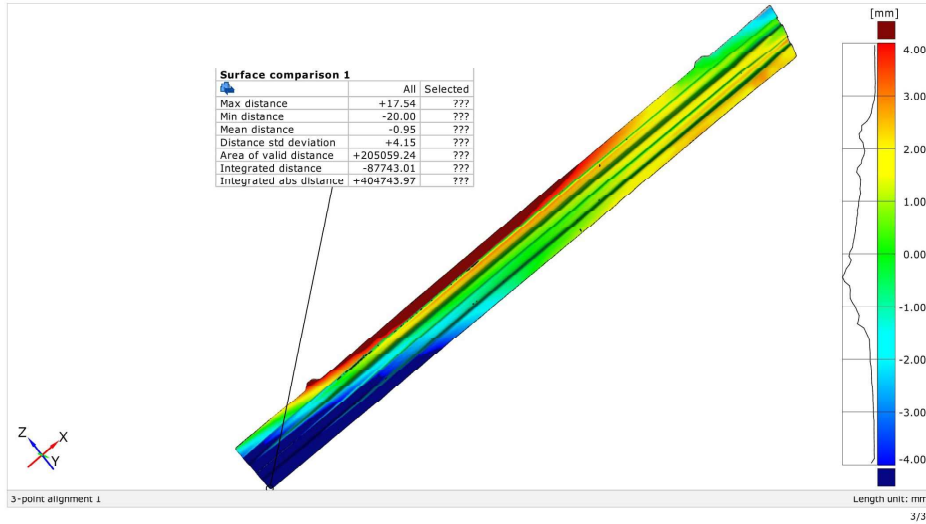


# 3D real MA03 higher\_simulation 1

Generated with GOM Inspect V8



Surface Comparison on CAD

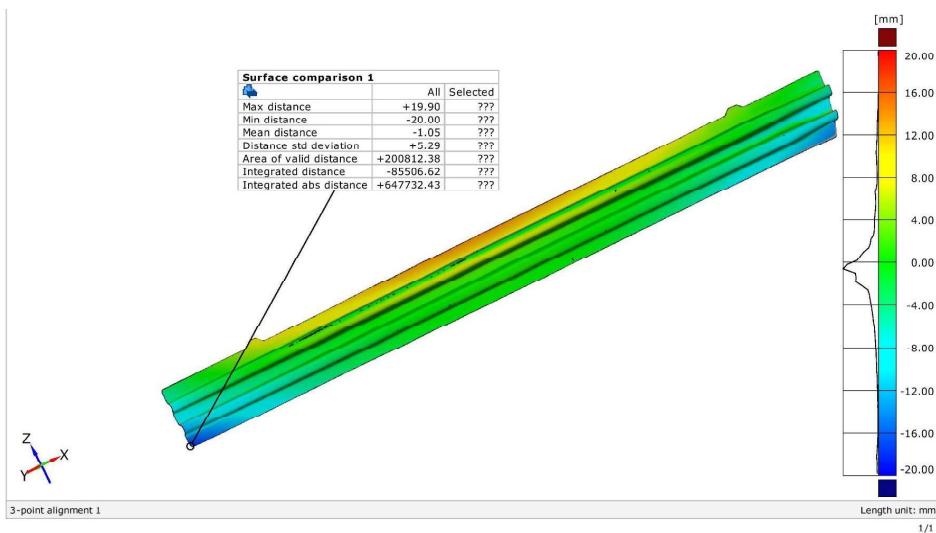


# 3D real MA03 higher\_simulation 2

Generated with GOM Inspect V8



surface comparison on cad

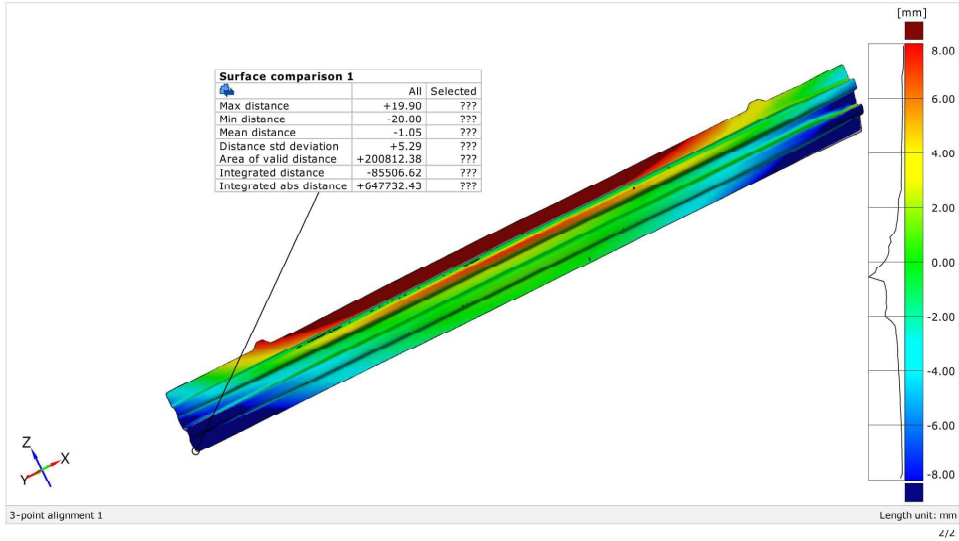


# 3D real MA03 higher\_simulation 2

Generated with GOM Inspect V8



Surface Comparison on CAD

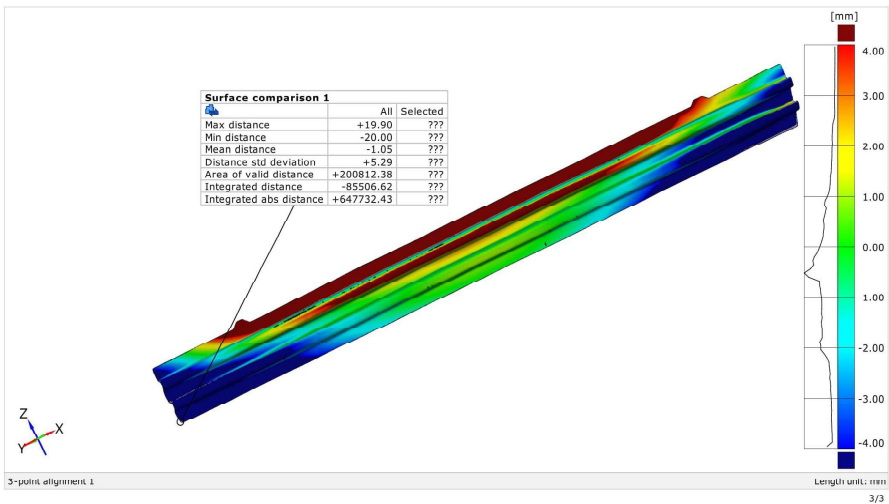


# 3D real MA03 higher\_simulation 2

Generated with GOM Inspect V8



Surface Comparison on CAD

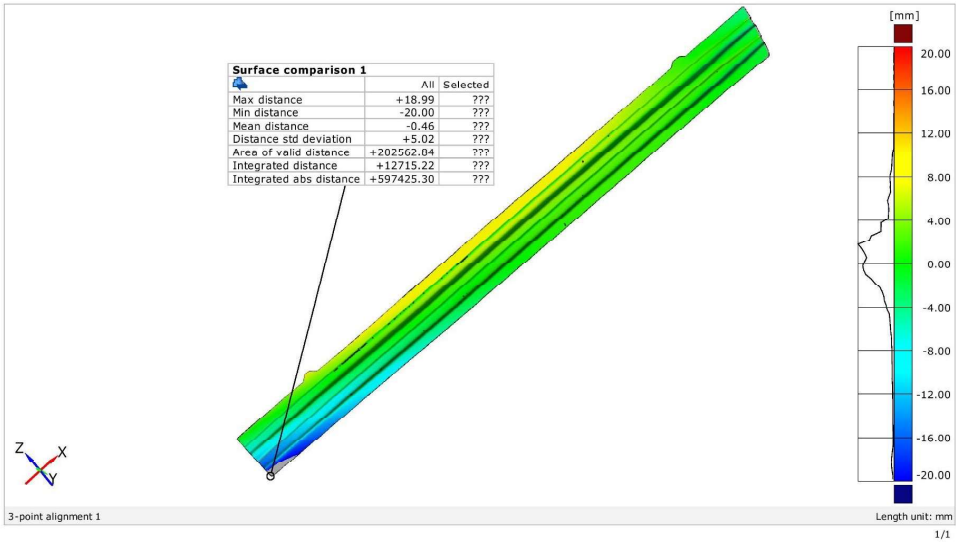


# 3D real MA03 higher\_simulation 3

Generated with GOM Inspect V8



surface comparison on cad

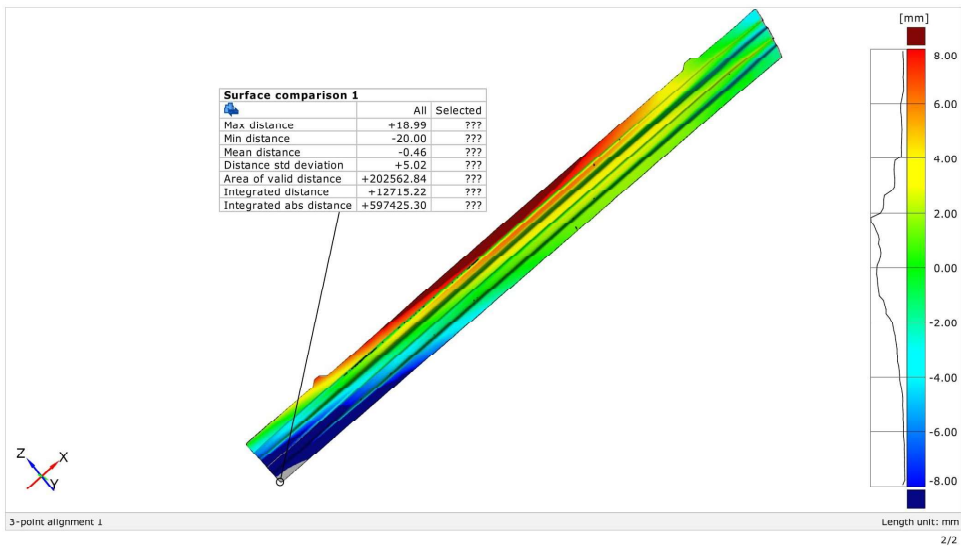


# 3D real MA03 higher\_simulation 3

Generated with GOM Inspect V8



Surface Comparison on CAD

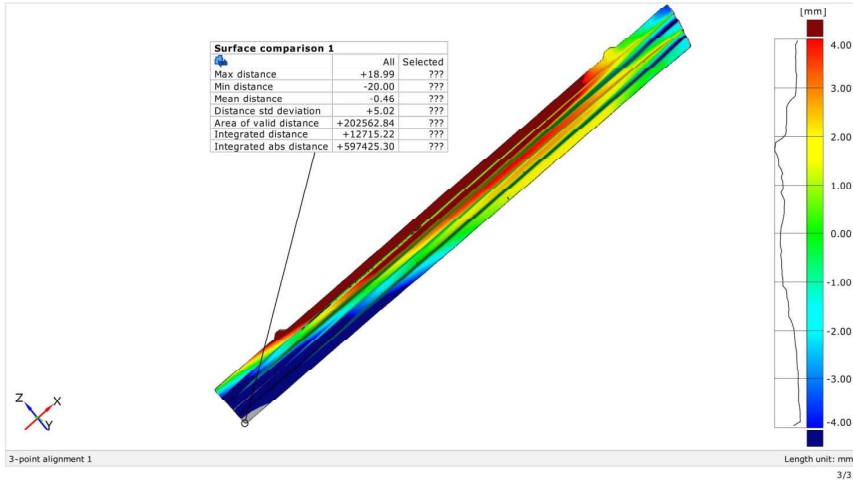


### 3D real MA03 higher\_simulation 3

Generated with GOM Inspect V8



Surface Comparison on CAD

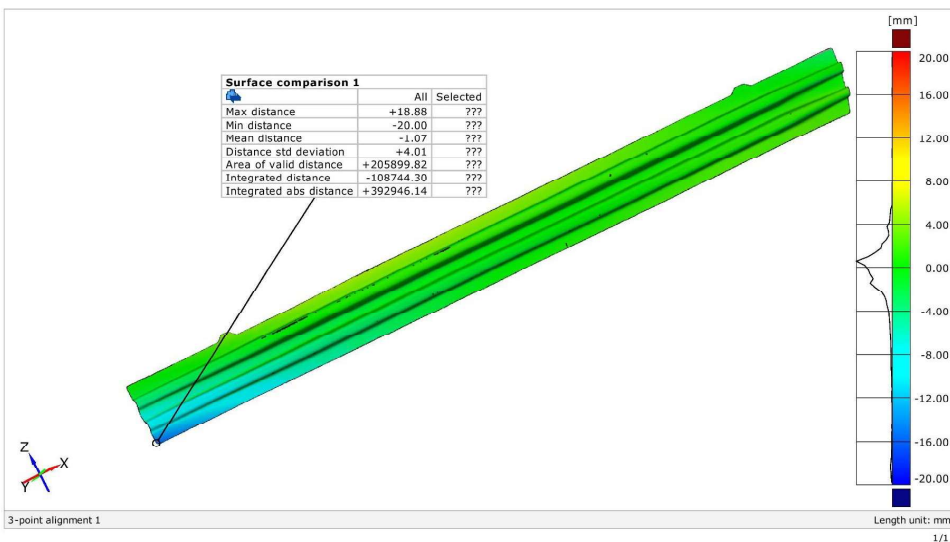


### 3D real MA03 higher\_simulation 4

Generated with GOM Inspect V8



surface comparison on cad

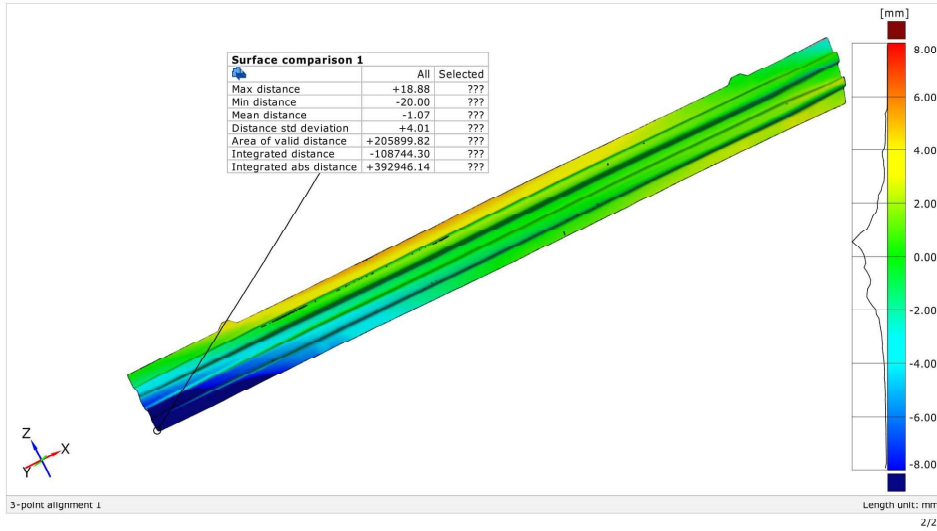


# 3D real MA03 higher\_simulation 4

Generated with GOM Inspect V8



Surface Comparison on CAD

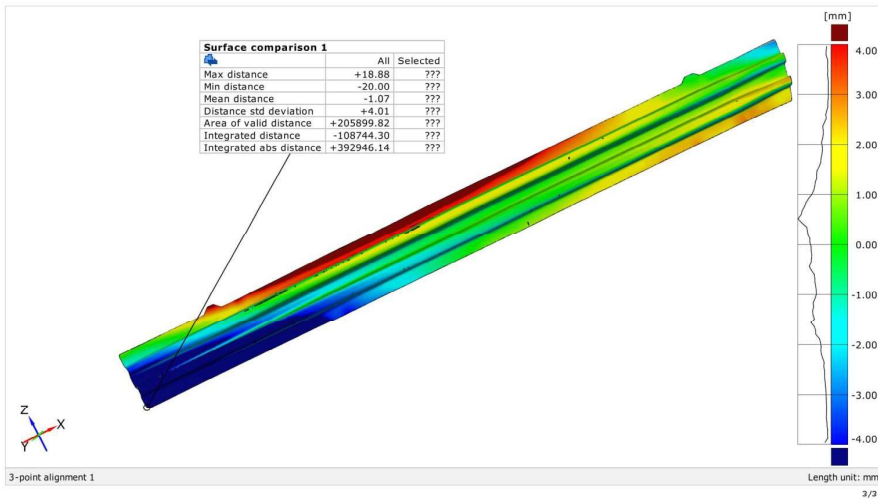


# 3D real MA03 higher\_simulation 4

Generated with GOM Inspect V8



Surface Comparison on CAD

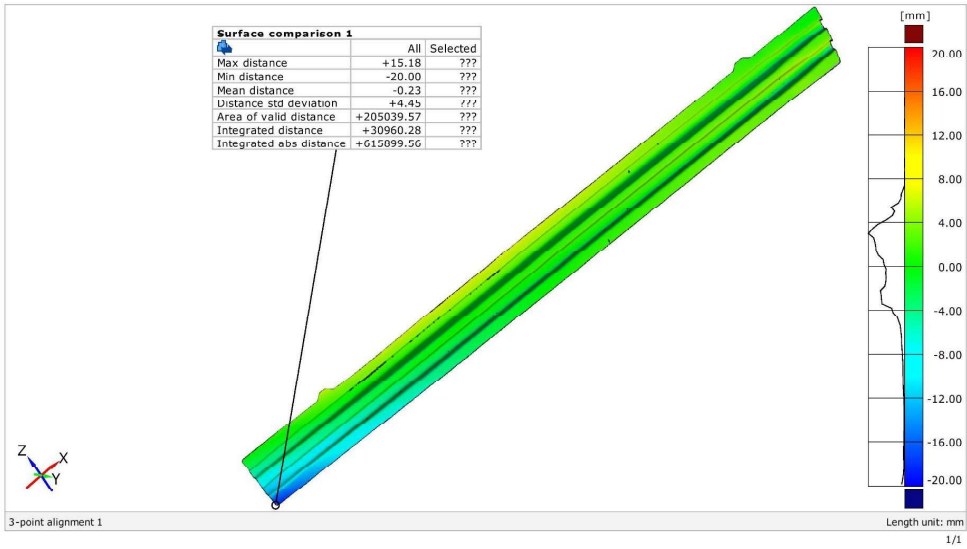


# 3D real MA03 higher\_simulation 5

Generated with GOM Inspect V8



surface comparison on cad

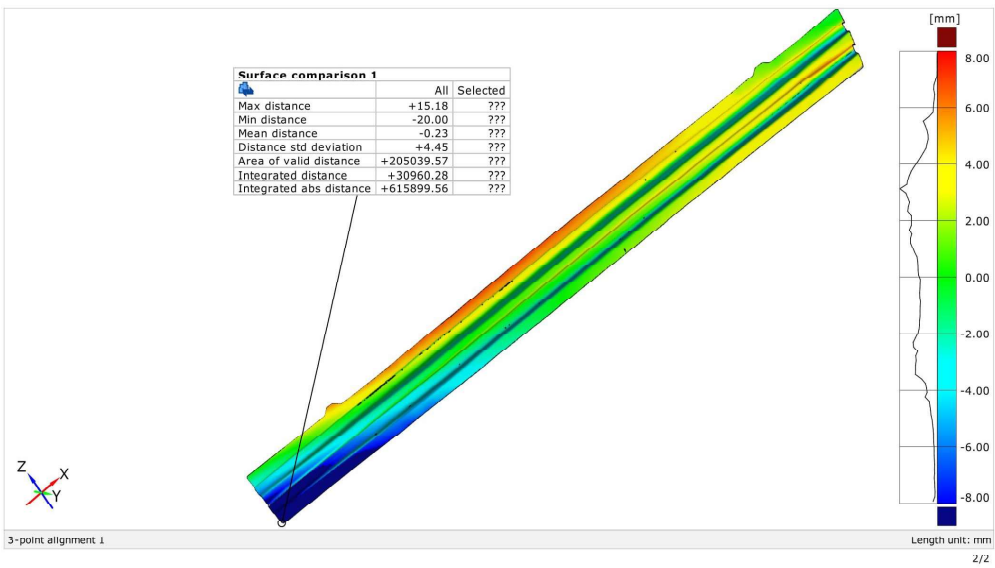


# 3D real MA03 higher\_simulation 5

Generated with GOM Inspect V8



Surface Comparison on CAD

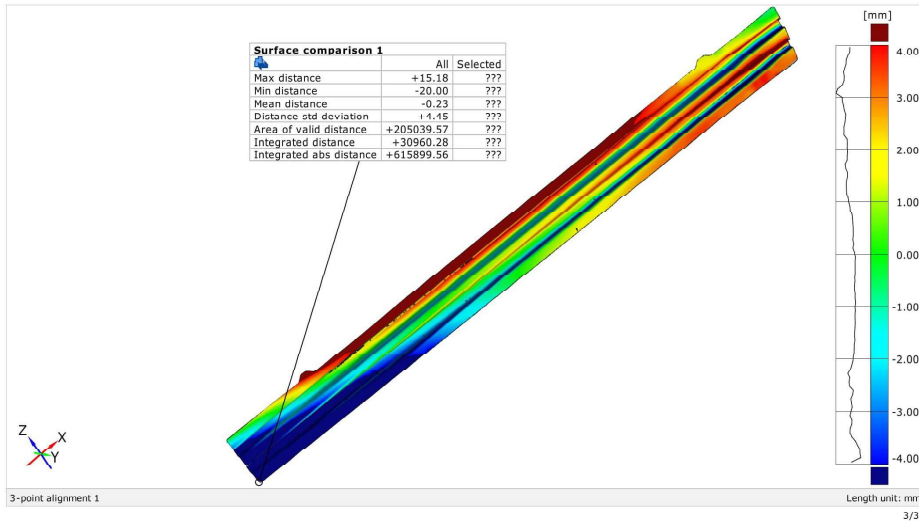


# 3D real MA03 higher\_simulation 5

Generated with GOM Inspect V8



Surface Comparison on CAD

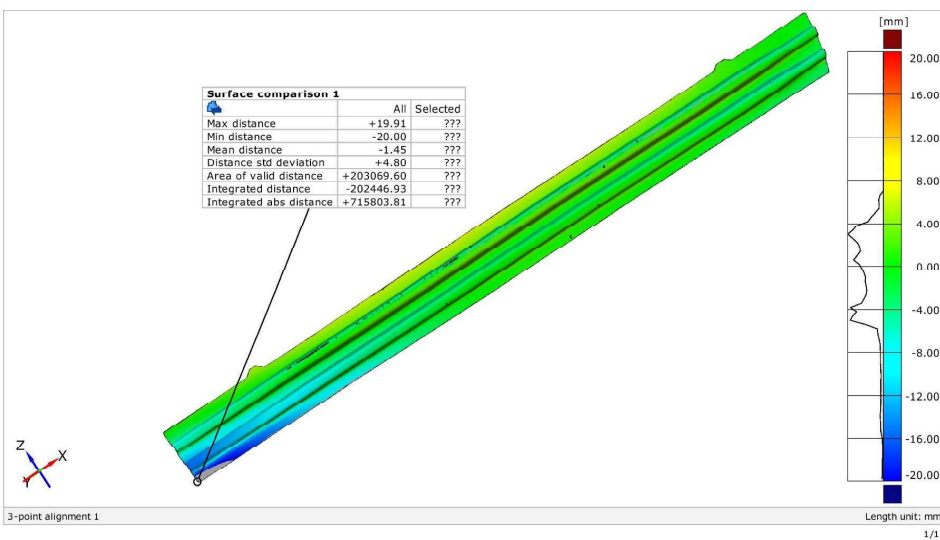


# 3D real MA03 higher\_simulation 6

Generated with GOM Inspect V8



surface comparison on cad

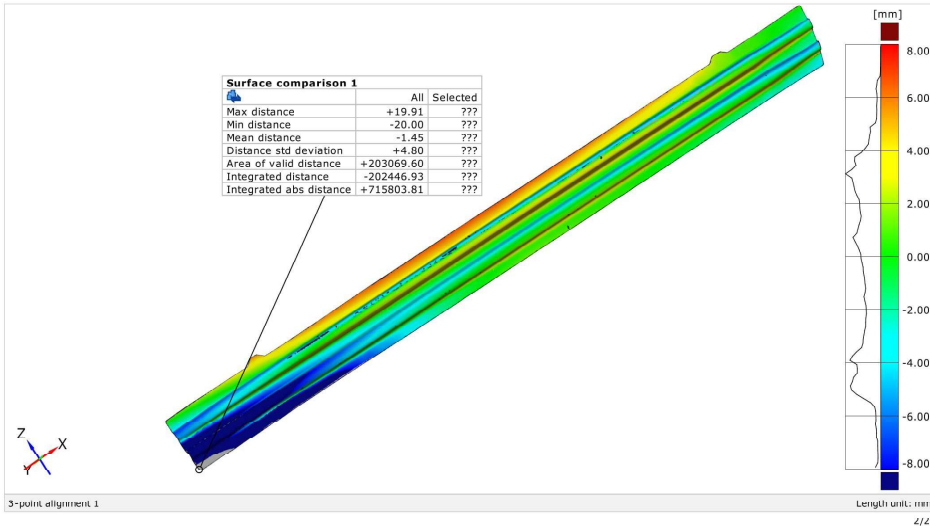


# 3D real MA03 higher\_simulation 6

Generated with GOM Inspect V8



Surface Comparison on CAD

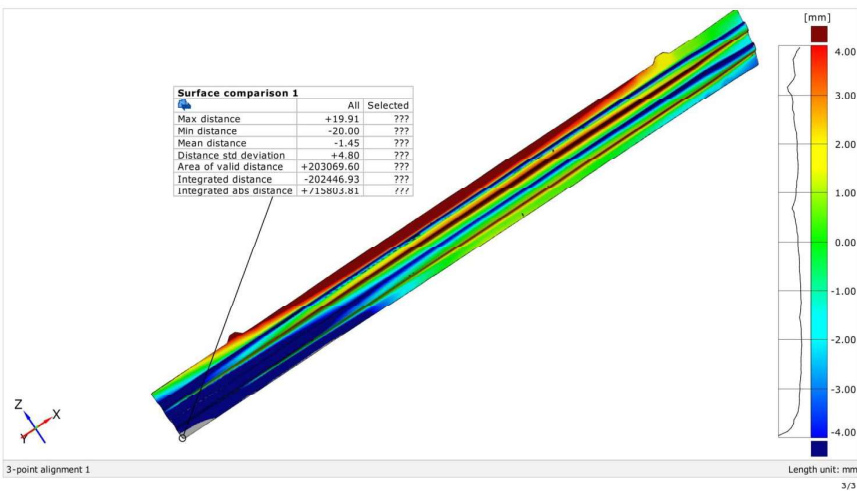


# 3D real MA03 higher\_simulation 6

Generated with GOM Inspect V8



Surface Comparison on CAD

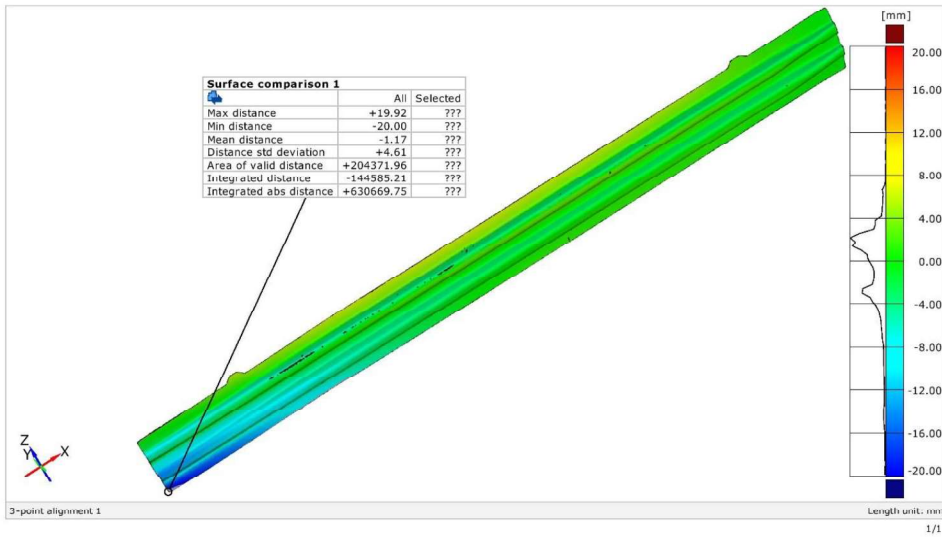


# 3D real MA03 higher\_simulation 7

Generated with GOM Inspect V8



surface comparison on cad

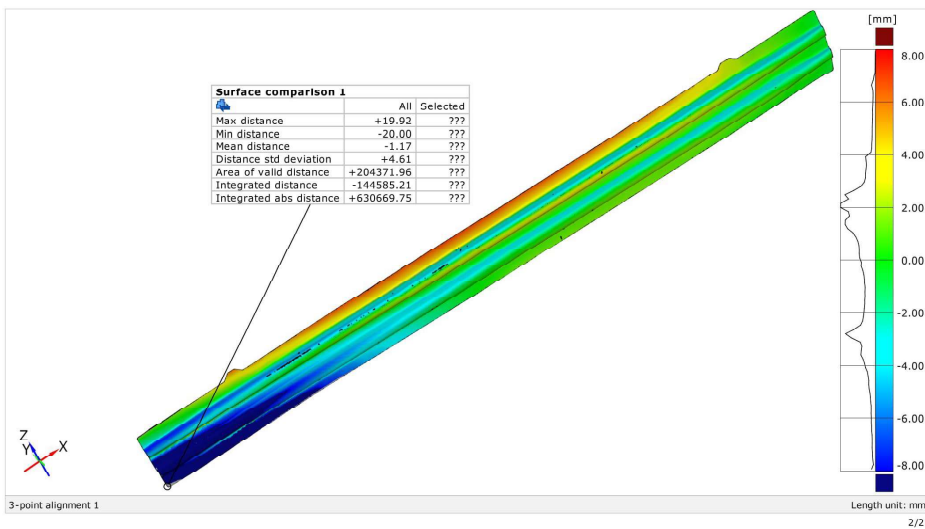


# 3D real MA03 higher\_simulation 7

Generated with GOM Inspect V8



Surface Comparison on CAD

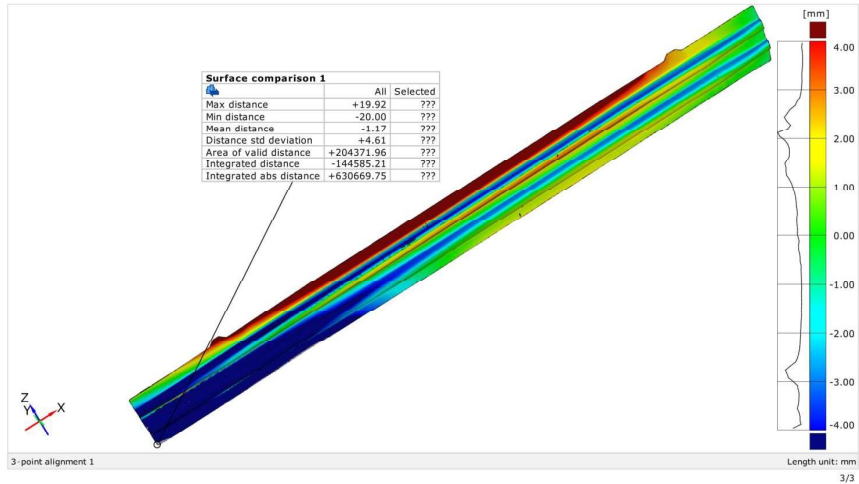


### 3D real MA03 higher\_simulation 7

Generated with GOM Inspect V8



Surface Comparison on CAD

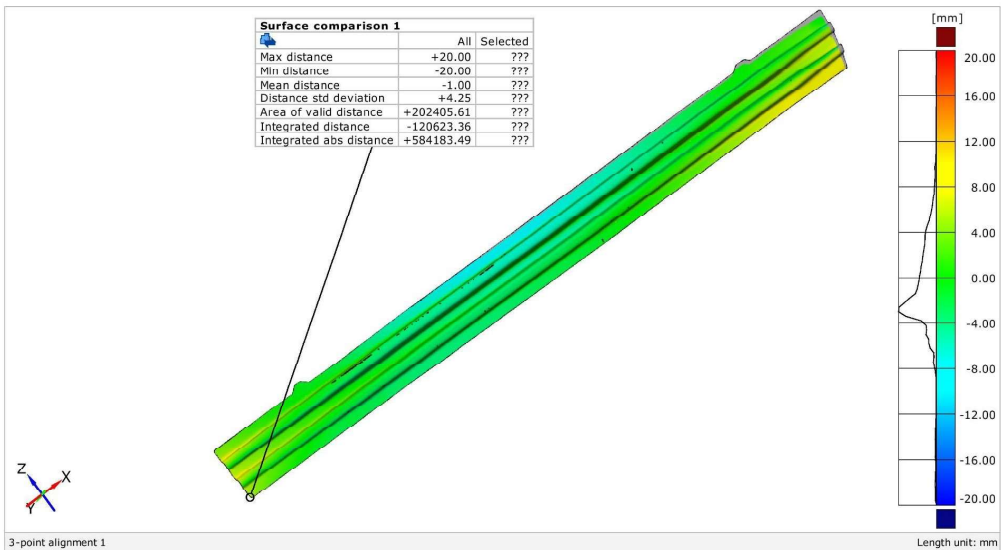


### 3D real MA03 higher\_simulation 8

Generated with GOM Inspect V8



Surface Comparison on CAD

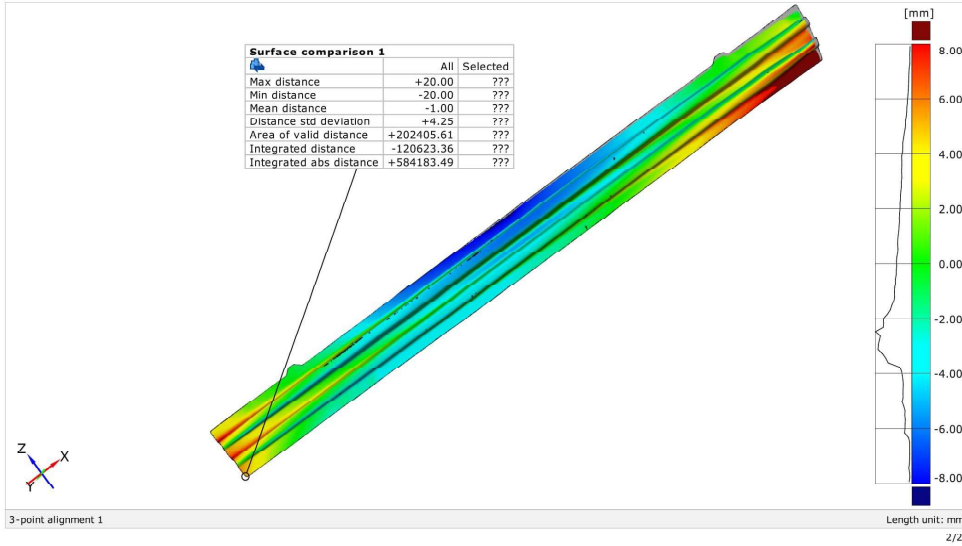


# 3D real MA03 higher\_simulation 8

Generated with GOM Inspect V8



Surface Comparison on CAD

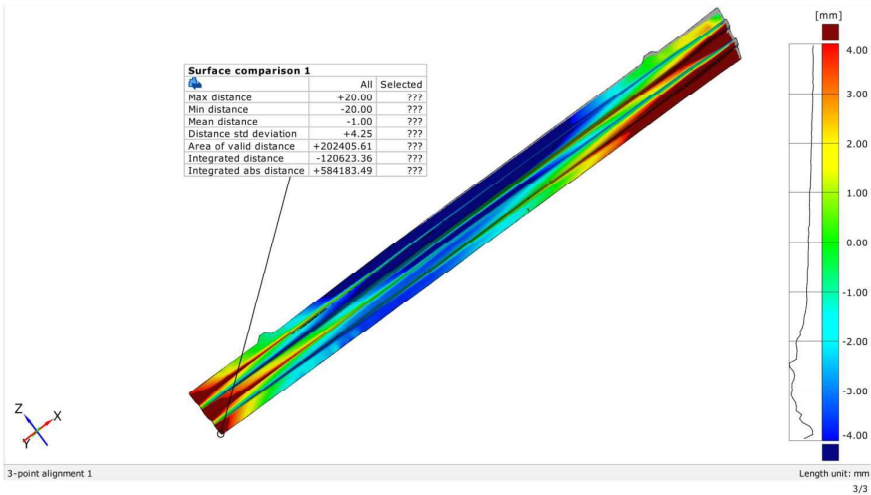


# 3D real MA03 higher\_simulation 8

Generated with GOM Inspect V8



Surface Comparison on CAD

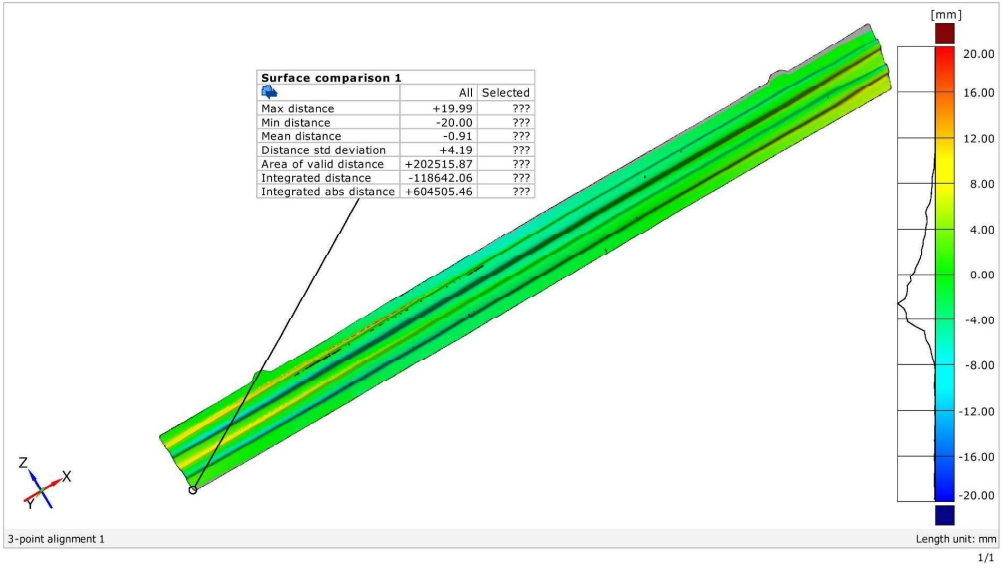


# 3D real MA03 higher\_simulation 9

Generated with GOM Inspect V8



Surface Comparison on CAD

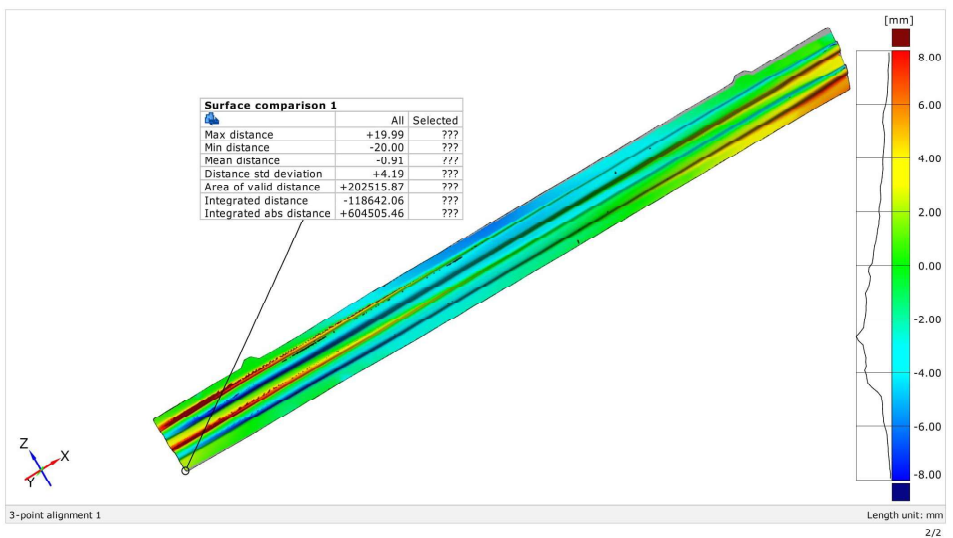


# 3D real MA03 higher\_simulation 9

Generated with GOM Inspect V8



Surface Comparison on CAD

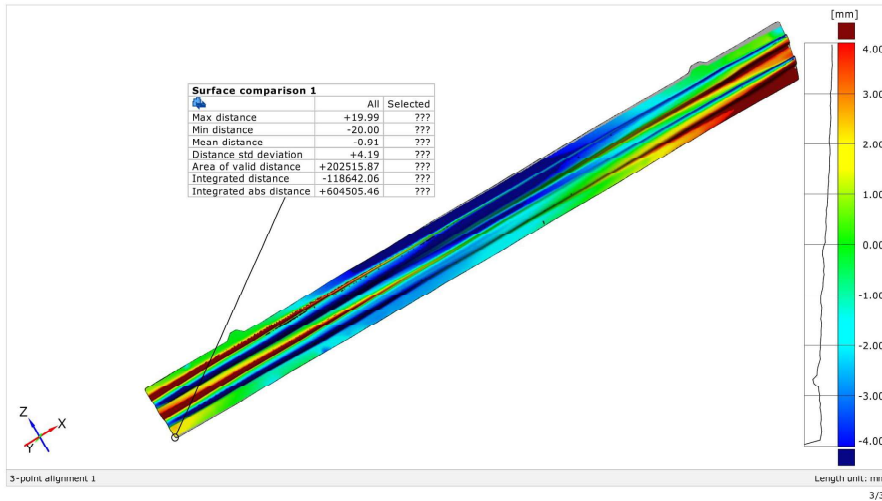


### 3D real MA03 higher\_simulation 9

Generated with GOM Inspect V8



Surface Comparison on CAD

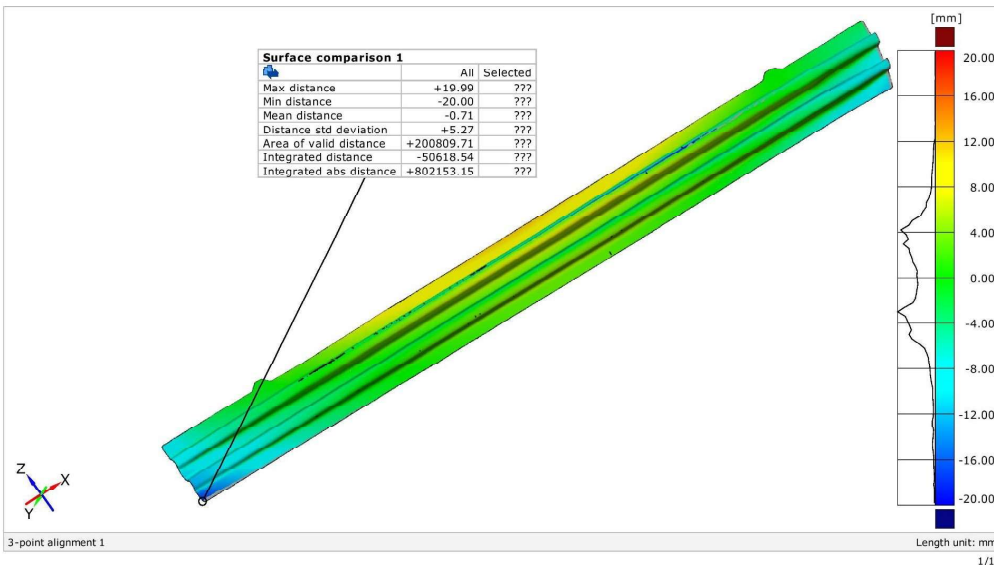


### 3D real MA03 higher\_simulation 10

Generated with GOM Inspect V8



Surface Comparison on CAD

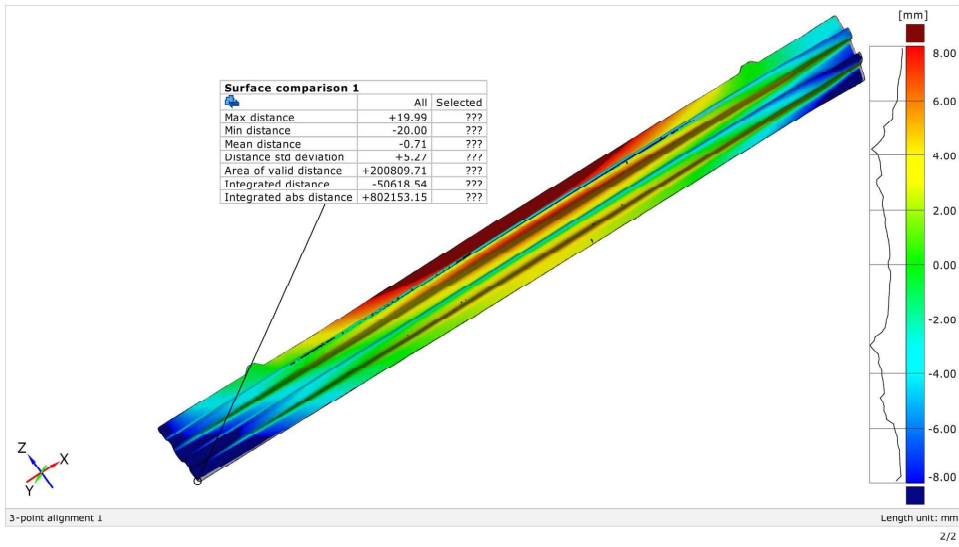


# 3D real MA03 higher simulation 10

Generated with GOM Inspect V8



Surface Comparison on CAD

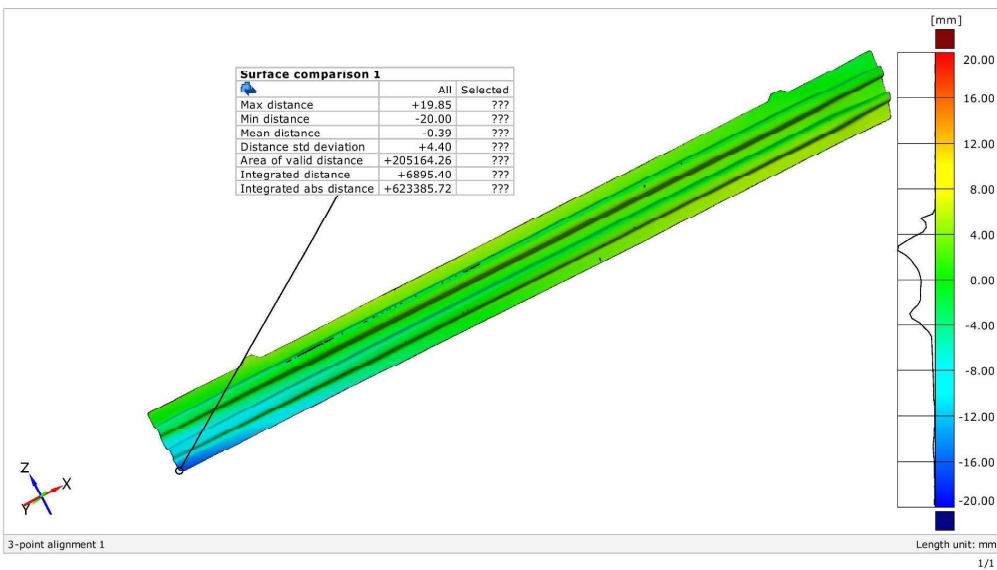


# 3D real MA03 higher\_simulation 11

Generated with GOM Inspect V8



Surface Comparison on CAD

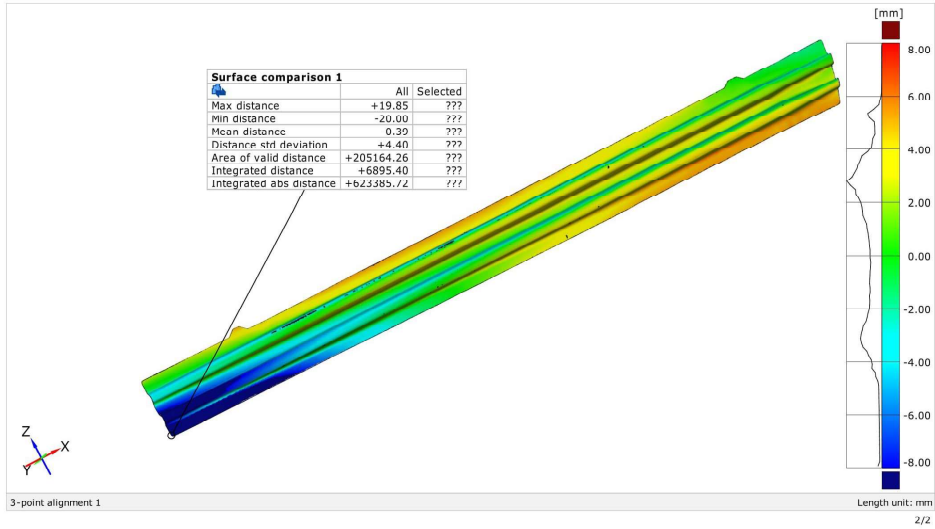


# 3D real MA03 higher\_simulation 11

Generated with GOM Inspect V8



Surface Comparison on CAD

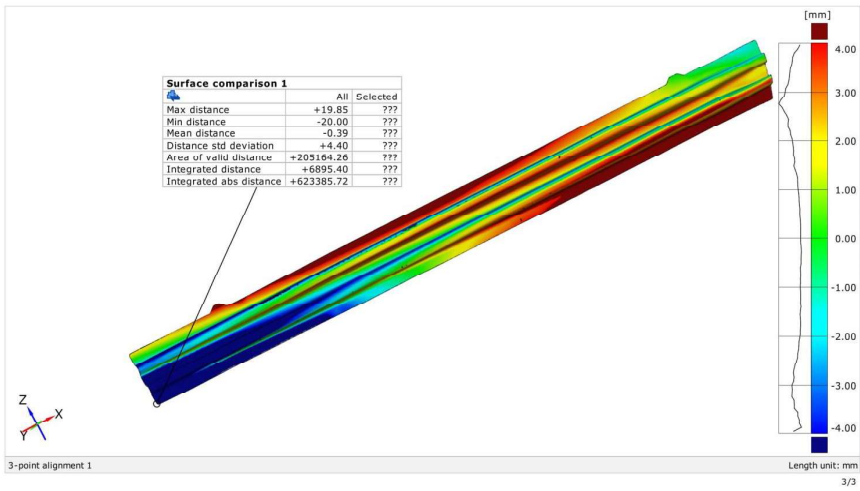


# 3D real MA03 higher\_simulation 11

Generated with GOM Inspect V8



Surface Comparison on CAD

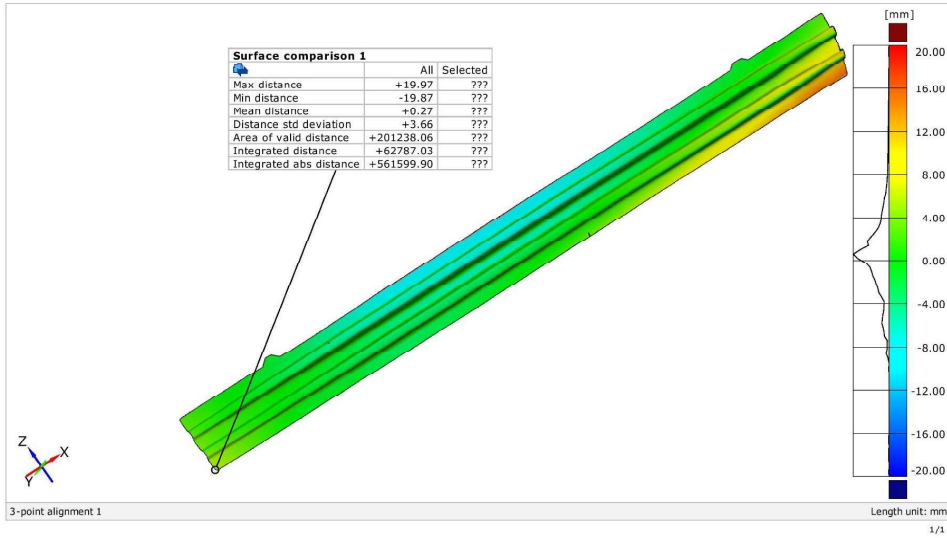


# 3D real MA03 lower\_simulation Autoform

Generated with GOM Inspect V8



surface comparison on cad

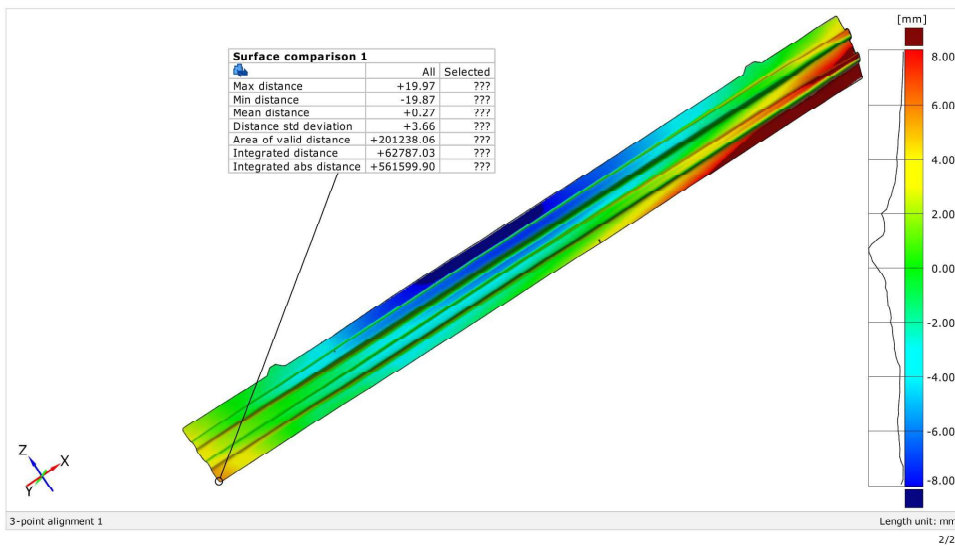


# 3D real MA03 lower\_simulation Autoform

Generated with GOM Inspect V8



Surface Comparison on CAD

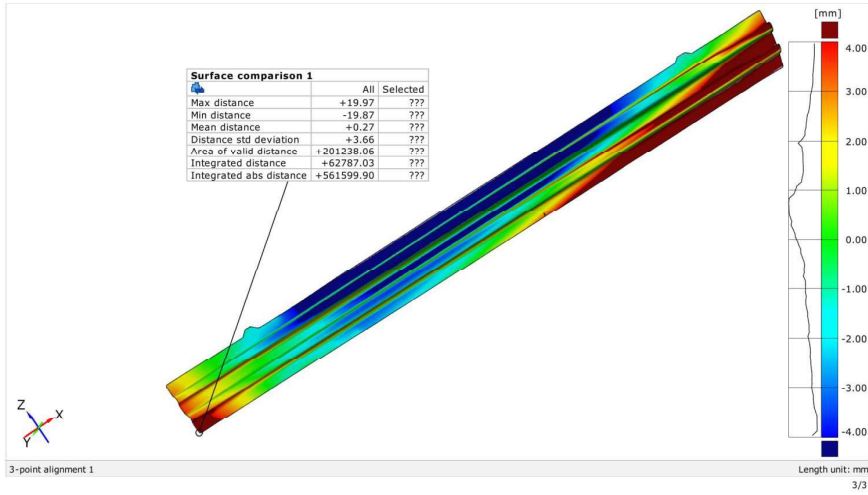


# 3D real MA03 lower\_simulation Autoform

Generated with GOM Inspect V8



Surface Comparison on CAD

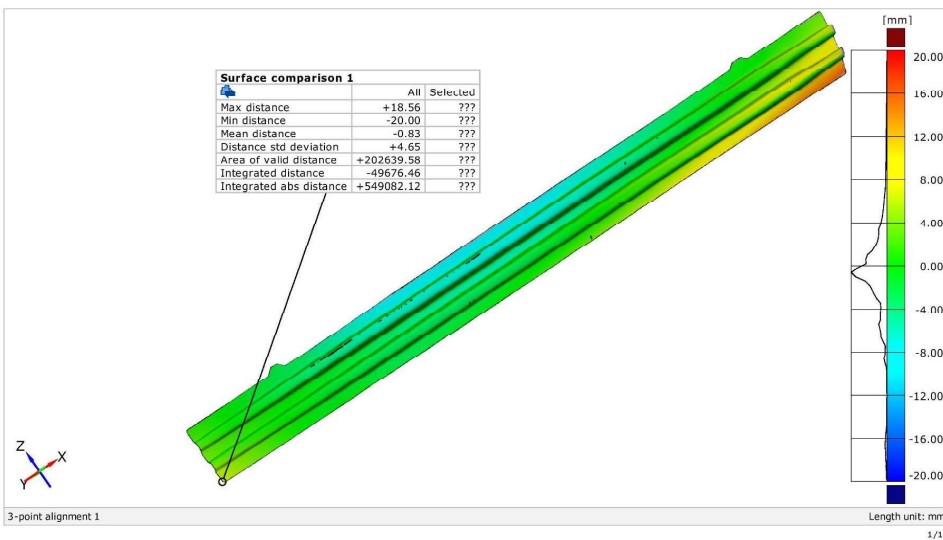


# 3D real MA03 higher\_simulation Autoform

Generated with GOM Inspect V8



surface comparison on cad

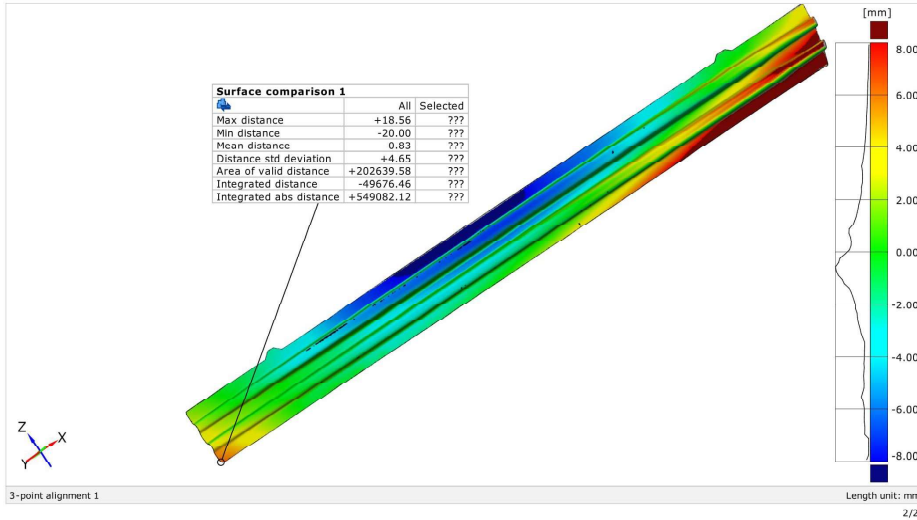


# 3D real MA03 higher\_simulation Autoform

Generated with GOM Inspect V8



Surface Comparison on CAD

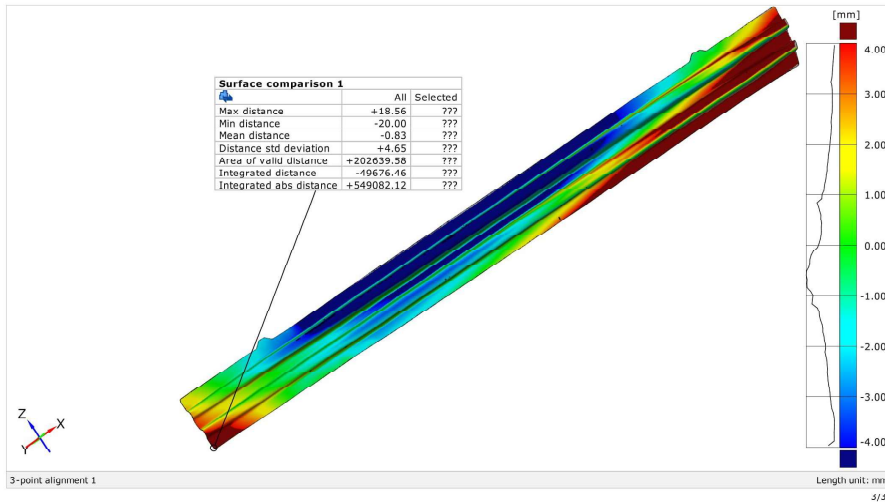


# 3D real MA03 higher\_simulation Autoform

Generated with GOM Inspect V8

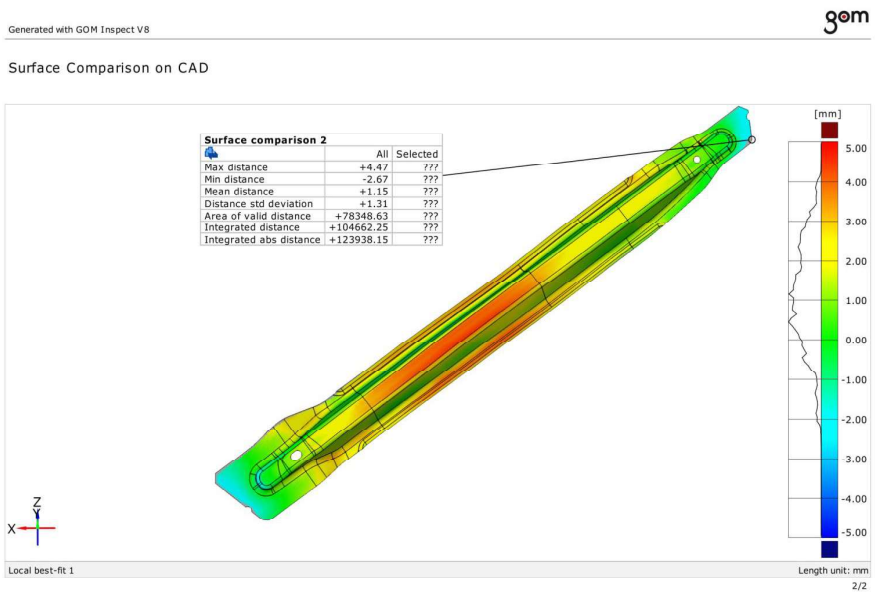


Surface Comparison on CAD



# ANNEX 16.1.7 COMPARISON BETWEEN THE CAD AND THE HYPERFORM SIMULATION

## Hyperform simulation\_CAD lower

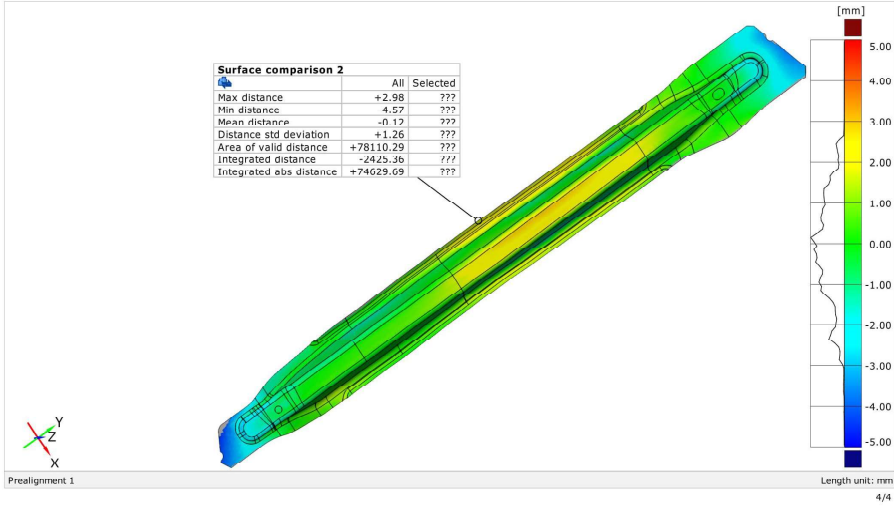


# Hyperform simulation\_CAD average

Generated with GOM Inspect V8



Surface Comparison on CAD

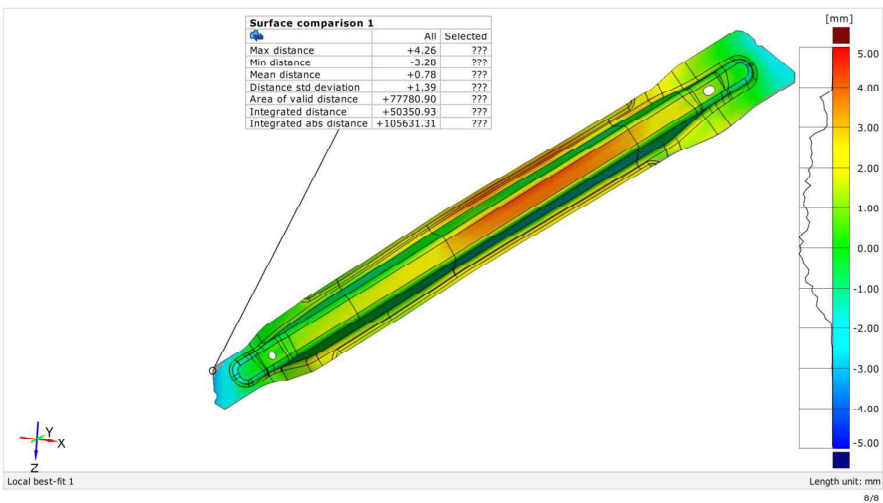


# Hyperform simulation\_CAD higher

Generated with GOM Inspect V8



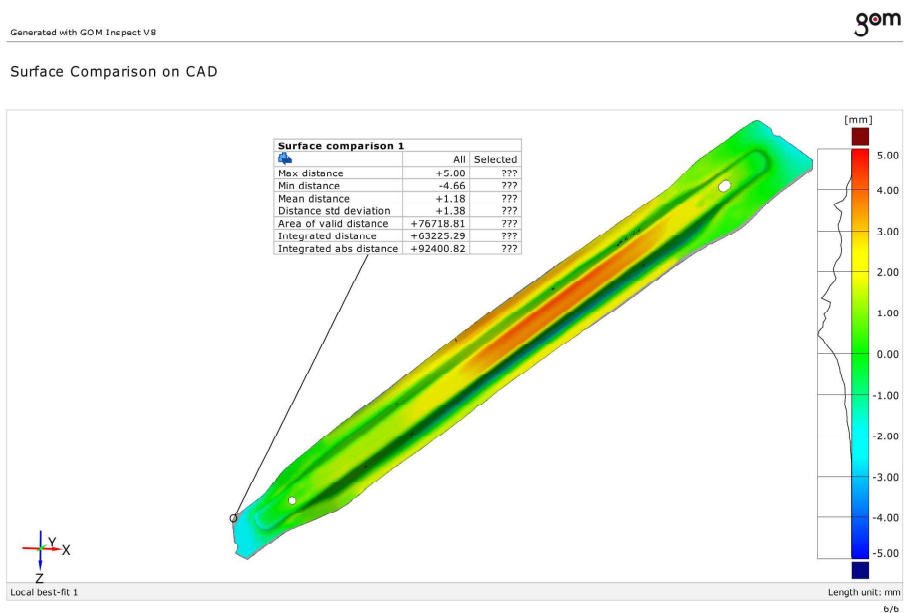
Surface Comparison on CAD



## ANNEX 16.1.8

### COMPARISON BETWEEN THE SCANNED GEOMETRY AND THE HYPERFORM SIMULATION

#### Hyperform simulation\_scanned lower

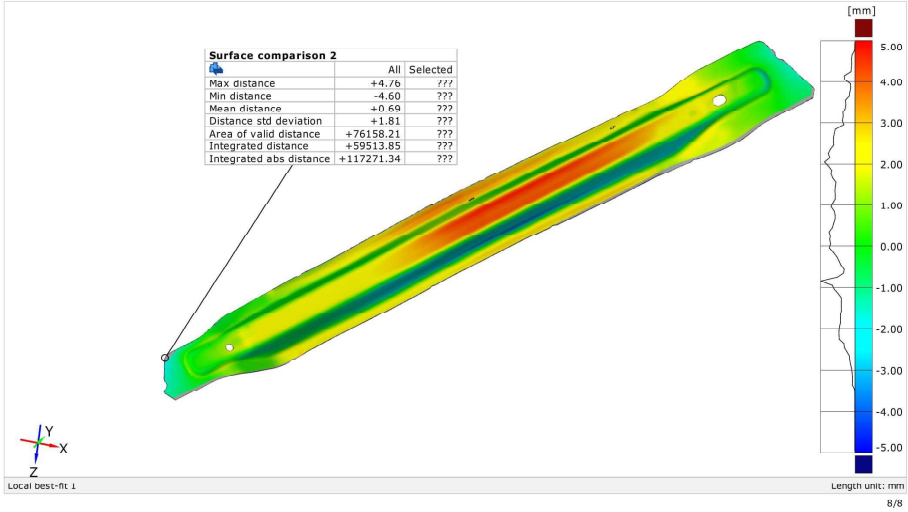


# Hyperform simulation\_scanned higher

Generated with GOM Inspect VR



## Surface Comparison on CAD



## ANNEX 16.2

### COMPARISON BETWEEN BEST RESULTS FROM HYPERFORM SIMULATION AND STAMPACK SIMULATION

#### Stampack Simulation 7 and Hyperform Simulation

Generated with GOM Inspect V8



Surface Comparison on CAD

